IMPERIAL

Imperial College London

Department of Mathematics

Phase-space approaches to decoherence and classicality in quantum theory

Rishindra Melanathuru

Supervised by: Prof. Dorje Brody, Dr. Eva-Maria Graefe.

2 October 2025

Submitted in part fulfilment of the requirements for the degree of Doctor of Philosophy in Mathematics of Imperial College London and the Diploma of Imperial College London.

Declaration of Originality

I, Rishindra Melanathuru

Supervised by: Prof. Dorje Brody, Dr. Eva-Maria Graefe., declare that the work in this thesis is my own. The work of others has been appropriately referenced. A full list of references is given in the bibliography.

Copyright

The copyright of this thesis rests with the author. Unless otherwise indicated, its contents are licensed under a Creative Commons Attribution-Non Commercial 4.0 International Licence (CC BY-NC). Under this licence, you may copy and redistribute the material in any medium or format. You may also create and distribute modified versions of the work. This is on the condition that: you credit the author and do not use it, or any derivative works, for a commercial purpose. When reusing or sharing this work, ensure you make the licence terms clear to others by naming the licence and linking to the licence text. Where a work has been adapted, you should indicate that the work has been changed and describe those changes.

Please seek permission from the copyright holder for uses of this work that are not included in this licence or permitted under UK Copyright Law.

Abstract

This thesis presents a comprehensive study of phase-space measurements, decoherence, and the emergence of classicality in quantum systems. Motivated by limitations of position-based localisation in standard decoherence models, we develop a phase-space decoherence formalism using coherent-state positive operator-valued measures (POVMs). These generalised measurements, constructed from overcomplete sets of coherent states, provide a natural and physically motivated framework for modelling coarse-grained quantum observations.

We develop an iterative measurement scheme for phase-space decoherence in systems with Heisenberg-Weyl, $\mathrm{SU}(2)$, $\mathrm{SU}(1,1)$, and $\mathrm{SU}(N)$ symmetries. In each case, repeated weak measurements gradually suppress quantum interference, driving the system toward a maximally mixed state. A universal structure is shown to emerge: a single iteration maps the Wigner function to the Husimi Q-function, removing negativity, while full decoherence maps the singular Glauber-Sudarshan P-function to the Q-function, eliminating all singularities. This establishes a group-independent mechanism by which phase-space measurements induce classicality.

We compare this model to Lindblad-type dynamics, which describe open quantum systems via completely positive, trace-preserving semigroups. For Heisenberg-Weyl and tomographic $\mathrm{SU}(N)$ systems, the measurement channel coincides exactly with isotropic Lindblad evolution. In $\mathrm{SU}(2)$ and $\mathrm{SU}(1,1)$ cases, the correspondence is only partial, with exact agreement in asymptotic regimes. A universal decoherence timescale, t_*, emerges beyond which quasi-probability distributions become strictly positive.

We then construct a stochastic unravelling based on Brownian motion on phase space, offering a geometric alternative to standard stochastic Schrödinger equations. This reveals that decoherence occurs without GKSL-type dynamics in noncompact systems. Such unravellings preserve the intrinsic phase-space symmetry and provide a natural setting for studying semiclassical limits and quantum-to-classical transitions.

Finally, we extend the framework to relativistic quantum systems by defining a covariant coherent-state POVM on the future tube and constructing a Bargmann transform to the forward light cone. Preliminary results on relativistic phase-space decoherence are presented, along with possible directions for future research.

Acknowledgements

I would like to express my deepest gratitude to my primary supervisor, **Prof. Dorje Brody**, whose remarkable expertise in mathematics and physics has been an inspiration throughout my PhD. Their guidance and mentorship have greatly shaped my understanding of the geometry and stochastic aspects of quantum theory. I am sincerely grateful for their support throughout this project.

I thank my second supervisor, **Dr. Eva-Maria Graefe**, whose thoughtful questions, keen insights and perspectives, both during my Master's and PhD, have had a positive impact on how I approach research problems.

I would also like to thank **Prof. Lane Hughston**, whose generous insights into relativistic quantum mechanics and valuable feedback on my conference poster have been greatly appreciated.

My gratitude extends to my group members, in particular **Wasim Rehman**, whose support has been invaluable, and **Simon Malzard**, for their advice and guidance during my PhD. I am also thankful to my colleagues in the group, especially **Katherine Holmes** and **Joseph Hall**, for the many stimulating conversations and the fun activities we shared, from games to writing haikus to our Countdown challenges, which made my time here all the more memorable.

I would like to express my deepest love and gratitude to my gods, my parents, **Venkata Ramana** and **Amrutha Lakshmi**, who have sacrificed so much to support my education. Their presence has been a source of comfort and strength throughout the ups and downs of this journey. They are the mountains on which I stand, the backbone of my life, and the light that guides me. I would like to dedicate this thesis to them.

I would like to thank **Anita**, for their love, patience and understanding throughout this journey. Their advice, unwavering support, and all the wonderful times shared have been invaluable.

I also wish to remember my late grandfather **Vedam Subba Raghavaiah**, who profoundly shaped my way of thinking and approaching life; my late uncle **Vedam Krishna Murthy**, whose example instilled in me the strength to help others; and my late sister **Venkata Padmavathi**, whose ever-present smile continues to remind me of the power of kindness. Their influence and spirit continue to inspire me every day.

I would also like to thank myself for persevering through this journey. Balancing financial challenges, working 20 hours a week to support myself and my loved ones, and still finding the time and energy to help those in need.

Finally, to all those who have been part of this journey, whether through a conversation, a shared moment, or a word of encouragement, thank you.

సాహసం సేయరా డింభకా

The phrase "Be Adventurous Man!" in Telugu

Contents

1 Introduction **9**

1.1 Motivation and context . . . 9

1.1.1 States and observables . . . 12

1.1.2 The density matrix formalism . . . 13

1.1.3 The Lüders rule . . . 13

1.2 Generalised measurements and POVMs . . . 14

1.3 Coherent states and phase-space methods . . . 16

1.4 Scope and outline of the thesis . . . 17

2 Phase-Space measurement and decoherence for quantum systems on the real line **20**

2.1 Introduction . . . 20

2.2 The physical system: quantum harmonic oscillator . . . 21

2.3 Canonical coherent states and phase space . . . 22

2.4 Coherent-state POVMs and iterative phase-space measurement . . . 24

2.5 Phase-space picture of decoherence . . . 28

2.6 Dynamical unravelling of phase-space measurement . . . 35

2.7 Discussion and conclusion . . . 39

3 Phase-space measurement and decoherence in $\mathrm{SU}(2)$ quantum systems **43**

3.1 Introduction . . . 43

3.2 $\mathrm{SU}(2)$ coherent states . . . 44

3.3 Coherent-state POVM measurement . . . 46

3.4 Coherent-state POVM measurement on the phase space . . . 50

3.5 Lindblad dynamics for the density matrix . . . 53

3.6 Dynamical unravelling on phase space . . . 55

3.6.1 Onset of classicality . . . 56

3.6.2 Negativity and lower bounds of quasi-probability distributions . . . 56

3.7 Discussion and conclusion . . . 58

4 Tomographic measurement and its dynamical unravelling for $\mathrm{SU}(N)$ quantum systems **62**

4.1 Introduction . . . 62

4.2 $\mathrm{SU}(N)$ group and its Lie algebra . . . 63

4.3 Tomographic POVM measurement . . . 65

4.4 Tomographic measurement on phase space . . . 67

4.5 Dynamical unravelling . . . 69

4.6 Discussion and conclusion . . . 73

5 Phase-Space measurement and decoherence in $\mathrm{SU}(1,1)$ quantum systems 74
5.1 Introduction . . . 74
5.2 $\mathrm{SU}(1,1)$ coherent states . . . 75
5.3 Coherent-state POVM measurement . . . 78
5.4 Coherent-state POVM measurement on phase-space . . . 80
5.5 Dynamical model for phase-space POVM measurement . . . 83
5.5.1 Husimi representation of the dynamical equation . . . 85
5.5.2 Solving the hyperbolic heat equation . . . 87
5.5.3 Onset of classicality . . . 89
5.6 Discussion and conclusion . . . 90

6 Stochastic unravelling of decoherence on phase space 91
6.1 Introduction . . . 91
6.2 Mathematical background . . . 92
6.2.1 Stochastic Schrödinger dynamics . . . 93
6.2.2 Density matrix and the Lindblad equation . . . 94
6.3 Continuous phase-space measurement and stochastic unravelling . . . 94
6.3.1 Stochastic evolution of canonical coherent states . . . 95
6.3.2 Martingale structure of the observables . . . 96
6.3.3 Coherent-state reduction and entropy functionals . . . 98
6.3.4 Lindblad-type evolution for the density matrix . . . 99
6.4 Stochastic dynamics on the Bloch sphere: The case of $\mathrm{SU}(2)$ . . . 99
6.4.1 Stochastic evolution of $\mathrm{SU}(2)$ coherent states . . . 100
6.4.2 Martingale structure of $\mathrm{SU}(2)$ observables . . . 102
6.4.3 Coherent-state reduction and information flow . . . 104
6.4.4 Lindblad-type evolution for the $\mathrm{SU}(2)$ density matrix . . . 106
6.5 Stochastic dynamics on the hyperbolic plane: The case of $\mathrm{SU}(1,1)$ . . . 106
6.5.1 Stochastic evolution of $\mathrm{SU}(1,1)$ coherent states . . . 106
6.5.2 Martingale structure of $\mathrm{SU}(1,1)$ observables . . . 108
6.5.3 Coherent-state reduction, entropy process and information flow . . . 109
6.5.4 Lindblad-type evolution for the $\mathrm{SU}(1,1)$ density matrix . . . 111
6.6 Discussion and conclusion . . . 111

7 Phase-space measurement in relativistic quantum mechanics 113
7.1 Introduction . . . 113
7.2 Phase space in relativistic classical mechanics . . . 114
7.3 Geometry of the future tube . . . 115
7.4 Phase space in relativistic quantum mechanics . . . 118
7.4.1 Space-time transformations on the future tube . . . 120
7.4.2 Quantum states on the future tube . . . 122
7.4.3 Coherent states on the future tube . . . 123
7.5 Bargmann transform . . . 123
7.5.1 Square-integrable functions on the interior of the light cone . . . 124

7.5.2 The Bargmann transform . . . 124
7.6 Coherent states on the interior of the forward light cone . . . 126
7.7 Conformal group and its generators . . . 128
7.8 Action of conformal generators on coherent states . . . 133
7.9 Quantum dynamics on the interior of the light cone . . . 136
7.10 Phase-space measurements via POVMs . . . 138
7.11 Discussion and conclusion . . . 140

8 Discussion, conclusion and future work **141**
8.1 Iterative POVMs vs Lindblad dynamics . . . 141
8.2 Hierarchy of phase-space distributions . . . 144
8.3 Lindblad dynamics vs stochastic descriptions . . . 145
8.4 Relativistic phase-space measurement and decoherence . . . 145
8.5 Towards a generalised framework . . . 146
8.5.1 Perelomov coherent states . . . 146
8.5.2 POVMs from generalised coherent states and Lindblad dynamics . . . 147
8.5.3 Connection to Lindblad dynamics . . . 149
8.5.4 Stochastic unravelling of coherent-state diffusions . . . 150

A Phase-space measurement in Fock-Segal-Bargmann representation **165**
A.1 Fock-Segal-Bargmann representation . . . 165
A.2 General POVM measurement . . . 170
A.3 Phase-space measurement . . . 171
A.4 Dynamical unravelling of the phase-space measurement . . . 173

B Solving Lindblad equations for phase-space distributions for the Heisenberg-Weyl case **177**
B.1 Mathematical preliminaries . . . 177
B.1.1 Moyal product and Lindblad operators . . . 177
B.1.2 Fourier transform on the real line . . . 178
B.1.3 Transforms on the phase space . . . 179
B.2 Double Fourier transform . . . 180
B.3 Lindblad equation for the free particle Hamiltonian . . . 182
B.3.1 Solving the Lindblad equation in Wigner representation . . . 184
B.3.2 Solving the Lindblad equation in the Husimi representation . . . 187
B.4 Lindblad equation for the harmonic oscillator . . . 192
B.4.1 Solving the Lindblad equation in Wigner representation . . . 193
B.4.2 Solving the Lindblad equation in the Husimi representation . . . 197

C Spherical harmonics, Husimi representation and other derivations **201**
C.1 Harmonic analysis on S^2 . . . 201
C.2 Proofs of technical results . . . 203
C.2.1 Proof of lemma 3.2 . . . 203
C.2.2 Proof of proposition 3.3 . . . 204
C.2.3 Proof of proposition 3.4 . . . 205
C.3 Coherent state POVM in $|s, m\rangle$ basis . . . 206
C.4 Lindblad dynamics for the density matrix in $|s, m\rangle$ basis . . . 211

D Hyperbolic harmonics, Husimi representation and other derivations **215**
D.1 Harmonic analysis on the hyperbolic plane . . . 215
D.2 Proofs of technical results . . . 218
D.2.1 Proof of proposition 5.1 . . . 218
D.2.2 Proof of proposition 5.2 . . . 220
D.2.3 Asymptotic limits of $\Phi_k(\lambda)$ . . . 221
D.2.4 SU(1,1)-covariance of Lindblad generators . . . 222
D.2.5 Deriving the heat equation and its solution . . . 225

E Stochastic processes, unravellings and other derivations **228**
E.1 Mathematical background . . . 228
E.2 Proofs of technical results . . . 231
E.2.1 Proof of lemma 6.1 . . . 231
E.2.2 Proof of proposition 6.1 . . . 232
E.2.3 Proof of proposition 6.2 . . . 233
E.2.4 Proof of proposition 6.6 . . . 234
E.2.5 Proof of proposition 6.7 . . . 235
E.2.6 Proof of lemma 6.2 . . . 236
E.2.7 Proof of lemma 6.3 . . . 236
E.2.8 Proof of proposition 6.9 . . . 237
E.2.9 Proof of proposition 6.14 . . . 239
E.2.10 Proof of lemma 6.4 . . . 240
E.2.11 Proof of lemma 6.5 . . . 241
E.2.12 Proof of proposition 6.15 . . . 241
E.2.13 Proof of proposition 6.20 . . . 242

F Relativistic phase-space measurement and related derivations **244**
F.1 Proofs of technical results . . . 244
F.1.1 Proof of proposition 7.2 . . . 244
F.1.2 Proof of proposition 7.3 . . . 247
F.1.3 Proof of proposition 7.5 . . . 249

List of Figures

1.1 Snapshots of the Wigner function illustrating phase-space decoherence. The plots show time evolution at $t = 0$, $t = \pi/4$, and $t = 8\pi$ (from left to right) under a diffusive open-system dynamics with rate $\gamma = 0.2$. The top row corresponds to an initial Schrödinger "cat" state in position; the middle row to a cat state in momentum; and the bottom row to the same momentum-cat state in the presence of an additional harmonic oscillator Hamiltonian ($\omega = m = 1$). Cat states are quantum superpositions of macroscopically distinct alternatives, which display strong Wigner-function negativity. This makes them especially useful for visualising how decoherence suppresses quantum interference and drives the system toward classical behaviour. 11

2.1 Density plots of the Wigner function evolved under the phase-space-decoherence Lindblad dynamics with $\gamma = 0.1$. Columns show times $t = 0$, $t = \pi/4$, and $t = 8\pi$. Top row: position Schrödinger-cat initial state; middle row: momentum cat; bottom row: same momentum-cat initial state evolved with an additional harmonic-oscillator Hamiltonian ($m = \omega = 1$). All other parameters and plotting conventions are identical to Fig. 1.1. Appendix B has the analytical solutions that were used to generate these plots. 41

3.1 *The Wigner (top row) and the Husimi (bottom row) functions of the initial state, the outcome state after a single phase-space measurement, and that after ten repeated measurements.* Starting from an initial spin-cat-like state for spin $s = 3$. The initial density matrix corresponds to a coherent superposition state: $|\psi\rangle = \frac{1}{\sqrt{2}}(|m = 3\rangle + |m = -3\rangle)$, exhibiting quantum coherence between these extremal spin states. The Wigner function initially displays pronounced negativity, which diminishes after a single phase-space measurement, and any residual interference effect vanishes entirely by the tenth measurement, resulting in a fully mixed state. The corresponding Husimi functions, which remain strictly positive throughout, similarly transforms into uniformity and converge to the maximally mixed state $\rho \approx \mathbb{1}/7$ after seven iterations. `Wigner3j.m` [120] function in MATLAB was used to make these plots. 52

3.2 (a) Minimum kernel eigenvalue $\lambda_{\min}^{(\sigma)}$ as a function of the ordering parameter σ for several spins s. At $\sigma = -1$ (Husimi) the minimum is 0 for all s; for $\sigma \geq 0$ the minimum becomes strictly negative and its magnitude grows rapidly with both σ and s. (b) Spin projection(s) $\kappa_\star(\sigma)$ that attain the minimum eigenvalue of $\hat{w}^{(\sigma)}$ (evaluated at the north pole). For $\sigma = -1$ the minimum is degenerate over all $\kappa \neq s$ (not shown), while for $\sigma \geq 0$ the minimiser consistently occurs at $\kappa_\star = s - 1$ (and symmetrically at $\kappa_\star = -(s - 1)$ when present). `Wigner3j.m` [120] function in MATLAB was used to make these plots. 58

4.1 (a) Minimum value of the quasi-probability distribution $F_{\min}^{(\sigma)}$ as a function of iteration number k, shown for several ordering parameters σ and Hilbert-space dimensions $N = 2, 3, 4, 5$. For each σ, the curves cross the classicality threshold (dashed line) at the universal iteration $k_* = \lceil(\sigma + 1)/2\rceil$, which is independent of the dimension N. (b) Phase diagram in the (σ, k) plane for $N = 4$, with the red line marking the boundary $\sigma - 2k = -1$ beyond which all quasi-probability distributions become non-negative. This illustrates the dimension-independent onset of classicality under tomographic measurements. 72

5.1 Spectral components of the $\mathrm{SU}(1,1)$ phase-space convolution. (a) Conical (Mehler) function $P_{\mathrm{i}\lambda-\frac{1}{2}}(\cosh\tau)$ as a function of τ for various values of λ. The function exhibits oscillatory behaviour that decays for larger τ, encoding the hyperbolic geometry of the $\mathrm{SU}(1,1)$ phase space. (b) Effective spectral weight $\lambda\tanh(\pi\lambda)\Phi_k(\lambda)$ as a function of λ, where $\Phi_k(\lambda)$ is the Plancherel weight. The decay in spectral weight for large λ reflects the suppression of high-frequency spectral contributions in the phase-space convolution. Together, these functions govern the smoothing effect of the $\mathrm{SU}(1,1)$ spectral convolution, progressively washing out quantum interference features in the Wigner function. The plots were generated using the `SpecFunPhys` MATLAB toolbox [176]. . 82

5.2 *The Wigner (top row) and the Husimi (bottom row) functions of the initial state, the outcome state after a single phase-space measurement, and that after ten repeated measurements.* Starting from an initial odd cat state $|\mathrm{cat}_-\rangle = \mathcal{N}_-\left(|\chi_0\rangle - |-\chi_0\rangle\right)$ with $k = 1$, $\chi_0 = \tanh(\tau_0/2)$ and $\tau_0 = 3.0$, exhibiting quantum coherence. The columns correspond to successive $\mathrm{SU}(1,1)$ phase-space convolutions with spectral power $n = 0, 1, 10$. The initial Wigner function exhibits strong negativities due to quantum interference, which are suppressed under successive convolutions, leading to a classical-like positive distribution. The corresponding Husimi functions, which remain strictly positive throughout, similarly transforms into uniformity. The plots were generated using the `SpecFunPhys` MATLAB toolbox [176]. 84

List of Tables

8.1 Comparison between coherent-state overlaps and heat kernel expansions for the HW group, $\mathrm{SU}(2)$, and $\mathrm{SU}(1,1)$. The agreement in HW explains the exact unravelling found in Chapter 2. For $\mathrm{SU}(2)$ and $\mathrm{SU}(1,1)$, the mismatch in spectral weights obstructs exact identification of POVM dynamics with diffusion. 142

A.1 Correspondence between the operators on the coordinate space and the Bargmann space. 175

Chapter 1

Introduction

1.1 Motivation and context

Quantum mechanics has been remarkably successful in predicting and explaining physical phenomena across a wide range of scales. However, the process of measurement remains one of its most conceptually and mathematically subtle aspects. The standard formalism of quantum mechanics involves two distinct types of evolution. When a system evolves in isolation, its dynamics are governed by the deterministic, unitary Schrödinger equation [1]. When a measurement is performed, however, the system's state is said to undergo a discontinuous and stochastic "collapse" to one of the eigenstates of the measured observable, with probabilities given by the Born rule. This dichotomy between unitary evolution and measurement-induced collapse is known as the *measurement problem* [2–4].

At the heart of the measurement problem lies the question of how can a theory that is linear and deterministic at the microscopic level produce definite, irreversible outcomes at the macroscopic level? The collapse postulate, while operationally successful, is not derived from the unitary dynamics of the theory and introduces a seemingly ad hoc rule for how and when measurements occur. Despite the fact that quantum mechanics does not predict the actual outcome of a single measurement, only its probability, it is consistently observed that macroscopic systems exhibit definite, classical behaviour. This raises the question of how does the classical world emerge from quantum theory, and in particular, how can superpositions of macroscopically distinct states become unobservable?

A significant step toward answering this is provided by the theory of *decoherence*, which describes how quantum coherence is dynamically suppressed due to the interaction of a system with its environment [5–9]. In this framework, the total system (including environment) evolves unitarily, but the reduced state of the system, obtained by tracing out the environmental degrees of freedom, appears to lose its off-diagonal elements in a preferred basis, sometimes known as pointer bases [10,11]. These bases are stable under environmental monitoring and behave approximately classically [11,12]. As a result, interference terms vanish, thus providing a mechanism by which classical-like statistical behaviour emerges from purely unitary dynamics.

Decoherence does not, however, solve the measurement problem in its entirety. It does not explain why a particular outcome is realised in a given run of an experiment, but rather why the superposition of macroscopic alternatives becomes dynamically inaccessible and observationally indistinguishable

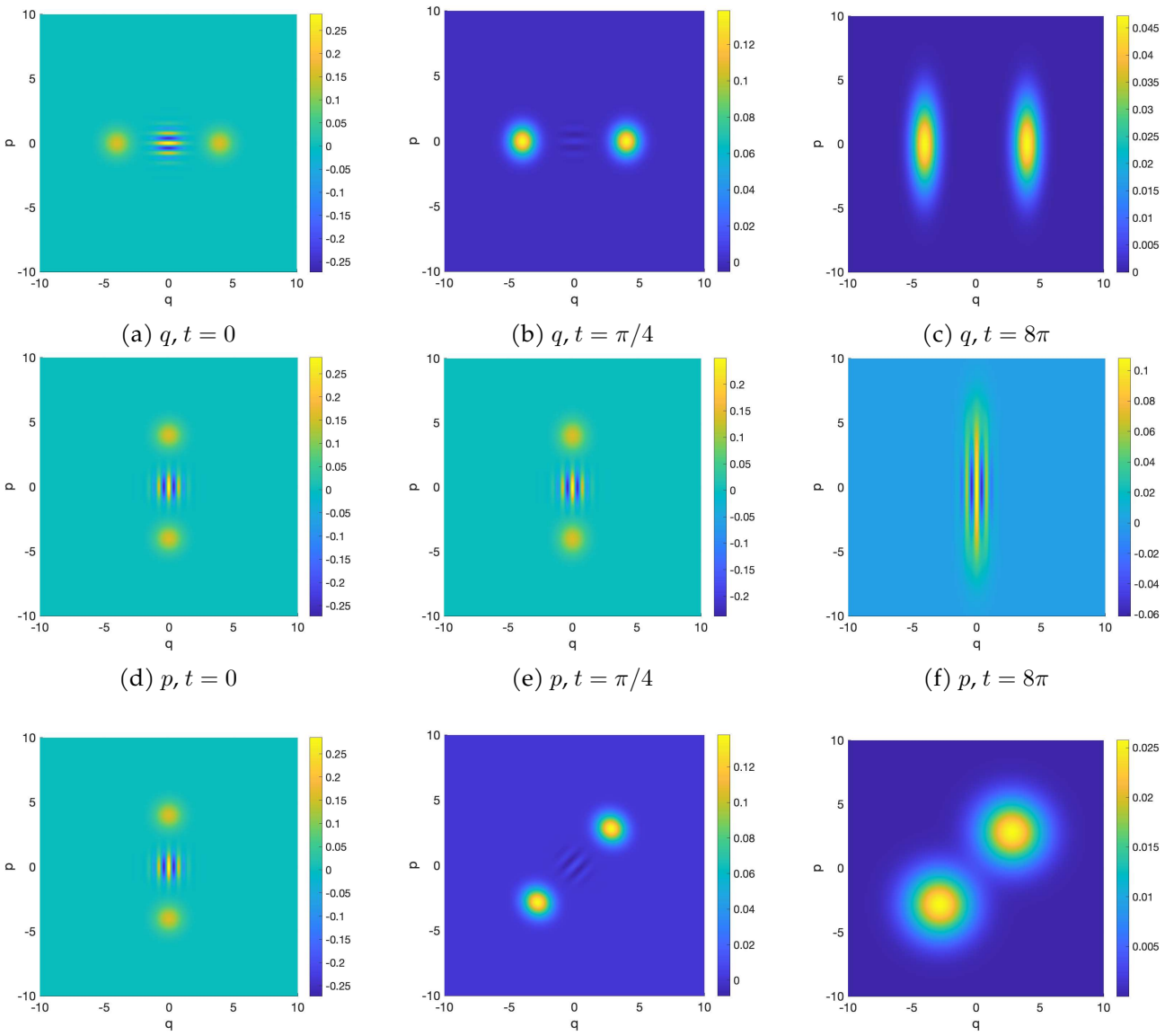
from a classical ensemble. Nonetheless, decoherence has become a cornerstone of modern quantum theory, playing a central role in quantum information [13], quantum cosmology [14–17], and foundational studies [8, 18–21], and offering a powerful framework for understanding the emergence of classicality.

Most traditional models of decoherence have focused on *spatial localisation*, wherein the environment is assumed to interact predominantly with the position of the system [5, 22]. These models are motivated by the fact that classical particles appear localised in space, making position a natural candidate for the preferred basis. However, classical physics, especially in the Hamiltonian formalism, describes systems not merely by their position but by their *entire phase-space configuration*, including both position and momentum. From this perspective, a particle existing in a superposition of distinct momenta is as unphysical as one being in two places at once [23].

Yet, position-based decoherence models suppress only spatial coherence, often leaving momentum coherence largely unaffected. This asymmetry becomes clear when visualised through the *Wigner function* [24–26], a quasi-probability distribution on phase space that captures both classical and quantum features. For instance, an initial superposition of momentum eigenstates may retain Wigner-function negativity even as spatial interference fringes are suppressed, signalling the persistence of nonclassical behaviour despite localisation as shown in Fig. 1.1. True classicality demands decoherence not only in position but also in momentum. Yet quantum mechanics forbids simultaneous sharp measurements of these conjugate variables; at best, one can perform joint measurements with limited resolution, constrained by the uncertainty principle [27, 28].

This limitation highlights the need for *phase-space-based models of decoherence*, in which both position and momentum are treated on an equal footing. This is *not* to be confused with position-based models formulated in phase space [26, 29–32]; rather, it refers to approaches where position and momentum jointly define the state and its evolution. This is achieved through the use of *coherent states* and their associated phase-space positive operator-valued measures (POVMs), which provide a symmetric, group-theoretic structure for modeling simultaneous, approximate measurements of noncommuting quantities [33, 34]. Unlike projective measurements, coherent-state POVMs form an overcomplete, smoothly varying set that allows for a more natural representation of quantum states in phase space [35, 36]. These measurements respect the symmetries of the system and suppress interference in both position and momentum, offering a compelling account of how classicality emerges through environmental monitoring [37, 38].

The central aim of this thesis is to systematically develop and analyse this phase-space-based approach to measurement and decoherence. We begin with canonical coherent states on the real line (associated with the Heisenberg-Weyl group), and extend the framework to systems with compact ($\mathrm{SU}(2)$) and noncompact ($\mathrm{SU}(1,1)$) symmetries, as well as higher-dimensional $\mathrm{SU}(N)$ systems [35, 39]. At each stage, we construct coherent-state POVMs, study the iterative application of these measurements, and analyse the resulting evolution of quantum states and phase-space distributions. We also explore stochastic unravellings of the measurement process and their connection to Lindblad-type master equations [40–44]. Finally, we propose a preliminary extension of this framework to relativistic quantum theory by constructing coherent states and phase-space observables on the future tube of complexified Minkowski space [45–47]. This serves as a potential foundation for understanding measurement and decoherence in Lorentz-invariant settings using phase-space methods.



(a) q, $t = 0$ (b) q, $t = \pi/4$ (c) q, $t = 8\pi$

(d) p, $t = 0$ (e) p, $t = \pi/4$ (f) p, $t = 8\pi$

(g) p_H, $t = 0$ (h) p_H, $t = \pi/4$ (i) p_H, $t = 8\pi$

Figure 1.1: Snapshots of the Wigner function illustrating phase-space decoherence. The plots show time evolution at $t = 0$, $t = \pi/4$, and $t = 8\pi$ (from left to right) under a diffusive open-system dynamics with rate $\gamma = 0.2$. The top row corresponds to an initial Schrödinger "cat" state in position; the middle row to a cat state in momentum; and the bottom row to the same momentum-cat state in the presence of an additional harmonic oscillator Hamiltonian ($\omega = m = 1$). Cat states are quantum superpositions of macroscopically distinct alternatives, which display strong Wigner-function negativity. This makes them especially useful for visualising how decoherence suppresses quantum interference and drives the system toward classical behaviour.

To rigorously investigate the ideas introduced above, particularly quantum measurement, decoherence, and the emergence of classicality, we begin by reviewing the formal structure of quantum theory. This includes the standard postulates, the density matrix formalism, and the mathematical representation of measurement processes. Special attention is given to the role of projective and generalised measurements, which form the theoretical basis for the phase-space POVM models developed later in this thesis.

1.1.1 States and observables

In the standard (Dirac-von Neumann) formulation of quantum mechanics, the state of a physical system is represented by a density matrix acting on the Hilbert space $\mathcal{H}$. A *Hilbert space* is a complex vector space equipped with an inner product $\langle \cdot, \cdot \rangle$ that is linear in its second argument and conjugate linear in its first, and is complete with respect to the norm induced by this inner product. That is, every Cauchy sequence in $\mathcal{H}$ converges to a limit in $\mathcal{H}$ [1, 48–51]. The inner product defines the geometry of the space, allowing the notions of orthogonality, projection, and length. For a normalised state $|\psi\rangle \in \mathcal{H}$, the inner product $\langle \psi, \psi \rangle = 1$ expresses total probability.

In quantum mechanics, a *measurement* refers to the extraction of classical information from a quantum system. Observables, measurable quantities such as position, momentum, spin, and energy, are represented by self-adjoint (Hermitian) operators acting on the Hilbert space $\mathcal{H}$. According to the spectral theorem, any self-adjoint operator $\hat{A}$ admits a decomposition

$$\hat{A} = \sum_i a_i \hat{P}_i, \tag{1.1}$$

where the $a_i \in \mathbb{R}$ are the *distinct* eigenvalues of $\hat{A}$, and $\hat{P}_i$ are the orthogonal projection operators onto the corresponding eigenspaces, satisfying $\hat{P}_i \hat{P}_j = \delta_{ij} \hat{P}_i$ and $\sum_i \hat{P}_i = \mathbb{1}$.

If the system is initially in a pure state, that is, a unit vector in the Hilbert space, $|\psi\rangle \in \mathcal{H}$, the probability of obtaining outcome a_i is given by the *Born rule*

$$\Pr(a_i) = \langle \psi | \hat{P}_i | \psi \rangle. \tag{1.2}$$

This probabilistic aspect reflects the inherent indeterminism of quantum measurement. Importantly, the act of measurement also modifies the state of the system. According to the *von Neumann projection postulate* [1], if outcome a_i is observed, then the state collapses to

$$|\psi\rangle \mapsto \frac{\hat{P}_i |\psi\rangle}{\sqrt{\langle \psi | \hat{P}_i | \psi \rangle}}. \tag{1.3}$$

This update rule characterises an idealised, instantaneous measurement process, commonly referred to as a *projective* or *sharp* measurement [1, 4]. Such measurements are repeatable i.e. immediately measuring the same observable again yields the same outcome with certainty.

Finally, time evolution of the state of a system between measurements is governed by the Schrödinger equation:

$$\mathrm{i}\hbar \frac{\mathrm{d}}{\mathrm{d}t} |\psi(t)\rangle = \hat{H} |\psi(t)\rangle, \tag{1.4}$$

where $\hat{H}$ is the Hamiltonian. The evolution is unitary, with a formal solution $|\psi(t)\rangle = \hat{U}(t)|\psi(0)\rangle$, where $\hat{U}(t) = \mathrm{e}^{-\mathrm{i}\hat{H}t/\hbar}$ preserves the norm and inner product structure.

1.1.2 The density matrix formalism

The state vector description of quantum mechanics, where pure states are represented by unit vectors $|\psi\rangle$ in a Hilbert space $\mathcal{H}$, is adequate for isolated systems in fully known states. However, many physically relevant situations involve incomplete information, classical uncertainty, or entanglement with external systems. To describe such cases, we require a more general framework: the *density matrix* (or *density operator*) formalism [50,51].

A *density operator* $\hat{\rho}$ is a positive semidefinite, trace-one operator acting on $\mathcal{H}$. That is

$$\hat{\rho} \geq 0, \qquad \mathrm{tr}(\hat{\rho}) = 1. \tag{1.5}$$

Any density operator can be expressed as a convex combination of pure states

$$\hat{\rho} = \sum_i p_i |\psi_i\rangle\langle\psi_i|, \quad p_i \geq 0, \quad \sum_i p_i = 1, \tag{1.6}$$

where $\{|\psi_i\rangle\}$ are unit vectors in $\mathcal{H}$, and the weights $\{p_i\}$ represent classical probabilities. Note that the summation here may be replaced by an integration with respect to a probability density.

A state is called *pure* if it can be written as $\hat{\rho} = |\psi\rangle\langle\psi|$ for some $|\psi\rangle \in \mathcal{H}$; such states satisfy $\hat{\rho}^2 = \hat{\rho}$ and $\mathrm{Tr}(\hat{\rho}^2) = 1$. A state is *mixed* if it cannot be written in this form, with $\mathrm{Tr}(\hat{\rho}^2) < 1$. Mixed states represent either statistical ensembles or subsystems of entangled systems.

The density matrix formalism is particularly indispensable in the context of composite systems. Let $\mathcal{H}_S \otimes \mathcal{H}_E$ denote the Hilbert space of a bipartite system (system + environment) in a joint state $\hat{\rho}_{SE}$. The state of the system alone is obtained by taking the *partial trace* over the environment

$$\hat{\rho}_S = \mathrm{tr}_E(\hat{\rho}_{SE}). \tag{1.7}$$

This procedure leads naturally to mixed states even when $\hat{\rho}_{SE}$ is pure, a key mechanism underlying decoherence.

Measurement theory is also naturally expressed in this formalism. For a projective measurement $\{\hat{P}_i\}$, the probability of obtaining outcome i in state $\hat{\rho}$ is given by

$$\Pr(i) = \mathrm{tr}(\hat{\rho}\hat{P}_i), \tag{1.8}$$

which generalises the Born rule.

This density matrix formalism allows for compact treatment of quantum operations and stochastic unravellings, both of which are central themes in this thesis.

1.1.3 The Lüders rule

The von Neumann projection postulate provides a state-update rule following the measurement of an observable with a nondegenerate spectrum. In that setting, the post-measurement state when

the outcomes is recorded, is a projection onto a single eigenvector corresponding to the observed eigenvalue. However, many physically relevant observables, such as angular momentum or energy in systems with symmetry, exhibit degeneracies. That is, multiple orthonormal eigenvectors may correspond to the same eigenvalue.

To extend the projection postulate to the degenerate case, Lüders proposed a generalised rule for the post-measurement state [52]. Let A be an observable with spectral decomposition $\hat{A} = \sum_i a_i \hat{P}_i$, where each $\hat{P}_i$ is an orthogonal projector onto the (possibly multidimensional) eigenspace associated with eigenvalue a_i. If the system is in state $\hat{\rho}$ and the measurement yields outcome a_i, the post-measurement state is given by the Lüders update rule

$$\hat{\rho} \mapsto \hat{\rho}_i = \frac{\hat{P}_i \hat{\rho} \hat{P}_i}{\mathrm{tr}(\hat{P}_i \hat{\rho})}. \tag{1.9}$$

This expression reduces to the standard von Neumann rule when the spectrum is nondegenerate (i.e., when $\hat{P}_i = |a_i\rangle\langle a_i|$). The Lüders rule ensures that the post-measurement state remains within the subspace corresponding to the measured eigenvalue, but preserves any coherences within the degenerate eigenspace.

Physically, this rule captures the idea that the measurement process projects the system onto a subspace which is not necessarily one-dimensional. Importantly, it retains the symmetry associated with the degenerate eigenspace and satisfies *repeatability*.

1.2 Generalised measurements and POVMs

The projective measurement framework described by the von Neumann and Lüders postulates assumes idealised measurement conditions such as instantaneous, perfectly sharp observables with mutually orthogonal eigenstates. While this framework is foundational, it does not adequately describe many realistic experimental scenarios, particularly in systems subject to noise, continuous monitoring, or limited resolution [4, 44]. In practice, measurement devices may have finite precision, may disturb the system in complex ways, and may only access coarse-grained or nonorthogonal properties of the system. To accommodate such scenarios, quantum measurement theory introduces a more general framework based on *positive operator-valued measures* (POVMs) [49,50].

A POVM is a collection of positive semidefinite operators $\{\hat{E}_i\}$ acting on the system's Hilbert space $\mathcal{H}$ such that

$$\hat{E}_i \geq 0, \quad \sum_i \hat{E}_i = \mathbb{1}. \tag{1.10}$$

Each $\hat{E}_i$ corresponds to a possible measurement outcome. Unlike projective measurements, the $\hat{E}_i$ need not be orthogonal projections, nor must they commute. The probability of obtaining outcome i when the system is in state $\hat{\rho}$ is given by the generalised Born rule

$$\Pr(i) = \mathrm{tr}(\hat{\rho} \hat{E}_i). \tag{1.11}$$

POVMs encompass a wide range of measurements, including:

- **Unsharp measurements:** where outcomes correspond to smeared projectors.
- **Weak measurements:** in which the system is only partially disturbed.
- **Continuous measurements:** modeled via time-resolved POVMs and quantum trajectories.
- **Simultaneous measurement of incompatible observables:** such as approximate position and momentum, as seen below in coherent-state POVMs.

An important result in this framework is *Naimark's dilation theorem*, which states that any POVM on a Hilbert space $\mathcal{H}$ can be realised as a projective measurement on a larger Hilbert space $\mathcal{K} \supset \mathcal{H}$, typically by embedding the system into a joint system-environment space and performing a projective measurement on the joint state [49, 50, 53–55].

Quantum instruments and post-measurement state update

While POVMs describe the statistics of quantum measurements, in themselves they do not specify how the system evolves as a result of the measurement. In many contexts, such as sequential measurement, feedback control, and open-system dynamics, it is necessary to describe not only the measurement outcome probabilities but also the corresponding post-measurement states. This leads to the concept of a *quantum instrument* [44, 54, 56].

A quantum instrument is a collection of completely positive (CP), trace-nonincreasing maps $\{\mathcal{I}_i\}$ such that

- Each $\mathcal{I}_i$ maps a density operator $\hat{\rho}$ to a (possibly unnormalised) post-measurement state $\mathcal{I}_i(\hat{\rho})$.
- The probability of outcome i is given by $\Pr(i) = \mathrm{tr}(\mathcal{I}_i(\hat{\rho}))$.
- The post-measurement state, conditioned on outcome i, is $\hat{\rho}_i = \mathcal{I}_i(\hat{\rho})/\,\mathrm{tr}(\mathcal{I}_i(\hat{\rho}))$.
- The overall transformation is trace-preserving: $\sum_i \mathrm{tr}(\mathcal{I}_i(\hat{\rho})) = 1$.

Each instrument $\mathcal{I}_i$ is associated with a POVM element $\hat{E}_i$ via $\mathrm{tr}(\mathcal{I}_i(\hat{\rho})) = \mathrm{tr}(\hat{\rho}\hat{E}_i)$, ensuring that instruments generalise both the statistical and dynamical content of quantum measurements.

Special cases include the Lüders instrument, where $\mathcal{I}_i(\hat{\rho}) = \hat{P}_i\hat{\rho}\hat{P}_i$, and more general operations described by Kraus operators $\{\hat{K}_{i\alpha}\}$:

$$\mathcal{I}_i(\hat{\rho}) = \sum_\alpha \hat{K}_{i\alpha}\hat{\rho}\hat{K}_{i\alpha}^\dagger. \tag{1.12}$$

Quantum instruments thus provide the most general framework for describing measurement as a physical process and will play a central role in our treatment of phase-space decoherence, stochastic unravellings, and iterative measurement schemes.

POVMs naturally arise in open-system dynamics, quantum optics, and quantum information, where measurements are often indirect or mediated by an auxiliary system. In this thesis, we will focus in particular on POVMs constructed from overcomplete sets of coherent states. These coherent-state POVMs enable a continuous phase-space representation of quantum measurements and will serve as the foundation for our models of decoherence and classicality.

1.3 Coherent states and phase-space methods

Coherent states occupy a central role in quantum theory as the states that most closely resemble classical points in phase space. They were first introduced in the setting of the quantum harmonic oscillator [57–59], where they appear as wave packets that follow classical trajectories and saturate the uncertainty principle. The concept was later generalised to a wide variety of physical systems, where coherent states are constructed not only for oscillators but also for spin systems, noncompact groups, and even relativistic symmetries [35, 60].

In all cases, coherent states share a number of key features

- They exhibit the smallest quantum fluctuations allowed by uncertainty relations, making them the most "classical-like" pure states.
- Expectation values of observables in coherent states evolve approximately like classical variables.
- They provide a natural localisation in phase space, while still respecting quantum uncertainty.
- They form an overcomplete set of states, which allows them to represent quantum states smoothly through phase-space distributions.
- They are covariant under the action of the symmetry group, i.e. the group action maps one coherent state to another within the family.

They provide a continuous family of states that can be used to build quasi-probability distributions such as the Wigner, Husimi Q, and Glauber–Sudarshan P functions [24, 25, 58, 59, 61–63]. Each of these distributions represents quantum states as functions on a classical-like phase space, offering a bridge between quantum theory and classical intuition.

In the context of measurement and decoherence, coherent states provide a natural framework for modelling the effect of environmental interactions. Such interactions can be interpreted as a continuous sequence of weak, unsharp measurements that probe the system in phase space. Mathematically, these are described by a coherent-state POVM

$$\{\hat{E}_\alpha = |\alpha\rangle\langle\alpha|\}_{\alpha\in\mathcal{M}}, \tag{1.13}$$

where $|\alpha\rangle$ denotes a coherent state labelled by a point α in the underlying phase space $\mathcal{M}$ (e.g. $\mathbb{C}$ for the Heisenberg–Weyl group, S^2 for $\mathrm{SU}(2)$, the Poincaré disk for $\mathrm{SU}(1,1)$, or $\mathbb{CP}^{N-1}$ for $\mathrm{SU}(N)$).

If the outcome α is registered, the system collapses into the corresponding coherent state $|\alpha\rangle$, localised around a phase-space point. In the more typical situation where the outcomes are not observed, the state is averaged over all possible results. This nonselective measurement induces decoherence i.e. interference is suppressed while classical-like localisation emerges in phase space.

From this perspective, decoherence arises not from an abrupt projection, but from the accumulation of unread phase-space information leaking into the environment. This picture underlies much of the discussion in this thesis, where phase-space methods are used to study how continuous measurement and environmental coupling drive quantum systems toward classical behavior.

1.4 Scope and outline of the thesis

The chapters of this thesis are outlined below.

Chapter summary

- **Chapter 2**: This chapter introduces the canonical coherent-state POVM for quantum systems on the real line, such as the harmonic oscillator, modelling simultaneous unsharp measurements of position and momentum. Explicit expressions for the density matrix after k iterations of nonselective coherent-state POVM measurement are derived in (2.29), and the corresponding transformations of the quasi-probability functions are given in (2.41, 2.52, 2.56). A central result (2.72) shows that these distributions are related by fractional iterations of the POVM: a single iteration maps the Wigner function to the Q-function, while two iterations map the singular P-function to the smooth Q-function. This reveals a group-independent mechanism for the suppression of quantum interference and emergence of classicality. We also show that this iterative process admits a continuous-time limit governed by a Lindblad equation (2.80), thereby linking measurement-induced decoherence to standard open-system dynamics. The Segal-Bargmann space is introduced as a holomorphic representation connected to the coherent-state transform, with further details in Appendix A. Appendix B provides explicit solutions of Lindblad equations for the free particle and harmonic oscillator. These results are new and have been published in [23].

- **Chapter 3**: This chapter develops the theory of $\mathrm{SU}(2)$ coherent states for spin systems, generalising canonical coherent states to compact phase spaces. We construct the associated coherent-state POVM and analyse the effect of iterative measurements both on density matrices and on the full family of σ-parametrised phase-space quasi-probability distributions. Explicit formulas are derived for the k-step evolved state (3.30) and its σ-distribution (3.48), providing a unified treatment that includes the Husimi Q-, Wigner, and Glauber-Sudarshan P-functions as special cases. We show that repeated measurements drive the system toward the maximally mixed state, modelling decoherence and the suppression of nonclassical features such as negativity and singularities. We then compare this discrete measurement-induced decoherence with Lindblad dynamics generated by isotropic diffusion (3.50). The two match exactly for spin-$\frac{1}{2}$ and asymptotically for large s, but differ at finite s, due to distinct eigenvalue spectra (3.58). Notably, we identify a characteristic timescale t_* (3.68) beyond which all σ-distributions become strictly positive, offering a quantitative criterion for the emergence of classicality. As an additional result, we numerically identify the minimum value attained by the σ-distributions over the Bloch sphere for arbitrary spin-s, yielding a quantitative signature of nonclassicality under coarse-grained measurement (Fig. 3.2). Supporting derivations and proofs are provided in Appendix C. These results are original and are currently being prepared for publication.

- **Chapter 4**: This chapter addresses tomographic measurement schemes in $\mathrm{SU}(N)$ quantum systems. We introduce an iterative measurement protocol based on informationally complete POVMs that enables full state reconstruction in finite-dimensional Hilbert spaces. The measurement channel acts on both density matrices and the full σ-parametrised family of phase-space quasi-probability distributions, with explicit formulas given for the k-step evolution (4.18) and (4.28). Unlike the $\mathrm{SU}(2)$ setting, where exact unravelling fails due to spectral mismatch, here the itera-

tive measurement scheme admits an *exact* dynamical unravelling. Specifically, we derive a Lindblad equation (4.31) whose generator is constructed from the $\mathrm{SU}(N)$ Lie algebra and exactly reproduces the POVM-induced decoherence. This establishes a rigorous correspondence between discrete and continuous-time models of open quantum dynamics in higher-dimensional systems. We also define a characteristic decoherence timescale t_* beyond which all such distributions become strictly positive, signalling the emergence of classical behaviour (4.45). Additionally, we identify a minimum value attained by the σ-distributions over the projective Hilbert space, offering a numerical signature of residual nonclassicality (4.49). The results of this chapter are currently under review for publication in Physical Review Research [64].

- **Chapter 5**: This chapter extends the analysis of coherent-state measurements to systems with noncompact symmetry, specifically the group $\mathrm{SU}(1,1)$, which arises naturally in quantum optics, squeezing phenomena, and hyperbolic geometry. We construct the $\mathrm{SU}(1,1)$ coherent states and associated POVM, and analyse the iterative decoherence process induced by repeated weak measurements. We compute the k-step evolution of the σ-parametrised quasi-probability distributions (5.43), which evolve under a discrete convolution with the $\mathrm{SU}(1,1)$ heat kernel on the hyperbolic plane. Unlike the $\mathrm{SU}(2)$ and $\mathrm{SU}(N)$ settings, the standard GKSL generator built from Lie algebra elements is not $\mathrm{SU}(1,1)$-covariant and fails to match the measurement-induced diffusion. To resolve this, we introduce a modified Lindblad generator with a flipped sign in the noncompact generator $\hat{K}_z$ (5.49), yielding trace-preserving, $\mathrm{SU}(1,1)$-covariant dynamics. Although not completely positive on all operators, this dynamics becomes physical when restricted to coherent-state-averaged observables. A characteristic decoherence time t_* is identified in the large-Bargmann index limit (5.78), beyond which all σ-distributions become positive, indicating the onset of classicality. Supporting calculations and derivations are provided in Appendix D. The results of this chapter are original and currently being prepared for publication.

- **Chapter 6**: This chapter develops a stochastic description of quantum evolution induced by repeated coherent-state POVM measurements. Starting from the iterative measurement framework developed in previous chapters, we derive stochastic differential equations (SDEs) governing the evolution of the system's state in phase space. These SDEs describe diffusive motion on the relevant group manifold, with the coherent state label evolving under Brownian motion, and serve as a geometric alternative to stochastic Schrödinger equations (SSEs). For Heisenberg-Weyl coherent states (6.9), the dynamics corresponds to planar Brownian motion in phase space; for $\mathrm{SU}(2)$ coherent states (6.38), it takes the form of rotational diffusion on the Bloch sphere; and for $\mathrm{SU}(1,1)$ coherent states (6.68), the motion occurs on the hyperbolic plane. In each case, the corresponding quantum state follows the trajectory of a moving coherent state, and the ensemble average over trajectories yields a decoherence channel. In compact cases such as Heisenberg-Weyl and $\mathrm{SU}(2)$, this stochastic unravelling reproduces completely positive, trace-preserving Lindblad evolution. However, in the noncompact $\mathrm{SU}(1,1)$ case, the resulting master equation is generated by the Laplace-Beltrami operator (Casimir element) on the hyperbolic plane, and preserves trace and covariance without complete positivity. We analyse the martingale structure of observables under this evolution, and show how entropy reduction and trajectory-wise purity gain differ from those in standard SSE models. Appendix E provides the stochastic calculus background and detailed derivations of the key results. The stochastic models developed here are novel and are being prepared for publication.

- **Chapter 7**: This chapter explores preliminary steps toward a relativistic theory of quantum measurement using phase-space methods. The analysis is based on the *future tube*, a domain in complexified Minkowski space that naturally encodes analyticity, causality, and Lorentz invariance, and serves as a natural candidate for relativistic phase space. Within this framework, we construct coherent states associated with unitary representations of the conformal group (7.54), and define a novel positive operator-valued measure (POVM) on the future tube. These coherent states generalise the Perelomov construction to a relativistically covariant setting. A new Bargmann-type integral transform (7.60) is introduced, mapping holomorphic functions on the future tube to square-integrable functions on the interior of the forward light cone. This transform defines a relativistic phase-space representation of quantum states, offering an explicit link between complex spacetime geometry and Hilbert space structure. We propose a framework for defining relativistic phase-space measurements (7.152) on the light cone and outline how such a model may underpin a future theory of relativistic open quantum systems. While a complete physical interpretation is still under development, the construction provides new tools for incorporating measurement and decoherence into relativistic settings. Appendix F contains the supporting analytic calculations and derivations. The coherent-state construction, Bargmann transform, and POVM formalism developed in this chapter are new and form a foundation for future research in relativistic quantum measurement theory.

- **Chapter 8**: This concluding chapter synthesizes the main contributions of the thesis, with a central focus on coherent-state POVM measurements as a unifying framework for modelling quantum decoherence and the emergence of classicality. We consolidate results from systems with flat phase space ($\mathbb{R}$), compact symmetry ($\mathrm{SU}(2)$), noncompact symmetry ($\mathrm{SU}(1,1)$), and the tomographic $\mathrm{SU}(N)$ case into a comprehensive comparative framework for iterative quantum measurement in phase space (8.12). It clarifies how phase-space geometry constrains the structure of physically admissible semigroups. We also examine the relationship between stochastic and dynamical unravellings, positioning the coherent-state trajectory picture as a geometric alternative to standard stochastic Schrödinger equations. The role of the Casimir generator, the emergence of a universal decoherence time scale t_* (8.5), and the corresponding positivity thresholds for quasi-probability distributions are unified across the studied symmetry groups. Importantly, we propose experimental schemes with testable predictions that may guide future developments in quantum control. We also introduce a preliminary framework for constructing stochastic differential equations (SDEs) governing coherent-state evolution for arbitrary Lie groups (8.22), and show that, under certain assumptions, the corresponding ensemble-averaged dynamics yields a master equation that is not necessarily of GKSL form (8.25). The chapter also discusses several avenues for future investigation.

With this structure in place, we now begin our investigation by considering phase-space measurement in the simplest nontrivial setting: quantum systems defined on the real line.

Chapter 2

Phase-Space measurement and decoherence for quantum systems on the real line

2.1 Introduction

In this chapter, we develop a model of measurement-induced decoherence in quantum systems with Heisenberg–Weyl symmetry, such as the quantum harmonic oscillator. These systems evolve on the real line, with a planar phase space, and are naturally described using the formalism of continuous variables. Our goal is to understand how repeated, weak, and unsharp measurements of phase-space observables drive quantum states toward classicality, and whether these measurements admit a consistent dynamical unravelling.

Such models underpin the theoretical description of decoherence and state reduction in quantum optics [43, 63], continuous quantum measurement [44], and quantum trajectory methods [65]. They are particularly relevant to experimental platforms such as optical cavities [66], superconducting resonators [67], and optomechanical systems [68], where quadrature measurements play a central role. These systems provide a natural setting for testing phase-space-based models of quantum-to-classical transition and for implementing quantum control protocols [44, 69].

We begin in Section 2.2 with a review of the harmonic oscillator and in Section 2.3 construct the canonical coherent states, displaced versions of the vacuum that form an overcomplete basis of Hilbert space [36,58]. An associated holomorphic (Segal-Bargmann) representation, $\psi(\alpha) = \langle \alpha | \psi \rangle$, provides a natural analytic phase-space description. These states generate a POVM that approximates simultaneous, unsharp measurements of position and momentum [33,34], which we introduce in Section 2.4 as the starting point for modelling decoherence.

The central analysis is carried out in Section 2.5, where we study how repeated nonselective POVM measurements modify both the density matrix and the standard quasi-probability distributions, namely the Husimi Q-function, the Wigner function, and the Glauber-Sudarshan P-representation [24,25,58, 59, 61, 62]. We show that successive measurements suppress quantum interference and drive the system toward classical-like distributions, with the Husimi function in particular satisfying a diffu-

sion equation on the complex plane. Building on this, we then extend the analysis to the full σ-parametrised family of quasi-probability distributions $F^{(\sigma)}(\alpha)$ [70–72], which are related by Gaussian convolutions and provide a unified framework encompassing the Q, W, and P functions as special cases.

In Section 2.6, we propose a Lindblad master equation with $\hat{x}$ and $\hat{p}$ as Lindblad operators, modelling the effect of simultaneous unsharp measurements of position and momentum [38, 44]. This dynamics reproduces the same phase-space diffusion observed in the iterative POVM scheme and can be expressed as a heat equation both on the (x, p) plane and in the Segal–Bargmann representation, thereby linking decoherence with classical diffusion and complex-analytic structures.

Finally, in Section 2.7, we discuss these results and present analytical plots of cat-state decoherence under free-particle and harmonic-oscillator Hamiltonians. Additional technical material is included in two appendices. Appendix A develops the Segal-Bargmann representation in more detail and explores phase-space measurement in this holomorphic setting, while Appendix B provides explicit solutions to Lindblad equations with $\hat{x}$ and $\hat{p}$ as Lindblad operators, which were used to generate the analytical plots in this chapter. Throughout, we work in natural units $\hbar = \omega = m = 1$, simplifying the algebra while preserving the essential structure of the theory.

2.2 The physical system: quantum harmonic oscillator

We consider the one-dimensional quantum harmonic oscillator with Hamiltonian [51, 73]

$$\hat{H} = \frac{\hat{p}^2}{2} + \frac{\hat{x}^2}{2}, \tag{2.1}$$

where $\hat{x}$ and $\hat{p}$ are the position and momentum operators, satisfying the canonical commutation relation $[\hat{q}, \hat{p}] = \mathrm{i}\mathbb{1}$.

The eigenvalues and eigenfunctions of the harmonic oscillator follow from the time-independent Schrödinger equation [73]

$$\hat{H}\phi_n(x) = E_n\phi_n(x), \tag{2.2}$$

yielding

$$E_n = \left(n + \frac{1}{2}\right), \quad \phi_n(x) = \frac{1}{\sqrt{2^n n!\sqrt{\pi}}} H_n(x)\mathrm{e}^{-x^2/2}, \tag{2.3}$$

where $H_n(x)$ are Hermite polynomials. They satisfy the recurrence relations [74]

$$H_{n+1}(x) = 2xH_n(x) - 2nH_{n-1}(x), \quad H_0(x) = 1,\ H_1(x) = 2x. \tag{2.4}$$

These eigenstates $\phi_n(x)$ form an orthonormal basis of the Hilbert space $L^2(\mathbb{R})$ of square-integrable functions. For any $f, g \in L^2(\mathbb{R})$, the inner product is

$$\langle f, g\rangle = \int_{-\infty}^{\infty} f(x)\overline{g(x)}\,\mathrm{d}x. \tag{2.5}$$

An alternative and more algebraic approach to the harmonic oscillator is due to Fock [75], who introduced ladder operators

$$\hat{a} = \frac{1}{\sqrt{2}}(\hat{x} + \mathrm{i}\hat{p}), \quad \hat{a}^\dagger = \frac{1}{\sqrt{2}}(\hat{x} - \mathrm{i}\hat{p}), \tag{2.6}$$

which satisfy the canonical commutation relation $[\hat{a}, \hat{a}^\dagger] = \mathbb{1}$. The Hamiltonian becomes

$$\hat{H} = \hat{a}^\dagger\hat{a} + \frac{1}{2} = \hat{N} + \frac{1}{2}, \tag{2.7}$$

where $\hat{N} = \hat{a}^\dagger\hat{a}$ is the number operator. Its eigenstates $|n\rangle$ satisfy

$$\hat{N}|n\rangle = n|n\rangle, \quad \hat{H}|n\rangle = \left(n + \frac{1}{2}\right)|n\rangle. \tag{2.8}$$

The wavefunctions $\phi_n(x)$ introduced in (2.3) are just the position representation of these Fock states, $\phi_n(x) = \langle x|n\rangle$.

While this chapter focuses on the one-dimensional oscillator, the algebraic formalism generalises naturally to higher dimensions by introducing independent mode operators $\hat{a}_i, \hat{a}_i^\dagger$. We will now introduce the canonical coherent states.

2.3 Canonical coherent states and phase space

As discussed in Chapter 1, coherent states provide the natural bridge between quantum and classical descriptions. In this chapter, we focus on canonical coherent states associated with the Heisenberg–Weyl group and their role in modelling measurement-induced decoherence.

These states can be defined as eigenstates of the annihilation operator

$$\hat{a}|\alpha\rangle = \alpha|\alpha\rangle, \quad \alpha \in \mathbb{C}, \tag{2.9}$$

and constructed explicitly as displaced vacuum states via the Weyl displacement operator

$$|\alpha\rangle = \hat{D}(\alpha)|0\rangle = \exp\left(\alpha\hat{a}^\dagger - \bar{\alpha}\hat{a}\right)|0\rangle. \tag{2.10}$$

where $\alpha = \frac{1}{\sqrt{2}}(x + \mathrm{i}p)$, parametrise these states so that the quantum phase space can be identified with the complex plane $\mathbb{C}$.

Coherent states possess several properties that reinforce their classical interpretation:

Minimum uncertainty. Coherent states saturate the Heisenberg uncertainty relation: $\Delta x\,\Delta p \geq \frac{\hbar}{2}$, achieving the minimum with equal uncertainties $\Delta x = \Delta p = \sqrt{\frac{\hbar}{2}}$. They are Gaussian wave packets centered at classical phase-space coordinates $(\mathrm{Re}(\alpha), \mathrm{Im}(\alpha))$, with isotropic spread.

Classical trajectories. Under the harmonic oscillator Hamiltonian $\hat{H} = \hat{a}^\dagger\hat{a} + \frac{1}{2}$, coherent states evolve along classical trajectories

$$|\alpha(t)\rangle = \mathrm{e}^{-\mathrm{i}\hat{H}t}|\alpha\rangle = \mathrm{e}^{-\mathrm{i}t/2}|\alpha\mathrm{e}^{-\mathrm{i}t}\rangle. \tag{2.11}$$

This corresponds to uniform circular motion in the complex plane, with the expectation values $\langle\hat{x}(t)\rangle$, $\langle\hat{p}(t)\rangle$ satisfying classical equations of motion.

Overcompleteness and POVMs. Coherent states are not orthogonal, namely, the overlap of two coherent states is given as

$$\langle\alpha|\beta\rangle = \exp\left(-\frac{1}{2}|\alpha|^2 - \frac{1}{2}|\beta|^2 + \bar{\alpha}\beta\right), \tag{2.12}$$

but they form an overcomplete set that resolves the identity

$$\int_{\mathbb{C}} \frac{\mathrm{d}^2\alpha}{\pi}\, |\alpha\rangle\langle\alpha| = \mathbb{1}, \tag{2.13}$$

where $\mathrm{d}^2\alpha = \frac{\mathrm{i}}{2}\mathrm{d}\alpha \wedge \mathrm{d}\bar{\alpha} = \mathrm{dRe}(\alpha)\,\mathrm{dIm}(\alpha)$.

Holomorphic structure and the Segal-Bargmann space

Although our primary formulation will remain in the Hilbert space $\mathcal{H} = L^2(\mathbb{R})$, coherent states naturally lead to a holomorphic representation. Given any quantum state $|\psi\rangle \in \mathcal{H}$, one defines a function on the complex plane by

$$\psi(\alpha) = \langle\alpha|\psi\rangle. \tag{2.14}$$

This function is entire due to the Gaussian structure of the coherent states. The collection of such functions, with inner product

$$\langle\psi|\phi\rangle = \int_{\mathbb{C}} \overline{\psi(\alpha)}\phi(\alpha)\, \frac{\mathrm{d}^2\alpha}{\pi}, \tag{2.15}$$

forms a reproducing kernel Hilbert space known as the Segal-Bargmann space [76,77]. While we do not adopt this as the main formalism in this thesis, the holomorphic structure will serve as a technical tool for analysing measurement dynamics and phase-space diffusion.

Explicitly, the coherent state wavefunction in position space is given by

$$\langle x|\alpha\rangle = \pi^{-1/4} \exp\left(-\frac{x^2}{2} + \sqrt{2}\alpha x - \frac{\alpha^2}{2} - \frac{|\alpha|^2}{2}\right), \tag{2.16}$$

which acts as the kernel of the Segal-Bargmann transform. This overlap not only links the real-line Hilbert space to holomorphic functions on $\mathbb{C}$, but also satisfies the reproducing kernel property

$$\psi(\alpha) = \langle\alpha|\psi\rangle = \int_{\mathbb{C}} \langle\alpha|\beta\rangle\, \psi(\beta)\, \frac{\mathrm{d}^2\beta}{\pi}, \tag{2.17}$$

demonstrating that coherent states encode all information about $|\psi\rangle$ through their inner products.

We will return to a more detailed mathematical discussion of the Segal-Bargmann representation and its role in phase-space dynamics in Appendix A.

In the sections that follow, we use these features to build a model of quantum measurement via

coherent-state POVMs. We study how repeated, unsharp phase-space measurements lead to decoherence and classical behavior, both in the density matrix and in phase-space representations.

2.4 Coherent-state POVMs and iterative phase-space measurement

In quantum mechanics, the uncertainty principle forbids assigning sharp simultaneous values to x and p, so a single classical phase-space point has no direct analogue. Nevertheless, coherent states, parametrised by $\alpha = \frac{1}{\sqrt{2}}(x + \mathrm{i}p)$, allow us to construct a family of phase-space measurements.

In particular, the overcompleteness of coherent states defines a positive operator-valued measure (POVM) describing unsharp, continuous measurements of position and momentum. It is given by

$$\hat{E}_\alpha = |\alpha\rangle\langle\alpha|, \qquad \alpha \in \mathbb{C}, \tag{2.18}$$

and satisfies the resolution of the identity

$$\int_{\mathbb{C}} \frac{\mathrm{d}^2\alpha}{\pi}\, \hat{E}_\alpha = \mathbb{1}. \tag{2.19}$$

For a system in state $\hat{\rho}$, the probability density for outcome α is

$$\Pr(\alpha) = \mathrm{tr}(\hat{\rho}\hat{E}_\alpha) = \langle\alpha|\hat{\rho}|\alpha\rangle, \tag{2.20}$$

which (up to normalisation) is precisely the Husimi Q-function [61]. Thus, the Q-function arises directly from coherent-state POVM statistics, providing a smooth, positive phase-space representation of quantum states.

In the context of decoherence, we are particularly interested in *nonselective* measurements, where the measurement is performed but the outcome α is not recorded. Rather than collapsing to a specific coherent state $|\alpha\rangle$, the system undergoes an ensemble-averaged transformation

$$\hat{\rho} \mapsto \int_{\mathbb{C}} \frac{\mathrm{d}^2\alpha}{\pi}\, |\alpha\rangle\langle\alpha|\hat{\rho}|\alpha\rangle\langle\alpha|. \tag{2.21}$$

This operation is trace preserving and maps pure states to mixed states in general. While the classical probability weights are retained at the ensemble level, coherence between distinct coherent states is progressively suppressed. In this way, the transformation models decoherence induced by environmental monitoring without conditioning on individual measurement outcomes.

Importantly, because coherent states are nonorthogonal, the POVM elements $\hat{E}_\alpha$ do *not* satisfy Zurek's repeatability criterion for measurements [11,78]. In Zurek's framework, a measurement is repeatable if, once an outcome is obtained, an immediate repetition yields the same result with certainty. This holds for projective measurements but fails for overcomplete POVMs like those formed by coherent states. As a result, the coherent-state POVM reflects a more realistic and noisy measurement process, one in which outcomes are inherently approximate and not sharply reproducible. To distinguish this post-measurement state from the original, we denote it by $\hat{\rho}^{(1)}$, the density matrix after a single iteration of the coherent-state POVM.

We now compute the resulting density matrix after one such nonselective measurement in the position representation.

Proposition 2.1. *After one application of the coherent-state POVM, the density matrix evolves as*

$$\rho^{(1)}(x,y) = \frac{1}{\sqrt{2\pi}} \exp\left(-\frac{(x-y)^2}{2}\right) \int_{-\infty}^{\infty} \exp\left(-\frac{\lambda^2}{2}\right) \rho(x+\lambda, y+\lambda)\, \mathrm{d}\lambda, \tag{2.22}$$

where $\rho(x,y)$ is the initial density matrix in the position representation, and $\rho^{(1)}(x,y)$ denotes the state after one application of the nonselective coherent-state POVM.

Proof. Sandwiching (2.21) between position eigenstates yields

$$\langle x|\rho^{(1)}|y\rangle = \int_{\mathbb{C}} \frac{\mathrm{d}^2\alpha}{\pi} \langle x|\alpha\rangle\langle\alpha|\hat{\rho}|\alpha\rangle\langle\alpha|y\rangle. \tag{2.23}$$

To evaluate the middle matrix element $\langle\alpha|\hat{\rho}|\alpha\rangle$, we insert a resolution of the identity in the position basis

$$\langle\alpha|\hat{\rho}|\alpha\rangle = \int_{\mathbb{R}^2} \mathrm{d}u\, \mathrm{d}v\, \langle\alpha|u\rangle\langle u|\hat{\rho}|v\rangle\langle v|\alpha\rangle = \int_{\mathbb{R}^2} \mathrm{d}u\, \mathrm{d}v\, \langle\alpha|u\rangle\, \rho(u,v)\, \langle v|\alpha\rangle. \tag{2.24}$$

Substituting this back, we obtain

$$\rho^{(1)}(x,y) = \int_{\mathbb{C}} \frac{\mathrm{d}^2\alpha}{\pi} \int_{\mathbb{R}^2} \mathrm{d}u\, \mathrm{d}v\, \langle x|\alpha\rangle\, \langle\alpha|u\rangle\, \rho(u,v)\, \langle v|\alpha\rangle\, \langle\alpha|y\rangle, \tag{2.25}$$

where we have defined $\langle x|\rho^{(1)}|y\rangle = \rho^{(1)}(x,y)$.
We now evaluate the integral

$$I = \int_{\mathbb{C}} \frac{\mathrm{d}^2\alpha}{\pi} \langle x|\alpha\rangle\, \langle\alpha|u\rangle\, \langle v|\alpha\rangle\, \langle\alpha|y\rangle,$$

where we make use of the position-space overlap (cf. (2.12)) and express the complex variable $\alpha = m + \mathrm{i}n \in \mathbb{C}$ in terms of real variables $m, n \in \mathbb{R}$. The measure becomes $\mathrm{d}^2\alpha = \mathrm{d}m\, \mathrm{d}n$.
Substituting the coherent state overlaps and simplifying the exponent, we obtain

$$I = \frac{1}{\pi^2} \exp\left(-\frac{x^2+y^2+a^2+b^2}{2}\right) \int \exp\left(\sqrt{2}\mathrm{i}n(a+y-x-b)\right) \times \left[\int \exp\left(-4m^2 + \sqrt{2}m(x+b+a+y)\right) \mathrm{d}m\right] \mathrm{d}n.$$

We first evaluate the Gaussian integral over m, using the standard identity

$$\int_{-\infty}^{\infty} \exp(-Am^2 + Bm)\, \mathrm{d}m = \sqrt{\frac{\pi}{A}} \exp\left(\frac{B^2}{4A}\right), \quad \text{for } A > 0,$$

with $A = 4$, $B = \sqrt{2}(x+b+a+y)$, yielding

$$I = \frac{1}{\pi^2} \exp\left(-\frac{x^2+y^2+a^2+b^2}{2}\right) \cdot \frac{\sqrt{\pi}}{2} \exp\left(\frac{(x+b+a+y)^2}{8}\right) \times \int \exp\left(\mathrm{i}\sqrt{2}n(a+y-x-b)\right) \mathrm{d}n. \tag{2.26}$$

The integral over n gives a delta function $\int \exp(\mathrm{i}cn)\mathrm{d}n = 2\pi\delta(c)$, and so we obtain

$$I = \frac{1}{\sqrt{2\pi}} \exp\left(-\frac{x^2+y^2+a^2+b^2}{2}\right) \exp\left(\frac{(x+b+a+y)^2}{8}\right) \delta(a+y-x-b). \tag{2.27}$$

Substituting this into (2.25), we get

$$\begin{aligned}\rho^{(1)}(x,y) &= \frac{1}{\sqrt{2\pi}} \exp\left(-\frac{x^2+y^2}{2}\right) \exp\left(\frac{(x+y)^2}{8}\right) \int\int \exp\left(-\frac{a^2+b^2}{2}\right) \\ &\quad \times \exp\left(\frac{(a+b)^2}{8} + \frac{(a+b)(x+y)}{4}\right) \delta(a+y-x-b)\, \rho(a,b)\, \mathrm{d}a\, \mathrm{d}b.\end{aligned}$$

We now evaluate the integral over a using the delta function, $\delta(a+y-x-b) \Rightarrow a = x-y+b$, which gives

$$\begin{aligned}\rho^{(1)}(x,y) &= \frac{1}{\sqrt{2\pi}} \exp\left(-\frac{x^2+y^2}{2}\right) \exp\left(\frac{(x+y)^2}{8}\right) \int \exp\left(-\frac{(x-y+b)^2+b^2}{2}\right) \\ &\quad \times \exp\left(\frac{(x+b-y+b)^2}{8} + \frac{(x+b-y+b)(x+y)}{4}\right) \rho(x-y+b,b)\, \mathrm{d}b.\end{aligned}$$

Simplifying the exponents, we eventually arrive at

$$\rho^{(1)}(x,y) = \frac{1}{\sqrt{2\pi}} \exp\left(-\frac{(x-y)^2}{2}\right) \int \exp\left(-\frac{\lambda^2}{2}\right) \rho(x+\lambda, y+\lambda)\, \mathrm{d}\lambda, \tag{2.28}$$

after performing the change of variable $\lambda = b - y$. □

The phase-space measurement suppresses off-diagonal terms by a Gaussian factor $\exp\left(-\frac{(x-y)^2}{2}\right)$, reflecting decoherence in the position basis. At the same time, the convolution over λ averages the density matrix over diagonal shifts, producing an additional Gaussian smoothing of the mean coordinate $\frac{x+y}{2}$. Thus, the measurement induces a double smoothing, damping quantum coherences and blurring the overall spatial profile, together capturing the gradual information loss that characterises environmentally induced decoherence.

To model continuous monitoring, as in environmental decoherence, we therefore consider k successive unrecorded applications of the coherent-state POVM.

Proposition 2.2. *After k applications of the coherent-state POVM, the density matrix evolves as*

$$\rho^{(k)}(x,y) = \frac{1}{\sqrt{2k\pi}} \exp\left(-\frac{k(x-y)^2}{2}\right) \int \exp\left(-\frac{\lambda^2}{2k}\right) \rho(x+\lambda, y+\lambda)\, \mathrm{d}\lambda. \tag{2.29}$$

where $\rho(x,y)$ is the initial density matrix in the position representation, and $\rho^{(k)}(x,y)$ denotes the state after k applications of the nonselective coherent-state POVM.

Proof. We prove the result by induction. For the base case $k = 1$, from the Proposition 2.1, we have

$$\rho^{(1)}(x,y) = \frac{1}{\sqrt{2\pi}} \exp\left(-\frac{(x-y)^2}{2}\right) \int \exp\left(-\frac{\lambda^2}{2}\right) \rho(x+\lambda, y+\lambda)\, \mathrm{d}\lambda, \tag{2.30}$$

which establishes the initial step. Assume the claim holds for some integer $k \geq 1$, that is,

$$\rho^{(k)}(x,y) = \frac{1}{\sqrt{2\pi k}} \exp\left(-\frac{(x-y)^2 k}{2}\right) \int \exp\left(-\frac{\lambda^2}{2k}\right) \rho(x+\lambda, y+\lambda)\, \mathrm{d}\lambda. \tag{2.31}$$

Applying the POVM update rule again, we obtain

$$\rho^{(k+1)}(x,y) = \frac{1}{\sqrt{2\pi}} \exp\left(-\frac{(x-y)^2}{2}\right) \int \exp\left(-\frac{\nu^2}{2}\right) \rho^{(k)}(x+\nu, y+\nu)\, \mathrm{d}\nu. \tag{2.32}$$

Substituting the inductive hypothesis (2.31) into the integrand

$$\begin{aligned} \rho^{(k+1)}(x,y) &= \frac{1}{2\pi\sqrt{k}} \exp\left(-\frac{(x-y)^2(k+1)}{2}\right) \\ &\quad \times \iint \exp\left(-\frac{\lambda^2}{2k} - \frac{\nu^2}{2}\right) \rho(x+\lambda+\nu, y+\lambda+\nu)\, \mathrm{d}\lambda\, \mathrm{d}\nu. \end{aligned} \tag{2.33}$$

We now make the change of variables $\eta = \lambda + \nu$, so that $\lambda = \eta - \nu$ and $\mathrm{d}\lambda\, \mathrm{d}\nu = \mathrm{d}\eta\, \mathrm{d}\nu$. Substituting gives

$$\begin{aligned} \rho^{(k+1)}(x,y) &= \frac{1}{2\pi\sqrt{k}} \exp\left(-\frac{(x-y)^2(k+1)}{2}\right) \\ &\quad \times \int \left[\int \exp\left(-\frac{(\eta-\nu)^2}{2k} - \frac{\nu^2}{2}\right) \mathrm{d}\nu\right] \rho(x+\eta, y+\eta)\, \mathrm{d}\eta. \end{aligned} \tag{2.34}$$

Evaluating the inner integral over ν, which is Gaussian, gives

$$\int \exp\left(-\frac{(\eta-\nu)^2}{2k} - \frac{\nu^2}{2}\right) \mathrm{d}\nu = \sqrt{2\pi \cdot \frac{k}{k+1}} \exp\left(-\frac{\eta^2}{2(k+1)}\right). \tag{2.35}$$

Substituting this back into the expression for $\rho^{(k+1)}$ in (2.34), we find

$$\begin{aligned} \rho^{(k+1)}(x,y) &= \frac{1}{2\pi\sqrt{k}} \sqrt{2\pi \frac{k}{k+1}} \exp\left(-\frac{(x-y)^2(k+1)}{2}\right) \int \exp\left(-\frac{\eta^2}{2(k+1)}\right) \rho(x+\eta, y+\eta)\, \mathrm{d}\eta, \\ &= \frac{1}{\sqrt{2\pi(k+1)}} \exp\left(-\frac{(x-y)^2(k+1)}{2}\right) \int \exp\left(-\frac{\eta^2}{2(k+1)}\right) \rho(x+\eta, y+\eta)\, \mathrm{d}\eta. \end{aligned} \tag{2.36}$$

This completes the inductive step, and the result follows for all $k \in \mathbb{N}$. □

The result in (2.29) shows that coherent-state POVM measurements induce two complementary effects on the density matrix. Off-diagonal coherence terms are suppressed by a Gaussian factor, driving the state toward diagonality in the position basis, while a convolution along the phase-space diagonal progressively blurs the spatial profile. After k iterations both effects accumulate, with suppression and smoothing becoming sharper as k increases.

The same structure appears in the momentum representation as well, by taking the double Fourier transform of (2.29), one obtains an identical expression with momentum variables (see Appendix B.2). Thus, iterative measurements induce both *dephasing* (suppression of off-diagonal terms) and *diffusion* (Gaussian smoothing), in both the position and momentum representations, together capturing the essence of environment-induced decoherence.

In the limit $k \to \infty$, the Gaussian prefactor tends to a delta function in the diagonal direction and zero elsewhere: $\exp\left(-\frac{(x-y)^2 k}{2}\right) \to \delta(x-y)$. Meanwhile, the smoothing kernel becomes broader and covers the entire real line: $\exp\left(-\frac{\lambda^2}{2k}\right) \to 1$. Thus, the density matrix $\rho^{(k)}(x,y)$ converges to a diagonal operator with its entries given by the marginal distribution of the original state

$$\rho^{(\infty)}(x,y) = \delta(x-y) \int \rho(x+\lambda, x+\lambda)\, \mathrm{d}\lambda. \tag{2.37}$$

While the resulting operator is formally diagonal, its diagonal entries are uniform over the entire space due to the infinite-width smoothing. This suggests that the final state approaches a *completely mixed state*, with minimal information about the initial coherences retained.

However, it's important to note that this limiting state may no longer be trace-class in the usual sense, and it may fail to represent a proper density operator. Rather, it can be interpreted as a distribution-valued object, e.g., a weak-* limit in the dual space of trace-class operators.

2.5 Phase-space picture of decoherence

The results above can be recast in the language of phase-space quasi-probability distributions [25, 43, 63], which provide complementary representations of quantum states. The Wigner function reveals interference through its negative regions [24], the Glauber-Sudarshan P-representation [58, 59, 79] expresses states as coherent-state mixtures (often singular), and the Husimi Q-function is smooth and positive, corresponding directly to coherent-state measurement probabilities [36, 61]. Under repeated POVM monitoring all three distributions are progressively smoothed, reflecting suppression of quantum coherence and decoherence manifests as a diffusion-like blurring in phase space [38, 44].

Husimi Q-function

The Husimi Q-function is defined as

$$Q(\alpha) = \langle \alpha | \hat{\rho} | \alpha \rangle, \tag{2.38}$$

where $|\alpha\rangle$ denotes the canonical coherent state labeled by a point $\alpha \in \mathbb{C}$. This function is smooth, positive-definite, and normalised over the complex plane, $\int_{\mathbb{C}} Q(\alpha) \frac{\mathrm{d}^2\alpha}{\pi} = 1$. Although it does not yield the correct marginal distributions for position or momentum, it is nonetheless a valid probability distribution on phase space, and it arises naturally as the probability distribution associated with a coherent-state POVM measurement.

In the context of a nonselective measurement, where no outcome is recorded, to determine the resulting Q-function after one iteration of the phase-space measurement, we sandwich both sides of (2.21) with the coherent state $|\alpha\rangle$, obtaining

$$Q^{(1)}(\alpha) = \langle \alpha | \hat{\rho}^{(1)} | \alpha \rangle = \int_{\mathbb{C}} \frac{\mathrm{d}^2\beta}{\pi} \, |\langle \alpha | \beta \rangle|^2 \langle \beta | \hat{\rho} | \beta \rangle, \tag{2.39}$$

where $Q^{(1)}(\alpha)$ is the Husimi function after one application of coherent-state POVM measurement and $\langle \beta | \hat{\rho} | \beta \rangle = Q(\beta)$ is the initial Husimi density function.

Using the known expression for the coherent-state overlap (2.12), we find that the post-measurement Q-function is a Gaussian convolution of the initial distribution

$$Q^{(1)}(\alpha) = \int_{\mathbb{C}} \frac{\mathrm{d}^2\beta}{\pi}\, \mathrm{e}^{-|\alpha-\beta|^2} Q(\beta). \tag{2.40}$$

This reveals that the effect of the measurement is to smooth the initial Q-function by a unit-variance Gaussian kernel. The smoothing originates directly from the Gaussian structure of the coherent-state overlap.

Just as we computed the density matrix after k nonselective measurements in the previous section for the density matrix, we now derive the corresponding evolution for the Husimi function.

Proposition 2.3. *After k successive nonselective coherent-state POVM measurements, the Husimi function evolves as*

$$Q^{(k)}(\alpha) = \int_{\mathbb{C}} \frac{\mathrm{d}^2\beta}{\pi k}\, \exp\left(-\frac{|\alpha-\beta|^2}{k}\right) Q(\beta). \tag{2.41}$$

That is, the initial Husimi function is convolved with a Gaussian of variance k, resulting in increasing smoothing over phase space with each iteration.

Proof. We proceed by induction on k.

For $k = 1$, we have already shown that in (2.40), which is the convolution of the initial Husimi function Q with a Gaussian of unit variance. This establishes the base case.

Assume the result holds for some $k \in \mathbb{N}$, i.e.,

$$Q^{(k)}(\alpha) = \int_{\mathbb{C}} \frac{\mathrm{d}^2\beta}{\pi k}\, \mathrm{e}^{-|\alpha-\beta|^2/k} Q(\beta). \tag{2.42}$$

We now compute $Q^{(k+1)}(\alpha)$ using the definition of the nonselective measurement update

$$\begin{aligned} Q^{(k+1)}(\alpha) &= \int_{\mathbb{C}} \frac{\mathrm{d}^2\gamma}{\pi}\, |\langle\alpha|\gamma\rangle|^2 Q^{(k)}(\gamma) \\ &= \int_{\mathbb{C}} \frac{\mathrm{d}^2\beta}{\pi k}\, Q(\beta) \int_{\mathbb{C}} \frac{\mathrm{d}^2\gamma}{\pi}\, \exp\left(-|\alpha-\gamma|^2 - \frac{|\gamma-\beta|^2}{k}\right). \end{aligned} \tag{2.43}$$

To evaluate the inner integral over γ, we complete the square. Define

$$A = 1 + \frac{1}{k}, \qquad \mu = \frac{\alpha + \beta/k}{A}. \tag{2.44}$$

Then

$$|\alpha-\gamma|^2 + \frac{1}{k}|\gamma-\beta|^2 = A|\gamma-\mu|^2 + \frac{|\alpha-\beta|^2}{k+1}. \tag{2.45}$$

Thus, the inner integral becomes

$$\int_{\mathbb{C}} \frac{\mathrm{d}^2\gamma}{\pi}\, \exp\left(-|\alpha-\gamma|^2 - \frac{|\gamma-\beta|^2}{k}\right) = \frac{\pi}{A} \exp\left(-\frac{|\alpha-\beta|^2}{k+1}\right). \tag{2.46}$$

Using $A = \frac{k+1}{k}$, we have $\frac{1}{A} = \frac{k}{k+1}$, so the full expression becomes

$$Q^{(k+1)}(\alpha) \quad = \quad \int_{\mathbb{C}} \frac{\mathrm{d}^2\beta}{\pi(k+1)} \exp\left(-\frac{|\alpha-\beta|^2}{k+1}\right) Q(\beta). \tag{2.47}$$

This completes the inductive step. Hence, by induction, the result holds for all $k \in \mathbb{N}$. □

This result shows that the effect of repeated nonselective coherent-state measurements is to iteratively smooth the Husimi Q-function by convolving it with a Gaussian kernel of increasing variance. In other words, the process generates a net convolution with a k-fold broadened Gaussian

$$Q^{(k)}(\alpha) = (Q^{(0)} * G_k)(\alpha), \tag{2.48}$$

where $G_k(\alpha) = \frac{1}{\pi k}\mathrm{e}^{-|\alpha|^2/k}$ is the normalised Gaussian of variance k.

As $k \to \infty$, this smoothing becomes more pronounced, and the Q-function spreads out over the entire phase space. In the limit, any initial structure in the state is washed out, and the distribution becomes increasingly flat. Formally, since the total integral of the Q-function is preserved (due to trace preservation of the quantum state), the distribution asymptotically approaches a uniform density over $\mathbb{C}$, though in practice this uniformity is always limited by the normalisation condition $\int_{\mathbb{C}} Q^{(k)}(\alpha)\,\frac{\mathrm{d}^2\alpha}{\pi} = 1$.

In the following section, we will explore phase-space measurement and decoherence through the P-function.

Glauber-Sudarshan P-function

The *Glauber–Sudarshan* P-function [58, 59, 62] represents the density operator as a diagonal mixture of coherent states,

$$\hat{\rho} = \int_{\mathbb{C}} \frac{\mathrm{d}^2\alpha}{\pi}\, P(\alpha)\, |\alpha\rangle\langle\alpha|. \tag{2.49}$$

In contrast to the Husimi Q-function, the P-function is often highly singular for nonclassical states, involving distributions such as derivatives of delta functions. Moreover, this representation is not unique, different generalised functions $P(\alpha)$ may correspond to the same density operator, reflecting the overcompleteness of the coherent-state basis. Although it cannot generally be interpreted as a genuine probability density, it remains a central tool in quantum optics for characterising nonclassicality relative to coherent states.

To explore how the coherent-state POVM acts on the P-function, we insert the diagonal P-representation of $\hat{\rho}$ into the expression for the Husimi function

$$Q(\alpha) = \langle\alpha|\hat{\rho}|\alpha\rangle = \int_{\mathbb{C}} \frac{\mathrm{d}^2\beta}{\pi}\, P(\beta)\, |\langle\alpha|\beta\rangle|^2. \tag{2.50}$$

Using the coherent state overlap from (2.12), we obtain the convolution form

$$Q(\alpha) = \int_{\mathbb{C}} \frac{\mathrm{d}^2\beta}{\pi}\, \mathrm{e}^{-|\alpha-\beta|^2}\, P(\beta). \tag{2.51}$$

This equation shows that the Husimi Q-function is the result of convolving the Glauber-Sudarshan P-function with a Gaussian kernel. In effect, a single coherent-state POVM measurement smooths the P-function, which may be highly singular or even distributional, into a well-behaved, positive-definite function on phase space.

Using this result, we observe that the k-fold application of the coherent-state POVM to the P-function produces the same Gaussian convolution structure as seen for the Husimi function. That is, the k^{th} iteration of the P-function evolves according to

$$P^{(k)}(\alpha) = \int_{\mathbb{C}} \frac{\mathrm{d}^2\beta}{\pi k}\, \mathrm{e}^{-|\alpha-\beta|^2/k}\, P(\beta). \tag{2.52}$$

In other words, repeated coherent-state measurements progressively smooth out the P-function, and in the large-k limit, the two phase-space distributions we have considered so far, Q, and P, approach increasingly classical, diffused forms.

We now turn to the Wigner function, a quasi-probability distribution that, unlike the Q-function, retains negative regions reflecting quantum interference.

Wigner function

The Wigner function $W(x,p)$ provides a central phase-space representation of quantum states [24,25]. Unlike the Husimi Q-function, it is not a genuine probability distribution, as it can take on negative values, a hallmark of nonclassicality. Nevertheless, it yields the correct marginal distributions

$$\int W(x,p)\,\mathrm{d}p = \langle x|\hat{\rho}|x\rangle, \quad \int W(x,p)\,\mathrm{d}x = \langle p|\hat{\rho}|p\rangle. \tag{2.53}$$

The Wigner function is related to the density matrix $\rho(x,y)$ via the Wigner-Weyl transform

$$W(x,p) = \frac{1}{2\pi}\int \mathrm{e}^{-\mathrm{i}p\lambda}\,\rho\left(x+\frac{\lambda}{2}, x-\frac{\lambda}{2}\right)\,\mathrm{d}\lambda, \tag{2.54}$$

with inverse transform

$$\rho(x,y) = \int \mathrm{e}^{\mathrm{i}p(x-y)}\,W\left(\frac{x+y}{2}, p\right)\,\mathrm{d}p. \tag{2.55}$$

We now analyse how repeated coherent-state POVM measurements affect the Wigner function. By applying the above transforms to the iterated density matrix $\rho^{(k)}(x,y)$, we will derive the resulting evolution of $W(x,p)$ and show that it too undergoes phase-space diffusion, reflecting a progressive loss of quantum coherence.

Proposition 2.4. *Under repeated coherent-state POVM measurements, the Wigner function evolves via a two-dimensional Gaussian convolution. Specifically, after n iterations, the Wigner function transforms according to:*

$$W^{(k)}(x,p) = \frac{1}{2n\pi}\iint \exp\left(-\frac{(x-u)^2}{2k} - \frac{(p-v)^2}{2k}\right) W(u,v)\,\mathrm{d}u\,\mathrm{d}v. \tag{2.56}$$

Proof. We begin with the expression for the density matrix after n iterations of the POVM measure-

ment

$$\rho^{(k)}(x,y) = \frac{1}{\sqrt{2n\pi}} \exp\left(-k\frac{(x-y)^2}{2}\right) \int \exp\left(-\frac{\mu^2}{2k}\right) \rho(x+\mu, y+\mu)\, \mathrm{d}\mu. \tag{2.57}$$

To obtain the Wigner function, we apply the Wigner transform

$$W^{(k)}(x,p) = \frac{1}{\pi} \int \rho^{(k)}(x+\mu, x-\mu) \exp(-2\mathrm{i}p\mu)\, \mathrm{d}\mu. \tag{2.58}$$

Substituting (2.57) into this expression yields

$$W^{(k)}(x,p) = \frac{1}{\pi\sqrt{2k\pi}} \int \mathrm{e}^{-2k\mu^2} \left[\int \mathrm{e}^{-\frac{\lambda^2}{2k}} \rho(x+\lambda+\mu, x+\lambda-\mu)\, \mathrm{d}\lambda\right] \mathrm{e}^{-2\mathrm{i}p\mu}\, \mathrm{d}\mu. \tag{2.59}$$

We now express ρ in terms of the initial Wigner function using the inverse Wigner transform

$$\rho(x',y') = \int W\left(\frac{x'+y'}{2}, \lambda\right) \mathrm{e}^{\mathrm{i}\lambda(x'-y')}\, \mathrm{d}\lambda. \tag{2.60}$$

With $x' = x+\lambda+\mu$ and $y' = x+\lambda-\mu$, we find

$$\rho(x+\lambda+\mu, x+\lambda-\mu) = \int W(x+\lambda, v) \mathrm{e}^{2\mathrm{i}v\mu}\, \mathrm{d}v. \tag{2.61}$$

Substituting back

$$W^{(k)}(x,p) = \frac{1}{\pi\sqrt{2k\pi}} \iint \left[\int \mathrm{e}^{-2k\mu^2} \mathrm{e}^{-2\mathrm{i}p\mu} \mathrm{e}^{2\mathrm{i}v\mu}\, \mathrm{d}\mu\right] \mathrm{e}^{-\frac{\lambda^2}{2k}}\, W(x+\lambda, v)\, \mathrm{d}\lambda\, \mathrm{d}v. \tag{2.62}$$

Evaluating the inner Gaussian integral over μ

$$\int \mathrm{e}^{-2k\mu^2} \mathrm{e}^{2\mathrm{i}(v-p)\mu} \mathrm{d}\mu = \sqrt{\frac{\pi}{2k}} \exp\left(-\frac{(p-v)^2}{2k}\right), \tag{2.63}$$

we obtain

$$W^{(k)}(x,p) = \frac{1}{2k\pi} \iint \exp\left(-\frac{\lambda^2}{2k} - \frac{(p-v)^2}{2n}\right) W(x+\lambda, v)\, \mathrm{d}\lambda\, \mathrm{d}v. \tag{2.64}$$

Finally, changing variables $u = x+\lambda$, we get

$$W^{(k)}(x,p) = \frac{1}{2k\pi} \iint \exp\left(-\frac{(x-u)^2}{2k} - \frac{(p-v)^2}{2k}\right) W(u,v)\, \mathrm{d}u\, \mathrm{d}v, \tag{2.65}$$

as required. □

Note that in complex coordinates, where phase space is parametrised by $\alpha = \frac{1}{\sqrt{2}}(x+\mathrm{i}p)$, the convolution form of this result mirrors the structure seen in the evolution of the Husimi Q-function and the P-function under coherent-state POVM measurements

$$W^{(k)}(\alpha) = \int_{\mathbb{C}} \frac{\mathrm{d}^2\beta}{\pi k} \exp\left(-\frac{|\alpha-\beta|^2}{k}\right) W(\beta), \tag{2.66}$$

expressing the action of the measurement as a Gaussian diffusion in phase space.

As $k \to \infty$, the Wigner function of the initial state is completely smoothed, losing all fine-scale quantum features (such as negativity) and approaching a uniform distribution, similar in spirit to the asymptotic forms of both the Q- and P-functions.

However, the smoothing induced by this POVM map is not restricted to integer iterations. Since each iteration corresponds to convolution with a Gaussian kernel of fixed variance, fractional iterations can be defined by convolution with a Gaussian of proportionally reduced variance. In particular, a half-iteration of the measurement map applied to the Wigner function yields precisely the Husimi Q-function.

Proposition 2.5. *The Husimi Q-function is related to the Wigner function via a Gaussian smoothing in phase space:*

$$Q(\alpha) = \frac{2}{\pi} \iint \exp\left(-2|\alpha - \beta|^2\right) W(\beta)\, \mathrm{d}^2\beta. \tag{2.67}$$

Proof. We expand the Husimi function using the position basis

$$Q(\alpha) = \int \mathrm{d}x\, \mathrm{d}y\, \langle\alpha|x\rangle\langle x|\hat{\rho}|y\rangle\langle y|\alpha\rangle. \tag{2.68}$$

Substituting the Weyl transform expression for the density matrix

$$\rho(x,y) = \int W\left(\frac{x+y}{2}, \lambda\right) \exp\left(\mathrm{i}\lambda(x-y)\right)\, \mathrm{d}\lambda, \tag{2.69}$$

and plugging into the Husimi formula

$$\begin{aligned} Q(\alpha) &= \iint \mathrm{d}x\, \mathrm{d}y\, \langle\alpha|x\rangle\, \langle y|\alpha\rangle \left[\int \mathrm{d}\lambda\, W\left(\frac{x+y}{2}, \lambda\right) \mathrm{e}^{\mathrm{i}\lambda(x-y)}\right] \\ &= \iiint \mathrm{d}x\, \mathrm{d}y\, \mathrm{d}\lambda\, \langle\alpha|x\rangle\, \langle y|\alpha\rangle\, \mathrm{e}^{\mathrm{i}\lambda(x-y)}\, W\left(\frac{x+y}{2}, \lambda\right). \end{aligned} \tag{2.70}$$

We then perform the change of variables $x + y = 2m$, so $x = 2m - y$, and integrate out y (a Gaussian integral). After simplifying, this results in

$$Q(\alpha) = \frac{1}{\pi} \iint \exp\left(-(m-x)^2 - (\lambda - p)^2\right) W(m, \lambda)\, \mathrm{d}m\, \mathrm{d}\lambda. \tag{2.71}$$

Finally relabelling $\alpha = \frac{x+\mathrm{i}p}{\sqrt{2}}$ and $\beta = \frac{m+\mathrm{i}\lambda}{\sqrt{2}}$, we obtain the desired result. This completes the proof. □

Together with the earlier results, this completes a unified picture

$$P \xrightarrow{\frac{1}{2}} W \xrightarrow{\frac{1}{2}} Q \tag{2.72}$$

The P-function, which may be singular, evolves into the Wigner function after a half-iteration of the phase-space measurement, and into the positive-definite Q-function after a second half-iteration. With further nonselective measurements, all distributions converge toward a uniform limit, reflecting maximal decoherence and the loss of nonclassical features.

Beyond the individual Q, P, and Wigner functions, all phase-space representations can be viewed as

members of a one-parameter family of quasi-probability distributions defined via the *Stratonovich–Weyl (SW) kernel* [25, 70–72]. For each ordering parameter $\sigma \in \mathbb{R}$, the kernel operator $\hat{w}^{(\sigma)}(\alpha)$ is defined as

$$\hat{w}^{(\sigma)}(\alpha) = \frac{1}{\pi} \int_{\mathbb{C}} \mathrm{e}^{\alpha\bar{\beta}-\bar{\alpha}\beta}\, \mathrm{e}^{\frac{\sigma}{2}|\beta|^2}\, \hat{D}(\beta)\, \mathrm{d}^2\beta, \tag{2.73}$$

where $\hat{D}(\beta) = \exp(\beta\hat{a}^\dagger - \bar{\beta}\hat{a})$ is the displacement operator. The corresponding quasi-probability distribution for a state $\hat{\rho}$ is

$$F^{(\sigma)}(\alpha) = \mathrm{tr}\left(\hat{\rho}\, \hat{w}^{(\sigma)}(\alpha)\right). \tag{2.74}$$

Special cases are obtained for $\sigma = -1, 0, +1$, yielding the Husimi Q-function, the Wigner function, and the Glauber-Sudarshan P-function, respectively.

Moreover, different members of this family are related by Gaussian convolutions. For $\sigma_2 < \sigma_1$,

$$F^{(\sigma_2)}(\alpha) = \frac{2}{\pi(\sigma_1 - \sigma_2)} \int_{\mathbb{C}} \exp\left(-\tfrac{2|\alpha-\beta|^2}{\sigma_1-\sigma_2}\right) F^{(\sigma_1)}(\beta)\, \mathrm{d}^2\beta. \tag{2.75}$$

Thus, the apparent distinctions between P, W, and Q are simply different orderings of the same underlying phase-space description, smoothly interpolated by the parameter σ.

Corollary 2.1. Let $F^{(\sigma)}(\alpha) = \mathrm{tr}\big(\hat{\rho}\, \hat{w}^{(\sigma)}(\alpha)\big)$ denote the Cahill-Glauber σ-parametrised quasi-probability distribution on the complex phase space $\alpha \in \mathbb{C}$ (HW case), and let $\mathcal{E}$ be a single unread coherent-state POVM measurement (Gaussian convolution on phase space). Then, for any integer $k \geq 1$,

$$\big(\mathcal{E}^k F^{(\sigma)}\big)(\alpha) \;=\; F^{(\sigma-2k)}(\alpha). \tag{2.76}$$

Moreover, the (spectral) half-iteration satisfies

$$\big(\mathcal{E}^{1/2} F^{(\sigma)}\big)(\alpha) \;=\; F^{(\sigma-1)}(\alpha). \tag{2.77}$$

Consequently, the minimal number of full iterations required to reach the Husimi distribution ($\sigma' = -1$) from a given σ is

$$k_{\min} \;=\; \left\lceil \frac{\sigma+1}{2} \right\rceil. \tag{2.78}$$

This result is significant because the Husimi distribution is strictly positive and free of quantum negativity. Thus, $k_{\min}$ provides a sharp upper bound on the number of phase-space measurements needed to guarantee classical behaviour, independently of the initial state.

The observation that phase-space quasi-distributions interpolate smoothly under fractional iterations naturally motivates a continuous-time formulation. We therefore shift our focus from discrete measurement steps to continuous dynamical evolution in the next section.

2.6 Dynamical unravelling of phase-space measurement

In the previous sections, we examined the effects of iterative coherent-state POVM measurements, showing how repeated nonselective measurements lead to a progressive smoothing of phase-space distributions. These discrete updates describe the step-by-step degradation of quantum coherence and the emergence of classical behavior. However, it is natural to ask whether this process admits a continuous-time description that captures the same decohering effect.

Such continuous models fall within the framework of open quantum systems, where the system of interest interacts weakly with an external environment. The dynamics of the reduced density matrix $\hat{\rho}(t)$ are then governed by a master equation of the Gorini-Kossakowski-Sudarshan-Lindblad (GKSL) form [40–42]

$$\frac{\mathrm{d}\hat{\rho}}{\mathrm{d}t} = -\mathrm{i}[\hat{H}, \hat{\rho}] + \sum_j \left(\hat{L}_j \hat{\rho} \hat{L}_j^\dagger - \frac{1}{2}\{\hat{L}_j^\dagger \hat{L}_j, \hat{\rho}\} \right), \tag{2.79}$$

where $\hat{H}$ is the system Hamiltonian, and the operators $\hat{L}_j$ encode the effects of decoherence or continuous measurement.

This form of the master equation ensures that the time evolution of the system is both completely positive and trace-preserving (CPTP), thereby guaranteeing the physical validity of the quantum state at all times [80, 81]. Complete positivity is particularly crucial for preserving positivity even when the system is entangled with ancillary degrees of freedom. The trace-preserving property, on the other hand, ensures conservation of total probability, i.e., $\mathrm{tr}(\hat{\rho}(t)) = 1$ for all t. Moreover, the Lindblad form emerges as the most general description of Markovian open system dynamics under the assumptions of weak system-environment coupling and negligible memory effects. Its structure ensures that the evolution preserves the physicality of the quantum state in all scenarios, even when the system is embedded within a larger entangled context [80,81].

To model phase-space decoherence induced by coherent-state POVMs, we take the Lindblad operators to be the canonical observables $\hat{x}$ and $\hat{p}$, reflecting the weak monitoring of position and momentum [82,83]. This choice, equivalent to using $\hat{a}$ and $\hat{a}^\dagger$, is adopted for its clearer physical interpretation.

We focus on the purely dissipative case, with no Hamiltonian contribution, in order to isolate the decoherence dynamics and hence consider the following master equation

$$\frac{\mathrm{d}\hat{\rho}}{\mathrm{d}t} = \gamma \left(\hat{x}\hat{\rho}\hat{x} - \frac{1}{2}\{\hat{x}^2, \hat{\rho}\} \right) + \gamma \left(\hat{p}\hat{\rho}\hat{p} - \frac{1}{2}\{\hat{p}^2, \hat{\rho}\} \right), \tag{2.80}$$

where $\gamma > 0$ controls the strength of decoherence.

To obtain the evolution equation in the position representation, we sandwich both sides of (2.80) between position eigenstates $|x\rangle$ and $|y\rangle$. Using the standard operator actions

$$\hat{x}|x\rangle = x|x\rangle, \quad \hat{p} = -\mathrm{i}\frac{\partial}{\partial x}, \quad \hat{p}|x'\rangle = -\mathrm{i}\frac{\partial}{\partial x}\delta(x - x'), \tag{2.81}$$

and applying the identities for the commutators in the coordinate basis, we find

$$\frac{\mathrm{d}\rho(x,y,t)}{\mathrm{d}t} = \gamma\left(-\frac{1}{2}(x-y)^2\rho(x,y,t) + \frac{\partial^2\rho(x,y,t)}{\partial x\,\partial y} + \frac{1}{2}\left(\frac{\partial^2}{\partial x^2} + \frac{\partial^2}{\partial y^2}\right)\rho(x,y,t)\right). \tag{2.82}$$

This partial differential equation governs the evolution of the density matrix elements in the position basis. The first term leads to exponential suppression of off-diagonal elements (i.e., spatial coherences), modeling the decoherence mechanism. The derivative terms induce a kind of diffusive spreading in the position variables, consistent with the intuitive picture of a noisy environment causing the system to undergo stochastic motion in phase space. We will now solve this Lindblad equation in the following proposition.

Proposition 2.6. *The solution to the Lindblad equation in position representation (2.82) with initial condition $\rho(x,y,0) = \rho(x,y)$, is given by*

$$\rho(x,y,t) = \frac{1}{\sqrt{2\pi\gamma t}}\exp\left(-\frac{(x-y)^2}{2}\gamma t\right)\int \exp\left(-\frac{\lambda^2}{2t\gamma}\right)\rho(x+\lambda,y+\lambda)\,\mathrm{d}\lambda. \tag{2.83}$$

Proof. Introduce centre/relative coordinates

$$u = \frac{x+y}{2}, \qquad v = x-y, \qquad \tilde{\rho}(u,v,t) = \rho(x,y,t). \tag{2.84}$$

A direct computation shows

$$\left(\frac{\partial}{\partial x} + \frac{\partial}{\partial y}\right) = \frac{\partial}{\partial u}, \qquad (x-y)^2 = v^2. \tag{2.85}$$

Hence, (2.82) becomes

$$\frac{\mathrm{d}\tilde{\rho}}{\mathrm{d}t}(u,v,t) = \frac{\gamma}{2}\frac{\partial^2\tilde{\rho}}{\partial u^2}(u,v,t) - \frac{\gamma}{2}\,v^2\,\tilde{\rho}(u,v,t), \qquad \tilde{\rho}(u,v,0) = \tilde{\rho}_0(u,v). \tag{2.86}$$

The generator splits into a sum of commuting parts: $\frac{1}{2}\partial_u^2$ (heat operator in u) and multiplication by $-\frac{1}{2}v^2$ (in v). Therefore, the solution factorises as

$$\tilde{\rho}(u,v,t) = \mathrm{e}^{-\frac{1}{2}v^2 t\gamma}\left(\mathrm{e}^{\frac{t\gamma}{2}\partial_u^2}\tilde{\rho}_0(\cdot,v)\right)(u). \tag{2.87}$$

The one–dimensional heat semigroup with diffusivity $D = \frac{1}{2}$ has kernel

$$G_{t\gamma}(\lambda) = \frac{1}{\sqrt{2\pi t\gamma}}\exp\Big(-\frac{\lambda^2}{2t\gamma}\Big), \qquad \left(\mathrm{e}^{\frac{\gamma t}{2}\partial_u^2}f\right)(u) = \int_{\mathbb{R}} G_{t\gamma}(\lambda)\,f(u+\lambda)\,\mathrm{d}\lambda. \tag{2.88}$$

Thus,

$$\tilde{\rho}(u,v,t) = \mathrm{e}^{-\frac{1}{2}v^2 t\gamma}\,\frac{1}{\sqrt{2\pi t\gamma}}\int_{\mathbb{R}}\exp\Big(-\frac{\lambda^2}{2t\gamma}\Big)\,\tilde{\rho}_0(u+\lambda,v)\,\mathrm{d}\lambda. \tag{2.89}$$

Returning to (x,y) variables (so that $u+\lambda \leftrightarrow (x+\lambda, y+\lambda)$, $v = x-y$) yields exactly (2.83). This completes the proof. □

This solution establishes a direct correspondence between the discrete and continuous descriptions

of phase-space decoherence. The Lindblad evolution plays the role of a continuous-time unravelling of the discrete POVM iterations, with the time parameter t corresponding to the iteration count k in (2.29). Both perspectives capture the same physical mechanism: the gradual loss of coherence induced by nonselective monitoring in the coherent-state basis.

We will now analyse the dynamical unravelling of phase-space measurement for Phase-space distributions starting with the Husimi Q-function.

Dynamical unravelling of phase-space measurement for phase-space distributions

We now derive the dynamical evolution of the Husimi Q-function under the Lindblad equation. Recall that the Q-function is defined as $Q(\alpha,t) = \langle\alpha|\rho(t)|\alpha\rangle$. To find its evolution, we take the time derivative

$$\frac{\mathrm{d}Q(\alpha,t)}{\mathrm{d}t} = \langle\alpha|\dot{\rho}(t)|\alpha\rangle. \tag{2.90}$$

Substituting (2.80) and using the identities $\hat{x}|\alpha\rangle = \frac{1}{\sqrt{2}}(\alpha+\bar{\alpha})|\alpha\rangle$, $\hat{p}|\alpha\rangle = \frac{1}{\sqrt{2}\mathrm{i}}(\alpha-\bar{\alpha})|\alpha\rangle$, and the well-known fact that coherent states are eigenstates of the annihilation operator $\hat{a}$, we evaluate

$$\frac{\mathrm{d}}{\mathrm{d}t}Q(\alpha,t) = \langle\alpha|\mathcal{L}[\rho]|\alpha\rangle = -\frac{1}{2}\langle\alpha|[\hat{x},[\hat{x},\rho]]|\alpha\rangle - \frac{1}{2}\langle\alpha|[\hat{p},[\hat{p},\rho]]|\alpha\rangle. \tag{2.91}$$

These expectation values simplify due to the Gaussian structure of coherent states. In particular, the action of these nested commutators reduces to Laplacians on the complex phase space, and we find

$$\frac{\mathrm{d}Q(\alpha,t)}{\mathrm{d}t} = \frac{\gamma}{2}\frac{\partial^2}{\partial\alpha\partial\bar{\alpha}}Q(\alpha,t) = \frac{\gamma}{2}\Delta_\alpha Q(\alpha,t). \tag{2.92}$$

This is the heat equation on the complex phase space, describing diffusion of the Husimi Q-function. In (x,p) coordinates, the Laplacian is given by $\partial_x^2+\partial_p^2$ with $\alpha = \frac{1}{\sqrt{2}}(x+\mathrm{i}p)$

This equation confirms our earlier intuition that the effect of continuous, nonselective coherent-state measurements is a diffusion in phase space, consistent with the iterative smoothing discussed previously [38, 43, 44, 84]. We now solve the heat equation in the following proposition.

Proposition 2.7. *Let $Q(\alpha,t)$ evolve under the heat equation (2.92), with $\gamma>0$. Then the solution at time t, given an initial Q-function $Q_0(\alpha)$, is*

$$Q(\alpha,t) = \int_{\mathbb{C}} \frac{\mathrm{d}^2\beta}{\pi\gamma t}\,\exp\left(-\frac{|\alpha-\beta|^2}{\gamma t}\right) Q_0(\beta). \tag{2.93}$$

Proof. It is well known that the fundamental solution (Green's function) of this equation is a Gaussian kernel

$$G(\alpha,\beta;t) = \frac{1}{\pi\gamma t}\exp\left(-\frac{|\alpha-\beta|^2}{\gamma t}\right), \tag{2.94}$$

which solves the initial-value problem with delta-function [85, 86]. By linearity, the solution with general initial condition $Q_0(\alpha)$ is the convolution

$$Q(\alpha,t) = \int_{\mathbb{C}} G(\alpha,\beta;t)Q_0(\beta)\,d^2\beta. \tag{2.95}$$

This proves the proposition. □

Lindblad equation in the Wigner representation

Having analysed the phase-space dynamics in the Husimi representation, we now turn to the Wigner function $W(x, p, t)$.

We begin by recalling that the Wigner function evolves under the Lindblad master equation through the Moyal product [87, 88] (see Appendix B.1.1), denoted by $\star$, which encodes the noncommutative nature of quantum observables in phase space. Applying the Lindblad equation to the Wigner representation, we obtain

$$\frac{\mathrm{d}W}{\mathrm{d}t} = x \star W \star x - \frac{1}{2}(x \star x \star W + W \star x \star x) + p \star W \star p - \frac{1}{2}(p \star p \star W + W \star p \star p), \tag{2.96}$$

where the star product is defined as

$$(f \star g)(x, p) = f(x, p) \exp\left[\frac{\mathrm{i}\hbar}{2}\left(\overleftarrow{\partial_x}\overrightarrow{\partial_p} - \overleftarrow{\partial_p}\overrightarrow{\partial_x}\right)\right] g(x, p). \tag{2.97}$$

In our case, since the Lindblad operators are linear in position $\hat{x}$ and momentum $\hat{p}$, the Moyal corrections vanish beyond second order, and the master equation simplifies significantly. Specifically, we find

$$\frac{\mathrm{d}W(x, p, t)}{\mathrm{d}t} = \frac{1}{2}\left(\frac{\partial^2 W}{\partial x^2} + \frac{\partial^2 W}{\partial p^2}\right), \tag{2.98}$$

which is exactly the classical heat equation in two dimensions.

Proposition 2.8. *The solution to (2.98) is given as*

$$W(x, p, t) = \frac{1}{2\pi t}\iint \mathrm{e}^{-\frac{(x-u)^2}{2t}}\mathrm{e}^{-\frac{(p-v)^2}{2t}} W_0(u, v)\,\mathrm{d}u\,\mathrm{d}v. \tag{2.99}$$

Proof. The proof follows the same reasoning as Proposition 2.7, but here we outline an equivalent approach based on the Fourier transform (see Appendix B.1.2).

Define the characteristic function

$$\chi_t(u, v) = \frac{1}{2\pi}\iint \mathrm{e}^{-\mathrm{i}ux}\mathrm{e}^{-\mathrm{i}vp}\, W(x, p, t)\,\mathrm{d}x\,\mathrm{d}y. \tag{2.100}$$

Then the heat equation in Fourier space becomes

$$\frac{\mathrm{d}\chi_t(u, v)}{\mathrm{d}t} = -\frac{1}{2}(u^2 + v^2)\chi_t(u, v), \tag{2.101}$$

which has the solution

$$\chi_t(u, v) = \chi_0(u, v) \exp\left(-\frac{1}{2}(u^2 + v^2)t\right). \tag{2.102}$$

Applying the inverse Fourier transform, we find the Wigner function at time t

$$W(x,p,t) = \frac{1}{2\pi t}\iint \mathrm{e}^{-\frac{(x-u)^2}{2t}}\mathrm{e}^{-\frac{(p-v)^2}{2t}} W_0(u,v)\,\mathrm{d}u\,\mathrm{d}v. \tag{2.103}$$

□

This confirms that the Wigner function, Husimi and also the P-function, undergoes Gaussian diffusion in phase space. All three thus evolve under the same heat-type dynamics, reinforcing the interpretation of decoherence as progressive phase-space smoothing, whereby singular or nonclassical features are gradually washed away.

More generally, the σ-parametrised family of distributions satisfies the heat equation on the complex plane

$$\frac{\mathrm{d}F^{(\sigma)}(\alpha,t)}{\mathrm{d}t} = \frac{\gamma}{2}\Delta_\alpha F^{(\sigma)}(\alpha,t), \tag{2.104}$$

whose solution is the Gaussian convolution

$$F^{(\sigma)}(\alpha,t) = \int_{\mathbb{C}} \frac{\mathrm{d}^2\beta}{\pi\gamma t}\,\exp\left(-\frac{|\alpha-\beta|^2}{\gamma t}\right) F^{(\sigma)}(\beta,0). \tag{2.105}$$

Equation (2.105) makes explicit that decoherence corresponds to diffusion on phase space, with variance growing linearly in time.

The minimum iteration count obtained earlier in (2.78) can be converted into a sufficient continuous-time threshold for the onset of classicality. Identifying the iteration number with γt, this yields a critical time

$$t_*(\sigma) = \frac{\sigma+1}{2\gamma}, \tag{2.106}$$

which specifies, for a given σ-parametrised quasi-probability distribution, the time after which all negativities are guaranteed to vanish.

2.7 Discussion and conclusion

In this chapter we showed that iterative coherent-state POVM measurements act as Gaussian smoothing operations in phase space, providing a natural model of decoherence. Working first in the density-matrix formalism, we demonstrated that each iteration suppresses off-diagonal coherence terms exponentially, while simultaneously smoothing the diagonal along the classical $x = y$ direction. This dual effect, *damping of coherence* and *diffusion along the diagonal*, provides a direct microscopic picture of how environmental monitoring drives quantum states toward classical mixtures.

Translated into the language of phase-space quasi-probability distributions, the Husimi Q-function was seen to evolve under a heat equation, spreading smoothly while remaining strictly positive. The Wigner function, initially capable of negativity, undergoes the same diffusion dynamics, with negativity gradually erased until it becomes indistinguishable from the Q-function. By contrast, the Glauber-Sudarshan P-function, which may be highly singular for nonclassical states, is progressively regu-

larised into a smooth distribution under iteration. Thus, all three representations are unified by the same underlying mechanism which is Gaussian diffusion in phase space.

This phase-space picture was confirmed dynamically by solving the Lindblad equation with $\hat{x}$ and $\hat{p}$ as Lindblad operators, yielding the same diffusion kernels as in the iterative measurement model. Hence, both discrete iterations and continuous-time unravellings describe a single mechanism, decoherence as diffusion in phase space.

Figure 2.1 illustrates this explicitly for the Wigner function of an initial Schrödinger-cat state. As time evolves under Lindblad dynamics, the interference fringes characteristic of quantum coherence are washed out, and the Wigner function becomes strictly positive, marking the transition to a classical-like probability distribution.

Maximum entropy principle for the Husimi Q-function

Beyond its dynamical role, the Husimi distribution is also the unique phase-space distribution that maximises entropy under natural constraints (normalisation, mean, variance), offering an information-theoretic justification for the Gaussian form arising from coherent-state POVMs and Lindblad evolution.

We consider the class of functions $Q(\alpha)$, defined on the complex plane $\alpha \in \mathbb{C}$, that maximise the Shannon entropy

$$S[Q] = -\int Q(\alpha) \log Q(\alpha) \, \frac{\mathrm{d}^2\alpha}{\pi}, \tag{2.107}$$

subject to the constraints of fixed normalisation, first and second moments

$$\int Q(\alpha) \, \frac{\mathrm{d}^2\alpha}{\pi} = 1, \quad \int \alpha \, Q(\alpha) \, \frac{\mathrm{d}^2\alpha}{\pi} = \bar{\alpha}, \quad \int |\alpha|^2 \, Q(\alpha) \, \frac{\mathrm{d}^2\alpha}{\pi} = \kappa. \tag{2.108}$$

We introduce Lagrange multipliers $\lambda_0 \in \mathbb{R}$, $\lambda_1 \in \mathbb{C}$, and $\lambda_2 \in \mathbb{R}$ to enforce the constraints. Define the functional

$$\begin{aligned} \mathcal{L}[Q] \;=\; & -\int Q(\alpha) \log Q(\alpha) \, \frac{\mathrm{d}^2\alpha}{\pi} + \lambda_0 \left(\int Q(\alpha) \, \frac{\mathrm{d}^2\alpha}{\pi} - 1 \right) + \lambda_1 \left(\int \alpha Q(\alpha) \, \frac{\mathrm{d}^2\alpha}{\pi} - \bar{\alpha} \right) \\ & + \bar{\lambda}_1 \left(\int \bar{\alpha} Q(\alpha) \, \frac{\mathrm{d}^2\alpha}{\pi} - \bar{\alpha}^* \right) + \lambda_2 \left(\int |\alpha|^2 Q(\alpha) \, \frac{\mathrm{d}^2\alpha}{\pi} - \kappa \right). \end{aligned} \tag{2.109}$$

We now set the functional derivative with respect to $Q(\alpha)$ to zero

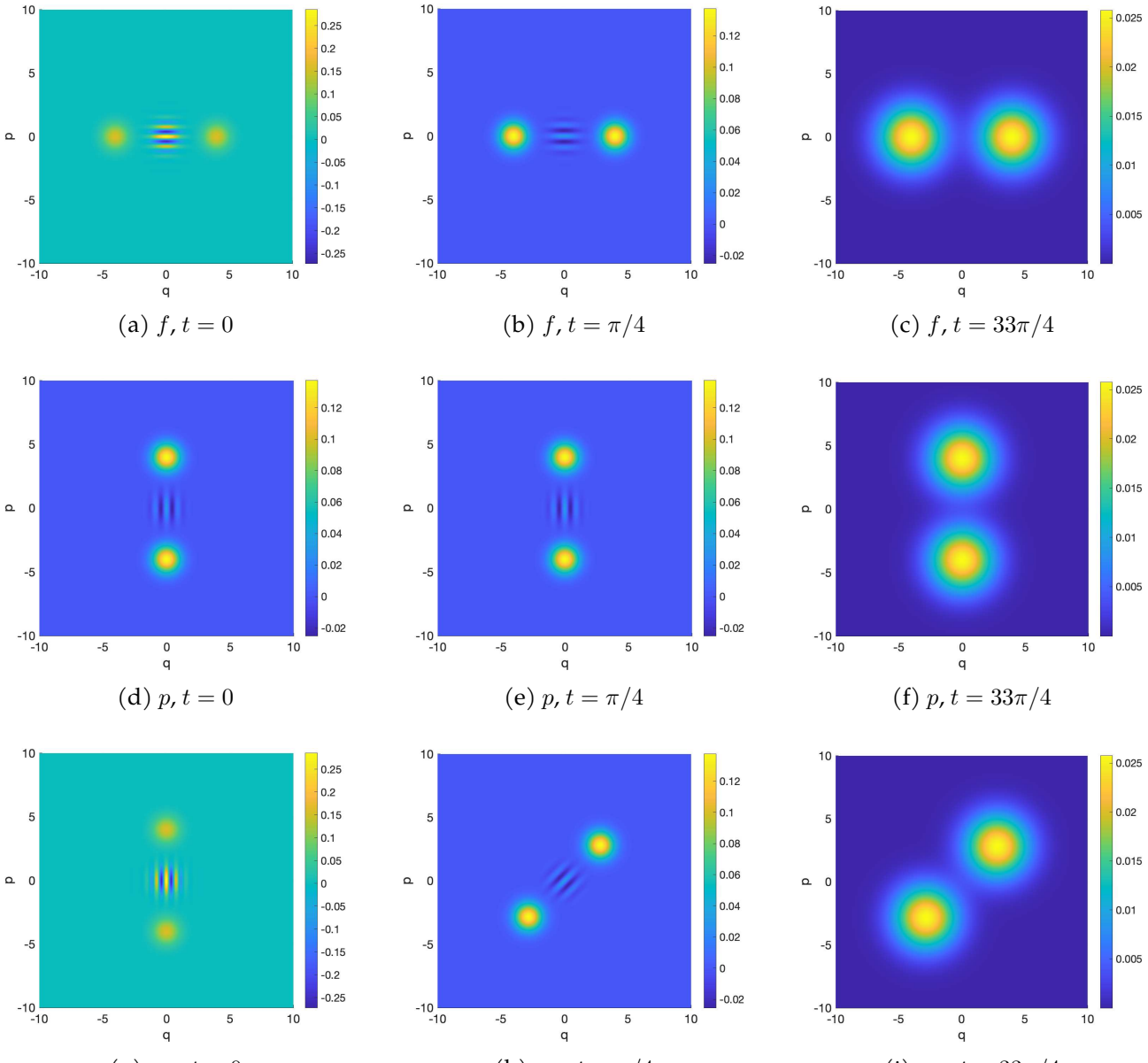
$$\frac{\delta \mathcal{L}}{\delta Q(\alpha)} = -(1 + \log Q(\alpha)) + \lambda_0 + \lambda_1 \alpha + \bar{\lambda}_1 \bar{\alpha} + \lambda_2 |\alpha|^2 = 0. \tag{2.110}$$

Solving for $Q(\alpha)$, we obtain

$$Q(\alpha) = \exp\left(\lambda_0 - 1 + \lambda_1 \alpha + \bar{\lambda}_1 \bar{\alpha} + \lambda_2 |\alpha|^2 \right). \tag{2.111}$$

To ensure that $Q(\alpha)$ is real and normalisable, we require $\lambda_2 < 0$, so that the exponential decays for large $|\alpha|$ and $\lambda_1 = -\bar{\lambda}_1$, i.e., purely imaginary, so that the linear term is real.

Using the constraints, it can be shown that $\lambda_1 = \frac{\bar{\alpha}}{\sigma^2}$, $\lambda_2 = -\frac{1}{\sigma^2}$, and so we absorb constants into the



(a) $f, t = 0$ (b) $f, t = \pi/4$ (c) $f, t = 33\pi/4$

(d) $p, t = 0$ (e) $p, t = \pi/4$ (f) $p, t = 33\pi/4$

(g) $p_H, t = 0$ (h) $p_H, t = \pi/4$ (i) $p_H, t = 33\pi/4$

Figure 2.1: Density plots of the Wigner function evolved under the phase-space-decoherence Lindblad dynamics with $\gamma = 0.1$. Columns show times $t = 0$, $t = \pi/4$, and $t = 8\pi$. Top row: position Schrödinger-cat initial state; middle row: momentum cat; bottom row: same momentum-cat initial state evolved with an additional harmonic-oscillator Hamiltonian ($m = \omega = 1$). All other parameters and plotting conventions are identical to Fig. 1.1. Appendix B has the analytical solutions that were used to generate these plots.

normalisation factor. Then the solution becomes

$$Q(\alpha) = \frac{1}{\sigma^2} \exp\left(-\frac{|\alpha - \bar{\alpha}|^2}{\sigma^2}\right), \tag{2.112}$$

where the variance is given by $\sigma^2 = \kappa - |\bar{\alpha}|^2$. This result shows that the entropy-maximising phase-space distribution is a circular Gaussian centered at the mean $\bar{\alpha}$ with variance σ^2. As the least biased estimate consistent with the known constraints, this distribution is the natural analogue of the canonical Gaussian in quantum optics and statistical mechanics [89–92].

In summary, the flat case shows that coherent-state POVMs act as Gaussian smoothing channels, erasing interference and driving states toward classicality. This process is equivalently captured by a Lindblad diffusion in phase space, providing a clear baseline framework for analysis in $\mathrm{SU}(2)$ and $\mathrm{SU}(1,1)$ cases.

Chapter 3

Phase-space measurement and decoherence in $\mathrm{SU}(2)$ quantum systems

3.1 Introduction

In Chapter 2, we analysed decoherence in systems with Heisenberg–Weyl (HW) symmetry, where flat phase space made it possible to relate iterative coherent-state POVM measurements and their Lindblad unravellings directly to diffusion. The Husimi Q-, Wigner, and Glauber-Sudarshan P-functions were shown to be connected by half-iterations of the measurement channel.

We now turn to systems with $\mathrm{SU}(2)$ symmetry. The $\mathrm{SU}(2)$ group arises naturally in many physical contexts: collective spin models in atomic physics and condensed matter [66, 93–95], polarisation states of light in quantum optics [69, 96], and qubits in quantum information processing [50]. Coherent states associated with $\mathrm{SU}(2)$ provide semiclassical descriptions of these systems, capturing spin-polarisation directions on the Bloch sphere as minimal-uncertainty states [35, 97].

Understanding decoherence in such systems is both fundamental and practical. On the conceptual side, the compact, curved phase space of $\mathrm{SU}(2)$ coherent states allows us to explore how curvature alters the diffusion-like behaviour observed in flat systems. On the applied side, spin decoherence is a key limitation in quantum memories, interferometers, and error-correcting codes [98, 99], making the study of measurement-induced dynamics in $\mathrm{SU}(2)$ systems highly relevant.

A central tool in this chapter is the σ-parametrised family of Stratonovich-Weyl distributions $F^{(\sigma)}$, which interpolate between the P-, W-, and Q-functions. We show that under repeated POVM measurements these distributions evolve via spectral damping factors expressed in terms of binomial coefficients, with each half-iteration reducing σ by one. As in the HW case, the P-, W-, and Q-functions are thus related by half-steps of the measurement channel. To develop this framework, we also employ irreducible tensor operators (ITOs), which form a natural representation-theoretic basis for analysing $\mathrm{SU}(2)$ decoherence dynamics. This language allows us to diagonalise both the POVM channel and the Lindblad semigroup, and to make precise statements about positivity, classicality thresholds, and the approach to the maximally mixed state.

The structure of this chapter is as follows: Section 3.3 constructs the $\mathrm{SU}(2)$ coherent-state POVM and its action on density matrices. Section 3.4 analyses the evolution of the $F^{(\sigma)}$ family of phase-space

distributions, including the P-, W-, and Q-functions as special cases. Section 3.5 introduces Lindblad dynamics generated by tensor operators and compares them with the POVM channel. Section 3.6 examines the phase-space evolution of $F^{(\sigma)}$, deriving sufficient conditions for classicality in terms of time and iteration number, and analysing the minimum values of quasi-probability distributions. Section 3.7 contains the discussion. Appendix C provides harmonic analysis on the sphere and supporting technical derivations.

3.2 $\mathrm{SU}(2)$ coherent states

We shall begin by introducing the $\mathrm{SU}(2)$ coherent states and some of their properties that are useful for ensuing analysis. Heuristically, coherent states associated with a given group G are a set of quantum states that are invariant under the action of G, or more generally, the unitary representation of G on Hilbert space, when G itself is not a unitary group. When G is a unitary group, such as the case for $\mathrm{SU}(2)$, the matter simplifies somewhat. In this case, every quantum state of a two-level system is de facto an $\mathrm{SU}(2)$ coherent state, because every element of the Hilbert space can be attained by the action of $\mathrm{SU}(2)$ group on a given element. However, in a three-dimensional Hilbert space, starting from a preferred element, the action of $\mathrm{SU}(2)$ will only exhaust a subset of the Hilbert space that can be reached from that element. The situation is analogous in higher dimensions. These subsets of states in turn form coherent states.

With these preliminaries, let us explore in more detail the action of the group $\mathrm{SU}(2)$. We begin by noting that the Lie algebra of the $\mathrm{SU}(2)$ is spanned by three spin operators $\hat{S}_x$, $\hat{S}_y$, and $\hat{S}_z$, satisfying the usual commutation relations

$$[\hat{S}_x, \hat{S}_y] = \mathrm{i}\hat{S}_z, \quad [\hat{S}_y, \hat{S}_z] = \mathrm{i}\hat{S}_x, \quad [\hat{S}_z, \hat{S}_x] = \mathrm{i}\hat{S}_y. \tag{3.1}$$

The squared magnitude of spin, or the Casimir operator $\hat{S}^2 = \hat{S}_x^2 + \hat{S}_y^2 + \hat{S}_z^2$, commutes with $\hat{S}_z$, so for a system with a fixed spin s we have the joint eigenstates $|s, m\rangle$, labelled by the eigenvalues $m \in \{-s, -s+1, \ldots, s\}$ of $\hat{S}_z$ and for a fixed s, such that

$$\hat{S}^2|s, m\rangle = s(s+1)|s, m\rangle \quad \text{and} \quad \hat{S}_z|s, m\rangle = m|s, m\rangle, \tag{3.2}$$

in units where $\hbar = 1$. For our analysis it will be useful to introduce the spin raising and lowering operators $\hat{S}_+ = \hat{S}_x + \mathrm{i}\hat{S}_y$ and $\hat{S}_- = \hat{S}_x - \mathrm{i}\hat{S}_y$, satisfying the commutation relations

$$[\hat{S}_+, \hat{S}_-] = 2\hat{S}_z \quad \text{and} \quad [\hat{S}_z, \hat{S}_\pm] = \pm\hat{S}_\pm. \tag{3.3}$$

Then the actions of these operators on $|s, m\rangle$ are given by

$$\begin{aligned} \hat{S}_+|s, m\rangle &= \sqrt{s(s+1) - m(m+1)}\,|s, m+1\rangle\,, \\ \hat{S}_-|s, m\rangle &= \sqrt{s(s+1) - m(m-1)}\,|s, m-1\rangle\,. \end{aligned} \tag{3.4}$$

From the first of these equations we deduce that the state $|s, m\rangle$ can be obtained from the lowest $\hat{S}_z$ state $|s, -s\rangle$ using the raising operator according to

$$|s, m\rangle = \sqrt{\binom{2s}{s+m}}\frac{1}{(s+m)!}(\hat{S}_+)^{s+m}|s, -s\rangle, \tag{3.5}$$

whereas the action of the lowering operator on the lowest state gives $\hat{S}_-|s,-s\rangle = 0$. Similarly, we have $\hat{S}_+|s,s\rangle = 0$ for the highest state.

The joint eigenstates $|s,m\rangle$ of $\hat{S}^2$ and $\hat{S}_z$ are evidently complete on the $(2s+1)$-dimensional Hilbert space

$$\sum_{m=-s}^{s} |s,m\rangle \langle s,m| = \mathbb{1}. \tag{3.6}$$

The coherent states for the group $\mathrm{SU}(2)$ are defined to be those states attainable by the action of the group on the preferred element $|s,-s\rangle$. There are different ways in which one can characterise the coherent states [100]; here we follow closely the characterisation due to Gilmore and Zhang [39]. Geometrically we can think of them as parametrised by the coordinates on the quotient space $\mathrm{SU}(2)/\mathrm{U}(1)$, where $\mathrm{U}(1)$ is the isotropy group for $\mathrm{SU}(2)$. The space $\mathrm{SU}(2)/\mathrm{U}(1)$ is diffeomorphic to the complex projective line $\mathbb{CP}^1$, a real two-dimensional manifold that is isomorphic to a two-sphere S^2 [39, 93, 94, 101]. In terms of the complex coordinate $\zeta = \tan(\theta/2)\exp(-\mathrm{i}\phi)$ of the sphere, where $\theta \in [0,\pi]$ and $\phi \in [0, 2\pi)$, we can define a coherent state $|\zeta\rangle$ according to the prescription

$$|\zeta\rangle = (1+|\zeta|^2)^{(-s)} \exp(\zeta \hat{S}_+)|s,-s\rangle. \tag{3.7}$$

Here the operator $\exp(\zeta\hat{S}_+)$ is an element of the group $\mathrm{SU}(2)/\mathrm{U}(1)$. The quotient space $\mathrm{SU}(2)/\mathrm{U}(1) \simeq S^2$ has the natural interpretation of representing the classical phase space of spin systems.
If we expand the exponential in (3.7) and make use of (3.4), we can express the coherent state as a series in ζ according to

$$|\zeta\rangle = (1+|\zeta|^2)^{-s} \sum_{m=-s}^{s} \sqrt{\binom{2s}{s+m}} \zeta^m |s,m\rangle\,. \tag{3.8}$$

A further substitution of $\zeta = \tan(\theta/2)\mathrm{e}^{-\mathrm{i}\phi}$ in here then gives us

$$\begin{aligned} |\zeta\rangle &= \sum_{m=-s}^{s} \sqrt{\binom{2s}{s+m}} \left(\cos\frac{\theta}{2}\right)^{s-m} \left(\sin\frac{\theta}{2}\exp(-\mathrm{i}\phi)\right)^{s+m} |s,m\rangle, \\ &= \sum_{m=-s}^{s} D^s_{m,-s}(\phi,\theta,-\phi)\,|s,m\rangle\,, \end{aligned} \tag{3.9}$$

where $D^s_{m,-s}$ is sometimes called the Wigner D-matrix [60, 102–105] and is defined according to

$$D^s_{m',m}(\alpha,\beta,\gamma) = \exp(-\mathrm{i}m'\alpha)\, d^s_{m'm}(\beta)\, \exp(-\mathrm{i}m\gamma). \tag{3.10}$$

Here α, β and γ are the Euler angles that describe rotations in three dimensions, and $d^s_{m',m}$, known as Wigner's small d-matrix, is defined by

$$\begin{aligned} d^s_{m'm}(\beta) &= \sum_{k=s_{\min}}^{s_{\max}} \frac{\sqrt{(s+m')!(s-m')!(s+m)!(s-m)!}}{(s+m-k)!k!(m'-m+k)!(s-m'-k)!} \\ &\quad \times \left(\cos\left(\frac{\beta}{2}\right)\right)^{2s+m-m'-2k} \left(\sin\left(\frac{\beta}{2}\right)\right)^{m'-m+2k} (-1)^k, \end{aligned} \tag{3.11}$$

where $s_{\min} = \max(0, m - m')$ and $s_{\max} = \min(s + m, s - m')$.

Let us mention some useful identities in relation to $\mathrm{SU}(2)$ coherent states. To begin, if we have a pair of coherent states parameterised by $\zeta = \tan(\theta/2)\mathrm{e}^{-\mathrm{i}\phi}$ and $\xi = \tan(\theta'/2)\mathrm{e}^{-\mathrm{i}\phi'}$, then their squared overlap is given by

$$|\langle\zeta|\xi\rangle|^2 = \cos^{4s}\left(\frac{\eta}{2}\right) = \frac{(1+\zeta\bar{\xi})^{2s}(1+\bar{\zeta}\xi)^{2s}}{(1+|\zeta|^2)^{2s}(1+|\xi|^2)^{2s}}, \tag{3.12}$$

where η is the angular separation between the points (θ, ϕ) and (θ', ϕ') on the two-sphere S^2, and is defined by the relation

$$\cos\eta = \cos\theta\cos\theta' + \sin\theta\sin\theta'\exp\left(\mathrm{i}(\phi - \phi')\right). \tag{3.13}$$

The coherent states satisfy the following resolution of the identity [39, 94]

$$\int |\zeta\rangle\langle\zeta|\,\mathrm{d}\mu^s_\zeta = \mathbb{1}, \tag{3.14}$$

where the relevant measure here takes the form

$$\mathrm{d}\mu^s_\zeta = \frac{2s+1}{\pi}\frac{1}{(1+|\zeta|^2)^2}\,\mathrm{d}^2\zeta, \qquad \mathrm{d}\mu^s_{\theta,\phi} = \frac{2s+1}{4\pi}\sin\theta\,\mathrm{d}\theta\,\mathrm{d}\phi\,. \tag{3.15}$$

Here $\mathrm{d}^2\zeta = -\mathrm{i}\frac{\mathrm{d}\zeta\wedge\mathrm{d}\bar{\zeta}}{2} = \mathrm{dRe}(\zeta)\,\mathrm{dIm}(\zeta)$. It follows that coherent states can be used to form a positive operator-valued measure (POVM) for characterising generalised measurements on spin systems.

In our analysis that follows, we shall alternate between complex coordinates and spherical coordinates, whichever is more convenient in the context of the analysis. With these mathematical preliminaries, let us now proceed to discuss phase-space measurements using the coherent-state POVM.

3.3 Coherent-state POVM measurement

We consider a spin-s system, whose associated classical phase space is represented by the $\mathrm{SU}(2)$ coherent states. If the emergence of classicality in spin systems is interpreted as the particle acquiring definite spin directions — or, equivalently, definite Stokes parameters [106] — in three dimensions, then this can be modelled in quantum theory by a joint *unsharp* measurement of the spin in three independent directions [107, 108]. The natural mathematical framework for such simultaneous, noisy measurements is provided by the $\mathrm{SU}(2)$ coherent-state POVM.

Building on from the discussion in Section 2.4, we now extend the analysis of phase-space measurement to the $\mathrm{SU}(2)$ setting, focusing on how iterative POVM measurements act on spin coherent states and how this process induces decoherence. In effect, this is a nonselective measurement performed on the system and in this case, the state of the system after the measurement is given by

$$\hat{\rho}_{\mathrm{out}} = \int Q_{\mathrm{in}}(\zeta)\,\hat{\Pi}(\zeta)\,\mathrm{d}\mu^s_\zeta. \tag{3.16}$$

Our first task is to evaluate the output state $\hat{\rho}^{(1)}$ after a single POVM measurement. Rather than attempting direct calculations in the standard basis $\{|s, m\rangle\}$, it is advantageous to take a representation-

theoretic approach. The key idea is that $\mathrm{SU}(2)$ symmetry naturally organises the operator space of the Hilbert space $\mathcal{H}_s$ into irreducible components. This is achieved through the use of *irreducible tensor operators* $\hat{T}^s_{k,q}$, which provide a canonical operator basis adapted to the group structure [103, 105, 109–114].

The utility of this basis is twofold. First, the tensor operators transform covariantly under $\mathrm{SU}(2)$ rotations, in complete analogy with spherical harmonics, making them ideally suited for expressing the action of coherent-state projectors and for analysing measurement-induced dynamics. Second, the Wigner-Eckart theorem reduces matrix elements of these operators to Clebsch–Gordan coefficients, enabling a systematic evaluation of quantities such as expectation values, overlaps, and phase-space functions without resorting to cumbersome summations.

The irreducible tensor operators are defined by their commutation relations with the spin generators

$$[\hat{S}_z,\, \hat{T}^s_{\ell,m}] = m\,\hat{T}^s_{\ell,m}, \quad [\hat{S}_\pm, \hat{T}^{(s)}_{\ell,m}] = \sqrt{(\ell \mp m)(L \pm m + 1)}\,\hat{T}^s_{\ell,m\pm1}, \tag{3.17}$$

and satisfy the Hermiticity relation $\left(\hat{T}^s_{\ell,m}\right)^\dagger = (-1)^m\,\hat{T}^s_{\ell,-m}$. An explicit construction in the $\{|m\rangle\}$ basis is

$$\hat{T}^s_{\ell,m} = \sqrt{\frac{2\ell+1}{2s+1}} \sum_{k,k'=-s}^{s} C^{\,s\,k'}_{s\,k;\,\ell\,m}\ |s,k'\rangle\,\langle s,k|\,, \tag{3.18}$$

where $C^{\,s\,k'}_{s\,k;\,\ell\,m}$ are Clebsch-Gordan coefficients (CGC) [103, 105, 109, 110](see Appendix C). They transform under $\mathrm{SU}(2)$ rotations like spherical harmonics of rank ℓ

$$U(R)\,\hat{T}^s_{\ell,m}\,U^\dagger(R) = \sum_{m'=-\ell}^{\ell} D^{(\ell)}_{m'm}(R)\,\hat{T}^s_{\ell,m'}, \tag{3.19}$$

and form a Hilbert-Schmidt orthonormal operator basis,

$$\mathrm{tr}\left(\hat{T}^s_{\ell,m}\,\hat{T}^{s\dagger}_{\ell',m'}\right) = \delta_{\ell,\ell'}\delta_{m,m'}, \tag{3.20}$$

and the unique scalar operator is given by $T^{(s)}_{0,0} = \frac{\mathbb{1}}{\sqrt{2s+1}}$, while all higher-rank tensors $L > 0$ are traceless, $\mathrm{tr}(T^{(s)}_{\ell,m}) = 0$.

Expanding the density operator $\hat{\rho}$, in this basis gives

$$\hat{\rho} \;=\; \sum_{\ell=0}^{2s}\sum_{m=-\ell}^{\ell} \rho_{\ell,m}\,\hat{T}^s_{\ell,m}, \qquad \rho_{\ell,m} \;=\; \mathrm{tr}\left(\left(\hat{T}^s_{\ell,m}\right)^\dagger\,\hat{\rho}\right). \tag{3.21}$$

Hermiticity $\hat{\rho}^\dagger = \hat{\rho}$ and $(\hat{T}^s_{\ell,m})^\dagger = (-1)^m\hat{T}^s_{\ell,-m}$ implies $\overline{\rho_{\ell,m}} = (-1)^m\,\rho_{\ell,-m}$. The matrix elements $\rho_{l,m}$ are the multipole components of the density matrix, $l = 0$ corresponds to the monopole (isotropic part), $l = 1$ to the dipole (orientation), $l = 2$ to the quadrupole (alignment), and so on [112, 114].

The trace condition $\mathrm{tr}\,\hat{\rho} = 1$ fixes the scalar component

$$1 \;=\; \mathrm{tr}\,\hat{\rho} \;=\; \sum_{\ell,m}\rho_{\ell,m}\,\mathrm{tr}\left(\hat{T}^s_{\ell,m}\right) \;=\; \sqrt{2s+1}\,\rho_{0,0}, \qquad \Rightarrow \qquad \rho_{0,0} \;=\; \frac{1}{\sqrt{2s+1}}. \tag{3.22}$$

With these preliminaries we now proceed to calculate the density matrix after one iteration of phase-space measurement.

Proposition 3.1. *Let $\hat{\rho}$ be a density operator for a spin-s system. After one iteration of the* $\mathrm{SU}(2)$ *coherent-state POVM measurement, the state can be expressed in the irreducible tensor operator basis as*

$$\hat{\rho}^{(1)} = \sum_{\ell=0}^{2s} \sum_{m=-\ell}^{\ell} \lambda_{s,\ell}\, \rho_{\ell,m}\, \hat{T}^{s}_{\ell,m}, \tag{3.23}$$

where $\hat{\rho} = \sum_{\ell,m} \rho_{\ell,m} \hat{T}^{s}_{\ell,m}$, and the eigenvalues are

$$\lambda_{s,\ell} = \frac{\binom{2s}{\ell}}{\binom{2s+\ell+1}{\ell}}. \tag{3.24}$$

Proof. We begin by expanding the coherent-state projector into irreducible tensor operators:

$$|\zeta\rangle\langle\zeta| = \sum_{\ell=0}^{2s} \sum_{m=-\ell}^{\ell} c_{\ell,m}(\zeta)\, \hat{T}^{s}_{\ell,m}, \tag{3.25}$$

where the coefficients are defined by ([35, 93, 105, 110])

$$c_{\ell,m}(\zeta) = \langle\zeta|\hat{T}^{(s)\dagger}_{\ell,m}|\zeta\rangle = \sqrt{\frac{2\ell+1}{2s+1}} \left(\frac{\binom{2s}{\ell}}{\binom{2s+\ell+1}{\ell}} \right)^{1/2} \overline{Y^{m}_{\ell}(\theta,\phi)} \tag{3.26}$$

Substituting for $\hat{\rho}$ and the coherent state in (3.16) we obtain

$$\hat{\rho}^{(1)} = \int \Big(\sum_{\ell,m} \rho_{\ell,m} \overline{c_{\ell,m}(\zeta)} \Big) \Big(\sum_{\ell',m'} c_{\ell',m'}(\zeta) \hat{T}^{s}_{\ell',m'} \Big)\, \mathrm{d}\mu^{s}_{\zeta}. \tag{3.27}$$

Using the orthogonality of spherical harmonics (for further details see Appendix C.1),

$$\int Y^{m}_{\ell}(\theta,\phi)\, \overline{Y^{m'}_{\ell'}(\theta,\phi)}\, \mathrm{d}\mu^{s}_{\theta,\phi} = \frac{2s+1}{2\ell+1} \delta_{\ell,\ell'} \delta_{m,m'}, \tag{3.28}$$

we find that

$$\hat{\rho}^{(1)} = \sum_{\ell,m} \frac{\binom{2s}{\ell}}{\binom{2s+\ell+1}{\ell}}\, \rho_{\ell,m} \hat{T}^{s}_{\ell,m}, \tag{3.29}$$

the density matrix elements get damped by the binomial ratio.

Thus, the coherent-state POVM channel is diagonal in the tensor operator basis, with eigenvalue $\lambda_{s,\ell}$ on each rank-ℓ sector. □

It follows immediately that after k successive applications of the POVM measurement channel, the action is

$$\hat{\rho}^{(k)} \;=\; \sum_{\ell,m} \left(\frac{\binom{2s}{\ell}}{\binom{2s+\ell+1}{\ell}} \right)^{k} \rho_{\ell,m} \hat{T}^{s}_{\ell,m}, \tag{3.30}$$

so that every multipole component of order ℓ decays geometrically with factor $\lambda_{s,\ell}^k$.

We would now like to analyse the behavior of the density matrix as $k \to \infty$. We consider the factor which we denote by $(\lambda_{s,\ell})^k$, with

$$\lambda_{s,\ell} = \frac{\binom{2s}{\ell}}{\binom{2s+\ell+1}{\ell}} = \frac{(2s)!\,(2s+1)!}{(2s-\ell)!\,(2s+\ell+1)!} = \prod_{j=1}^{\ell} \frac{2s+1-j}{2s+1+j}. \tag{3.31}$$

Large-k limit

For $\ell = 0$, one has $\lambda_{s,0} = 1$. For $\ell \geq 1$, every factor in the product satisfies $(2s+1-j)/(2s+1+j) < 1$, so that

$$0 < \lambda_{s,\ell} < 1 \qquad (\ell \geq 1). \tag{3.32}$$

Therefore,

$$\lim_{k\to\infty} (\lambda_{s,\ell})^k = \begin{cases} 1, & \ell = 0, \\ 0, & 1 \leq \ell \leq 2s. \end{cases} \tag{3.33}$$

Thus, in the long-iteration limit, only the $\ell = 0$ mode survives, while higher-ℓ components are exponentially suppressed in k.

This implies that the density matrix becomes the following

$$\lim_{k\to\infty} \hat{\rho}^{(k)} = \rho_{0,0} \hat{T}^s_{0,0} = \frac{\mathbb{1}}{2s+1}, \tag{3.34}$$

and this is the maximally mixed state. This result shows that under repeated coherent-state POVM measurements, all nonisotropic components of the state are exponentially suppressed, and the system is driven irreversibly toward the maximally mixed state.

It is also interesting to ask how this behavior changes as the spin quantum number s increases. The large-s limit corresponds to the semiclassical regime, where $\mathrm{SU}(2)$ coherent states become more sharply localised on the Bloch sphere and quantum fluctuations diminish relative to the system size.

Large-s limit (with fixed ℓ)

For $s \gg \ell$, we expand

$$\log\left(\frac{2s+1-j}{2s+1+j}\right) = \log\left(1 - \frac{j}{2s+1}\right) - \log\left(1 + \frac{j}{2s+1}\right) = -\frac{2j}{2s+1} + O\left(\frac{j^3}{(2s+1)^3}\right). \tag{3.35}$$

Summing over $j = 1, \ldots, \ell$ gives

$$\log \lambda_{s,\ell} = -\frac{2}{2s+1} \sum_{j=1}^{\ell} j + O\left(\frac{\ell^3}{(2s+1)^3}\right) = -\frac{\ell(\ell+1)}{2s+1} + O\left(\frac{\ell^3}{(2s+1)^3}\right). \tag{3.36}$$

Hence,

$$\lambda_{s,\ell} = \exp\left(-\frac{\ell(\ell+1)}{2s+1} + O\left(\frac{\ell^3}{(2s+1)^3}\right)\right), \qquad (\lambda_{s,\ell})^k \;\approx\; \exp\left(-\frac{k\,\ell(\ell+1)}{2s+1}\right). \tag{3.37}$$

For large s with fixed ℓ, the decay rate is $\ell(\ell+1)/(2s+1)$, and we will show later that this coincides with the eigenvalue of the Laplacian on the sphere S^2. Thus, the iterative measurement procedure reproduces the action of a heat kernel on the two-sphere for large spins, progressively smoothing the state until only the isotropic component remains.

3.4 Coherent-state POVM measurement on the phase space

Having understood the iterative action of coherent-state POVMs on the density matrix, it is natural to ask how these effects manifest directly in phase space. In order to track the loss of coherence and the approach to classicality, it is often more transparent to work with quasi-probability distributions rather than with operator expressions. To this end, we now consider the Stratonovich-Weyl (SW) family of quasi-probability distributions on the $\mathrm{SU}(2)$ phase space [70, 112, 115–119]. These distributions provide a unifying framework that interpolates between the Husimi Q, Wigner W, and Glauber-Sudarshan P functions, and hence allow us to study decoherence at different levels of smoothing.

For any density matrix $\hat{\rho}$, we define this σ parametrised family of quasi-probability distributions as

$$F^{(\sigma)}(\theta,\phi) \;=\; \mathrm{tr}\big(\hat{\rho}\,\hat{w}^{(\sigma)}(\theta,\phi)\big), \tag{3.38}$$

on the spherical phase space associated with a given quantum state $\hat{\rho}$, where the kernel operator is given as

$$\hat{w}^{(\sigma)}(\theta,\phi) = \frac{1}{\sqrt{2s+1}} \sum_{\ell=0}^{2s} \sum_{m=-\ell}^{\ell} \sqrt{2\ell+1} \left(\frac{\binom{2s}{\ell}}{\binom{2s+\ell+1}{\ell}}\right)^{-\sigma/2} \overline{Y_\ell^m(\theta,\phi)}\, \hat{T}^s_{\ell,m}. \tag{3.39}$$

The family $F^{(\sigma)}$ includes, in particular, the Husimi Q function ($\sigma = -1$), the Wigner W function ($\sigma = 0$), and the Glauber-Sudarshan P function ($\sigma = +1$), for $\mathrm{SU}(2)$ systems. The kernel satisfies properties of the Stratonovich-Weyl correspondence, normalisation, $\int \hat{w}^{(\sigma)}(\theta,\phi)\,\mathrm{d}\mu^s_{\theta,\phi} = \mathbb{1}$ and has unit trace $\mathrm{tr}(\hat{w}^{(\sigma)}(\theta,\phi)) = 1$.

Lemma 3.1. The SW kernel $\hat{w}^{(\sigma)}(\theta,\phi)$ satisfies the completeness relation

$$\int \hat{w}^{(\sigma)}(\theta,\phi)\,\mathrm{d}\mu^s_\zeta = \mathbb{1}. \tag{3.40}$$

Proof. This follows by direct computation

$$\begin{aligned}
\int \hat{w}^{(\sigma)}(\theta,\phi)\,\mathrm{d}\mu^s_\zeta \;&=\; \frac{1}{\sqrt{2s+1}} \int \sum_{\ell=0}^{2s} \sqrt{2\ell+1} \left(\frac{\binom{2s}{\ell}}{\binom{2s+\ell+1}{\ell}}\right)^{-\sigma/2} \sum_{m=-\ell}^{\ell} \overline{Y_\ell^m(\theta,\phi)}\, \hat{T}^s_{\ell,m}\,\mathrm{d}\mu^s_\zeta, \\
&=\; \frac{1}{\sqrt{2s+1}} \sum_{\ell=0}^{2s} \sqrt{2\ell+1} \left(\frac{\binom{2s}{\ell}}{\binom{2s+\ell+1}{\ell}}\right)^{-\sigma/2} \sum_{m=-\ell}^{\ell} \hat{T}^s_{\ell,M} \int \overline{Y_\ell^m(\theta,\phi)}\,\mathrm{d}\mu^s_\zeta.
\end{aligned} \tag{3.41}$$

From $Y_0^0 = 1$ and the orthogonality of spherical harmonics, we deduce that

$$\int \overline{Y_\ell^m}\, \mathrm{d}\mu_\zeta^\ell = \int \overline{Y_\ell^m} Y_0^0\, \mathrm{d}\mu_\zeta^\ell = \delta_{\ell,0}\, \delta_{m,0}. \tag{3.42}$$

Thus, only the $\ell = m = 0$ term survives, yielding

$$\int \hat{w}^{(\sigma)}(\theta,\phi)\, \mathrm{d}\mu_\zeta^s \;\; = \;\; \sqrt{2s+1}\hat{T}_{0,0}^s = \mathbb{1}. \tag{3.43}$$

□

A direct consequence of the above Lemma is the following

$$\int F^{(\sigma)}(\theta,\phi)\, \mathrm{d}\mu_{\theta,\phi}^s = 1. \tag{3.44}$$

We will now analyse the effect of repeated phase-space measurement on the family of quasi-probability distributions. As the iterative POVM measurement map is diagonalised by the irreducible tensor operators, we find that after k iterations of phase-space measurement, the function $F^{(\sigma)}$ transforms as

$$F_k^{(\sigma)}(\theta,\phi) = \mathrm{tr}(\hat{\rho}^{(k)} \hat{w}^{(\sigma)}(\theta,\phi)) \tag{3.45}$$

Substituting (3.30) into the above expression we find

$$F_k^{(\sigma)}(\theta,\phi) = \frac{1}{\sqrt{2s+1}} \sum_{\ell=0}^{2s} \sum_{m=-\ell}^{\ell} \sqrt{2\ell+1} \left(\frac{\binom{2s}{\ell}}{\binom{2s+\ell+1}{\ell}} \right)^{-\sigma/2} \lambda_{s,\ell}^k\, \rho_{\ell,m}\, Y_\ell^m(\theta,\phi), \tag{3.46}$$

where $\rho_{\ell,m} = \mathrm{tr}(\hat{\rho}\, \hat{T}_{\ell,m}^s)$. Using the orthogonality of the spherical harmonics we can express $\rho_{\ell,m}$ as

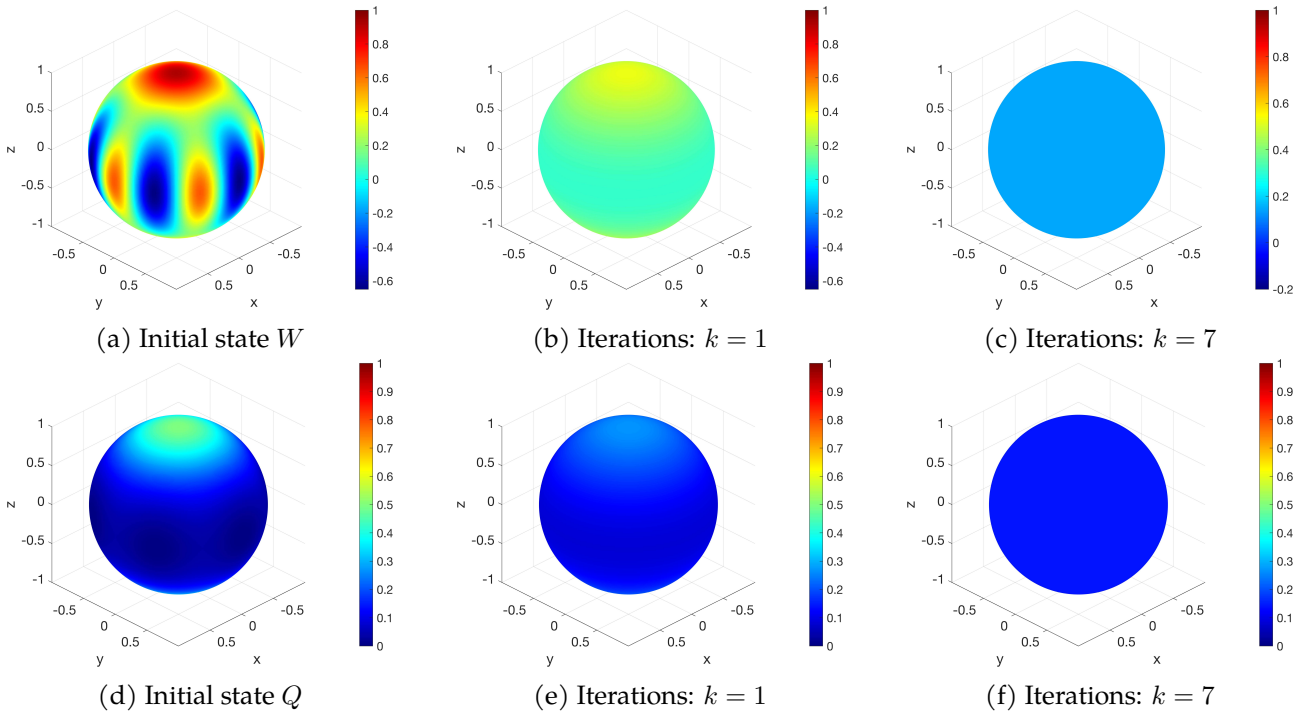
$$\sqrt{\frac{2\ell+1}{2s+1}} \left(\frac{\binom{2s}{\ell}}{\binom{2s+\ell+1}{\ell}} \right)^{-\sigma/2} \rho_{\ell,m} = \int F^{(\sigma)}(\theta,\phi) \overline{Y_\ell^m(\theta,\phi)}\, \mathrm{d}\mu_{\theta,\phi}^\ell. \tag{3.47}$$

and so $F_k^{(\sigma)}$ admits the integral kernel representation

$$F_k^{(\sigma)}(\theta,\phi) = \sum_{\ell=0}^{2s} \lambda_{s,\ell}^k \int P_\ell(\cos\eta)\, F^{(\sigma)}(\theta',\phi')\, \mathrm{d}\mu_{\theta',\phi'}^\ell, \tag{3.48}$$

where we have used the addition theorem for spherical harmonics (see Appendix C.1) and $\cos\eta = \cos\theta\cos\theta' + \sin\theta\sin\theta'\cos(\phi-\phi')$.
From the above equation it follows that $F_k^{(\sigma)}(\theta,\phi) = F^{(\sigma-2k)}$. In particular, a single nonselective $\mathrm{SU}(2)$ coherent-state POVM measurement maps $F^{(\sigma)} \mapsto F^{(\sigma-2)}$, while even a half-iteration already produces $F^{(\sigma)} \mapsto F^{(\sigma-1)}$.

The foregoing observations reveal an interesting hierarchy between the three principal phase-space representations, namely, the Wigner W-function, the Husimi Q-function, and the Glauber-Sudarshan P-function, represented in the forms $Q = W^{(1/2)} = P^{(1)}$ and $W = P^{(1/2)}$. In other words, each of these quasi-probability distributions can be obtained from another through a fractional number of iterations of the $\mathrm{SU}(2)$ coherent-state POVM measurement.



(a) Initial state W (b) Iterations: $k = 1$ (c) Iterations: $k = 7$

(d) Initial state Q (e) Iterations: $k = 1$ (f) Iterations: $k = 7$

Figure 3.1: *The Wigner (top row) and the Husimi (bottom row) functions of the initial state, the outcome state after a single phase-space measurement, and that after ten repeated measurements.* Starting from an initial spin-cat-like state for spin $s = 3$. The initial density matrix corresponds to a coherent superposition state: $|\psi\rangle = \frac{1}{\sqrt{2}}(|m = 3\rangle + |m = -3\rangle)$, exhibiting quantum coherence between these extremal spin states. The Wigner function initially displays pronounced negativity, which diminishes after a single phase-space measurement, and any residual interference effect vanishes entirely by the tenth measurement, resulting in a fully mixed state. The corresponding Husimi functions, which remain strictly positive throughout, similarly transforms into uniformity and converge to the maximally mixed state $\rho \approx \mathbb{1}/7$ after seven iterations. `Wigner3j.m` [120] function in MATLAB was used to make these plots.

As discussed in [121], Wigner functions for spin-s systems can exhibit significant regions of negativity, serving as a hallmark of nonclassicality. However, as shown in Fig. 3.1, even a single iteration of the coarse-graining process rapidly suppresses this negativity, and by the seventh iteration already, the Wigner function has become completely mixed, indicating a full transition to classicality. We also show the corresponding Husimi functions after each iteration; as expected, they remain strictly positive throughout and progressively become more mixed, approaching a uniform distribution.

Within this formalism, negativity, a hallmark of nonclassicality, is gradually suppressed as σ decreases, reaching the strictly positive Husimi function at $\sigma = -1$. For $\sigma < -1$, the distributions $F^{(\sigma)}$ remain positive, corresponding to increasingly classical behaviour. Hence, after at most $\lceil(\sigma + 1)/2\rceil$ POVM iterations, any initial $F^{(\sigma)}$ becomes positive, providing a clear mechanism by which coherent-state POVMs filter out high-frequency components and drive the system toward classicality.

As in the case of the density matrix, the function $F^{(\sigma)}$ is getting damped by the binomial factor $\lambda_{s,\ell}$ after each iteration of the phase-space measurement. In the large-k limit, the function converges to the following

$$\lim_{k\to\infty} F_k^{(\sigma)}(\theta, \phi) = \int F^{(\sigma)}(\theta', \phi')\, \mathrm{d}\mu^{\ell}_{\theta',\phi'} = \frac{1}{2s+1}, \tag{3.49}$$

signifying the complete mixed state.

The way in which these 'half' iterations enter the analysis is highly suggestive of the existence of an underlying continuous-time dynamical model of a Lindblad type that interpolates the discrete iterated POVM measurements, whereby the iteration step k plays the role of time. It turns out that it is not so straightforward to identify such continuous-time model. However, it is possible to find a dynamical equation that approximately interpolates the POVM decoherence very closely, which we shall present below.

3.5 Lindblad dynamics for the density matrix

Our aim here is to model the decoherence effect resulting from phase-space monitoring of the spin system using the coherent-state POVM within a continuous-time dynamical setup. In Chapter 2, Section 2.6, we have examined an analogous problem on a flat phase space. In the case of a flat phase space, the decoherence effect resulting from successive coherent-state POVM measurements can be replicated exactly by considering a Lindblad equation [40–42] for which the two driving Lindblad operators are the position $\hat{x}$ and the momentum $\hat{p}$ operators [82, 83].

This motivates us to explore properties of the Lindblad equation driven by the three angular momentum operators $\hat{S}_x$, $\hat{S}_y$, and $\hat{S}_z$. Such an equation models isotropic spin decoherence, corresponding to continuous, unsharp monitoring of all spin components simultaneously. We show in what follows that such an equation, perhaps unexpectedly, does not exactly match the iterative POVM measurements based on coherent states by working out the solution to the Lindblad equation.

The Lindblad master equation that we shall investigate is given by

$$\frac{\mathrm{d}\hat{\rho}}{\mathrm{d}t} = \gamma \left(\hat{S}_x \hat{\rho} \hat{S}_x + \hat{S}_y \hat{\rho} \hat{S}_y + \hat{S}_z \hat{\rho} \hat{S}_z - \frac{1}{2} \left(\hat{S}_x^2 \hat{\rho} + \hat{\rho} \hat{S}_x^2 \right) - \frac{1}{2} \left(\hat{S}_y^2 \hat{\rho} + \hat{\rho} \hat{S}_y^2 \right) - \frac{1}{2} \left(\hat{S}_z^2 \hat{\rho} + \hat{\rho} \hat{S}_z^2 \right) \right), \tag{3.50}$$

where $\gamma > 0$ is a parameter that determines the decoherence rate. We will now solve the Lindblad equation as follows:

Proposition 3.2. *Consider a spin-s system with Lindblad master equation as in (3.50) Each $\hat{T}^s_{\ell,m}$ is an eigenoperator of the generator*

$$\mathcal{L}[\hat{T}^s_{\ell,m}] \;=\; -\,\Gamma_\ell\, \hat{T}^s_{\ell,m}, \qquad \Gamma_\ell \;=\; \tfrac{\gamma}{2}\,\ell(\ell+1). \tag{3.51}$$

(ii) Writing the density operator as

$$\hat{\rho}(0) = \sum_{\ell=0}^{2s} \sum_{m=-\ell}^{\ell} \rho_{\ell,m}(0)\, \hat{T}^s_{\ell,m}, \tag{3.52}$$

the exact solution is

$$\hat{\rho}(t) \;=\; \sum_{\ell=0}^{2s} \sum_{m=-\ell}^{\ell} \mathrm{e}^{-\frac{\gamma}{2}\ell(\ell+1)\,t}\; \rho_{\ell,m}(0)\, \hat{T}^s_{\ell,m}. \tag{3.53}$$

Proof. For Hermitian jump operators the Lindblad dissipator can be written as a double commutator

$$\hat{S}_i\hat{\rho}\hat{S}_i - \tfrac{1}{2}\{\hat{S}_i^2, \hat{\rho}\} = -\tfrac{1}{2}\,[\hat{S}_i, [\hat{S}_i, \hat{\rho}]]. \tag{3.54}$$

Therefore,

$$\mathcal{L}[\cdot] = \gamma \sum_i \left(\hat{S}_i(\cdot)\hat{S}_i - \tfrac{1}{2}\{\hat{S}_i^2, \cdot\}\right) = -\tfrac{\gamma}{2}\sum_i [\hat{S}_i, [\hat{S}_i, \cdot\,]]. \tag{3.55}$$

The superoperator $\mathcal{C}[\cdot] = \sum_i [\hat{S}_i, [\hat{S}_i, \cdot]]$ is the adjoint action of the quadratic Casimir $\hat{S}^2 = \hat{S}_x^2 + \hat{S}_y^2 + \hat{S}_z^2$. By standard tensor-operator theory (see, e.g., [103], [105]), the set $\{\hat{T}^s_{\ell,m}\}_{m=-\ell}^{\ell}$ furnishes an irreducible spin-ℓ representation under the adjoint action, and thus

$$\sum_i [\hat{S}_i, [\hat{S}_i, \hat{T}^s_{\ell,m}]] \;=\; \ell(\ell+1)\,\hat{T}^s_{\ell,m}. \tag{3.56}$$

Inserting this into (3.55) yields (3.51)

$$\mathcal{L}[\hat{T}^s_{\ell,m}] \;=\; -\tfrac{\gamma}{2}\,\ell(\ell+1)\,\hat{T}^s_{\ell,m}. \tag{3.57}$$

Expanding $\hat{\rho}$ in the irreducible tensor operator basis and applying the semigroup $\mathrm{e}^{t\mathcal{L}}$ gives (3.53). □

We see therefore that the decoherence effect resulting from the Lindblad equation 3.50 is to exponentially suppress the matrix elements. In the long time limit as $t \to \infty$, the only surviving elements are $\ell = 0, m = 0$ and using (3.22) and hence $\hat{\rho}_\infty = \frac{\mathbb{1}}{2s+1}$, the state of complete ignorance.

We would now like to compare the decoherence induced by iterative POVM measurements with that generated dynamically by Lindblad evolution. At first sight, this structural similarity suggests that the two descriptions might coincide. To investigate this, we compare the decay rates governing the two channels.

$$\gamma \leftrightarrow -\frac{2}{\ell(\ell+1)} \log\left(\frac{\binom{2s}{\ell}}{\binom{2s+\ell+1}{\ell}}\right). \tag{3.58}$$

The fact that the right side of (3.58) is dependent on the summation variable ℓ shows that there is no decay rate γ of the Lindblad dynamics that matches the decay rate of the iterated POVM measurements except in the case $s = 1/2$ and for large spin, $s >> \ell$ (3.37), where the Lindblad equation exactly matches the sequential POVM transformations. Other than this, the structure of the dynamics is essentially identical, and in both cases, asymptotically as $t \to \infty$, the density matrix approaches the state of complete ignorance, independent of the choice of the basis in which the density matrix is represented.

It is also worth remarking that the Lindblad equation (3.50) retains full covariance under the action of the symmetry group in the sense that the dynamical equation is invariant under $\mathrm{SU}(2)$ transformations. This ensures that the dynamics remain isotropic in phase space and treats all spin directions equivalently.

3.6 Dynamical unravelling on phase space

Our final analysis concerns the phase-space representation of the Lindblad equation (3.50) and its solution, which provides an alternative perspective of the dynamics.

Before proceeding, we recall the following standard result regarding the adjoint action of the Lindblad generator.

Lemma 3.2. Let $\mathcal{L} : \mathcal{B}(\mathcal{H}) \to \mathcal{B}(\mathcal{H})$ be the Lindblad generator

$$\mathcal{L}(\hat{\rho}) \;=\; -\mathrm{i}[\hat{H},\hat{\rho}] + \sum_k \Big(\hat{L}_k\hat{\rho}\hat{L}_k^\dagger - \tfrac{1}{2}\{\hat{L}_k^\dagger\hat{L}_k,\hat{\rho}\}\Big). \tag{3.59}$$

Then its adjoint $\mathcal{L}^\dagger$ acts on observables $\hat{A}$ as

$$\mathcal{L}^\dagger(\hat{A}) \;=\; \mathrm{i}[\hat{H},\hat{A}] + \sum_k \Big(\hat{L}_k^\dagger\hat{A}\hat{L}_k - \tfrac{1}{2}\{\hat{L}_k^\dagger\hat{L}_k,\hat{A}\}\Big). \tag{3.60}$$

Moreover, for all density operators $\hat{\rho}$ and bounded operators $\hat{A}$,

$$\mathrm{tr}\big(\mathcal{L}(\hat{\rho})\,\hat{A}\big) = \mathrm{tr}\big(\hat{\rho}\,\mathcal{L}^\dagger(\hat{A})\big). \tag{3.61}$$

The proof is given in Appendix C.2.1. This relation will allow us to move the Lindblad generator under the trace when working with phase-space quasi-probability distributions.

The Lindblad equation for these σ-parameter distributions on the phase-space of $\mathrm{SU}(2)$ transforms into the heat equation and can be solved as follows:

Proposition 3.3. *$F^{(\sigma)}(\theta,\phi,t)$ satisfies the heat equation*

$$\partial_t F^{(\sigma)}(\theta,\phi,t) \;=\; \frac{\gamma}{2}\,\Delta_{\mathbb{S}^2}\,F^{(\sigma)}(\theta,\phi,t), \tag{3.62}$$

and the solution is given as

$$F^{(\sigma)}(\theta,\phi,t) = \sum_{\ell,m} \mathrm{e}^{\left(-\frac{\gamma}{2}\ell(\ell+1)\right)} \left(\frac{\binom{2s}{\ell}}{\binom{2s+\ell+1}{\ell}}\right)^{-\sigma/2} \rho_{\ell,m}(0)\,Y_\ell^m(\theta,\phi). \tag{3.63}$$

or equivalently in the integral representation as

$$F^{(\sigma)}(\theta,\phi,t) = \sum_{\ell=0}^{2s} \mathrm{e}^{-\frac{\gamma}{2}\ell(\ell+1)t} \left(\int P_\ell(\cos\eta)\,F^{(\sigma)}(\theta',\phi',0)\,\mathrm{d}\mu^\ell_{\theta,\phi}\right), \tag{3.64}$$

where $\cos\eta = \cos\theta\cos\theta' + \sin\theta\sin\theta'\cos(\phi-\phi')$ *and* $\mathrm{d}\mu^\ell_{\theta,\phi} = \frac{2\ell+1}{4\pi}\sin\theta\,\mathrm{d}\theta\,\mathrm{d}\phi$.

The proof is given in Appendix C.2.2. So we see that the phase-space representation of the Lindblad equation shows that the dynamics gives rise to a heat equation associated with a Brownian motion on phase space. The solution asymptotically converges to the uniform distribution $F^{(\sigma)}(\theta,\phi,t) \;\longrightarrow\; (2s+1)^{-1}$ on the sphere S^2. This follows from the solution, which shows that in the large–time limit the only surviving term in the sum is the term with $\ell = 0$, but $P_0 = 1$ and the normalisation condition

$\int F^{(\sigma)}(\theta,\phi,t)\,\mathrm{d}\mu^{s}_{\theta,\phi} = 1$ is preserved. Thus, irrespective of the value of σ, all Stratonovich-Weyl phase-space quasidistributions $F^{(\sigma)}$ obey the same heat equation on the sphere.

3.6.1 Onset of classicality

A natural question to ask is: *how long does it take for the quasi-probability distribution $F^{(\sigma)}(\theta,\phi,t)$ to become a genuine probability density?* That is, after what time t are all negativities removed so that the distribution admits a classical interpretation?
From (3.63), under isotropic diffusion with rate γ, the evolution of each multipole component of rank ℓ is damped by $\mathrm{e}^{-\frac{\gamma}{2}\,\ell(\ell+1)\,t}\,\lambda_{s,\ell}^{-\sigma/2}$. Classicality is guaranteed once

$$\mathrm{e}^{-\frac{\gamma}{2}\,\ell(\ell+1)\,t}\,\lambda_{s,\ell}^{-\sigma/2} \;\le\; \lambda_{s,\ell}^{1/2}, \qquad \forall\,\ell \ge 1, \tag{3.65}$$

that is, when the damped σ-kernel is no sharper than the Husimi ($\sigma = -1$) kernel.

The critical time $t_*(\sigma)$ is thus obtained from the worst-case multipole, which occurs at $\ell = 2s$

$$t_*(\sigma) \;=\; \frac{\sigma+1}{\gamma\,(2s)(2s+1)}\,\log\binom{4s+1}{2s}. \tag{3.66}$$

At this time, the highest-rank moments have decayed to Husimi level; for all $t \ge t_*(\sigma)$ the quasi-probability distribution $F^{(\sigma)}$ is strictly nonnegative. We may therefore interpret t_* as the *onset of classicality* for the σ-ordered representation. For a given initial state, classicality may arise earlier, but t_* provides a sharp, state-independent threshold.

It is instructive to examine the scaling with spin. For large s, Stirling's approximation yields [122,123]

$$\log\binom{4s+1}{2s} \;\sim\; 4s\log 2, \;\Longrightarrow\; t_*(\sigma) \;\approx\; \frac{(\sigma+1)\log 2}{\gamma\, s}, \qquad s \gg 1. \tag{3.67}$$

Thus, larger spins classicalise more rapidly, consistent with the intuition that the macroscopic limit accelerates the loss of quantum interference. Moreover, $t_* \propto 1/\gamma$ so stronger diffusion accelerates positivity, and $t_* \propto (\sigma+1)$, so the closer one is to the Husimi case ($\sigma = -1$), the earlier positivity occurs.

The worst-case choice $\ell = 2s$ yields a tight, state-independent bound but is conservative. If one fixes the multipole rank ℓ and lets $s \to \infty$, substituting into the positivity condition, one finds the sharper scaling

$$t_*(\sigma,\ell) = \frac{\sigma+1}{2\gamma\, S} \;+\; O\Big(\frac{1}{S^2}\Big), \qquad S \gg 1,\ \ell \text{ fixed}. \tag{3.68}$$

Thus, the "typical" onset time at fixed ℓ is smaller than the worst-case bound by a factor $\frac{1/2}{\log 2} \approx 0.72$.

3.6.2 Negativity and lower bounds of quasi-probability distributions

In addition to studying when $F^{(\sigma)}$ becomes strictly positive, it is natural to ask how negative these quasi-probability distributions can be for a given spin s and parameter σ. We therefore analyse the spectral bounds of $F^{(\sigma)}$, identifying the minimal values these distributions may attain before positivity is guaranteed.

The SU(2) Stratonovich-Weyl kernels transform covariantly

$$U(R)\,\hat{w}^{(\sigma)}(\theta,\phi)\,U^{\dagger}(R) \;=\; \hat{w}^{(\sigma)}\big(R\cdot(\theta,\phi)\big), \tag{3.69}$$

for every rotation R. Hence, all kernels $\hat{w}^{(\sigma)}(\theta,\phi)$ are unitarily similar and *share the same spectrum*, independently of (θ,ϕ). We may therefore evaluate the eigenvalues at the north pole (NP), $(\theta,\phi) = (0, \text{arbitrary})$, where only the $m = 0$ spherical harmonics contribute. Writing the spin projection as $\kappa \in \{-s, -s{+}1, \ldots, s\}$, we consider

$$\lambda_{\kappa}^{(\sigma)} \;=\; \langle s,\kappa|\hat{w}^{(\sigma)}(\mathrm{NP})|s,\kappa\rangle. \tag{3.70}$$

With $Y_{\ell}^{m}(\mathrm{NP}) = \delta_{m,0}$, we obtain

$$\lambda_{\kappa}^{(\sigma)} \;=\; \frac{1}{\sqrt{2s+1}}\sum_{\ell=0}^{2s}\sqrt{2\ell+1}\left(\frac{\binom{2s}{\ell}}{\binom{2s+\ell+1}{\ell}}\right)^{-\sigma/2}\langle s,\kappa|\,\hat{T}^{s}_{\ell,0}\,|s,\kappa\rangle. \tag{3.71}$$

The diagonal tensor matrix element can be written as

$$\langle s,\kappa|\,\hat{T}^{s}_{\ell,0}\,|s,\kappa\rangle \;=\; \frac{\sqrt{2\ell+1}}{\sqrt{2s+1}}\,\big\langle s\,\kappa;\,\ell\,0\,\big|\,s\,\kappa\big\rangle, \tag{3.72}$$

which follows from (3.18). Substituting (3.72) into (3.71) yields the compact CGC form

$$\lambda_{\kappa}^{(\sigma)} \;=\; \frac{1}{2s+1}\sum_{\ell=0}^{2s}(2\ell+1)\left(\frac{\binom{2s}{\ell}}{\binom{2s+\ell+1}{\ell}}\right)^{-\sigma/2}\big\langle s\,\kappa;\,\ell\,0\,\big|\,s\,\kappa\big\rangle. \tag{3.73}$$

Since $F^{(\sigma)}(\theta,\phi) = \mathrm{tr}(\hat{\rho}\,\hat{w}^{(\sigma)}(\theta,\phi))$ is the expectation value of a Hermitian operator, if we diagonalise $\hat{w}^{(\sigma)}(\theta,\phi) = \sum_{i=1}^{2s+1}\lambda_i^{(\sigma)}\,|i\rangle\langle i|$ then $F^{(\sigma)}(\theta,\phi) = \sum_i p_i\,\lambda_i^{(\sigma)}$ with $p_i = \langle i|\hat{\rho}|i\rangle \geq 0$, $\sum_i p_i = 1$. Therefore,

$$\lambda_{\min}^{(\sigma)} \;\leq\; F^{(\sigma)}(\theta,\phi) \;\leq\; \lambda_{\max}^{(\sigma)}, \tag{3.74}$$

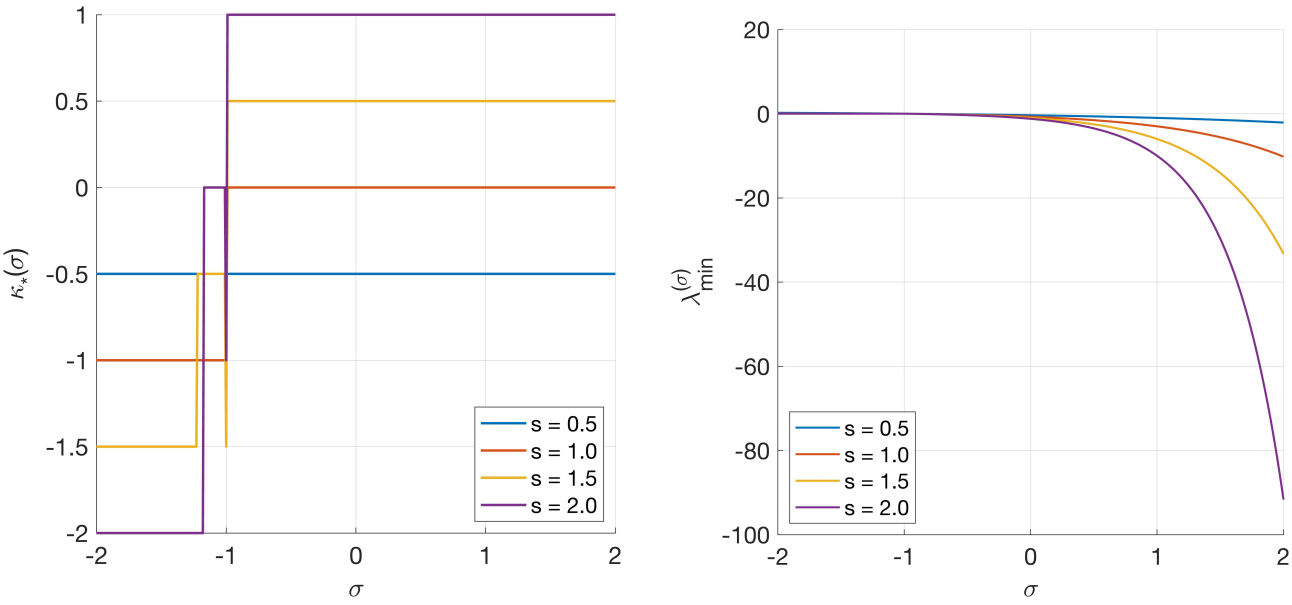
and the bounds are saturated by pure states aligned with the eigenvectors corresponding to $\lambda_{\min}^{(\sigma)}$ and $\lambda_{\max}^{(\sigma)}$. Because the spectrum is independent of (θ,ϕ), the extremal values can be read off from (3.73) by taking $\lambda_{\min}^{(\sigma)} = \min_{\kappa}\lambda_{\kappa}^{(\sigma)}$ and $\lambda_{\max}^{(\sigma)} = \max_{\kappa}\lambda_{\kappa}^{(\sigma)}$.

The closed form (3.73) enables straightforward numerical evaluation of the kernel spectrum. Figure 3.2 shows the minimum eigenvalue $\lambda_{\min}^{(\sigma)}$ as a function of σ for several spins s. At $\sigma = -1$ (the Husimi case) the spectrum is $\{1, 0, \ldots, 0\}$, so the minimum is 0 independently of s. For $\sigma \geq 0$ the minimum becomes strictly negative, and its magnitude grows rapidly with both σ and s.

In particular, for the P-function ($\sigma = 1$) the minimum eigenvalue takes the simple closed form

$$\lambda_{\min}^{(1)} = -\,s\,(2s+1), \tag{3.75}$$

realised at $\kappa_{\star} = s-1$ (and symmetrically at $\kappa_{\star} = -(s-1)$ when present). This compact expression suggests a deeper algebraic structure underlying the spectrum of $\hat{w}^{(\sigma)}$, which we leave for future work to explore.



(a) Phase plot for σ, k

(b) $F^{\sigma}_{\min}$ for different values of σ

Figure 3.2: (a) Minimum kernel eigenvalue $\lambda^{(\sigma)}_{\min}$ as a function of the ordering parameter σ for several spins s. At $\sigma = -1$ (Husimi) the minimum is 0 for all s; for $\sigma \geq 0$ the minimum becomes strictly negative and its magnitude grows rapidly with both σ and s. (b) Spin projection(s) $\kappa_\star(\sigma)$ that attain the minimum eigenvalue of $\hat{w}^{(\sigma)}$ (evaluated at the north pole). For $\sigma = -1$ the minimum is degenerate over all $\kappa \neq s$ (not shown), while for $\sigma \geq 0$ the minimiser consistently occurs at $\kappa_\star = s - 1$ (and symmetrically at $\kappa_\star = -(s-1)$ when present). `Wigner3j.m` [120] function in MATLAB was used to make these plots.

3.7 Discussion and conclusion

We have worked out the effect of decoherence induced by repeated $\mathrm{SU}(2)$ coherent-state POVM measurements on general spin systems from multiple complementary perspectives, namely, the density matrix formalism, and the phase-space probability and quasi-probability distributions. It is shown, in particular, that starting with an arbitrary initial quantum state of the system, the decoherence resulting from a single POVM measurement based on coherent states is to turn both the Wigner function and the Glauber-Sudarshan P-function positive, thus washing out any quantum interference effect.

We next consider a Lindblad equation with the three spin components as independent Lindblad operators. Its solution provides a natural continuous-time analogue of the iterative POVM measurement and, in many regimes, offers a close approximation. In the flat (Heisenberg-Weyl) case, we have seen that an iterated coherent-state POVM can be matched *exactly* by a Lindblad equation generated by position and momentum operators. For spin systems, however, the analogous formulation with $\hat{S}_x, \hat{S}_y, \hat{S}_z$ does not reproduce the POVM dynamics exactly, except in the special case $s = \frac{1}{2}$ or asymptotically in the large-spin limit ($s \gg \ell$).

The discrepancy between the isotropic diffusion and the coherent-state POVM measurement can be traced to the fact that, although both are $\mathrm{SU}(2)$-covariant and possess the semigroup property, they are governed by different spectra. The diffusion has decay rates determined by the quadratic Casimir, while the POVM channel has damping factors given by binomial ratios. Thus, except in the special case of spin-$\frac{1}{2}$ and in the semiclassical large-s limit, the two channels represent genuinely distinct semigroups.

Since the Lindblad dynamics generated by the spin operators $\{\hat{S}_x, \hat{S}_y, \hat{S}_z\}$ does not reproduce the measurement-induced evolution, we are led to consider a more symmetric choice. The action of the coherent-state POVM damps all irreducible tensor sectors of the density matrix, not just the rank-one components. This motivates a Lindblad equation whose generators are taken to be *all* irreducible tensor operators of all ranks. In this way we test whether the complete representation-theoretic operator basis can capture the POVM dynamics. As we show, even this fully symmetric Lindbladian fails to coincide with the POVM channel, underlining a structural mismatch between the two models of decoherence.

Proposition 3.4. *Let $\hat{\rho}(t)$ be the state of a spin-s system evolving under a Lindblad equation with irreducible tensor operators $\hat{T}^s_{\ell,m}$ as Lindblad operators:*

$$\frac{\mathrm{d}}{\mathrm{d}t}\hat{\rho}(t) \;=\; \sum_{\ell=1}^{2s}\gamma_\ell \sum_{m=-\ell}^{\ell}\Big(\hat{T}^s_{\ell,m}\hat{\rho}(t)\hat{T}^{s\,\dagger}_{\ell,m} - \tfrac{1}{2}\{\hat{T}^{s\,\dagger}_{\ell,m}\hat{T}^s_{\ell,m}, \hat{\rho}(t)\}\Big). \tag{3.76}$$

Then the solution is diagonal in the tensor operator basis,

$$\hat{\rho}(t) \;=\; \sum_{\ell=0}^{2s}\sum_{m=-\ell}^{\ell} \mathrm{e}^{-\Gamma_\ell t}\,\rho_{\ell,m}(0)\,\hat{T}^s_{\ell,m}, \tag{3.77}$$

where $\hat{\rho}(0) = \sum_{\ell,m}\rho_{\ell,m}(0)\hat{T}^s_{\ell,m}$ and $\Gamma_\ell \geq 0$ are effective decay rates determined by the coefficients γ_ℓ and

$$\Gamma_{\ell'} \;=\; \sum_{\ell=0}^{2s}\gamma_\ell\left[\frac{2\ell+1}{2s+1} - (2\ell+1)(-1)^{2s+\ell'}\begin{Bmatrix} s & s & \ell \\ s & s & \ell' \end{Bmatrix}\right], \tag{3.78}$$

and $\begin{Bmatrix}\cdot\end{Bmatrix}$ denotes the Wigner $6j$ symbol [103, 105]. In particular, $\Gamma_0 = 0$, so that the trace is preserved, while higher-rank sectors $\ell \geq 1$ decay exponentially.

The proof is discussed in Appendix C.2.3. Here we see that Γ_ℓ is not linear in its dependence on γ_ℓ, the decoherence rates associated with each ℓ-sector, suggesting that even though both channels appear isotropic, their spectra originate from fundamentally different algebraic structures: Casimir-driven for the diffusion semigroup, and binomially weighted for the POVM measurement and hence there is no exact unravelling. For example lets look at the case for spin-1.

Spin-1 case: irreducible tensor operators and isotropic channels

For concreteness, let us work out explicitly the case $s = 1$. In the $\hat{S}_z$ eigenbasis $\{|1\rangle, |0\rangle, |-1\rangle\}$ one can construct the irreducible tensor operators (ITOs) of rank $0, 1, 2$ in Hilbert–Schmidt orthonormal form

$$\begin{aligned}
T^1_{0,0} &= \frac{1}{\sqrt{3}}\begin{pmatrix}1&0&0\\0&1&0\\0&0&1\end{pmatrix}, \qquad T^1_{1,0} = \frac{1}{\sqrt{2}}\begin{pmatrix}1&0&0\\0&0&0\\0&0&-1\end{pmatrix},\\
T^1_{1,1} &= -\tfrac{1}{\sqrt{2}}\left(|1\rangle\langle 0| + |0\rangle\langle -1|\right), \qquad T^1_{1,-1} = \tfrac{1}{\sqrt{2}}\left(|0\rangle\langle 1| + |-1\rangle\langle 0|\right),\\
T^1_{2,0} &= \tfrac{1}{\sqrt{6}}\begin{pmatrix}1&0&0\\0&-2&0\\0&0&1\end{pmatrix}, \qquad T^1_{2,\pm 2} = |\pm 1\rangle\langle \mp 1|,\\
T^1_{2,+1} &= \tfrac{1}{\sqrt{2}}\left(-|1\rangle\langle 0| + |0\rangle\langle -1|\right), \qquad T^1_{2,-1} = \tfrac{1}{\sqrt{2}}\left(|0\rangle\langle 1| - |-1\rangle\langle 0|\right).
\end{aligned} \tag{3.79}$$

These satisfy orthonormality. The recoupling relation reads

$$\sum_{m=-\ell}^{\ell} \hat{T}^s_{\ell,m}\, \hat{T}^s_{\ell',q}\, \hat{T}^{s\,\dagger}_{\ell,m} = c_{\ell\to\ell'}\, \hat{T}^s_{\ell',q} = (2\ell+1)(-1)^{2s+\ell'} \begin{Bmatrix} s & s & \ell \\ s & s & \ell' \end{Bmatrix} \hat{T}^s_{\ell',q}, \tag{3.80}$$

with coefficients (independent of q) that can be computed either by explicit matrix multiplication or from Wigner $6j$-symbols [103, 105]. For $s = 1$ one finds

$c_{\ell\to\ell'}$	$\ell' = 0$	$\ell' = 1$	$\ell' = 2$
$\ell = 1$	1	$\frac{1}{2}$	$-\frac{1}{2}$
$\ell = 2$	$\frac{5}{3}$	$-\frac{5}{6}$	$\frac{1}{6}$

(3.81)

so that the ITO basis indeed diagonalises the isotropic channel. Now consider a Lindblad generator that is isotropic at the tensorial level,

$$\mathcal{L}_\ell[X] = \gamma_\ell \sum_{m=-\ell}^{\ell} \Big(\hat{T}^s_{\ell,m} X \hat{T}^{s\,\dagger}_{\ell,m} - \tfrac{1}{2}\{\hat{T}^{s\,\dagger}_{\ell,m}\hat{T}^s_{\ell,m},\, X\}\Big). \tag{3.82}$$

Using $\sum_m \hat{T}^{s\,\dagger}_{\ell,m}\hat{T}^s_{\ell,m} = \frac{2\ell+1}{2s+1}\,\mathbb{1}$ and the above recoupling coefficients, one finds that $\mathcal{L}_\ell$ acts diagonally on each rank-ℓ' subspace

$$\mathcal{L}_\ell[\hat{T}^s_{\ell',q}] = \alpha_{\ell\to\ell'}\, \hat{T}^s_{\ell',q}, \qquad \alpha_{\ell\to\ell'} = c_{\ell\to\ell'} - \frac{2\ell+1}{2s+1}. \tag{3.83}$$

For $s = 1$ this gives

$\alpha_{\ell\to\ell'}$	$\ell' = 0$	$\ell' = 1$	$\ell' = 2$
$\ell = 1$	0	$-\frac{1}{2}$	$-\frac{3}{2}$
$\ell = 2$	0	$-\frac{5}{2}$	$-\frac{3}{2}$

(3.84)

The full generator $\mathcal{L} = \mathcal{L}_1 + \mathcal{L}_2$ is therefore diagonal on the tensor operator basis, with decay rates

$$\Gamma_{\ell'} = -\sum_{\ell=1}^{2} \gamma_\ell\, \alpha_{\ell\to\ell'}. \tag{3.85}$$

These can be compared to the eigenvalues of the $\mathrm{SU}(2)$ coherent-state POVM channel. For $s = 1$ the one-step eigenvalues are

$$\lambda_0 = 1, \qquad \lambda_1 = \tfrac{1}{2}, \qquad \lambda_2 = \tfrac{1}{10}, \tag{3.86}$$

so that after k iterations, $\Gamma_{\ell'} = -\log \lambda_{s,\ell'}^k$. This yields the linear system

$$\Gamma_1 = \tfrac{1}{2}\,\gamma_1 + \tfrac{5}{2}\,\gamma_2 = k \log 2, \qquad \Gamma_2 = \tfrac{3}{2}\,\gamma_1 + \tfrac{3}{2}\,\gamma_2 = k \log 10, \tag{3.87}$$

whose solution is

$$\gamma_1 = \frac{k}{6}\,(5 \log 10 - 3 \log 2)\,, \qquad \gamma_2 = \frac{k}{6}\,(3 \log 2 - \log 10)\,. \tag{3.88}$$

The important point is that $\gamma_2 < 0$ for $k > 0$, which violates complete positivity of the Lindblad generator. Thus, while the isotropic tensor-operator Lindbladian is diagonal in the same ITO basis as the coherent-state POVM channel, their spectra cannot be matched with nonnegative rates. This shows concretely that the POVM channel and the heat-kernel diffusion, though both isotropic, are genuinely different dynamical semigroups.

In summary, while the coherent-state POVM provides a natural and physically motivated model of decoherence in spin systems, its dynamics cannot be exactly unravelled by a Lindblad semigroup, even when the full tensor operator algebra is included. This persistent mismatch highlights a structural distinction between measurement-induced channels and dynamical master equations on compact phase spaces. Together, these results clarify both the scope and the limits of phase-space models of spin decoherence, and set the stage for exploring analogous phenomena in noncompact systems such as $\mathrm{SU}(1,1)$.

Chapter 4

Tomographic measurement and its dynamical unravelling for $\mathrm{SU}(N)$ quantum systems

4.1 Introduction

In the preceding chapter, we examined phase-space measurement and dynamical unravelling for systems with $\mathrm{SU}(2)$ symmetry. A key observation was that, while iterative coherent-state POVM measurements provide a natural mechanism for decoherence, the mismatch between coherent-state overlaps and the associated heat kernels prevents an exact dynamical unravelling. This limitation motivates the search for measurement schemes that probe the full Hilbert space and admit a consistent dynamical description.

Remarkably, in the spin-$\frac{1}{2}$ case, every quantum state is a coherent state, and the corresponding measurement scheme effectively performs quantum state tomography. This special case, where the coherent-state POVM spans the full Hilbert space and aligns with the heat-kernel dynamics, highlights the potential for consistent unravelling when such conditions are met. It thus motivates the construction of generalised measurement schemes that extend this tomographic property to higher-dimensional systems.

In this chapter, we extend the framework to finite-dimensional quantum systems with $\mathrm{SU}(N)$ symmetry. Such systems include higher-spin particles [124–126], multi-level atoms [98, 127, 128], qudits [129–132], and collective spin ensembles [128, 133], all of which are central to quantum information processing, quantum simulation, and quantum control [50, 99, 134, 135].

In this setting, the relevant measurements are essentially tomographic, i.e., they form informationally complete POVMs that probe the entire Hilbert space, rather than only the classical phase-space variables as in the coherent-state POVM. This difference is crucial: while coherent-state POVMs access coarse-grained phase-space information, tomographic POVMs resolve all operator components. As a consequence, for $\mathrm{SU}(N)$ systems, the measurement-induced decoherence channel coincides exactly with a Lindblad semigroup generated by the $\mathrm{SU}(N)$ algebra, establishing a clean correspondence between nonselective measurements and continuous-time dynamics.

We model decoherence as arising from the iterative application of $\mathrm{SU}(N)$ tomographic POVM measurements. Section 4.2 introduces the $\mathrm{SU}(N)$ algebra and its associated coherent states. In Section 4.3, we construct the POVM and analyse its action on the density matrix, before turning in Section 4.4 to the induced dynamics on phase space, represented as probability distributions over the complex projective space $\mathbb{CP}^{N-1}$. A spectral analysis of the measurement map reveals how fractional iterations interpolate between different quasi-probability distributions, and in particular shows that a half-iteration suffices to remove all negativity from the Wigner representation, thereby providing a sharp threshold for classicality.

In Section 4.5, we derive a $\mathrm{SU}(N)$-covariant Lindblad master equation that continuously unravels the measurement process, both at the operator level and in the phase-space representation. We conclude with a discussion in Section 4.6, highlighting the implications of exact unravelling in $\mathrm{SU}(N)$ systems for decoherence theory and quantum information applications.

4.2 $\mathrm{SU}(N)$ group and its Lie algebra

The special unitary group $\mathrm{SU}(N)$ consists of all $N \times N$ unitary matrices with unit determinant.

Its associated Lie algebra, $\mathfrak{su}(N)$, comprises all traceless Hermitian matrices and forms the natural space of observables for an N-level quantum system [136–140].

The generators $\{\lambda_\alpha\}_{\alpha=1}^{N^2-1}$ of the Lie algebra, $\mathfrak{su}(N)$, satisfy: **Hermiticity**: $\lambda_\alpha^\dagger = \lambda_\alpha$, **Tracelessness**: $\mathrm{tr}(\lambda_\alpha) = 0$, **Orthonormality** (Hilbert-Schmidt inner product), $\mathrm{tr}(\lambda_\alpha \lambda_\beta) = 2\delta_{\alpha\beta}$.

These generators obey the commutation and anticommutation relations

$$[\lambda_\alpha, \lambda_\beta] = 2\mathrm{i} \sum_{\gamma=1}^{N^2-1} f_{\alpha\beta\gamma} \lambda_\gamma, \tag{4.1}$$

$$\{\lambda_\alpha, \lambda_\beta\} = \frac{4}{N}\delta_{\alpha\beta}\mathbb{1} + 2 \sum_{\gamma=1}^{N^2-1} d_{\alpha\beta\gamma} \lambda_\gamma, \tag{4.2}$$

where $f_{\alpha\beta\gamma}$ and $d_{\alpha\beta\gamma}$ are the totally antisymmetric and symmetric structure constants of $\mathfrak{su}(N)$, respectively.

We now turn to the space of pure quantum states for an N-level system, which is naturally identified with the complex projective space $\mathbb{CP}^{N-1}$.

Quantum states in $\mathbb{CP}^{N-1}$

A pure quantum state in an N-level system corresponds to a ray in Hilbert space, represented by a normalised vector $|z(x)\rangle \in \mathbb{C}^N$ with $\langle z(x)|z(x)\rangle = 1$, defined up to a global phase [91, 141–143]. The space of such rays is the complex projective space $\mathbb{CP}^{N-1}$, which we parametrise using local real coordinates $x \in \mathbb{R}^{2N-2}$.

The group $\mathrm{SU}(N)$ acts transitively on $\mathbb{CP}^{N-1}$, endowing it with a homogeneous and isotropic structure. This geometry is captured by the Fubini–Study metric, which defines the distance between two pure states $|z\rangle$ and $|z'\rangle$ as

$$\mathrm{d_{FS}}([z],[z']) = \arccos\left(\left|\langle z|z'\rangle\right|\right). \tag{4.3}$$

This expression is independent of the choice of global phase and depends only on the equivalence classes $[z], [z'] \in \mathbb{CP}^{N-1}$.

Locally, the infinitesimal form of the Fubini–Study metric yields the line element

$$\mathrm{d}s^2 = \langle \partial_i z | \partial_j z \rangle \, \mathrm{d}x^i \mathrm{d}x^j - \langle z | \partial_i z \rangle \langle \partial_j z | z \rangle \, \mathrm{d}x^i \mathrm{d}x^j, \tag{4.4}$$

where $\partial_i = \frac{\partial}{\partial x^i}$, and derivatives are evaluated on the normalised representative $|z(x)\rangle$. This defines a Kähler metric on $\mathbb{CP}^{N-1}$, and the corresponding volume form plays an important role in tomographic reconstruction and the statistical analysis of quantum ensembles.

A general quantum state $\hat{\rho}$ on $\mathbb{C}^N$ is represented by a density matrix, a positive semi-definite, Hermitian operator with unit trace. In the context of $\mathrm{SU}(N)$, such a state admits a Bloch-like decomposition in terms of the identity and the generators of the Lie algebra $\mathfrak{su}(N)$

$$\hat{\rho} = \frac{\mathbb{1}}{N} + \frac{1}{2} \sum_{\alpha=1}^{N^2-1} r_\alpha \lambda_\alpha, \tag{4.5}$$

where $\{\lambda_\alpha\}$ are the generalised Gell-Mann matrices (or any orthonormal basis of traceless Hermitian $\mathrm{SU}(N)$ generators), and $\vec{r} = (r_1, \ldots, r_{N^2-1}) \in \mathbb{R}^{N^2-1}$ is known as the Bloch vector, encoding the state's orientation in the space of traceless observables. The coefficients $r_\alpha = \mathrm{tr}(\lambda_\alpha \hat{\rho})$.

We define the Husimi function on projective Hilbert space $\mathbb{CP}^{N-1}$ as the normalised probability density

$$Q(z) = \langle z | \hat{\rho} | z \rangle, \tag{4.6}$$

where $|z\rangle \in \mathbb{C}^N$ is a normalised state representing the ray $[z] \in \mathbb{CP}^{N-1}$. To integrate functions over $\mathbb{CP}^{N-1}$, we use the Fubini–Study volume form $\mathrm{d}\mu_{\mathrm{FS}}(z)$, which is the unique unitarily invariant measure on projective Hilbert space. In homogeneous coordinates, it takes the form

$$\mathrm{d}\mu_{\mathrm{FS}}(z) = A_N \, \delta \left(\sum_{j=1}^{N} |z_j|^2 - 1 \right) \prod_{j=1}^{N} \mathrm{d}^2 z_j, \tag{4.7}$$

with normalisation constant A_N fixed by $\int_{\mathbb{CP}^{N-1}} \mathrm{d}\mu_{\mathrm{FS}}(z) = 1$, and the resolution of the identity

$$\int_{\mathbb{CP}^{N-1}} |z\rangle\langle z| \, \mathrm{d}\mu_{\mathrm{FS}}(z) = \frac{\mathbb{1}}{N}, \tag{4.8}$$

the Husimi function integrates to unity

$$N \int_{\mathbb{CP}^{N-1}} Q(z) \, \mathrm{d}\mu_{\mathrm{FS}}(z) = \mathrm{tr}(\hat{\rho}) = 1. \tag{4.9}$$

Thus, $Q(z)$ is a bona fide probability density on $\mathbb{CP}^{N-1}$, nonnegative by construction and bounded as $0 \leq Q(z) \leq 1$.

We now turn to tomographic measurements on quantum phase space, which serve not only to reconstruct quantum states but also to model decoherence as an emergent phenomenon. Unlike coherent-state POVMs, which probe lower-dimensional submanifolds (such as complex quadrics in $\mathbb{CP}^{N-1}$),

tomographic POVMs are informationally complete and span the entire space of density operators.

4.3 Tomographic POVM measurement

We consider a quantum system with $\mathrm{SU}(N)$ symmetry, where classicality is modeled as the emergence of definite values for observables spanning the full operator space. This perspective motivates the use of informationally complete measurements, specifically, tomographic POVMs, that probe all directions in the space of Hermitian operators.

We now consider a tomographic measurement on a quantum system described by an initial density matrix $\hat{\rho}$. The POVM elements are rank-one projectors onto normalised state vectors $|z\rangle \in \mathbb{C}^N$, labeled by points $[z] \in \mathbb{CP}^{N-1}$. Upon obtaining the outcome corresponding to $[z]$, the system collapses to the pure state $|z\rangle$, and the post-measurement state becomes the projector $|z\rangle\langle z|$.

Just like in the previous chapters, the post-measurement state in the nonselective setting, denoted by $\hat{\rho}^{(1)}$, is then obtained by averaging over all possible outcomes

$$\hat{\rho}^{(1)} = N \int_{\mathbb{CP}^{N-1}} \mathrm{tr}(\hat{\rho}\,\hat{\Pi}(z))\,\hat{\Pi}(z)\,\mathrm{d}\mu_{\mathrm{FS}}(z), \tag{4.10}$$

The prefactor N ensures that $\hat{\rho}$ is correctly normalised under the resolution of the identity.

We now proceed to calculate the density matrix after one iteration of nonselective tomographic measurement.

Proposition 4.1. *After one iteration of a nonselective tomographic POVM measurement, the post-measurement state is given by*

$$\hat{\rho}^{(1)} = \frac{\mathbb{1} + \hat{\rho}}{N+1}. \tag{4.11}$$

Thus, the Bloch vector contracts by a factor of $1/(N+1)$ *after one iteration.*

Proof. We start by expanding $\hat{\rho}$ in the Bloch representation (4.5). The Born rule gives the probability density for outcome z

$$\langle z|\hat{\rho}|z\rangle = \frac{1}{N} + \frac{1}{2}\sum_{\alpha=1}^{N^2-1} r_\alpha \langle z|\lambda_\alpha|z\rangle. \tag{4.12}$$

Next, we expand the projector $|z\rangle\langle z|$ in its own Bloch representation

$$|z\rangle\langle z| = \frac{\mathbb{1}}{N} + \frac{1}{2}\sum_{\beta=1}^{N^2-1} \langle z|\lambda_\beta|z\rangle \lambda_\beta. \tag{4.13}$$

Thus, the post-measurement state becomes

$$\hat{\rho}^{(1)} \;=\; N\int \left(\frac{1}{N} + \frac{1}{2}\sum_\alpha r_\alpha \langle z|\lambda_\alpha|z\rangle\right)\left(\frac{\mathbb{1}}{N} + \frac{1}{2}\sum_\beta \langle z|\lambda_\beta|z\rangle\lambda_\beta\right)\mathrm{d}\mu_{\mathrm{FS}}(z). \tag{4.14}$$

Expanding the product, we obtain three types of terms. The identity term integrates to

$$\int \frac{1}{N} \cdot \frac{\mathbb{1}}{N} \, \mathrm{d}\mu_{\mathrm{FS}}(z) = \frac{\mathbb{1}}{N^2},$$

since the Fubini-Study measure is normalised. The cross terms vanish due to the tracelessness of the generators and $\mathrm{SU}(N)$ invariance of the measure: $\int \langle z|\lambda_\alpha|z\rangle \, \mathrm{d}\mu_{\mathrm{FS}}(z) = 0$. Using the integral identity, derived from ensemble averages over projective Hilbert space [139, 144], is

$$\int_{\mathbb{CP}^{N-1}} \langle z|\lambda_\alpha|z\rangle\langle z|\lambda_\beta|z\rangle \, \mathrm{d}\mu_{\mathrm{FS}}(z) = \frac{2}{N(N+1)}\delta_{\alpha\beta}, \tag{4.15}$$

the second-order term becomes

$$\frac{1}{4}\sum_\alpha r_\alpha \cdot \frac{2}{N(N+1)}\lambda_\alpha = \frac{1}{2N(N+1)}\sum_\alpha r_\alpha \lambda_\alpha.$$

Adding these terms, we find

$$\hat{\rho}^{(1)} = \frac{\mathbb{1}}{N} + \frac{1}{2(N+1)} \sum_{\alpha=1}^{N^2-1} r_\alpha \lambda_\alpha. \tag{4.16}$$

Substituting for $\sum_\alpha r_\alpha \lambda_\alpha$ in terms of the initial density matrix $\hat{\rho}$, we find the desired result

$$\hat{\rho}^{(1)} = \frac{\mathbb{1} + \hat{\rho}}{N+1}. \tag{4.17}$$

This completes the proof. □

From the result we can see that after a single iteration of the nonselective tomographic measurement, the density matrix undergoes a uniform transformation that reflects the isotropic averaging over the full projective Hilbert space.

As this measurement is nonorthogonal, it does not fully project the system onto a basis state. Instead, it produces a partial, symmetry-respecting reduction of the state. To capture the full evolution of the system under ongoing environmental monitoring, we consider the iterative application of the tomographic measurement. We find that the density matrix after k iterations of the tomographic measurement, denoted $\hat{\rho}^{(k)}$, is given by

Proposition 4.2. *After k iterations of the tomographic measurement we get*

$$\hat{\rho}^{(k)} = \frac{\mathbb{1}}{N}\left(1 - \frac{1}{(N+1)^k}\right) + \frac{\hat{\rho}}{(N+1)^k}. \tag{4.18}$$

Proof. We will prove this by induction. Base case is when $k = 1$, substituting for $k = 1$ in (4.18) we get the same result as in (4.11). We will now proceed to prove the induction step using the induction hypothesis.

We consider the density matrix after $(k+1)^{\mathrm{th}}$ iteration of the tomographic measurement and we have from (4.11)

$$\hat{\rho}^{(k+1)} = \frac{1}{N+1}(\mathbb{1} + \hat{\rho}^{(k)}). \tag{4.19}$$

Using the induction hypothesis, substituting for $\hat{\rho}^{(k)}$ from (4.18) in the above equation we obtain

$$\hat{\rho}^{(k+1)} = \frac{\mathbb{1}}{N+1} + \frac{1}{N+1}\left(\frac{\mathbb{1}}{N}\left(1 - \frac{1}{(N+1)^k}\right) + \frac{\hat{\rho}}{(N+1)^k}\right). \tag{4.20}$$

Expanding the above expression yields

$$\hat{\rho}^{(k+1)} = \left(\frac{\mathbb{1}}{N+1} + \frac{\mathbb{1}}{N(N+1)} - \frac{\mathbb{1}}{N(N+1)^{k+1}}\right) + \frac{\hat{\rho}}{(N+1)^{k+1}}, \tag{4.21}$$

which on simplifying gives

$$\hat{\rho}^{(k+1)} = \left(\frac{\mathbb{1}}{N} - \frac{\mathbb{1}}{N(N+1)^{k+1}}\right) + \frac{\hat{\rho}}{(N+1)^{k+1}}, \tag{4.22}$$

which gives us the density matrix after $(k+1)^{\text{th}}$ iteration, completing the induction step and thereby completing the proof. □

As seen from (4.18) the off-diagonal elements of the density matrix are progressively damped by a geometric factor of $(N+1)$ with each measurement step. This cumulative suppression reflects the systematic erosion of quantum coherence due to repeated nonselective tomographic measurements. While the diagonal elements (populations) are also attenuated, their relative weight increases due to the decay of coherence, and the overall evolution asymptotically drives the system toward the maximally mixed state. In the long-time limit, the density matrix approaches

$$\lim_{k\to\infty} \hat{\rho}^{(k)} = \frac{\mathbb{1}}{N}, \tag{4.23}$$

representing a state of maximal entropy and minimal information, a completely incoherent and isotropic distribution over the quantum state space.

In the next section, we reformulate the dynamics of iterative tomographic measurements in terms of phase-space representations.

4.4 Tomographic measurement on phase space

We define the σ-parametrised Stratonovich–Weyl (SW) kernel [144,145] $\hat{w}^{(\sigma)}(z)$ on the $\mathrm{SU}(N)$ phase space by

$$\hat{w}^{(\sigma)}(z) = \frac{\mathbb{1}}{N} + \frac{1}{2}\sqrt{(N+1)^{1+\sigma}} \sum_{\alpha=1}^{\mathrm{N}^2-1} \langle z|\lambda_\alpha|z\rangle \lambda_\alpha. \tag{4.24}$$

The associated σ-parametrised quasi-probability distribution is then defined as

$$F^{(\sigma)}(z) = \mathrm{tr}\left(\hat{\rho}\,\hat{w}^{(\sigma)}(z)\right) \tag{4.25}$$

which generalises the Q-function ($\sigma = -1$), Wigner function ($\sigma = 0$), and P-function ($\sigma = +1$) to finite-dimensional $\mathrm{SU}(N)$ systems.

Proposition 4.3. *Then, under one iteration of a nonselective tomographic POVM measurement, the σ-parametrised*

quasi-probability distribution $F^{(\sigma)}$ gets mapped to $F^{(\sigma-2)}$.

Proof. After one iteration of nonselective tomographic measurement the σ-parametrised function is given as

$$F_1^{(\sigma)}(z) = \mathrm{tr}(\hat{\rho}^{(1)}\hat{\mathrm{w}}^{(\sigma)}(\mathrm{z})) \tag{4.26}$$

Substituting for the SW kernel we get

$$F_1^{(\sigma)}(z) = \frac{1}{N} + \frac{1}{2}\sqrt{(N+1)^{1+\sigma}} \sum_{\alpha=1}^{N^2-1} \langle z|\lambda_\alpha|z\rangle \,\mathrm{tr}(\hat{\rho}^{(1)}\lambda_\alpha).$$

Substituting the result for $\hat{\rho}^{(1)}$ from (4.11) we find

$$F_1^{(\sigma)}(z) = \frac{1}{N} + \frac{1}{2}\sqrt{(N+1)^{1+\sigma}} \sum_{\alpha=1}^{N^2-1} \langle z|\lambda_\alpha|z\rangle \,\mathrm{tr}\left(\left(\frac{\mathbb{1}+\hat{\rho}}{N+1}\right)\lambda_\alpha\right).$$

Using the fact that $\mathrm{tr}(\lambda_\alpha) = 0$ we find that

$$F_1^{(\sigma)}(z) = \frac{1}{N} + \frac{1}{2}\sqrt{(N+1)^{\sigma-1}} \sum_{\alpha=1}^{N^2-1} \langle z|\lambda_\alpha|z\rangle \,\mathrm{tr}(\hat{\rho}\lambda_\alpha), \tag{4.27}$$

and this is exactly $F^{(\sigma-2)}(z)$. This completes the proof. □

Since the process is linear and preserves the Bloch decomposition structure, it follows that each half iteration of the measurement map induces a smoothing step, that maps $F^{(\sigma)}$ to $F^{(\sigma-1)}$.

This is remarkable as it shows that the Wigner function lies precisely midway between the P- and Q-representations in this measurement-induced hierarchy $P(z) \xrightarrow{\frac{1}{2}} W(z) \xrightarrow{\frac{1}{2}} Q(z)$. This sequence has immediate implications for the suppression of negativity. Since the Husimi Q-function is manifestly nonnegative, any negativity present in the initial P- or W-function is necessarily eliminated after a single full iteration of the tomographic measurement.

It follows from (4.27), that after k-iterations of the tomographic measurement the function $F^{(\sigma)}$ gets updated as

$$F_k^{(\sigma)}(z) = \frac{1}{N} + \frac{1}{2}\sqrt{(N+1)^{\sigma+1-2k}} \sum_{\alpha=1}^{N^2-1} \langle z|\lambda_\alpha|z\rangle \,\mathrm{tr}(\hat{\rho}\lambda_\alpha) = F^{(\sigma-2k)}. \tag{4.28}$$

In the limit $k \to \infty$, the probability density function resulting from the iterative tomographic measurement converges to the uniform distribution over phase space

$$\lim_{k\to\infty} F_k^{(\sigma)}(z) = \frac{1}{N}. \tag{4.29}$$

The phase-space distribution thus becomes fully uniform, reflecting the complete erasure of information through repeated, informationally incomplete measurements.

Since the Husimi Q-function ($\sigma = -1$) is strictly positive, any quasi-probability negativity is eliminated once the measurement iterations drive σ to -1. This requires at most

$$k_* = \left\lceil \tfrac{\sigma+1}{2} \right\rceil \tag{4.30}$$

full iterations (or half as many half-iterations). Unlike bounds with N-dependent corrections [146], this threshold is purely geometric, depending only on the initial σ-ordering.

These fractional iterations highlight that the tomographic measurement process admits a continuous interpolation, rather than being confined to discrete steps. This suggests the existence of an underlying dynamical model, a continuous-time evolution that unravels the effect of tomographic measurements. In the next section, we construct such a model in the form of a Lindblad-type master equation, which captures the smoothing action of measurement in a time-resolved and symmetry-preserving framework.

4.5 Dynamical unravelling

We now turn to a continuous-time description of the decoherence process induced by repeated tomographic measurements. Specifically, we propose a dynamical model that unravels the effect of the iterative measurement process described above. This leads naturally to a Lindblad-type master equation [40–42] governing the evolution of the system's density matrix under continuous, isotropic monitoring by the environment.

We will now show that the Lindblad equation with the $\mathrm{SU}(N)$ generators as the Lindblad operators, gives rise to the continuous-time unravelling of the iterative tomographic measurement. This is in line with the interpretation that a Hermitian Lindbladian corresponds to a monitoring of the relevant observable.

We have

$$\frac{\mathrm{d}\rho}{\mathrm{d}t} = \gamma \left(\sum_{i=1}^{N^2-1} \left(\lambda_i \rho \lambda_i^\dagger - \frac{1}{2}\{\lambda_i^\dagger \lambda_i, \hat{\rho}\} \right) \right), \tag{4.31}$$

where λ_i are the generators of the $\mathrm{SU}(N)$ Lie algebra.

Proposition 4.4. *The Linbdlad master equation in (4.31) simplifies to*

$$\frac{\mathrm{d}\hat{\rho}}{\mathrm{d}t} = 2\gamma \left(\mathbb{1} - N\hat{\rho} \right). \tag{4.32}$$

Proof. Consider the term $\sum_\alpha \lambda_\alpha \hat{\rho} \lambda_\alpha$. Substituting the Bloch expansion of the density matrix from (4.5), we obtain

$$\begin{aligned} \sum_\alpha \lambda_\alpha \hat{\rho} \lambda_\alpha &= \sum_\alpha \lambda_\alpha \left(\frac{\mathbb{1}}{N} + \frac{1}{2} \sum_\beta r_\beta \lambda_\beta \right) \lambda_\alpha, \\ &= \frac{1}{N} \sum_\alpha \lambda_\alpha^2 + \frac{1}{2} \sum_{\alpha,\beta} r_\beta \lambda_\alpha \lambda_\beta \lambda_\alpha. \end{aligned} \tag{4.33}$$

Using the completeness relation $\sum_{\alpha=1}^{N^2-1} \lambda_\alpha^2 = \frac{2(N^2-1)}{N}\mathbb{1}$, the first term evaluates to

$$\frac{1}{N}\sum_\alpha \lambda_\alpha^2 = \frac{2(N^2-1)}{N^2}\mathbb{1}. \tag{4.34}$$

The second term simplifies by the identity $\sum_\alpha \lambda_\alpha\lambda_\beta\lambda_\alpha = -\frac{2}{N}\lambda_\beta$, and hence it becomes

$$\frac{1}{2}\sum_\beta r_\beta\left(-\frac{2}{N}\lambda_\beta\right) = -\frac{1}{N}\sum_\beta r_\beta\lambda_\beta.$$

Recalling that $\sum_\beta r_\beta\lambda_\beta = 2\left(\hat{\rho} - \frac{\mathbb{1}}{N}\right)$, we have

$$\sum_\alpha \lambda_\alpha\hat{\rho}\lambda_\alpha = \frac{2(N^2-1)}{N^2}\mathbb{1} - \frac{2}{N}\left(\hat{\rho} - \frac{\mathbb{1}}{N}\right).$$

Simplifying this expression yields

$$\sum_\alpha \lambda_\alpha\hat{\rho}\lambda_\alpha = 2\left(\mathbb{1} - \frac{\hat{\rho}}{N}\right). \tag{4.35}$$

For the anticommutator term, note that λ_α^2 is proportional to identity for all α, so

$$\sum_\alpha \{\lambda_\alpha^2, \hat{\rho}\} = \frac{4(N^2-1)}{N}\hat{\rho}.$$

Substituting these results into the Lindblad equation, we obtain

$$\begin{aligned}\frac{\mathrm{d}\hat{\rho}}{\mathrm{d}t} &= \gamma\left(2\left(\mathbb{1} - \frac{\hat{\rho}}{N}\right) - \frac{2(N^2-1)}{N}\hat{\rho}\right), \\ &= 2\gamma\left(\mathbb{1} - N\hat{\rho}\right).\end{aligned} \tag{4.36}$$

This completes the proof. □

Having found the Lindblad equation for the density matrix we will now proceed to solve it.

Proposition 4.5. *The solution to the Lindblad equation in (4.32) is given by*

$$\hat{\rho}(t) = \frac{\mathbb{1}}{N}(1 - \exp\left(-2\gamma N t\right)) + \hat{\rho}_0\exp\left(-2\gamma N t\right), \tag{4.37}$$

where $\hat{\rho}(0) = \hat{\rho}_0$.

Proof. We will verify that the result in the proposition is correct by taking its derivative. Taking the derivative of (4.37), we get

$$\dot{\hat{\rho}}(t) = (2\gamma N)\left(\exp\left(-2\gamma N t\right) - \hat{\rho}_0\exp\left(-2\gamma N t\right)\right). \tag{4.38}$$

Substituting the solution in the left hand side of (4.32) we get

$$\dot{\hat{\rho}}(t) = 2\gamma\left(\mathbb{1} - N\left(\frac{\mathbb{1}}{N}(1 - \exp\left(-2\gamma N t\right)) + \hat{\rho}_0\exp\left(-2\gamma N t\right)\right)\right). \tag{4.39}$$

Expanding and simplifying gives

$$\begin{aligned}\dot{\hat{\rho}}(t) &= 2\gamma\left(\mathbb{1} - \mathbb{1} + N\exp\left(-2\gamma N t\right) - \hat{\rho}_0\exp\left(-2\gamma N t\right)\right), \\ &= (2\gamma N)\left(\exp\left(-2\gamma N t\right) - \hat{\rho}_0\exp\left(-2\gamma N t\right)\right), \end{aligned} \tag{4.40}$$

which is the same as the right hand side of (4.38) and this completes the proof. □

Solving the Lindblad equation confirms the qualitative behavior observed in the iterative scheme which is that the off-diagonal elements of the density matrix decay exponentially, and the system evolves toward the maximally mixed state in the long-time limit, $t \to \infty$. The dynamical model thus provides a continuous-time unravelling of the discrete tomographic measurement process, with both frameworks capturing the same asymptotic behavior. By equating

$$\exp\left(-2\gamma N t\right) \leftrightarrow \frac{1}{(N+1)^k}, \tag{4.41}$$

and setting γ to be

$$\gamma = \frac{1}{2}\frac{\log\left(N+1\right)}{N}, \tag{4.42}$$

we have thus dynamically unravelled the iterative tomographic measurement scheme within a continuous-time framework.

We will now transform the Lindblad equation to the phase-space representation to get

$$\frac{\mathrm{d}F^{(\sigma)}(z,t)}{\mathrm{d}t} = 2\gamma\left(1 - NF^{(\sigma)}(z,t)\right). \tag{4.43}$$

which can be solved by

$$F^{(\sigma)}(z,t) = \frac{1}{N} + \left(F_0^{(\sigma)}(z) - \frac{1}{N}\right)\mathrm{e}^{-2\gamma N t}, \tag{4.44}$$

where $F_0^{(\sigma)}(z) = F^{(\sigma)}(z, t=0)$.

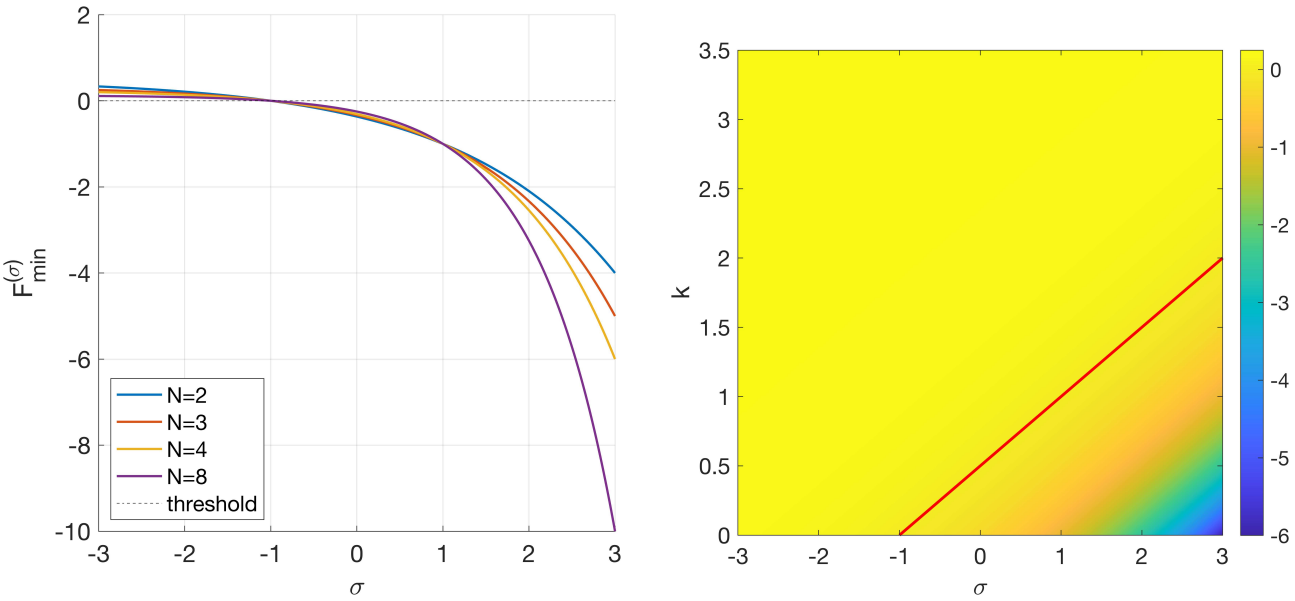
This solution shows that the function $F^{(\sigma)}$ exponentially relaxes toward the uniform distribution $F^{(\sigma)}(z,t) \to \frac{1}{N}$ as $t \to \infty$, consistent with the density matrix approaching the maximally mixed state $\hat{\rho} = \frac{\mathbb{1}}{N}$. The rate of decay is governed by the factor $2\gamma N$, which encapsulates both the intrinsic decoherence rate γ and the dimensionality of the Hilbert space.

Onset of classicality

Using the correspondence between discrete iterations and the continuous-time Lindblad dynamics (4.42), this translates into a physical time-to-classicality

$$t_*(\sigma) = \max\left\{0,\ \frac{(\sigma+1)\ \ln(N+1)}{4N\,\gamma}\right\}, \tag{4.45}$$

that is, the minimal evolution time after which the σ-parametrised distribution has been smoothed to the Husimi Q-function (or beyond) and hence becomes everywhere nonnegative.



(a) $F^{\sigma}_{\min}$ for different values of σ

(b) Phase plot for σ, k

Figure 4.1: (a) Minimum value of the quasi-probability distribution $F^{(\sigma)}_{\min}$ as a function of iteration number k, shown for several ordering parameters σ and Hilbert-space dimensions $N = 2, 3, 4, 5$. For each σ, the curves cross the classicality threshold (dashed line) at the universal iteration $k_* = \lceil(\sigma + 1)/2\rceil$, which is independent of the dimension N. (b) Phase diagram in the (σ, k) plane for $N = 4$, with the red line marking the boundary $\sigma - 2k = -1$ beyond which all quasi-probability distributions become nonnegative. This illustrates the dimension-independent onset of classicality under tomographic measurements.

We now construct the most negative value a σ-parametrised distribution can take for a given value of N. The argument is as follows: Substituting (4.5) in (4.25) we obtain

$$F^{(\sigma)}(z) = \frac{1}{N} + \frac{(N+1)^{(\sigma+1)/2}}{2} \sum_a r_a \langle z|\lambda_a|z\rangle. \tag{4.46}$$

At the same time taking the expectation value of (4.5) with respect to $|z\rangle$ we find

$$\langle z|\hat{\rho}|z\rangle = \frac{1}{N} + \frac{1}{2} \sum_a r_a \langle z|\lambda_a|z\rangle. \tag{4.47}$$

Substituting (4.46) in (4.47) we find that

$$F^{(\sigma)}(z) = \frac{1}{N} + (N+1)^{(\sigma+1)/2} \left(\langle z|\hat{\rho}|z\rangle - \frac{1}{N} \right). \tag{4.48}$$

As $0 \leq \langle z|\hat{\rho}|z\rangle \leq 1$, the function attains a minimum value when $\langle z|\hat{\rho}|z\rangle = 0$, which gives

$$F^{(\sigma)}_{\min}(z) = \frac{1 - (N+1)^{(\sigma+1)/2}}{N}. \tag{4.49}$$

The attainability of $Q(z) = 0$ follows from the spectral properties of $\hat{\rho}$. As $\hat{\rho} \succeq 0$, one has

$$\lambda_{\min}(\hat{\rho}) \;\leq\; Q(z) \;\leq\; \lambda_{\max}(\hat{\rho}).$$

If $\hat{\rho}$ is full rank, then $Q(z) > 0$ everywhere. If $\hat{\rho}$ is rank-deficient, however, then there exists a state $|z\rangle$ in the kernel of $\hat{\rho}$ such that $Q(z) = 0$. In particular, for any pure state $\hat{\rho} = |\psi\rangle\langle\psi|$, one has $Q(z) = 0$ whenever $|z\rangle$ is orthogonal to $|\psi\rangle$. Thus, when both $\hat{\rho}$ and $|z\rangle$ are varied, the minimum achievable value is always

$$\min_{\rho,\, z} Q(z) = 0,$$

independent of N.

In particular, for the Husimi case this yields $F_{\min}^{(-1)} = 0$ consistent with the positivity of the Q-function, $Q(z) = \langle z|\hat{\rho}|z\rangle \geq 0$. By contrast, the expression reported in [146] gives $F_{\min}^{(-1)} = \frac{2-N}{N}$, which is negative for $N > 2$. This contradiction indicates that the extremal state assumed in [146], while correctly normalised to unit trace, does not define a valid density operator because it violates positivity.

Fig. 4.1 makes clear that the negativity threshold is crossed at the same universal iteration $k_* = \lceil(\sigma + 1)/2\rceil$, independent of N, confirming analytically derived bounds and visually highlighting the geometry-driven nature of the transition.

4.6 Discussion and conclusion

In this chapter, we investigated a measurement-based model of decoherence in finite-dimensional quantum systems with $\mathrm{SU}(N)$ symmetry. We distinguished between two classes of POVMs with different physical roles. Coherent-state POVMs provide a phase-space representation, probing classical-like variables such as orientations or amplitudes on the homogeneous space G/H. By contrast, tomographic POVMs are informationally complete i.e. they uniformly sample the entire Hilbert space and thereby resolve all operator components, not just the classical directions. This distinction highlights two complementary routes to classicality, coarse-graining onto effective classical variables, or full suppression of coherence across the operator algebra.

In the $\mathrm{SU}(N)$ setting, we employed tomographic measurements to construct a physically motivated mechanism for decoherence. The nonselective version of these measurements induces a gradual suppression of coherence, driving the system toward the maximally mixed state. To connect this discrete picture with a continuous-time framework, we proposed a Lindblad-type dynamical model that unravels the tomographic process. The solution of the master equation reproduced the same qualitative features observed in the iterative scheme, demonstrating the consistency between the two descriptions and offering a clear physical interpretation of decoherence as continuous, isotropic environmental monitoring without readout.

A key distinction from the $\mathrm{SU}(2)$ case is that, in the fundamental representation of $\mathrm{SU}(N)$, the operator space decomposes only into the identity and adjoint sectors. This ensures that the tomographic POVM channel acts with a single nontrivial eigenvalue, exactly matching the spectral action of a Lindblad semigroup generated by the $\mathrm{SU}(N)$ Lie algebra elements. By contrast, for $\mathrm{SU}(2)$ (beyond spin-$\frac{1}{2}$) the operator space contains higher-rank tensor sectors, leading to a spectral mismatch and only approximate unravellings.

This structural simplicity explains why the $\mathrm{SU}(N)$ case admits an exact Lindblad description, providing a particularly clean and general framework for quantum measurement dynamics in N dimensions.

Chapter 5

Phase-Space measurement and decoherence in $\mathrm{SU}(1,1)$ quantum systems

5.1 Introduction

Having seen that iterative phase-space measurement in compact settings such as $\mathrm{SU}(2)$ admits an asymptotic dynamical unravelling, where the measurement-induced decoherence channel approaches a Lindblad evolution in the large-spin limit, and that tomographic measurements in $\mathrm{SU}(N)$ systems yield an exact correspondence with isotropic Lindblad dynamics, we are now led to explore whether a similar unravelling exists for systems with $\mathrm{SU}(1,1)$ symmetry. In this chapter, we investigate whether repeated coherent-state POVM measurements on the hyperbolic phase space induce a decoherence process that can be described by a continuous-time dynamical model, and what structural constraints arise from the noncompact nature of the group.

Compared to $\mathrm{SU}(2)$ and Heisenberg-Weyl systems, $\mathrm{SU}(1,1)$ systems have been less extensively studied due to the noncompact nature of the group and the complexity of its representation theory. While $\mathrm{SU}(2)$ supports only finite-dimensional irreducible representations, $\mathrm{SU}(1,1)$ admits infinite-dimensional representations, including the discrete, continuous, and supplementary series. Despite this mathematical richness, $\mathrm{SU}(1,1)$ systems play a central role in quantum optics, particularly in the study of two-photon processes, parametric amplification [147–150], and nonlinear quantum interferometry [96, 151], where they exhibit squeezing and enhanced metrological sensitivity [152, 153]. They also find applications in areas such as time-frequency analysis and signal processing [154].

In this chapter, we develop a framework for decoherence in $\mathrm{SU}(1,1)$ systems based on iterative coherent-state POVM measurements. Focusing on the positive discrete series of representations, we employ the Stratonovich–Weyl (SW) correspondence to construct a one-parameter family of phase-space quasi-probability distributions $F^{(\sigma)}$. Similar to the $\mathrm{SU}(2)$ case, this provides a unified treatment of the Husimi Q-, Wigner W-, and Glauber-Sudarshan P-functions, which appear as special cases at $\sigma = -1, 0, +1$, respectively, and which we show are related by half-iterations of the POVM map.

Section 5.2 introduces the $\mathrm{SU}(1,1)$ algebra and coherent states, together with their geometric realisation on the hyperbolic plane. Section 5.3 formulates the coherent-state POVM and its action on quantum states. In Section 5.4, we study the effect of repeated nonselective measurements on the

family $F^{(\sigma)}$, showing that the dynamics act as a spectral filter suppressing high-frequency modes and driving all distributions toward the maximally mixed state. The relation between Q, P, and W functions then follows as a special case of this family.

In Section 5.5, we turn to dynamical unravellings. Using $\mathrm{SU}(1,1)$ generators, we construct a master equation that is $\mathrm{SU}(1,1)$ covariant, exhibiting diffusion-like behaviour in the Q-representation. However, we demonstrate that this dynamics is not of GKSL form and fails to be completely positive at the operator level. Interestingly, when reinterpreted through coherent-state averaging, the resulting dynamics do preserve positivity and trace, thereby exposing a structural distinction between operator-level and phase-space-level descriptions of decoherence. This difference highlights fundamental limits on GKSL-type diffusion models in noncompact quantum systems. We conclude with a discussion in Section 5.6.

Appendix D reviews harmonic analysis on the hyperbolic plane and the spectral decomposition underpinning the SW correspondence. It also discusses $\mathrm{SU}(1,1)$ covariance of Lindblad generators by analysing conjugation under $\hat{K}_z$ rotations and $\hat{K}_x$ boosts (which together generate the full group), we show that the flipped Lindblad operator is covariant. Finally, the appendix establishes the D-algebra representation for $\mathrm{SU}(1,1)$ generators, which forms the technical basis for deriving the POVM dynamics and master equations in this chapter.

5.2 $\mathrm{SU}(1,1)$ coherent states

We begin by introducing the Lie group $\mathrm{SU}(1,1)$ and its Lie algebra $\mathfrak{su}(1,1)$, its Hermitian generators, and the associated unitary representations that will play a central role in our analysis.

The group $\mathrm{SU}(1,1)$ is a noncompact, simple Lie group. Unlike compact groups such as $\mathrm{SU}(2)$, all unitary irreducible representations (UIRs) of $\mathrm{SU}(1,1)$ are infinite-dimensional. These representations are classified into three distinct families, namely, the discrete series, the continuous series, and the supplementary series [35, 148, 155].

In this chapter, we focus exclusively on the positive discrete series representations, denoted $\mathcal{D}^{+}(k)$, which are the most commonly encountered in physical applications. These representations are labeled by the Bargmann index $k \in \frac{1}{2}\mathbb{Z}_{>0}$, and are realised on Hilbert spaces with orthonormal bases indexed by nonnegative integers.

The algebra $\mathfrak{su}(1,1)$ is generated by three Hermitian operators $\hat{K}_x$, $\hat{K}_y$, and $\hat{K}_z$, which satisfy the commutation relations

$$[\hat{K}_x, \hat{K}_y] = -\mathrm{i}\hat{K}_z, \quad [\hat{K}_y, \hat{K}_z] = \mathrm{i}\hat{K}_x, \quad [\hat{K}_z, \hat{K}_x] = \mathrm{i}\hat{K}_y. \tag{5.1}$$

The corresponding Hilbert space admits an orthonormal basis labeled by $|k, k+m\rangle$, where k is a fixed positive parameter and $m \in \mathbb{N} \cup \{0\}$, satisfying the resolution of identity

$$\sum_{m=0}^{\infty} |k, k+m\rangle\langle k, k+m| = \mathbb{1}. \tag{5.2}$$

These states are eigenstates of the operator $\hat{K}_z$

$$\hat{K}_z|k, k+m\rangle = (k+m)|k, k+m\rangle. \tag{5.3}$$

The quadratic Casimir operator $\hat{K}^2$, which commutes with all generators of the algebra and characterises irreducible representations, is given by

$$\hat{K}^2 = \hat{K}_z^2 - \hat{K}_x^2 - \hat{K}_y^2. \tag{5.4}$$

It acts on these basis states as

$$\hat{K}^2|k, k+m\rangle = k(k-1)|k, k+m\rangle. \tag{5.5}$$

To further explore the structure of this representation, we define the ladder operators

$$\hat{K}_+ = \mathrm{i}(\hat{K}_x + \mathrm{i}\hat{K}_y), \quad \hat{K}_- = -\mathrm{i}(\hat{K}_x - \mathrm{i}\hat{K}_y), \tag{5.6}$$

which satisfy the commutation relations

$$[\hat{K}_z, \hat{K}_\pm] = \pm\hat{K}_\pm, \quad [\hat{K}_+, \hat{K}_-] = -2\hat{K}_z. \tag{5.7}$$

These operators act as raising and lowering operators within the representation space

$$\begin{aligned} \hat{K}_+|k, k+m\rangle &= \sqrt{(m+1)(2k+m)}\,|k, k+m+1\rangle, \\ \hat{K}_-|k, k+m\rangle &= \sqrt{m(2k+m-1)}\,|k, k+m-1\rangle, \end{aligned} \tag{5.8}$$

where $|k, k\rangle$ is defined to be the ground state, $\hat{K}_-|k, k\rangle = 0$. The states $|k, k+m\rangle$ can also be got from the action of the ladder operator, $\hat{K}_+$, on the state $|k, k\rangle$ as follows:

$$|k, k+m\rangle = \sqrt{\frac{\Gamma(2k)}{m!\,(\Gamma(2k+m))}}(\hat{K}_+)^m\,|k, k\rangle. \tag{5.9}$$

The coherent states used in this work are the Perelomov $\mathrm{SU}(1,1)$ coherent states [35, 156, 157], which generalise the canonical Glauber coherent states of the Heisenberg–Weyl group to the noncompact $\mathrm{SU}(1,1)$ setting. They are constructed within the positive discrete series representation $\mathcal{D}^+(k)$, characterised by the Bargmann index $k > 0$. Perelomov coherent states are obtained by acting on this lowest-weight state with a group displacement operator

$$|\chi\rangle = \hat{D}(\chi)|k, k\rangle, \qquad |\chi| < 1, \tag{5.10}$$

where χ is a complex parameter inside the unit disc.

Geometrically, these states are labelled by points on the coset space $\mathrm{SU}(1,1)/\mathrm{U}(1)$, which is diffeomorphic to the two-dimensional hyperbolic plane $\mathbb{H}^2$. This space can be represented either as the upper sheet of the two-sheeted hyperboloid

$$x_0^2 - x_1^2 - x_2^2 = 1, \qquad x_0 > 0,$$

or equivalently by the unit disc (the Poincaré disc model), with the relation

$$\chi = \tanh\left(\tfrac{\tau}{2}\right) \mathrm{e}^{-\mathrm{i}\phi}, \quad x_0 = \cosh\tau, \quad x_1 = \sinh\tau\cos\phi, \quad x_2 = \sinh\tau\sin\phi. \tag{5.11}$$

Thus, each coherent state $|\chi\rangle$ may be viewed as a quantum analogue of a point on the hyperbolic phase space, parametrised by the hyperbolic Bloch vector $\vec{n}(\tau,\phi) = (\cosh\tau, \sinh\tau\cos\phi, \sinh\tau\sin\phi)$. For comparison, we note that Barut-Girardello coherent states [158] are instead defined as eigenstates of the lowering operator $\hat{K}_-$, but in this work we restrict attention to the Perelomov family, which is most naturally adapted to the phase-space and POVM framework.
The displacement operator, representing a coset element in $\mathrm{SU}(1,1)/\mathrm{U}(1)$, takes the explicit form

$$\hat{D}(\chi) = (1-|\chi|^2)^k \exp(\chi\hat{K}_+). \tag{5.12}$$

and the resulting coherent state can be explicitly written as

$$|\chi\rangle = (1-|\chi|^2)^k \sum_{m=0}^{\infty} \sqrt{\frac{\Gamma(2k+m)}{m!\,\Gamma(2k)}}\, \chi^m\, |k, k+m\rangle. \tag{5.13}$$

In hyperbolic polar coordinates (τ,ϕ), the coherent state becomes

$$|\chi\rangle = \sum_{m=0}^{\infty} \sqrt{\frac{\Gamma(2k+m)}{m!\,\Gamma(2k)}} \left(\cosh\left(\frac{\tau}{2}\right)\right)^{-2k-m} \left(\mathrm{e}^{-\mathrm{i}\phi}\sinh\left(\frac{\tau}{2}\right)\right)^m |k, k+m\rangle. \tag{5.14}$$

These states form an overcomplete family and satisfy the resolution of identity

$$\int |\chi\rangle\langle\chi|\, \mathrm{d}\mu_\chi^k = \mathbb{1}, \tag{5.15}$$

with the $\mathrm{SU}(1,1)$-invariant measure in disc coordinates given by

$$\mathrm{d}\mu_\chi^k = \frac{2k-1}{\pi} \frac{1}{(1-|\chi|^2)^2}\, \mathrm{d}^2\chi, \quad \text{for } k > \frac{1}{2}, \tag{5.16}$$

where $\mathrm{d}^2\chi = -\frac{\mathrm{i}}{2}\mathrm{d}\chi\wedge\mathrm{d}\bar{\chi} = \mathrm{dRe}(\chi)\,\mathrm{dIm}(\chi)$ and for when $k = 1/2$, we take the limit of the expression as $k \to 1/2$. In hyperbolic polar coordinates, this becomes

$$\mathrm{d}\mu_{\tau,\phi}^k = \frac{2k-1}{4\pi}\sinh\tau\,\mathrm{d}\tau\,\mathrm{d}\phi. \tag{5.17}$$

Alternatively in terms of the $\mathrm{SU}(1,1)$ equivalent to $\mathrm{SU}(2)$ Wigner D-matrices the coherent states can be written as

$$|\chi\rangle = \sum_{m=0}^{\infty} D^k_{k+m,k}(\phi,\tau,-\phi)\,|k, k+m\rangle, \tag{5.18}$$

where $D^k_{k+\mu,k+\mu'}(\alpha,\beta,\gamma)$ [159–161] is defined as

$$D^k_{k+\mu,k+\mu'}(\alpha,\beta,\gamma) = \exp\left(-\mathrm{i}\mu\alpha\right) d^k_{\mu,\mu'}(\tau)\, \exp\left(-\mathrm{i}\mu'\gamma\right), \tag{5.19}$$

and the little $d^k_{\mu,\mu'}$ is defined to be

$$d^k_{\mu,\mu'}(\tau) = \sqrt{\frac{\Gamma(\mu+k)\Gamma(\mu-k+1)}{\Gamma(\mu'+k)\Gamma(\mu'-k+1)}}\frac{1}{-\Gamma(\mu'+\mu+1)}\,{}_2F_1\left(k-\mu', k+\mu, \mu-\mu'+1; \tanh^2\left(\frac{\tau}{2}\right)\right) \times\left(\cosh\left(\frac{\tau}{2}\right)\right)^{-2k+\mu'-\mu}\left(\sinh\left(\frac{\tau}{2}\right)\right)^{\mu-\mu'}. \tag{5.20}$$

Using (5.13) and the orthogonality of the states $|k, k+m\rangle$, we can calculate the overlap between coherent states parametrised by χ_1, χ_2 as

$$\langle\chi_1|\chi_2\rangle = (1-|\chi_1|^2)^k(1-|\chi_2|^2)^k\sum_{n=0}^{\infty}\frac{\Gamma(2k+n)}{n!\,\Gamma(2k)}\bar{\chi}_1^n\chi_2^n = \frac{(1-|\chi_1|^2)^k(1-|\chi_2|^2)^k}{(1-\bar{\chi}_1\chi_2)^{2k}}. \tag{5.21}$$

If $\chi_1 = \tanh\left(\frac{\tau_1}{2}\right)e^{-i\phi_1}$ and $\chi_2 = \tanh\left(\frac{\tau_2}{2}\right)e^{-i\phi_2}$ then the square modulous of the overlap [35, 162] is also given as

$$|\langle\chi_1|\chi_2\rangle|^2 = \left(\frac{1+\cosh\eta}{2}\right)^{-2k}, \tag{5.22}$$

where $\cosh\eta = \cosh\tau_1\cosh\tau_2 - \sinh\tau_1\sinh\tau_2\cos(\phi_1-\phi_2)$, the hyperbolic distance between χ_1, χ_2.

To conclude this overview, we briefly review the continuous series representations of the group $\mathrm{SU}(1,1)$ [35, 163], which play a complementary role to the discrete series and are fundamental to the harmonic analysis of noncompact Lie groups. In the continuous series, the irreducible unitary representations of $\mathrm{SU}(1,1)$ are labeled by a real parameter $\lambda \in \mathbb{R}_{>0}$ and a discrete quantum number $\mu \in \mathbb{Z}$ (or half-integers, depending on the realisation). The Hilbert space is spanned by states $|\lambda, \mu\rangle$, which are simultaneous eigenstates of the Casimir operator $\hat{K}^2$ and the generator $\hat{K}_z$

$$\hat{K}^2|\lambda,\mu\rangle = \left(\lambda^2+\frac{1}{4}\right)|\lambda,\mu\rangle, \qquad \hat{K}_z|\lambda,\mu\rangle = \mu|\lambda,\mu\rangle. \tag{5.23}$$

The ladder operators $\hat{K}\pm$ act on these states as

$$\hat{K}_+|\lambda,\mu\rangle = \left(\frac{1}{2}-i\lambda+\mu\right)|\lambda,\mu+1\rangle, \qquad \hat{K}_-|\lambda,\mu\rangle = \left(-\frac{1}{2}+i\lambda+\mu\right)|\lambda,\mu-1\rangle. \tag{5.24}$$

Unlike the discrete series, where the spectrum of $\hat{K}_z$ is bounded from below, in the continuous series it is unbounded in both directions. These representations are unitary and essential for applications such as the Plancherel decomposition and the representation theory of the Poincaré upper half-plane, where they appear in the spectral resolution of the Laplace-Beltrami operator [164–166](see Appendix D.1).

We now shift focus to the central theme of this work, namely, modeling quantum measurements using coherent state positive operator-valued measures (POVMs).

5.3 Coherent-state POVM measurement

We consider a quantum system with $\mathrm{SU}(1,1)$ symmetry, characterised by the Bargmann index k in the positive discrete series. Its classical limit is described by the hyperbolic phase space of SU(1,1)

coherent states, which encode minimal-uncertainty configurations for the generators $\hat{K}_x$, $\hat{K}_y$, and $\hat{K}_z$ of the $\mathfrak{su}(1,1)$ algebra.

To model phase-space decoherence in this setting, we employ a positive operator-valued measure (POVM) constructed from the coherent states. The POVM provides a resolution of the identity (5.16) over phase space and captures the emergence of classical behaviour through coarse-grained phase-space localisation.

Following the same idea as in Chapter 2, 3, we now consider the scenario in which a phase-space measurement is performed, but the measurement outcome is not recorded and the post-measurement state is given by

$$\hat{\rho}_{\text{out}} = \int \mathrm{d}\mu(\chi)\, \langle\chi|\hat{\rho}_{\text{in}}|\chi\rangle\, |\chi\rangle\langle\chi|. \tag{5.25}$$

This map represents a completely positive, trace-preserving operation that captures the loss of quantum coherence due to unobserved measurement interactions.

Although the analysis could in principle be carried out entirely in the operator formalism, the non-compact structure of $\mathrm{SU}(1,1)$ presents major difficulties. Unlike $\mathrm{SU}(2)$, which admits finite-dimensional representations and closed Clebsch–Gordan coefficients, $\mathrm{SU}(1,1)$ has only infinite-dimensional representations, and its Irreducible tensor operators or the Clebsch-Gordan coefficients are generally known only in sums of hypergeometric functions or complicated series form [167–170].

Nevertheless, the effect of a single coherent-state POVM measurement can still be obtained analytically. While this approach does not scale to repeated iterations, it captures the operator-level structure of decoherence and highlights the role of $\mathrm{SU}(1,1)$ Clebsch–Gordan coefficients. For clarity, we denote by $\hat{\rho}^{(1)}$ the output of one POVM measurement applied to an initial state $\hat{\rho}$, as established in the following proposition.

Proposition 5.1. *After one iteration of the coherent-state POVM measurement, the density matrix decoheres as*

$$\rho^{(1)}_{m_1,m_2} = \sum_{\lambda=\lambda_{\min}}^{\lambda_{\max}} \rho_{m_1+\lambda,m_2+\lambda} \sum_{K=K_{\min}}^{K_{\max}} C^{K,2k+m_1+m_2+\lambda}_{k,k+m_1;k,k+m_2+\lambda}\, C^{K,2k+m_1+m_2+\lambda}_{k,k+m_2;k,k+m_1+\lambda} \left(C^{K,2k}_{k,k;k,k}\right)^2 \frac{2k-1}{2K-1}, \tag{5.26}$$

where $\rho^{(1)}_{m_1,m_2} = \langle k, k+m_1|\hat{\rho}^{(1)}|k, k+m_2\rangle$, and the summation ranges are given by $\lambda_{\min} = \max(-m_1, -m_2)$, $\lambda_{\max} = \infty$, $K_{\min} = 2k + \min(0, m_1 - m_2)$, $K_{\max} = \infty$. The coefficients $C^{K,K+M}_{k_1,k_1+m_1;k_2,k_2+m_2}$ are the Clebsch-Gordan coefficients for the $\mathrm{SU}(1,1)$ group [167–172], defined by

$$C^{K,K+M}_{k_1,k_1+m_1;k_2,k_2+m_2} = \langle k_1, k_1+m_1; k_2, k_2+m_2|K, K+M\rangle, \tag{5.27}$$

where the right-hand side denotes the scalar product between a tensor product basis state and a coupled basis state

$$\langle k_1, k_1+m_1; k_2, k_2+m_2|K, K+M\rangle = \langle k_1, k_1+m_1| \otimes \langle k_2, k_2+m_2||K, K+M\rangle. \tag{5.28}$$

Remark. In the derivation above, the state $|K, K+M\rangle$ appearing on the right-hand side of the Clebsch-Gordan decomposition is defined as the simultaneous eigenstate of the total Casimir operator and the total Cartan generator of the combined system. That is, we define the total $\mathrm{SU}(1,1)$ generators via

$$\hat{K}^{\mathrm{tot}} = \hat{K}_1 \otimes \mathbb{1} + \mathbb{1} \otimes \hat{K}_2, \tag{5.29}$$

$$\hat{K}_z^{\mathrm{tot}} = \hat{K}_{1,z} \otimes \mathbb{1} + \mathbb{1} \otimes \hat{K}_{2,z}. \tag{5.30}$$

The total Casimir operator is then

$$(\hat{K}^{\mathrm{tot}})^2 = (\hat{K}_z^{\mathrm{tot}})^2 - (\hat{K}_x^{\mathrm{tot}})^2 - (\hat{K}_y^{\mathrm{tot}})^2, \tag{5.31}$$

and the state $|K, K+M\rangle$ satisfies the eigenvalue equations

$$(\hat{K}^{\mathrm{tot}})^2 |K, K+M\rangle = K(K-1)|K, K+M\rangle, \tag{5.32}$$

$$\hat{K}_z^{\mathrm{tot}} |K, K+M\rangle = (K+M)|K, K+M\rangle. \tag{5.33}$$

By definition, the state $|K, K+M\rangle$ decomposes into the uncoupled basis $|k_1, k_1+m_1\rangle \otimes |k_2, k_2+m_2\rangle$ according to

$$|K, K+M\rangle = \sum_{m_1,m_2} C^{K,K+M}_{k_1,k_1+m_1;k_2,k_2+m_2} |k_1, k_1+m_1\rangle \otimes |k_2, k_2+m_2\rangle, \tag{5.34}$$

where the Clebsch-Gordan coefficients $C^{K,K+M}_{k_1,k_1+m_1;k_2,k_2+m_2}$ ensure proper angular momentum (weight) addition $m_1 + m_2 = M$. These coefficients satisfy the orthogonality relation

$$\sum_{m_1,m_2} C^{K,K+M}_{k_1,k_1+m_1;k_2,k_2+m_2} C^{K',K'+M}_{k_1,k_1+m_1;k_2,k_2+m_2} = \delta_{K,K'}, \tag{5.35}$$

ensuring that total $\mathrm{SU}(1,1)$ states with different Casimir labels remain orthogonal.

The proof is provided in detail in Appendix D.2.1. So we see from (5.26) that after a single application of the coherent-state POVM measurement, the density matrix elements are damped by a weighted sum over Clebsch–Gordan coefficients. In addition, the nontrivial index couplings in (5.26) prevent the map from taking a simple recursive form. One cannot iterate the same transformation matrix on the density operator; each step requires a fresh convolution involving Clebsch-Gordan coefficients.

To overcome these difficulties, and to establish a clearer link with classical phase-space, we turn instead to the phase-space formulation of quantum mechanics. In this representation, the action of the POVM becomes diagonal in a suitable spectral basis, allowing repeated measurements to be described as a spectral filter acting on phase-space quasi-probability distributions.

5.4 Coherent-state POVM measurement on phase-space

Following the construction in [162, 173–175], we define the σ-parametrised kernel operators $\hat{w}^{(\sigma)}(\chi)$ on the $\mathrm{SU}(1,1)$ phase space, thereby extending the Cahill–Glauber formalism to noncompact symmetric spaces. In this setting, the relevant harmonic analysis is carried out on the Lobachevsky (hyperbolic) plane, where the natural basis functions are given by the conical (Mehler) functions $P_{\mathrm{i}\lambda-\frac{1}{2}}(\cosh\eta)$, which play the role of spherical harmonics in this noncompact geometry. Appendix D.1

provides further details on this representation theory and the harmonic analysis underlying these kernels.

With this structure in place, the σ-parametrised kernels admit the following spectral integral representation

$$\begin{aligned}\hat{w}^{(\sigma)}(\chi') &= \frac{2}{2k-1}\int \mathrm{d}\mu_\chi^k \int \mathrm{d}\nu_\lambda\, P_{\mathrm{i}\lambda-\frac{1}{2}}(\cosh\eta)\,\Phi_k(\lambda)^{1/2-\sigma/2}\,\hat{w}^+(\chi),\\ &= \frac{2}{2k-1}\int \mathrm{d}\mu_\chi^k \int \mathrm{d}\nu_\lambda\, P_{\mathrm{i}\lambda-\frac{1}{2}}(\cosh\eta)\,\Phi_k(\lambda)^{-1/2-\sigma/2}\,\hat{w}^-(\chi),\end{aligned} \tag{5.36}$$

where the spectral weight is given by

$$\Phi_k(\lambda) = \frac{(2k-1)|\Gamma(2k-\frac{1}{2}+\mathrm{i}\lambda)|^2}{\Gamma^2(2k)}, \tag{5.37}$$

and $\cosh\eta = \cosh\tau\cosh\tau' - \sinh\tau\sinh\tau'\cos(\phi-\phi')$, the variables $\chi = \tanh(\frac{\tau}{2})\mathrm{e}^{-\mathrm{i}\phi}$ and $\chi' = \tanh(\frac{\tau'}{2})\mathrm{e}^{-\mathrm{i}\phi'}$ parametrise points on the Poincaré disk.

Here $\hat{w}^+(\chi)$ and $\hat{w}^-(\chi)$ denote, respectively, the inverse and direct coherent-state projectors. These generate the familiar Glauber-Sudarshan P- [58,59,62] and Q-functions [61],

$$P(\chi) = \mathrm{tr}(\hat{\rho}\,\hat{w}^+(\chi)), \qquad Q(\chi) = \mathrm{tr}(\hat{\rho}\,\hat{w}^-(\chi)), \tag{5.38}$$

with $\hat{w}^-(\chi) = |\chi\rangle\langle\chi|$. The P-function further provides a reconstruction of the density operator,

$$\hat{\rho} = \int |\chi\rangle P(\chi)\langle\chi|\,\mathrm{d}\mu_\chi^k. \tag{5.39}$$

By construction, the kernels $\hat{w}^{(\sigma)}(\chi)$ satisfy the normalisation condition $\mathrm{tr}[\hat{w}^{(\sigma)}(\chi)] = 1$ and obey the resolution of the identity $\int \mathrm{d}\mu_\chi^k\,\hat{w}^{(\sigma)}(\chi) = \mathbb{1}$.

The corresponding σ-parametrised phase-space quasi-probability distributions are defined as

$$\begin{aligned}F^{(\sigma)}(\chi) &= \mathrm{tr}[\hat{\rho}\,\hat{w}^{(\sigma)}(\chi)],\\ &= \frac{2}{2k-1}\int \mathrm{d}\mu_{\chi'}^k \int \mathrm{d}\nu_\lambda\, P_{\mathrm{i}\lambda-\frac{1}{2}}(\cosh\eta)\,\Phi_k(\lambda)^{1/2-\sigma/2}\,\mathrm{tr}(\hat{\rho}\hat{w}^+(\chi')),\\ &= \frac{2}{2k-1}\int \mathrm{d}\mu_{\chi'}^k \int \mathrm{d}\nu_\lambda\, P_{\mathrm{i}\lambda-\frac{1}{2}}(\cosh\eta)\,\Phi_k(\lambda)^{-1/2-\sigma/2}\,\langle\chi'|\hat{\rho}|\chi'\rangle.\end{aligned} \tag{5.40}$$

For $\sigma = -1, 0, +1$, these distributions reduce to the $\mathrm{SU}(1,1)$ analogues of the Husimi Q-function, the Wigner function, and the Glauber-Sudarshan P-function, respectively. In particular, the $\sigma = -1$ case corresponds to the Mehler-Fock transform on the hyperbolic plane, which plays the role of the spherical harmonic expansion in the noncompact setting (see Appendix D.2.5).

We will now analyse the application of the coherent-state POVM measurement to the general function $F^{(\sigma)}$ as follows

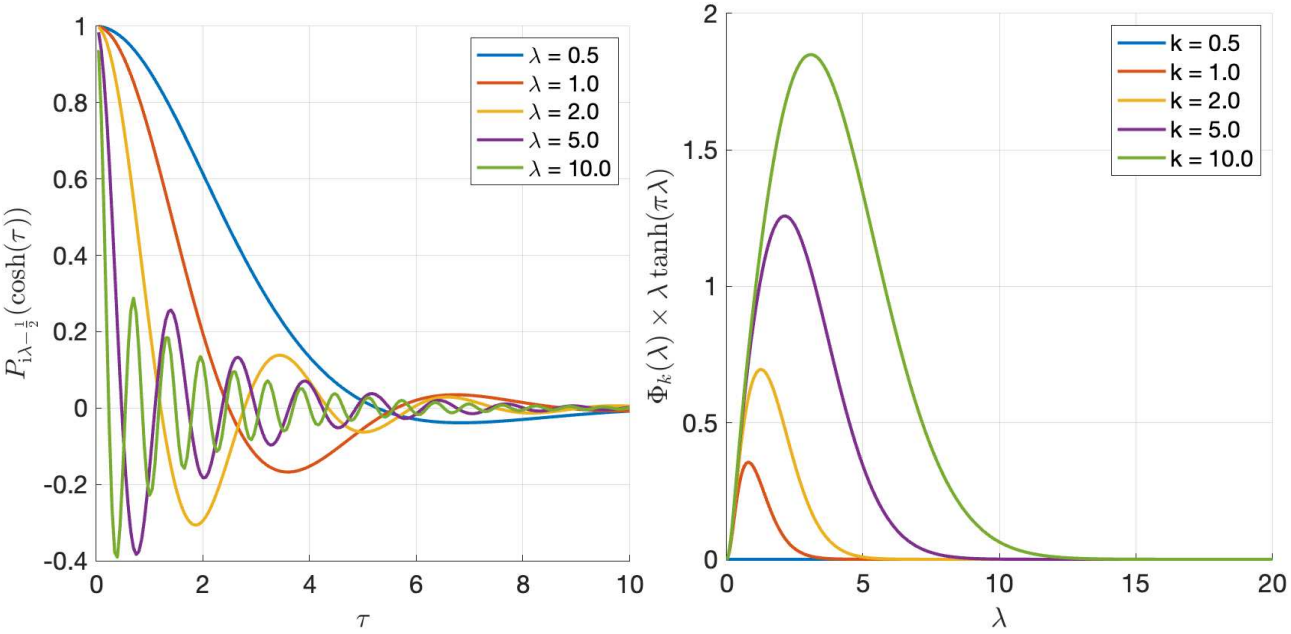
Proposition 5.2. *After one iteration of coherent-state POVM measurement*

$$F_1^{(\sigma)}(\chi) = \frac{2}{2k-1}\int \mathrm{d}\mu_{\chi'}^k \int \mathrm{d}\nu_\lambda\, P_{\mathrm{i}\lambda-\frac{1}{2}}(\cosh\eta)\,\Phi_k(\lambda)\,F^{(\sigma)}(\chi'), \tag{5.41}$$

where $F_1^{(\sigma)}(\chi)$ is the distribution after the nonselective measurement or equivalently

$$F_1^{(\sigma)}(\chi) \;=\; \frac{2}{2k-1}\int \mathrm{d}\mu^k_{\chi'}\,\langle\chi'|\hat{\rho}|\chi'\rangle \int \mathrm{d}\nu_\lambda\, P_{\mathrm{i}\lambda-\frac{1}{2}}(\cosh\eta)\,\Phi_k(\lambda)^{1/2-\sigma/2}. \tag{5.42}$$

The proof is discussed in Appendix D.2.2. So after one iteration of the coherent-state POVM measurement, we see that the distribution $F^{(\sigma)}(\chi)$ gets damped by a factor $\Phi_k(\lambda)$. Notably, this multiplicative factor $\Phi_k(\lambda)$ acts as a spectral filter on the λ-modes. Since this ratio decays as $|\lambda|$ increases (see Fig. 5.1), it suppresses contributions from higher-frequency components in the Legendre expansion. As a result, the transformation damps fine-grained structure in the input distribution, thereby implementing a coarse-graining of the phase-space density. This mechanism reflects the intrinsic smoothing behaviour of the coherent-state POVM, analogous to diffusion processes on the hyperbolic plane.



(a) Conical (Mehler) function $P_{i\lambda-\frac{1}{2}}(\cosh\tau)$ (b) Spectral weight $\lambda\tanh(\pi\lambda)\Phi_k(\lambda)$

Figure 5.1: Spectral components of the $\mathrm{SU}(1,1)$ phase-space convolution. (a) Conical (Mehler) function $P_{\mathrm{i}\lambda-\frac{1}{2}}(\cosh\tau)$ as a function of τ for various values of λ. The function exhibits oscillatory behaviour that decays for larger τ, encoding the hyperbolic geometry of the $\mathrm{SU}(1,1)$ phase space. (b) Effective spectral weight $\lambda\tanh(\pi\lambda)\Phi_k(\lambda)$ as a function of λ, where $\Phi_k(\lambda)$ is the Plancherel weight. The decay in spectral weight for large λ reflects the suppression of high-frequency spectral contributions in the phase-space convolution. Together, these functions govern the smoothing effect of the $\mathrm{SU}(1,1)$ spectral convolution, progressively washing out quantum interference features in the Wigner function. The plots were generated using the `SpecFunPhys` MATLAB toolbox [176].

Comparing (5.42) with (5.40), we find that the exponent of $\Phi_k(\lambda)$ shifts by $+1$, implying $F_1^{(\sigma)} = F^{(\sigma-2)}$. Thus, a nonselective $\mathrm{SU}(1,1)$ coherent-state POVM measurement acts by reducing the σ-parameter of the phase-space distribution by two, $F^{(\sigma)}(\chi) \;\mapsto\; F^{(\sigma-2)}(\chi)$, with half-iteration of the measurement doing $F^{(\sigma)}(\chi) \;\mapsto\; F^{(\sigma-1)}(\chi)$.

Remarkably, this shows that the familiar quasi-probability distributions are related by fractional iterations of the same measurement process, the Glauber-Sudarshan P function, the Wigner W function, and the Husimi Q function correspond respectively to $F^{(1)}$, $F^{(0)}$, and $F^{(-1)}$, each separated by a half-iteration. As a consequence, the singular behaviour of the P distribution and the negativity of the W

distribution are completely eliminated after just a single full iteration, so that classicality, in the sense of positivity in phase space, is achieved immediately.

An immediate consequence of Proposition 5.2 is that after n iterations of the POVM measurement the distribution $F^{(\sigma)}$ transforms as

$$F_n^{(\sigma)}(\chi) = \frac{2}{2k-1} \int \mathrm{d}\mu_\chi^k \int \mathrm{d}\nu_\lambda \, P_{\mathrm{i}\lambda-\frac{1}{2}}(\cosh\eta) \, (\Phi_k(\lambda))^n \, F^{(\sigma)}(\chi') = F^{(\sigma-2n)}. \tag{5.43}$$

The n-step convolution has the same form as the single-iteration case, with the spectral damping factor $\Phi_k(\lambda)$ raised to the n^{th} power.

Since $0 \leq \Phi_k(\lambda) < 1$ for all $\lambda \in \mathbb{R}$ and $k \geq \frac{1}{2}$ (see Appendix D.2.3), repeated iterations exponentially suppress every nonzero spectral mode. By dominated convergence, we may exchange the $n \to \infty$ limit with the spectral integral, yielding the trivial uniform steady state

$$\lim_{n\to\infty} F_n^{(\sigma)}(\tau', \phi') = 0. \tag{5.44}$$

This reflects the fact that the function $F^{(\sigma)}$ becomes completely delocalised under repeated measurement, spreading uniformly across the infinite-volume hyperbolic phase space. The probability density at any specific point vanishes, even though the total integral remains normalised to unity.

Following the same spectral-iteration argument used for $\mathrm{SU}(2)$, the $\mathrm{SU}(1,1)$ case also admits a natural route toward classicality. The classical boundary occurs at $\sigma = -1$, where the Husimi function becomes pointwise positive, and further POVM iterations ($\sigma \mapsto \sigma - 2$ per step) only increase the smoothing. Thus, any initial $F^{(\sigma)}$ converges to a positive classical distribution after at most $\lceil(\sigma+1)/2\rceil$ iterations, providing an upper bound on the number of POVM steps required to suppress interference in hyperbolic phase space.

The appearance of fractional iterations in the POVM framework naturally suggests the possibility of an underlying continuous-time dynamical model, one in which the iteration index n plays the role of time. While identifying an exact Lindblad-type equation that reproduces the discrete POVM evolution is nontrivial, it is possible to construct a continuous dynamical model that approximates it closely.

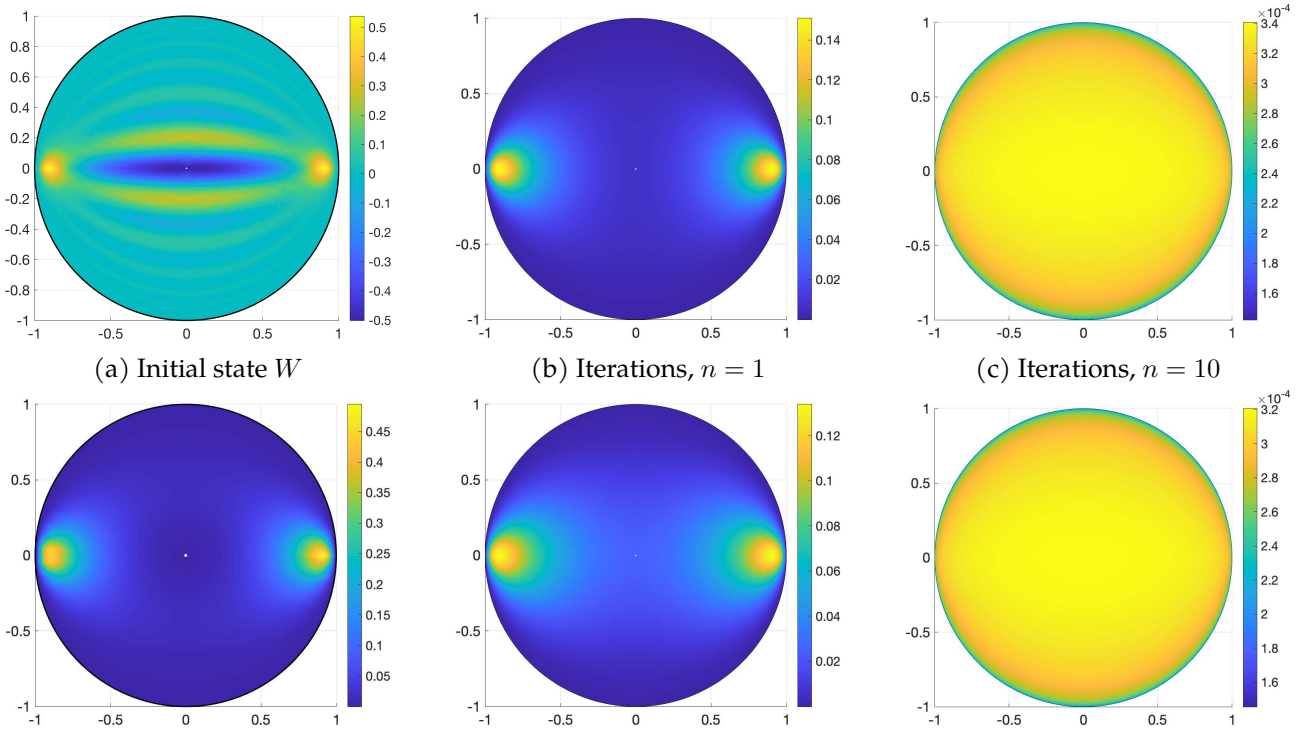
5.5 Dynamical model for phase-space POVM measurement

Just like in the HW and $\mathrm{SU}(2)$ cases (see Sections 2.6, 3.5), we consider a purely decohering Lindblad equation [40–42] for the density matrix $\hat{\rho}$ of the form

$$\dot{\hat{\rho}} = \gamma \sum_k \left(\hat{L}_k \hat{\rho} \hat{L}_k^\dagger - \frac{1}{2}\{\hat{L}_k^\dagger \hat{L}_k, \hat{\rho}\} \right), \tag{5.45}$$

where $\gamma > 0$ is a decoherence rate and $\hat{L}_k$ are the Lindblad operators chosen to be

$$\hat{L}_1 = \frac{\hat{K}_+}{\sqrt{2}}, \qquad \hat{L}_2 = \frac{\hat{K}_-}{\sqrt{2}}, \qquad \hat{L}_3 = \hat{K}_z. \tag{5.46}$$



(a) Initial state W (b) Iterations, $n = 1$ (c) Iterations, $n = 10$

(d) Initial state Q (e) Iterations: $n = 1$ (f) Iterations: $n = 10$

Figure 5.2: *The Wigner (top row) and the Husimi (bottom row) functions of the initial state, the outcome state after a single phase-space measurement, and that after ten repeated measurements.* Starting from an initial odd cat state $|\text{cat}_-\rangle = \mathcal{N}_-\left(|\chi_0\rangle - |-\chi_0\rangle\right)$ with $k = 1$, $\chi_0 = \tanh(\tau_0/2)$ and $\tau_0 = 3.0$, exhibiting quantum coherence. The columns correspond to successive $\mathrm{SU}(1,1)$ phase-space convolutions with spectral power $n = 0, 1, 10$. The initial Wigner function exhibits strong negativities due to quantum interference, which are suppressed under successive convolutions, leading to a classical-like positive distribution. The corresponding Husimi functions, which remain strictly positive throughout, similarly transforms into uniformity. The plots were generated using the `SpecFunPhys` MATLAB toolbox [176].

However, due to the noncompact nature of $\mathrm{SU}(1,1)$, the Casimir operator involves a negative contribution from the compact direction, $\hat{K}_z^2$. To correctly reproduce diffusion and preserve $\mathrm{SU}(1,1)$ covariance on the hyperbolic phase space, the contribution of $\hat{K}_z$ in the Lindblad equation must therefore enter with an effective negative sign (see Appendix D.2.4). This sign flip ensures the correct balance between the compact and noncompact directions of the algebra and is essential for obtaining the hyperbolic heat equation as the effective phase-space dynamics.

It should be emphasized, however, that the resulting "flipped" Lindblad equation although is trace-preserving, is *not* completely positive at the operator level, since the associated Kossakowski matrix is not positive semidefinite. Nevertheless, when averaged over coherent states the induced dynamics of the Husimi Q-function is governed by the heat kernel on the hyperbolic plane, which *is* positivity preserving and trace preserving, thereby providing a physically consistent effective description of decoherence in phase space. In fact, one can go further: a stochastic unravelling based on Brownian motion of $\mathrm{SU}(1,1)$ coherent states yields, upon ensemble averaging, precisely this diffusive (flipped) Lindblad equation (see Chapter 6).

The generator for the diffusive motion is given by

$$\dot{\hat{\rho}} = \gamma\left(\frac{1}{2}\hat{K}_+\hat{\rho}\hat{K}_- - \frac{1}{4}\{\hat{K}_-\hat{K}_+,\hat{\rho}\} + \frac{1}{2}\hat{K}_-\hat{\rho}\hat{K}_+ - \frac{1}{4}\{\hat{K}_+\hat{K}_-,\hat{\rho}\} - \left(\hat{K}_z\hat{\rho}\hat{K}_z - \frac{1}{2}\{\hat{K}_z^2,\hat{\rho}\}\right)\right). \quad (5.47)$$

By combining terms, this can be simplified to the more compact form

$$\dot{\hat{\rho}} = \gamma\left(\frac{1}{2}\left(\hat{K}_+\hat{\rho}\hat{K}_- + \hat{K}_-\hat{\rho}\hat{K}_+\right) - \hat{K}_z\hat{\rho}\hat{K}_z + \frac{1}{4}\left\{2\hat{K}_z^2 - \hat{K}_+\hat{K}_- - \hat{K}_-\hat{K}_+,\hat{\rho}\right\}\right). \quad (5.48)$$

Using the identity for the Casimir operator in $\mathcal{D}^+(k)$, $\hat{K}^2 = k(k-1)\mathbb{1}$, the dynamical equation simplifies to

$$\dot{\hat{\rho}} = \gamma\left(\frac{1}{2}\left(\hat{K}_+\hat{\rho}\hat{K}_- + \hat{K}_-\hat{\rho}\hat{K}_+\right) + \hat{K}_z\hat{\rho}\hat{K}_z + k(k-1)\hat{\rho}\right). \quad (5.49)$$

We now transform (5.49) to the coherent state representation and obtain an explicit expression for the time evolution of the Husimi Q-function, which we proceed to solve.

5.5.1 Husimi representation of the dynamical equation

To derive the Husimi representation of (5.49), we calculate the expectation value of (5.49) in the $\mathrm{SU}(1,1)$ coherent state $|\chi\rangle$, obtaining

$$\langle\chi|\dot{\hat{\rho}}|\chi\rangle = \gamma\left\langle\chi\middle|\frac{1}{2}\hat{K}_+\hat{\rho}\hat{K}_- + \frac{1}{2}\hat{K}_-\hat{\rho}\hat{K}_+ - \hat{K}_z\hat{\rho}\hat{K}_z + k(k-1)\hat{\rho}\middle|\chi\right\rangle. \quad (5.50)$$

The left-hand side defines the time derivative of the Husimi Q-function,

$$\dot{Q}(\chi) = \langle\chi|\dot{\hat{\rho}}|\chi\rangle, \quad (5.51)$$

while the right side involves matrix elements of operator products evaluated between coherent states.

The required differential representations of $\mathrm{SU}(1,1)$ generators in the coherent-state basis are derived

in Appendix D.2.5. Using these results, one obtains a closed partial differential equation for $Q(\chi, t)$, which takes the form of a heat equation on the hyperbolic plane [177]

$$\frac{\mathrm{d}Q}{\mathrm{d}t} = \frac{\gamma}{2}(1-|\chi|^2)^2 \frac{\partial^2 Q}{\partial \chi \partial \bar{\chi}} = \frac{\gamma}{2}\Delta_{\mathbb{H}^2} Q, \tag{5.52}$$

In hyperbolic coordinates this becomes

$$\frac{\mathrm{d}Q(\tau,\phi)}{\mathrm{d}t} = \frac{\gamma}{2}\left(\frac{\partial^2}{\partial \tau^2} + \frac{1}{\sinh^2(\tau)}\frac{\partial^2}{\partial \phi^2} + \coth(\tau)\frac{\partial}{\partial \tau}\right) Q(\tau,\phi). \tag{5.53}$$

Using the fact that the Husimi distribution satisfies the heat equation on the Hyperbolic plane we now show that the σ-parameter family of functions also satisfy the same heat equation.

Proposition 5.3. *Assume $Q(\chi, t)$ solves the hyperbolic heat equation $\partial_t Q(\chi, t) = \frac{\gamma}{2}\Delta_{\mathbb{H}^2} Q(\chi, t)$, with $\gamma > 0$. Then for each fixed σ, $F^{(\sigma)}(\chi, t)$ also solves*

$$\partial_t F^{(\sigma)}(\chi, t) = \frac{\gamma}{2}\Delta_{\mathbb{H}^2} F^{(\sigma)}(\chi, t). \tag{5.54}$$

Proof. Write $F^{(\sigma)}$ as a *zonal convolution* of the Husimi density Q for $\mathrm{SU}(1,1)$, meaning a convolution with a kernel that depends only on the invariant geodesic distance between phase-space points,

$$F^{(\sigma)}(\chi, t) = \int Q(\chi', t)\, G_\sigma(\chi, \chi')\, \mathrm{d}\mu^k_{\chi'}. \tag{5.55}$$

where

$$G_\sigma(\rho) = \frac{2}{2k-1}\int \mathrm{d}\nu_\lambda\, P_{\mathrm{i}\lambda-\frac{1}{2}}(\cosh\eta)\, \Phi_k(\lambda)^{-\frac{1}{2}-\frac{\sigma}{2}}. \tag{5.56}$$

and $G_\sigma(\chi, \chi') = G_\sigma\big(\eta(\chi, \chi')\big)$ is group invariant and depends only on the geodesic distance ρ. The hyperbolic conical functions $P_{\mathrm{i}\lambda-\frac{1}{2}}(\cosh\eta)$ diagonalise Δ in either variable with the same eigenvalue, hence

$$\Delta_\chi\, G_\sigma(\chi, \chi') = \Delta_{\chi'}\, G_\sigma(\chi, \chi'). \tag{5.57}$$

Assuming $Q(\cdot, t)$ is smooth and satisfies $\partial_t Q = \frac{\gamma}{2}\Delta_{\chi'} Q$, and using dominated convergence plus the self-adjointness of Δ with respect to the invariant measure $\mathrm{d}\mu^k_\chi$, we obtain

$$\begin{aligned}
\partial_t F^{(\sigma)}(\chi, t) &= \int (\partial_t Q)(\chi', t)\, G_\sigma(\chi, \chi')\, \mathrm{d}\mu^k_{\chi'}, \\
&= \frac{\gamma}{2}\int (\Delta_{\chi'} Q)(\chi', t)\, G_\sigma(\chi, \chi')\, \mathrm{d}\mu^k_{\chi'}, \\
&= \frac{\gamma}{2}\int Q(\chi', t)\, (\Delta_{\chi'} G_\sigma)(\chi, \chi')\, \mathrm{d}\mu^k_{\chi'}, \\
&= \frac{\gamma}{2}\int Q(\chi', t)\, (\Delta_{\chi} G_\sigma)(\chi, \chi')\, \mathrm{d}\mu^k_{\chi'}, \\
&= \frac{\gamma}{2}\Delta_\chi\left[\int Q(\chi', t)\, G_\sigma(\chi, \chi')\, \mathrm{d}\mu^k_{\chi'}\right] = \frac{\gamma}{2}\Delta_\chi F^{(\sigma)}(\chi, t).
\end{aligned} \tag{5.58}$$

This proves that $F^{(\sigma)}$ obeys the same heat equation as Q. □

5.5.2 Solving the hyperbolic heat equation

We now solve the hyperbolic heat equation derived in the previous section. It is important to emphasize that the Q-function we consider here is associated with a quantum system in the positive discrete series representation of $\mathrm{SU}(1,1)$ with Bargmann index $k > \frac{1}{2}$. As such, it is normalised with respect to the $\mathrm{SU}(1,1)$-invariant measure $\mathrm{d}\mu^k_{\tau,\phi}$ (which depends on k), rather than the standard Riemannian volume measure on $\mathbb{H}^2$, $\mathrm{d}\omega_{\tau,\phi}$ (see Appendix D.1).

Proposition 5.4. *The solution to the hyperbolic heat equation (5.53) with initial condition $Q(\tau,\phi,0) = Q_0(\tau,\phi)$, is given by*

$$Q(\tau,\phi,t) = \int \left[\int \mathrm{e}^{-\frac{\gamma t}{2}(\lambda^2+\frac{1}{4})} P_{\mathrm{i}\lambda-\frac{1}{2}}(\cosh\eta)\,\mathrm{d}\nu_\lambda \right] Q_0(\tau',\phi')\,\mathrm{d}\omega_{\tau',\phi'}, \tag{5.59}$$

where $\eta = \eta(\tau,\phi;\tau',\phi')$ is the hyperbolic distance given by

$$\cosh\eta = \cosh\tau\cosh\tau' - \sinh\tau\sinh\tau'\cos(\phi-\phi'), \tag{5.60}$$

and the measure $\mathrm{d}\omega_{\tau',\phi'} = \frac{1}{2\pi}\sinh(\tau)\,\mathrm{d}\tau\,\mathrm{d}\phi$ and $\mathrm{d}\nu_\lambda = \lambda\tanh(\pi\lambda)\,\mathrm{d}\lambda$ is the spectral Plancherel measure.

Proof. We begin by expanding the initial condition $Q_0(\tau,\phi)$ in terms of eigenfunctions of the hyperbolic Laplacian on $\mathbb{H}^2$, which are given by generalised spherical harmonics $\psi_{\lambda,\mu}(\tau,\phi)$

$$Q_0(\tau,\phi) = \sum_{\mu=-\infty}^{\infty} \int f_{\lambda,\mu}\,\psi_{\lambda,\mu}(\tau,\phi)\,\mathrm{d}\nu_\lambda, \tag{5.61}$$

with spectral coefficients given by the projection onto this basis

$$f_{\lambda,\mu} = \int Q_0(\tau',\phi')\psi^*_{\lambda,\mu}(\tau',\phi')\,\mathrm{d}\omega_{\tau',\phi'}. \tag{5.62}$$

The heat operator acts diagonally on this basis, so the time evolution is given by

$$Q(\tau,\phi,t) = \sum_{\mu=-\infty}^{\infty} \int \mathrm{e}^{-\frac{\gamma t}{2}(\lambda^2+\frac{1}{4})} f_{\lambda,\mu}\psi_{\lambda,\mu}(\tau,\phi)\,\mathrm{d}\nu_\lambda. \tag{5.63}$$

Substituting the expression for $f_{\lambda,\mu}$, we get

$$Q(\tau,\phi,t) = \sum_{\mu=-\infty}^{\infty} \int \mathrm{e}^{-\frac{\gamma t}{2}(\lambda^2+\frac{1}{4})} \left[\int Q_0(\tau',\phi')\psi^*_{\lambda,\mu}(\tau',\phi')\,\mathrm{d}\omega_{\tau',\phi'} \right] \psi_{\lambda,\mu}(\tau,\phi)\,\mathrm{d}\nu_\lambda. \tag{5.64}$$

Now, using the addition theorem (reproducing kernel identity) for the eigenfunctions from (D.7), we find

$$Q(\tau,\phi,t) = \int \left[\int \mathrm{e}^{-\frac{\gamma t}{2}(\lambda^2+\frac{1}{4})} P_{\mathrm{i}\lambda-\frac{1}{2}}(\cosh\eta)\,\mathrm{d}\nu_\lambda \right] Q_0(\tau',\phi')\,\mathrm{d}\omega_{\tau',\phi'}, \tag{5.65}$$

which completes the proof. □

Similarly it can be shown that

$$F^{(\sigma)}(\tau,\phi,t)=\int\left[\int \mathrm{e}^{-\frac{\gamma t}{2}(\lambda^2+\frac{1}{4})}P_{\mathrm{i}\lambda-\frac{1}{2}}(\cosh\eta)\,\mathrm{d}\nu_\lambda\right]F^{(\sigma)}(\tau',\phi',0)\,\mathrm{d}\omega_{\tau',\phi'}. \tag{5.66}$$

The solution to the heat equation (5.66) expresses the time-evolved Husimi function $F^{(\sigma)}(\tau,\phi,t)$ as a convolution of the initial distribution $F^{(\sigma)}(\tau',\phi',0)$ with a kernel of associated Legendre functions $P_{\mathrm{i}\lambda-\frac{1}{2}}(\cosh\eta)$, weighted by an exponentially decaying factor. High-λ modes are rapidly suppressed, while low-λ modes dominate at long times, driving the distribution toward a smooth uniform state.

In contrast, the iterative POVM dynamics derived earlier introduce a geometric damping factor of the form $(\Phi_k(\lambda))^n$, where $\Phi_k(\lambda)<1$ for all $\lambda\neq 0$. Both frameworks, discrete POVM iteration and continuous dynamical evolution, act as spectral filters that dampen fine-grained features of the quantum state, effectively driving it toward a classical-like configuration.

To compare the two approaches quantitatively, one may attempt to identify a correspondence between the damping factors by equating their decay rates

$$\exp\left(-\frac{\gamma t}{2}\left(\lambda^2+\frac{1}{4}\right)\right)\quad\leftrightarrow\quad(\Phi_k(\lambda))^n\,. \tag{5.67}$$

Taking logarithms yields the relation

$$\gamma\leftrightarrow-\frac{2}{\lambda^2+\frac{1}{4}}\log\Phi_k(\lambda). \tag{5.68}$$

This expression makes it evident that no single choice of γ can match the entire spectrum of λ values unless $\Phi_k(\lambda)$ is itself exponential in λ^2, which it is not.

However, in the large-k limit, with λ fixed, the spectral factor simplifies considerably. Applying Stirling's expansion to the logarithm of the Gamma functions [122,123], one finds

$$\ln\Phi_k(\lambda)=-\frac{\lambda^2+\frac{1}{4}}{2k}+O\left(\frac{1}{k^2}\right). \tag{5.69}$$

Thus, to leading order,

$$\Phi_k(\lambda)\;\simeq\;\exp\left(-\frac{\lambda^2+\frac{1}{4}}{2k}\right). \tag{5.70}$$

After n measurement iterations, the damping factor becomes

$$\Phi_k(\lambda)^n\;\simeq\;\exp\Big(-\frac{n}{2k}\left(\lambda^2+\frac{1}{4}\right)\Big). \tag{5.71}$$

This coincides with the eigenvalue of the hyperbolic heat kernel, with the effective diffusion time identified as $t=\frac{n}{2k}$.

In the limit $t\to\infty$, assuming sufficient regularity of $F^{(\sigma)}(\tau,\phi,0)$, we may exchange the limit and the

integral via dominated convergence

$$\begin{aligned}\lim_{t\to\infty} F^{(\sigma)}(\tau,\phi,t) &= \lim_{t\to\infty}\int\left[\int \mathrm{e}^{-\frac{\gamma t}{2}(\lambda^2+\frac{1}{4})}P_{\mathrm{i}\lambda-\frac{1}{2}}(\cosh\eta)\,\mathrm{d}\nu_\lambda\right]F^{(\sigma)}(\tau',\phi',0)\,\mathrm{d}\mu^k_{\tau',\phi'},\\ &= 0.\end{aligned} \tag{5.72}$$

5.5.3 Onset of classicality

Similar to the $\mathrm{SU}(2)$ case, we identify the earliest time t_* for which the heat-kernel evolution (5.66) produces a distribution $F^{(\sigma)}(\tau,\phi,t)$ that is everywhere nonnegative. The key observation is that one iteration of the $\mathrm{SU}(1,1)$ coherent-state POVM measurement corresponds to multiplication by $\Phi_k(\lambda)$ in the spectral domain, while the continuous-time dynamics multiplies each spectral mode by $\exp[-\gamma t(\lambda^2+1/4)]$. Thus, after $(\sigma+1)/2$ iterations, the exact number required to wash out negativity and singularities, the spectral damping factor is $\Phi_k(\lambda)^{(\sigma+1)/2}$. Positivity is therefore guaranteed once

$$\mathrm{e}^{-\gamma t(\lambda^2+\frac{1}{4})} \;\le\; \Phi_k(\lambda)^{\frac{\sigma+1}{2}} \quad \text{for all } \lambda\in\mathbb{R}. \tag{5.73}$$

The ratio

$$R_k(\lambda)=\frac{\log\big(1/\Phi_k(\lambda)\big)}{\lambda^2+\frac{1}{4}} \tag{5.74}$$

is maximised at $\lambda=0$, which sets the critical positivity time

$$t_*(\sigma,k,\gamma)=\frac{\sigma+1}{2\gamma}\,\sup_{\lambda\in\mathbb{R}}R_k(\lambda)=\frac{2(\sigma+1)}{\gamma}\,\log\left[\frac{\Gamma(2k)}{\sqrt{2k-1}\,\Gamma(2k-\frac{1}{2})}\right]. \tag{5.75}$$

For all $t>t_*(\sigma,k,\gamma)$ the distribution $F^{(\sigma)}(\tau,\phi,t)$ is strictly positive, signalling the onset of classicality.

As an example, when $k=1$ one finds $\Phi_1(0)=\pi/4$, giving

$$t_*(\sigma,1,\gamma)\approx 0.482\,\frac{\sigma+1}{\gamma}. \tag{5.76}$$

In the large-k limit, Stirling's approximation yields

$$\log\left(\frac{1}{\Phi_k(0)}\right)\sim\frac{1}{8k}, \tag{5.77}$$

so that

$$t_*(\sigma,k,\gamma)\;\sim\;\frac{\sigma+1}{4\gamma k},\qquad (k\to\infty). \tag{5.78}$$

Thus, for fixed (σ,γ) the onset time decreases inversely with the Bargmann index, reflecting the accelerated emergence of classicality in the semiclassical, large-representation limit.

5.6 Discussion and conclusion

In this chapter, we developed a coherent framework for modelling decoherence in quantum systems with $\mathrm{SU}(1,1)$ symmetry using phase-space measurements based on coherent-state POVMs. Focusing on the positive discrete series, we showed that iterative, unread POVM measurements act as spectral filters, progressively damping high-frequency modes of the σ-parametrised quasi-probability distributions $F^{(\sigma)}$ on the hyperbolic plane. This process establishes a natural hierarchy in which successive iterations shift $\sigma \mapsto \sigma - 2$, with fractional iterations connecting the entire family $\{F^{(\sigma)}\}$ and recovering the familiar P-, W-, and Q-functions as special cases. In particular, we identified the Husimi function ($\sigma = -1$) as the universal classical threshold, for any initial $F^{(\sigma)}$, classicality is guaranteed after at most $\lceil(\sigma+1)/2\rceil$ iterations, providing a sharp, state-independent bound on the onset of positivity.

To complement this discrete picture, we introduced a continuous-time master equation based on the $\mathfrak{su}(1,1)$ generators, which yields a heat-like evolution on the hyperbolic plane. Although the corresponding generator differs from the standard GKSL form and fails to ensure complete positivity at the operator level, it preserves $\mathrm{SU}(1,1)$ covariance and reproduces hyperbolic diffusion when interpreted in the coherent-state representation. Here, complete positivity and trace preservation are recovered under phase-space averaging. Unlike the POVM framework, however, the dynamical onset of classicality is state-dependent, with the decoherence time controlled by the spectral weight of the initial distribution. This contrast highlights the complementary roles of measurement-based and dynamical descriptions, one offers a universal sufficiency bound, while the other encodes state-specific decay rates.

This completes our analysis of $\mathrm{SU}(1,1)$ phase-space measurement and decoherence. We now turn to tomographic measurement schemes for $\mathrm{SU}(N)$ quantum systems, and examine how phase-space decoherence manifests in that setting.

Chapter 6

Stochastic unravelling of decoherence on phase space

6.1 Introduction

In the previous chapters, we developed measurement-based and Lindblad descriptions of decoherence across different symmetry groups. In this chapter, we turn to a complementary approach, focusing instead on stochastic trajectory descriptions of phase-space measurements.

The dynamics of open quantum systems, especially under continuous observation, are fundamentally stochastic in nature. While the unitary Schrödinger equation describes closed systems evolving in isolation, realistic quantum systems are invariably coupled to external degrees of freedom such as thermal reservoirs, measurement devices, and uncontrolled environments. This interaction leads to decoherence, information loss, and effective irreversibility, all of which are encoded in the general theory of quantum master equations and the framework of completely positive trace-preserving (CPTP) maps [43, 44, 50, 81, 92].

Among the most important such descriptions is the Lindblad master equation [40–42], which governs the Markovian evolution of the density matrix for a system undergoing environmental noise or continuous measurement. A deeper understanding of this dynamics is provided by the theory of quantum trajectories and stochastic Schrödinger equations (SSEs), which represent the evolution of a pure quantum state under continuous monitoring as a stochastic process in Hilbert space [43, 44, 65]. These unravelings not only reproduce the Lindblad equation upon ensemble averaging but also reveal the underlying informational and physical mechanisms of decoherence and measurement backaction (the effect, disturbance or alteration of a quantum state due to the act of observing it).

In this chapter we investigate the dynamics of coherent states undergoing stochastic evolution induced by continuous monitoring of phase-space observables. By formulating a stochastic process for the coherent-state label, we derive stochastic differential equations (SDEs) that govern the conditioned evolution of the quantum state within the family of coherent states. We show that the ensemble average of the outer product of the stochastic trajectories yields a trace-preserving quantum dynamical semigroup. In the Heisenberg–Weyl and $\mathrm{SU}(2)$ cases this semigroup coincides with the Gorini–Kossakowski–Sudarshan–Lindblad (GKSL) master equation, with Lindblad operators corresponding

to the generators of the Lie algebra associated with the coherent-state manifold. For $\mathrm{SU}(1,1)$, however, the resulting dynamics is not completely positive and departs from the standard GKSL form as we saw in Chapter 5, instead taking the structure of a diffusion equation generated by the quadratic Casimir on the noncompact phase space. In addition, we analyse the stochastic properties of quantum observables along these trajectories, identifying martingale structures and entropy processes that reflect the underlying symmetries.

The structure of this chapter is as follows: Section 6.2 provides a brief overview of the probabilistic and stochastic framework needed to define and interpret the stochastic Schrödinger equation. This includes a short discussion of probability spaces, filtrations, martingales, and Itô calculus. A full account of this background is presented in Appendix E.

Section 6.2.1 presents the normalised stochastic Schrödinger equation (SSE), discusses its key properties such as norm preservation, and derives the associated Lindblad master equation through ensemble averaging. In Section 6.3, we introduce continuous phase-space measurements within the framework of canonical coherent states and derive the stochastic differential equation (SDE) governing the evolution of the coherent-state label under such measurements. Section 6.4 extends this treatment to generalised coherent states associated with the $\mathrm{SU}(2)$ group, formulating the corresponding SDE on the Bloch sphere and analysing the induced stochastic dynamics. Section 6.5 generalises this approach further to $\mathrm{SU}(1,1)$ coherent states, deriving the SDE on the Poincaré disk and examining the evolution, with particular attention to boundary effects and amplification dynamics. In Sections 6.3, 6.4 and 6.5, we also investigate the martingale properties of observables under different measurement schemes, highlighting their connection to conservation laws and symmetries. Finally we conclude with a discussion in Section 6.6. For clarity of presentation, many of the detailed derivations and lengthy proofs are deferred to Appendix E.

6.2 Mathematical background

In this section we outline the key probabilistic concepts required for the stochastic dynamics developed in this chapter. Rather than providing formal definitions, we briefly summarise the tools that will be used in the main text, including probability spaces, filtrations, martingales, and Itô calculus. A rigorous treatment, with precise definitions and supporting results, is given in Appendix E.1.

When a quantum system interacts continuously with an environment or measurement apparatus, its evolution becomes inherently random and nonunitary. The deterministic Schrödinger equation is then replaced by a stochastic Schrödinger equation (SSE), which describes the conditioned evolution of the system's wavefunction. These dynamics are naturally framed within the language of stochastic processes and stochastic differential equations (SDEs).

A stochastic process is a collection of random variables indexed by time, whose evolution is described by SDEs comprising deterministic drift and random fluctuations (diffusion). The latter are modeled mathematically by Brownian motion (Wiener processes). The formal structure of such processes is built on a probability space, with a filtration that encodes the accumulation of information over time, enabling precise definitions of adapted processes, martingales, and conditional expectations.

Central to our analysis are Itô processes, stochastic analogues of ordinary differential equations, whose evolution is governed by SDEs in differential form. The calculus of such processes is encapsulated in

Itô's lemma, a stochastic chain rule that accounts for the nondifferentiable nature of Brownian paths through second-order correction terms arising from their quadratic variation.

Given that quantum states reside in complex Hilbert spaces, we extend Itô calculus to complex-valued processes using Wirtinger derivatives. This complex stochastic framework preserves analytic structure and is particularly suited to quantum optics, coherent states, and measurement-induced dynamics.

The concepts introduced here provide the mathematical foundation for constructing and analysing stochastic Schrödinger equations, and for understanding the probabilistic structure of quantum systems subject to noise, feedback, and continuous observation. For detailed expositions, see Øksendal [178], Karatzas & Shreve [179], Gardiner [180] and [181] for Itô's lemma. For quantum measurement theory and SSEs, see Wiseman & Milburn [44] and Barchielli & Gregoratti [65].

With these preliminaries, we begin by reviewing the Stochastic Schrödinger equation.

6.2.1 Stochastic Schrödinger dynamics

Let $\mathcal{H}$ be a finite-dimensional complex Hilbert space of dimension N, equipped with the inner product $\langle\cdot|\cdot\rangle$. The quantum state is described by a family of state vectors $\{|\psi_t\rangle\}_{t\geq 0}$, where for each $t \in [0,\infty)$, the state vector $|\psi_t\rangle \in \mathcal{H}$ is a random variable defined on a filtered probability space $(\Omega, \mathcal{F}, \{\mathcal{F}_t\}_{t\geq 0}, \mathbb{P})$. We assume that $\{|\psi_t\rangle\}$ is adapted to the filtration $\{\mathcal{F}_t\}$, and satisfies the required integrability conditions so that stochastic integrals are well-defined. Physically, $|\psi_t\rangle$ represents a pure-state trajectory undergoing random evolution due to its coupling to a noisy environment or a continuous measurement process.

Let $\hat{H}$ denote the Hamiltonian of the system, and let $\{\hat{L}^k\}$ be a fixed collection of Lindblad operators on the Hilbert space $\mathcal{H}$. Each $\hat{L}^k$ corresponds to an independent channel of decoherence or continuous measurement acting on the quantum system. We assume the existence of a collection $\{W_t^k\}_{t\geq 0}$ of mutually independent standard Wiener processes, one for each Lindblad operator, all defined on the same filtered probability space and adapted to the filtration $\{\mathcal{F}_t\}_{t\geq 0}$.

The evolution of the quantum state $|\psi_t\rangle \in \mathcal{H}$ under continuous environmental interaction or observation is modeled by a normalised Itô-type stochastic Schrödinger equation (SSE) [182–187]

$$\mathrm{d}|\psi_t\rangle = -\frac{\mathrm{i}}{\hbar}\hat{H}|\psi_t\rangle\,\mathrm{d}t - \frac{\sigma^2}{8}\left(\left(\hat{L}^k\right)^\dagger \hat{L}^k - 2\overline{L_t^k}\hat{L}^k + |L_t^k|^2\right)|\psi_t\rangle\,\mathrm{d}t + \frac{\sigma}{2}\sum_k\left(\hat{L}^k - L_t^k\right)|\psi_t\rangle\,\mathrm{d}W_t^k, \quad (6.1)$$

where $\sigma > 0$ is a fixed coupling constant that controls the strength of the stochastic fluctuations, and

$$L_t^k = \frac{\langle\psi_t|\hat{L}^k|\psi_t\rangle}{\langle\psi_t|\psi_t\rangle} \quad (6.2)$$

denotes the expectation value of the operator $\hat{L}^k$ at time t. The nonlinearity in (6.1) arises from the dependence of the drift and diffusion terms on this expectation value.

In the special case where all Lindblad operators are self-adjoint, $\hat{L}^k = \left(\hat{L}^k\right)^\dagger$, the SDE simplifies to

$$\mathrm{d}|\psi_t\rangle = -\frac{\mathrm{i}}{\hbar}\hat{H}|\psi_t\rangle\,\mathrm{d}t - \frac{\sigma^2}{8}\sum_k \left(\hat{L}^k - L_t^k\right)^2 |\psi_t\rangle\,\mathrm{d}t + \frac{\sigma}{2}\sum_k \left(\hat{L}^k - L_t^k\right)|\psi_t\rangle\,\mathrm{d}W_t^k, \tag{6.3}$$

which is often used in the literature for systems undergoing real-valued measurement processes (e.g., homodyne detection [43, 44, 92]).

A defining feature of the stochastic Schrödinger equation (SSE) is the preservation of the norm of the quantum state vector at all times.

Lemma 6.1. Let $|\psi_t\rangle$ evolve according to the normalised stochastic Schrödinger equation 6.1. Then the norm is conserved almost surely for all $t \geq 0$, regardless of whether the Lindblad operators $\hat{L}_k$ are Hermitian.

The detailed proof is presented in Appendix E.2.1.

6.2.2 Density matrix and the Lindblad equation

We now consider the corresponding mixed-state description of the system. For a given realisation of the stochastic process, we define the instantaneous pure-state projector as $\hat{R}_t = |\psi_t\rangle\langle\psi_t|$. The statistical state of the system, which accounts for classical uncertainty due to the stochasticity of the measurement record or environmental noise, is given by the ensemble average of these pure-state projectors: $\hat{\rho}_t = \mathbb{E}[\hat{R}_t]$. By construction, $\hat{\rho}_t$ is a legitimate density matrix, i.e. it is Hermitian, positive semidefinite, and normalised to unit trace.

Proposition 6.1. *Let $|\psi_t\rangle$ evolve according to (6.1). Then the ensemble average $\hat{\rho}_t = \mathbb{E}[\hat{R}_t]$ satisfies the deterministic Lindblad master equation*

$$\frac{\mathrm{d}\hat{\rho}_t}{\mathrm{d}t} = -\frac{\mathrm{i}}{\hbar}[\hat{H}, \hat{\rho}_t] + \frac{\sigma^2}{4}\sum_k \left(\hat{L}^k\hat{\rho}_t(\hat{L}^k)^\dagger - \frac{1}{2}\left\{(\hat{L}^k)^\dagger\hat{L}^k, \hat{\rho}_t\right\}\right), \tag{6.4}$$

where $\{\cdot,\cdot\}$ denotes the anti-commutator.

The proof is discussed in detail in Appendix E.2.2. This result shows that the Lindblad equation emerges naturally as the ensemble average of stochastic pure-state evolutions, thus providing the rigorous basis for interpreting stochastic Schrödinger equations as microscopic unravellings of open-system dynamics.

6.3 Continuous phase-space measurement and stochastic unravelling

The stochastic Schrödinger equation (SSE) provides a general framework for describing the conditioned evolution of a quantum state under continuous measurement. When the measured observables are linked to phase space, such as position and momentum, or their analogues in systems with Lie group symmetries, the quantum state undergoes a gradual, stochastic evolution driven by measurement backaction, rather than an instantaneous collapse.

In many relevant scenarios, as we have seen in the previous chapters, this evolution remains confined to a manifold of coherent states. This motivates describing the dynamics through a stochastic

differential equation (SDE) for the coherent-state label, viewed as a diffusion process on the corresponding phase-space manifold. While this approach is well established for canonical coherent states of the Heisenberg–Weyl group [43,44,188], it extends naturally to generalised coherent states associated with Lie groups such as $\mathrm{SU}(2)$ and $\mathrm{SU}(1,1)$. In these cases, the geometry of the coherent-state manifold, the Bloch sphere or the Poincaré disk, constrains the stochastic dynamics, leading to group-structured diffusion processes.

We begin by developing this construction explicitly for the coherent states of the Heisenberg–Weyl group, before extending it to $\mathrm{SU}(2)$ and $\mathrm{SU}(1,1)$.

6.3.1 Stochastic evolution of canonical coherent states

In Chapter 2, we introduced Heisenberg-Weyl coherent states as phase-space localised states providing a natural POVM for modelling measurement-induced decoherence. We now extend this construction dynamically by considering a time-dependent family of coherent states, indexed by a stochastic process $\{\alpha_t\}_{t\geq 0}$. This allows us to describe decoherence as a diffusion process directly on phase space. Formally, similar to (2.10), we define the coherent-state stochastic process

$$|\alpha_t\rangle = \hat{D}(\alpha_t)|0\rangle = \exp(\alpha_t \hat{a}^\dagger - \bar{\alpha_t}\hat{a})|0\rangle, \tag{6.5}$$

where $\alpha_t = \frac{1}{\sqrt{2}}(x_t + \mathrm{i}p_t)$, with x_t, p_t real-valued stochastic processes given by

$$x_t = \sigma W_t^x, \quad p_t = \sigma W_t^p. \tag{6.6}$$

Here, W_t^x and W_t^p are independent standard Brownian motions, and $\sigma > 0$ is a fixed parameter governing the strength of the stochastic fluctuations.

The process α_t is a complex Itô diffusion adapted to the filtration $\{\mathcal{F}_t\}$ generated by the Wiener processes. As such, the coherent state $|\alpha_t\rangle$ becomes a stochastic process in the Hilbert space $\mathcal{H}$, adapted and measurable with respect to the same filtration.

The differential of α_t satisfies

$$\mathrm{d}\alpha_t = \frac{1}{\sqrt{2}}\sigma\,\mathrm{d}W_t^x + \frac{\mathrm{i}}{\sqrt{2}}\sigma\,\mathrm{d}W_t^p, \tag{6.7}$$

from which we immediately obtain the Itô identities $(\mathrm{d}\alpha_t)^2 = (\mathrm{d}\bar{\alpha_t})^2 = 0$, $\mathrm{d}\alpha_t\,\mathrm{d}\bar{\alpha_t} = \sigma^2\mathrm{d}t$.

Using this we now derive the SDE satisfied by the coherent-state stochastic process to be

Proposition 6.2. *Let α_t be a complex-valued Itô process as defined above, and let $|\alpha_t\rangle$ denote the corresponding time-dependent Heisenberg-Weyl coherent state. Then $|\alpha_t\rangle$ satisfies the stochastic differential equation*

$$\begin{aligned}
\mathrm{d}|\alpha_t\rangle \;=\; & \frac{\sigma}{\sqrt{2}}\left(\hat{a}^\dagger - \frac{\bar{\alpha_t}}{2}\right)|\alpha_t\rangle\,\mathrm{d}W_t^x + \frac{\mathrm{i}\sigma}{\sqrt{2}}\left(\hat{a}^\dagger - \frac{\bar{\alpha_t}}{2}\right)|\alpha_t\rangle\,\mathrm{d}W_t^p \\
& -\frac{\sigma}{\sqrt{2}}\left(\hat{a} - \frac{\alpha_t}{2}\right)|\alpha_t\rangle\,\mathrm{d}W_t^x + \frac{\mathrm{i}\sigma}{\sqrt{2}}\left(\hat{a} - \frac{\alpha_t}{2}\right)|\alpha_t\rangle\,\mathrm{d}W_t^p \\
& -\frac{\sigma^2}{2}\left(\hat{a}\hat{a}^\dagger + \hat{a}^\dagger\hat{a} - \hat{a}\bar{\alpha_t} - \hat{a}^\dagger\alpha_t + \frac{|\alpha_t|^2}{2}\right)|\alpha_t\rangle\,\mathrm{d}t.
\end{aligned} \tag{6.8}$$

The detailed derivation of (6.8), using Itô calculus and the differential representation of displacement operators, is provided in Appendix E.2.3. This result provides the explicit stochastic evolution of a coherent-state-valued process $|\alpha_t\rangle$, driven by Brownian motion in phase space.

Expressing the dynamics in terms of the canonical quadrature operators $\hat{x} = \frac{1}{\sqrt{2}}(\hat{a} + \hat{a}^\dagger)$ and $\hat{p} = \frac{1}{\sqrt{2}\mathrm{i}}(\hat{a} - \hat{a}^\dagger)$, and using the decomposition $\alpha_t = \frac{1}{\sqrt{2}}(x_t + \mathrm{i}p_t)$, the stochastic differential equation becomes

$$\begin{aligned} \mathrm{d}|\alpha_t\rangle \;=\; & -\mathrm{i}\sigma\left(\hat{p} - \frac{p_t}{2}\right)|\alpha_t\rangle\,\mathrm{d}W_t^x + \mathrm{i}\sigma\left(\hat{x} - \frac{x_t}{2}\right)|\alpha_t\rangle\,\mathrm{d}W_t^p \\ & -\frac{\sigma^2}{2}\left[\left(\hat{x} - \frac{x_t}{2}\right)^2 + \left(\hat{p} - \frac{p_t}{2}\right)^2\right]|\alpha_t\rangle\,\mathrm{d}t. \end{aligned} \tag{6.9}$$

Here, $x_t = \langle\alpha_t|\hat{x}|\alpha_t\rangle$ and $p_t = \langle\alpha_t|\hat{p}|\alpha_t\rangle$ are precisely the expectation values of position and momentum in the coherent state $|\alpha_t\rangle$, consistent with the parametrisation $\alpha_t = \frac{1}{\sqrt{2}}(x_t + \mathrm{i}p_t)$.

This equation captures the coherent state's response to phase-space noise, with each Brownian term coupling to the quadrature conjugate to its label, namely, $\mathrm{d}W_t^x$ drives the momentum operator $\hat{p}$, while $\mathrm{d}W_t^p$ drives position $\hat{x}$. This structure differs from the stochastic Schrödinger equation (SSE) formulation, where each noise term is directly associated with a specific operator (Lindblad operator), and the stochastic increments act independently on their corresponding Hilbert-space operators. In contrast, the phase-space representation reflects the canonical conjugacy of position and momentum, leading to a cross-coupling between the noise terms and the quadrature directions in the SDE for the coherent-state label.

Crucially, this evolution preserves the normalisation $\langle\alpha_t|\alpha_t\rangle = 1$ at all times.

Proposition 6.3. *Let $|\alpha_t\rangle = \hat{D}(\alpha_t)|0\rangle$ be the coherent-state process defined as in (6.5), then it has constant norm*

$$\langle\alpha_t|\alpha_t\rangle = 1 \quad \textit{for all } t \geq 0. \tag{6.10}$$

Proof. Since $\hat{D}(\alpha_t)$ is unitary for all $\alpha_t \in \mathbb{C}$, and the vacuum state $|0\rangle$ is normalised, we have

$$\langle\alpha_t|\alpha_t\rangle = \langle 0|\hat{D}^\dagger(\alpha_t)\hat{D}(\alpha_t)|0\rangle = \langle 0|0\rangle = 1. \tag{6.11}$$

□

Thus, the evolution is well-defined and the coherent state remains properly normalised throughout the stochastic dynamics.

6.3.2 Martingale structure of the observables

We now analyse the martingale nature of the phase-space observables x_t and p_t.

Proposition 6.4. *Let $|\alpha_t\rangle$ satisfy the coherent-state-valued stochastic differential equation in (6.8). Then the processes $x_t = \langle\alpha_t|\hat{x}|\alpha_t\rangle$ and $p_t = \langle\alpha_t|\hat{p}|\alpha_t\rangle$ are* martingales *with respect to the filtration generated by the Brownian motions W_t^x and W_t^p.*

Proof. We apply Itô's lemma to the function $x_t = \langle\alpha_t|\hat{x}|\alpha_t\rangle$. Using the differential of a quadratic form

of a stochastic process, we compute

$$\mathrm{d}x_t = \langle \mathrm{d}\alpha_t|\hat{x}|\alpha_t\rangle + \langle \alpha_t|\hat{x}|\mathrm{d}\alpha_t\rangle + \langle \mathrm{d}\alpha_t|\hat{x}|\mathrm{d}\alpha_t\rangle. \tag{6.12}$$

Each of these terms can be expanded using the explicit form of the SDE for $|\alpha_t\rangle$. After simplification, we find that the drift term vanishes, and the result is purely stochastic

$$\mathrm{d}x_t = \sigma \mathrm{d}W_t^x. \tag{6.13}$$

Hence, the conditional expectation of x_t satisfies $\mathbb{E}[x_t|\mathcal{F}_s] = x_s$, which verifies the martingale property. The same argument applies to p_t using Itô's lemma with $\hat{p}$, $\mathrm{d}p_t = \sigma \mathrm{d}W_t^p$. Thus, both x_t and p_t are martingales. □

We now explore the martingale structure of the variances of the observables $\hat{x}$ and $\hat{p}$.

Proposition 6.5. *Let $|\alpha_t\rangle$ evolve according to the stochastic differential equation for Heisenberg-Weyl coherent states in (6.8). Then, the variance processes*

$$\mathrm{Var}_{\alpha_t}(\hat{x}) = \langle \alpha_t|\hat{x}^2|\alpha_t\rangle - \langle \alpha_t|\hat{x}|\alpha_t\rangle^2, \quad \mathrm{Var}_{\alpha_t}(\hat{p}) = \langle \alpha_t|\hat{p}^2|\alpha_t\rangle - \langle \alpha_t|\hat{p}|\alpha_t\rangle^2 \tag{6.14}$$

are constant in time. That is, for all $t \geq 0$, $\mathrm{d}\,\mathrm{Var}_{\alpha_t}(\hat{x}) = \mathrm{d}\,\mathrm{Var}_{\alpha_t}(\hat{p}) = 0$.

Proof. We apply Itô's lemma to compute the differential of the variance of $\hat{x}$

$$\mathrm{dVar}_{\alpha_t}(\hat{x}) \quad = \quad \mathrm{d}\langle \hat{x}^2\rangle_t - 2x_t\,\mathrm{d}x_t - (\mathrm{d}x_t)^2, \tag{6.15}$$

where $x_t = \langle \alpha_t|\hat{x}|\alpha_t\rangle$.

Using Itô's lemma, we compute

$$\mathrm{d}(x_t^2) = 2x_t\,\mathrm{d}x_t + (\mathrm{d}x_t)^2. \tag{6.16}$$

From Proposition 6.4, we have $\mathrm{d}x_t = \sigma\,\mathrm{d}W_t^x$. Therefore, $(\mathrm{d}x_t)^2 = \sigma^2\,\mathrm{d}t$, and:

$$\mathrm{d}(x_t^2) = 2\sigma x_t\,\mathrm{d}W_t^x + \sigma^2\,\mathrm{d}t. \tag{6.17}$$

Substituting into (6.15), we obtain

$$\mathrm{dVar}_{\alpha_t}(\hat{x}) \quad = \quad \left(2\sigma x_t\,\mathrm{d}W_t^x + \sigma^2\,\mathrm{d}t\right) - 2x_t\cdot\sigma\,\mathrm{d}W_t^x - \sigma^2\,\mathrm{d}t = 0. \tag{6.18}$$

Thus, the variance of $\hat{x}$ remains constant in time. A completely analogous computation shows that $\mathrm{d}\,\mathrm{Var}_{\alpha_t}(\hat{p}) = 0$. This confirms that both $\mathrm{Var}_{\alpha_t}(\hat{x})$ and $\mathrm{Var}_{\alpha_t}(\hat{p})$ are preserved under the coherent-state process and are trivially Martingale. □

The preservation of the variances of $\hat{x}$ and $\hat{p}$ under the coherent-state stochastic process has a clear physical meaning. Since coherent states are minimum-uncertainty states that saturate the Heisenberg relation $\Delta\hat{x}\cdot\Delta\hat{p} = \frac{1}{2}$, this result implies that the wavepacket retains its fixed Gaussian shape throughout the evolution.

We will now explore some further properties of the coherent state SDE.

6.3.3 Coherent-state reduction and entropy functionals

Let $\{|\beta\rangle\}_{\beta\in\mathbb{C}}$ denote the standard overcomplete set of Heisenberg-Weyl coherent states. For a time-evolving coherent state $|\alpha_t\rangle$, we define the *coherent-state reduction process*

$$P_t(\beta) = |\langle\beta|\alpha_t\rangle|^2. \tag{6.19}$$

This quantity describes the instantaneous overlap between the current state and a reference coherent state $|\beta\rangle$.

As is well known, the overlap of two coherent states has the closed-form expression (2.12),

$$P_t(\beta) = \exp\left(-|\alpha_t|^2 - |\beta|^2 + \bar{\beta}\alpha_t + \bar{\alpha}_t\beta\right) = \exp\left(-|\alpha_t - \beta|^2\right). \tag{6.20}$$

Thus, $P_t(\beta)$ behaves as a smooth, positive probability-like function on phase space, satisfying

$$\int_{\mathbb{C}} P_t(\beta)\,\mathrm{d}\mu_\beta = 1, \tag{6.21}$$

with $\mathrm{d}\mu_\beta = \frac{1}{\pi}\mathrm{d}^2\beta$, the standard Gaussian measure on phase space.

Since $P_t(\beta)$ depends explicitly on the stochastic process α_t, its evolution is governed by a stochastic differential equation. We now compute this explicitly via Itô's lemma to be

Proposition 6.6.

$$\begin{aligned}\mathrm{d}P_t(\beta) \;=\; & \sqrt{2}\sigma\,\mathrm{Re}\left[\beta - \alpha_t\right]\; P_t(\beta)\,\mathrm{d}W_t^x + \sqrt{2}\sigma\,\mathrm{Im}\left[\beta - \alpha_t\right]\; P_t(\beta)\,\mathrm{d}W_t^p \\ & +\sigma^2\left(-1 + |\alpha_t|^2 + |\beta|^2 - \beta\bar{\alpha}_t - \bar{\beta}\alpha_t\right)\; P_t(\beta)\,\mathrm{d}t.\end{aligned} \tag{6.22}$$

The proof is given in Appendix E.2.4.

To quantify this localisation more systematically, we turn to an information-theoretic perspective by examining the Shannon entropy of $P_t(\beta)$. This provides a natural measure of how the distribution spreads or concentrates under the action of continuous phase-space monitoring. Explicitly

$$S_t = -\int_{\mathbb{C}} P_t(\beta)\log P_t(\beta)\,\mathrm{d}\mu_\beta. \tag{6.23}$$

Substituting (6.20) into (6.23), we obtain

$$S_t = \int_{\mathbb{C}} |\beta - \alpha_t|^2 \exp(-|\beta - \alpha_t|^2)\,\mathrm{d}\mu_\beta. \tag{6.24}$$

Making the change of variables $\gamma = \beta - \alpha_t$, so that $\mathrm{d}\mu_\gamma = \mathrm{d}\mu_\beta$, this becomes

$$S_t = \int_{\mathbb{C}} |\gamma|^2\,\exp(-|\gamma|^2)\,\mathrm{d}\mu_\gamma. \tag{6.25}$$

and this is a standard Gaussian integral over the complex plane. Therefore, the Shannon entropy

evaluates to the constant

$$S_t = 1. \tag{6.26}$$

Although the coherent-state process $|\alpha_t\rangle$ evolves stochastically over time, the transition probability density $P_t(\beta)$ retains a fixed Gaussian profile centered at the moving point α_t. As a result, the shape of $P_t(\beta)$ does not change, only its center drifts in phase space. Since the Shannon entropy measures the spread or uncertainty of a distribution, and this spread remains constant under translations, the entropy S_t remains invariant and is a Martingale.

6.3.4 Lindblad-type evolution for the density matrix

While the stochastic process $|\alpha_t\rangle$ captures the conditioned evolution along a single measurement trajectory, physical predictions typically concern the ensemble behaviour obtained by averaging over all possible realisations of the noise. We therefore consider the ensemble-averaged evolution of the stochastic pure-state process and derive the equation governing the mixed state $\hat{\rho}_t = \mathbb{E}[\,|\alpha_t\rangle\langle\alpha_t|\,]$.

Proposition 6.7. *Let $|\alpha_t\rangle$ be a stochastic process as defined in (6.5). Then $\hat{\rho}_t = \mathbb{E}[|\alpha_t\rangle\langle\alpha_t|]$, satisfies the master equation*

$$\frac{\mathrm{d}\hat{\rho}_t}{\mathrm{d}t} = \sigma^2 \left(\hat{a}^\dagger \hat{\rho}_t \hat{a} + \hat{a} \hat{\rho}_t \hat{a}^\dagger - \frac{1}{2} \left\{ \hat{a}^\dagger \hat{a} + \hat{a}\hat{a}^\dagger, \hat{\rho}_t \right\} \right), \tag{6.27}$$

where $\{\cdot,\cdot\}$ denotes the anti-commutator. This is a Lindblad equation with non-Hermitian Lindblad operators $\hat{a}$ and $\hat{a}^\dagger$, and represents a purely diffusive quantum dynamical semigroup.

Alternatively substituting for $\hat{a}, \hat{a}^\dagger$ in terms of $\hat{q}$ and $\hat{p}$, we find that the Lindblad equation is given by

$$\frac{\mathrm{d}\hat{\rho}_t}{\mathrm{d}t} = \sigma^2 \left(\hat{x} \hat{\rho}_t \hat{x} + \hat{p} \hat{\rho}_t \hat{p}^\dagger - \frac{1}{2} \{ \hat{x}^2 + \hat{p}^2, \hat{\rho}_t \} \right), \tag{6.28}$$

The proof is discussed in Appendix E.2.5. In summary, averaging over stochastic trajectories of the coherent-state process $|\alpha_t\rangle$ recovers the deterministic Lindblad evolution, with the flat geometry of the Heisenberg–Weyl phase space shaping the diffusion in x- and p-quadratures. This establishes the link between individual noisy trajectories and the ensemble description of decoherence.

We now extend this framework beyond flat phase space to non-Abelian settings. In the following sections, we analyse two canonical examples: the compact group $\mathrm{SU}(2)$, whose coherent states describe spin systems on the Bloch sphere, and the noncompact group $\mathrm{SU}(1,1)$, whose coherent states capture squeezing dynamics on the hyperbolic plane.

6.4 Stochastic dynamics on the Bloch sphere: The case of $\mathrm{SU}(2)$

Extending the flat-space analysis to the compact case, we now turn to stochastic dynamics of $\mathrm{SU}(2)$ coherent states, where the label evolves as a diffusion process on the Bloch sphere. In Chapter 3, we showed that iterative POVM measurements drive decoherence in terms of the stereographic coordinate ζ. Here, we develop a complementary description, instead of discrete iterations, we let ζ_t undergo Brownian motion on the sphere and derive the corresponding stochastic differential equation (SDE)

for the evolving state $|\zeta_t\rangle$. This provides a continuous-time unravelling of the measurement-induced dynamics.

6.4.1 Stochastic evolution of SU(2) coherent states

Using the stereographic parameterisation ζ_t from (3.7), we model the effect of continuous phase-space noise as a stochastic process on the Bloch sphere. Each state in the process takes the form

$$|\zeta_t\rangle = \frac{1}{(1+|\zeta_t|^2)^s}\, \mathrm{e}^{\zeta_t \hat{S}_+}|s,-s\rangle, \tag{6.29}$$

where $\zeta_t \in \mathbb{C}\cup\{\infty\} \cong \mathbb{CP}^1$ is now promoted to a time-dependent complex stochastic variable.

We start by explicitly computing the dynamics of the coordinate process ζ_t, viewed as a function of the spherical angles θ_t and ϕ_t, and then later substitute this into the SDE for $|\zeta_t\rangle$.

Proposition 6.8. *Let $\zeta_t = \tan(\theta_t/2)\mathrm{e}^{-\mathrm{i}\phi_t}$ be the stereographic coordinate on the Bloch sphere. Suppose the angles θ_t and ϕ_t evolve according to the stochastic differential equations that describe the Brownian motion on the sphere*

$$\mathrm{d}\theta_t = \sigma\left(\frac{1}{2}\cot\theta_t\,\mathrm{d}t + \mathrm{d}W_t^\theta\right), \quad \mathrm{d}\phi_t = \sigma\left(\frac{1}{\sin\theta_t}\mathrm{d}W_t^\phi\right), \tag{6.30}$$

where $\sigma > 0$ is a strength parameter, and W_t^θ, W_t^ϕ are independent standard Brownian motions. Then the complex process ζ_t satisfies the stochastic differential equation

$$\mathrm{d}\zeta_t = \sigma\frac{(1+|\zeta_t|^2)\zeta_t}{2|\zeta_t|}\left(\mathrm{d}W_t^\theta - \mathrm{i}\,\mathrm{d}W_t^\phi\right). \tag{6.31}$$

This describes a purely noise-driven evolution of the complex coordinate ζ_t on the stereographic chart of the sphere, induced by isotropic Brownian motion on the Bloch sphere.

Proof. Differentiating gives $\zeta_t = \tan\left(\frac{\theta_t}{2}\right)\mathrm{e}^{-\mathrm{i}\phi_t}$ gives

$$\partial_\theta\zeta_t = \frac{1}{2}\sec^2\left(\frac{\theta_t}{2}\right)\mathrm{e}^{-\mathrm{i}\phi_t}, \quad \partial_\phi\zeta_t = -\mathrm{i}\zeta_t, \quad \partial^2_{\theta\theta}\zeta_t = \frac{1}{4}\sec^2\left(\frac{\theta_t}{2}\right)\tan\left(\frac{\theta_t}{2}\right)\mathrm{e}^{-\mathrm{i}\phi_t},$$
$$\partial^2_{\phi\phi}\zeta_t = -\zeta_t, \quad \partial^2_{\theta\phi}\zeta_t = -\frac{\mathrm{i}}{2}\sec^2\left(\frac{\theta_t}{2}\right)\mathrm{e}^{-\mathrm{i}\phi_t}. \tag{6.32}$$

We now apply Itô's lemma to the process ζ_t to obtain

$$\mathrm{d}\zeta_t = \partial_\theta\zeta_t\,\mathrm{d}\theta_t + \partial_\phi\zeta_t\,\mathrm{d}\phi_t + \frac{1}{2}\partial^2_{\theta\theta}\zeta_t\,(\mathrm{d}\theta_t)^2 + \frac{1}{2}\partial^2_{\phi\phi}\zeta_t\,(\mathrm{d}\phi_t)^2 + \partial^2_{\theta\phi}\zeta_t\,\mathrm{d}\theta_t\,\mathrm{d}\phi_t. \tag{6.33}$$

After substituting the trigonometric identities in terms of ζ_t and simplifying, we obtain

$$\mathrm{d}\zeta_t = \frac{1+|\zeta_t|^2}{2}\frac{\zeta_t}{|\zeta_t|}\,\mathrm{d}\theta_t - \mathrm{i}\zeta_t\,\mathrm{d}\phi_t + \frac{(1+|\zeta_t|^2)\zeta_t}{4}\,(\mathrm{d}\theta_t)^2 - \frac{\zeta_t}{2}\,(\mathrm{d}\phi_t)^2 - \mathrm{i}(1+|\zeta_t|^2)\frac{\zeta_t}{|\zeta_t|}\,\mathrm{d}\theta_t\,\mathrm{d}\phi_t. \tag{6.34}$$

Substitute the expressions for $\mathrm{d}\theta_t$ and $\mathrm{d}\phi_t$ from (6.30), and collect all $\mathrm{d}t, \mathrm{d}W_t^\theta$, and $\mathrm{d}W_t^\phi$ terms. This yields the final form in (6.31). □

Immediately from the above proposition, we can calculate the following Itô's identities

$$(\mathrm{d}\zeta_t)^2 = 0, \quad (\mathrm{d}\bar{\zeta}_t)^2 = 0, \quad \mathrm{d}\zeta_t\,\mathrm{d}\bar{\zeta}_t = \sigma^2\frac{(1+|\zeta_t|^2)^2}{2}\,\mathrm{d}t. \tag{6.35}$$

Before deriving the stochastic differential equation for the coherent-state stochastic process $|\zeta_t\rangle$, it is convenient to establish a pair of algebraic identities satisfied by $\mathrm{SU}(2)$ coherent states. These relations, already implicit in the representation-theoretic construction of coherent states discussed in Chapter 3, will greatly simplify the subsequent computations.

Lemma 6.2. Let $|\zeta_t\rangle$ be the normalised $\mathrm{SU}(2)$ coherent state as in (6.29), then the following operator identity holds

$$\left(\hat{S}_- + 2\zeta_t\hat{S}_z - \zeta_t^2\hat{S}_+\right)|\zeta_t\rangle = 0. \tag{6.36}$$

Lemma 6.3. Let $|\zeta_t\rangle$ be the normalised $\mathrm{SU}(2)$ coherent state defined by (6.29), then the following identity holds

$$\left(\hat{S}_+\zeta_t + \hat{S}_-\bar{\zeta}_t + |\zeta_t|^2\hat{S}_z\right)|\zeta_t\rangle = \left(\hat{S}_z + s(1+|\zeta_t|^2)\right)|\zeta_t\rangle. \tag{6.37}$$

The proofs are discussed in Appendix E.2.6, E.2.7. These lemmas encapsulate the way the Lie algebra generators act on the coherent-state manifold parametrised by $\zeta_t \in \mathbb{CP}^1$.

Using Lemmas 6.2 and 6.3, we can simplify the action of the $\mathrm{SU}(2)$ generators on the coherent state and thereby obtain the stochastic differential equation governing the process $|\zeta_t\rangle$

Proposition 6.9.

$$\begin{aligned}\mathrm{d}|\zeta_t\rangle \;=\; & -\frac{\sigma^2}{4}\left(\hat{S}_-\hat{S}_+ + \hat{S}_+\hat{S}_- + 2\hat{S}_z^2 + 2s\hat{S}_z(1+|\zeta_t|^2)\right)|\zeta_t\rangle\,\mathrm{d}t + \sigma\left(\frac{\hat{S}_+\zeta_t - \hat{S}_-\bar{\zeta}_t}{2|\zeta_t|}\right)\mathrm{d}W_t^\theta\,|\zeta_t\rangle \\ & -\sigma\left(\frac{\mathrm{i}(\hat{S}_+\zeta_t + \hat{S}_-\bar{\zeta}_t) + 2\mathrm{i}|\zeta_t|^2\hat{S}_z}{2|\zeta_t|}\right)\mathrm{d}W_t^\phi\,|\zeta_t\rangle.\end{aligned} \tag{6.38}$$

The proof is given in Appendix E.2.8. The stochastic differential equation above describes the evolution of an $\mathrm{SU}(2)$ coherent state subject to classical noise in the angular coordinates θ_t and ϕ_t. As in the Heisenberg-Weyl case, the dynamics remain confined to the projective Hilbert space trajectory i.e. the evolution is always tangent to the coherent-state manifold, with no component orthogonal to it. This allows the process to be viewed as a quantum analogue of classical diffusion on a curved phase space.

Equivalently in terms of the Hermitian generators $\hat{S}_x, \hat{S}_y, \hat{S}_z$, the SDE for the coherent state process is given by

$$\begin{aligned}\mathrm{d}|\zeta_t\rangle \;=\; & -\frac{\sigma^2}{2}\left(\hat{S}_x^2 + \hat{S}_y^2 + \hat{S}_z^2 + s\hat{S}_z(1+|\zeta_t|^2)\right)|\zeta_t\rangle\,\mathrm{d}t + \sigma\left(\frac{\hat{S}_x(\zeta_t-\bar{\zeta}_t) - \mathrm{i}\hat{S}_y(\zeta_t+\bar{\zeta}_t)}{2|\zeta_t|}\right)\mathrm{d}W_t^\theta\,|\zeta_t\rangle \\ & -\sigma\left(\frac{\mathrm{i}(\hat{S}_x(\zeta_t+\bar{\zeta}_t) + \mathrm{i}\hat{S}_y(\zeta_t-\bar{\zeta}_t)) + 2\mathrm{i}|\zeta_t|^2\hat{S}_z}{2|\zeta_t|}\right)\mathrm{d}W_t^\phi\,|\zeta_t\rangle.\end{aligned} \tag{6.39}$$

We note that the stochastic differential equation obtained here differs in structure from the stochastic Schrödinger equation with $\hat{S}_x, \hat{S}_y, \hat{S}_z$ as Lindblad operators. In our formulation, the noise is encoded in the stochastic evolution of the coherent-state label ζ_t, which directly parameterises the state $|\zeta_t\rangle$. By contrast, the SSE with spin operators involves operator-valued noise terms acting on a fixed Hilbert-space basis, without reference to the geometric coordinate ζ_t on the Bloch sphere.

A key feature of this evolution is that it preserves the norm of the state vector. That is, $\frac{\mathrm{d}}{\mathrm{d}t}\langle\zeta_t|\zeta_t\rangle = 0$, which follows from the structure of the SDE and reflects the unitarity of the underlying group action.

6.4.2 Martingale structure of $\mathrm{SU}(2)$ observables

We now investigate the Martingale structrue of the expectation values of the $\mathrm{SU}(2)$ spin observables $\hat{S}_x, \hat{S}_y, \hat{S}_z$, under the stochastic evolution of the coherent state $|\zeta_t\rangle$, driven by Brownian motion on the Bloch sphere.

Proposition 6.10. *Let $|\zeta_t\rangle$ be a stochastic $\mathrm{SU}(2)$ coherent-state process. Then, the processes $\langle\hat{S}_x\rangle_t$, $\langle\hat{S}_y\rangle_t$, $\langle\hat{S}_z\rangle_t$ are not, in general, martingales.*

Proof. Instead of applying Itô's lemma directly to the expectation values $\langle\zeta_t|\hat{S}_a|\zeta_t\rangle$, we exploit the geometric structure of the coherent states and the simplified form of the SDE for ζ_t. The expectation values of the generators $\hat{S}_x, \hat{S}_y, \hat{S}_z$ are given by [35]

$$\langle\zeta_t|\hat{S}_x|\zeta_t\rangle = s\,\frac{\zeta_t+\bar{\zeta}_t}{1+|\zeta_t|^2}, \qquad \langle\zeta_t|\hat{S}_y|\zeta_t\rangle = s\,\frac{\zeta_t-\bar{\zeta}_t}{\mathrm{i}(1+|\zeta_t|^2)}, \qquad \langle\zeta_t|\hat{S}_z|\zeta_t\rangle = s\,\frac{1-|\zeta_t|^2}{1+|\zeta_t|^2}. \tag{6.40}$$

Let us define

$$f(\zeta_t,\bar{\zeta}_t) = \frac{\zeta_t+\bar{\zeta}_t}{1+|\zeta_t|^2}. \tag{6.41}$$

We compute $\mathrm{d}f(\zeta_t,\bar{\zeta}_t)$ using Itô's lemma for functions of complex variables as

$$\mathrm{d}f(\zeta_t,\bar{\zeta}_t) = \frac{\partial f}{\partial\zeta_t}\,\mathrm{d}\zeta_t + \frac{\partial f}{\partial\bar{\zeta}_t}\,\mathrm{d}\bar{\zeta}_t + \frac{\partial^2 f}{\partial\zeta_t\partial\bar{\zeta}_t}\,\mathrm{d}\zeta_t\,\mathrm{d}\bar{\zeta}_t, \tag{6.42}$$

as all the other terms are zero because of (6.35).

We now compute the partial derivatives

$$\frac{\partial f}{\partial\zeta_t} = \frac{1-(\bar{\zeta}_t)^2}{(1+|\zeta_t|^2)^2}, \qquad \frac{\partial f}{\partial\bar{\zeta}_t} = \frac{1-\zeta_t^2}{(1+|\zeta_t|^2)^2}, \qquad \frac{\partial^2 f}{\partial\zeta_t\partial\bar{\zeta}_t} = \frac{-2(\zeta_t+\bar{\zeta}_t)}{(1+|\zeta_t|^2)^3}. \tag{6.43}$$

Substituting the expressions and simplifying, the full stochastic differential for $\langle\hat{S}_x\rangle_t = s\,f(\zeta_t,\bar{\zeta}_t)$ is

$$\mathrm{d}\langle\hat{S}_x\rangle_t = \frac{s\sigma\left(1-|\zeta_t|^2\right)}{2|\zeta_t|(1+|\zeta_t|^2)}(\zeta_t+\bar{\zeta}_t)\,\mathrm{d}W_t^{\theta} + \frac{\mathrm{i}s\sigma}{2|\zeta_t|}(-\zeta_t+\bar{\zeta}_t)\,\mathrm{d}W_t^{\phi} - \sigma^2 s\frac{\zeta_t+\bar{\zeta}_t}{1+|\zeta_t|^2}\,\mathrm{d}t. \tag{6.44}$$

Hence, $\langle\hat{S}_x\rangle_t$ evolves stochastically with a nonzero drift, proportional to $(\zeta_t+\bar{\zeta}_t)/(1+|\zeta_t|^2)$, and therefore is not a martingale.

Similarly $\langle \hat{S}_y \rangle_t$ is calculated to be

$$\mathrm{d}\langle \hat{S}_y \rangle_t = \frac{s\sigma(1-|\zeta_t|^2)}{2\mathrm{i}(1+|\zeta_t|^2)|\zeta_t|}(\zeta_t - \bar{\zeta}_t)\,\mathrm{d}W_t^{\theta} - \frac{s\sigma}{2|\zeta_t|}(\zeta_t + \bar{\zeta}_t)\,\mathrm{d}W_t^{\phi} - \sigma^2 s\frac{\zeta_t - \bar{\zeta}_t}{\mathrm{i}(1+|\zeta_t|^2)}\,\mathrm{d}t. \tag{6.45}$$

and finally $\langle \hat{S}_z \rangle_t$

$$\mathrm{d}\langle \hat{S}_z \rangle_t = \frac{-2s\sigma|\zeta_t|}{(1+|\zeta_t|^2)}\mathrm{d}W_t^{\theta} - \sigma^2 s\frac{(1-|\zeta_t|^2)}{1+|\zeta_t|^2}\,\mathrm{d}t. \tag{6.46}$$

The drift terms are nonzero and hence $\langle \hat{S}_y \rangle_t$, and $\langle \hat{S}_z \rangle_t$ are not martingales. □

The sign and magnitude of the drift depend explicitly on the complex stereographic coordinate ζ_t. Specifically, for $\langle \hat{S}_x \rangle_t$ and $\langle \hat{S}_y \rangle_t$, the drift is proportional to the real and imaginary parts of ζ_t (through $\zeta_t + \bar{\zeta}_t$ and $\zeta_t - \bar{\zeta}_t$, respectively), while for $\langle \hat{S}_z \rangle_t$, the drift is proportional to $1 - |\zeta_t|^2$, corresponding to the radial distance from the north pole on the Bloch sphere. As a result, near the equator of the sphere (where $|\zeta_t| \approx 1$), the drift term in $\langle \hat{S}_z \rangle_t$ approximately vanishes, making it behave almost like a martingale. Similarly, $\langle \hat{S}_x \rangle_t$ and $\langle \hat{S}_y \rangle_t$ approach martingale behavior when the real or imaginary parts of ζ_t are small. In general, depending on the region of the sphere, these observables may behave either as submartingales (if the drift is positive) or supermartingales (if the drift is negative).

This behaviour contrasts with the standard stochastic Schrödinger equation (SSE) formulation, where the expectation values of observables are true martingales. Here, in the coherent-state reduction, the drift terms survive, so the observables only approximate martingale behaviour in special regions of the Bloch sphere. This situation also contrasts with the Heisenberg-Weyl case, where the position and momentum observables $\hat{x}$ and $\hat{p}$ evolved exactly as true martingales under the coherent-state stochastic process, with no drift terms. These distinctions underlie that the geometry of the coherent-state manifold modifies the stochastic structure of quantum trajectories, leading to curvature-dependent deviations from the SSE picture.

In contrast, the Casimir operator $\hat{S}^2$ remains constant in time as $\langle \zeta_t | \hat{S}^2 | \zeta_t \rangle = s(s+1)$, and is trivially a martingale, reflecting the conservation of total spin under the stochastic evolution.

Proposition 6.11. *Let $|\zeta_t\rangle$ be a $\mathrm{SU}(2)$ coherent-state process evolving according to (6.38). Then, at any time t, the variances of the spin operators $\hat{S}_x, \hat{S}_y, \hat{S}_z$ satisfy the relations*

$$\mathrm{Var}_{\zeta_t}(\hat{S}_x) = \mathrm{Var}_{\zeta_t}(\hat{S}_y) = \mathrm{Var}_{\zeta_t}(\hat{S}_z) \quad = \tfrac{s}{2}. \tag{6.47}$$

Proof. For any generator $\hat{S}_a$ (with $a = x, y, z$) of the $\mathrm{SU}(2)$ Lie algebra, the variance in a coherent state is defined as

$$\mathrm{Var}_{\zeta_t}(\hat{S}_a) = \langle \zeta_t | \hat{S}_a^2 | \zeta_t \rangle - \Big(\langle \zeta_t | \hat{S}_a | \zeta_t \rangle \Big)^2. \tag{6.48}$$

It is a known property of $\mathrm{SU}(2)$ coherent states that [35]

$$\langle \zeta_t | \hat{S}_a^2 | \zeta_t \rangle = \Big(\langle \zeta_t | \hat{S}_a | \zeta_t \rangle \Big)^2 + \frac{s}{2}, \tag{6.49}$$

where s is the spin quantum number. Substituting into the variance formula gives

$$\mathrm{Var}_{\zeta_t}(\hat{S}_a) = \frac{s}{2}. \tag{6.50}$$

Thus, the variance of each spin component is constant in time and equal to $s/2$, independent of the specific coherent state $|\zeta_t\rangle$. □

Since the variances $\mathrm{Var}_{\zeta_t}(\hat{S}_x)$, $\mathrm{Var}_{\zeta_t}(\hat{S}_y)$, and $\mathrm{Var}_{\zeta_t}(\hat{S}_z)$ are constant in time and equal to $s/2$, they are trivially martingales under the stochastic evolution of the coherent state, $|\zeta_t\rangle$.

6.4.3 Coherent-state reduction and information flow

We now turn to the overlap of SU(2) coherent states, viewed as a stochastic process. For a spin-s system, the overlap between two coherent states $|\zeta\rangle$ and $|\zeta'\rangle$, given in (3.12), defines the transition probability amplitude between different points on the Bloch sphere. From this, we construct the associated probability density, which encodes the coherent-state reduction of the stochastic dynamics to the phase-space level.

$$P_t(\xi) = |\langle\xi|\zeta_t\rangle|^2 = \left(\frac{|1+\bar{\xi}\zeta_t|^2}{(1+|\zeta_t|^2)(1+|\xi|^2)}\right)^{2s}. \tag{6.51}$$

This function $P_t(\xi)$ defines a transition probability kernel on S^2, peaked around $\xi = \zeta_t$, and exhibits Gaussian behavior in the large-s limit. It describes the probability of finding a coherent state near ξ given that it was initially peaked at ζ_t.

Proposition 6.12. *The overlap probability density satisfies the following SDE*

$$\begin{aligned} \mathrm{d}P_t(\xi) \;=\; & \frac{s\sigma P_t(\xi)}{|\zeta_t|}\left(\frac{(\bar{\xi}-\bar{\zeta}_t)\zeta_t}{(1+\zeta_t\bar{\xi})}+\frac{(\xi-\zeta_t)\bar{\zeta}_t}{(1+\bar{\zeta}_t\xi)}\right)\mathrm{d}W_t^{\theta} + \frac{\mathrm{i}s\sigma P_t(\xi)}{|\zeta_t|}\left(-\frac{(\bar{\xi}-\bar{\zeta}_t)\zeta_t}{(1+\zeta_t\bar{\xi})}+\frac{(\xi-\zeta_t)\bar{\zeta}_t}{(1+\bar{\zeta}_t\xi)}\right)\mathrm{d}W_t^{\phi} \\ & +\sigma^2 s P_t(\xi)\left(\frac{(\xi-\zeta_t)(\bar{\xi}-\bar{\zeta}_t)}{(1+\bar{\xi}\zeta_t)(1+\xi\bar{\zeta}_t)}-1\right)\mathrm{d}t \end{aligned} \tag{6.52}$$

then the right-hand side is completely explicit in $\zeta_t, \bar{\zeta}_t$ via the formulas above.

Proof. We apply the complex version of Itô's lemma on $P_t(\xi)$ to get

$$\mathrm{d}P_t(\xi) = \partial_{\zeta_t}P_t(\xi)\,\mathrm{d}\zeta_t + \partial_{\bar{\zeta}_t}P_t(\xi)\,\mathrm{d}\bar{\zeta}_t + \partial^2_{\zeta_t\bar{\zeta}_t}P_t(\xi)\,\mathrm{d}\zeta_t\,\mathrm{d}\bar{\zeta}_t, \tag{6.53}$$

where the other terms are zero because of (6.35). Taking the derivatives of $P_t(\xi)$ we get

$$\begin{aligned} \frac{\partial P_t(\xi)}{\partial\zeta_t} &= 2sP_t(\xi)\frac{(\bar{\xi}-\bar{\zeta}_t)}{(1+|\zeta_t|^2)(1+\bar{\xi}\zeta_t)}, \\ \frac{\partial P_t(\xi)}{\partial\zeta_t} &= 2sP_t(\xi)\frac{(\xi-\zeta_t)}{(1+|\zeta_t|^2)(1+\xi\bar{\zeta}_t)}, \\ \frac{\partial^2 P_t(\xi)}{\partial\zeta_t\partial\bar{\zeta}_t} &= \frac{2sP_t(\xi)}{(1+|\zeta_t|^2)^2}\left(\frac{(\xi-\zeta_t)(\bar{\xi}-\bar{\zeta}_t)}{(1+\xi\bar{\zeta}_t)(1+\bar{\xi}\zeta_t)}-1\right). \end{aligned} \tag{6.54}$$

Substituting (6.31) into (6.53) we get the desired result. □

This stochastic differential equation makes explicit how the overlap probability density evolves under Brownian motion of the coherent-state label. The noise terms describe random fluctuations induced by the underlying angular diffusion, while the drift term encodes the deterministic damping and spreading of $P_t(\xi)$. Together, these effects drive the overlap distribution toward uniformity on the sphere, reflecting the approach to the maximally mixed state under continuous monitoring.

We now turn to a global measure of information loss by studying the associated Shannon entropy process, which quantifies how continuous monitoring drives the system toward classicality.

Proposition 6.13. *Let $(\zeta_t)_{t\geq 0}$ be a stochastic process on the Bloch sphere, and define*

$$S_t \;=\; -\int_{S^2} P_t(\xi)\,\log P_t(\xi)\,\mathrm{d}\mu^s_\xi, \tag{6.55}$$

where $\mathrm{d}\mu^s_\xi = \frac{2s+1}{\pi}\frac{1}{(1+|\xi|^2)^2}\mathrm{d}^2\xi$. Then

$$S_t = \frac{2s}{2s+1} \tag{6.56}$$

for all t, hence $(S_t)_{t\geq 0}$ is constant and therefore a martingale with respect to any filtration.

Proof. Rotational invariance implies that $P_t(\zeta)$ depends only on the angular separation $\theta \in [0,\pi]$ between ξ and ζ_t and so

$$P_t(\xi) = \Big(\cos^2\frac{\theta}{2}\Big)^{2s} \;=\; \Big(\frac{1+\cos\theta}{2}\Big)^{2s}. \tag{6.57}$$

Substituting this in the integral for Shannon entropy, we obtain

$$S_t = -\frac{2s+1}{2}\int_0^\pi \sin\theta\,\Big(\frac{1+\cos\theta}{2}\Big)^{2s}\log\Big(\frac{1+\cos\theta}{2}\Big)^{2s}\,\mathrm{d}\theta. \tag{6.58}$$

With the substitution $u = \frac{1+\cos\theta}{2} \in [0,1]$ (so that $\sin\theta\,\mathrm{d}\theta = -2\,\mathrm{d}u$), we get

$$S_t \;=\; -(2s+1)\,2s\int_0^1 u^{2s}\,\log u\,\mathrm{d}u. \tag{6.59}$$

Using $\displaystyle\int_0^1 u^a\log u\,\mathrm{d}u = -\frac{1}{(a+1)^2}$ for $a>-1$, we obtain

$$S_t \;=\; -(2s+1)\,2s\left(-\frac{1}{(2s+1)^2}\right) \;=\; \frac{2s}{2s+1}. \tag{6.60}$$

This value is independent of ζ_t and of t, completing the proof. □

Thus, the entropy process remains constant and is a Martingale, throughout the stochastic evolution, highlighting that while individual trajectories fluctuate, the informational content of the overlap distribution is preserved under $\mathrm{SU}(2)$-covariant noise.

6.4.4 Lindblad-type evolution for the $\mathrm{SU}(2)$ density matrix

Having established the Itô SDE governing the evolution of the $\mathrm{SU}(2)$ coherent state vector $|\zeta_t\rangle$ under stochastic motion on the Bloch sphere, we now lift this trajectory to the level of the density matrix. In particular, we are interested in the ensemble-averaged evolution $\hat{\rho}_t = \mathbb{E}[|\zeta_t\rangle\langle\zeta_t|]$.

Proposition 6.14. *The expectation value of the outer product of the coherent-state SDE in (6.38) satisfies the following Lindblad-type master equation*

$$\begin{aligned}\frac{\mathrm{d}\hat{\rho}_t}{\mathrm{d}t} &= \sigma^2\left(\frac{\hat{S}_+}{\sqrt{2}}\hat{\rho}_t\frac{\hat{S}_-}{\sqrt{2}} + \frac{\hat{S}_-}{\sqrt{2}}\hat{\rho}_t\frac{\hat{S}_+}{\sqrt{2}} + \hat{S}_z\hat{\rho}_t\hat{S}_z\right)\\ &\quad -\frac{\sigma^2}{2}\left(\frac{\hat{S}_+\hat{S}_-}{2}\hat{\rho}_t + \frac{\hat{S}_-\hat{S}_+}{2}\hat{\rho}_t + \hat{S}_z^2\hat{\rho}_t + \hat{\rho}_t\hat{S}_z^2 + \hat{\rho}_t\frac{\hat{S}_+\hat{S}_-}{2} + \hat{\rho}_t\frac{\hat{S}_-\hat{S}_+}{2}\right).\end{aligned} \tag{6.61}$$

The proof is detailed in Appendix E.2.9. This equation captures the dissipative dynamics of a quantum spin system undergoing angular noise on the Bloch sphere. The effective Lindblad operators $\frac{\hat{S}_+}{\sqrt{2}}, \frac{\hat{S}_-}{\sqrt{2}}, \hat{S}_z$ reflect the fundamental $\mathrm{SU}(2)$ symmetries, with each term describing a decoherence channel aligned with the structure of the Lie algebra. This equation can also be written using the Lindblad operators $\hat{S}_x, \hat{S}_y$ and $\hat{S}_z$.

While each trajectory $|\zeta_t\rangle$ remains confined to the coherent-state manifold, the ensemble average $\hat{\rho}_t$ typically lies outside this manifold due to its nonlinear and nonconvex geometry. As a result, $\hat{\rho}_t$ is generally a mixed state. Nevertheless, the evolution of $\hat{\rho}_t$ preserves the underlying symmetry, i.e., the master equation is built entirely from $\mathrm{SU}(2)$ generators, faithfully encoding the geometry and algebraic structure of the coherent-state framework.

6.5 Stochastic dynamics on the hyperbolic plane: The case of $\mathrm{SU}(1,1)$

We now turn to the stochastic dynamics of $\mathrm{SU}(1,1)$ coherent states (see Chapter 5) under time-dependent noise in the parameters τ_t and ϕ_t. These parameters evolve stochastically on the upper sheet of the hyperbolic plane, and the corresponding coherent state vector remains confined to the manifold of $\mathrm{SU}(1,1)$ coherent states.

6.5.1 Stochastic evolution of $\mathrm{SU}(1,1)$ coherent states

We define the stochastic process $\{\chi_t\}_{t\geq 0}$ by

$$\chi_t = \tanh\left(\frac{\tau_t}{2}\right)\mathrm{e}^{-\mathrm{i}\phi_t}, \tag{6.62}$$

and the associated time-dependent coherent state as

$$|\chi_t\rangle = (1-|\chi_t|^2)^k \exp(\chi_t\hat{K}_+)|k,k\rangle. \tag{6.63}$$

The derivational framework parallels the $\mathrm{SU}(2)$ case discussed in the previous section, and we therefore omit detailed intermediate steps that are formally analogous. Instead, we highlight the key structural differences, present the resulting stochastic differential equations, and derive the corresponding Lindblad-type master equation. Full proofs of the intermediate lemmas and operator identities are

given in Appendix E.

Similar to the $\mathrm{SU}(2)$ case it can be shown that the coherent-state label evolves as

$$\mathrm{d}\chi_t = \sigma \frac{(1-|\chi_t|^2)^2 \chi_t}{2|\chi_t|}(\mathrm{d}W_t^\tau - \mathrm{i}\,\mathrm{d}W_t^\phi). \tag{6.64}$$

We calculate the Itô products, $\mathrm{d}\chi_t \mathrm{d}\bar{\chi}_t, \mathrm{d}\bar{\chi}_t \mathrm{d}\bar{\chi}_t$ and $\mathrm{d}\chi_t \mathrm{d}\chi_t$ to be

$$\mathrm{d}\chi_t \mathrm{d}\bar{\chi}_t = \sigma^2 \left(\frac{(1-|\chi_t|^2)^2}{2}\right)\mathrm{d}t, \quad \mathrm{d}\bar{\chi}_t \mathrm{d}\bar{\chi}_t = 0, \quad \mathrm{d}\chi_t \mathrm{d}\chi_t = 0. \tag{6.65}$$

We will now proceed to derive the SDE for the coherent state vector in (6.62). Similar to the $\mathrm{SU}(2)$ case we use the following identities

Lemma 6.4.

$$(\hat{K}_- - 2\chi_t \hat{K}_z + \chi_t^2 \hat{K}_+)\,|\chi_t\rangle = 0 \tag{6.66}$$

Lemma 6.5.

$$(\hat{K}_+ \chi_t + \hat{K}_- \bar{\chi}_t - |\chi_t|^2 \hat{K}_z)\,|\chi_t\rangle = (\hat{K}_z - k(1-|\chi_t|^2))\,|\chi_t\rangle\,. \tag{6.67}$$

The proofs of these results follow from a direct application of the Baker-Campbell-Hausdorff (BCH) formula, together with the $\mathfrak{su}(1,1)$ commutation relations and are detailed in Appendix E.2.10, E.2.11. Specifically, one can use the disentangled form of the $\mathrm{SU}(1,1)$ coherent state and systematically commute the generators to bring the operators to normal-ordered forms.

Using the identities and Itô's lemma, we can derive the coherent-state SDE to be

Proposition 6.15.

$$\begin{aligned}\mathrm{d}|\chi_t\rangle \;=\; & -\frac{\sigma^2}{4}\left(\hat{K}_-\hat{K}_+ + \hat{K}_+\hat{K}_- - 2\hat{K}_z^2 + 2k\hat{K}_z(1-|\chi_t|^2)\right)|\chi_t\rangle\,\mathrm{d}t + \sigma\left(\frac{\hat{K}_+\chi_t - \hat{K}_-\bar{\chi}_t}{2|\chi_t|}\right)\mathrm{d}W_t^\tau\,|\chi_t\rangle \\ & -\sigma\left(\frac{\mathrm{i}(\hat{K}_+\chi_t + \hat{K}_-\bar{\chi}_t)}{2|\chi_t|} - \frac{\mathrm{i}|\chi_t|^2\hat{K}_z}{|\chi_t|}\right)\mathrm{d}W_t^\phi\,|\chi_t\rangle.\end{aligned} \tag{6.68}$$

The proof is in Appendix E.2.12. Equation (6.68) describes the stochastic evolution of an $\mathrm{SU}(1,1)$ coherent state $|\chi_t\rangle$ under classical noise in the hyperbolic angular coordinates τ_t and ϕ_t. The complex parameter χ_t undergoes stochastic motion on the Poincaré disk, reflecting the hyperbolic geometry of the $\mathrm{SU}(1,1)$ phase space. Equivalently the SDE can be written in terms of $\hat{K}_x, \hat{K}_y, \hat{K}_z$ to be

$$\begin{aligned}\mathrm{d}|\chi_t\rangle \;=\; & -\frac{\sigma^2}{2}\left(\hat{K}_x^2 + \hat{K}_y^2 - \hat{K}_z^2 + 2k\hat{K}_z(1-|\chi_t|^2)\right)|\chi_t\rangle\,\mathrm{d}t + \sigma\left(\frac{\mathrm{i}\hat{K}_x(\chi_t+\bar{\chi}_t) - \hat{K}_y(\chi_t-\bar{\chi}_t)}{2|\chi_t|}\right)\mathrm{d}W_t^\tau\,|\chi_t\rangle \\ & -\sigma\left(\frac{(\hat{K}_x(\bar{\chi}_t-\chi_t) - \mathrm{i}\hat{K}_y(\chi_t+\bar{\chi}_t))}{2|\chi_t|} - \frac{\mathrm{i}|\chi_t|^2\hat{K}_z}{|\chi_t|}\right)\mathrm{d}W_t^\phi\,|\chi_t\rangle.\end{aligned} \tag{6.69}$$

The evolution preserves the norm of the state and is confined to the coherent-state manifold due to

the group-theoretic structure. Noise terms account for angular diffusion, while drift terms represent deterministic dynamics such as external driving or weak continuous measurements.

6.5.2 Martingale structure of $\mathrm{SU}(1,1)$ observables

We now analyse the stochastic evolution of the expectation values of the $\mathrm{SU}(1,1)$ Lie algebra generators $\hat{K}_x, \hat{K}_y, \hat{K}_z$ under the coherent-state process $|\chi_t\rangle$.

Proposition 6.16. *Let $|\chi_t\rangle$ be a stochastic $\mathrm{SU}(1,1)$ coherent-state process evolving under the simplified SDE (6.64). Then, the expectation value processes*

$$\langle \hat{K}_x \rangle_t, \quad \langle \hat{K}_y \rangle_t, \quad \langle \hat{K}_z \rangle_t \tag{6.70}$$

are not, in general, martingales.

Proof. The expectation values of the generators $\hat{K}_x, \hat{K}_y, \hat{K}_z$ in the state $|\chi_t\rangle$ are given by [35]

$$\langle \chi_t | \hat{K}_x | \chi_t \rangle = k \, \frac{\chi_t + \bar{\chi}_t}{1 - |\chi_t|^2}, \qquad \langle \chi_t | \hat{K}_y | \chi_t \rangle = k \, \frac{\chi_t - \bar{\chi}_t}{\mathrm{i}(1 - |\chi_t|^2)}, \qquad \langle \chi_t | \hat{K}_z | \chi_t \rangle = k \, \frac{1 + |\chi_t|^2}{1 - |\chi_t|^2}. \tag{6.71}$$

We analyse the martingale structure by computing the Itô differential of the observable $\langle \hat{K}_x \rangle_t$. Let us define the real-valued function

$$f(\chi_t, \bar{\chi}_t) = \langle \hat{K}_x \rangle_t = \frac{\chi_t + \bar{\chi}_t}{1 - |\chi_t|^2}, \tag{6.72}$$

and apply Itô's lemma for functions of complex variables

$$\mathrm{d}f = \frac{\partial f}{\partial \chi_t} \mathrm{d}\chi_t + \frac{\partial f}{\partial \bar{\chi}_t} \mathrm{d}\bar{\chi}_t + \frac{1}{2} \left(2 \frac{\partial^2 f}{\partial \chi_t \partial \bar{\chi}_t} \mathrm{d}\chi_t \mathrm{d}\bar{\chi}_t \right). \tag{6.73}$$

We compute the partial derivatives

$$\frac{\partial f}{\partial \chi_t} = \frac{1 + (\bar{\chi}_t)^2}{(1 - |\chi_t|^2)^2}, \quad \frac{\partial f}{\partial \bar{\chi}_t} = \frac{1 + \chi_t^2}{(1 - |\chi_t|^2)^2}, \quad \frac{\partial^2 f}{\partial \chi_t \partial \bar{\chi}_t} = \frac{2(\chi_t + \bar{\chi}_t)}{(1 - |\chi_t|^2)^3}. \tag{6.74}$$

Now substituting the expression for $\mathrm{d}\chi_t$ and its complex conjugate, we obtain a stochastic differential for $\langle \hat{K}_x \rangle_t = k \, f(\chi_t, \bar{\chi}_t)$ of the form

$$\mathrm{d}\langle \hat{K}_x \rangle_t = \frac{k\sigma}{2|\chi_t|} \left(\frac{(\chi_t + \bar{\chi}_t)(1 + |\chi_t|^2)}{(1 - |\chi_t|^2)} \right) \mathrm{d}W_t^\tau + \frac{k\sigma \mathrm{i}}{2|\chi_t|} (\bar{\chi}_t - \chi_t) \, \mathrm{d}W_t^\phi + k\sigma^2 \, \frac{(\chi_t + \bar{\chi}_t)}{(1 - |\chi_t|^2)} \, \mathrm{d}t. \tag{6.75}$$

This reveals a nonzero drift term, proportional to $\chi_t + \bar{\chi}_t$, and hence $\langle \hat{K}_x \rangle_t$ is not a martingale.

A similar computation reveals

$$\mathrm{d}\langle \hat{K}_y \rangle_t \quad = \quad \frac{k\sigma(1 + |\chi_t|^2)}{2\mathrm{i}(1 - |\chi_t|^2)|\zeta_t|} (\chi_t - \bar{\chi}_t) \, \mathrm{d}W_t^\tau - \frac{k\sigma}{2|\chi_t|} (\chi_t + \bar{\chi}_t) \, \mathrm{d}W_t^\phi + \sigma^2 k \frac{\chi_t - \bar{\chi}_t}{\mathrm{i}(1 - |\chi_t|^2)} \, \mathrm{d}t, \tag{6.76}$$

and finally $\langle \hat{K}_z \rangle_t$

$$\mathrm{d}\langle \hat{K}_z \rangle_t = \frac{2k\sigma|\chi_t|}{(1 - |\chi_t|^2)} \mathrm{d}W_t^\tau + \sigma^2 k \frac{(1 + |\chi_t|^2)}{1 - |\zeta_t|^2} \, \mathrm{d}t. \tag{6.77}$$

In all cases, the presence of a deterministic drift confirms that none of these expectation processes is a martingale. □

As in the $\mathrm{SU}(2)$ case, none of the expectation values of the generators define martingale processes as each evolution equation contains a deterministic drift term. However, the structure of this drift depends sensitively on the underlying geometry. On the Bloch sphere (compact $\mathrm{SU}(2)$ case) the drift reflects the positive curvature, while on the Poincaré disk (noncompact $\mathrm{SU}(1,1)$ case) it reflects the negative curvature. Thus, although martingale behaviour is absent in both settings, the way stochastic fluctuations combine with deterministic drift encodes the curvature and symmetry of the phase-space manifold.

Proposition 6.17. *Let $|\chi_t\rangle$ be a stochastic $\mathrm{SU}(1,1)$ coherent-state process, and let $\hat{K}_j \in \{\hat{K}_x, \hat{K}_y, \hat{K}_z\}$ be any of the generators of $\mathfrak{su}(1,1)$. Then, the quantum variance of $\hat{K}_j$ in the state $|\chi_t\rangle$,*

$$\mathrm{Var}_{\chi_t}(\hat{K}_j) = \langle\chi_t|\hat{K}_j^2|\chi_t\rangle - \langle\chi_t|\hat{K}_j|\chi_t\rangle^2, \tag{6.78}$$

is constant in time and satisfies

$$\mathrm{Var}_{\chi_t}(\hat{K}_j) = \frac{k}{2}, \quad \textit{for all } t \geq 0. \tag{6.79}$$

This follows from the known formula for variances of $\mathrm{SU}(1,1)$ observables [35]. Since the quantum variance remains constant for all time t, it trivially satisfies the martingale property $\mathbb{E}[\mathrm{Var}_{\chi_t}(\hat{K}_j) \,|\, \mathcal{F}_s] = \mathrm{Var}_{\chi_s}(\hat{K}_j)$, for all $t \geq s$, with respect to the natural filtration $\mathcal{F}_s$ of the stochastic process.

6.5.3 Coherent-state reduction, entropy process and information flow

We now consider the overlap of $\mathrm{SU}(1,1)$ coherent states as a probabilistic, or more precisely, a stochastic process. The overlap between two coherent states $|\chi_1\rangle$ and $|\chi_2\rangle$ is given by (5.21),

$$\langle\chi_1|\chi_2\rangle = \frac{(1-|\chi_1|^2)^{2k}(1-|\chi_2|^2)^{2k}}{(1-\bar{\chi}_1\chi_2)^{2k}(1-\bar{\chi}_2\chi_1)^{2k}}. \tag{6.80}$$

From this, we define the associated probability density

$$P_t(\eta) = |\langle\eta|\chi_t\rangle|^2 = \frac{(1-|\chi_t|^2)^{2k}(1-|\rho|^2)^{2k}}{(1-\bar{\chi}_t\rho)^{2k}(1-\bar{\eta}\chi_t)^{2k}}, \tag{6.81}$$

which gives the likelihood of observing the system in the coherent state labelled by η, given that its stochastic trajectory is currently peaked around χ_t.

Proposition 6.18. *The overlap probability density satisfies the following SDE*

$$\begin{aligned} \mathrm{d}P_t(\eta) \;=\; & \frac{k\sigma P_t(\eta)}{|\zeta_t|}\left(\frac{(\bar{\eta}-\bar{\chi}_t)\chi_t}{(1-\chi_t\bar{\eta})} + \frac{(\eta-\chi_t)\bar{\chi}_t}{(1-\bar{\chi}_t\eta)}\right)\mathrm{d}W_t^{\tau} + \frac{\mathrm{i}k\sigma P_t(\eta)}{|\zeta_t|}\left(-\frac{(\bar{\eta}-\bar{\chi}_t)\chi_t}{(1-\chi_t\bar{\rho})} + \frac{(\eta-\chi_t)\bar{\chi}_t}{(1-\bar{\chi}_t\eta)}\right)\mathrm{d}W_t^{\phi} \\ & + \sigma^2 k P_t(\eta)\left(\frac{(\eta-\chi_t)(\bar{\eta}-\bar{\chi}_t)}{(1-\bar{\eta}\chi_t)(1-\eta\bar{\chi}_t)} - 1\right)\mathrm{d}t \end{aligned} \tag{6.82}$$

then the right-hand side is completely explicit in $\chi_t, \bar{\chi}_t$ via the formulas above.

Proof. We use the complex version of Itô's lemma on $P_t(\eta)$ to get

$$\mathrm{d}P_t(\eta) = \partial_{\chi_t} P_t(\eta)\,\mathrm{d}\chi_t + \partial_{\bar{\chi}_t} P_t(\eta)\,\mathrm{d}\bar{\chi}_t + \partial^2_{\chi_t\bar{\chi}_t} P_t(\eta)\,\mathrm{d}\chi_t\,\mathrm{d}\bar{\chi}_t, \tag{6.83}$$

where the other terms are zero because of (6.65). Taking the derivatives of $P_t(\eta)$, we find that

$$\begin{aligned}
\frac{\partial P_t(\eta)}{\partial \chi_t} &= 2kP_t(\eta)\frac{(\bar{\eta}-\bar{\chi}_t)}{(1-|\chi_t|^2)(1-\bar{\eta}\chi_t)},\\
\frac{\partial P_t(\eta)}{\partial \chi_t} &= 2kP_t(\eta)\frac{(\eta-\chi_t)}{(1-|\chi_t|^2)(1-\eta\bar{\chi}_t)},\\
\frac{\partial^2 P_t(\eta)}{\partial \chi_t \partial \bar{\chi}_t} &= \frac{2sP_t(\eta)}{(1-|\chi_t|^2)^2}\left(\frac{(\eta-\chi_t)(\bar{\eta}-\bar{\chi}_t)}{(1-\eta\bar{\chi}_t)(1-\bar{\eta}\chi_t)}-1\right).
\end{aligned} \tag{6.84}$$

Substituting (6.31) into (6.53) we get the desired result. □

As in the $\mathrm{SU}(2)$ case, this stochastic formulation provides a natural probabilistic interpretation of coherent-state overlaps, encoding both classical transport and quantum spreading in a unified geometric framework.

Finally, we explore the stochastic evolution of the entropy process.

Proposition 6.19. *Let $(\chi_t)_{t\geq 0}$ be a stochastic process taking values in the unit disk $\mathbb{D} = \{\chi \in \mathbb{C} : |\chi| < 1\}$, and define*

$$S_t = -\int_{\mathbb{D}} P_t(\eta)\,\log P_t(\eta)\,\mathrm{d}\mu^k_\eta, \tag{6.85}$$

where $\mathrm{d}\mu^k_\eta = \frac{2k-1}{\pi}\frac{1}{(1-|\eta|^2)^2}\,\mathrm{d}^2\eta$. Then, for all t,

$$S_t = \frac{2k}{2k-1}, \tag{6.86}$$

so $(S_t)_{t\geq 0}$ is constant in t (hence a martingale with respect to any filtration).

Proof. By $\mathrm{SU}(1,1)$ covariance (disk automorphisms), we may assume $\chi_t = 0$ without loss of generality. For Perelomov $\mathrm{SU}(1,1)$ coherent states, the squared overlap with the vacuum state at the origin is

$$P_t(\eta) = |\langle \eta\,|\,0\rangle|^2 = (1-|\eta|^2)^{2k}. \tag{6.87}$$

Substituting this in the integral for Shannon entropy, we obtain

$$\begin{aligned}
S_t &= -\int_{\mathbb{D}} (1-|\eta|^2)^{2k}\,\log(1-|\eta|^2)^{2k}\,\frac{2k-1}{\pi}\,\frac{\mathrm{d}^2\eta}{(1-|\eta|^2)^2},\\
&= -\frac{2k-1}{\pi}\int_0^{2\pi}\int_0^1 (1-r^2)^{2k-2}\left(2k\log(1-r^2)\right) r\,\mathrm{d}r\,\mathrm{d}\theta,\\
&= -2(2k-1)k\int_0^1 (1-r^2)^{2k-2}\,\log(1-r^2)\,r\,\mathrm{d}r.
\end{aligned} \tag{6.88}$$

Using $u = r^2$ (so $r\,\mathrm{d}r = \frac{1}{2}\,\mathrm{d}u$) in the above integral expression, we get

$$\begin{aligned} S_t &= -(2k-1)\,2k \int_0^1 (1-u)^{2k-2}\,\log(1-u)\,\frac{\mathrm{d}u}{2}, \\ &= -(2k-1)\,2k \int_0^1 v^{2k-2}\,\log v\,\mathrm{d}v \quad (v = 1-u). \end{aligned} \tag{6.89}$$

Using $\int_0^1 v^{a-1}\log v\,\mathrm{d}v = -\dfrac{1}{a^2}$ for $a > 0$ with $a = 2k-1$, we obtain

$$S_t = -(2k-1)\,2k\left(-\tfrac{1}{(2k-1)^2}\right) = \tfrac{2k}{2k-1}. \tag{6.90}$$

This value is independent of χ_t and of t, completing the proof. □

6.5.4 Lindblad-type evolution for the $\mathrm{SU}(1,1)$ density matrix

We now consider the ensemble-averaged evolution of a quantum system undergoing $\mathrm{SU}(1,1)$ coherent-state diffusion. As in the $\mathrm{SU}(2)$ case, we compute the time evolution of the density matrix $\hat{\rho}_t = \mathbb{E}[|\chi_t\rangle\langle\chi_t|]$, where the expectation is taken over stochastic trajectories governed by the Itô SDE in (6.68).

Proposition 6.20. *The expectation value of the stochastic evolution equation (6.68) leads to the following Lindblad-type master equation*

$$\begin{aligned} \frac{\mathrm{d}\hat{\rho}_t}{\mathrm{d}t} &= \sigma^2\left(\frac{\hat{K}_+}{\sqrt{2}}\hat{\rho}_t\frac{\hat{K}_-}{\sqrt{2}} + \frac{\hat{K}_-}{\sqrt{2}}\hat{\rho}_t\frac{\hat{K}_+}{\sqrt{2}} - \hat{K}_z\hat{\rho}_t\hat{K}_z\right) \\ &\quad -\frac{\sigma^2}{2}\left(\frac{\hat{K}_+\hat{K}_-}{2}\hat{\rho}_t + \frac{\hat{K}_-\hat{K}_+}{2}\hat{\rho}_t - \hat{K}_z^2\hat{\rho}_t - \hat{\rho}_t\hat{K}_z^2 + \hat{\rho}_t\frac{\hat{K}_+\hat{K}_-}{2} + \hat{\rho}_t\frac{\hat{K}_-\hat{K}_+}{2}\right). \end{aligned} \tag{6.91}$$

The proof is given in Appendix E.2.13. At first sight, the resulting master equation for $\hat{\rho}_t = \mathbb{E}[|\chi_t\rangle\langle\chi_t|]$ does not take the standard Gorini-Kossakowski-Sudarshan-Lindblad (GKSL) form because of the minus signs in the dissipative terms. This deviation is a direct consequence of the noncompact nature of $\mathrm{SU}(1,1)$. While GKSL dynamics guarantee complete positivity in general finite-dimensional settings, the present equation instead preserves trace and is $\mathrm{SU}(1,1)$-covariant. Thus, although it is not of GKSL form, it remains physically meaningful within the hyperbolic geometry of the $\mathrm{SU}(1,1)$ phase space.

This observation links naturally to the analysis in Chapter 5, particularly Section 5.5, where iterative POVM measurements were shown to induce diffusion on the hyperbolic plane. Here we see the same geometric structure re-emerging from the stochastic unravelling, the Itô SDE on the unit disc leads, upon averaging, to a hyperbolic diffusion equation that is consistent with the $\mathrm{SU}(1,1)$ symmetry.

With this, we conclude our exploration of stochastic dynamics on the coherent-state manifolds for HW, $\mathrm{SU}(2)$ and $\mathrm{SU}(1,1)$ groups.

6.6 Discussion and conclusion

We have developed a stochastic phase-space formulation of continuous quantum measurement for coherent states associated with three key symmetry groups: the Heisenberg–Weyl group, $\mathrm{SU}(2)$,

and $\mathrm{SU}(1,1)$. Starting from the normalised stochastic Schrödinger equation, we identified situations where the conditioned quantum state remains confined to the corresponding coherent-state manifold, with its phase-space label evolving according to a complex Itô diffusion. For each group, we derived the explicit form of the coherent-state SDE, demonstrated norm preservation, and showed that the ensemble average of the pure-state projectors recovers the appropriate master equation, with operators identified with the group generators. We also analysed the martingale properties of relevant observables, as well as the behaviour of entropy processes under measurement-induced noise.

A notable distinction from the standard SSE framework is that in the latter, observables constructed from the Lindblad operators are martingales, and the dynamics are insensitive to the underlying geometry. In contrast, in the coherent-state formulation developed here, the geometry of the phase space (flat, spherical, or hyperbolic) enters explicitly into the drift and diffusion terms. This geometric dependence prevents the corresponding observables from being strict martingales, but at the same time allows the coherent-state SDEs to encode phase-space decoherence in a more natural and physically transparent way than the geometry-free SSE picture.

In Chapter 8 we propose a general framework, based on the calculations here, that extends this stochastic coherent-state approach to arbitrary Lie groups. From a mathematical standpoint, it would be valuable to rigorously establish the general Lie-group formulation and characterise the associated diffusion processes on noncompact and higher-rank coherent-state manifolds. From a physical perspective, extending this approach to multi-mode and multi-spin systems could open new possibilities for modelling complex quantum networks and symmetry-protected dynamics. Finally, the framework may serve as a foundation for designing measurement-based control protocols, where the stochastic phase-space representation offers both analytic tractability and geometric insight.

Chapter 7

Phase-space measurement in relativistic quantum mechanics

7.1 Introduction

So far, in the previous chapters, we have studied phase-space measurements, decoherence, classicality, and the stochastic unravelling of coherent-state POVMs in the nonrelativistic setting. We now turn to the formulation of phase-space measurements in relativistic quantum mechanics.

Constructing a relativistic phase space presents conceptual and mathematical challenges. In nonrelativistic mechanics, both classical and quantum, phase space is equipped with a natural symplectic structure and global time evolution. In relativistic systems, however, the absence of a preferred time coordinate, together with the demands of Lorentz invariance and causality, obstructs a straightforward extension of these ideas [189, 190]. This motivates the search for alternative structures that respect relativistic symmetry while retaining a phase-space-like interpretation.

One such structure is the *future tube*, a complexified extension of Minkowski space that preserves causal order and admits holomorphic realisations of relativistic quantum states [191–202]. The future tube supports a natural reproducing-kernel Hilbert space of square-integrable holomorphic functions that is invariant under unitary action of the conformal group [47, 190]. This symmetry extends the familiar Poincaré group by including dilations and special conformal transformations. Within this setting, one can construct relativistic coherent states that localise phase-space information in a Lorentz-covariant way, thereby bridging classical phase-space intuition with relativistic quantum kinematics [35, 76]. Beyond its role in the present construction, the future tube has been extensively studied in mathematical physics as the natural analyticity domain of relativistic quantum fields. In particular, it underpins the analytic continuation of Wightman functions and plays a central role in axiomatic approaches to quantum field theory (QFT) [190, 203, 204, 209].

In this chapter, we develop these ideas systematically. We begin in Section 7.2 by recalling the role of phase space in classical mechanics and highlighting the difficulties of extending the usual cotangent-bundle construction to relativistic settings. Motivated by these issues, we turn in Section 7.4 to the geometry of the *future tube*, a complexified domain of Minkowski space that naturally incorporates analyticity, causality, and Lorentz invariance, and discuss its significance for relativistic quantum theory.

The transformation properties of this domain under the conformal group are analysed in Section 7.4.1.

We then construct coherent states on the future tube and analyse their fundamental properties, including normalisation, overcompleteness, and the associated reproducing kernel. Section 7.5 introduces the Bargmann transform, a unitary map from the holomorphic Hilbert space of the future tube to a square-integrable function space on the interior of the forward light cone. This mapping provides a concrete representation of relativistic quantum states in terms of measurable quantities such as position and momentum eigenvalues, and parallels the Segal-Bargmann representation discussed in Appendix A.

Using this transform, Section 7.6 defines coherent states directly on the interior of the forward light cone and verifies their mathematical structure, while Section 7.7 analyses their transformation under the conformal group and its Lie algebra generators on the interior of the forward light cone. Finally, in Section 7.10, we turn to measurement theory, constructing POVMs from coherent states on both the future tube and the light cone and performing phase-space measurement within this relativistic framework.

7.2 Phase space in relativistic classical mechanics

We begin by reviewing the notion of phase space in relativistic classical mechanics [205–208]. The natural starting point is Minkowski spacetime $\mathbb{M}$, a four-dimensional Lorentzian manifold that provides the configuration space of events. It is equipped with the Minkowski metric $g_{\mu\nu} = \mathrm{diag}(1, -1, -1, -1)$, which determines the invariant line element $\mathrm{d}s^2 = g_{\mu\nu}\,\mathrm{d}x^\mu \mathrm{d}x^\nu$. Each point in $\mathbb{M}$ corresponds to a position four-vector x^μ, with $\mu = 0, 1, 2, 3$. Given two events $x^a, y^a \in \mathbb{M}$, their separation is characterised by the vector $q^a = x^a - y^a$.

The nature of the separation is determined by the sign of $g_{ab}q^a q^b$

- If $g_{ab}q^a q^b > 0$, the separation is *timelike*, meaning that a signal traveling at or below the speed of light can connect the two points.
- If $g_{ab}q^a q^b < 0$, the separation is *spacelike*, implying that no causal signal can connect them.
- If $g_{ab}q^a q^b = 0$, the separation is *lightlike* or *null*, corresponding to motion at the speed of light.

The associated relativistic phase space is then given by the cotangent bundle $T^*\mathbb{M}$, an eight dimensional manifold, whose points (x^μ, p_μ) consist of spacetime positions together with conjugate four-momenta. This phase space inherits a natural symplectic structure from the canonical one-form $p_\mu\, dx^\mu$, but its interpretation is complicated by the mass-shell constraint $p_\mu p^\mu = m^2$ and the absence of a global time parameter.

Given a smooth function $H : T^*\mathbb{M} \to \mathbb{R}$, interpreted as the Hamiltonian, the dynamics on relativistic phase space are governed by Hamilton's equations

$$\frac{\mathrm{d}x^a}{\mathrm{d}s} = g^{ab}\frac{\partial H}{\partial p^b}, \quad \frac{\mathrm{d}p^a}{\mathrm{d}s} = -g^{ab}\frac{\partial H}{\partial x^b}, \tag{7.1}$$

where s is typically referred to as the proper time, and the metric g_{ab} is used to raise and lower indices via $p^a = g^{ab}p_b$. A solution to Hamilton's equations defines a trajectory $(x^a(s), p_a(s)) \in T^*\mathbb{M}$,

parametrised by proper time $s \in \mathbb{R}^+$.

While this approach is natural from a classical perspective, it presents several difficulties when extended to relativistic systems, as discussed in [47]. Some of the key issues are:

1. **Causality violations**: The momentum p_a can become spacelike or even past-pointing during evolution. Although one can impose conditions to avoid this on a case-by-case basis, a more fundamental resolution is desirable.

2. **Lack of complex structure**: The cotangent bundle $T^*\mathbb{M}$ does not naturally admit a complex structure that would combine position and momentum into a unified complex variable. Complex structures are essential in quantum field theory for distinguishing between positive and negative frequency modes, and their absence limits the cotangent bundle approach.

3. **Ambiguity in proper time for many-body systems**: When dealing with multiple particles, it becomes unclear which particle's proper time should serve as the evolution parameter for the overall system. A natural question arises: is there a way to define a universal proper time when analysing many-body relativistic systems?

To address these issues, we seek an alternative framework for phase-space in relativistic mechanics, one that maintains causal consistency, incorporates a complex structure naturally, and provides a universal evolution parameter suitable for many-body systems. This leads us toward the consideration of complexified phase spaces such as the future tube, which we shall explore next.

7.3 Geometry of the future tube

We begin with the complexification of Minkowski spacetime, denoted $\mathbb{CM}$, where each point is of the form $z^a = x^a + \mathrm{i}y^a$, with $x^a, y^a \in \mathbb{R}^4$. The complexified spacetime inherits the Minkowski metric [47].

Within $\mathbb{CM}$, the *future tube* Γ^+ is defined as the subset consisting of points

$$z^a = x^a - \mathrm{i}r^a \tag{7.2}$$

where r^a satisfies two conditions, $r^a r_a > 0$ (the imaginary part is timelike), $r^0 > 0$ (future-directed). These conditions ensure that Γ^+ consists entirely of complex points respecting the causal structure of spacetime [47].

A simple illustration is seen in one dimension, $z = x - \mathrm{i}r$ with $r > 0$, which parametrises a half-plane $\mathrm{Im}\, z < 0$. Up to a change of sign in the imaginary coordinate, this is equivalent to the standard Poincaré upper half-plane.

Although each point on Γ^+ is expressed as $z^a = x^a - \mathrm{i}r^a$, the physical meaning of r^a requires careful interpretation. Dimensionally, r^a must carry the units of length. One insightful idea is to treat r^a as related to the inverse of the momentum [47]. This relation is made precise through the *Kelvin transform*, connecting r^a and p^a via

$$r^a = \frac{\hbar\, p^a}{p_c p^c}, \quad p^a = \frac{\hbar\, r^a}{r_c r^c}. \tag{7.3}$$

A straightforward dimensional analysis confirms that r^a indeed has units of length

$$[r^a] = \frac{[\mathrm{ML}^2\mathrm{T}^{-1}]\,[\mathrm{MLT}^{-1}]}{[\mathrm{MLT}^{-1}][\mathrm{MLT}^{-1}]} = [\mathrm{L}]. \tag{7.4}$$

Thus the Kelvin transform defines an invertible correspondence between the future-directed timelike cone in the cotangent bundle $T^*\mathbb{M}$ and the future tube Γ^+.

By complex conjugation, one obtains the *past tube* Γ^-, defined by $\bar{z}^a = x^a + \mathrm{i}r^a$, $r^0 > 0$, which is simply the complex conjugate of Γ^+ and corresponds to the analytic continuation associated with past-directed timelike separations.

We will now prove the following result regarding the geometry of the future tube which will be useful for later calculations.

Proposition 7.1. *Let $x^a - \mathrm{i}r^a$ be a point on the future tube Γ^+. Then the Kelvin inversion of the conjugate point $x^a + \mathrm{i}r^a$*

$$\frac{x^a + \mathrm{i}r^a}{(x^b + \mathrm{i}r^b)\cdot(x_b + \mathrm{i}r_b)} \in \Gamma^+, \tag{7.5}$$

also lies in the future tube.

Proof. The idea for this argument was kindly suggested by Prof. Lane Hughston. Expanding the denominator of (7.5), we have

$$\frac{x^a + \mathrm{i}r^a}{(x^b + \mathrm{i}r^b)\cdot(x_b + \mathrm{i}r_b)} = \frac{x^a + \mathrm{i}r^a}{x^2 - r^2 + 2\mathrm{i}\,x\cdot r}, \tag{7.6}$$

where $x^2 = x^a x_a$, $r^2 = r^b r_b$ and $x \cdot r = x^c r_c$. We rationalise the above expression by multiplying numerator and denominator by the complex conjugate $(x^2 - r^2 - 2\mathrm{i}\,x\cdot r)$. Then the numerator becomes $(x^a + \mathrm{i}r^a)(x^2 - r^2 - 2\mathrm{i}\,x\cdot r)$ which expands to $x^a(x^2 - r^2) + r^a\,x\cdot r + \mathrm{i}\left[r^a(x^2 - r^2) - 2x^a\,x\cdot r\right]$ and the denominator modulus-squared is $(x^2 - r^2)^2 + 4(x\cdot r)^2$. Therefore the transformed point has the form

$$\frac{x^a + \mathrm{i}r^a}{(x^b + \mathrm{i}r^b)\cdot(x_b + \mathrm{i}r_b)} = \frac{x^a(x^2 - r^2) + r^a\,x\cdot r + \mathrm{i}\left[r^a(x^2 - r^2) - 2x^a\,x\cdot r\right]}{(x^2 - r^2)^2 + 4(x\cdot r)^2}. \tag{7.7}$$

Observe that the denominator is strictly positive. To prove the transformed point is in the future tube, it suffices to show that the imaginary part of the numerator is future-directed timelike. We define

$$v^a = r^a(x^2 - r^2) - 2x^a\,x\cdot r. \tag{7.8}$$

First, we show it is timelike

$$v^a v_a = r^2(x^2 - r^2)^2 + 4r^2(x\cdot r)^2, \tag{7.9}$$

which is strictly positive since r^a is timelike with $r^0 > 0$. To check that v^a is past-directed, we contract it with r_a to get

$$r_a v^a = r^2(x^2 - r^2) - 2(x\cdot r)^2. \tag{7.10}$$

Substituting (7.8) into the above expression we get

$$\left[r^a\left(x^2-r^2\right)-2x^a\,x\cdot r\right]r_a=r^2x^2-(r^2)^2-2(x\cdot r)^2. \tag{7.11}$$

We now define the unit timelike vector $t^a=\frac{r^a}{\sqrt{r^2}}$, so that $x\cdot r=x\cdot t\sqrt{r^2}$, with which we introduce an orthonormal basis

$$\{t^a,\ell^a,m^a,n^a\} \tag{7.12}$$

with t^a unit timelike and the others spacelike. We now expand x^a in this orthonormal basis as

$$x^a=T\,t^a+X\,\ell^a+Y\,m^a+Z\,n^a. \tag{7.13}$$

Contracting x^a with itself gives

$$x^2=T^2-X^2-Y^2-Z^2,\quad x\cdot t=T. \tag{7.14}$$

Substituting this in (7.11) we obtain

$$r^2x^2-(r^2)^2-2(x\cdot r)^2=r^2\left[T^2-X^2-Y^2-Z^2\right]-(r^2)^2-2\,r^2T^2. \tag{7.15}$$

Simplifying the above expression gives

$$=-r^2\left[T^2+X^2+Y^2+Z^2\right]-(r^2)^2, \tag{7.16}$$

which is strictly negative. Therefore the imaginary part of the Kelvin-transformed point is past-directed timelike, confirming that it lies in the past tube. □

We now turn to dynamics on the future tube. To derive Hamilton's equations on Γ^+, we first compute how derivatives with respect to p^a translate into derivatives with respect to r^a. Using the chain rule we find $\frac{\partial}{\partial p^a}$ in terms of $\frac{\partial}{\partial r^b}$ as

$$\frac{\partial}{\partial p^a}=\frac{\partial r^b}{\partial p^a}\frac{\partial}{\partial r^b}=\frac{\partial}{\partial p^a}\left(\frac{\hbar p^b}{p^cp_c}\right)\frac{\partial}{\partial r^b}=\hbar\left(\frac{\delta^b_a}{p^cp_c}-\frac{2p^bp_a}{(p^cp_c)^2}\right)\frac{\partial}{\partial r^b}=\frac{1}{\hbar}r^cr_c\left(\delta^b_a-\frac{2r^br_a}{r^cr_c}\right)\frac{\partial}{\partial r^b}, \tag{7.17}$$

where we have used (7.3). Contracting (7.17) with the metric g^{da}, we get

$$\hbar g^{da}\frac{\partial}{\partial p^a}=r^cr_c\left(g^{db}-\frac{2r^br^d}{r^cr_c}\right)\frac{\partial}{\partial r^b}. \tag{7.18}$$

Similarly, applying the chain rule, we can express the derivative of p^a with respect to s, the proper time as

$$\frac{\mathrm{d}p^a}{\mathrm{d}s}=\frac{\mathrm{d}p^a}{\mathrm{d}r^b}\frac{\mathrm{d}r^b}{\mathrm{d}s}=\hbar\left(\frac{\delta^a_b}{r^cr_c}-\frac{2r^ar_b}{(r^cr_c)^2}\right)\frac{\mathrm{d}r^b}{\mathrm{d}s}. \tag{7.19}$$

Contracting the above expression by g_{ad} leads to

$$\frac{1}{\hbar}g_{ad}\frac{\mathrm{d}p^a}{\mathrm{d}s}=\frac{1}{r_cr^c}\left(g_{bd}-\frac{2r_br_d}{r_cr^c}\right)\frac{\mathrm{d}r^b}{\mathrm{d}s}. \tag{7.20}$$

Recognising the structure in these expressions, we introduce two tensors h_{ab} and k^{ab}:

$$h_{ab} = -\frac{1}{r_c r^c}\left(g_{ab} - \frac{2r_a r_b}{r_c r^c}\right), \quad k^{ab} = -r_c r^c\left(g^{ab} - \frac{2r^a r^b}{r_c r^c}\right), \tag{7.21}$$

which satisfy $h_{ab}k^{bd} = \delta_a^d$. Thus, h_{ab} and k^{ab} are inverses of each other.

Using these calculations, we can now express Hamilton's equations on the future tube as

$$\begin{aligned}\frac{\mathrm{d}x^a}{\mathrm{d}s} &= g^{ab}\frac{\partial H}{\partial p^b} = \frac{g^{ab}}{\hbar}r^c r_c\left(\delta_b^d - \frac{2r^d r_b}{r^c r_c}\right)\frac{\partial H}{\partial r^d} = \frac{-k^{ad}}{\hbar}\frac{\partial H}{\partial r^d},\\ \frac{\mathrm{d}r^a}{ds} &= \frac{\mathrm{d}r^a}{\mathrm{d}p^b}\frac{\mathrm{d}p^b}{\mathrm{d}s} = -\frac{\mathrm{d}r^a}{\mathrm{d}p^b}g^{bd}\frac{\partial H}{\partial x^d} = -\frac{r_c r^c}{\hbar}\left(g^{ad} - \frac{2r^a r^d}{r_c r^c}\right)\frac{\partial H}{\partial x^d} = \frac{k^{ad}}{\hbar}\frac{\partial H}{\partial x^d}.\end{aligned} \tag{7.22}$$

An interesting feature emerging from this structure is that the effective metric h_{ab} is *positive definite* [47], in contrast to the indefinite Minkowski metric g_{ab}. This provides a Riemannian structure on the future tube, where the natural quadratic form is given by $\mathrm{d}s^2 = h_{ab}(\mathrm{d}x^a\mathrm{d}x^b + \mathrm{d}r^a\mathrm{d}r^b)$. This positive definite structure on Γ^+ plays a crucial role in defining a well-behaved relativistic phase space suitable for quantum theory.

7.4 Phase space in relativistic quantum mechanics

We now turn to the construction of a phase-space framework for relativistic quantum mechanics based on the future tube Γ^+. In analogy with the role of the Segal-Bargmann space (see Appendix A) in the nonrelativistic setting, the natural Hilbert space associated with Γ^+ is the space of square-integrable holomorphic functions. Accordingly, we define

$$L^{2,h}(\Gamma^+) = \left\{f : \Gamma^+ \to \mathbb{C} \,\middle|\, f \text{ holomorphic and } \langle f, f\rangle < \infty\right\}. \tag{7.23}$$

This space is a closed subspace of $\mathcal{L}^2(\Gamma^+)$, the Hilbert space of all square-integrable complex-valued functions on Γ^+. Equivalently, in sheaf-theoretic language, one may write $L^2(\Gamma^+, \mathcal{O})$ to refer to the square-integrable global sections of the sheaf of holomorphic functions on Γ^+ [47].

The inner product on $L^{2,h}(\Gamma^+)$ is defined as

$$\langle g, f\rangle = \int_{\Gamma^+} \overline{g(z)}f(z)\,\mathrm{d}\mu_z, \tag{7.24}$$

where $\mathrm{d}\mu_z$ is the Lebesgue measure on Γ^+ given by

$$\mathrm{d}\mu_z = \frac{1}{16}\,\mathrm{d}^4z\,\mathrm{d}^4\overline{z}. \tag{7.25}$$

Using this inner product, we define the norm on $L^{2,h}(\Gamma^+)$ in the standard way

$$||f|| = \left(\int_{\Gamma^+} \overline{f(z)}f(z)\,\mathrm{d}\mu_z\right)^{1/2}. \tag{7.26}$$

An important structural feature of $L^{2,h}(\Gamma^+)$ is the existence of a *reproducing kernel*, the Bergman kernel [210], associated with the space. If $\{\Phi_n(z)\}_{n\in I}$ denotes an orthonormal basis of $L^{2,h}(\Gamma^+)$ (with I

some indexing set), the Bergman kernel $K(z, \overline{w})$ is defined as

$$K(z, \overline{w}) = \sum_{n \in I} \overline{\Phi_n(w)} \Phi_n(z). \tag{7.27}$$

This kernel satisfies the fundamental *reproducing property*: for any $f \in L^{2,h}(\Gamma^+)$,

$$f(z) = \langle K_z, f \rangle = \int_{\Gamma^+} K(z, \overline{z'}) f(z') \, \mathrm{d}\mu_{z'}, \tag{7.28}$$

where $K_w(z) = K(z, \overline{w})$.

In addition, the Bergman kernel acts as an identity operator on the space, satisfying the composition rule

$$\int_{\Gamma^+} K(x, \overline{y}) K(y, \overline{z}) \, \mathrm{d}\mu_y = K(x, \overline{z}), \tag{7.29}$$

which confirms its role as the fundamental two-point function on Γ^+ [47].

For the specific case of the future tube Γ^+, the Bergman kernel has been found explicitly [47] to be

$$K(z, \overline{w}) = \frac{2^3 \times 4!}{\pi^4} \frac{1}{\left(g_{ab}(z^a - \overline{w}^a)(z^b - \overline{w}^b)\right)^4}. \tag{7.30}$$

Here, g_{ab} is the Minkowski metric, and the denominator emphasizes the role of causal structure (through the Minkowski inner product) even in the complexified setting.

Moreover, the geometry of the future tube inherits a natural *Kähler structure* from the properties of the Bergman kernel. Specifically, the Kähler metric h_{ab} on Γ^+, discussed previously, can also be obtained by taking the mixed second derivatives of the logarithm of the kernel

$$h_{ab} = \frac{\partial^2}{\partial z^a \, \partial \overline{z}^b} \log K(z, \overline{z}). \tag{7.31}$$

This metric h_{ab} is positive definite, providing a Riemannian structure on Γ^+ that will be essential for the definition of coherent states and the discussion of quantum measurements on relativistic phase space.

Using the expression for the Kähler metric given in (7.31), we can explicitly recover the metric h_{ab} on the future tube Γ^+ previously introduced in (7.21). Starting from

$$\begin{aligned} \frac{\partial^2 \log K(z, \overline{z})}{\partial z^a \partial \overline{z}^b} &= \frac{\partial}{\partial z^a} \left(\frac{1}{K(z, \overline{z})} \frac{\partial K(z, \overline{z})}{\partial \overline{z}^b} \right), \\ &= -\frac{1}{(K(z, \overline{z}))^2} \frac{\partial K(z, \overline{z})}{\partial z^a} \frac{\partial K(z, \overline{z})}{\partial \overline{z}^b} + \frac{1}{K(z, \overline{z})} \frac{\partial^2 K(z, \overline{z})}{\partial z^a \partial \overline{z}^b}, \end{aligned} \tag{7.32}$$

we proceed by explicitly computing the required derivatives of $K(z, \overline{z})$.

The first partial derivatives are

$$\frac{\partial K(z,\overline{z})}{\partial z^a} = -\frac{8g_{ad}(z^d-\overline{z}^d)}{g_{cd}(z^c-\overline{z}^c)(z^d-\overline{z}^d)}K(z,\overline{z}), \tag{7.33}$$

$$\frac{\partial K(z,\overline{z})}{\partial \overline{z}^b} = \frac{8g_{bf}(z^f-\overline{z}^f)}{g_{cd}(z^c-\overline{z}^c)(z^d-\overline{z}^d)}K(z,\overline{z}). \tag{7.34}$$

The mixed second derivative is computed to be

$$\begin{aligned}\frac{\partial^2 K(z,\overline{z})}{\partial z^a \partial \overline{z}^b} = &-\frac{64g_{ad}g_{bf}(z^d-\overline{z}^d)(z^f-\overline{z}^f)}{(g_{cd}(z^c-\overline{z}^c)(z^d-\overline{z}^d))^2}K(z,\overline{z}) + \frac{8g_{ab}}{g_{cd}(z^c-\overline{z}^c)(z^d-\overline{z}^d)}K(z,\overline{z}) \\ &-\frac{16g_{bf}g_{ad}(z^d-\overline{z}^d)(z^f-\overline{z}^f)}{(g_{cd}(z^c-\overline{z}^c)(z^d-\overline{z}^d))^2}K(z,\overline{z}).\end{aligned} \tag{7.35}$$

Substituting the results from (7.33),(7.34), and (7.35) into (7.32), we obtain

$$\frac{\partial^2 \log K(z,\overline{z})}{\partial z^a \partial \overline{z}^b} = \frac{8g_{ab}}{g_{cd}(z^c-\overline{z}^c)(z^d-\overline{z}^d)} - \frac{16g_{bf}g_{ad}(z^d-\overline{z}^d)(z^f-\overline{z}^f)}{(g_{cd}(z^c-\overline{z}^c)(z^d-\overline{z}^d))^2}. \tag{7.36}$$

Now, recalling that points on the future tube Γ^+ are of the form $z^a = x^a - \mathrm{i}r^a$, with $r^0 > 0$ and $r_a r^a > 0$, we have, $z^a - \overline{z}^a = -2\mathrm{i}r^a$. Substituting this into the above expression yields

$$\begin{aligned}\frac{\partial^2 \log K(z,\overline{z})}{\partial z^a \partial \overline{z}^b} &= \frac{8g_{ab}}{(-2i)^2 g_{cd}r^c r^d} - \frac{16g_{bf}g_{ad}(-2\mathrm{i}r^d)(-2\mathrm{i}r^f)}{(-2i)^4(g_{cd}r^c r^d)^2}, \\ &= \frac{2}{r_c r^c}g_{ab} - \frac{4r_a r_b}{(r_c r^c)^2}, \\ &= \frac{2}{r_c r^c}\left(g_{ab} - \frac{2r_a r_b}{r_c r^c}\right).\end{aligned} \tag{7.37}$$

Thus, we recover

$$\frac{\partial^2 \log K(z,\overline{z})}{\partial z^a \partial \overline{z}^b} = 2h_{ab}, \tag{7.38}$$

where h_{ab} is exactly the Kähler metric introduced earlier in (7.21).

This explicit computation shows that the positive-definite Kähler metric on the future tube is directly derived from the geometry of the Bergman kernel. It also establishes the underlying complex-symplectic structure crucial for defining relativistic quantum phase space dynamics.

7.4.1 Space-time transformations on the future tube

It is now natural to ask how fundamental spacetime symmetries, especially those of the Poincaré and conformal groups, act on the Hilbert space of holomorphic square-integrable functions defined on the future tube. Since the future tube is a complexified domain, one must construct explicit unitary representations of these transformations acting on its Hilbert space $\mathcal{H}$ [47].

The future tube Γ^+ is invariant under the action of the conformal group, which preserves its causal structure and complex-analytic properties. In particular, conformal transformations act as biholomorphic automorphisms of Γ^+, mapping holomorphic functions to holomorphic functions and preserving the domain of analyticity. This ensures that the induced action on $\mathcal{H}$ is compatible with the

holomorphic structure and admits a unitary realisation with respect to the natural reproducing-kernel inner product. At this stage, we only highlight this geometric invariance, deferring a systematic introduction of conformal transformations and their generators to Section 7.7, where we study their explicit action on coherent states and measurements

The Poincaré transformations can be described in coordinate form as

$$z^a \mapsto L^a_b z^b + B^a, \tag{7.39}$$

where B^a is a real four-vector representing a translation, and L^a_b is a Lorentz transformation satisfying

$$g_{ab} L^a_c L^b_d = g_{cd}. \tag{7.40}$$

This transformation rule defines the action of the Poincaré group on the future tube.

On the Hilbert space of holomorphic functions, these coordinate transformations are implemented by a family of unitary operators $\widehat{U}_P$ with the explicit kernel form

$$U(x, \overline{y}) = K\big(L^a_b x^b + B^a, \overline{y}\big), \tag{7.41}$$

where $K(x, \overline{y})$ is the Bergman kernel of the future tube. This operator preserves the inner product on $\mathcal{H}$, guaranteeing unitarity, as can be checked by verifying

$$\widehat{U}\widehat{U}^\dagger = \mathbb{1} \tag{7.42}$$

using the reproducing property of the Bergman kernel. Explicitly, one verifies [47]

$$\int U(x, \overline{y})\, \overline{U(y, \overline{z})}\, \mathrm{d}\mu_y = K(x, \overline{z}) \tag{7.43}$$

by using the invariance of the measure under the group action. This demonstrates that these unitary operators form a representation of the Poincaré group on the Hilbert space of the future tube.

Special conformal transformations

In addition to the Poincaré subgroup, one can also represent special conformal transformations, of the form

$$z^a \mapsto \frac{z^a + z^2 \lambda^a}{1 + 2\lambda \cdot z + \lambda^2 z^2}, \tag{7.44}$$

where λ^a is a real four-vector parameter and $z^2 = g_{ab} z^a z^b$. Geometrically, these can be interpreted as an inversion, followed by a translation, followed by a second inversion. The corresponding unitary operator acting on $\mathcal{H}$ takes the form

$$U(x, \overline{y}) = \frac{1}{\big(1 + 2\lambda \cdot x + \lambda^2 x^2\big)^4}\, K\left(\frac{x^a + x^2 \lambda^a}{1 + 2\lambda \cdot x + \lambda^2 x^2}, \overline{y}\right), \tag{7.45}$$

and satisfies the appropriate group composition laws for special conformal transformations.

Dilations

The future tube also admits dilations of the form

$$z^a \mapsto \Lambda\, z^a \tag{7.46}$$

for positive Λ. The corresponding unitary operator on $\mathcal{H}$ is

$$U(x,\overline{y}) = \Lambda^4\, K\big(\Lambda x^a, \overline{y}\big), \tag{7.47}$$

where the Λ^4 prefactor ensures preservation of the Hilbert space norm and unitarity.

Together, these transformations, translations, Lorentz transformations, dilations, and special conformal transformations, generate a representation of the full 15-dimensional conformal group on the future tube Hilbert space. The kernel formalism guarantees these operators are unitary and preserve the holomorphic inner product.

Every infinitesimal generator of these transformations, such as the four-momentum operator associated with translations,

$$\widehat{P}_a = -\mathrm{i}\hbar \frac{\partial}{\partial x^a}, \tag{7.48}$$

can be represented explicitly by acting on the Bergman kernel, yielding a phase-space representation as worked out in [47]. For instance, the phase-space representation of the four-momentum operator takes the form

$$P_a(z,\overline{w}) = -\frac{3\cdot 2^9 \hbar\,\mathrm{i}}{\pi^4}\, \frac{g_{ab}\big(z^b - \overline{w}^b\big)}{\big[g_{ab}\big(z^a - \overline{w}^a\big)\big(z^b - \overline{w}^b\big)\big]^5}. \tag{7.49}$$

These explicit representations make manifest how symmetry generators act on the relativistic phase-space structure provided by the future tube.

7.4.2 Quantum states on the future tube

Having established the structure of the future tube Γ^+, we now turn to the description of quantum states defined on this space.

A general quantum state on $L^{2,h}(\Gamma^+)$ is represented by a *density matrix* $R(z,\overline{w})$, a bi-holomorphic function belonging to $L^{2,h}(\Gamma^+) \times L^{2,h}(\Gamma^+)$. The density matrix must satisfy the following conditions:

1. **Hermiticity:** $R(z,\overline{w}) = \overline{R(w,\overline{z})}$,
2. **Positivity:** For all $\Psi(w) \in L^{2,h}(\Gamma^+)$,

$$\int_{\Gamma^+} \overline{\Psi(z)}\, R(z,\overline{w})\, \Psi(w)\, \mathrm{d}\mu_z\, \mathrm{d}\mu_w \geq 0, \tag{7.50}$$

3. **Normalisation:** The trace condition

$$\int_{\Gamma^+} R(z,\overline{z})\, \mathrm{d}\mu_z = 1 \tag{7.51}$$

must hold.

In particular, *pure states* correspond to density matrices of the form

$$R(z,\overline{w}) = \Psi(z)\,\overline{\Psi(w)}, \tag{7.52}$$

where $\Psi(w) \in L^{2,h}(\Gamma^+)$ has unit norm. The diagonal function $R(z,\overline{w})$ describes the probability density associated with the state.

7.4.3 Coherent states on the future tube

The structure of the Hilbert space $L^{2,h}(\Gamma^+)$ allows a natural construction of *coherent states* based on the Bergman kernel $K(z,\overline{w})$. Let $\Gamma^+ \ni \alpha_\sigma$ be a family of points smoothly parametrised by $\sigma \in [0,1]$. For each σ, we define a corresponding coherent state as

$$\Psi_\sigma(z) = C\,K(z,\overline{\alpha_\sigma}), \tag{7.53}$$

where the constant C is fixed to satisfy the resolution of identity. These coherent states form an *overcomplete* set in $L^{2,h}(\Gamma^+)$, ensuring that they provide a complete description of the quantum state space, even after removal of finitely many elements [35]. They minimise uncertainty and are therefore well-suited for describing phase-space localisation in relativistic quantum dynamics.

The normalisation constant C is determined so that $\int_{\Gamma^+} \overline{\Psi_\alpha(z)}\,\Psi_\alpha(z)\,\mathrm{d}\mu_z = \mathbb{1}$, guaranteeing a resolution of identity and the explicit form of the normalised coherent state may be written as

$$\Psi_w(z) = \frac{K(z,\bar{w})}{\sqrt{K(w,\bar{w})}} = \frac{8\sqrt{3}}{\pi^2}\,\frac{\big(g_{ab}(w^a-\bar{w}^a)(w^b-\bar{w}^b)\big)^2}{\big(g_{ab}(z^a-\bar{w}^a)(z^b-\bar{w}^b)\big)^4}, \tag{7.54}$$

where $K(z,\bar{w})$ is the Bergman kernel on $L^{2,h}(\Gamma^+)$.

Having established how spacetime symmetries, including the full conformal group, act unitarily on the holomorphic Hilbert space of the future tube, we are now in a position to link these structures to physically meaningful measurements and phase-space descriptions on real Minkowski space. In particular, we shall next introduce the Bargmann transform, which provides a unitary map from the holomorphic domain of the future tube to the real forward light cone. This transform allows us to reinterpret the coherent states and symmetry generators developed above in a physically observable representation, and sets the stage for constructing coherent-state-based measurement frameworks consistent with relativistic causality.

7.5 Bargmann transform

In relativistic quantum theory formulated on the future tube $\Gamma^+ \subset \mathbb{C}^4$, the Hilbert space of states is taken to be the space of square-integrable holomorphic functions, denoted $L^{2,h}(\Gamma^+)$, equipped with a Lorentz-invariant measure. While this framework captures the analytic and geometric richness of complexified spacetime, physical observables, particularly momentum eigenvalues, are naturally defined on the real forward light cone

$$\mathcal{C}_+^\circ = \left\{ q \in \mathbb{R}^{1,3} \,\middle|\, q^0 > 0,\; q^\mu q_\mu > 0 \right\}, \tag{7.55}$$

i.e., the set of all future-directed timelike four-vectors in Minkowski space.

7.5.1 Square-integrable functions on the interior of the light cone

Before we construct the Bargmann transform, let us consider the space of square-integrable functions defined on the interior of the forward light cone. We define the Hilbert space $L^2(\mathcal{C}_+^\circ)$ to be the space of complex-valued measurable functions $\phi(q)$ on $\mathcal{C}_+^\circ$ that are square-integrable with respect to the Lorentz-invariant measure

$$\mathrm{d}\nu_q = \frac{1}{8\pi^5}\,(q^a q_a)^2\,\mathrm{d}q^a. \tag{7.56}$$

The corresponding inner product on $L^2(\mathcal{C}_+^\circ)$ is given by

$$\langle \phi_1, \phi_2 \rangle = \int_{\mathcal{C}_+^\circ} \overline{\phi_1(q)}\,\phi_2(q)\,\frac{1}{8\pi^5}(q^a q_a)^2\,\mathrm{d}q^a. \tag{7.57}$$

7.5.2 The Bargmann transform

We now define the Bargmann transform as a unitary map between the space of holomorphic square-integrable functions on the future tube $\Gamma^+ \subset \mathbb{C}^4$ and the space of square-integrable functions on the interior of the forward light cone $\mathcal{C}_+^\circ \subset \mathbb{R}^{1,3}$.

Let $A(q, \bar{z})$ be the Bargmann kernel, a jointly measurable function defined on $\Gamma^+ \times \mathcal{C}_+^\circ$. The Bargmann transform

$$\mathcal{B} : L^{2,h}(\Gamma^+) \longrightarrow L^2(\mathcal{C}_+^\circ) \tag{7.58}$$

is defined by the integral operator

$$(\mathcal{B}\psi)(q) = \int_{\Gamma^+} A(q, \bar{z})\,\Psi(z)\,\mathrm{d}\mu_z, \tag{7.59}$$

where $\mathrm{d}\mu_z$ is the invariant measure on Γ^+, (7.25), and $A(q, \bar{z})$ is given by

$$A(q, \bar{z}) = \frac{1}{(-\mathrm{i}\bar{z}^b \bar{z}_b)^4} \exp\left(-\frac{\mathrm{i}q_a \bar{z}^a}{\bar{z}^b \bar{z}_b}\right). \tag{7.60}$$

The transform is constructed such that if $z^a \in \Gamma^+$, the future tube with the units of position, then $\bar{z}^a$ is the past tube with the units of position. The Kelvin inverse transforms it into the future tube in momentum units and we are multiplying it with q^a which has the units of position.

The inverse transform

$$\mathcal{B}^{-1} : L^2(\mathcal{C}_+^\circ) \longrightarrow \mathcal{H}^2(\Gamma^+) \tag{7.61}$$

is given by

$$(\mathcal{B}^{-1}\Phi)(z) = \int_{\mathcal{C}_+^\circ} \overline{A(q, \bar{z})}\,\phi(q)\,\mathrm{d}\nu_q, \tag{7.62}$$

where $\mathrm{d}\nu_q$ is the Lorentz-invariant measure defined earlier in (7.56).

In this section, we will prove the two fundamental properties of the Bargmann transform:

1. Unitarity: The Bargmann transform $\mathcal{B}$ is an isometry:

$$\langle \psi_1, \psi_2 \rangle_{\mathcal{H}^2(\Gamma^+)} = \langle \mathcal{B}\psi_1, \mathcal{B}\psi_2 \rangle_{L^2(\mathcal{C}_+^\circ)}. \tag{7.63}$$

2. Reproducing kernel property: The Bargmann kernel satisfies the identity

$$\int_{\mathcal{C}_+^\circ} \overline{A(q,\bar{z})}\, A(q,\bar{w})\, \mathrm{d}\nu_q = K(z,\bar{w}), \tag{7.64}$$

where $K(z,\bar{w})$ is the reproducing kernel for the space $L^{2,h}(\Gamma^+)$.

These two properties ensure that the Bargmann transform is not only unitary but also provides a bridge between complexified momentum space and real relativistic position space.

Proposition 7.2. *Let $A(q,\bar{z})$ be the Bargmann kernel associated with the Bargmann transform $\mathcal{B} : L^{2,h}(\Gamma^+) \to L^2(\mathcal{C}_+^\circ)$, where $z, w \in \Gamma^+$ and $q \in \mathcal{C}_+^\circ$*

$$A(q,\bar{z}) = \frac{1}{(-\mathrm{i}\bar{z}^c \bar{z}_c)^4} \exp\left(-\frac{\mathrm{i} q_a \bar{z}^a}{\bar{z}^b \bar{z}_b}\right) \tag{7.65}$$

Then the kernel satisfies the reproducing identity

$$\int_{\mathcal{C}_+^\circ} \overline{A(q,\bar{z})}\, A(q,\bar{w})\, \mathrm{d}\nu_q = K(z,\bar{w}), \tag{7.66}$$

where $K(z,\bar{w})$ is the reproducing kernel of the Hilbert space $L^{2,h}(\Gamma^+)$.

The proof is given in Appendix F.1.1. For completeness, we also establish the corresponding inverse property.

Proposition 7.3. *Let $A(q,\bar{z})$ denote the Bargmann kernel and let $A(z,\bar{w})$ be the reproducing kernel for the Hilbert space $L^{2,h}(\Gamma^+)$. Then the following inverse resolution of the identity holds:*

$$\int_{\Gamma} A(q,\bar{z})\, \overline{A(q',\bar{z})}\, \mathrm{d}\mu_z = \delta^{(4)}(q-q'), \tag{7.67}$$

in the sense of distributions on $L^2(\mathcal{C}_+^\circ)$.

The proof is detailed in Appendix F.1.2. Taken together, these two properties establish the foundation for the following theorem, which demonstrates that the Bargmann transform is an isometry.

Theorem 7.1. *Let $\mathcal{B} : L^{2,h}(\Gamma^+) \to L^2(\mathcal{C}_+^\circ)$ be the Bargmann transform defined by*

$$(\mathcal{B}\psi)(q) = \int_{\Gamma}^{+} A(q,\bar{z})\, \Psi(z)\, \mathrm{d}\mu_z, \tag{7.68}$$

where $A(q,\bar{z})$ is the Bargmann kernel, and $\mathrm{d}\mu_z$ is the invariant measure on Γ^+. Then $\mathcal{B}$ is a unitary operator. That is,

$$\langle \Psi_1, \Psi_2 \rangle_{L^{2,h}(\Gamma^+)} = \langle \mathcal{B}\psi_1, \mathcal{B}\psi_2 \rangle_{L^2(\mathcal{C}_+^\circ)}, \tag{7.69}$$

for all $\Psi_1, \Psi_2 \in L^{2,h}(\Gamma^+)$, and $\mathcal{B}$ is surjective.

Proof. We proceed in two steps: first, we verify that $\mathcal{B}$ is an isometry, and then we show that its image is the whole of $L^2(\mathcal{C}_+^\circ)$.

$\mathcal{B}$ is an isometry.

Let $\psi_1, \psi_2 \in L^{2,h}(\Gamma^+)$. Then the inner product of their images under $\mathcal{B}$ is

$$\begin{aligned}\langle \mathcal{B}\psi_1, \mathcal{B}\psi_2\rangle_{L^2(\mathcal{C}_+^\circ)} &= \int_{\mathcal{C}_+^\circ} \overline{(\mathcal{B}\psi_1)(q)}\,(\mathcal{B}\psi_2)(q)\,\mathrm{d}\nu_q, \\ &= \int_{\mathcal{C}_+^\circ} \left[\int_{\Gamma^+} \overline{A(q,\bar{z})}\,\overline{\Psi_1(z)}\,\mathrm{d}\mu_z\right]\left[\int_{\Gamma^+} A(q,\bar{w})\,\Psi_2(w)\,\mathrm{d}\mu_w\right]\mathrm{d}\nu_q. \end{aligned} \tag{7.70}$$

We now interchange the order of integration (justified by Fubini's theorem, assuming integrability of the kernel) to write

$$\langle \mathcal{B}\psi_1, \mathcal{B}\psi_2\rangle_{L^2(\mathcal{C}_+^\circ)} = \int_{\Gamma^+}\int_{\Gamma^+} \overline{\Psi_1(z)}\,\Psi_2(w)\left[\int_{\mathcal{C}_+^\circ} \overline{A(q,\bar{z})}\,A(q,\bar{w})\,\mathrm{d}\nu_q\right]\mathrm{d}\mu_z\,\mathrm{d}\mu_w. \tag{7.71}$$

The expression in brackets is, by assumption, equal to the reproducing kernel $A(z,\bar{w})$, so we obtain:

$$\begin{aligned}\langle \mathcal{B}\psi_1, \mathcal{B}\psi_2\rangle_{L^2(\mathcal{C}_+^\circ)} &= \int_{\Gamma^+}\int_{\Gamma^+} \overline{\Psi_1(z)}\,K(z,\bar{w})\,\Psi_2(w)\,\mathrm{d}\mu_z\,\mathrm{d}\mu_w, \\ &= \langle \Psi_1, \Psi_2\rangle_{L^{2,h}(\Gamma^+)}, \end{aligned} \tag{7.72}$$

where the last equality follows from the reproducing property of $K(z,\bar{w})$ in $L^{2,h}(\Gamma^+)$.

Surjectivity of $\mathcal{B}$.

Since $\mathcal{B}$ is an isometry between two Hilbert spaces and has dense image (as it maps an orthonormal basis in $L^{2,h}(\Gamma^+)$ to an orthonormal system in $L^2(\mathcal{C}_+^\circ)$), it follows that $\mathcal{B}$ is surjective. Therefore, $\mathcal{B}$ is unitary. □

This result sets the stage for the introduction of relativistic coherent states in the next section. There, we will use the isometry to construct a family of normalised states with optimal phase-space localisation, and examine their mathematical structure and physical interpretation within the relativistic framework.

7.6 Coherent states on the interior of the forward light cone

In this section, we construct a family of normalised relativistic coherent states, first on the future tube and then, via the unitary Bargmann transform, on the interior of the forward light cone. These states retain the hallmark features of coherent-state systems, normalisation, overcompleteness, and geometric labelling, thereby providing an informationally complete family in the Hilbert space. They furnish a natural phase-space description within the holomorphic framework, while their representation on the interior of the forward light cone makes their physical interpretation in terms of spacetime variables transparent. This construction forms the foundation for our subsequent treatment of relativistic phase-space measurements and their operational meaning.

Proposition 7.4. *Let $\Psi_w \in L^{2,h}(\Gamma^+)$ denote the coherent state on the future tube, defined by*

$$\Psi_w(z) = \frac{K(z,\overline{w})}{\sqrt{K(w,\overline{w})}}, \tag{7.73}$$

where K is the Bergman kernel on Γ^+. Then the image of Ψ_w under the unitary Bargmann transform $\mathcal{B}$ defines a coherent state on the interior of the forward light cone, given by

$$\psi_w(q) = (\mathcal{B}\Psi_z)(q) = \int A(q,\bar{z})\Psi_w(z)\,\mathrm{d}\mu_z. \tag{7.74}$$

This family $\{\psi_w\}$ forms an overcomplete set in $L^2(\mathcal{C}_+^\circ)$ and preserves the geometric labeling, normalisation, and resolution-of-identity properties of the coherent states on Γ^+.

Proof. Using the explicit expression for the coherent state on the future tube from (7.54), and applying the Bargmann transform, we define

$$\psi_w(q) = (\mathcal{B}\Psi_w)(q) = \frac{1}{\sqrt{K(w,\overline{w})}} \int_{\Gamma^+} A(q,\bar{z})\,K(z,\overline{w})\,\mathrm{d}\mu_z, \tag{7.75}$$

where $A(w,q)$ is the Bargmann kernel.

By the reproducing kernel property for the Bargmann kernel, we have

$$\int_{\Gamma^+} A(q,\bar{z})\,K(z,\overline{w})\,\mathrm{d}\mu_z = A(q,\bar{w}), \tag{7.76}$$

so that

$$\psi_w(q) = \frac{A(q,\bar{w})}{\sqrt{K(w,\overline{w})}} = \frac{\pi^2}{\sqrt{192}}\left((w^d-\bar{w}^d)(w_d-\bar{w}_d)\right)^2 \frac{1}{(-\mathrm{i}\bar{w}^b\bar{w}_b)^4}\exp\left(-\frac{\mathrm{i}q_a\bar{w}^a}{\bar{w}^c\bar{w}_c}\right) \tag{7.77}$$

This defines the coherent state on the interior of the forward light cone up to the same geometric labeling w. We will now verify that these coherent states are indeed normalised on $L^2(\mathcal{C}_+^\circ)$.

Using the definition of the inner product on the interior of the forward light cone we have

$$|\psi_w(q)|^2 = \frac{1}{8\pi^5}\int_{\mathcal{C}_+^\circ} \overline{\psi_w(q)}\psi_w(q)\,(q^bq_b)^2\,\mathrm{d}q^a. \tag{7.78}$$

Substituting for the coherent state gives

$$\begin{aligned} |\psi_w(q)|^2 &= \frac{1}{8\pi^5}\left(\frac{\pi^2}{\sqrt{192}}\frac{\left((w^d-\bar{w}^d)(w_d-\bar{w}_d)\right)^2}{(-\mathrm{i}w^cw_c)^2(-\mathrm{i}\bar{w}^g\bar{w}_g)^2}\right)^2 \int_{\mathcal{C}_+^\circ}\exp\left(\frac{\mathrm{i}q_aw^a}{w^ew_e}-\frac{\mathrm{i}q_a\bar{w}^a}{\bar{w}^f\bar{w}_f}\right)(q^bq_b)^2\,\mathrm{d}q^a, \\ &= \frac{1}{1536\pi}(m^dm_d)^4\int_{\mathcal{C}_+^\circ}\exp\left(\mathrm{i}q_am^a\right)(q^bq_b)^2\,\mathrm{d}q^a \end{aligned} \tag{7.79}$$

where we have substituted the following

$$m^a = \frac{z^a}{z^bz_b}-\frac{\bar{z}^a}{\bar{z}^c\bar{z}_c}. \tag{7.80}$$

Using Proposition 7.2 (proved in Appendix F.1.1), the integral evaluates to $\frac{1536\pi}{(m^am_a)^4}$. Substituting this

result into the expression above, we obtain

$$|\psi_w(q)|^2 = 1, \tag{7.81}$$

which confirms the normalisation of the state.

The overcompleteness of the transformed coherent states on the interior of the forward light cone follows immediately from the inverse resolution of identity established earlier for the Bargmann transform in Proposition 7.3. Since the transform is unitary and bijective, the coherent states on the future tube, which are known to be overcomplete, are mapped to a family of coherent states on the light cone that also satisfy a resolution of the identity. This guarantees that the transformed coherent states provide a redundant spanning set for the Hilbert space $L^2(\mathcal{C}_+^\circ)$ without requiring an explicit recomputation of their integral kernel. □

Remark 7.6.1. Let $\psi_w(q)$ denote the image of a normalised coherent state on the future tube under the Bargmann transform, taking the explicit form

$$\psi_w(q) = \frac{\pi^2}{\sqrt{192}} \Big((w^d - \bar{w}^d)(w_d - \bar{w}_d)\Big)^2 \frac{1}{(-\mathrm{i}\bar{w}^c\bar{w}_c)^4} \exp\left(-\frac{\mathrm{i}q_a\bar{w}^a}{\bar{w}^b\bar{w}_b}\right), \tag{7.82}$$

Since the Bargmann transform is unitary, the state $\psi(q)$ is normalised in the Hilbert space of square-integrable functions on the interior of the forward light cone. It is often convenient to regroup the normalisation constants, defining

$$\tilde{\psi}_w(q) = \frac{\pi^2}{\sqrt{192}} \frac{\Big((w^d - \bar{w}^d)(w_d - \bar{w}_d)\Big)^2}{(-\mathrm{i}w^c w_c)^2(-\mathrm{i}\bar{w}^e\bar{w}_e)^2} \exp\left(-\frac{\mathrm{i}q_a\bar{w}^a}{\bar{w}^b\bar{w}_b}\right), \tag{7.83}$$

which preserves the same norm because

$$\|\tilde{\psi}\|^2 = \|\psi\|^2 = 1. \tag{7.84}$$

7.7 Conformal group and its generators

Having established the overcompleteness of coherent states on the interior of the forward light cone, we now return to the role of symmetry transformations in this setting. While in Section 7.4.1 we examined the conformal action on the future tube, here we focus on its realisation directly on the light cone.

In classical and quantum physics, symmetry principles provide a unifying framework for understanding conservation laws, particle classifications, and interactions. The Poincaré group, combining spacetime translations and Lorentz transformations, is fundamental to special relativity since it preserves the Minkowski metric. However, certain physical systems and field theories possess an even richer symmetry structure that preserves angles rather than distances; these are described by the conformal group. The role of the conformal group in relativistic field theories has been thoroughly developed in both mathematical and physical contexts [211–214], providing essential tools for the study of symmetries, operator product expansions, and renormalisation.

The defining feature of a conformal transformation is that it preserves the causal structure of Minkowski

space, mapping lightcones to lightcones, and thereby preserves the notion of angle, though not necessarily lengths.

In this section, we will systematically define the conformal group on Minkowski space, classify its transformations, derive the explicit form of its generators, and explain how these transformations act on spacetime coordinates. This will lay a solid mathematical foundation for applications in relativistic quantum theories with conformal invariance.

Definition of conformal transformations

Let $\mathbb{M}^d$ denote d-dimensional Minkowski space with metric $g_{\mu\nu} = \mathrm{diag}(1, -1, -1, \ldots, -1)$. A conformal transformation is a smooth, invertible map

$$x^\mu \mapsto x'^\mu(x) \tag{7.85}$$

such that the metric is preserved up to a local positive scaling factor

$$g_{\rho\sigma}\, dx'^\rho dx'^\sigma = \Omega(x)^2\, g_{\mu\nu}\, dx^\mu dx^\nu, \tag{7.86}$$

for some positive, smooth function $\Omega(x)$. In other words, conformal transformations preserve the light-cone structure and hence causal relationships, though they do not globally preserve lengths.

In infinitesimal form, the conformal condition may be expressed as

$$\partial_\mu x'^\rho(x)\, \partial_\nu x'^\sigma(x)\, g_{\rho\sigma} = \Omega(x)^2\, g_{\mu\nu}. \tag{7.87}$$

A coordinate transformation satisfying this relation is called a conformal isometry of Minkowski space.

The conformal group is the group of all such transformations, forming a Lie group whose dimension is $\frac{(d+1)(d+2)}{2}$, and whose Lie algebra is isomorphic to $\mathfrak{so}(d, 2)$. In $d = 4$, this yields 15 generators in total. These generators consist of

- spacetime translations (4),
- Lorentz rotations and boosts (6),
- dilations (1),
- special conformal transformations (4).

This group dramatically enlarges the symmetry structure beyond the Poincaré group, with important implications in relativistic field theories.

Translations as conformal transformations

We first consider the infinitesimal translation

$$x'^\mu = x^\mu + a^\mu, \tag{7.88}$$

where a^μ is a constant parameter. In infinitesimal notation, this corresponds to $\epsilon^\mu(x) = a^\mu$. Since a^μ is constant, its derivatives vanish: $\partial_\mu \epsilon_\nu = 0$. Substituting into the conformal Killing equation

$$\partial_\mu \epsilon_\nu + \partial_\nu \epsilon_\mu = f(x)\, g_{\mu\nu}, \tag{7.89}$$

we find

$$0 + 0 = f(x)\, g_{\mu\nu} \implies f(x) = 0. \tag{7.90}$$

Therefore translations satisfy the conformal condition with a trivial scaling factor $\Omega(x) = 1$, preserving the Minkowski metric exactly. Translations map lightcones to lightcones without local rescaling and are thus genuine conformal transformations. The associated generators are the momentum operators

$$P_\mu = -\mathrm{i}\, \partial_\mu. \tag{7.91}$$

Lorentz transformations as conformal transformations

Next, consider the infinitesimal Lorentz transformation

$$x'^\mu = x^\mu + \omega^\mu{}_\nu x^\nu, \tag{7.92}$$

where $\omega^\mu{}_\nu$ is antisymmetric, $\omega^{\mu\nu} = -\omega^{\nu\mu}$. This corresponds to $\epsilon^\mu(x) = \omega^\mu{}_\nu x^\nu$. Taking the derivative, $\partial_\alpha \epsilon_\beta = \omega_{\beta\alpha}$, where indices are lowered with the Minkowski metric. Substituting into the conformal Killing equation $\partial_\mu \epsilon_\nu + \partial_\nu \epsilon_\mu = f(x)\, g_{\mu\nu}$, yields

$$\omega_{\nu\mu} + \omega_{\mu\nu} = f(x)\, g_{\mu\nu}. \tag{7.93}$$

Since $\omega_{\mu\nu}$ is antisymmetric, the sum vanishes, which implies

$$f(x) = 0. \tag{7.94}$$

Hence Lorentz transformations also satisfy the conformal Killing equation with $\Omega(x) = 1$, preserving the Minkowski metric exactly, and map lightcones to lightcones without any local scaling. Their generators are the familiar angular momentum and boost operators:

$$M_{\mu\nu} = \mathrm{i}\left(x_\mu \partial_\nu - x_\nu \partial_\mu\right). \tag{7.95}$$

Dilations as conformal transformations

Consider a global scaling, or dilation, defined infinitesimally by

$$x'^\mu = (1 + \lambda)\, x^\mu \tag{7.96}$$

with a small parameter λ. This can be rewritten in infinitesimal form as $\epsilon^\mu(x) = \lambda\, x^\mu$. Taking its derivative gives $\partial_\nu \epsilon_\mu = \lambda\, \delta_{\mu\nu}$. Substituting into the conformal Killing equation $\partial_\mu \epsilon_\nu + \partial_\nu \epsilon_\mu = f(x)\, g_{\mu\nu}$,

results in

$$\lambda\,\delta_{\nu\mu} + \lambda\,\delta_{\mu\nu} = f(x)\,g_{\mu\nu}. \tag{7.97}$$

Since $\delta_{\mu\nu} = g_{\mu\nu}$ in index-free notation, this simplifies to

$$2\lambda\,g_{\mu\nu} = f(x)\,g_{\mu\nu} \implies f(x) = 2\lambda. \tag{7.98}$$

Therefore, dilations are conformal transformations with a constant conformal factor

$$\Omega(x) = 1 + \lambda, \tag{7.99}$$

scaling all distances uniformly. Dilations thus preserve lightcones up to an overall rescaling of the metric. Their associated generator is

$$D = -\mathrm{i}\,x^\mu \partial_\mu. \tag{7.100}$$

Special conformal transformations as conformal transformations

Special conformal transformations (SCTs) are defined by

$$x'^\mu = \frac{x^\mu - b^\mu x^2}{1 - 2b\cdot x + b^2 x^2}, \tag{7.101}$$

where b^μ is a small constant parameter. For an infinitesimal b^μ, expand to first order

$$x'^\mu \approx x^\mu - b^\mu x^2 + 2x^\mu (b\cdot x). \tag{7.102}$$

Hence the infinitesimal form is

$$\epsilon^\mu(x) = -b^\mu x^2 + 2x^\mu (b\cdot x). \tag{7.103}$$

Let us compute its derivative

$$\partial_\nu \epsilon_\mu = -b_\mu 2x_\nu + 2\,\delta_{\mu\nu}(b\cdot x) + 2x_\mu b_\nu. \tag{7.104}$$

Substituting this in the conformal Killing equation yields

$$\begin{aligned}\partial_\mu\epsilon_\nu + \partial_\nu\epsilon_\mu &= -2b_\nu x_\mu - 2b_\mu x_\nu + 2g_{\mu\nu}(b\cdot x) + 2x_\mu b_\nu + 2x_\nu b_\mu,\\ &= 2\,g_{\mu\nu}(b\cdot x).\end{aligned}$$

Hence

$$f(x) = 2\,b\cdot x. \tag{7.105}$$

Therefore special conformal transformations satisfy the conformal Killing equation with a position-dependent conformal factor

$$\Omega(x) = 1 + b\cdot x \tag{7.106}$$

to first order in b. These transformations preserve the lightcone structure while performing an inversion–translation–inversion sequence geometrically. Their generators are

$$K_\mu = -\mathrm{i}\left(2x_\mu x^\nu \partial_\nu - x^2 \partial_\mu\right). \tag{7.107}$$

Commutation relations of the conformal algebra

To analyse how relativistic coherent states transform, it is useful to recall the generators of the conformal Lie algebra. The conformal group is generated by spacetime translations P_μ, Lorentz transformations $M_{\mu\nu}$, dilations D, and special conformal transformations K_μ

$$\{P_\mu,\, M_{\mu\nu},\, D,\, K_\mu\}. \tag{7.108}$$

These operators close under commutation to form the Lie algebra $\mathfrak{so}(d,2)$, which in four dimensions yields a total of 15 generators.

The satisfy the following commutation relations:

$$\begin{aligned}
[M_{\mu\nu}, M_{\rho\sigma}] &= \mathrm{i}\left(g_{\nu\rho}M_{\mu\sigma} - g_{\mu\rho}M_{\nu\sigma} - g_{\nu\sigma}M_{\mu\rho} + g_{\mu\sigma}M_{\nu\rho}\right), \\
[M_{\mu\nu}, P_\rho] &= \mathrm{i}\left(g_{\nu\rho}P_\mu - g_{\mu\rho}P_\nu\right), \\
[M_{\mu\nu}, K_\rho] &= \mathrm{i}\left(g_{\nu\rho}K_\mu - g_{\mu\rho}K_\nu\right), \\
[D, P_\mu] &= -\mathrm{i}P_\mu, \quad [D, K_\mu] = \mathrm{i}K_\mu, \\
[P_\mu, K_\nu] &= 2\mathrm{i}\left(g_{\mu\nu}D - M_{\mu\nu}\right).
\end{aligned}$$

All other commutators vanish:

$$[D, M_{\mu\nu}] = 0, \quad [P_\mu, P_\nu] = 0, \quad [K_\mu, K_\nu] = 0. \tag{7.109}$$

Geometric interpretation

These relations exhibit the following structural features:

- **Lorentz subalgebra:** $M_{\mu\nu}$ satisfy the familiar Lorentz algebra, preserving the Minkowski metric and describing rotations and boosts.
- **Poincaré consistency:** P_μ transform as Lorentz vectors, showing translations are consistent with Poincaré symmetry. Likewise, K_μ also transform as Lorentz vectors under $M_{\mu\nu}$.
- **Dilation weights:** The commutators with D reveal that P_μ has scaling dimension -1 while K_μ has scaling dimension $+1$, consistent with their geometric roles under scale transformations.
- **Interplay of P and K:** The commutator $[P_\mu, K_\nu]$ produces both a dilation generator and a Lorentz generator, demonstrating how translations and special conformal transformations are linked in a nonabelian structure.
- **Remaining vanishing commutators:** These confirm no further hidden structure is present beyond these relations, closing the algebra.

Geometrically, the conformal group preserves the causal structure of Minkowski spacetime. Translations and Lorentz transformations rigidly move the lightcones, while dilations scale them uniformly. Special conformal transformations can be seen as a sequence of inversion, translation, and inversion, preserving angles and mapping null rays to null rays.

7.8 Action of conformal generators on coherent states

We now examine how these conformal symmetry operations act directly on the coherent states themselves. Since coherent states provide a phase-space-localised basis of quantum states, their transformation properties under the conformal group encode valuable information about covariance, stability, and the dynamics of phase-space measurements in relativistic settings. Although the conformal algebra is defined globally on Minkowski space, in this exposition we restrict its action to the Hilbert space of states supported on the interior of the forward light cone, where the generators remain well-defined as differential operators acting on smooth functions within this causally consistent domain.

Momentum like operator - translations on coherent states

We begin by considering the infinitesimal translation generator P_μ, which acts on states by shifting their argument in Minkowski space. When applied to a relativistic coherent state $\psi_w(q)$, we have the following in position representation

$$P_\mu \tilde{\psi}_w(q) = -\mathrm{i}\frac{\partial}{\partial q^\mu}\tilde{\psi}_w(q), \tag{7.110}$$

which reflects the standard differential action of translations on wavefunctions.

Substituting for the coherent state and taking its derivative we see that

$$\begin{aligned} P_\mu \tilde{\psi}_w(q) &= -\frac{\mathrm{i}\pi^2}{\sqrt{192}}\frac{-\mathrm{i}\bar{w}^\mu}{\bar{w}^b\bar{w}_b}\frac{\left((w^d-\bar{w}^d)(w_d-\bar{w}_d)\right)^2}{(-\mathrm{i}w^c w_c)^2(-\mathrm{i}\bar{w}^b\bar{w}_b)^2}\exp\left(-\frac{\mathrm{i}q_a\bar{w}^a}{\bar{w}^b\bar{w}_b}\right) \\ &= -\frac{\bar{w}_\mu}{\bar{w}^c\bar{w}_c}\tilde{\psi}_w(q). \end{aligned} \tag{7.111}$$

and so the coherent state is an eigenfunction of the translation operator.

The expectation value of the translation operator in the coherent state basis is given as

$$\left\langle -\mathrm{i}\frac{\partial}{\partial q^\mu}\right\rangle_{\tilde{\psi}_w(q)} = -\frac{\bar{w}_\mu}{\bar{w}^c\bar{w}_c}. \tag{7.112}$$

From Proposition 7.1, We know that if $w^a \in \Gamma^+$ and has the units of position, then $\frac{\bar{w}^\mu}{\bar{w}^c\bar{w}_c}$ also lies in the future tube, Γ^+, with the units of momentum. So this translation operator looks like a complex *momentum* operator.

Turning to the finite translation group element, generated by the unitary operator

$$U(a) = \mathrm{e}^{-\mathrm{i}a^\mu P_\mu}. \tag{7.113}$$

In position representation, the coherent-state wavefunction transforms accordingly as

$$\tilde{\psi}_w(q) \mapsto \tilde{\psi}_w(q-a), \tag{7.114}$$

which shifts the phase-space localisation of the coherent state. This behaviour illustrates how relativistic coherent states transform naturally under translations, preserving their interpretation as localised, covariant wavepackets.

Position like operator

In addition to the translation generator P_μ, one may consider the position-like operator Q^μ, defined by multiplication with the coordinate variable q^μ.

$$Q^\mu \tilde{\psi}_w(q) = q^\mu \tilde{\psi}_w(q). \tag{7.115}$$

We will now calculate the expectation value of this operator in the coherent state basis, $\psi_w(q)$. We consider the following

$$\langle Q^\mu \rangle_{\tilde{\psi}_w(q)} = \int_{\mathcal{C}_+^\circ} q^\mu \tilde{\psi}_w(q) \overline{\tilde{\psi}_w(q)}\, \mathrm{d}\nu_q \tag{7.116}$$

Substituting for the coherent state $\psi_w(q)$ the above expression can be written as

$$\langle Q^\mu \rangle_{\tilde{\psi}_w(q)} = \int_{\mathcal{C}_+^\circ} q^\mu \frac{\pi^4}{192} \frac{\left((w^d - \bar{w}^d)(w_d - \bar{w}_d)\right)^4}{(-\mathrm{i}w^c w_c)^4 (-\mathrm{i}\bar{w}^b \bar{w}_b)^4} \exp\left(\frac{\mathrm{i}q_a w^a}{w^e w_e} - \frac{\mathrm{i}q_a \bar{w}^a}{\bar{w}^f \bar{w}_f}\right) \mathrm{d}\nu_q \tag{7.117}$$

By letting m^a to be

$$m^a = \frac{w^a}{w^b w_b} - \frac{\bar{w}^a}{\bar{w}^c \bar{w}_c} \tag{7.118}$$

the integral becomes

$$\langle Q^\mu \rangle_{\tilde{\psi}_w(q)} = \int_{\mathcal{C}_+^\circ} \frac{q^\mu}{1536\pi} (m^d m_d)^4 \exp\left(\mathrm{i}q_a m^a\right) \mathrm{d}q^a \tag{7.119}$$

Let us now consider the normalisation condition for the coherent state

$$\|\tilde{\psi}_w\|^2 = \frac{1}{1536\pi} \int_{\mathcal{C}_+^\circ} (m^d m_d)^4 \exp\left(\mathrm{i}q^a m_a\right) \mathrm{d}q^a = 1. \tag{7.120}$$

Let us now differentiate it by m^a

$$\begin{aligned} \frac{\mathrm{d}}{\mathrm{d}m_\mu} \|\tilde{\psi}_w\|^2 &= \frac{1}{1536\pi} \int_{\mathcal{C}_+^\circ} \mathrm{i}q^\mu (m^d m_d)^4 \exp\left(\mathrm{i}q^a m_a\right) \mathrm{d}q^a, \\ &\quad + \frac{1}{1536\pi} \int_{\mathcal{C}_+^\circ} 8(m^d m_d)^3 m^\mu \exp\left(\mathrm{i}q^a m_a\right) \mathrm{d}q^a. \end{aligned} \tag{7.121}$$

The first term is the expectation of the position like operator and the second integral can be evaluated from the normalisation. So we have

$$\frac{\mathrm{d}}{\mathrm{d}m_\mu}\|\tilde{\psi}_w\|^2 = \mathrm{i}\,\langle Q^\mu\rangle + \frac{8m^\mu}{m^d m_d} = 0. \tag{7.122}$$

Solving for the expectation value of Q^μ we get

$$\langle Q^\mu\rangle = \frac{8\mathrm{i}m^\mu}{m^d m_d}. \tag{7.123}$$

We will now argue that this expectation value is real and positive. Consider the quantity $m^a = \frac{w^a}{w_b w^b} - \frac{\bar{w}^a}{\bar{w}_b \bar{w}^b}$ with $w^a \in \Gamma^+$, where $w^a = x^a - \mathrm{i}r^a$ and r^a is future-directed timelike. Its complex conjugate is $\bar{w}^a = x^a + \mathrm{i}r^a$, which belongs to the past tube Γ^-. Each term in m^a has the form $\frac{w^a}{w_b w^b}$, which carries the units of inverse length, consistent with momentum, since w^a has dimension of length and $w_b w^b$ has dimension of length^2. Because w^a lies in the future tube, its denominator has a negative imaginary part, so its reciprocal maps into the upper half-plane, behaving essentially like an element of Γ^-.

Taking the difference between these two terms yields m^a, which is purely imaginary with a positive imaginary part. Therefore $\mathrm{i}\,m^a$ is real and negative.

Next, consider its norm $m^c m_c$. Since m^a is purely imaginary and timelike, its norm squared is negative. As a result, the entire expectation value

$$\frac{\mathrm{i}\,m^\mu}{m^c m_c} \in \mathbb{R}_{>0} \tag{7.124}$$

has a negative numerator (since $\mathrm{i}\,m^\mu$ is real and negative) and negative denominator, producing a final answer that is real and positive overall, having the units of position, consistent with the physical interpretation of a phase-space observable.

Using (7.110), (7.115), we wish to compute their commutator acting on an arbitrary smooth test function $\psi(q)$. Let us expand explicitly

$$\begin{aligned}
[Q^\mu, P_\nu]\,\psi(q) &= Q^\mu P_\nu \psi(q) - P_\nu Q^\mu \psi(q), \\
&= q^\mu\left(-\mathrm{i}\frac{\partial}{\partial q^\nu}\psi(q)\right) + \mathrm{i}\frac{\partial}{\partial q^\nu}\left(q^\mu\psi(q)\right).
\end{aligned} \tag{7.125}$$

Expanding the derivative in the second term we get

$$\frac{\partial}{\partial q^\nu}\left(q^\mu\psi(q)\right) = \delta^\mu_\nu\psi(q) + q^\mu\frac{\partial\psi}{\partial q^\nu}. \tag{7.126}$$

Substituting back, we obtain

$$\begin{aligned}
[Q^\mu, P_\nu]\,\psi(q) &= -\mathrm{i}q^\mu\frac{\partial\psi}{\partial q^\nu} + \mathrm{i}\left(\delta^\mu_\nu\psi(q) + q^\mu\frac{\partial\psi}{\partial q^\nu}\right), \\
&= \mathrm{i}\delta^\mu_\nu\psi(q),
\end{aligned} \tag{7.127}$$

where the terms involving $q^\mu \partial_\nu \psi$ cancel exactly. Hence the commutator operator identity is

$$[Q^\mu, P_\nu] = \mathrm{i}\, \delta^\mu_\nu. \tag{7.128}$$

This confirms that the relativistic position-like and momentum-like operators satisfy the standard canonical commutation relation, consistent with their role as conjugate variables even within the domain of the forward light cone.

Dilation operator

We now consider the action of the dilation operator, $D = -\mathrm{i}\, q^\mu \frac{\partial}{\partial q^\mu}$, on the coherent states $\tilde{\psi}_w(q)$ constructed previously. Substituting for the coherent state

$$D\tilde{\psi}_w(q) = -\mathrm{i}\, q^\mu \frac{\partial}{\partial q^\mu}\tilde{\psi}_w(q) = -\frac{q^\mu \bar{w}_\mu}{\bar{w}^c \bar{w}_c}\tilde{\psi}_w(q), \tag{7.129}$$

where we have used the result from (7.111). Let us now calculate the expectation of the Dilation operator in the coherent state basis, this amounts to calculating the following integral

$$\langle D\rangle_{\tilde{\psi}_w(q)} = \left\langle \tilde{\psi}_w(q), -\mathrm{i}q^\mu \frac{\partial}{\partial q^\mu}\tilde{\psi}_w(q)\right\rangle = -\frac{\bar{w}_\mu}{\bar{w}^c \bar{w}_c}\left\langle \tilde{\psi}_w(q), q^\mu \tilde{\psi}_w(q)\right\rangle \tag{7.130}$$

and this is the expectation of the position operator and substituting (7.123) we get

$$\langle D\rangle_{\tilde{\psi}_w(q)} = \frac{8\mathrm{i}m^\mu \bar{w}_\mu}{m^d m_d}, \tag{7.131}$$

where

$$m^\mu = \frac{w^\mu}{w^d w_d} - \frac{\bar{w}^\mu}{\bar{w}^d \bar{w}_d}. \tag{7.132}$$

The expectation value is a Lorentz scalar but is not necessarily real.

We now explore Quantum dynamics on the interior of the Forward light cone.

7.9 Quantum dynamics on the interior of the light cone

Describing relativistic quantum dynamics consistently inside the forward light cone requires the introduction of an appropriate evolution parameter. Unlike in nonrelativistic quantum mechanics, where the Hamiltonian generates evolution with respect to a globally defined Newtonian time, relativistic frameworks do not admit a preferred global time coordinate. Proper time along a worldline provides a natural invariant parameter for classical particles, but it cannot be straightforwardly applied to interacting or quantum systems, where superpositions of trajectories and indefinite causal structure appear.

A widely used resolution is the *Stückelberg parameter* [189, 215]. This parameter, often denoted by τ, is introduced as an additional evolution variable, distinct from the spacetime coordinates x^μ. It plays the role of a covariant analogue of proper time, with two crucial features:

1. **Lorentz covariance:** τ is invariant under Lorentz transformations, ensuring that the dynamical

evolution does not privilege any particular inertial frame.

2. **Hamiltonian structure:** τ permits a Hamiltonian formulation in which the canonical coordinates are (x^μ, p_μ) with the usual Poisson brackets, while the Hamiltonian generates translations in τ.

This construction, sometimes called *Stückelberg–Horwitz–Piron dynamics*, extends standard relativistic quantum mechanics by embedding trajectories in a five-dimensional phase space $(x^\mu, p_\mu; \tau)$. The dynamical equations then resemble a Schrödinger-type equation in the evolution parameter τ,

$$\mathrm{i}\frac{\partial}{\partial\tau}\psi(x^\mu,\tau) = H\psi(x^\mu,\tau), \tag{7.133}$$

where H is a Hamiltonian constraint encoding the mass-shell condition and possible interactions.

We consider a relativistic quantum evolution on the interior of the forward light cone, governed by a Stückelberg-type Schrödinger equation with the symmetrised Hamiltonian

$$H = \frac{1}{2}\left(P^\mu Q_\mu + Q^\mu P_\mu\right), \tag{7.134}$$

where $P_\mu = -\mathrm{i}\frac{\partial}{\partial q^\mu}$, $Q^\mu = q^\mu$. Expanding,

$$H\psi(q) = \frac{1}{2}\left[-\mathrm{i}\, q^\mu\frac{\partial}{\partial q^\mu} + q^\mu\left(-\mathrm{i}\frac{\partial}{\partial q^\mu}\right)\right]\psi(q). \tag{7.135}$$

Observing the commutator

$$[P_\mu, Q^\mu] = -\mathrm{i}\,\delta^\mu_\mu = -4\mathrm{i}, \tag{7.136}$$

one rewrites

$$Q^\mu P_\mu = P_\mu Q^\mu + [Q^\mu, P_\mu] = P_\mu Q^\mu + \mathrm{i}\,4. \tag{7.137}$$

Thus the Hamiltonian becomes

$$H = \frac{1}{2}\left(P^\mu Q_\mu + Q^\mu P_\mu\right) = -\mathrm{i}\, q^\mu\partial_\mu - 2\mathrm{i}, \tag{7.138}$$

and the evolution equation becomes

$$\mathrm{i}\frac{\partial\psi}{\partial\tau} = -\mathrm{i}\left(q^\mu\partial_\mu + 2\right)\psi \quad\Longrightarrow\quad \frac{\partial\psi}{\partial\tau} = \left(q^\mu\partial_\mu + 2\right)\psi. \tag{7.139}$$

This is a first-order PDE suitable for the method of characteristics. The characteristic flow satisfies

$$\frac{\mathrm{d}q^\mu}{\mathrm{d}\tau} = q^\mu, \tag{7.140}$$

which integrates to

$$q^\mu(\tau) = q^\mu(0)\,\mathrm{e}^\tau. \tag{7.141}$$

Along these curves, the evolution of ψ obeys

$$\frac{\mathrm{d}\psi}{\mathrm{d}\tau} = 2\psi \qquad \Longrightarrow \qquad \psi(\tau) = \psi(0)\,\mathrm{e}^{2\tau}. \tag{7.142}$$

Hence the complete solution is

$$\psi(q,\tau) = \mathrm{e}^{2\tau}\, f\left(q\,\mathrm{e}^{-\tau}\right) \tag{7.143}$$

where f is arbitrary initial data specified at $\tau = 0$.

7.10 Phase-space measurements via POVMs

In the nonrelativistic settings explored in earlier chapters, phase-space measurements were modelled using coherent-state POVMs naturally adapted to the underlying symmetry group, whether the Heisenberg-Weyl group or its compact and noncompact analogues. We now extend this perspective to the relativistic domain. Our goal is to develop a framework for phase-space measurement in relativistic quantum mechanics, using a POVM construction intrinsically adapted to the geometry of the future tube Γ^+. This allows us to formulate relativistic measurements in close analogy with the nonrelativistic case, while respecting the analytic and causal structure of Minkowski spacetime. We now adapt the coherent-state POVM formalism, first introduced in Chapter 1, to the relativistic setting.

Formally, a POVM on phase space is defined by a family of positive operators $\{\phi_A(y,\overline{z})\}_{A\in\mathcal{B}}$, where $\mathcal{B}$ is the Borel σ-algebra generated by open subsets of Γ^+. Each measurable set $A \in \mathcal{B}$ is associated with a positive operator ϕ_A satisfying the following properties:

1. **Positivity:** $\phi_A(y,\overline{z})$ is a positive operator for every $A \in \mathcal{B}$;

2. **Normalisation:** The operator corresponding to the full phase space satisfies

$$\phi_{\Gamma^+}(y,\overline{z}) = K(y,\overline{z}), \tag{7.144}$$

   where $K(y,\overline{z})$ is the Bergman kernel;

3. **Countable additivity:** For any countable collection of disjoint measurable sets $\{A_n\}_{n\in\mathbb{N}}$ with union $A = \bigcup_n A_n$, we have

$$\phi_A(x,\overline{z}) = \sum_n \phi_{A_n}(x,\overline{z}). \tag{7.145}$$

The POVM corresponding to the detection of an event within a measurable subset $A \subset \Gamma^+$ is explicitly given by

$$\phi_A(x,\overline{z}) = \int_{y\in A} K(x,\overline{y})K(y,\overline{z})\,\mathrm{d}\mu_y, \quad A \in \mathcal{B}. \tag{7.146}$$

Given a quantum state described by a density matrix $R(z,\overline{y})$, the probability that an event occurs

within the set A is computed as

$$\mathbb{P}(A) \quad = \quad \int_{\Gamma^+} \phi_A(y,\overline{z}) R(z,\overline{y})\, \mathrm{d}\mu_y\, \mathrm{d}\mu_z = \int_{z\in A} R(z,\overline{z})\, \mathrm{d}\mu_z, \tag{7.147}$$

where $R(z,\overline{z})$ is the diagonal probability density associated with the state.

To describe the transformation of the quantum state after a measurement, we introduce the associated *Kraus operator* for the region $A \in \mathcal{B}$, defined by

$$T_A(u,v,\overline{x},\overline{y}) = \int_{w\in A} \frac{K(u,\overline{w})K(v,\overline{w})K(w,\overline{x})K(w,\overline{y})}{K(w,\overline{w})}\, \mathrm{d}\mu_w. \tag{7.148}$$

The Kraus operator describes the coherent interaction of the system with the measurement region.

Importantly, taking the partial trace over one pair of variables recovers the POVM operator

$$\int_{\Gamma^+} T_A(x,y,\overline{y},\overline{z})\, \mathrm{d}\mu_y = \phi_A(x,\overline{z}). \tag{7.149}$$

Suppose the system initially occupies the state $R_{\text{in}}(y,\overline{v})$. After the measurement associated with detecting an event in A, the updated (post-measurement) state is given by

$$\begin{aligned} R_{\text{out}}(u,\overline{x}) \quad &= \quad \frac{\int_{\Gamma^+} T_A(u,v,\overline{x},\overline{y}) R_{\text{in}}(y,\overline{v})\, \mathrm{d}\mu_v\, \mathrm{d}\mu_y}{\int_{\Gamma^+} T_A(z,v,\overline{z},\overline{y}) \rho_{\text{in}}(y,\overline{v})\, \mathrm{d}\mu_v\, \mathrm{d}\mu_y\, \mathrm{d}\mu_z} \\ &= \quad \frac{\int_{z\in A} \frac{K(u,\overline{z})K(z,\overline{x})}{K(z,\overline{z})} R_{\text{in}}(z,\overline{z})\, \mathrm{d}\mu_z}{\int_{z\in A} R_{\text{in}}(z,\overline{z})\, \mathrm{d}\mu_z}. \end{aligned} \tag{7.150}$$

Here, the numerator describes the projection onto the region A, weighted by the original state, and the denominator ensures normalisation. Thus, the POVM formalism allows for the consistent definition of both the probability of measurement outcomes and the evolution of quantum states under localised measurements in relativistic phase space.

Iterative phase-space measurement

To study repeated phase-space measurements in the relativistic setting, we first require a suitable representation of quantum states. In the holomorphic framework on the future tube Γ^+, the state of the system is described by a holomorphic density kernel $R(z,\bar{w})$, which encodes statistical mixtures and coherences in a form compatible with analyticity and the geometry of Γ^+.

The Bargmann transform provides a unitary map between this holomorphic representation and the density matrix on the interior of the forward light cone. Explicitly, we define

$$\rho(q,q') = \int_{\Gamma^+\times\Gamma^+} A(q,\bar{z})\, R(z,\bar{w})\, \overline{A(q',\bar{w})}\, \mathrm{d}\mu_z\, \mathrm{d}\mu_w, \tag{7.151}$$

where $A(q,\bar{z})$ is the Bargmann kernel introduced earlier.

Because the transform is unitary, $\rho(q,q')$ inherits the usual algebraic properties of a density matrix, Hermiticity, positivity, and unit trace, while its support is restricted to the forward light cone, thereby ensuring compatibility with relativistic causality.

As in the nonrelativistic cases studied in earlier chapters, a phase-space measurement can be viewed as asking which coherent state best describes the system. A selective measurement projects onto a specific phase-space point, while a nonselective measurement, the case of interest here, averages over all outcomes, yielding a partially decohered state. In the relativistic framework, this motivates the study of *iterative phase-space measurements*, where successive applications of the coherent-state POVM gradually suppress quantum interference and drive the density matrix toward classical-like behaviour.

Proposition 7.5. *After one iteration of the coherent-state POVM measurement, the density matrix becomes*

$$\rho^{(1)}(q,q') = \frac{15\times 2^5}{\pi}\int_{\mathcal{C}_+^\circ} \frac{\rho(\lambda+q,\lambda+q')}{((q^a+\lambda^a+q'^a)(\lambda_a+q_a+q'_a))^6}((\lambda^a+q^a)(\lambda_a+q_a))^4\,\mathrm{d}\lambda^a. \tag{7.152}$$

The proof is discussed in detail in Appendix F.1.3. This result illustrates explicitly how the density matrix becomes damped under a single phase-space measurement, with the off-diagonal terms suppressed through integrals with the terms $(\lambda_a+q_a)^8\big(q_a+\lambda_a+q'_a\big)^{-12}$, which encode the smoothing action of the POVM.

While the first iteration can be evaluated in closed form, subsequent iterations involve increasingly complicated nested integrals that are not easily reducible to compact expressions. A systematic analysis of these higher-order terms is deferred to future work.

7.11 Discussion and conclusion

In this final chapter, we have extended the phase-space measurement framework to the relativistic setting. To overcome the difficulties inherent in defining phase space via the usual cotangent bundle construction, we instead worked with the *future tube*, a complexified domain that provides a natural arena for relativistic quantum mechanics. Within this setting, we constructed a POVM on the future tube and established a unitary Bargmann transform mapping states from the forward light cone to the future tube. This construction yields a family of coherent states associated with the conformal group, thereby embedding relativistic quantum systems into the broader framework of group-theoretic coherent states.

We further examined Hamiltonian evolution in this setting using the Stückelberg formulation of time, and formulated phase-space measurements for density matrices defined on the interior of the forward light cone. By applying the Bargmann transform we related these to states on the future tube, and computed the effect of a single coherent-state POVM iteration on the density matrix. In contrast to the nonrelativistic cases studied earlier, however, this process does not admit a simple recursive structure, and further iterations remain an open challenge.

This underscores both the novelty and the complexity of relativistic phase-space measurements, to which we return to in the general discussion in Chapter 8.

Chapter 8

Discussion, conclusion and future work

This thesis has explored *phase-space approaches to decoherence and classicality in quantum theory*. The overarching question has been: *to what extent can phase-space methods, grounded in coherent states and their associated measurements, provide a unifying description of decoherence, Lindblad dynamics, and the quantum-to-classical transition?* By analysing coherent-state POVMs, quasi-probability distributions, and stochastic unravellings across different symmetry groups, we have sought to clarify how measurement and environmental interactions shape quantum dynamics.

Our strategy has been twofold. First, we examined the effect of repeated coherent-state POVM measurements, which provide a natural operational model of unsharp phase-space observation. This led to explicit iterative and discrete-time descriptions of density-matrix dynamics, revealing how quantum coherences are progressively suppressed through convolution-like smoothing in phase space. Second, we compared these measurement-induced dynamics with those generated by Lindblad master equations, the standard framework for Markovian open-system evolution. In this way, we sought to identify conditions under which decoherence may be understood as phase-space diffusion, and to clarify the role played by symmetry, geometry, and representation theory.

Our investigation revealed a rich interplay between group symmetries, Lindblad semigroups, and informationally complete POVMs. In some cases (such as the flat Heisenberg-Weyl phase space and $\mathrm{SU}(N)$) the correspondence is exact, while in others (such as $\mathrm{SU}(2)$ and $\mathrm{SU}(1,1)$) the relationship is more subtle and requires alternative measurement schemes or even modifications of the dynamics.

Rather than treating each group in isolation, we now bring out the structural themes that unify the diverse symmetry settings studied in this thesis. These include, the interpretation of iterative coherent-state POVM measurements as covariant smoothing channels on phase space; the emergence of continuous-time diffusion generated by quadratic Casimirs; the discrete-to-continuous hierarchy of quasi-probability distributions; and the role of underlying geometry in shaping both deterministic and stochastic dynamics.

8.1 Iterative POVMs vs Lindblad dynamics

The fundamental distinction between the Iterative POVM measurement and Lindblad dynamics lies in the nature of these two constructions. POVM channels are defined by coherent-state overlaps,

resulting in covariant smoothing maps, while Lindblad dynamics arise from heat kernels generated by the quadratic Casimir, forming diffusion semigroups.

Despite both being isotropic on phase space, these channels generally have different spectra in the natural harmonic basis, as summarised in Table 8.1. Exact agreement occurs only in the HW case, where the POVM channel and Lindblad diffusion coincide fully, yielding an exact stochastic unravelling. For $\mathrm{SU}(2)$ and $\mathrm{SU}(1,1)$, the spectra differ but converge in certain limits, spin-$\frac{1}{2}$ and large-s ($s > 5$ is sufficient) for $\mathrm{SU}(2)$; large-k semiclassical scaling for $\mathrm{SU}(1,1)$. Interestingly, the $\mathrm{SU}(N)$ case exhibits full spectral agreement, with both channels admitting a common decomposition in terms of the $\mathfrak{su}(N)$ generators.

Group	**Coherent-state overlap** $\lvert\langle\Omega\rvert\Omega'\rangle\rvert^2$	**Heat Kernel Expansion**
HW	$\exp\big(-\lvert\alpha-\alpha'\rvert^2\big)$	$\dfrac{1}{(4\pi t)^{1/2}}\exp\!\left(-\dfrac{\lvert\alpha-\alpha'\rvert^2}{4t}\right)$
SU(2)	$\left(\cos\dfrac{\rho}{2}\right)^{2s}=\displaystyle\sum_{\ell=0}^{2s}a_\ell P_\ell(\cos\rho),$ $a_\ell=\dfrac{\binom{2s}{\ell}}{\binom{2s+\ell+1}{\ell}}$	$\displaystyle\sum_{\ell=0}^{2s}e^{-\ell(\ell+1)t}P_\ell(\cos\rho)$
SU(1,1)	$\left(\cosh\dfrac{\tau}{2}\right)^{-2k}=\displaystyle\int_0^\infty c_k(\lambda)\,P_{\mathrm{i}\lambda-\frac{1}{2}}(\cosh\tau)\,\mathrm{d}\lambda,$ $c_k(\lambda)=\dfrac{(2k-1)\lvert\Gamma(2k-\frac{1}{2}+\mathrm{i}\lambda)\rvert^2}{\Gamma^2(2k)}$	$\displaystyle\int_0^\infty \lambda\tanh(\pi\lambda)\,\mathrm{e}^{-t(\lambda^2+1/4)}\,P_{\mathrm{i}\lambda-\frac{1}{2}}(\cosh\tau)\,\mathrm{d}\lambda$

Table 8.1: Comparison between coherent-state overlaps and heat kernel expansions for the HW group, $\mathrm{SU}(2)$, and $\mathrm{SU}(1,1)$. The agreement in HW explains the exact unravelling found in Chapter 2. For $\mathrm{SU}(2)$ and $\mathrm{SU}(1,1)$, the mismatch in spectral weights obstructs exact identification of POVM dynamics with diffusion.

Both channels described above can be understood within the broader framework of quantum dynamical semigroups, families of completely positive, trace-preserving (CPTP) maps $\Phi_t, t \geq 0$ satisfying the semigroup composition law $\Phi_{t+s} = \Phi_t \circ \Phi_s$. For Lindblad diffusion, t is continuous and corresponds to physical time; for POVM iteration, k is discrete and counts successive nonselective measurements.

Diffusion semigroup. Generated by the Laplace-Beltrami operator (or equivalently, the quadratic Casimir), the diffusion channel acts on the eigenbasis f_λ as

$$\Phi_t^{\mathrm{diff}}[f_\lambda] = \mathrm{e}^{-\mathcal{C}_2(\lambda)t}\, f_\lambda, \tag{8.1}$$

where $\mathcal{C}_2(\lambda)$ is the quadratic-Casimir eigenvalue associated with the irreducible component labeled by λ.

POVM semigroup. Iterated coherent-state measurements define a discrete-time semigroup via

$$\Phi_k^{\mathrm{POVM}}[f_\lambda] = (\lambda_{\mathrm{POVM}})^k(\lambda)\, f_\lambda, \tag{8.2}$$

where the eigenvalues $\lambda_{\mathrm{POVM}}(\lambda)$ arise from the harmonic decomposition of the coherent-state overlap kernel, Gaussian for HW, binomial ratios for $\mathrm{SU}(2)$, and $\Phi_k(\lambda)$ weights for $\mathrm{SU}(1,1)$. Operator-theoretically, these eigenvalues define the spectrum of the Berezin transform [216–218], which captures how the POVM channel smooths phase-space structure through nonselective measurement.

In all symmetry settings the tension can be traced to the structure of the invariant operator algebra. For the Heisenberg-Weyl (HW) case, coherent-state convolution kernels shrink in phase space and converge to Gaussian heat kernels, so the Berezin channel coincides with the GKSL diffusion generated by $\hat{a}, \hat{a}^\dagger$. For $\mathrm{SU}(2)$ and $\mathrm{SU}(1,1)$, however, the coherent-state Berezin map is an invariant convolution operator with a finite-width kernel on the curved phase space (sphere or hyperboloid). The only $\mathrm{SU}(2)$ or $\mathrm{SU}(1,1)$-covariant local diffusive GKSL generators are multiples of the Laplace-Beltrami operator (quadratic Casimir), by standard classification of invariant diffusions on homogeneous spaces. These two invariant algebras, differential vs. convolution, do not coincide for finite kernel width; the Berezin increment already contains higher even angular moments that cannot be captured by a single second-order local operator.

By contrast, in tomographic $\mathrm{SU}(N)$ measurements the situation is trivialised by representation theory: $\mathrm{SU}(N)$ covariance reduces operator space to just two irreps (identity and adjoint), so both the tomographic channel and the depolarising Lindbladian act as scalars on the same blocks, and can be matched by tuning a single rate. Thus, only in the HW/flat and $\mathrm{SU}(N)$ tomographic cases do the measurement-induced Berezin channels coincide with simple GKSL diffusions, while for finite-spin $\mathrm{SU}(2)$ and $\mathrm{SU}(1,1)$ the structural mismatch is unavoidable.

This parallel structure raises a natural question: Can these two dynamics, diffusion and POVM smoothing, be experimentally distinguished? To address this, we now turn to the task of discrimination between semigroups via physically measurable quantities.

Experimental discrimination for decoherence models

Given that both mechanisms POVM measurement and the Lindblad dynamics are *a priori* plausible, deciding which one captures physical decoherence is ultimately an experimental question. A minimal and decisive test for $\mathrm{SU}(2)$ case is offered by a spin-1 system, where there are two nontrivial multipole sectors (dipole $\ell = 1$ and quadrupole $\ell = 2$).

For the isotropic Lindblad model, the rank-ℓ mode decays with rate $\Lambda_\ell = \frac{\gamma}{2}\,\ell(\ell+1)$. For the coherent-state POVM channel, a single iteration multiplies the rank-ℓ coefficient by $\lambda_{s,\ell} = \binom{2s}{\ell} / \binom{2s+\ell+1}{\ell}$; in an exponential fit per iteration (or per unit time after a suitable calibration) the effective decay rate is $\lambda_\ell = -\log \lambda_{s,\ell}$. For $s = 1$ this gives

$$\frac{\Lambda_2}{\Lambda_1} = 3, \qquad \frac{\lambda_2}{\lambda_1} = \frac{\log 10}{\log 2} \approx 3.32, \tag{8.3}$$

a dimensionless discrepancy that cannot be absorbed into a rescaling of γ.

Working in the irreducible tensor basis for spin 1, where the orientation (dipole) sector is encoded in $\rho_{1,m}$ and the alignment (quadrupole) sector in $\rho_{2,m}$ [112, 114]. Because isotropic channels damp all components within a fixed rank at the same rate, it suffices to monitor any nonzero pair $\rho_{1,m}(t)$ and

$\rho_{2,m}(t)$ and form

$$R = \frac{-\log\big(\rho_{2,m}(t)/\rho_{2,m}(0)\big)}{-\log\big(\rho_{1,m'}(t)/\rho_{1,m'}(0)\big)}. \tag{8.4}$$

Then $R \approx 3$ supports Lindblad diffusion, while $R \approx 3.32$ supports POVM-induced smoothing. In practice, $\rho_{1,m}$ can be read out from single-spin expectations (QND Faraday rotation / spin-squeezing), and $\rho_{2,m}$ from alignment observables via alignment-to-orientation conversion (AOC) with Raman coupling; see, e.g., [220–223].

In tomographic measurement, any isotropic Lindblad built from the Lie algebra generators likewise gives a single adjoint decay rate. Consequently, the ratio test becomes trivial ($R \equiv 1$ at the spectral level after normalisation), i.e. spin-1 (SU(2) with $s > 1/2$) is the minimal setting that *can* discriminate the two mechanisms spectrally.

For noncompact symmetry the standard GKSL with Hermitian generators is not $\mathrm{SU}(1,1)$-covariant; the "flipped" (Casimir-diffusive) variant restores covariance but is not a conventional CP Lindbladian at the operator level. Designing an experimental analogue of the above ratio test thus requires an implementation-specific route to alignment/orientation observables in the positive-discrete series and remains an open direction.

8.2 Hierarchy of phase-space distributions

The comparison of POVM and diffusion semigroups reveals how measurement-induced decoherence reflects the spectral structure of each symmetry group. A complementary perspective is offered by the Stratonovich-Weyl (SW) family of quasi-probability distributions $F^{(\sigma)}$, which interpolate between the singular P-function ($\sigma = 1$), the Wigner function ($\sigma = 0$), and the smooth, positive Husimi Q-function ($\sigma = -1$).

As shown in earlier chapters, coherent-state POVM iterations generate this hierarchy, acting as discrete shifts $\sigma \mapsto \sigma - 2$, with half-iterations shifting $\sigma \mapsto \sigma - 1$. Repeated measurements therefore drive any initial quasi-distribution toward the Q-function, defining a natural regularisation process in which singularities are smoothed, negativities eliminated, and classicality emerges.

In this language, the onset of classicality can be characterised by a sufficient bound

$$t_* \;=\; \max_{\lambda} \frac{1+\sigma}{\gamma\, \mathcal{C}_2(\lambda)} \log \Lambda_\lambda, \tag{8.5}$$

where $\gamma > 0$ is the decoherence strength parameter. The equation is expressed in terms of the representation labels λ, with $\mathcal{C}_2(\lambda)$ the quadratic Casimir and Λ_λ the Berezin eigenvalue for the associated mode. This bound marks the time after which all nontrivial modes are suppressed below the POVM threshold, ensuring positivity of the quasi-probability distribution.

Whether the same sufficiency bound applies in more general settings, and, more broadly, whether universal decoherence time scales can be identified for arbitrary Lie group representations, remains an open and compelling direction for future investigation.

Another promising avenue is the study of the minimum attainable value of a given quasi-probability

distribution $F^{(\sigma)}$, which quantifies its nonclassicality through the extent of negativity. Understanding how this minimum evolves under POVM-induced smoothing could offer a more refined measure of classicality onset, complementing the sufficiency bounds based on positivity alone. In Chapter 3 we presented numerical simulations for the $\mathrm{SU}(2)$ case, showing how the lowest value of $F^{(\sigma)}$ depends on spin s. In Chapter 4 we derived an analytical value for the minimum of a quasi-probability distribution. Extending this analysis to a more rigorous theoretical framework, and generalising it to noncompact settings such as $\mathrm{SU}(1,1)$, would further clarify the role of negativity as a quantitative witness of nonclassicality.

8.3 Lindblad dynamics vs stochastic descriptions

The Lindblad equation provides the most general algebraic framework for Markovian open-system dynamics, with a generator that is linear, completely positive, and trace-preserving. However, the choice of Lindblad operators is largely unconstrained and need not respect the symmetries of the underlying system, so group covariance is not guaranteed in general.

By contrast, the POVM and stochastic approaches developed in this thesis are symmetry-adapted from the outset. Coherent states are defined as group orbits, and their overlaps reflect the geometry of the associated homogeneous space. The stochastic unravellings we construct, driven by Brownian motion on the phase space, preserve this geometric structure, confining trajectories to the coherent-state manifold and yielding dynamics that are automatically group-covariant.

In this framework, the generator is fixed by geometry: Brownian motion implies that evolution is governed by the Laplace-Beltrami operator, tied to the quadratic Casimir of the group. This results in diffusion-type semigroups. In contrast, GKSL master equations can describe a broader class of noise processes, but they are not generally derived from an underlying phase-space geometry. The case of $\mathrm{SU}(1,1)$ highlights this distinction. Standard GKSL dynamics break group covariance, while the coherent-state SDE construction retains it, yielding Casimir-driven diffusion.

Thus, Lindblad dynamics offer algebraic generality, while the coherent-state approach provides a geometric, symmetry-aware model of decoherence, more constrained, but deeply connected to the underlying phase space. This opens a natural direction for future work which is to explore how alternative noise models on the coherent-state manifold, beyond Brownian motion, can lead to different classes of dynamical equations, and whether such models can capture the full structure of POVM-induced channels [224,225]. Doing so could bridge the gap between geometric stochastic unravellings and the algebraic richness of Lindblad dynamics.

8.4 Relativistic phase-space measurement and decoherence

Finally, we turned to relativistic quantum mechanics, a subject often bypassed in favour of quantum field theory (QFT). While QFT provides the dominant framework for relativistic phenomena, it comes with well-known challenges such as divergences requiring renormalisation, the absence of a natural phase-space structure, and limited tools for analysing entanglement and decoherence.

Motivated by these shortcomings, we constructed a relativistic phase-space representation based on the unitary Bargmann transform between the future tube and the forward light cone. This enabled the

definition of coherent states of the conformal group and an associated POVM, thereby establishing a measurement-theoretic phase-space picture for relativistic systems. We also introduced iterative measurement and outlined preliminary dynamical considerations, pointing toward a broader programme of relativistic phase-space methods.

Although this analysis is preliminary, it opens several promising directions for future work. One avenue is to develop a systematic understanding of iterative measurement processes in the relativistic setting, which may require new mathematical tools beyond those used in the nonrelativistic case. Another is to explore dynamical aspects more fully, including the possibility of defining causal and covariant Brownian motion on the future tube or the forward light cone, providing a relativistic analogue of the stochastic unravelling models introduced earlier. Such developments could offer new insights into decoherence, classicality, and entanglement in relativistic quantum systems, and may ultimately suggest a finite, measurement-based alternative to QFT that avoids divergences while retaining covariance.

8.5 Towards a generalised framework

The results presented in the previous chapters suggest the possibility of a generalised framework for modelling decoherence and classicality in quantum theory. At its heart, this approach is based on generalised coherent states and their associated POVMs, which encode the geometry of the underlying symmetry group and provide a natural bridge between Hilbert space and classical phase space. Within this tentative framework:

- Coherent states represent the geometry of phase space (flat, compact, noncompact, or relativistic).
- POVM measurements generate diffusion-like processes that drive states toward classicality.
- Lindblad semigroups can be interpreted as the continuous-time limit of such measurements, though the correspondence depends on the symmetry group and measurement choice.
- Stochastic unravellings can be modelled as Brownian motion of coherent-state labels on phase space, with ensemble averages reproducing Lindblad dynamics.

We now sketch how these ideas can be formalised by introducing generalised coherent states, constructing the associated POVMs, and extending the discussion to stochastic unravellings.

8.5.1 Perelomov coherent states

A natural starting point for a generalised phase-space framework is the construction of Perelomov coherent states [35] (briefly discussed in 3.2), which generalise the canonical coherent states of the harmonic oscillator to arbitrary Lie groups.

Let G be a Lie group with a unitary irreducible representation (UIR) $U(g)$ on a Hilbert space $\mathcal{H}$. Fix a normalised *fiducial vector* $|\psi_0\rangle \in \mathcal{H}$, often chosen as a ground state or vacuum. The family of coherent states is then defined as the group orbit

$$|\psi_g\rangle = U(g)|\psi_0\rangle, \qquad g \in G. \tag{8.6}$$

In general, the fiducial state is invariant up to a phase under a stabiliser subgroup $H \subset G$,

$$H = \{h \in G \,|\, U(h)|\psi_0\rangle = \mathrm{e}^{\mathrm{i}\phi(h)}|\psi_0\rangle\}. \tag{8.7}$$

Thus, the physically distinct coherent states are naturally labelled by the coset space G/H. The resulting set $\{|\psi_{gH}\rangle\}_{gH\in G/H}$ is overcomplete in $\mathcal{H}$ and provides a resolution of the identity.

Properties

These coherent-states satsify the following properties.

Normalisation. Each state is normalised by construction, $\langle\psi_g|\psi_g\rangle = 1$.

Overcompleteness. The coherent states form an overcomplete set on the phase space G/H, satisfying a resolution of the identity

$$\int_{G/H} \mathrm{d}\mu(gH)\, |\psi_{gH}\rangle\langle\psi_{gH}| = \mathbb{1},$$

where $\mathrm{d}\mu$ is an invariant measure. This underpins their use in POVM-based measurements and phase-space quantisation.

Nonorthogonality. Coherent states are nonorthogonal, with overlaps $\langle\psi_g|\psi_{g'}\rangle \neq 0$. These overlaps define a reproducing kernel, endowing the coherent-state manifold with the structure of a reproducing kernel Hilbert space (RKHS) [33].

Semiclassicality. Coherent states often minimize uncertainty relations and follow trajectories on G/H that approximate classical motion, making them natural candidates for describing the quantum-to-classical transition under decoherence.

8.5.2 POVMs from generalised coherent states and Lindblad dynamics

In this section, we describe how we can construct coherent-state based POVMs, discuss their interpretational significance in measurement theory, and show how they provide a physically motivated model for decoherence when viewed as nonselective environmental interactions.

Construction of the POVM

Given a set of generalised coherent states $\{|\psi_{gH}\rangle\}_{gH\in G/H}$, we define a coherent-state POVM as the map

$$\mathcal{E} : B(G/H) \to \mathcal{B}(\mathcal{H}), \quad \mathcal{E}(\Omega) = \int_{\Omega} \mathrm{d}\mu(gH)\, |\psi_{gH}\rangle\langle\psi_{gH}|, \tag{8.8}$$

where $B(G/H)$ is the Borel σ-algebra of the homogeneous space G/H, $\mathcal{B}(\mathcal{H})$ denotes bounded operators on $\mathcal{H}$, and $\mathrm{d}\mu$ is a normalised invariant measure over G/H. The completeness of the POVM

follows from the resolution of the identity.

This defines an informationally complete measurement, any quantum state $\hat{\rho} \in \mathcal{B}(\mathcal{H})$ is fully specified by the probability distribution

$$p(gH) = \mathrm{tr}(\hat{\rho}\,|\psi_{gH}\rangle\langle\psi_{gH}|). \tag{8.9}$$

These POVMs are also covariant with respect to the symmetry group G, meaning that for all $g \in G$, we have

$$U(g)\,\mathcal{E}(\Omega)\,U(g)^{\dagger} = \mathcal{E}(g\Omega), \tag{8.10}$$

where $g\Omega = \{gh \,|\, h \in \Omega\}$. This covariance ensures that the measurement respects the underlying physical symmetries of the system.

This completeness, combined with the minimal disturbance from nonselective application, makes them ideal tools for modeling decoherence and the emergence of classicality in symmetry-rich quantum systems [11,54].

Selective and nonselective measurement

Suppose a measurement is performed using this POVM, and the outcome corresponds to a specific point $gH \in G/H$. Then, the post-measurement state (under the Lüders update rule) becomes

$$\hat{\rho} \mapsto \frac{|\psi_{gH}\rangle\langle\psi_{gH}|}{\langle\psi_{gH}|\hat{\rho}|\psi_{gH}\rangle}. \tag{8.11}$$

This describes a *selective measurement*, where the outcome is known, and the system collapses to the coherent state labeled by the observed point in phase space.

However, to model decoherence, particularly as induced by an environment that is constantly monitoring the system without revealing the outcome, we must consider *nonselective* measurements. This corresponds to averaging over all possible outcomes, leading to a completely positive trace-preserving (CPTP) map

$$\hat{\rho} \mapsto \int_{G/H} \mathrm{d}\mu(gH)\,|\psi_{gH}\rangle\langle\psi_{gH}|\,\hat{\rho}\,|\psi_{gH}\rangle\langle\psi_{gH}|. \tag{8.12}$$

Since coherent states are nonorthogonal, this measurement is *fuzzy*, it does not fully distinguish between basis elements, which reflects physical limitations of precision and information extraction in realistic environments and thus can be used as an environmental model of decoherence.

Having established that nonselective coherent-state POVMs lead to decoherence by averaging over phase-space outcomes, we now consider a dynamical perspective: What happens when such measurements are applied repeatedly, as a sequence of weak, symmetry-respecting interventions? This leads to the notion of *iterative coherent-state POVMs*, which serves as a bridge between static measurement models and continuous-time open system dynamics.

Iterated nonselective measurements

Let $\mathcal{E}$ be the CPTP map associated with a nonselective coherent-state measurement:

$$\mathcal{E}[\hat{\rho}] = \int_{G/H} \mathrm{d}\mu(gH)\, |\psi_{gH}\rangle\langle\psi_{gH}|\, \hat{\rho}\, |\psi_{gH}\rangle\langle\psi_{gH}|. \tag{8.13}$$

Suppose this operation is applied iteratively at discrete time steps. After n applications, the state evolves as

$$\hat{\rho}^{(n)} = \mathcal{E}^n[\hat{\rho}^{(0)}], \tag{8.14}$$

where $\hat{\rho}^{(0)}$ is the initial state. As $n \to \infty$, under mild conditions, the state converges to a fixed point, typically a diagonal mixture over the coherent states, representing a classical-like state with suppressed coherence in the phase space.

To analyse this evolution, one can exploit the structure of a reproducing kernel Hilbert space (RKHS). The coherent states satisfy

$$\langle\psi_{gH}|\psi_{g'H}\rangle = K(gH, g'H), \tag{8.15}$$

where K is a positive-definite reproducing kernel. In many cases, we can expand the kernel in an orthonormal basis $\{\phi_k\}$ of $L^2(G/H, \mathrm{d}\mu)$

$$K(gH, g'H) = \sum_k \lambda_k\, \phi_k(gH)\, \overline{\phi_k(g'H)}. \tag{8.16}$$

This expansion provides a way to study the effect of repeated POVM application on the matrix elements of $\hat{\rho}$ in this basis.

8.5.3 Connection to Lindblad dynamics

A natural question is whether the discrete-time evolution induced by iterative POVM measurement can be approximated by a continuous-time master equation. In the weak-measurement limit, such dynamics often reduce to a Lindblad-type generator of the form

$$\frac{\mathrm{d}\hat{\rho}}{\mathrm{d}t} = \sum_j \left(\hat{L}_j \hat{\rho} \hat{L}_j^\dagger - \frac{1}{2}\{\hat{L}_j^\dagger \hat{L}_j, \hat{\rho}\} \right), \tag{8.17}$$

where the $\hat{L}_j$ are Lindblad operators.

For systems with Lie-group symmetry G, it is natural to construct these operators from the generators $\{T_j\}$ of the Lie algebra $\mathfrak{g}$, represented on Hilbert space via

$$\hat{L}_j = X_j, \quad \text{where} \quad X_j = \frac{\mathrm{d}}{\mathrm{d}t} U(\exp(tT_j))\Big|_{t=0}. \tag{8.18}$$

This choice ensures complete positivity and trace preservation, but not necessarily covariance under G.

Indeed, general GKSL dynamics are not group-covariant unless the generator commutes with the

adjoint action of G. This requires the dissipator to transform appropriately under the group, which imposes additional constraints beyond the algebraic GKSL form. In compact groups such as $\mathrm{SU}(2)$, isotropic Lindblad generators constructed from the spin operators do satisfy covariance. For noncompact groups like $\mathrm{SU}(1,1)$, however, covariance is generally broken due to the indefinite metric in the adjoint representation.

An alternative, symmetry-respecting construction arises by endowing $\mathfrak{g}$ with the Killing form and taking the Lindblad generator to be proportional to the quadratic Casimir operator as

$$\frac{\mathrm{d}\hat{\rho}}{\mathrm{d}t} = \sum_{i,j} \kappa^{ij} \left(\hat{L}_i \hat{\rho} \hat{L}_j^\dagger - \frac{1}{2} \left\{ \hat{L}_j^\dagger \hat{L}_i, \hat{\rho} \right\} \right), \tag{8.19}$$

where κ^{ij} is the inverse of the Killing form matrix $\kappa_{ij} = \kappa(X_i, X_j)$, assuming it's nondegenerate.

This yields a diffusion semigroup whose generator is the Laplace–Beltrami operator on the group manifold, and hence automatically group-covariant. Such dynamics are precisely those obtained from the coherent-state Brownian-motion framework developed in this thesis, providing a geometrically natural and symmetry-aware alternative to general GKSL evolution.

8.5.4 Stochastic unravelling of coherent-state diffusions

In what follows, we describe the structure of these group-based SDEs and outline their potential role in modeling open quantum systems via diffusion on coherent-state manifolds. While a complete formulation of this idea remains to be developed, we outline here a tentative framework aimed at generalising these constructions.

Geometric construction

Consider the left-invariant Itô SDE on G [226–230]

$$\mathrm{d}g_t \, g_t^{-1} = X_a \, \mathrm{d}\omega_t^a, \qquad \mathrm{d}\omega_t^a = \mu^a \, \mathrm{d}t + \sigma^a{}_k \, \mathrm{d}W_t^k, \tag{8.20}$$

where $\{X_a\}$ is a basis of $\mathfrak{g}$, $\{W_t^k\}$ are independent standard Wiener processes.

Define the coherent-state process

$$|\psi_{g,t}\rangle = U(g_t) \, |\psi_0\rangle. \tag{8.21}$$

Writing $U_*(X_a)$ for the differential of the representation, Itô's formula gives

$$\mathrm{d}|\psi_{g,t}\rangle = \Big(U_*(X_a) \, \mathrm{d}\omega_t^a + \frac{1}{2} \, \Gamma^{ab} \, U_*(X_a) U_*(X_b) \, \mathrm{d}t \Big) \, |\psi_{g,t}\rangle, \tag{8.22}$$

and $\Gamma^{ab} = \sum_k \sigma^a{}_k \sigma^b{}_k$.
The general SDE above accommodates arbitrary diffusion structures in the Lie algebra directions through the noise coefficients σ^a_k. In many physically relevant scenarios, however, the noise is uncorrelated and acts independently along each generator of the Lie algebra. This yields the *diagonal noise case*, in which the diffusion matrix Γ^{ab} is diagonal.

Such a structure arises naturally in models of decoherence, weak continuous measurement, or symmetry-

preserving diffusion, where each generator of the symmetry algebra undergoes independent stochastic fluctuations. We record this as a corollary.

Corollary 8.1. Suppose the noise is uncorrelated and aligned with the Lie algebra basis, so that

$$\mathrm{d}\omega_t^a = \sqrt{\gamma}\,\mathrm{d}W_t^a, \qquad \mathrm{d}\omega_t^a\,\mathrm{d}\omega_t^b = \gamma\,g^{ab}\,\mathrm{d}t, \tag{8.23}$$

where g^{ab} is the inverse of the invariant bilinear form (e.g. the Killing form) on the Lie algebra. Then the coherent-state SDE is

$$\mathrm{d}|\psi_{g,t}\rangle = \left(\sum_a U_*(X_a)\,\mathrm{d}\omega_t^a + \tfrac{1}{2}\,\gamma\sum_{a,b} g^{ab}\,U_*(X_a)U_*(X_b)\,\mathrm{d}t\right)|\psi_{g,t}\rangle. \tag{8.24}$$

This form closely resembles the standard diffusive stochastic Schrödinger equation (SSE) used in open quantum systems, with the differential representation operators $U_*(X_a)$ playing the role of Lindblad operators. The key distinction is that the diffusion coefficients are weighted by the invariant metric g^{ab} of the Lie algebra: for compact groups (e.g. $\mathrm{SU}(2)$) this reduces to the familiar positive-definite case, while for noncompact groups (e.g. $\mathrm{SU}(1,1)$) the indefinite signature of g^{ab} leads to sign changes in the drift terms. In all cases, however, the evolution remains confined to the coherent-state manifold and incorporates quantum noise consistent with continuous measurement or environmental decoherence.

We now show that under the diagonal noise dynamics, the ensemble-averaged state $\hat{\rho}_t = \mathbb{E}[\hat{R}_t] = \mathbb{E}[|\psi_{g,t}\rangle\langle\psi_{g,t}|]$ satisfies a master equation.

Proposition 8.1. *Let $|\psi_{g,t}\rangle$ be the coherent-state process defined by (8.24) with Gaussian noises satisfying $\mathbb{E}[\mathrm{d}\omega_t^a] = 0$ and $\mathrm{d}\omega_t^a\,\mathrm{d}\omega_t^b = \gamma\,g^{ab}\,\mathrm{d}t$. Then the ensemble-averaged density matrix $\hat{\rho}_t = \mathbb{E}[\,|\psi_{g,t}\rangle\langle\psi_{g,t}|\,]$ evolves according to*

$$\frac{\mathrm{d}\hat{\rho}_t}{\mathrm{d}t} = \gamma\left(g^{ab}\,U_*(X_a)\,\hat{\rho}_t\,U_*(X_b) - \tfrac{1}{2}\,\{g^{ab}\,U_*(X_a)U_*(X_b),\,\hat{\rho}_t\}\right). \tag{8.25}$$

Proof. This follows directly from Itô's lemma applied to the stochastic process $\hat{R}_t$, using the quadratic variation $\mathrm{d}\omega_t^a\,\mathrm{d}\omega_t^b = \gamma g^{ab}\,\mathrm{d}t$ and collecting the drift terms. □

This concludes the discussion on the stochastic unravelling framework for generalised coherent states.

Conclusion and outlook

This thesis has developed a phase-space framework for decoherence and the emergence of classicality, using generalised coherent states and their associated POVMs as the central unifying structure. By examining the connections between iterative POVM-induced smoothing, Lindblad-type diffusion, and stochastic unravellings on phase space, we have uncovered both universal mechanisms underlying measurement-induced decoherence and group-specific subtleties arising from the geometry of the underlying symmetry.

These results point toward a deeper synthesis of quantum measurement theory, open-system dynamics, and geometric methods, and suggest several avenues for future work as discussed.

Bibliography

[1] von Neumann J. 1955 *Mathematical Foundations of Quantum Mechanics* (Princeton University Press).

[2] Bell J. S. 1990 Against measurement *Physics World* **3**, 33–40.

[3] Maudlin T. 1995 Three measurement problems *Topoi* **14**, 7–15.

[4] Busch P., Lahti P. and Mittelstaedt P. 1996 *The Quantum Theory of Measurement* (Springer).

[5] Zeh H. D. 1970 On the interpretation of measurement in quantum theory *Foundations of Physics* **1**, 69–76.

[6] Joos E. and Zeh H. D. 1985 The emergence of classical properties through interaction with the environment *Zeitschrift für Physik B* **59**, 223–243.

[7] Zurek W. H. 1991 Decoherence and the transition from quantum to classical *Physics Today* **44**(10), 36–44.

[8] Schlosshauer M. 2007 *Decoherence and the Quantum-to-Classical Transition* (Springer).

[9] Schlosshauer M. 2019 Quantum decoherence *Physics Reports* **831**, 1–57.

[10] Joos E., Zeh H. D., Kiefer C., Giulini D., Kupsch J., and Stamatescu I.-O. 2003 *Decoherence and the Appearance of a Classical World in Quantum Theory*, 2nd ed. (Springer).

[11] Zurek W. H. 2003 Decoherence, einselection, and the quantum origins of the classical *Reviews of Modern Physics* **75**, 715–775.

[12] Paz J. P. and Zurek W. H. 2001 Environment-induced decoherence and the transition from quantum to classical in Heiss D. (ed.), *Lecture Notes in Physics* **587**, (Springer).

[13] Heiss D. 2008 *Fundamentals of Quantum Information: Quantum Computation, Communication, Decoherence and All That* (Springer, Vol. 587).

[14] Halliwell J. J. 1989 Decoherence in quantum cosmology *Physical Review D* **39**(10), 2912–2923.

[15] Barvinsky A., Kamenshchik A., Kiefer C. and Mishakov I. 1998 Decoherence in quantum cosmology at the onset of inflation *Modern Physics Letters A* **13**(38), 3245–3253.

[16] Halliwell J. J. 2009 Probabilities in quantum cosmological models: A decoherent histories analysis *Physical Review D* **80**, 124032.

[17] Asselmeyer-Maluga T. and Krol J. 2013 Decoherence in quantum cosmology and the cosmological constant *Modern Physics Letters A* **28**, 1350158.

[18] Bacciagaluppi G. and Hemmo M. 1996 Modal interpretations, decoherence and measurements *Studies in History and Philosophy of Modern Physics* **27** 239–277.

[19] Bacciagaluppi G. 2000 Delocalized properties in the modal interpretation of a continuous model of decoherence *Foundations of Physics* **30**(9), 1431–1444.

[20] Bacciagaluppi G. 2007 Probability, arrow of time and decoherence *arXiv preprint* arXiv:quant-ph/0701225.

[21] Bacciagaluppi G. 2012 The role of decoherence in quantum mechanics In E. Zalta (ed.), *The Stanford Encyclopedia of Philosophy*, summer 2020 ed.

[22] Caldeira A. O. and Leggett A. J. 1983 Path integral approach to quantum Brownian motion *Physica A* **121**, 587–616.

[23] Brody D. C., Graefe E.-M. and Melanathuru R. 2025 Phase-space measurements, decoherence, and classicality *Physical Review Letters* **134**(12), 120201.

[24] Wigner E. P. 1932 On the quantum correction for thermodynamic equilibrium *Physical Review* **40**, 749–759.

[25] Hillery M., O'Connell R. F., Scully M. O. and Wigner E. P. 1984 Distribution functions in physics: Fundamentals *Physics Reports* **106**, 121–167.

[26] Davidovich L. 1999 Decoherence, Wigner functions, and the classical limit of quantum mechanics in cavity QED *AIP Conference Proceedings* **461**, 151–162.

[27] Arthurs E. and Kelly J. L., Jr. 1965 On the simultaneous measurement of a pair of conjugate observables *Bell System Technical Journal* **44**(4), 725–729.

[28] Busch P. 1985 Indeterminacy relations and simultaneous measurements in quantum theory *International Journal of Theoretical Physics* **24**(1), 63–92.

[29] Diósi L. and Halliwell J. J. 1998 Coupling classical and quantum variables using continuous quantum measurement theory *Physical Review Letters* **81**, 2846–2849.

[30] Murakami M., Ford G. W. and O'Connell R. F. 2003 Decoherence in phase space *Laser Physics* **13**, 180–183.

[31] De Pasquale A., Foti C., Cuccoli A., Giovannetti V. and Verrucchi P. 2019 Dynamical model for positive-operator-valued measures *Physical Review A* **100**, 012130.

[32] Bohmann M., Agudelo E. and Sperling J. 2020 Probing nonclassicality with matrices of phase-space distributions *Quantum* **4**, 343.

[33] Ali S. T., Antoine J.-P. and Gazeau J.-P. 2000 *Coherent States, Wavelets, and Their Generalizations* (Springer).

[34] Busch P. 1991 Informationally complete sets of physical quantities *International Journal of Theoretical Physics* **30**, 1217–1227.

[35] Perelomov A. 1986 *Generalized Coherent States and Their Applications* (Springer).

[36] Klauder J. R. and Skagerstam B.-S. 1985 *Coherent States: Applications in Physics and Mathematical Physics* (World Scientific).

[37] Habib S., Shizume K. and Zurek W. H. 1998 Decoherence, chaos, and the correspondence principle *Physical Review Letters* **80**, 4361–4365.

[38] Brun T. A. 2000 Continuous measurements, quantum trajectories, and decoherent histories *Physical Review A* **61**, 042107.

[39] Zhang W.-M., Feng D. H. and Gilmore R. 1990 Coherent states: theory and some applications *Reviews of Modern Physics* **62**, 867–927.

[40] Kossakowski A. 1972 On quantum statistical mechanics of non-Hamiltonian systems *Reports on Mathematical Physics* **3**, 247–274.

[41] Lindblad G. 1976 On the generators of quantum dynamical semigroups *Communications in Mathematical Physics* **48**, 119–130.

[42] Gorini V., Kossakowski A. and Sudarshan E. C. G. 1976 Completely positive dynamical semigroups of N-level systems *Journal of Mathematical Physics* **17**, 821–825.

[43] Carmichael H. J. 1993 *An Open Systems Approach to Quantum Optics* (Springer).

[44] Wiseman H. M. and Milburn G. J. 2010 *Quantum Measurement and Control* (Cambridge University Press).

[45] Bros J. and Buchholz D. 1990 Analyticity and crossing symmetry in quantum field theory *Physics Letters B* **246**, 315–319.

[46] Nussbaum A. 1995 The future tube and quantum field theory *Journal of Mathematical Physics* **36**, 2841–2855.

[47] Brody D. C. and Hughston L. P. 2021 Quantum measurement of space-time events *Journal of Physics A: Mathematical and Theoretical* **54**, 235304.

[48] Reed M. and Simon B. 1980 *Functional Analysis* (*Methods of Modern Mathematical Physics, Vol. I*) (Academic Press).

[49] Hall B. C. 2013 *Quantum Theory for Mathematicians* (Springer).

[50] Nielsen M. A. and Chuang I. L. 2010 *Quantum Computation and Quantum Information*, 10th Anniversary ed. (Cambridge University Press).

[51] Sakurai J. J. and Napolitano J. 1994 *Modern Quantum Mechanics*, 2nd ed. (Addison-Wesley).

[52] Lüders G. 1951 Über die Zustandsänderung durch den Meßprozess *Annalen der Physik* **443**(5–8), 322–328. [English translation: Concerning the state change due to the measurement process *Annalen der Physik* (*Leipzig*) **15**, 663–670 (2006).]

[53] Davies E. B. 1976 *Quantum Theory of Open Systems* (Academic Press, London).

[54] Holevo A. S. 2001 *Statistical Structure of Quantum Theory* (Springer).

[55] Peres A. 2002 *Quantum Theory: Concepts and Methods* (Kluwer Academic Publishers).

[56] Davies E. B. and Lewis J. T. 1970 An operational approach to quantum probability *Communications in Mathematical Physics* **17**, 239–260.

[57] Schrödinger E. 1926 Der stetige Übergang von der Mikro- zur Makromechanik *Naturwissenschaften* **14**, 664–666.

[58] Glauber R. J. 1963 Coherent and incoherent states of the radiation field *Physical Review* **131**, 2766–2788.

[59] Glauber R. J. 1963 The quantum theory of optical coherence *Physical Review* **130**, 2529–2539.

[60] Gilmore R. 1972 Geometry of symmetrized states *Annals of Physics* **74**(2), 391–463.

[61] Husimi K. 1940 Some formal properties of the density matrix *Proceedings of the Physico-Mathematical Society of Japan* **22**, 264–314.

[62] Sudarshan E. C. G. 1963 Equivalence of semiclassical and quantum mechanical descriptions of statistical light beams *Physical Review Letters* **10**(7), 277–279.

[63] Schleich W. P. 2001 *Quantum Optics in Phase Space* (Wiley-VCH).

[64] Brody D. C. and Melanathuru R. 2025 Decoherence from universal tomographic measurements *arXiv preprint* arXiv:2511.07369.

[65] Barchielli A. and Gregoratti M. 2009 *Quantum Trajectories and Measurements in Continuous Time* (Springer).

[66] Haroche S. and Raimond J. M. 2006 *Exploring the Quantum: Atoms, Cavities, and Photons* (Oxford University Press).

[67] Blais A., Grimsmo A. L., Girvin S. M., and Wallraff A. 2021 Circuit quantum electrodynamics *Reviews of Modern Physics* **93**, 025005.

[68] Aspelmeyer M., Kippenberg T. J., and Marquardt F. 2014 Cavity optomechanics *Reviews of Modern Physics* **86**, 1391-–1452.

[69] Walls D. F. and Milburn G. J. 2008 *Quantum Optics*, 2nd ed. (Springer).

[70] Stratonovich H. L. 1955 On distributions in representation space *Soviet Physics JETP* **4**(6), 891–898.

[71] Cahill K. E. and Glauber R. J. 1969 Ordered expansions in boson amplitude operators *Physical Review* **177**, 1857–1881.

[72] Agarwal G. S. and Wolf E. 1970 Calculus for functions of noncommuting operators and general phase-space methods in quantum mechanics. I. Mapping theorems and ordering of functions of noncommuting operators *Physical Review D* **2**, 2161–2186.

[73] Cohen-Tannoudji C., Diu B. and Laloe F. 1977 *Quantum Mechanics*, Vol. 1 (Wiley).

[74] Arfken G. B., Weber H. J. and Harris F. E. 2012 *Mathematical Methods for Physicists*, 7th ed. (Academic Press).

[75] Fock V. 1928 Verallgemeinerung und Lösung der Diracschen statistischen Gleichung *Zeitschrift für Physik* **49**, 339–357.

[76] Bargmann V. 1961 On a Hilbert space of analytic functions and an associated integral transform *Communications on Pure and Applied Mathematics* **14**, 187–214.

[77] Hall B. C. 2000 Holomorphic methods in analysis and mathematical physics *Contemporary Mathematics* **260**, American Mathematical Society.

[78] Zurek W. H. 1981 Pointer basis of quantum apparatus: Into what mixture does the wave packet collapse? *Physical Review D* **24**(6), 1516–1525.

[79] Diósi L. and Kiefer C. 2002 Exact positivity of the Wigner and P-functions of a Markovian open system *Journal of Physics A: Mathematical and General* **35**, 2675–2683.

[80] Rivas Á. and Huelga S. F. 2012 *Open Quantum Systems: An Introduction* (Springer).

[81] Breuer H.-P. and Petruccione F. 2002 *The Theory of Open Quantum Systems* (Oxford University Press).

[82] Hertz A. and De Bièvre S. 2020 Quadrature coherence scale driven fast decoherence of bosonic quantum field states *Physical Review Letters* **124**, 090402.

[83] De Bièvre S., Horoshko D. B., Patera G. and Kolobov M. I. 2019 Measuring nonclassicality of bosonic field quantum states via operator ordering sensitivity *Physical Review Letters* **122**, 080402.

[84] Gardiner C. W. and Zoller P. 2004 *Quantum Noise*, 3rd ed. (Springer).

[85] Strauss W. A. 2007 *Partial Differential Equations: An Introduction*, 2nd ed. (John Wiley & Sons).

[86] Evans L. C. 2010 *Partial Differential Equations* (American Mathematical Society, Graduate Studies in Mathematics, Vol. 19).

[87] Moyal J. E. 1949 Quantum mechanics as a statistical theory *Proceedings of the Cambridge Philosophical Society* **45**, 99–124.

[88] Curtright T., Fairlie D. and Zachos C. 2012 *A Concise Treatise on Quantum Mechanics in Phase Space* (World Scientific).

[89] Jaynes E. T. 1957 Information theory and statistical mechanics *Physical Review* **106**(4), 620–630.

[90] Cover T. M. and Thomas J. A. 2006 *Elements of Information Theory*, 2nd ed. (Wiley-Interscience).

[91] Bengtsson I. and Życzkowski K. 2006 *Geometry of Quantum States* (Cambridge University Press).

[92] Holevo A. S. 2011 *Probabilistic and Statistical Aspects of Quantum Theory* (Edizioni della Normale).

[93] Arecchi T. F., Courtens E., Gilmore R. and Thomas H. 1972 Atomic coherent states in quantum optics *Physical Review A* **6**(6), 2211–2237.

[94] Radcliffe M. J. 1971 Some properties of coherent spin states *Journal of Physics A: General Physics* **4**(3), 313–323.

[95] Brune M., Haroche S., Raimond J. M., Davidovich L. and Zagury N. 1992 Manipulation of photons in a cavity by dispersive atom-field coupling: Quantum-nondemolition measurements and generation of Schrödinger cat states *Physical Review A* **45**, 5193–5214.

[96] Gerry C. C. and Knight P. L. 2005 *Introductory Quantum Optics* (Cambridge University Press).

[97] Gazeau J. P. 2009 *Coherent States in Quantum Physics* (Wiley-VCH).

[98] Hammerer K., Sørensen A. S. and Polzik E. S. 2010 Quantum interface between light and atomic ensembles *Reviews of Modern Physics* **82**(2), 1041–1093.

[99] Brif C., Chakrabarti R. and Rabitz H. 2010 Control of quantum phenomena: past, present and future *New Journal of Physics* **12**, 075008.

[100] Brody D. C. and Graefe E.-M. 2010 Coherent states and rational surfaces *Journal of Physics A: Mathematical and Theoretical* **43**(25), 255205.

[101] Berman G. P., Bulgakov E. N. and Holm D. D. 1994 *Crossover-Time in Quantum Boson and Spin Systems* (Springer Science & Business Media).

[102] Biedenharn L. C., Louck J. D. and Carruthers P. A. 1984 *Angular Momentum in Quantum Physics: Theory and Application* (Addison-Wesley).

[103] Edmonds A. R. 1996 *Angular Momentum in Quantum Mechanics* (Princeton University Press).

[104] Rose M. E. 1995 *Elementary Theory of Angular Momentum* (Courier Corporation).

[105] Varshalovich D. A., Moskalev N. M. and Khersonskii V. K. 1988 *Quantum Theory of Angular Momentum* (World Scientific).

[106] Rivas A. and Luis A. 2013 SU(2)-invariant depolarization of quantum states of light *Physical Review A* **88**(5), 052120.

[107] Weigert S. and Busch P. 2003 Lüders theorem for coherent-state POVMs *Journal of Mathematical Physics* **44**(12), 5474–5486.

[108] Appleby D. M. 2000 Optimal measurements of spin direction *International Journal of Theoretical Physics* **39**, 2231–2252.

[109] Racah G. 1942 Theory of complex spectra. II *Physical Review* **62**, 438–462.

[110] Klimov A. B. and Chumakov S. M. 2009 *A Group-Theoretical Approach to Quantum Optics: Models of Atom-Field Interactions* (Wiley-VCH).

[111] Fano U. 1957 Description of states in quantum mechanics by density matrix and operator techniques *Reviews of Modern Physics* **29**, 74–93.

[112] Agarwal G. S. 1981 Relation between atomic coherent-state representation, state multipoles, and generalized phase-space distributions *Physical Review A* **24**(6), 2889–2896.

[113] Blum K. 2012 *Density Matrix Theory and Applications*, 3rd ed. (Springer).

[114] Budker D. and Jackson Kimball D. F. 2013 *Optical Magnetometry* (Cambridge University Press).

[115] Gilmore R. 1976 Q and P representatives for spherical tensors *Journal of Physics A: Mathematical and General* **9**(7), 65–78.

[116] Klimov A. B. 2002 Exact evolution equations for SU(2) quasidistribution functions *Journal of Mathematical Physics* **43**(5), 2202–2213.

[117] Klimov A. B. and Chumakov S. M. 2002 On the SU(2) Wigner function dynamics *Revista Mexicana de Física* **48**(4), 317–324.

[118] Gilmore R. 2005 Wigner distribution on SU(2) in *The Physics of Phase Space: Nonlinear Dynamics and Chaos, Geometric Quantization, and Wigner Function* (Springer), pp. 211–213.

[119] Klimov A. B., Romero J. L. and De Guise H. 2017 Generalized SU(2) covariant Wigner functions and some of their applications *Journal of Physics A: Mathematical and Theoretical* **50**(32), 325301.

[120] Terr D. 2025 *Wigner3j.m*, MATLAB Central File Exchange. https://www.mathworks.com/matlabcentral/fileexchange/5275-wigner3j-m. Retrieved September 7, 2025.

[121] Davis J., Kumari M., Mann R. B. and Ghose S. 2021 Wigner negativity in spin-j systems *Physical Review Research* **3**, 033134.

[122] Gradshteyn I. S. and Ryzhik I. M. 2007 *Table of Integrals, Series, and Products*, 7th ed. (Academic Press), edited by Jeffrey A. and Zwillinger D.

[123] Abramowitz M. and Stegun I. A. (eds.) 1964 *Handbook of Mathematical Functions with Formulas, Graphs, and Mathematical Tables* (U.S. Government Printing Office, Washington, D.C.).

[124] Gorshkov A. V., Hermele M., Gurarie V., Xu C., Julienne P. S., Ye J., Zoller P., Demler E., Lukin M. D. and Rey A. M. 2010 Two-orbital SU(N) magnetism with ultracold alkaline-earth atoms *Nature Physics* **6**, 289–295.

[125] Jin F., Willsch D., Willsch M., Lagemann H., Michielsen K. and De Raedt H. 2021 Random state technology *Journal of the Physical Society of Japan* **90**(1), 012001.

[126] Dukalski B., Müller M. M. and Žnidarič M. 2020 Controllability of high-dimensional quantum systems *Physical Review Letters* **125**(14), 140403.

[127] Eleuch H. and Hiluf D. 2021 Influence of the dissipation on the N-level atom interacting with two two-level atoms *Scientific Reports* **11**, 6042.

[128] Periwal A., Cooper J., Cao Q. and Schleier-Smith M. H. 2021 Collective spin-light and light-mediated spin-spin interactions in an optical cavity *PRX Quantum* **2**, 020308.

[129] Wang Y., Hu Z., Sanders B. C. and Kais S. 2020 Qudits and high-dimensional quantum computing *Frontiers in Physics* **8**, 589504.

[130] Thew R. T., Nemoto K., White A. G. and Munro W. J. 2002 Qudit quantum-state tomography *Physical Review A* **66**(1), 012303.

[131] Lanyon B. P., Barbieri M., Almeida M. P. and White A. G. 2009 Simplifying quantum logic using higher-dimensional Hilbert spaces *Nature Physics* **5**, 134–140.

[132] Kiktenko E. O., Fedorov A. K., Man'ko O. V. and Man'ko V. I. 2015 Multilevel superconducting circuits as two-qudit quantum processors *Physical Review A* **91**(4), 042312.

[133] Julsgaard B., Kozhekin A. and Polzik E. S. 2001 Experimental long-lived entanglement of two macroscopic objects *Nature* **413**, 400–403.

[134] Georgi H. 1999 *Lie Algebras in Particle Physics: From Isospin to Unified Theories*, 2nd ed. (Westview Press).

[135] Dong D. and Petersen I. R. 2010 Quantum control theory and applications: a survey *IET Control Theory & Applications* **4**(12), 2651–2671.

[136] Hioe F. T. 1985 Gell-Mann dynamic symmetry for N-level quantum systems *Physical Review A* **32**(5), 2824–2827.

[137] Weigert S. 1997 Baker–Campbell–Hausdorff relation for special unitary groups *Journal of Physics A: Mathematical and General* **30**(24), 8739–8749.

[138] Nemoto K. 2000 Generalized coherent states for SU(n) systems *Journal of Physics A: Mathematical and General* **33**(17), 3493–3506.

[139] Bertlmann R. A. and Krammer P. 2008 Bloch vectors for qudits *Journal of Physics A: Mathematical and Theoretical* **41**(23), 235303.

[140] Zhong W., Sun Z., Ma J., Wang X. and Nori F. 2013 Fisher information under decoherence in Bloch representation *Physical Review A* **87**(2), 022337.

[141] Gibbons G. W. 1992 Typical states and density matrices *Journal of Geometry and Physics* **8**(1–4), 147–162.

[142] Brody D. C. and Hughston L. P. 2001 Geometric quantum mechanics *Journal of Geometry and Physics* **38**(1), 19–53.

[143] Brody D. C. and Hughston L. P. 2015 Universal quantum measurements *Journal of Physics: Conference Series* **624**, 012002.

[144] Tilma T., Everitt M. J., Samson J. H., Munro W. J. and Nemoto K. 2016 Wigner functions for arbitrary quantum systems *Physical Review Letters* **117**, 180401.

[145] Runeson J. E. and Richardson J. O. 2021 Generalized spin mapping for quantum-classical dynamics *The Journal of Chemical Physics* **155**(12), 124105.

[146] Xu Z. 2025 Quantum-to-classical transition via single-shot generalized measurements *arXiv preprint* arXiv:2507.13174.

[147] Yurke B., McCall S. L. and Klauder J. R. 1986 SU(2) and SU(1,1) interferometers *Physical Review A* **33**(6), 4033–4054.

[148] Gerry C. C. 1985 Dynamics of SU(1,1) coherent states *Physical Review A* **31**(4), 2721–2725.

[149] Caves C. M. and Schumaker B. L. 1985 New formalism for two-photon quantum optics. I. Quadrature phases and squeezed states *Physical Review A* **31**(5), 3068–3092.

[150] Bužek V. 1990 SU(1,1) squeezing of SU(1,1) generalized coherent states *Journal of Modern Optics* **37**(3), 303–316.

[151] Trifonov D. A. 1994 Generalized intelligent states and squeezing *Journal of Mathematical Physics* **35**(5), 2297–2307.

[152] Marian P. and Marian T. A. 1992 Squeezed states with SU(1,1) symmetry: correlations and distributions *Physical Review A* **45**(3), 2044–2053.

[153] Liu J., Yuan H., Lu X.-M. and Wang X. 2020 Quantum Fisher information matrix and multiparameter estimation *Journal of Physics A: Mathematical and Theoretical* **53**(2), 023001.

[154] Lenz R. 2017 The Mehler-Fock transform in signal processing *Entropy* **19**(6), 289.

[155] Novaes M. 2004 Some basics of SU(1,1) *Revista Brasileira de Ensino de Física* **26**, 351–357.

[156] Matsumoto H. 1988 Coherent states of SU(1,1) and uncertainty relation *Progress of Theoretical Physics* **79**(1), 217–226.

[157] Brif C., Vourdas A. and Mann A. 1996 Analytic representations based on SU(1,1) coherent states and their applications *Journal of Physics A: Mathematical and General* **29**(18), 5873–5888.

[158] Barut A. O. and Girardello L. 1971 New coherent states associated with non-compact groups *Communications in Mathematical Physics* **21**(1), 41–55.

[159] Bargmann V. 1947 Irreducible unitary representations of the Lorentz group *Annals of Mathematics* **48**(3), 568–640.

[160] Perelomov A. M. 1971 On the connection of matrix elements of the SU(1,1) discrete series representations with SU(2) matrix elements *Reports on Mathematical Physics* **2**(4), 277–281.

[161] Inomata A., Kuratsuji H. and Gerry C. C. 1992 *Path Integrals and Coherent States of SU(2) and SU(1,1)* (World Scientific).

[162] Klimov A. B., Seyfarth U., de Guise H. and Sánchez-Soto L. L. 2021 SU(1,1) covariant s-parametrized maps *Journal of Physics A: Mathematical and Theoretical* **54**(6), 065301.

[163] Lindblad G. and Nagel B. 1970 Continuous bases for unitary irreducible representations of $\mathrm{SU}(1,1)$ *Annales de l'Institut Henri Poincaré Section A: Physique Théorique* **13**(1), 27–56.

[164] Vilenkin N. I. 1978 *Special Functions and the Theory of Group Representations* (American Mathematical Society).

[165] Vilenkin N. J. and Klimyk A. U. 1991 *Representation of Lie Groups and Special Functions*, Vol. 1: Group Representations and Harmonic Analysis (Springer).

[166] Terras A. 2013 *Harmonic Analysis on Symmetric Spaces: Euclidean Space, the Sphere, and the Poincaré Upper Half-Plane* (Springer).

[167] Holman W. J. III and Biedenharn L. C. Jr. 1966 Complex angular momenta and the groups SU(1,1) and SU(2) *Annals of Physics* **39**(1), 1–42.

[168] Holman W. J. III and Biedenharn L. C. Jr. 1968 A general study of the Wigner coefficients of SU(1,1) *Annals of Physics* **47**(2), 205–231.

[169] Ui H. 1970 Clebsch–Gordan formulas of the SU(1,1) group *Progress of Theoretical Physics* **44**(3), 689–702.

[170] Gerry C. C. 2004 On the Clebsch–Gordan problem for SU(1,1): Coupling nonstandard representations *Journal of Mathematical Physics* **45**(3), 1180–1190.

[171] Biedenharn L. C., Nuyts J. and Straumann N. 1965 On the unitary representations of SU(1,1) and SU(2,1) *Annales de l'Institut Henri Poincaré Section A: Physique Théorique* **3**(1), 13–39.

[172] Brif C. 1997 SU(2) and SU(1,1) algebra eigenstates: A unified analytic approach to coherent and intelligent states *International Journal of Theoretical Physics* **36**, 1651–1682.

[173] Seyfarth U., Klimov A. B., de Guise H., Leuchs G. and Sánchez-Soto L. L. 2020 Wigner function for SU(1,1) *Quantum* **4**, 317.

[174] Baltazar M., Valtierra I. F. and Klimov A. B. 2022 Correspondence rules for SU(1,1) quasidistribution functions and quantum dynamics in the hyperbolic phase space *Entropy* **24**(11), 1580.

[175] Fabre N., Klimov A. B., Leuchs G. and Sánchez-Soto L. L. 2023 Local sampling of the SU(1,1) Wigner function *AVS Quantum Science* **5**(1), 016801.

[176] Schweizer W. 2021 *Special Functions in Physics with MATLAB* (Springer).

[177] Kubo R. 1988 Geometry, heat equation and path integrals on the Poincaré upper half-plane *Progress of Theoretical Physics* **79**(1), 217–226.

[178] Øksendal B. 2003 *Stochastic Differential Equations: An Introduction with Applications*, 6th ed. (Springer).

[179] Karatzas I. and Shreve S. E. 1991 *Brownian Motion and Stochastic Calculus*, 2nd ed. (Springer).

[180] Gardiner C. 2009 *Stochastic Methods: A Handbook for the Natural and Social Sciences*, 4th ed. (Springer).

[181] Itô K. 1951 On stochastic differential equations *Memoirs of the American Mathematical Society* **4**, 1–51.

[182] Gisin N. 1984 Quantum measurements and stochastic processes *Physical Review Letters* **52**, 1657–1660.

[183] Diósi L. 1988 Quantum stochastic processes as models for state vector reduction *Journal of Physics A: Mathematical and General* **21**, 2885–2898.

[184] Diósi L. 1988 Continuous quantum measurement and Itô formalism *Physics Letters A* **129**, 419–423.

[185] Diósi L. 1988 Models for universal reduction of macroscopic quantum fluctuations *Physics Letters A* **132**, 233–236.

[186] Gisin N. 1989 Stochastic quantum dynamics and relativity *Helvetica Physica Acta* **62**, 363–371.

[187] Gisin N. and Percival I. C. 1992 The quantum-state diffusion model applied to open systems *Journal of Physics A: Mathematical and General* **25**, 5677–5691.

[188] Percival I. C. 1994 Primary state diffusion *Proceedings of the Royal Society of London A* **447**, 189–209.

[189] Horwitz L. P. and Piron C. 1973 Relativistic dynamics *Helvetica Physica Acta* **46**, 316–326.

[190] Bros J. and Moschella U. 1996 Two-point functions and quantum fields on the universal covering of anti-de Sitter space *Reviews in Mathematical Physics* **8**(3), 327–391.

[191] Uhlmann A. 1963 Remark on the future tube *Acta Physica Polonica* **24**, 293.

[192] Kobayashi S. and Nomizu K. 1969 *Foundations of Differential Geometry*, Vol. II (John Wiley & Sons, New York).

[193] Uhlmann A. 1972 Some properties of the future tube Karl Marx Universität, HEP-7209, 1–14.

[194] Rühl W. 1972 Distributions on Minkowski space and their connection with analytic representations of the conformal group *Communications in Mathematical Physics* **27**, 53–86.

[195] Rühl W. 1973 Field representations of the conformal group with continuous mass spectrum *Communications in Mathematical Physics* **30**, 287–302.

[196] Odzijewicz A. 1976 A model of conformal kinematics *International Journal of Theoretical Physics* **15**, 575–593.

[197] Carey A. L. 1977 Induced representations, reproducing kernels and the conformal group *Communications in Mathematical Physics* **52**, 77–101.

[198] Coquereaux R. and Jadczyk A. 1990 Conformal theories, curved phase spaces, relativistic wavelets and the geometry of complex domains *Reviews in Mathematical Physics* **2**, 1–44.

[199] Odzijewicz A. 1992 Coherent states and geometric quantization *Communications in Mathematical Physics* **150**, 385–413.

[200] Segreev A. G. and Vladimirov V. S. 1994 Complex analysis in the future tube in *Several Complex Variables II*, eds. Khenkin G. M. and Vitushkin A. G. (Springer, New York).

[201] Gibbons G. W. 2000 Holography and the future tube *Classical and Quantum Gravity* **17**, 1071–1079.

[202] Krantz S. G. 1982 *Function Theory of Several Complex Variables* (John Wiley & Sons, New York).

[203] Bros J., Epstein H. and Glaser V. 1965 A proof of the crossing property for two-particle amplitudes in general quantum field theory *Communications in Mathematical Physics* **1**, 240–264.

[204] Bros J. and Buchholz D. 1996 Axiomatic analyticity properties and representations of particles in thermal quantum field theory *Annales de l'Institut Henri Poincaré Section A: Physique Théorique* **64**(4), 495–521.

[205] Nikolov P. A. and Todorov I. T. 1982 Space-time versus phase-space approach to relativistic particle dynamics in *Twistor Geometry and Non-Linear Systems* ed. Doebner H. D. and Palev T. D. (Springer-Verlag, Berlin)

[206] Marsden J. E., Montgomery R., Morrison P. J. and Thompson W. B. 1986 Covariant Poisson brackets for classical fields *Annals of Physics* **169**, 29–47.

[207] Sorge H., Stöcker H. and Greiner W. 1989 Poincaré invariant Hamiltonian dynamics: Modelling multi-hadronic interactions in a phase-space approach *Annals of Physics* **192**, 266–306.

[208] Woodhouse N. M. J. 1992 *Geometric Quantization*, 2nd ed. (Oxford University Press).

[209] Streater R. F. and Wightman A. S. 2000 *PCT, Spin and Statistics, and All That* (Princeton University Press).

[210] Bergman S. and Schiffer M. 1951 Kernel functions and conformal mapping *Compositio Mathematica* **8**, 205–249.

[211] Ferrara S., Grillo A. and Gatto R. 1973 Conformal algebra in space-time and operator product expansions *Annals of Physics* **76**, 161–188.

[212] Weinberg S. 1996 *The Quantum Theory of Fields, Volume II: Modern Applications* (Cambridge University Press).

[213] Di Francesco P., Mathieu P. and Sénéchal D. 1997 *Conformal Field Theory* (Springer).

[214] Blumenhagen R. and Plauschinn E. 2009 *Introduction to Conformal Field Theory* (Springer).

[215] Stückelberg E. C. G. 1941 La signification du temps propre en mécanique ondulatoire *Helvetica Physica Acta* **14**, 588–594.

[216] Berezin F. A. 1972 Covariant and contravariant symbols of operators *Mathematics of the USSR-Izvestija* **6**(5), 1117–1151.

[217] Axler S. 1998 The Berezin transform on the Bergman space *Contemporary Mathematics* **213**, 1–17.

[218] Schlichenmaier M. 2010 Berezin–Toeplitz quantization for compact Kähler manifolds: a review of results *Advances in Mathematical Physics* **2010**, 927280.

[219] Budker D., Kimball D. F. and DeMille D. P. 2002 Optical magnetometry. *Reviews of Modern Physics* **74**, 1153–1201.

[220] Rochester S. M. and Budker D. 2001 Nonlinear magneto-optical rotation with frequency-modulated light in the geophysical field range. *American Journal of Physics* **69**, 450–454.

[221] Geremia J. M., Stockton J. K. and Mabuchi H. 2005 Suppression of spin projection noise in broadband atomic magnetometry. *Physical Review Letters* **94**, 203002.

[222] Sewell R. J, Koschorreck M, Napolitano M, Dubost B, Behbood N and Mitchell M W 2012 Magnetic sensitivity beyond the projection noise limit by spin squeezing. *Physical Review Letters* **109**,253605.

[223] Rochester S M, Ledbetter M P, Zigdon T, Wilson-Gordon A D and Budker D 2012 Orientation-to-alignment conversion and spin squeezing. *Physical Review A* **85**, 022125.

[224] Jackson C. S. and Caves C. M. 2023 Simultaneous momentum and position measurement and the instrumental Weyl-Heisenberg group *Entropy* **25**(8), 1221.

[225] Jackson C. S. and Caves C. M. 2023 How to perform the coherent measurement of a curved phase space by continuous isotropic measurement. I. Spin and the Kraus-operator geometry of $\mathrm{SL}(2,\mathbb{C})$ *Quantum* **7**, 1085.

[226] Hunt G. A. 1956 Semi-groups of measures on Lie groups *Transactions of the American Mathematical Society* **81**(2), 264–293.

[227] Stroock D. W. and Varadhan S. R. S. 1972 On the support of diffusion processes with applications to the strong maximum principle *Proceedings of the Sixth Berkeley Symposium on Mathematical Statistics and Probability*, Vol. 3, 333–359.

[228] Elworthy K. D. 1982 *Stochastic Differential Equations on Manifolds* (Cambridge University Press).

[229] Kunita H. 1984 Stochastic differential equations and stochastic flows of diffeomorphisms *École d'Été de Probabilités de Saint-Flour XII—1982*, Lecture Notes in Mathematics, Vol. 1097 (Springer).

[230] Albeverio S., Arede T. and Haba Z. 1990 On left invariant Brownian motions and heat kernels of nilpotent Lie groups *Journal of Mathematical Physics* **31**(2), 278–286.

[231] Groenewold H. J. 1946 On the principles of elementary quantum mechanics *Physica* **12**, 405–460.

[232] Bateman H. and Erdélyi A. 1953 *Higher Transcendental Functions* (McGraw-Hill).

[233] Bateman H., Erdélyi A., Magnus W. and Oberhettinger F. 1954 *Tables of Integral Transforms* (McGraw-Hill).

[234] Silverman R. A. 1972 *Special Functions and Their Applications* (Courier Corporation).

[235] Lucht P. 1976 The generalized-Legendre addition theorems, SU(1,1), and the diagonalization of convolution equations Lawrence Berkeley Laboratory Technical Report LBL-5527, University of California, Berkeley, October 11.

[236] Lucht P. 1978 The SU(1,1) addition theorems and their use in diagonalizing integral equations Technical Report, University of California, Berkeley, June.

[237] Oberhettinger F. and Higgins T. P. 1961 *Tables of Lebedev, Mehler and Generalized Mehler Transforms* NASA Technical Note D-246.

[238] Gautschi W. 1959 Some inequalities for the gamma and psi functions *Mathematics of Computation* **13**, 240–244.

[239] Olver F. W. J., Lozier D. W., Boisvert R. F., and Clark C. W. (eds.) 2010 *NIST Handbook of Mathematical Functions* (Cambridge University Press).

Appendix A

Phase-space measurement in Fock-Segal-Bargmann representation

This appendix develops the Fock-Segal-Bargmann (FSB) representation as a holomorphic framework for phase-space analysis. We first formulate phase-space measurements and Lindblad dynamics in this representation, showing how coherent-state kernels naturally appear. Together, these results provide a complementary viewpoint to the main text in Chapter 2.

A.1 Fock-Segal-Bargmann representation

Although our primary formulation remains in the Hilbert space $\mathcal{H} = L^2(\mathbb{R})$, coherent states naturally give rise to a space of holomorphic functions via their overlap with quantum states. For any state $|\psi\rangle \in \mathcal{H}$, we define a function on the complex plane by

$$\psi(\alpha) = \langle \alpha | \psi \rangle, \quad \alpha \in \mathbb{C}. \tag{A.1}$$

This function $\psi(\alpha)$ is entire (analytic) on all of $\mathbb{C}$, due to the exponential structure of coherent states. The space of such functions, equipped with the Gaussian-weighted inner product

$$\langle \psi | \phi \rangle = \int_{\mathbb{C}} \overline{\psi(\alpha)} \phi(\alpha) \, \frac{\mathrm{d}^2 \alpha}{\pi}, \tag{A.2}$$

defines a reproducing kernel Hilbert space known as the *Fock-Segal-Bargmann (FSB) space* [75–77].

Note that the measure used here differs from that in Chapter 2, where a flat (Lebesgue) phase-space measure was employed for POVM-based analysis. The Gaussian weight in the Bargmann space ensures square-integrability of holomorphic functions and aligns with the canonical quantisation of the harmonic oscillator. This space, often denoted $\mathcal{F}_1$, is a Hilbert space of entire functions $f(z)$ such that

$$\|f\|^2 = \int_{\mathbb{C}} |f(z)|^2 \, \mathrm{d}\mu_z < \infty. \tag{A.3}$$

We now discuss the Quantum harmonic oscillator in the holomorphic representation.

Quantum harmonic oscillator in the FSB representation

In the FSB representation, the annihilation and creation operators act as differential and multiplicative operators $\hat{a} = \frac{\mathrm{d}}{\mathrm{d}z}$, $\hat{a}^\dagger = z$. Consequently, the harmonic oscillator Hamiltonian $\hat{H} = \hat{a}^\dagger\hat{a} + \frac{1}{2}$ becomes $\hat{H}_z = z\frac{\mathrm{d}}{\mathrm{d}z} + \frac{1}{2}$.

Proposition A.1. *The eigenvalues and eigenfunctions of $\hat{H}_z$ in the holomorphic representation are given by*

$$\hat{H}_z\Phi_n(z) = E_n\Phi_n(z), \quad n \in \mathbb{Z}_{\geq 0}, \tag{A.4}$$

where

$$\Phi_n(z) = \frac{z^n}{\sqrt{n!}}, \quad E_n = n + \frac{1}{2}. \tag{A.5}$$

These functions $\Phi_n(z)$ form an orthonormal basis of the Segal-Bargmann space $\mathcal{F}_1$. They correspond to the Fock number states $|n\rangle$ under the Segal-Bargmann transform $\Phi_n(z) = \langle z|n\rangle$. Thus, the entire structure of the harmonic oscillator, its spectrum, ladder structure, and time evolution, admits a clean analytic formulation in terms of holomorphic functions, which proves especially useful in analysing the phase-space structure of quantum states.

Proof. We start with the time independent Schrödinger equation

$$\hat{H}_z\Phi_n(z) = \left(z\frac{\mathrm{d}}{\mathrm{d}z} + \frac{1}{2}\right)\Phi_n(z) = E_n\Phi_n(z), \tag{A.6}$$

This equation can be solved for $\Phi_n(z)$ and integration leads to

$$\log(\Phi_n(z)) = \left(E_n - \frac{1}{2}\right)\log(z) + k, \tag{A.7}$$

where k is a constant of integration.
Taking the exponential of the above equation results in the following

$$\Phi_n(z) = cz^{\left(E_n - \frac{1}{2}\right)}, \tag{A.8}$$

where $c = \mathrm{e}^k$ is a constant.
To ensure that these functions form a valid basis in the Hilbert space $\mathcal{F}_1$, we impose the orthonormality condition. Using the inner product on $\mathcal{F}_1$ (A.2) and (A.8), we compute

$$\langle\Phi_n, \Phi_m\rangle = \frac{|c|^2}{\pi}\int_{\mathbb{C}} \overline{z}^{E_n - \frac{1}{2}}\, z^{E_m - \frac{1}{2}}\mathrm{e}^{-|z|^2}\,\mathrm{d}^2z. \tag{A.9}$$

Using $z = r\mathrm{e}^{\mathrm{i}\theta}$ and $\mathrm{d}^2z = r\,\mathrm{d}r\,\mathrm{d}\theta$, we get

$$\langle\Phi_n, \Phi_m\rangle = \frac{|c|^2}{\pi}\int_0^{2\pi}\int_0^{\infty} r^{E_n+E_m}\,\mathrm{e}^{\mathrm{i}\theta(E_n-E_m)}\,\mathrm{e}^{-r^2}r\,\mathrm{d}r\,\mathrm{d}\theta. \tag{A.10}$$

We now examine this expression for two cases.

Case 1: $n = m$**.** Then $E_n = E_m$ and the angular integral evaluates to 2π

$$\langle \Phi_n, \Phi_n \rangle = 2|c|^2 \int_0^\infty r^{2E_n} \mathrm{e}^{-r^2} \, \mathrm{d}r = |c|^2 \Gamma\left(E_n + \frac{1}{2}\right). \tag{A.11}$$

Normalising to 1 gives

$$c = \frac{1}{\sqrt{\Gamma\left(E_n + \frac{1}{2}\right)}}. \tag{A.12}$$

Case 2: $n \neq m$**.** From (A.10), the θ-integral evaluates to

$$\int_0^{2\pi} \mathrm{e}^{\mathrm{i}\theta(E_n - E_m)} \, \mathrm{d}\theta = 0 \quad \text{iff } E_n - E_m \notin \mathbb{Z}. \tag{A.13}$$

So orthogonality requires

$$E_n - E_m \in \mathbb{Z}. \tag{A.14}$$

Holomorphicity constraint. In the Segal-Bargmann space $\mathcal{F}_1$, wavefunctions must be entire (holomorphic on $\mathbb{C}$). This rules out negative or noninteger powers of z, since

- If $E_n - \frac{1}{2} < 0$, $\Phi_n(z)$ has a pole at $z = 0$.
- If $E_n - \frac{1}{2} \in \mathbb{Q} \setminus \mathbb{Z}$, $\Phi_n(z)$ has branch cuts.

Therefore, the only acceptable values are

$$E_n - \frac{1}{2} = n \in \mathbb{Z}^+ \cup \{0\} \quad \Rightarrow \quad E_n = n + \frac{1}{2}, \tag{A.15}$$

and thus

$$\Phi_n(z) = \frac{z^n}{\sqrt{\Gamma(n+1)}} = \frac{z^n}{\sqrt{n!}}. \tag{A.16}$$

□

Having established an orthonormal basis, we can now construct the reproducing kernel, which encodes the inner product structure of the Hilbert space.

Reproducing kernel. The eigenfunctions $\{\Phi_n(z)\}_{n=0}^\infty$ form an orthonormal basis of $\mathcal{F}_1$. The Bergman kernel (reproducing kernel) [210] is given by

$$K(z, \overline{w}) = \sum_{n=0}^\infty \Phi_n(z) \overline{\Phi_n(w)} = \sum_{n=0}^\infty \frac{(z\overline{w})^n}{n!} = \exp(z\overline{w}). \tag{A.17}$$

We shall now verify its identity and reproducing properties.

Proposition A.2. *The kernel reproduces the identity function:*

$$\langle 1, K(z, \overline{w}) \rangle = 1. \tag{A.18}$$

Proof. Using (A.2)

$$\begin{aligned}\langle 1, K(z,\overline{w})\rangle &= \frac{1}{\pi}\int_{\mathbb{C}} K(z,\overline{w})\,\mathrm{e}^{-|w|^2}\,\mathrm{d}^2w = \frac{1}{\pi}\int_{\mathbb{R}^2}\exp(z(x-\mathrm{i}y))\mathrm{e}^{-(x^2+y^2)}\,\mathrm{d}x\,\mathrm{d}y \\ &= \int_{-\infty}^{\infty}\frac{1}{\sqrt{\pi}}\exp\left(-\frac{1}{4}(2y+\mathrm{i}z)^2\right)\,\mathrm{d}y = 1. \end{aligned} \tag{A.19}$$

□

This confirms that the reproducing kernel correctly maps the constant function 1 to itself, validating a key property of such kernels in a Hilbert space.

Proposition A.3. *The kernel satisfies the reproducing property*

$$\int K(z,\overline{w})K(w,\bar{t})\,\mathrm{d}\mu_w = K(z,\bar{t}). \tag{A.20}$$

Proof.

$$\int_{\mathbb{C}} K(z,\overline{w})K(w,\bar{t})\,\mathrm{e}^{-|w|^2}\,\mathrm{d}^2w = \int_{\mathbb{C}}\exp(z\overline{w}+w\bar{t}-|w|^2)\,\mathrm{d}\mu_w. \tag{A.21}$$

Using $w = x + \mathrm{i}y$ and integrating yields

$$\int \exp((z+\bar{t})x + \mathrm{i}y(\bar{t}-z) - x^2 - y^2)\,\mathrm{d}x\,\mathrm{d}y = \exp(z\bar{t}), \tag{A.22}$$

as expected. □

Having constructed the Bargmann space $\mathcal{F}_1$ as our phase space, we are now in a position to define coherent states on it. These states are quantum analogs of classical points in phase space and are known for their minimal uncertainty and Gaussian localisation as discussed in Chapters 1, 2. In $\mathcal{F}_1$, coherent states are generated by translating the vacuum state using the symmetry group of the phase space. Explicitly, we define a coherent state centered at $w \in \mathbb{C}$ as

$$\Psi_w(z) = CK(z,\overline{w}), \tag{A.23}$$

where C is a normalisation constant to be determined.
To ensure that Ψ_w is normalised with respect to the inner product on $\mathcal{F}_1$, we require

$$\langle \Psi_w, \Psi_w\rangle = \int_{\mathbb{C}} \overline{\Psi_w(z)}\Psi_w(z)\,\mathrm{d}\mu_z = 1, \tag{A.24}$$

Substituting (A.23) in the above expression

$$\int_{\mathbb{C}} |C|^2 K(w,\overline{z})K(z,\overline{w})\,\mathrm{d}\mu_z \quad = |C|^2K(w,\bar{w}) = 1, \tag{A.25}$$

where we have used the reproducing kernel property of the kernel function. Assuming that C is real and substituting for the kernel we find that $C = \exp\left(-\frac{|w|^2}{2}\right)$. Thus, the normalised coherent state on

$\mathcal{F}_1$ becomes

$$\Psi_w(z) = \exp\left(-\frac{|w|^2}{2}\right)\exp(z\overline{w}). \tag{A.26}$$

We can now compute the modulus squared of this state, which gives the probability density in phase space

$$|\Psi_w(z)|^2 = \exp\left(-|w|^2 - |z|^2 + 2\,\mathrm{Re}(z\overline{w})\right). \tag{A.27}$$

Letting $z = x + \mathrm{i}p$ and $w = \alpha + \mathrm{i}\beta$, we find $|\psi_w(z)|^2 = \exp\left(-(x-\alpha)^2 - (p-\beta)^2\right)$.

This shows that the coherent state is a Gaussian centered at the point $w = \alpha + \mathrm{i}\beta$ in phase space.

Thus, the space of holomorphic functions associated with coherent states provides an analytic framework in which to express and understand the effect of phase-space measurements on quantum states.

Coherent States in $\mathcal{L}^2(\mathbb{R})$: We now derive the form of a coherent state in the Hilbert space $\mathcal{L}^2(\mathbb{R})$ using the inverse Bargmann transform.

Proposition A.4. *The coherent state in position space $\psi(q)$ corresponding to the Bargmann space coherent state $\psi_w(z)$ is given by:*

$$\psi(q) = \frac{1}{\pi^{1/4}}\exp\left(-\frac{|w|^2}{2}\right)\exp\left(-\frac{q^2}{2} + \sqrt{2}qw - \frac{w^2}{2}\right). \tag{A.28}$$

Proof. By introducing a resolution of identity we obtain

$$\psi(q) = \langle q|\psi\rangle = \int_{\mathbb{C}} \langle q|z\rangle\,\langle z|\psi\rangle\,\mathrm{d}\mu_z, \tag{A.29}$$

where $A(q,z) = \langle q|z\rangle$ is the Bargmann kernel given by [75,77,159]

$$A(q,z) = \frac{1}{\pi^{1/4}}\exp\left(-\frac{z^2}{2} + \sqrt{2}zq - \frac{q^2}{2}\right). \tag{A.30}$$

Substituting for $\Psi_w(z)$ we get

$$\psi(q) \;=\; \frac{1}{\pi^{1/4}}\exp\left(-\frac{|w|^2}{2}\right)\int_{\mathbb{C}}\exp\left(-\frac{z^2}{2} + \sqrt{2}zq - \frac{q^2}{2} + \bar{z}w\right)\mathrm{d}\mu_z. \tag{A.31}$$

We now express $z = x + \mathrm{i}y$, so that $\mathrm{d}\mu_z = \pi^{-1}\mathrm{e}^{-x^2-y^2}\,\mathrm{d}x\,\mathrm{d}y$, and compute

$$\begin{aligned}\psi(q) \;=\; & \frac{1}{\pi^{5/4}}\exp\left(-\frac{q^2+|w|^2}{2}\right)\\ & \times\iint_{\mathbb{R}^2}\exp\left(-\frac{(x+\mathrm{i}y)^2}{2} + \sqrt{2}q(x+\mathrm{i}y) + (x-\mathrm{i}y)w - x^2 - y^2\right)\mathrm{d}x\,\mathrm{d}y.\end{aligned} \tag{A.32}$$

Expanding the exponentials and collecting terms

$$\begin{aligned}\psi(q) &= \frac{1}{\pi^{5/4}}\exp\left(-\frac{q^2+|w|^2}{2}\right)\int_{-\infty}^{\infty}\int_{-\infty}^{\infty}\exp\left(-\frac{3x^2}{2}+x(-\mathrm{i}y+\sqrt{2}q+w)\right)\\ &\quad\times\exp\left(-\frac{y^2}{2}+\mathrm{i}y(\sqrt{2}q-w)\right)\mathrm{d}x\,\mathrm{d}y. \end{aligned} \tag{A.33}$$

Both integrals are Gaussian and can be evaluated using standard results

$$\int_{-\infty}^{\infty}\exp\left(-ax^2+bx\right),\mathrm{d}x=\sqrt{\frac{\pi}{a}}\exp\left(\frac{b^2}{4a}\right). \tag{A.34}$$

Applying this to both x and y integrations, simplifying the exponents and collecting terms, we ultimately arrive at

$$\psi(q)=\frac{1}{\pi^{1/4}}\exp\left(-\frac{|w|^2}{2}\right)\exp\left(-\frac{q^2}{2}+\sqrt{2}qw-\frac{w^2}{2}\right), \tag{A.35}$$

as claimed. □

This coherent state is indeed normalised as we have seen in Chapter 2.

A.2 General POVM measurement

Having defined the space of holomorphic functions $\mathcal{F}_1$, constructed the Bergman kernel, and introduced coherent states, we now proceed to define general quantum states on $\mathcal{F}_1$ [47].

A general quantum state on $\mathcal{F}_1$ is defined to be a density state $R(u,\overline{v})\in\mathcal{F}_1\times\mathcal{F}_1$ satisfying the properties:

1. $R(u,\overline{v})$ is Hermitian i.e. $R(u,\overline{v})=\overline{R(v,\overline{u})}$ and
2. $R(u,\overline{v})$ is positive i.e
$$\int_{\mathbb{C}}\int_{\mathbb{C}}\overline{\psi(u)}R(u,\overline{v})\psi(v)\,\mathrm{d}\mu_u\,\mathrm{d}\mu_v\geq 0, \tag{A.36}$$
where $\psi(u)\in\mathcal{F}_1$ and finally
3. $R(u,\overline{v})$ has unit trace i.e.
$$\int_{\mathbb{C}}\int_{\mathbb{C}}K(u,\overline{v})R(v,\overline{u})\,\mathrm{d}\mu_u\,\mathrm{d}\mu_v=\int_{\mathbb{C}}R(v,\overline{v})\,\mathrm{d}\mu_v=1. \tag{A.37}$$

The diagonal $R(v,\overline{v})$ defines the probability density associated with the quantum state ψ on the phase space.

A pure state on $\mathcal{F}_1$ is represented by the rank-one operator

$$R(u,\overline{v})=\psi(u)\overline{\psi(v)}, \tag{A.38}$$

where $\psi(u)\in\mathcal{F}_1$ is a holomorphic function normalised such that $|\psi|=1$.

To describe measurements on phase space, we introduce a Positive Operator-Valued Measure (POVM). An explicit realisation of the POVM is given by [47]

$$\Phi_A(x,\bar{z}) = \int_{y\in A} K(x,\bar{y})K(y,\bar{z})\,\mathrm{d}\mu_y, \quad A\in\mathcal{B}, \tag{A.39}$$

which acts on $\mathcal{F}_1$ as an integral operator with a kernel built from the Bergman kernel.

Given a quantum state described by the kernel $R(z,\bar{y})$, the probability that a measurement yields a value within the set A is computed as

$$\mathbb{P}(A) = \iint \Phi_A(y,\bar{z})R(z,\bar{y})\,\mathrm{d}\mu_y\,\mathrm{d}\mu_z = \int_{z\in A} R(z,\bar{z})\,\mathrm{d}\mu_z. \tag{A.40}$$

This expression reduces to integrating the diagonal of the density kernel over A, highlighting the role of $R(z,\bar{z})$ as the probability density on $\mathbb{C}$.

Suppose the initial state is given by $R(y,\bar{v})$. Then, the output state after a measurement yielding a result in A is

$$R^{(1)}(u,\bar{x}) \quad = \quad \frac{\int_{z\in A}\frac{K(u,\bar{z})K(z,\bar{x})}{K(z,\bar{z})}R(z,\bar{z})\,\mathrm{d}\mu_z}{\int_{z\in A}R(z,\bar{z})\,\mathrm{d}\mu_z}. \tag{A.41}$$

This formula describes the updated state conditioned on the measurement outcome falling within the region A of phase space. The numerator integrates a "filtered" version of the initial state, modulated by the kernel's reproducing property, while the denominator ensures normalisation. We now turn to the question of quantum measurement on phase space.

A.3 Phase-space measurement

Suppose a measurement is performed on the phase space $\mathcal{F}_1$, and the outcome corresponds to detecting a specific phase-space point $z\in\mathbb{C}$. In this case, the quantum state collapses to the coherent state centered at z, denoted by $\Psi_w(z)$.

Nonselective or "unread" or unconditioned measurements naturally lead to environmental decoherence, and they can be modeled within our formalism by averaging over all possible outcomes on phase space as

$$R^{(1)}(u,\bar{x}) = \int \frac{K(u,\bar{w})K(w,\bar{x})}{K(w,\bar{w})}R(w,\bar{w})\,\mathrm{d}\mu_w, \tag{A.42}$$

where R_{in} is the initial density matrix and R_{out} is the state of the system after such a nonselective measurement.

Substituting the expression for the Bergman kernel into the phase-space measurement update ((A.41)), we obtain an explicit formula for the output density matrix

$$R^{(1)}(u,\bar{v}) = \int_{\mathbb{C}} \exp\left(w\bar{v}+u\bar{w}-|w|^2\right)R(w,\bar{w})\,\mathrm{d}\mu_w. \tag{A.43}$$

However, this single application does not fully capture the cumulative effect of environmental mon-

itoring as the coherent states are nonorthogonal. Therefore, we extend the model by iterating this transformation i.e. we apply the same phase-space measurement process multiple times to model the progressive decohering of the quantum state.

Let us now derive a general expression for the density matrix after n such measurement steps. Starting from $R^{(0)} = R$, we compute the density matrix after n measurements to be

Proposition A.5.

$$R^{(n)}(u,\bar{v}) \quad = \quad \frac{1}{n}\exp\left(\frac{(n-1)u\bar{v}}{n}\right)\int_{\mathbb{C}}\exp\left(\frac{w\bar{v}+u\bar{w}-|w|^2}{n}\right)R(w,\bar{w})\,\mathrm{d}\mu_w,\ n\in\mathbb{N}_0. \tag{A.44}$$

Proof. We will prove the result by induction. Starting with the base case $n = 1$, we have

$$R^{(1)}(u,\bar{v}) = \int_{\mathbb{C}}\exp\left(w\bar{v}+u\bar{w}-|w|^2\right)R(w,\bar{w})\,\mathrm{d}\mu_w, \tag{A.45}$$

and this is the same as (A.43).
We will now perform the induction step by calculating the density matrix after the $(n+1)$th iteration of phase-space measurement. We have from (A.43)

$$R^{(n+1)}(u,\bar{v}) = \int_{\mathbb{C}}\exp\left(w\bar{v}+u\bar{w}-|w|^2\right)R^{(n)}(w,\bar{w})\,\mathrm{d}\mu_w. \tag{A.46}$$

Substituting for $R^{(n)}$ from (A.43) in the above expression and rearranging the terms we have

$$\begin{aligned} R^{(n+1)}(u,\bar{v}) \quad = \quad & \frac{1}{n}\int_{\mathbb{C}}\left[\int_{\mathbb{C}}\exp\left(w\bar{v}+u\bar{w}-|w|^2\right)\exp\left(\frac{(n-1)|w|^2}{n}\right)\exp\left(\frac{z\bar{w}+w\bar{z}}{n}\right)\mathrm{d}\mu_w\right] \\ & \times\exp\left(\frac{-|z|^2}{n}\right)R(z,\bar{z})\,\mathrm{d}\mu_z. \end{aligned} \tag{A.47}$$

We will now compute the inner integral in the above equation as follows:

$$I = \frac{1}{n}\int\exp\left(w\bar{v}+u\bar{w}-|w|^2\right)\exp\left(\frac{(n-1)|w|^2}{n}\right)\exp\left(\frac{z\bar{w}+w\bar{z}}{n}\right)\mathrm{d}\mu_w. \tag{A.48}$$

By making the substitution $w = x + \mathrm{i}y$, so that $\mathrm{d}\mu_w = \pi^{-1}\exp\left(-x^2-y^2\right)\mathrm{d}x\,\mathrm{d}y$, we have

$$\begin{aligned} I \quad = \quad & \frac{1}{\pi n}\iint\exp\left(x\left(\bar{v}+u+\frac{z+\bar{z}}{n}\right)\right)\exp\left(\mathrm{i}y\left(\bar{v}-u+\frac{\bar{z}-z}{n}\right)\right) \\ & \times\exp\left(-\frac{(n+1)(x^2+y^2)}{n}\right)\mathrm{d}x\,\mathrm{d}y. \end{aligned} \tag{A.49}$$

Since the expression consists of two separable Gaussian integrals, we can evaluate each one independently using standard techniques to give

$$I = \frac{1}{(n+1)}\exp\left(\frac{n\left(\bar{v}+u+\frac{\bar{z}+z}{n}\right)^2}{4(n+1)}\right)\exp\left(-\frac{n\left(\bar{v}-u+\frac{\bar{z}-z}{n}\right)^2}{4(n+1)}\right), \tag{A.50}$$

which on simplfication evaluates to

$$I = \frac{1}{(n+1)}\exp\left(\frac{(z+\bar{v}n)(\bar{z}+un)}{(n+1)n}\right). \tag{A.51}$$

Having now evaluated the inner integral I in (A.47), we substitute it back into the expression to obtain

$$R^{(n+1)}(u,\bar{v}) = \frac{1}{n+1}\exp\left(\frac{nu\bar{v}}{n+1}\right)\int \exp\left(\frac{z\bar{v}+u\bar{z}-|z|^2}{n+1}\right)R(z,\bar{z})\,\mathrm{d}\mu_z, \tag{A.52}$$

giving us the expression for the density matrix after $(n+1)^{\text{th}}$ iteration of the phase-space measurement, thereby completing the proof. □

This result reveals a fundamental feature of the iterative measurement process which is that the density matrix undergoes exponential damping inside the integral along with an additional overall exponential damping through the factor $\exp\left(-\frac{nu\bar{v}}{n+1}\right)$. As the number of iterations n increases, this damping becomes more pronounced, leading to a progressive suppression of quantum coherences.

A.4 Dynamical unravelling of the phase-space measurement

In this section, we derive a dynamical equation in the Fock-Segal-Bargmann representation and solve it to show how the effect of phase-space measurement can be encoded into a time-continuous dynamical evolution of the quantum state. Since our measurements are performed in phase space, it is natural to consider the position and momentum operators, $\hat{x}$ and $\hat{p}$, as the relevant Lindblad operators [40–42]

$$\frac{\mathrm{d}\hat{\rho}}{\mathrm{d}t} = \hat{x}\hat{\rho}\hat{x}^\dagger - \frac{1}{2}(\hat{x}^\dagger\hat{x}\hat{\rho} + \hat{\rho}\hat{x}^\dagger\hat{x}) + \hat{p}\hat{\rho}\hat{p}^\dagger - \frac{1}{2}(\hat{p}^\dagger\hat{p}\hat{\rho} + \hat{\rho}\hat{p}^\dagger\hat{p}). \tag{A.53}$$

Having introduced the Lindblad master equation, we now proceed to express it in the Fock-Segal-Bargmann (FSB) representation.

To do so, we recall that the density operator $\hat{\rho}$ on $\mathcal{L}^2(\mathbb{R})$ is related to the kernel representation $R(u,\bar{v})$ on $\mathcal{F}_1$ via the Bargmann transform

$$R(u,\bar{v}) = \int_{\mathbb{R}^2} A(u,x)\,\rho(x,y)\,\overline{A(v,y)}\,\mathrm{d}x\,\mathrm{d}y, \tag{A.54}$$

where $A(z,q)$ denotes the Bargmann kernel. Equivalently, we write this as

$$R(u,\bar{v}) = \langle\xi_{\bar{u}}|\hat{\rho}|\xi_{\bar{v}}\rangle, \tag{A.55}$$

with the state $|\xi_{\bar{u}}\rangle$ defined by its action on $\psi \in \mathcal{L}^2(\mathbb{R})$ as

$$\langle\xi_{\bar{u}}|\psi\rangle = \int A(x,u)\psi(x)\,\mathrm{d}x. \tag{A.56}$$

We now apply the Bargmann transform to the Lindblad master equation, translating it into a partial differential equation for the phase-space kernel $R(u,\bar{v},t)$ on $\mathcal{F}_1$.

Specifically, we consider the action of composite operator expressions like $\hat{x}\hat{\rho}\hat{x}^\dagger$ and $\hat{p}\hat{\rho}\hat{p}^\dagger$, and demonstrate how these translate to differential operators acting on $R(u,\bar{v})$. The remaining terms follow analogously.

Let us now evaluate the action of the operator $\hat{x}\hat{\rho}\hat{x}^\dagger$ on the phase space. We show the following

Proposition A.6.

$$\frac{1}{2}\left(\bar{v}+\frac{\partial}{\partial\bar{v}}\right)\left(u+\frac{\partial}{\partial u}\right)R(u,\bar{v})=\langle\xi_{\bar{u}}(x)\,|\,\hat{x}\hat{\rho}\hat{x}^{\dagger}\,|\,\xi_{\bar{v}}(y)\rangle. \tag{A.57}$$

Proof. We begin by expressing $R(u,\bar{v})$ via the Bargmann transform

$$R(u,\bar{v})=\int A(x,u)\,\rho(x,y)\,A(y,\bar{v})\,\mathrm{d}x\,\mathrm{d}y. \tag{A.58}$$

Applying the differential operators one after the other gives

$$\begin{aligned}\frac{1}{2}\left(\bar{v}+\frac{\partial}{\partial\bar{v}}\right)\left(u+\frac{\partial}{\partial u}\right)R(u,\bar{v}) &= \frac{1}{2}\left(\bar{v}+\frac{\partial}{\partial\bar{v}}\right)\int A(x,u)\,\rho(x,y)\,\sqrt{2}x,A(y,\bar{v})\,\mathrm{d}x\,\mathrm{d}y,\\ &= \int A(x,u)\,xy,\rho(x,y)\,A(y,\bar{v})\,\mathrm{d}x\,\mathrm{d}y.\end{aligned} \tag{A.59}$$

This is precisely the kernel representation of $\hat{x}\hat{\rho}\hat{x}^{\dagger}$ in the Fock-Segal-Bargmann space:

$$\langle\xi_{\bar{u}}(x)\,|\,\hat{x}\hat{\rho}\hat{x}^{\dagger}\,|\,\xi_{\bar{v}}(y)\rangle=\int A(x,u)\,xy\,\rho(x,y)\,A(y,\bar{v})\,\mathrm{d}x\,\mathrm{d}y. \tag{A.60}$$

□

Similarly, we now evaluate the action of the operator $\hat{p}\hat{\rho}\hat{p}^{\dagger}$ on phase space

Proposition A.7.

$$\frac{1}{2}\left(\bar{v}-\frac{\partial}{\partial\bar{v}}\right)\left(u-\frac{\partial}{\partial u}\right)R(u,\bar{v})=\langle\xi_{\bar{u}}(x)\,|\,\hat{p}\hat{\rho}\hat{p}^{\dagger}\,|\,\xi_{\bar{v}}(y)\rangle. \tag{A.61}$$

Proof. We again begin with the Bargmann representation of the density matrix

$$R(u,\bar{v})=\int A(x,u)\,\rho(x,y)\,A(y,\bar{v})\;\mathrm{d}x\,\mathrm{d}y. \tag{A.62}$$

Applying the differential operator, we compute

$$\frac{1}{2}\left(\bar{v}-\frac{\partial}{\partial\bar{v}}\right)\left(u-\frac{\partial}{\partial u}\right)R(u,\bar{v})=\frac{1}{2}\left(\bar{v}-\frac{\partial}{\partial\bar{v}}\right)\left(u-\frac{\partial}{\partial u}\right)\int A(x,u)\,\rho(x,y)\,A(y,\bar{v})\,\mathrm{d}x\,\mathrm{d}y. \tag{A.63}$$

Using the known action of differential operators on $A(x,u)$ and $A(y,\bar{v})$, we obtain

$$\begin{aligned}\frac{1}{2}\left(\bar{v}-\frac{\partial}{\partial\bar{v}}\right)\left(u-\frac{\partial}{\partial u}\right)R(u,\bar{v}) &= \frac{1}{2}\left(\bar{v}-\frac{\partial}{\partial\bar{v}}\right)\int A(x,u)\,\rho(x,y)\,A(y,\bar{v})\,(2u-\sqrt{2}x)\,\mathrm{d}x\,\mathrm{d}y,\\ &= \int A(x,u)\,(\sqrt{2}u-x)(\sqrt{2}\bar{v}-y)\,\rho(x,y)\,A(y,\bar{v})\,\mathrm{d}x\,\mathrm{d}y.\end{aligned} \tag{A.64}$$

Finally, recognising the second-order derivative structure in this expression, we can rewrite it as

$$\begin{aligned}\frac{1}{2}\left(\bar{v}-\frac{\partial}{\partial\bar{v}}\right)\left(u-\frac{\partial}{\partial u}\right)R(u,\bar{v}) &= \int A(x,u)\,\frac{\partial^2\rho(x,y)}{\partial x,\partial y}\,A(y,\bar{v})\,\mathrm{d}x\,\mathrm{d}y,\\ &= \langle\xi_{\bar{u}}(x)\,|\,\hat{p}\hat{\rho}\hat{p}^{\dagger}\,|\,\xi_{\bar{v}}(y)\rangle.\end{aligned} \tag{A.65}$$

□

These computations confirm that the action of position and momentum operators (and their adjoints) within the Lindblad equation can be naturally expressed as differential operators acting on the kernel $R(u, \bar{v})$. The table below summarizes the full set of such operator mappings, providing a practical dictionary between Hilbert space expressions and their FSB counterparts.

Coordinate Space $\leftrightarrow$ Bargmann Space
$\hat{x} \leftrightarrow \frac{1}{\sqrt{2}}\left(z + \frac{\partial}{\partial z}\right)$
$\hat{p} \leftrightarrow \frac{i}{\sqrt{2}}\left(z - \frac{\partial}{\partial z}\right)$
$\hat{x}\hat{\rho} \leftrightarrow \frac{1}{\sqrt{2}}\left(z + \frac{\partial}{\partial z}\right)$
$\hat{p}\hat{\rho} \leftrightarrow \frac{1}{\sqrt{2}\mathrm{i}}\left(z - \frac{\partial}{\partial z}\right)$
$\hat{\rho}\hat{x} \leftrightarrow \frac{1}{\sqrt{2}}\left(\bar{z} + \frac{\partial}{\partial \bar{z}}\right)$
$\hat{\rho}\hat{p} \leftrightarrow \frac{-1}{\sqrt{2}\mathrm{i}}\left(\bar{z} - \frac{\partial}{\partial \bar{z}}\right)$
$\hat{x}\hat{\rho}\hat{x}^\dagger \leftrightarrow \frac{1}{2}\left(z + \frac{\partial}{\partial z}\right)\left(\bar{z} + \frac{\partial}{\partial \bar{z}}\right)$
$\hat{p}\hat{\rho}\hat{p}^\dagger \leftrightarrow \frac{1}{2}\left(z - \frac{\partial}{\partial z}\right)\left(\bar{z} - \frac{\partial}{\partial \bar{z}}\right)$
$\hat{x}^\dagger\hat{x}\hat{\rho} \leftrightarrow \frac{1}{2}\left(\bar{z} + \frac{\partial}{\partial \bar{z}}\right)\left(\bar{z} + \frac{\partial}{\partial \bar{z}}\right)$
$\hat{p}^\dagger\hat{p}\hat{\rho} \leftrightarrow -\frac{1}{2}\left(\bar{z} - \frac{\partial}{\partial \bar{z}}\right)\left(\bar{z} - \frac{\partial}{\partial \bar{z}}\right)$
$\hat{\rho}\hat{x}^\dagger\hat{x} \leftrightarrow \frac{1}{2}\left(z + \frac{\partial}{\partial z}\right)\left(z + \frac{\partial}{\partial z}\right)$
$\hat{\rho}\hat{p}^\dagger\hat{p} \leftrightarrow -\frac{1}{2}\left(z - \frac{\partial}{\partial z}\right)\left(z - \frac{\partial}{\partial z}\right)$

Table A.1: Correspondence between the operators on the coordinate space and the Bargmann space.

Proposition A.8. *The Lindblad equation in the Fock-Segal-Bargmann representation for the density matrix $R(u, \bar{v})$ is given as*

$$\frac{\mathrm{d}R(u,\bar{v})}{\mathrm{d}t} = \frac{\partial^2 R(u,\bar{v})}{\partial u \partial \bar{v}} - u\frac{\partial R(u,\bar{v})}{\partial u} - \bar{v}\frac{\partial R(u,\bar{v})}{\partial \bar{v}} + (u\bar{v} - 1)R(u,\bar{v}). \tag{A.66}$$

Proof. Substituting the correspondence rules for the operator expressions into the Lindblad equation, we obtain

$$\begin{aligned}\frac{\mathrm{d}R(u,\bar{v})}{\mathrm{d}t} &= \frac{1}{2}\left(\bar{v} + \frac{\partial}{\partial \bar{v}}\right)\left(u + \frac{\partial}{\partial u}\right)R(u,\bar{v}) - \frac{1}{4}\left(\bar{v} + \frac{\partial}{\partial \bar{v}}\right)\left(\bar{v} + \frac{\partial}{\partial \bar{v}}\right)R(u,\bar{v}) \\ &\quad -\frac{1}{4}\left(u + \frac{\partial}{\partial u}\right)\left(u + \frac{\partial}{\partial u}\right)R(u,\bar{v}) + \frac{1}{2}\left(\bar{v} - \frac{\partial}{\partial \bar{v}}\right)\left(u - \frac{\partial}{\partial u}\right)R(u,\bar{v}) \\ &\quad +\frac{1}{4}\left(\bar{v} - \frac{\partial}{\partial \bar{v}}\right)\left(\bar{v} - \frac{\partial}{\partial \bar{v}}\right)R(u,\bar{v}) + \frac{1}{4}\left(u - \frac{\partial}{\partial u}\right)\left(u - \frac{\partial}{\partial u}\right)R(u,\bar{v}).\end{aligned} \tag{A.67}$$

Expanding and simplifying the terms gives

$$\frac{\mathrm{d}R(u,\bar{v})}{\mathrm{d}t} = \frac{\partial^2 R(u,\bar{v})}{\partial u \partial \bar{v}} - u\frac{\partial R(u,\bar{v})}{\partial u} - \bar{v}\frac{\partial R(u,\bar{v})}{\partial \bar{v}} + (u\bar{v} - 1)R(u,\bar{v}), \tag{A.68}$$

completing the proof. □

The Lindblad equation, once expressed in the Fock-Segal-Bargmann (FSB) representation, admits the following explicit solution for the density matrix kernel $R(u, \bar{v}, t)$.

Proposition A.9. *The solution to* (A.68) *is given as*

$$R(u, \bar{v}, t) = \frac{1}{t} \exp\left(\frac{(t-1)u\bar{v}}{t}\right) \int_{\mathbb{C}} \exp\left(\frac{w\bar{v} + \bar{w}u - |w|^2}{t}\right) R_0(w, \bar{w})\, \mathrm{d}\mu_w. \tag{A.69}$$

Proof. A direct substitution of the proposed solution (A.69) into the Lindblad equation (A.68) verifies that it satisfies the required time evolution. Since the equation is linear and homogeneous, uniqueness of solutions guarantees that this expression is indeed the correct propagator of the initial density matrix kernel. □

In this way the phase-space decoherence model discussed in Chapter 2 can be reproduced in the FSB representation.

Appendix B

Solving Lindblad equations for phase-space distributions for the Heisenberg-Weyl case

This appendix reviews mathematical preliminaries relevant to phase-space methods, including the Moyal representation and the Fourier transform on phase space. We then demonstrate, via a double Fourier transform, that the density matrix undergoes identical decoherence in both the momentum and position representations. We finally examine the evolution of quadratures under Lindblad dynamics, and explicitly solve the Lindblad equations for both the free particle and harmonic oscillator Hamiltonians with position and momentum Lindblad operators. The solutions are presented in both the Wigner and Husimi representations, highlighting how decoherence manifests differently in these phase-space pictures.

B.1 Mathematical preliminaries

B.1.1 Moyal product and Lindblad operators

In the phase-space formulation of the Lindblad equation, the action of Lindblad jump operators linear in position and momentum can be systematically expressed using the Moyal product [87,88,231]. Let us denote generic Lindblad operators

$$\hat{L}_j = a_j \hat{x} + b_j \hat{p} \tag{B.1}$$

where $a_j, b_j \in \mathbb{C}$. Their effect on the Wigner function requires evaluating terms like $\hat{L}_j \hat{\rho} \hat{L}_j^\dagger$ translated to phase space via the Moyal product. We expand the Moyal product for x and p explicitly, which yields derivative corrections that capture noncommutativity. To this end, note the standard Moyal product identity

$$f \star g = f\, g + \frac{\mathrm{i}\hbar}{2}\{f, g\}_{\mathrm{PB}} - \frac{\hbar^2}{8}\{\{f, g\}_{\mathrm{PB}}, g\}_{\mathrm{PB}} + \cdots \tag{B.2}$$

where $\{\cdot, \cdot\}_{\mathrm{PB}}$ is the classical Poisson bracket. Applying this systematically gives the following expansions:

Position operator

$$x \star W(x,p) = x\, W(x,p) + \frac{\mathrm{i}\hbar}{2}\frac{\partial W}{\partial p}, \quad W(x,p) \star x = x\, W(x,p) - \frac{\mathrm{i}\hbar}{2}\frac{\partial W}{\partial p}, \tag{B.3}$$

leading to

$$x \star W \star x = x^2\, W + \mathrm{i}\hbar\, x\frac{\partial W}{\partial p} - \frac{\hbar^2}{4}\frac{\partial^2 W}{\partial p^2}. \tag{B.4}$$

Momentum operator

$$p \star W(x,p) = p\, W(x,p) - \frac{\mathrm{i}\hbar}{2}\frac{\partial W}{\partial x}, \quad W(x,p) \star p = p\, W(x,p) + \frac{\mathrm{i}\hbar}{2}\frac{\partial W}{\partial x}, \tag{B.5}$$

yielding

$$p \star W \star p = p^2\, W - \mathrm{i}\hbar\, p\frac{\partial W}{\partial x} - \frac{\hbar^2}{4}\frac{\partial^2 W}{\partial x^2}. \tag{B.6}$$

Mixed terms which appear in many Lindblad cross-operator terms

$$x \star W \star p = xp\, W + \frac{\mathrm{i}\hbar}{2}x\frac{\partial W}{\partial x} + \frac{\mathrm{i}\hbar}{2}p\frac{\partial W}{\partial p} - \frac{\hbar^2}{4}\frac{\partial^2 W}{\partial x \partial p}, \tag{B.7}$$

$$p \star W \star x = px\, W - \frac{\mathrm{i}\hbar}{2}p\frac{\partial W}{\partial p} - \frac{\mathrm{i}\hbar}{2}x\frac{\partial W}{\partial x} - \frac{\hbar^2}{4}\frac{\partial^2 W}{\partial x \partial p}. \tag{B.8}$$

These expansions are directly applied in the derivation of the phase-space Lindblad equation

$$\frac{\mathrm{d}W}{\mathrm{d}t} = \text{Moyal}\left(\hat{L}_j \hat{\rho} \hat{L}_j^\dagger - \tfrac{1}{2}\{\hat{L}_j^\dagger \hat{L}_j, \hat{\rho}\}_+\right) \tag{B.9}$$

where $\{\cdot,\cdot\}_+$ denotes the anticommutator. The derivative corrections from the Moyal product systematically account for quantum corrections to the dissipative terms, recovering the classical Fokker-Planck structure in the limit $\hbar \to 0$.

B.1.2 Fourier transform on the real line

We shall now briefly review the double Fourier transform on $\mathcal{L}^2(\mathbb{R})$. The Fourier transform, and its inverse are defined as follows:

$$\xi(u,v) = \frac{1}{2\pi}\iint \exp\left(-\frac{\mathrm{i}xu}{\hbar}\right)\exp\left(-\frac{\mathrm{i}pv}{\hbar}\right)W(x,p)\,\mathrm{d}x\,\mathrm{d}p, \tag{B.10}$$

and

$$W(x,p) = \frac{1}{2\pi\hbar^2}\iint \exp\left(\frac{\mathrm{i}xu}{\hbar}\right)\exp\left(\frac{\mathrm{i}pv}{\hbar}\right)\xi(u,v)\,\mathrm{d}u\,\mathrm{d}v. \tag{B.11}$$

Now let us verify if they are indeed inverses of each other. So we have

$$\xi(u,v) = \frac{1}{2\pi}\iint \exp\left(-\frac{\mathrm{i}xu}{\hbar}\right)\exp\left(-\frac{\mathrm{i}pv}{\hbar}\right)W(x,p)\,\mathrm{d}x\,\mathrm{d}p. \tag{B.12}$$

Substituting for $W(x,p)$ in the above equation we have

$$\begin{aligned}\xi(u,v) &= \frac{1}{4\pi^2\hbar^2}\iint \exp\left(-\frac{\mathrm{i}xu}{\hbar}\right)\exp\left(-\frac{\mathrm{i}pv}{\hbar}\right)\\ &\quad\times\left[\iint \exp\left(\frac{\mathrm{i}xu'}{\hbar}\right)\exp\left(\frac{\mathrm{i}pv'}{\hbar}\right)\xi(u',v')\,\mathrm{d}u'\mathrm{d}v'\right]\mathrm{d}x\,\mathrm{d}p. \end{aligned}\tag{B.13}$$

Rearranging the terms gives

$$\xi(u,v)=\frac{1}{4\pi^2\hbar^2}\iint\left[\int\exp\left(\frac{\mathrm{i}xu'-\mathrm{i}xu}{\hbar}\right)\mathrm{d}x\right]\left[\int\exp\left(\frac{\mathrm{i}pv'-\mathrm{i}pv}{\hbar}\right)\mathrm{d}p\right]\xi(u',v')\,\mathrm{d}u'\mathrm{d}v'\tag{B.14}$$

Evaluating the integrals for p and x gives

$$\xi(u,v)=\frac{1}{4\pi^2\hbar^2}\iint(2\pi\hbar\,\delta(u-u'))(2\pi\hbar\,\delta(v-v'))\,\xi(u',v')\,\mathrm{d}u'\mathrm{d}v'.\tag{B.15}$$

and evaluating the integrals for u' and v' gives $\xi(u,v)=\xi(u,v)$.

B.1.3 Transforms on the phase space

We now discuss the analogous Fourier transforms in phase-space complex coordinates.

Proposition B.1. *The pair of transforms*

$$H(z,\bar z) = \frac{1}{\pi}\int\exp(-z\bar w+w\bar z)\,Q(w,\bar w)\,\mathrm{d}^2w,\tag{B.16}$$

$$Q(w,\bar w) = \frac{1}{\pi}\int\exp(-w\bar z+z\bar w)\,H(z,\bar z)\,\mathrm{d}^2z,\tag{B.17}$$

are inverses of each other and d^2w *is the Lebesgue measure on* $\mathbb{C}$.

Proof. Substituting the expression for H into the inverse transform gives

$$\begin{aligned}Q(z,\bar z) &= \frac{1}{\pi}\int \mathrm{e}^{-z\bar w+w\bar z}\left[\frac{1}{\pi}\int\mathrm{e}^{-w\bar u+u\bar w}\,Q(u,\bar u)\,\mathrm{d}^2u\right]\mathrm{d}^2w,\\ &= \frac{1}{\pi^2}\iint\exp\bigl(-z\bar w+w\bar z-w\bar u+u\bar w\bigr)\,Q(u,\bar u)\,\mathrm{d}^2u\,\mathrm{d}^2w.\end{aligned}\tag{B.18}$$

Define the kernel

$$K(z,u;\bar z,\bar u)=\frac{1}{\pi^2}\int\exp\left(-z\bar w+w\bar z-w\bar u+u\bar w\right)\mathrm{d}^2w.\tag{B.19}$$

Set $A=\bar z-\bar u,\quad B=u-z$, so that $-w\bar z+w\bar z-w\bar u+u\bar w=wA+\bar wB$. Writing $w=x+\mathrm{i}y$ gives $\bar w=x-\mathrm{i}y$ and hence

$$wA+\bar wB=x(A+B)+\mathrm{i}y(A-B).\tag{B.20}$$

Define $C=A+B$, $D=A-B$, then

$$K(z,u)=\frac{1}{\pi^2}\iint\exp\bigl(xC+\mathrm{i}yD\bigr)\,\mathrm{d}x\,\mathrm{d}y.\tag{B.21}$$

This integral is well-defined in the distribution sense. One interprets

$$\int \mathrm{e}^{xC}\,\mathrm{d}x \propto \delta(\mathrm{Re}\,C), \quad \int \mathrm{e}^{\mathrm{i}yD}\,\mathrm{d}y = 2\pi\delta(D), \tag{B.22}$$

so $K(z,u) \propto \delta(\mathrm{Re}\,C)\,\delta(D)$. Substituting back

$$C = (\bar{z} - \bar{u}) + (u - z) = \bar{z} + u - \bar{u} - z, \tag{B.23}$$

$$D = (\bar{z} - \bar{u}) - (u - z) = \bar{z} - u - \bar{u} + z. \tag{B.24}$$

Setting these to zero forces $z = u$, meaning the kernel acts as a delta function. Thus,

$$Q(z,\bar{z}) = \int \delta^2(z-u)\,Q(u,\bar{u})\,\mathrm{d}^2u = Q(z,\bar{z}) \tag{B.25}$$

as claimed. □

B.2 Double Fourier transform

In this section we shall show that (2.22) has the same structure in the momentum representation using the double Fourier transform. We have the result for a density matrix after a single iteration of nonselective phase-space measurement

$$\rho^{(1)}(x,y) = \frac{1}{\sqrt{2\pi}} \exp\left(-\frac{(x-y)^2}{2}\right) \int \exp\left(-\frac{\lambda^2}{2}\right) \rho(x+\lambda, y+\lambda)\,\mathrm{d}\lambda. \tag{B.26}$$

For momentum variables s,t the double Fourier transform of the density matrix $\tilde{\rho}(s,t)$ is given as

$$\rho(x,y) = \frac{1}{2\pi} \iint \exp\left(\mathrm{i}sx - \mathrm{i}ty\right) \tilde{\rho}(s,t)\,\mathrm{d}s\,\mathrm{d}t. \tag{B.27}$$

Let us now define the double Fourier transform of $\rho(x,y)$ from the coordinate space representation to momentum space representation in variables p and q as

$$\tilde{\rho}^{(1)}(p,q) = \frac{1}{2\pi} \iint \exp\left(-\mathrm{i}px + \mathrm{i}qy\right) \rho^{(1)}(x,y)\,\mathrm{d}x\,\mathrm{d}y. \tag{B.28}$$

Now substituting (B.26) for $\rho^{(1)}$ in the above equation, we get

$$\begin{aligned} \tilde{\rho}^{(1)}(p,q) \;=\; & \frac{1}{\sqrt{(2\pi)^3}} \iint \mathrm{e}^{-\mathrm{i}px+\mathrm{i}qy} \exp\left(-\frac{(x-y)^2}{2}\right) \\ & \times \left[\int \exp\left(-\frac{\lambda^2}{2}\right) \rho(x+\lambda, y+\lambda)\,\mathrm{d}\lambda\right] \mathrm{d}x\,\mathrm{d}y. \end{aligned} \tag{B.29}$$

Substituting for ρ from (B.27) and rearranging the terms, the above equation becomes

$$\begin{aligned} \tilde{\rho}^{(1)}(p,q) \;=\; & \frac{1}{\sqrt{(2\pi)^5}} \iint \left[\int \left[\iint \exp\left(\mathrm{i}x(-p+s) + \mathrm{i}y(t-q)\right) \exp\left(-\frac{(x-y)^2}{2}\right) \mathrm{d}x\mathrm{d}y\right] \right. \\ & \left. \times \exp\left(\mathrm{i}s\lambda - \mathrm{i}t\lambda\right) \exp\left(-\frac{\lambda^2}{2}\right) \mathrm{d}\lambda\right] \tilde{\rho}(s,t)\,\mathrm{d}s\,\mathrm{d}t. \end{aligned} \tag{B.30}$$

Looking at the inner integral we have

$$\iint \exp\left(\mathrm{i}x(-p+s)+\mathrm{i}y(t-q)\right)\exp\left(-\frac{(x-y)^2}{2}\right)\mathrm{d}x\mathrm{d}y = \int \exp\left(-\frac{y^2}{2}-\mathrm{i}y(t-q)\right) \times\left[\int \exp\left(-\frac{x^2}{2}+x(y+\mathrm{i}(s-p))\right)\mathrm{d}x\right]\mathrm{d}y. \quad \text{(B.31)}$$

Evaluating the x integral gives

$$\begin{aligned}\iint \exp\left(\mathrm{i}x(-p+s)+\mathrm{i}y(t-q)\right)\exp\left(-\frac{(x-y)^2}{2}\right)\mathrm{d}x\mathrm{d}y &= \sqrt{2\pi}\int \exp\left(-\frac{y^2}{2}-\mathrm{i}y(t-q)\right)\\ &\quad\times\exp\left(-\frac{(y+\mathrm{i}(s-p))^2}{2}\right)\mathrm{d}y\\ &= \sqrt{2\pi}\int \exp\left(-\mathrm{i}y(t-q-(s-p))\right)\\ &\quad\times\exp\left(-\frac{(s-p)^2}{2}\right)\mathrm{d}y. \quad \text{(B.32)}\end{aligned}$$

Now evaluating the y integral and simplifying the terms gives

$$\iint \mathrm{e}^{(\mathrm{i}x(-p+s)+\mathrm{i}y(t-q))}\exp\left(-\frac{(x-y)^2}{2}\right)\mathrm{d}x\mathrm{d}y = \sqrt{(2\pi)^3}\exp\left(-\tfrac{(s-p)^2}{2}\right)\delta(q+s-p-t). \quad \text{(B.33)}$$

Now (B.30) becomes

$$\begin{aligned}\tilde{\rho}^{(1)}(p,q) &= \frac{1}{2\pi}\iiint \exp\left(-\frac{(s-p)^2}{2}\right)\delta(q+s-p-t)\exp\left(-\frac{\lambda^2}{2}\right)\exp\left(\mathrm{i}\lambda(s-t)\right)\tilde{\rho}(s,t)\,\mathrm{d}s\,\mathrm{d}t\,\mathrm{d}\lambda.\\ &= \frac{1}{2\pi}\iint\left[\int \exp\left(-\frac{\lambda^2}{2}+\mathrm{i}\lambda(s-t)\right)\mathrm{d}\lambda\right]\\ &\quad\times\exp\left(-\frac{(s-p)^2}{2}\right)\delta(s-(q+t-p))\tilde{\rho}(s,t)\,\mathrm{d}s\,\mathrm{d}t. \quad \text{(B.34)}\end{aligned}$$

Evaluating the λ integral in the above equation gives

$$\tilde{\rho}^{(1)}(p,q) = \frac{1}{\sqrt{2\pi}}\iint\left[\exp\left(-\frac{(s-t)^2}{2}\right)\right]\exp\left(-\frac{(s-p)^2}{2}\right)\delta(s-(q+t-p))\tilde{\rho}(s,t)\,\mathrm{d}s\,\mathrm{d}t. \quad \text{(B.35)}$$

Now evaluating the s integral in the above equation with the delta function, we get

$$\tilde{\rho}^{(1)}(p,q) = \frac{1}{\sqrt{2\pi}}\int \exp\left(-\frac{(q+t-p-t)^2}{2}\right)\exp\left(-\frac{(p-q+t-p)^2}{2}\right)\tilde{\rho}(p+t-q,t)\,\mathrm{d}t, \quad \text{(B.36)}$$

which after simplifying becomes

$$\tilde{\rho}^{(1)}(p,q) = \frac{1}{\sqrt{2\pi}}\int \exp\left(-\frac{(q-p)^2}{2}\right)\exp\left(-\frac{(t-q)^2}{2}\right)\tilde{\rho}(p+t-q,t)\,\mathrm{d}t. \quad \text{(B.37)}$$

Now making the substitution $t-q=\mu$ we get

$$\tilde{\rho}^{(1)}(p,q) = \frac{1}{\sqrt{2\pi}}\exp\left(-\frac{(q-p)^2}{2}\right)\int \exp\left(-\frac{\mu^2}{2}\right)\tilde{\rho}(p+\mu,q+\mu)\,\mathrm{d}\mu, \quad \text{(B.38)}$$

which is the same as the result we had in the coordinate space in (B.26).

B.3 Lindblad equation for the free particle Hamiltonian

In this section, we examine the phase-space dynamics of a free particle subject to linear Lindblad decoherence. The free particle Hamiltonian is given by

$$\hat{H} = \frac{\hat{p}^2}{2m}. \tag{B.39}$$

We include two Lindblad operators representing dissipative couplings in position and momentum

$$\hat{L}_1 = \sqrt{\gamma_x}\,\hat{x}, \qquad \hat{L}_2 = \sqrt{\gamma_p}\,\hat{p}, \tag{B.40}$$

where $\gamma_x, \gamma_p \geq 0$ are decoherence rates associated with position and momentum, respectively.

Our objective is to derive the time evolution of the first and second statistical moments of the system

$$\langle \hat{x}(t) \rangle, \quad \langle \hat{p}(t) \rangle, \quad \mathrm{Var}(\hat{x}(t)), \quad \mathrm{Var}(\hat{p}(t)). \tag{B.41}$$

We will first derive the moment equations for the most general case in which both Lindblad operators are present. Subsequently, we will specialise these results to the limiting cases in which either γ_x or γ_p is set to zero, to examine how purely position or purely momentum decoherence affects the dynamics.

Position and Momentum Lindbladians Together

The Lindblad master equation is given by

$$\frac{\mathrm{d}\hat{\rho}}{\mathrm{d}t} = -\frac{\mathrm{i}}{\hbar}[\hat{H}, \hat{\rho}] + \gamma_x \left(\hat{x}\hat{\rho}\hat{x} - \tfrac{1}{2}\{\hat{x}^2, \hat{\rho}\} \right) + \gamma_p \left(\hat{p}\hat{\rho}\hat{p} - \tfrac{1}{2}\{\hat{p}^2, \hat{\rho}\} \right). \tag{B.42}$$

Our goal is to obtain the time evolution of the first and second moments of position and momentum.

First Moments Let us define

$$\langle \hat{x} \rangle = \mathrm{tr}(\hat{\rho}\hat{x}), \quad \langle \hat{p} \rangle = \mathrm{tr}(\hat{\rho}\hat{p}). \tag{B.43}$$

Applying the master equation and using standard commutators, one obtains the Ehrenfest equations

$$\frac{\mathrm{d}}{\mathrm{d}t}\langle \hat{x} \rangle = \frac{1}{m}\langle \hat{p} \rangle, \quad \frac{\mathrm{d}}{\mathrm{d}t}\langle \hat{p} \rangle = 0. \tag{B.44}$$

The dissipative terms involving symmetric Lindblad operators do not alter the first moments, because for Hermitian operators, the mean drift vanishes.

With initial conditions

$$\langle \hat{x}(0) \rangle = x_0, \quad \langle \hat{p}(0) \rangle = p_0, \tag{B.45}$$

the solutions are

$$\langle \hat{p}(t) \rangle \quad = p_0, \quad \langle \hat{x}(t) \rangle \quad = x_0 + \frac{p_0}{m}t. \tag{B.46}$$

Second Moments Let us next define the second-order moments

$$X^2(t) = \langle \hat{x}^2 \rangle, \quad P^2(t) = \langle \hat{p}^2 \rangle, \quad XP(t) = \frac{1}{2}\langle \hat{x}\hat{p} + \hat{p}\hat{x} \rangle. \tag{B.47}$$

Their evolution equations are obtained from the master equation:

- For $\langle \hat{x}^2 \rangle$

$$\frac{\mathrm{d}}{\mathrm{d}t}\langle \hat{x}^2 \rangle = \frac{1}{m}\langle \hat{x}\hat{p} + \hat{p}\hat{x} \rangle = \frac{2}{m}\, XP(t). \tag{B.48}$$

- For $\langle \hat{p}^2 \rangle$

$$\frac{\mathrm{d}}{\mathrm{d}t}\langle \hat{p}^2 \rangle = 0 + \gamma_x \hbar^2, \tag{B.49}$$

  because the Moyal expansion of the $\hat{x}$-based dissipator gives momentum diffusion with strength $\gamma_x \hbar^2$.

- Finally for the symmetric correlator

$$\frac{\mathrm{d}}{\mathrm{d}t}\, XP(t) = \frac{1}{m}\langle \hat{p}^2 \rangle, \tag{B.50}$$

  as there is no contribution from the Lindblad part to cross-terms.

Therefore the closed set of second-moment ODEs is

$$\frac{\mathrm{d}}{\mathrm{d}t}X^2(t) = \frac{2}{m}\, XP(t), \quad \frac{\mathrm{d}}{\mathrm{d}t}P^2(t) = \gamma_x \hbar^2, \quad \frac{\mathrm{d}}{\mathrm{d}t}XP(t) = \frac{1}{m}P^2(t), \tag{B.51}$$

with initial conditions

$$X^2(0) = k_2, \quad P^2(0) = k_1, \quad XP(0) = k_3. \tag{B.52}$$

The equation for P^2 can be solved immediately:

$$P^2(t) = k_1 + \gamma_x \hbar^2\, t. \tag{B.53}$$

Then

$$\frac{\mathrm{d}}{\mathrm{d}t}XP(t) = \frac{1}{m}P^2(t) = \frac{1}{m}\left(k_1 + \gamma_x \hbar^2 t\right). \tag{B.54}$$

This integrates to

$$XP(t) = k_3 + \frac{k_1}{m}t + \frac{\gamma_x \hbar^2}{2m}t^2. \tag{B.55}$$

Finally

$$\frac{\mathrm{d}}{\mathrm{d}t}X^2(t) = \frac{2}{m}XP(t) \tag{B.56}$$

which gives

$$\frac{\mathrm{d}}{\mathrm{d}t}X^2(t) = \frac{2}{m}\left(k_3 + \frac{k_1}{m}t + \frac{\gamma_x\hbar^2}{2m}t^2\right), \tag{B.57}$$

so

$$X^2(t) = k_2 + \frac{2k_3}{m}t + \frac{k_1}{m^2}t^2 + \frac{\gamma_x\hbar^2}{3m^2}t^3. \tag{B.58}$$

Variances We can collect the variances by noting

$$\mathrm{Var}(\hat{x}) = X^2(t) - \langle\hat{x}(t)\rangle^2, \quad \mathrm{Var}(\hat{p}) = P^2(t) - \langle\hat{p}(t)\rangle^2. \tag{B.59}$$

Explicitly,

$$\mathrm{Var}(\hat{x})(t) = k_2 + \frac{2k_3}{m}t + \frac{k_1}{m^2}t^2 + \frac{\gamma_x\hbar^2}{3m^2}t^3 - \left(x_0 + \frac{p_0}{m}t\right)^2, \tag{B.60}$$

and

$$\mathrm{Var}(\hat{p})(t) = k_1 + \gamma_x\hbar^2 t - p_0^2. \tag{B.61}$$

The results reveal key features of Lindblad decoherence for a free particle in phase space. In the absence of dissipation, the free Hamiltonian conserves momentum moments, leading to ballistic spreading of position variance. Introducing Lindblad terms alters this picture depending on the noise channel: a position-coupled Lindblad operator ($\hat{L} = \sqrt{\gamma_x}\hat{x}$) induces momentum diffusion, causing cubic growth in position variance over time due to kinetic coupling. Conversely, a momentum-coupled dissipator ($\hat{L} = \sqrt{\gamma_p}\hat{p}$) leads to linear growth in position uncertainty from both ballistic and diffusive contributions, while leaving momentum moments unaffected. When both couplings are present, position and momentum undergo simultaneous diffusion, producing enhanced spreading in both quadratures. This reflects the backaction trade-off in continuously monitoring noncommuting observables.

We will now solve the Lindblad equation for a free particle Hamiltonian with position and momentum Lindblad operators (B.42)in both the Wigner and Husimi representation.

B.3.1 Solving the Lindblad equation in Wigner representation

In phase space, the master equation takes the form

$$\begin{aligned}\frac{\mathrm{d}W(x,p,t)}{\mathrm{d}t} &= -\frac{\mathrm{i}}{2m\hbar}\left(p^2\star W - W\star p^2\right) + \gamma_1\left(x\star W\star x - \frac{1}{2}\left(x^2\star W + W\star x^2\right)\right)\\ &\quad +\gamma_2\left(p\star W\star p - \frac{1}{2}\left(p^2\star W + W\star p^2\right)\right),\end{aligned} \tag{B.62}$$

where $\star$ denotes the Moyal product [87]. After evaluating the Moyal brackets, this simplifies to the partial differential equation

$$\frac{\mathrm{d}W(x,p,t)}{\mathrm{d}t} = -\frac{p}{m}\frac{\partial W}{\partial x} + \frac{\hbar^2}{2}\left(\gamma_1\frac{\partial^2 W}{\partial x^2} + \gamma_2\frac{\partial^2 W}{\partial p^2}\right), \tag{B.63}$$

which describes a linear Fokker–Planck-type evolution in phase space. Its explicit solution can be stated as follows:.

Proposition B.2. *The solution of equation* (B.63) *is given by*

$$\begin{aligned} W(x,p,t) &= \sqrt{\frac{3}{\pi^2\left(t^4+12t^2\right)}}\iint \exp\left[-\frac{6\left(x-x'-p't\right)^2}{t^3+12t}\right] \\ &\quad\times\exp\left[-\frac{2\left(p-p'\right)^2\left(t^2+3\right)}{t^3+12t}\right] W_0(x',p')\,\mathrm{d}x'\,\mathrm{d}p', \end{aligned} \tag{B.64}$$

where $W_0(x',p')$ is the initial Wigner function at $t=0$.

Proof. We begin by taking the Fourier transform of equation (B.63), which yields

$$\frac{\mathrm{d}\xi(u,v,t)}{\mathrm{d}t} = \frac{u}{m}\frac{\partial\xi(u,v,t)}{\partial v} - \frac{1}{2}\left(\gamma_1 u^2+\gamma_2 v^2\right)\xi(u,v,t). \tag{B.65}$$

To solve this equation, we apply the method of characteristics. The characteristic system is given by

$$\frac{\mathrm{d}t}{\mathrm{d}s}=1, \qquad \frac{\mathrm{d}v}{\mathrm{d}s}=-\frac{u}{m}, \qquad \frac{\mathrm{d}u}{\mathrm{d}s}=0, \qquad \frac{\mathrm{d}\xi}{\mathrm{d}s}=-\frac{1}{2}\left(\gamma_1 u^2+\gamma_2 v^2\right)\xi(u,v,s). \tag{B.66}$$

We choose initial conditions

$$u(s=0)=u_0, \quad v(s=0)=v_0, \quad \xi(u,v,s=0)=\xi_0(u,v), \quad t(s=0)=0, \tag{B.67}$$

and solve for the characteristic curves:

$$t(s)=s, \qquad u(s)=u_0, \qquad v(s)=v_0-\frac{u_0}{m}s. \tag{B.68}$$

Next, let us compute the integrals appearing in the exponential solution. First,

$$\int u^2\,\mathrm{d}s = u_0^2 s. \tag{B.69}$$

Similarly,

$$\int v^2\,\mathrm{d}s = \int\left(v_0-\frac{u_0}{m}s\right)^2\mathrm{d}s = \int\left(\frac{u_0^2 s^2}{m^2}+v_0^2-\frac{2u_0v_0s}{m}\right)\mathrm{d}s = \frac{u_0^2s^3}{3m^2}+v_0^2 s-\frac{u_0v_0s^2}{m}. \tag{B.70}$$

Using these results, the ODE for ξ becomes

$$\frac{\mathrm{d}\xi}{\mathrm{d}s} = -\frac{1}{2}\left(\gamma_1 u_0^2+\gamma_2\left(v_0-\frac{u_0}{m}s\right)^2\right)\xi(s), \tag{B.71}$$

which integrates to

$$\begin{aligned} \log\xi(s) &= -\frac{1}{2}\int\left(\gamma_1 u_0^2+\gamma_2\left(v_0-\frac{u_0}{m}s\right)^2\right)\mathrm{d}s, \\ &= -\left[\frac{\gamma_1}{2}u_0^2 s+\frac{\gamma_2}{2}\left(\frac{u_0^2s^3}{3m^2}+v_0^2 s-\frac{u_0v_0s^2}{m}\right)\right]. \end{aligned} \tag{B.72}$$

Making the substitutions $s = t$, $u = u_0$, and $v_0 = v + \frac{ut}{m}$, we obtain the general solution of the Fourier-transformed PDE

$$\xi(u, v, t) = \xi_0 \left(u,\, v + \frac{ut}{m} \right) \exp\left(-\frac{\gamma_1 u^2 t}{2} - \frac{\gamma_2 v^2 t}{2} - \frac{\gamma_2 u^2 t^3}{6m^2} - \frac{uvt^2\gamma_2}{2m} \right). \tag{B.73}$$

To recover the Wigner function, we apply the inverse Fourier transform

$$W(x, p, t) = \frac{1}{2\pi\hbar^2} \iint \exp\left(\frac{\mathrm{i}xu}{\hbar} \right) \exp\left(\frac{\mathrm{i}pv}{\hbar} \right) \xi(u, v, t)\, \mathrm{d}u\, \mathrm{d}v. \tag{B.74}$$

Substituting $\xi(u, v, t)$ from above gives

$$\begin{aligned} W(x, p, t) \;=\; & \frac{1}{2\pi\hbar^2} \iint \exp\left(\frac{\mathrm{i}xu}{\hbar} \right) \exp\left(\frac{\mathrm{i}pv}{\hbar} \right) \\ & \times \xi_0 \left(u,\, v + \frac{ut}{m} \right) \exp\left(-\frac{\gamma_1 u^2 t}{2} - \frac{\gamma_2 v^2 t}{2} - \frac{\gamma_2 u^2 t^3}{6m^2} - \frac{uvt^2\gamma_2}{2m} \right) \mathrm{d}u\, \mathrm{d}v. \end{aligned} \tag{B.75}$$

Now, expressing the initial characteristic function in terms of the initial Wigner function,

$$\xi_0 \left(u,\, v + \frac{ut}{m} \right) = \frac{1}{2\pi} \iint \exp\left(\frac{-\mathrm{i}x'u}{\hbar} \right) \exp\left(\frac{-\mathrm{i}p' \left(v + \frac{ut}{m} \right)}{\hbar} \right) W_0(x', p')\, \mathrm{d}x'\, \mathrm{d}p', \tag{B.76}$$

which substituted back and and collecting terms, simplifies to

$$\begin{aligned} W(x, p, t) \;=\; & \frac{1}{4\pi^2\hbar^2} \iint \iint \exp\left(u \left(\frac{2\mathrm{i}\left(m(x - x') - p't \right) - \gamma_2 v t^2 \hbar}{2m\hbar} \right) - \frac{3m^2\gamma_1 u^2 t + \gamma_2 u^2 t^3}{6m^2} \right) \mathrm{d}u \\ & \times \exp\left(v \left(\frac{\mathrm{i}(p - p')}{\hbar} \right) - \frac{\gamma_2 v^2 t}{2} \right) \mathrm{d}v\, W_0(x', p')\, \mathrm{d}x'\, \mathrm{d}p'. \end{aligned} \tag{B.77}$$

Integrating with respect to u, we obtain

$$\begin{aligned} W(x, p, t) \;=\; & \frac{1}{4\pi^2\hbar^2} \iiint \sqrt{\frac{6m^2\pi}{3m^2\gamma_1 t + \gamma_2 t^3}} \exp\left(\frac{3\left(2\mathrm{i}m(x - x') - 2\mathrm{i}p't - \gamma_2 v t^2 \hbar \right)^2}{8\hbar^2 \left(3m^2\gamma_1 t + \gamma_2 t^3 \right)} \right) \\ & \times \exp\left(v \frac{\mathrm{i}(p - p')}{\hbar} - \frac{\gamma_2 v^2 t}{2} \right) \mathrm{d}v\, W_0(x', p')\, \mathrm{d}x'\, \mathrm{d}p'. \end{aligned} \tag{B.78}$$

Expanding the quadratic terms and rearranging leads to

$$\begin{aligned} W(x, p, t) \;=\; & \frac{1}{4\pi^2\hbar^2} \sqrt{\frac{6m^2\pi}{3m^2\gamma_1 t + \gamma_2 t^3}} \iiint \exp\left(-\frac{3\left(m(x - x') - p't \right)^2}{2\hbar^2 \left(3m^2\gamma_1 t + \gamma_2 t^3 \right)} \right) \\ & \times \exp\left(-v^2 \left(\frac{4\gamma_2 t \left(3m^2\gamma_1 t + \gamma_2 t^3 \right) - 3\gamma_2^2 t^4}{8\left(3m^2\gamma_1 t + \gamma_2 t^3 \right)} \right) \right) \\ \times \exp\left(\mathrm{i}v \left(\frac{2(p - p')\left(3m^2\gamma_1 t + \gamma_2 t^3 \right) - 3\left(m(x - x') - p't \right)\gamma_2 t^2}{2\hbar\left(3m^2\gamma_1 t + \gamma_2 t^3 \right)} \right) \right) & \mathrm{d}v\, W_0(x', p')\, \mathrm{d}x'\, \mathrm{d}p'. \end{aligned} \tag{B.79}$$

Integrating with respect to v gives

$$\begin{aligned} W(x,p,t) &= \frac{1}{4\pi^2\hbar^2}\sqrt{\frac{6m^2\pi}{3m^2\gamma_1 t+\gamma_2 t^3}}\sqrt{\frac{8\pi\left(3m^2\gamma_1 t+\gamma_2 t^3\right)}{4\gamma_2 t\left(3m^2\gamma_1 t+\gamma_2 t^3\right)-3\gamma_2^2 t^4}} \\ &\quad\times\iint\exp\left(-\frac{3\left(m(x-x')-p't\right)^2}{2\hbar^2\left(3m^2\gamma_1 t+\gamma_2 t^3\right)}\right) \\ &\quad\times\exp\left(-\frac{\left(2(p-p')\left(3m^2\gamma_1 t+\gamma_2 t^3\right)-3\left(m(x-x')-p't\right)\gamma_2 t^2\right)^2}{2\hbar^2\left(3m^2\gamma_1 t+\gamma_2 t^3\right)\left(4\gamma_2 t\left(3m^2\gamma_1 t+\gamma_2 t^3\right)-3\gamma_2^2 t^4\right)}\right) \\ &\quad\times W_0(x',p')\,\mathrm{d}x'\,\mathrm{d}p'. \end{aligned} \tag{B.80}$$

Further simplification gives the final form

$$\begin{aligned} W(x,p,t) &= \frac{\sqrt{3}m}{\pi\hbar^2}\sqrt{\frac{1}{12m^2\gamma_1\gamma_2 t^2+\gamma_2^2 t^4}} \\ &\quad\times\iint\exp\left(-\frac{2(p-p')^2\left(3m^2\gamma_1+\gamma_2 t^2\right)}{12m^2\gamma_1\gamma_2 t+\gamma_2^2 t^3}\right) \\ &\quad\times\exp\left(-\frac{6\left(m(x-x')-p't\right)\left(m(x-x')-pt\right)}{\hbar^2\left(12m^2\gamma_1 t+\gamma_2 t^3\right)}\right)W_0(x',p')\,\mathrm{d}x'\,\mathrm{d}p'. \end{aligned} \tag{B.81}$$

In the special case where $\hbar=\gamma_1=\gamma_2=m=1$, the solution simplifies to

$$\begin{aligned} W(x,p,t) &= \sqrt{\frac{3}{\pi^2\left(t^4+12t^2\right)}}\iint\exp\left(\frac{-6\left(x-x'-p't\right)\left(x-x'-pt\right)}{t^3+12t}\right) \\ &\quad\times\exp\left(-\frac{2(p-p')^2\left(t^2+3\right)}{t^3+12t}\right)W_0(x',p')\,\mathrm{d}x'\,\mathrm{d}p'. \end{aligned} \tag{B.82}$$

□

B.3.2 Solving the Lindblad equation in the Husimi representation

In the holomorphic (FSB) representation, the Lindblad equation takes the following form:

$$\begin{aligned} \frac{\mathrm{d}R(u,\bar{v},t)}{\mathrm{d}t} &= \frac{-\mathrm{i}\Omega}{4}\left(\left(u-\frac{\partial}{\partial u}\right)\left(u-\frac{\partial}{\partial u}\right)-\left(\bar{v}-\frac{\partial}{\partial\bar{v}}\right)\left(\bar{v}-\frac{\partial}{\partial\bar{v}}\right)\right)R(u,\bar{v}) \\ &\quad+\frac{\gamma_1}{m\Omega}\left(\frac{1}{2}\left(\bar{v}+\frac{\partial}{\partial\bar{v}}\right)\left(u+\frac{\partial}{\partial u}\right)R(u,\bar{v})-\frac{1}{4}\left(\bar{v}+\frac{\partial}{\partial\bar{v}}\right)\left(\bar{v}+\frac{\partial}{\partial\bar{v}}\right)R(u,\bar{v})\right. \\ &\quad\left.-\frac{1}{4}\left(u+\frac{\partial}{\partial u}\right)\left(u+\frac{\partial}{\partial u}\right)R(u,\bar{v})\right)+\gamma_2 m\Omega\left(\frac{1}{2}\left(\bar{v}-\frac{\partial}{\partial\bar{v}}\right)\left(u-\frac{\partial}{\partial u}\right)R(u,\bar{v})\right. \\ &\quad\left.+\frac{1}{4}\left(\bar{v}-\frac{\partial}{\partial\bar{v}}\right)\left(\bar{v}-\frac{\partial}{\partial\bar{v}}\right)R(u,\bar{v})+\frac{1}{4}\left(u-\frac{\partial}{\partial u}\right)\left(u-\frac{\partial}{\partial u}\right)R(u,\bar{v})\right). \end{aligned} \tag{B.83}$$

Expanding the differential operators yields , collecting and grouping the terms gives

$$\begin{aligned}\frac{\mathrm{d}R(u,\bar{v},t)}{\mathrm{d}t} &= \left(\frac{-\mathrm{i}\Omega(u^2-\bar{v}^2)}{4}-\frac{\gamma_1(u-\bar{v})^2}{4m\Omega}+\frac{\gamma_2 m\Omega(u+\bar{v})^2}{4}-\frac{\gamma_1}{2m\Omega}-\frac{\gamma_2 m\Omega}{2}\right)R(u,\bar{v})\\ &+\left(\frac{\mathrm{i}\Omega u}{2}+\frac{\gamma_1(\bar{v}-u)}{2m\Omega}-\frac{\gamma_2 m\Omega(\bar{v}+u)}{2}\right)\frac{\partial R(u,\bar{v})}{\partial u}\\ &+\left(\frac{-\mathrm{i}\Omega\bar{v}}{2}+\frac{\gamma_1(u-\bar{v})}{2m\Omega}-\frac{\gamma_2 m\Omega(\bar{v}+u)}{2}\right)\frac{\partial R(u,\bar{v})}{\partial \bar{v}}\\ &+\left(\frac{\gamma_2 m\Omega}{4}-\frac{\gamma_1}{4m\Omega}-\frac{\mathrm{i}\Omega}{4}\right)\frac{\partial^2 R(u,\bar{v})}{\partial u^2}+\left(\frac{\gamma_2 m\Omega}{4}-\frac{\gamma_1}{4m\Omega}+\frac{\mathrm{i}\Omega}{4}\right)\frac{\partial^2 R(u,\bar{v})}{\partial \bar{v}^2}\\ &+\left(\frac{\gamma_1}{2m\Omega}+\frac{\gamma_2 m\Omega}{2}\right)\frac{\partial^2 R(u,\bar{v})}{\partial u\partial\bar{v}}. \end{aligned} \tag{B.84}$$

Restricting to the diagonal elements $u=z$, $\bar{v}=\bar{z}$ gives in terms of the Husimi function $Q(z,\bar{z})$

$$\begin{aligned}\frac{\mathrm{d}Q(z,\bar{z},t)}{\mathrm{d}t} &= \frac{\partial Q}{\partial z}\left(\frac{-\mathrm{i}\Omega\bar{z}+\mathrm{i}\Omega z}{2}\right)+\frac{\partial Q}{\partial \bar{z}}\left(\frac{-\mathrm{i}\Omega\bar{z}+\mathrm{i}\Omega z}{2}\right)\\ &+\frac{\partial^2 Q}{\partial z^2}\left(\frac{\gamma_2 m\Omega}{4}-\frac{\gamma_1}{4m\Omega}-\frac{\mathrm{i}\Omega}{4}\right)+\frac{\partial^2 Q}{\partial \bar{z}^2}\left(\frac{\gamma_2 m\Omega}{4}-\frac{\gamma_1}{4m\Omega}+\frac{\mathrm{i}\Omega}{4}\right)\\ &+\left(\frac{\gamma_1}{2m\Omega}+\frac{\gamma_2 m\Omega}{2}\right)\frac{\partial^2 Q(z,\bar{z})}{\partial z\partial\bar{z}}. \end{aligned} \tag{B.85}$$

Proposition B.3. *Consider the Lindblad equation for the Husimi Q-function in the holomorphic representation. In the special case when*

$$m=\gamma_1=\gamma_2=\Omega=1, \tag{B.86}$$

the solution for the diagonal Husimi function is explicitly given by

$$\begin{aligned}Q(z,\bar{z},t) &= \sqrt{\frac{12}{\pi^2\left(t^4+9t^2\right)}}\int \exp\left(\frac{(\bar{\alpha}-\alpha)^2}{4t}\right)\exp\left(\frac{-3(\bar{\alpha}+\alpha)^2}{t^3+9t}\right)\\ &\times\exp\left(\frac{3\mathrm{i}(\bar{\alpha}^2-\alpha^2)(t-1)}{t^3+9t}\right)\exp\left(\frac{3(t-1)^2(\bar{\alpha}-\alpha)^2}{4(t^3+9t)}\right)Q_0(u,\bar{u})\,\mathrm{d}^2u, \end{aligned} \tag{B.87}$$

where

$$\alpha=z-u+\mathrm{i}ut,\quad \bar{\alpha}=\bar{z}-\bar{u}-\mathrm{i}\bar{u}t. \tag{B.88}$$

Upon explicitly substituting these expressions, the solution becomes

$$\begin{aligned}Q(z,\bar{z},t) &= \sqrt{\frac{12}{\pi^2\left(t^4+9t^2\right)}}\int \exp\left(\frac{\left(z-u-\bar{z}+\bar{u}\right)^2}{4t}\right)\exp\left(\frac{-3\left(z-u+\bar{z}-\bar{u}+\mathrm{i}ut-\mathrm{i}\bar{u}t\right)^2}{t^3+9t}\right)\\ &\times\exp\left(\frac{3(t-1)^2\left(z-u-\bar{z}+\bar{u}\right)^2}{4(t^3+9t)}\right)\\ &\times\exp\left(\frac{3\mathrm{i}(t-1)\left(z-u+\bar{z}-\bar{u}+\mathrm{i}ut-\mathrm{i}\bar{u}t\right)\left(z-u-\bar{z}+\bar{u}\right)}{t^3+9t}\right)Q_0(u,\bar{u})\,\mathrm{d}^2u. \end{aligned} \tag{B.89}$$

Proof. We begin by introducing the holomorphic transform

$$H(w,\bar{w},t) = \frac{1}{\pi}\int \exp\left(-w\bar{z}+z\bar{w}\right) Q(z,\bar{z})\,\mathrm{d}^2 z, \tag{B.90}$$

which maps the Husimi Q-function to the Segal–Bargmann kernel representation. Applying this transform to the Lindblad equation yields

$$\begin{aligned}\frac{\mathrm{d}H}{\mathrm{d}t} &= \frac{\partial H}{\partial \bar{w}}\left(\frac{-\mathrm{i}\Omega\bar{w}+\mathrm{i}\Omega w}{2}\right)+\frac{\partial H}{\partial w}\left(\frac{-\mathrm{i}\Omega\bar{w}+\mathrm{i}\Omega w}{2}\right)\\ &\quad+\left(\frac{\gamma_2 m\Omega(w-\bar{w})^2}{4}-\frac{\gamma_1(w+\bar{w})^2}{4m\Omega}+\frac{\mathrm{i}\Omega(w^2-\bar{w}^2)}{4}\right)H.\end{aligned} \tag{B.91}$$

Using the method of characteristics, we have the following system of ODEs

$$\frac{\mathrm{d}t}{\mathrm{d}s}=1,\quad \frac{\mathrm{d}w}{\mathrm{d}s}=\frac{\mathrm{i}\Omega\bar{w}-\mathrm{i}\Omega w}{2},\quad \frac{\mathrm{d}\bar{w}}{\mathrm{d}s}=\frac{\mathrm{i}\Omega\bar{w}-\mathrm{i}\Omega w}{2}, \tag{B.92}$$

together with

$$\frac{\mathrm{d}H}{\mathrm{d}s}=\left(\frac{\gamma_2 m\Omega(w-\bar{w})^2}{4}-\frac{\gamma_1(w+\bar{w})^2}{4m\Omega}+\frac{\mathrm{i}\Omega(w^2-\bar{w}^2)}{4}\right)H. \tag{B.93}$$

Solving the first three characteristic equations with initial data

$$s=0,\quad w(0)=w_0,\quad \bar{w}(0)=\bar{w}_0,\quad H(w,\bar{w},0)=H_0(w_0,\bar{w}_0), \tag{B.94}$$

yields

$$t(s)=s,\quad w(s) = \mathrm{i}\Omega\left(\frac{\bar{w}_0-w_0}{2}\right)s+w_0,\quad \bar{w}(s)=\mathrm{i}\Omega\left(\frac{\bar{w}_0-w_0}{2}\right)s+\bar{w}_0. \tag{B.95}$$

Inverting these, one finds

$$w_0=-\mathrm{i}\Omega\left(\frac{\bar{w}-w}{2}\right)s+w,\quad \bar{w}_0=-\mathrm{i}\Omega\left(\frac{\bar{w}-w}{2}\right)s+\bar{w}. \tag{B.96}$$

The ODE for the amplitude is then

$$\frac{\mathrm{d}H}{\mathrm{d}s}=\left(\frac{\gamma_2 m\Omega(w-\bar{w})^2}{4}-\frac{\gamma_1(w+\bar{w})^2}{4m\Omega}+\frac{\mathrm{i}\Omega(w^2-\bar{w}^2)}{4}\right)H, \tag{B.97}$$

which integrates to

$$\begin{aligned}\log H &= \int\left(\frac{\gamma_2 m\Omega(w-\bar{w})^2}{4}-\frac{\gamma_1(w+\bar{w})^2}{4m\Omega}+\frac{\mathrm{i}\Omega(w^2-\bar{w}^2)}{4}\right)\mathrm{d}s,\\ &= \frac{\gamma_2 m\Omega(w-\bar{w})^2 s}{4}+\frac{\gamma_1\Omega(\bar{w}-w)^2 s^3}{12m}+\frac{\mathrm{i}\gamma_1(\bar{w}^2-w^2)s^2}{4m}\\ &\quad-\frac{\gamma_1(w+\bar{w})^2 s}{4m\Omega}+\frac{\mathrm{i}\Omega(w^2-\bar{w}^2)s}{4}-\frac{\Omega^2 s^2(w-\bar{w})^2}{8}.\end{aligned} \tag{B.98}$$

Hence the solution to the PDE is

$$\begin{aligned} H(w,\bar{w},t) &= H_0\left(-\mathrm{i}\Omega\left(\frac{\bar{w}-w}{2}\right)t+w,-\mathrm{i}\Omega\left(\frac{\bar{w}-w}{2}\right)t+\bar{w}\right) \\ &\times\exp\left(\frac{\gamma_2 tm\Omega(w-\bar{w})^2}{4}+\frac{\gamma_1\Omega(\bar{w}-w)^2t^3}{12m}+\frac{\mathrm{i}\gamma_1(\bar{w}^2-w^2)t^2}{4m}\right) \\ &\times\exp\left(-\frac{\gamma_1(w+\bar{w})^2t}{4m\Omega}+\frac{\mathrm{i}\Omega(w^2-\bar{w}^2)t}{4}-\frac{\Omega^2t^2(w-\bar{w})^2}{8}\right). \end{aligned} \tag{B.99}$$

The initial function $H_0(w_0,\bar{w}_0)$ can be expressed as

$$H_0(w_0,\bar{w}_0)=\frac{1}{\pi}\int\exp\left(\mathrm{i}\Omega\left(\frac{\bar{w}-w}{2}\right)t\bar{u}-w\bar{u}-\mathrm{i}\Omega\left(\frac{\bar{w}-w}{2}\right)tu+\bar{w}u\right)Q_0(u,\bar{u})\,\mathrm{d}^2u. \tag{B.100}$$

We now reconstruct the solution in terms of the Husimi Q-function

$$\begin{aligned} Q(z,\bar{z},t) &= \frac{1}{\pi^2}\iint\exp\left(-z\bar{w}+w\bar{z}+\mathrm{i}\Omega\left(\frac{\bar{w}-w}{2}\right)t\bar{u}-w\bar{u}-\mathrm{i}\Omega\left(\frac{\bar{w}-w}{2}\right)tu+\bar{w}u\right) \\ &\times\exp\left(\frac{\gamma_2 tm\Omega(w-\bar{w})^2}{4}+\frac{\gamma_1\Omega(\bar{w}-w)^2t^3}{12m}+\frac{\mathrm{i}\gamma_1(\bar{w}^2-w^2)t^2}{4m}-\frac{\gamma_1(w+\bar{w})^2t}{4m\Omega}+\frac{\mathrm{i}\Omega(w^2-\bar{w}^2)t}{4}\right) \\ &\times\exp\left(-\frac{\Omega^2t^2(w-\bar{w})^2}{8}\right)Q_0(u,\bar{u})\,\mathrm{d}^2w\,\mathrm{d}^2u. \end{aligned} \tag{B.101}$$

Introducing $\alpha=z-\frac{\mathrm{i}\Omega t\bar{u}}{2}+\frac{\mathrm{i}\Omega tu}{2}-u$, this becomes

$$\begin{aligned} Q(z,\bar{z},t) &= \frac{1}{\pi^2}\iint\exp\left(-\alpha\bar{w}+w\bar{\alpha}\right) \\ &\times\exp\left(\frac{\gamma_2 tm\Omega(w-\bar{w})^2}{4}+\frac{\gamma_1\Omega(\bar{w}-w)^2t^3}{12m}+\frac{\mathrm{i}\gamma_1(\bar{w}^2-w^2)t^2}{4m}-\frac{\gamma_1(w+\bar{w})^2t}{4m\Omega}+\frac{\mathrm{i}\Omega(w^2-\bar{w}^2)t}{4}\right) \\ &\times\exp\left(-\frac{\Omega^2t^2(w-\bar{w})^2}{8}\right)Q_0(u,\bar{u})\,\mathrm{d}^2w\,\mathrm{d}^2u. \end{aligned} \tag{B.102}$$

Making the substitution $w=a+\mathrm{i}b$, we find

$$\begin{aligned} Q(z,\bar{z},t) &= \frac{1}{\pi^2}\iiint\exp\left(-a^2\left(\frac{\gamma_1 t}{m\Omega}\right)+a\left(\frac{m(\bar{\alpha}-\alpha)+bt(\gamma_1 t-\Omega m)}{m}\right)\right) \\ &\times\exp\left(-b^2\left(\frac{6\gamma_2m^2\Omega t+2\gamma_1\Omega t^3-3m\Omega^2t^2}{6m}\right)+\mathrm{i}b(\bar{\alpha}+\alpha)\right)\mathrm{d}a\,\mathrm{d}b\,Q_0(u,\bar{u})\,\mathrm{d}^2u. \end{aligned} \tag{B.103}$$

Integrating with respect to a gives

$$\begin{aligned} Q(z,\bar{z},t) &= \frac{1}{\pi^2}\sqrt{\frac{m\Omega\pi}{\gamma_1 t}}\iint\exp\left(\frac{\left(m(\bar{\alpha}-\alpha)+bt(\gamma_1 t-\Omega m)\right)^2\Omega}{4m\gamma_1 t}\right) \\ &\times\exp\left(-b^2\left(\frac{6\gamma_2m^2\Omega t+2\gamma_1\Omega t^3-3m\Omega^2t^2}{6m}\right)+\mathrm{i}b(\bar{\alpha}+\alpha)\right)\mathrm{d}b\,H_0(u,\bar{u})\,\mathrm{d}^2u. \end{aligned} \tag{B.104}$$

Expanding the terms gives

$$\begin{aligned} Q(z,\bar{z},t) &= \frac{1}{\pi^2}\sqrt{\frac{m\Omega\pi}{\gamma_1 t}}\iint \exp\left(\frac{(\bar{\alpha}-\alpha)^2 m\Omega}{4\gamma_1 t}\right)\exp\left(\frac{b^2 t(\gamma_1 t-\Omega m)^2\Omega}{4m\gamma_1}\right)\exp\left(\frac{b(\gamma_1 t-\Omega m)(\bar{\alpha}-\alpha)}{2\gamma_1}\right) \\ &\quad\times\exp\left(-b^2\left(\frac{6\gamma_2 m^2\Omega t+2\gamma_1\Omega t^3-3m\Omega^2 t^2}{6m}\right)+\mathrm{i}b(\bar{\alpha}+\alpha)\right)\mathrm{d}b\,H_0(u,\bar{u})\,\mathrm{d}^2u. \end{aligned} \tag{B.105}$$

Simplifying yields

$$\begin{aligned} Q(z,\bar{z},t) &= \frac{1}{\pi^2}\sqrt{\frac{m\Omega\pi}{\gamma_1 t}}\int\exp\left(\frac{(\bar{\alpha}-\alpha)^2 m\Omega}{4\gamma_1 t}\right) \\ &\quad\times\int\exp\left(-b^2\left(\frac{12\gamma_1\gamma_2 m^2\Omega t+4\gamma_1^2\Omega t^3-6m\Omega^2 t^2\gamma_1-3\Omega t(\gamma_1 t-\Omega m)^2}{12m\gamma_1}\right)\right) \\ &\quad\times\exp\left(\frac{2\mathrm{i}\gamma_1(\bar{\alpha}+\alpha)+(\gamma_1 t-\Omega m)(\bar{\alpha}-\alpha)}{2\gamma_1}b\right)\mathrm{d}b\,H_0(u,\bar{u})\,\mathrm{d}^2u. \end{aligned} \tag{B.106}$$

Integrating with respect to b then gives

$$\begin{aligned} Q(z,\bar{z},t) &= \frac{1}{\pi^2}\sqrt{\frac{m\Omega\pi}{\gamma_1 t}}\sqrt{\frac{12\pi\gamma_1}{12\gamma_1\gamma_2 m^2\Omega t-3m^2\Omega^3 t+\Omega t^3\gamma_1^2}} \\ &\quad\times\int\exp\left(\frac{(\bar{\alpha}-\alpha)^2 m\Omega}{4\gamma_1 t}\right)\exp\left(\frac{3m\left(2\mathrm{i}\gamma_1(\bar{\alpha}+\alpha)+(\gamma_1 t-\Omega m)(\bar{\alpha}-\alpha)\right)^2}{4\gamma_1\left(12\gamma_1\gamma_2 m^2\Omega t-3m^2\Omega^3 t+\Omega t^3\gamma_1^2\right)}\right)H_0(u,\bar{u})\,\mathrm{d}^2u. \end{aligned}$$

Expanding out gives

$$\begin{aligned} Q(z,\bar{z},t) &= \sqrt{\frac{12m}{\pi^2 t\left(12\gamma_1\gamma_2 m^2 t+t^3\gamma_1^2-3m^2\Omega^2 t\right)}} \\ &\quad\times\int\exp\left(\frac{(\bar{\alpha}-\alpha)^2 m\Omega}{4\gamma_1 t}\right)\exp\left(\frac{3m(\gamma_1 t-\Omega m)^2(\bar{\alpha}-\alpha)^2}{4\gamma_1\left(12\gamma_1\gamma_2 m^2\Omega t-3m^2\Omega^3 t+\Omega t^3\gamma_1^2\right)}\right) \\ &\quad\times\exp\left(\frac{-3m\gamma_1(\bar{\alpha}+\alpha)^2}{\gamma_1\left(12\gamma_1\gamma_2 m^2\Omega t-3m^2\Omega^3 t+\Omega t^3\gamma_1^2\right)}\right) \\ &\quad\times\exp\left(\frac{3\mathrm{i}m(\alpha+\bar{\alpha})(\bar{\alpha}-\alpha)(\gamma_1 t-\Omega m)}{\gamma_1\left(12\gamma_1\gamma_2 m^2\Omega t-3m^2\Omega^3 t+\Omega t^3\gamma_1^2\right)}\right)H_0(u,\bar{u})\,\mathrm{d}^2u. \end{aligned} \tag{B.107}$$

In the case where $m=\gamma_1=\gamma_2=\Omega=1$, we have the simplified form

$$\begin{aligned} Q(z,\bar{z},t) &= \sqrt{\frac{12}{\pi^2\left(t^4+9t^2\right)}}\int\exp\left(\frac{(\bar{\alpha}-\alpha)^2}{4t}\right)\exp\left(\frac{-3(\bar{\alpha}+\alpha)^2}{t^3+9t}\right) \\ &\quad\times\exp\left(\frac{3\mathrm{i}(\bar{\alpha}^2-\alpha^2)(t-1)}{t^3+9t}\right)\exp\left(\frac{3(t-1)^2(\bar{\alpha}-\alpha)^2}{4(t^3+9t)}\right)H_0(u,\bar{u})\,\mathrm{d}^2u, \end{aligned} \tag{B.108}$$

with $\alpha=z-u+\mathrm{i}ut,\quad \bar{\alpha}=\bar{z}-\bar{u}-\mathrm{i}\bar{u}t.$ □

B.4 Lindblad equation for the harmonic oscillator

Just as in the free-particle case, we now analyse the effect of Lindblad decoherence on a damped harmonic oscillator governed by the Hamiltonian

$$\hat{H} = \frac{\hat{p}^2}{2m} + \frac{k\hat{x}^2}{2}. \tag{B.109}$$

We focus on the evolution of the first and second moments

$$\langle \hat{x}(t) \rangle, \quad \langle \hat{p}(t) \rangle, \quad \mathrm{Var}\big(\hat{x}(t)\big), \quad \mathrm{Var}\big(\hat{p}(t)\big), \tag{B.110}$$

under continuous monitoring of position and momentum via Lindblad operators. Our analysis will primarily treat the case of simultaneous monitoring, with the position-only and momentum-only scenarios obtained as limiting cases. This provides a unified framework for understanding how decoherence and measurement backaction shape the oscillator's phase-space dynamics.

First and Second Moments

The combined Lindblad equation describing a harmonic oscillator under simultaneous position and momentum monitoring can be written as

$$\frac{\mathrm{d}\hat{\rho}}{\mathrm{d}t} = -\frac{\mathrm{i}}{\hbar}\left[\frac{\hat{p}^2}{2m} + \frac{k\hat{x}^2}{2}, \hat{\rho}\right] + \gamma_1\left(\hat{x}\hat{\rho}\hat{x} - \frac{1}{2}\left\{\hat{x}^2, \hat{\rho}\right\}\right) + \gamma_2\left(\hat{p}\hat{\rho}\hat{p} - \frac{1}{2}\left\{\hat{p}^2, \hat{\rho}\right\}\right). \tag{B.111}$$

From this master equation, one obtains the differential equations for the relevant expectation values

$$\begin{aligned}
\frac{\mathrm{d}}{\mathrm{d}t}\left(\mathrm{tr}(\hat{\rho}\hat{x})\right) &= \frac{1}{m}\,\mathrm{tr}(\hat{\rho}\hat{p}), \\
\frac{\mathrm{d}}{\mathrm{d}t}\left(\mathrm{tr}(\hat{\rho}\hat{p})\right) &= -k\,\mathrm{tr}(\hat{\rho}\hat{x}), \\
\frac{\mathrm{d}}{\mathrm{d}t}\left(\mathrm{tr}(\hat{\rho}\hat{x}^2)\right) &= \frac{2}{m}\mathrm{tr}(\hat{\rho}\hat{p}\hat{x}) + \frac{\mathrm{i}\hbar}{m} + \gamma_2\hbar^2, \\
\frac{\mathrm{d}}{\mathrm{d}t}\left(\mathrm{tr}(\hat{\rho}\hat{p}^2)\right) &= -2k\,\mathrm{tr}(\hat{\rho}\hat{p}\hat{x}) - \mathrm{i}\hbar + \gamma_1\hbar^2, \\
\frac{\mathrm{d}}{\mathrm{d}t}\left(\mathrm{tr}(\hat{\rho}\hat{p}\hat{x})\right) &= \frac{1}{m}\,\mathrm{tr}(\hat{\rho}\hat{p}^2) - k\,\mathrm{tr}(\hat{\rho}\hat{x}^2).
\end{aligned} \tag{B.112}$$

Given the initial conditions

$$\mathrm{tr}(\hat{\rho}\hat{x})(0) = x_0, \quad \mathrm{tr}(\hat{\rho}\hat{p})(0) = p_0, \quad \mathrm{tr}(\hat{\rho}\hat{p}\hat{x})(0) = k_1, \quad \mathrm{tr}(\hat{\rho}\hat{x}^2)(0) = k_2, \tag{B.113}$$

the solutions are

$$\begin{aligned}
\mathrm{tr}(\hat{\rho}\hat{x}) &= x_0\cos(\omega t) + \frac{p_0}{m\omega}\sin(\omega t), \\
\mathrm{tr}(\hat{\rho}\hat{p}) &= p_0\cos(\omega t) - m\omega x_0\sin(\omega t), \\
\mathrm{tr}(\hat{\rho}\hat{x}^2) &= \frac{k_1}{m\omega}\sin(2\omega t) + k_2\cos(2\omega t) + \hbar^2\gamma_2 t, \\
\mathrm{tr}(\hat{\rho}\hat{p}^2) &= -\frac{kk_1}{\omega}\sin(2\omega t) - mkk_2\cos(2\omega t) + \hbar^2\gamma_1 t, \\
\mathrm{tr}(\hat{\rho}\hat{p}\hat{x}) &= k_1\cos(2\omega t) - m\omega k_2\sin(2\omega t) - \frac{\mathrm{i}\hbar}{2}.
\end{aligned} \tag{B.114}$$

The variances can then be determined explicitly as

$$\begin{aligned}\mathrm{Var}(\hat{x}(t)) &= \mathrm{tr}(\hat{\rho}\hat{x}^2) - (\mathrm{tr}(\hat{\rho}\hat{x}))^2\,, \\ &= \hbar^2\gamma_2 t + k_2\cos(2\omega t) + \frac{k_1 - p_0 x_0}{m\omega}\sin(2\omega t) - x_0^2\cos^2(\omega t) - \frac{p_0^2}{m^2\omega^2}\sin^2(\omega t), \end{aligned} \tag{B.115}$$

and

$$\begin{aligned}\mathrm{Var}(\hat{p}(t)) &= \mathrm{tr}(\hat{\rho}\hat{p}^2) - (\mathrm{tr}(\hat{\rho}\hat{p}))^2\,, \\ &= \hbar^2\gamma_1 t - \frac{kk_1}{\omega}\cos(2\omega t) \\ &\quad - (mkk_2 - m\omega x_0 p_0)\sin(2\omega t) - p_0^2\cos^2(\omega t) - m^2\omega^2 x_0^2\sin^2(\omega t). \end{aligned} \tag{B.116}$$

The solutions show that simultaneous position (γ_1) and momentum (γ_2) monitoring leads to linearly growing variances in both observables, reflecting measurement-induced diffusion superimposed on harmonic oscillations. When only one Lindblad operator is active, the corresponding variance grows directly, while the other evolves indirectly via oscillator coupling. Thus, position-only ($\gamma_1 > 0$) or momentum-only ($\gamma_2 > 0$) decoherence results in asymmetric phase-space diffusion, while both active channels produce symmetric delocalisation and enhanced spreading.

We now proceed to solve the Lindblad equation for the harmonic oscillator (B.111) in both the Wigner and Husimi representations highlighting how the phase-space diffusion affects the oscillator dynamics.

B.4.1 Solving the Lindblad equation in Wigner representation

On phase space, the above Lindblad equation maps to the following form:

$$\begin{aligned}\frac{\mathrm{d}W(x,p,t)}{\mathrm{d}t} &= -\frac{\mathrm{i}}{\hbar}\left(\hat{H} * W(x,p) - W(x,p) * \hat{H}\right) + \gamma_1\left(x * W(x,p) * x - \frac{1}{2}\left(x^2 * W + W * x^2\right)\right) \\ &\quad + \gamma_2\left(p * W(x,p) * p - \frac{1}{2}\left(p^2 * W + W * p^2\right)\right), \end{aligned} \tag{B.117}$$

where $*$ denotes the Moyal star product. Expanding the Moyal brackets to second order in $\hbar$, one obtains

$$\frac{\mathrm{d}W(x,p,t)}{\mathrm{d}t} = -\frac{p}{m}\frac{\partial W}{\partial x} + kq\frac{\partial W}{\partial p} + \frac{\hbar^2}{2}\left(\gamma_1\frac{\partial^2 W}{\partial x^2} + \gamma_2\frac{\partial^2 W}{\partial p^2}\right), \tag{B.118}$$

which is a Fokker-Planck-type equation describing diffusive evolution of the Wigner function under harmonic confinement.

Proposition B.4. *A formal solution to the Wigner equation for the harmonic oscillator with simultaneous*

position and momentum Lindblad operators (B.118) is given by

$$
\begin{aligned}
W(x,p,t) \;=\; & \frac{2m\omega^2}{\pi\hbar^2}\sqrt{\frac{1}{4\omega^2\left(\gamma_1 m^2\omega^2 t+\gamma_2 t\right)^2-\left(\gamma_1 m^2\omega^2-\gamma_2\right)^2}} \\
& \times\iint \exp\left(-\frac{\left(m\omega\big(x-x'\cos(\omega t)\big)-p'\sin(\omega t)\right)^2}{\omega^2\hbar^2\left(m^2\gamma_1 t+\gamma_2 t\right)}\right) \\
& \times\exp\left(-\frac{4\omega^2\left(m^2\gamma_1\omega^2 t+\gamma_2 t\right)\left(p-p'\cos(\omega t)+x' m\omega\sin(\omega t)\right)^2}{\hbar^2\left(4\omega^2\left(\gamma_1 m^2\omega^2 t+\gamma_2 t\right)^2-\left(\gamma_1 m^2\omega^2-\gamma_2\right)^2\right)}\right) \\
& \times\exp\left(-\frac{\left(m\omega\big(x-x'\cos(\omega t)\big)-p'\sin(\omega t)\right)^2\left(\gamma_1 m^2\omega^2-\gamma_2\right)^2}{\left[4\omega^2\left(\gamma_1 m^2\omega^2 t+\gamma_2 t\right)^2-\left(\gamma_1 m^2\omega^2-\gamma_2\right)^2\right]\left(m^2\omega^2\gamma_1 t+\gamma_2 t\right)}\right) \\
& \times\exp\left(-\frac{4\omega\left(m\omega\big(x-x'\cos(\omega t)\big)-p'\sin(\omega t)\right)\left(\gamma_1 m^2\omega^2-\gamma_2\right)\left(p-p'\cos(\omega t)+x' m\omega\sin(\omega t)\right)}{4\omega^2\left(\gamma_1 m^2\omega^2 t+\gamma_2 t\right)^2-\left(\gamma_1 m^2\omega^2-\gamma_2\right)^2}\right) \\
& \times W_0(x',p')\,\mathrm{d}x'\,\mathrm{d}p'. \qquad \text{(B.119)}
\end{aligned}
$$

Proof. Taking the Fourier transform of the Wigner equation gives

$$
\frac{\mathrm{d}\xi(u,v,t)}{\mathrm{d}t}=\frac{u}{m}\frac{\partial\xi}{\partial v}-kv\frac{\partial\xi}{\partial u}-\frac{1}{2}\left(\gamma_1 u^2+\gamma_2 v^2\right)\xi. \qquad \text{(B.120)}
$$

We use the method of characteristics, introducing the system

$$
\frac{\mathrm{d}\xi}{\mathrm{d}s}=-\frac{1}{2}\left(\gamma_1 u^2+\gamma_2 v^2\right)\xi,\quad \frac{\mathrm{d}u}{\mathrm{d}s}=kv,\quad \frac{\mathrm{d}v}{\mathrm{d}s}=-\frac{u}{m},\quad \frac{\mathrm{d}t}{\mathrm{d}s}=1, \qquad \text{(B.121)}
$$

with initial conditions

$$
u(s=0)=u_0,\quad v(s=0)=v_0,\quad \xi(0)=\xi_0(u_0,v_0),\quad s=0. \qquad \text{(B.122)}
$$

From $\frac{\mathrm{d}t}{\mathrm{d}s}=1 \implies s=t$, and a second-order equation for u

$$
\frac{\mathrm{d}^2u}{\mathrm{d}s^2}=-\frac{k}{m}u, \qquad \text{(B.123)}
$$

with solution

$$
\begin{aligned}
u(s) &= u_0\cos(\omega s)+\frac{v_0 k}{\omega}\sin(\omega s), \\
v(s) &= -\frac{\omega u_0}{k}\sin(\omega s)+v_0\cos(\omega s). \qquad \text{(B.124)}
\end{aligned}
$$

Rewriting these gives

$$
\begin{aligned}
u_0 &= u\cos(\omega s)-\frac{kv}{\omega}\sin(\omega s), \\
v_0 &= \frac{u\omega}{k}\sin(\omega s)+v\cos(\omega s). \qquad \text{(B.125)}
\end{aligned}
$$

Next, for

$$
\int u^2\mathrm{d}s=\int\left(u_0^2\cos^2(\omega s)+\frac{v_0^2k^2}{\omega^2}\sin^2(\omega s)+\frac{u_0v_0k}{\omega}\sin(2\omega s)\right)\mathrm{d}s, \qquad \text{(B.126)}
$$

one finds

$$= \frac{s}{2}\left(u_0^2 + \frac{v_0^2 k^2}{\omega^2}\right) + \frac{\sin(2\omega s)}{4\omega}\left(u_0^2 - \frac{v_0^2 k^2}{\omega^2}\right) - \frac{u_0 v_0 k}{2\omega^2}\cos(2\omega s). \tag{B.127}$$

Substituting back gives the simplified result

$$\int u^2 \mathrm{d}s = \frac{s}{2}\left(u^2 + \frac{v^2 k^2}{\omega^2}\right) - \frac{ukv}{2\omega^2}. \tag{B.128}$$

Similarly

$$\int v^2 \mathrm{d}s = \int \left(\frac{u_0^2\omega^2}{k^2}\sin^2(\omega s) + v_0^2\cos^2(\omega s) - \frac{u_0 v_0 k}{\omega}\sin(2\omega s)\right)\mathrm{d}s \tag{B.129}$$

leads to

$$= \frac{s}{2}\left(\frac{u_0^2\omega^2}{k^2} + v_0^2\right) + \frac{\sin(2\omega s)}{4\omega}\left(-\frac{u_0^2\omega^2}{k^2} + v_0^2\right) + \frac{u_0 v_0}{2\omega}\cos(2\omega s), \tag{B.130}$$

and simplifying gives

$$\int v^2 \mathrm{d}s = \frac{s}{2}\left(\frac{u^2\omega^2}{k^2} + v^2\right) + \frac{uv}{2k}. \tag{B.131}$$

Therefore, integrating

$$\frac{\mathrm{d}\xi}{\mathrm{d}s} = -\frac{1}{2}\left(\gamma_1 u^2 + \gamma_2 v^2\right)\xi \tag{B.132}$$

yields

$$\log\xi = -\frac{\gamma_1}{2}\left(\frac{u^2 t}{2} + \frac{v^2 k^2}{2\omega^2}t - \frac{ukv}{2\omega^2}\right) - \frac{\gamma_2}{2}\left(\frac{u^2\omega^2}{2k^2}t + \frac{v^2 t}{2} + \frac{uv}{2k}\right). \tag{B.133}$$

Hence the solution is

$$\begin{aligned}\xi(u,v,t) &= \xi_0\left(u\cos(\omega t) - \frac{kv}{\omega}\sin(\omega t), \frac{u\omega}{k}\sin(\omega t) + v\cos(\omega t)\right)\\ &\quad\times\exp\left(-\frac{\gamma_1}{2}\left(\frac{u^2 t}{2} + \frac{v^2 k^2}{2\omega^2}t - \frac{ukv}{2\omega^2}\right) - \frac{\gamma_2}{2}\left(\frac{u^2\omega^2}{2k^2}t + \frac{v^2 t}{2} + \frac{uv}{2k}\right)\right).\end{aligned} \tag{B.134}$$

We now take the inverse Fourier transform to recover the Wigner function:

$$W(x,p,t) = \frac{1}{2\pi\hbar^2}\iint \exp\left(\frac{\mathrm{i}xu}{\hbar}\right)\exp\left(\frac{\mathrm{i}pv}{\hbar}\right)\xi(u,v,t)\,\mathrm{d}u\,\mathrm{d}v. \tag{B.135}$$

Substituting for $\xi(u,v,t)$, we have

$$\begin{aligned}W(x,p,t) &= \frac{1}{2\pi\hbar^2}\iint \exp\left(\frac{\mathrm{i}xu}{\hbar}\right)\exp\left(\frac{\mathrm{i}pv}{\hbar}\right)\\ &\quad\times\xi_0\left(u\cos(\omega t) - \frac{vk}{\omega}\sin(\omega t), \frac{u\omega}{k}\sin(\omega t) + v\cos(\omega t)\right)\\ &\quad\times\exp\left(-\frac{\gamma_1}{2}\left(\frac{u^2 t}{2} + \frac{v^2 k^2 t}{2\omega^2} - \frac{ukv}{2\omega^2}\right) - \frac{\gamma_2}{2}\left(\frac{u^2\omega^2 t}{2k^2} + \frac{v^2 t}{2} + \frac{uv}{2k}\right)\right)\mathrm{d}u\,\mathrm{d}v.\end{aligned} \tag{B.136}$$

Using

$$\xi_0\left(\dots\right) = \frac{1}{2\pi}\iint \exp\left(-\frac{\mathrm{i}q'}{\hbar}\left(u\cos(\omega t) - \frac{vk}{\omega}\sin(\omega t)\right)\right)$$
$$\times \exp\left(-\frac{\mathrm{i}p'}{\hbar}\left(\frac{u\omega}{k}\sin(\omega t) + v\cos(\omega t)\right)\right) W_0(x',p')\,\mathrm{d}x'\,\mathrm{d}p', \tag{B.137}$$

the Wigner function then becomes

$$\begin{aligned} W(x,p,t) &= \frac{1}{4\pi^2\hbar^2}\iiint \exp\left(-u^2\frac{\gamma_1 m^2\omega^2 t + \gamma_2 t}{4m^2\omega^2}\right) \\ &\times \exp\left(u\frac{4\mathrm{i}\left(m\omega^2\left(x - x'\cos(\omega t)\right) - p'\sin(\omega t)\omega\right) + \hbar\left(\gamma_1 v m^2\omega^2 - \gamma_2 v\right)}{4m\omega^2\hbar}\right) \\ &\times \exp\left(-v^2\frac{\gamma_1 m^2\omega^2 t + \gamma_2 t}{4}\right)\exp\left(v\frac{\mathrm{i}\left(p - p'\cos(\omega t) + x' m\omega\sin(\omega t)\right)}{\hbar}\right) \\ &\times W_0(x',p')\,\mathrm{d}x'\,\mathrm{d}p'\,\mathrm{d}u\,\mathrm{d}v. \end{aligned} \tag{B.138}$$

Evaluating the integral with respect to u gives

$$\begin{aligned} W(x,p,t) &= \frac{1}{4\pi^2\hbar^2}\sqrt{\frac{4m^2\omega^2\pi}{m^2\omega^2\gamma_1 t + \gamma_2 t}}\iiint \\ &\times \exp\left(\frac{\left[4\mathrm{i}\left(m\omega^2(x - x'\cos(\omega t)) - p'\sin(\omega t)\omega\right) + \hbar\left(\gamma_1 v m^2\omega^2 - \gamma_2 v\right)\right]^2}{16\omega^2\hbar^2(m^2\omega^2\gamma_1 t + \gamma_2 t)}\right) \\ &\times \exp\left(-v^2\frac{m^2\omega^2\gamma_1 t + \gamma_2 t}{4}\right)\exp\left(v\frac{\mathrm{i}\left(p - p'\cos(\omega t) + x' m\omega\sin(\omega t)\right)}{\hbar}\right) \\ &\times W_0(x',p')\,\mathrm{d}x'\,\mathrm{d}p'\,\mathrm{d}v. \end{aligned} \tag{B.139}$$

Expanding out the numerator of the exponential we obtain

$$\begin{aligned} W(x,p,t) &= \frac{1}{4\pi^2\hbar^2}\sqrt{\frac{4m^2\omega^2\pi}{m^2\omega^2\gamma_1 t + \gamma_2 t}}\iiint \exp\left(\frac{-\left(m\omega(x - x'\cos(\omega t)) - p'\sin(\omega t)\right)^2}{\omega^2\hbar^2\left(m^2\gamma_1 t + \gamma_2 t\right)}\right) \\ &\times \exp\left(\frac{\left(\gamma_1 v m^2\omega^2 - \gamma_2 v\right)^2}{16\omega^2\left(m^2\omega^2\gamma_1 t + \gamma_2 t\right)}\right)\exp\left(\frac{\mathrm{i}\left(m\omega(x - x'\cos(\omega t)) - p'\sin(\omega t)\right)\left(\gamma_1 v m^2\omega^2 - \gamma_2 v\right)}{2\omega\hbar\left(m^2\omega^2\gamma_1 t + \gamma_2 t\right)}\right) \\ &\times \exp\left(-v^2\frac{4\omega^2\left(m^2\omega^2\gamma_1 t + \gamma_2 t\right)^2 - \left(m^2\omega^2\gamma_1 - \gamma_2\right)^2}{16\omega^2\left(m^2\omega^2\gamma_1 t + \gamma_2 t\right)}\right) \\ &\times \exp\left(v\frac{\mathrm{i}\left(p - p'\cos(\omega t) + x' m\omega\sin(\omega t)\right)}{\hbar}\right) W_0(x',p')\,\mathrm{d}x'\,\mathrm{d}p'\,\mathrm{d}v. \end{aligned} \tag{B.140}$$

Evaluating the integral with respect to v gives

$$\begin{aligned}
W(x,p,t) &= \frac{2m\omega^2}{\pi\hbar^2}\sqrt{\frac{1}{4\omega^2\left(\gamma_1 m^2\omega^2 t+\gamma_2 t\right)^2-\left(\gamma_1 m^2\omega^2-\gamma_2\right)^2}} \\
&\quad\times\iint\exp\left(\frac{-\left(m\omega(x-x'\cos(\omega t))-p'\sin(\omega t)\right)^2}{\omega^2\hbar^2\left(m^2\gamma_1 t+\gamma_2 t\right)}\right) \\
&\quad\times\exp\left(\frac{-4\omega^2\left(m^2\gamma_1\omega^2 t+\gamma_2 t\right)\left(p-p'\cos(\omega t)+x'm\omega\sin(\omega t)\right)^2}{\hbar^2\left(4\omega^2\left(\gamma_1 m^2\omega^2 t+\gamma_2 t\right)^2-\left(\gamma_1 m^2\omega^2-\gamma_2\right)^2\right)}\right) \\
&\quad\times\exp\left(\frac{-\left(m\omega(x-x'\cos(\omega t))-p'\sin(\omega t)\right)^2\left(\gamma_1 m^2\omega^2-\gamma_2\right)^2}{\left(4\omega^2\left(\gamma_1 m^2\omega^2 t+\gamma_2 t\right)^2-\left(\gamma_1 m^2\omega^2-\gamma_2\right)^2\right)\left(m^2\omega^2\gamma_1 t+\gamma_2 t\right)}\right) \\
&\quad\times\exp\left(\frac{-4\omega\left(m\omega(x-x'\cos(\omega t))-p'\sin(\omega t)\right)\left(\gamma_1 m^2\omega^2-\gamma_2\right)\left(p-p'\cos(\omega t)+x'm\omega\sin(\omega t)\right)}{4\omega^2\left(\gamma_1 m^2\omega^2 t+\gamma_2 t\right)^2-\left(\gamma_1 m^2\omega^2-\gamma_2\right)^2}\right) \\
&\quad\times W_0(x',p')\,\mathrm{d}x'\,\mathrm{d}p'. \qquad \text{(B.141)}
\end{aligned}$$

In the special case $\gamma_1=\gamma_2=\hbar=k=\omega=m=1$, the solution reduces to

$$\begin{aligned}
W(x,p,t) &= \frac{1}{2\pi t}\iint\exp\left(-\frac{\left(x-x'\cos(t)-p'\sin(t)\right)^2}{2t}\right) \\
&\quad\times\exp\left(-\frac{\left(p-p'\cos(t)+x'\sin(t)\right)^2}{2t}\right)W_0(x',p')\,\mathrm{d}x'\,\mathrm{d}p'. \qquad \text{(B.142)}
\end{aligned}$$

□

B.4.2 Solving the Lindblad equation in the Husimi representation

We have the Lindblad equation

$$\frac{\mathrm{d}\hat\rho}{\mathrm{d}t}=-\frac{\mathrm{i}}{\hbar}[\hat H,\hat\rho]+\frac{\gamma_1}{\hbar}\left(\hat x\hat\rho\hat x^\dagger-\frac{1}{2}\{\hat x^\dagger\hat x,\hat\rho\}\right)+\frac{\gamma_2}{\hbar}\left(\hat p\hat\rho\hat p^\dagger-\frac{1}{2}\{\hat p^\dagger\hat p,\hat\rho\}\right), \qquad \text{(B.143)}$$

with the Hamiltonian

$$\hat H=\frac{\hat p^2}{2m}+\frac{k\hat x^2}{2}=\hbar\Omega\left(\hat a^\dagger\hat a+\frac{1}{2}\right), \qquad \text{(B.144)}$$

where $\Omega=\sqrt{\frac{k}{m}}$. On the Segal-Bargmann space of holomorphic functions, this becomes Expanding the operators yields

$$\begin{aligned}
\frac{\mathrm{d}R(u,\bar v,t)}{\mathrm{d}t} &= \left(-\frac{\gamma_1(u-\bar v)^2}{4m\Omega}+\frac{\gamma_2 m\Omega(u+\bar v)^2}{4}-\frac{\gamma_1}{2m\Omega}-\frac{\gamma_2 m\Omega}{2}\right)R(u,\bar v) \\
&\quad+\left(\mathrm{i}\Omega u+\frac{\gamma_1(\bar v-u)}{2m\Omega}-\frac{\gamma_2 m\Omega(\bar v+u)}{2}\right)\frac{\partial R}{\partial u} \\
&\quad+\left(-\mathrm{i}\Omega\bar v+\frac{\gamma_1(u-\bar v)}{2m\Omega}-\frac{\gamma_2 m\Omega(\bar v+u)}{2}\right)\frac{\partial R}{\partial\bar v} \\
&\quad+\left(\frac{\gamma_2 m\Omega}{4}-\frac{\gamma_1}{4m\Omega}\right)\left(\frac{\partial^2 R}{\partial u^2}+\frac{\partial^2 R}{\partial\bar v^2}\right)+\left(\frac{\gamma_1}{2m\Omega}+\frac{\gamma_2 m\Omega}{2}\right)\frac{\partial^2 R}{\partial u\partial\bar v}. \qquad \text{(B.145)}
\end{aligned}$$

Similarly, restricting to the diagonal $u = z$, $\bar{v} = \bar{z}$, we get in terms of the Husimi function $Q(z, \bar{z}, t)$, the equation is

$$\frac{\mathrm{d}Q}{\mathrm{d}t} = \mathrm{i}\Omega z\frac{\partial Q}{\partial z} - \mathrm{i}\Omega\bar{z}\frac{\partial Q}{\partial \bar{z}} + \left(\frac{\gamma_2 m\Omega}{4} - \frac{\gamma_1}{4m\Omega}\right)\left(\frac{\partial^2 Q}{\partial z^2} + \frac{\partial^2 Q}{\partial \bar{z}^2}\right) + \left(\frac{\gamma_1}{2m\Omega} + \frac{\gamma_2 m\Omega}{2}\right)\frac{\partial^2 Q}{\partial z \partial \bar{z}}. \quad \text{(B.146)}$$

Proposition B.5. *The solution to (B.146) is given by*

$$\begin{aligned} Q(z,\bar{z},t) &= \frac{4m\Omega^2}{\pi}\sqrt{\frac{1}{4\Omega^2\left(\gamma_2 m^2\Omega^2 t + \gamma_1 t\right)^2 - \left(\gamma_2 m^2\Omega^2 - \gamma_1\right)^2}} \\ &\times \int \exp\left(\frac{m\Omega(\bar{\alpha}-\alpha)^2}{2\left(\gamma_2 m^2\Omega^2 t + \gamma_1 t\right)}\right)\exp\left(\frac{-2(\alpha+\bar{\alpha})^2 m\Omega^3\left(\gamma_2 m^2\Omega^2 t + \gamma_1 t\right)}{4\Omega^2\left(\gamma_2 m^2\Omega^2 t + \gamma_1 t\right)^2 - \left(\gamma_2 m^2\Omega^2 - \gamma_1\right)^2}\right) \\ &\times \exp\left(\frac{(\bar{\alpha}-\alpha)^2\left(\gamma_2 m^2\Omega^2 - \gamma_1\right)^2}{2m\Omega^3\left(\gamma_2 m^2\Omega^2 t + \gamma_1 t\right)\left(4\Omega^2\left(\gamma_2 m^2\Omega^2 t + \gamma_1 t\right)^2 - \left(\gamma_2 m^2\Omega^2 - \gamma_1\right)^2\right)}\right) \\ &\times \exp\left(\frac{-2\mathrm{i}(\bar{\alpha}^2 - \alpha^2)\left(\gamma_2 m^2\Omega^2 - \gamma_1\right)}{4\Omega^2\left(\gamma_2 m^2\Omega^2 t + \gamma_1 t\right)^2 - \left(\gamma_2 m^2\Omega^2 - \gamma_1\right)^2}\right) Q_0(u,\bar{u})\,\mathrm{d}^2 u. \end{aligned} \quad \text{(B.147)}$$

where Q_0 is the initial Husimi function.

Proof. To solve the differential equation, we will make use of the following transform

$$H(w,\bar{w}) = \frac{1}{\pi}\int \exp\left(-w\bar{z} + z\bar{w}\right) Q(z,\bar{z})\,\mathrm{d}^2 z \quad \text{(B.148)}$$

The above PDE now becomes

$$\frac{\mathrm{d}H(w,\bar{w},t)}{\mathrm{d}t} = -\mathrm{i}\Omega\bar{w}\frac{\partial H}{\partial \bar{w}} + \mathrm{i}\Omega w\frac{\partial H}{\partial w} + \left(\frac{\gamma_2(w-\bar{w})^2 m\Omega}{4} - \frac{\gamma_1(w+\bar{w})^2}{4m\Omega}\right)H. \quad \text{(B.149)}$$

We will use the method of characteristics to solve this PDE. We have the following system of ODEs

$$\frac{\mathrm{d}t}{\mathrm{d}s} = 1, \quad \frac{\mathrm{d}w}{\mathrm{d}s} = -\mathrm{i}\Omega w, \quad \frac{\mathrm{d}\bar{w}}{\mathrm{d}s} = \mathrm{i}\Omega\bar{w}, \quad \frac{\mathrm{d}H}{\mathrm{d}s} = \left(\frac{\gamma_2(w-\bar{w})^2 m\Omega}{4} - \frac{\gamma_1(w+\bar{w})^2}{4m\Omega}\right)H. \quad \text{(B.150)}$$

With initial conditions $s = 0$, $w(s=0) = w_0$ and $H(w,\bar{w},s=0) = H_0(w,\bar{w})$, we find

$$t = s, \quad w = w_0\exp(-\mathrm{i}\Omega s), \quad \bar{w} = \bar{w}_0\exp(\mathrm{i}\Omega s). \quad \text{(B.151)}$$

Let us now solve

$$\frac{\mathrm{d}H}{\mathrm{d}s} = \left(\frac{\gamma_2(w-\bar{w})^2 m\Omega}{4} - \frac{\gamma_1(w+\bar{w})^2}{4m\Omega}\right)H \quad \text{(B.152)}$$

Integrating on both sides gives

$$\begin{aligned} \log H &= \int\left(\frac{\gamma_2 m\Omega}{4}(w-\bar{w})^2 - \frac{\gamma_1}{4m\Omega}(w+\bar{w})^2\right)\mathrm{d}s \\ &= \left(\frac{\gamma_2 m\Omega}{4}\left(-2|w|^2 t - \frac{\mathrm{i}(w^2-\bar{w}^2)}{2\Omega}\right) - \frac{\gamma_1}{4m\Omega}\left(2|w|^2 t - \frac{\mathrm{i}(w^2-\bar{w}^2)}{2\Omega}\right)\right). \end{aligned} \quad \text{(B.153)}$$

Hence the solution to the PDE is

$$\begin{aligned} H(w,\bar{w},t) &= H_0\big(w\exp(\mathrm{i}\Omega t),\bar{w}\exp(-\mathrm{i}\Omega t)\big) \\ &\quad\times\exp\left(\frac{\gamma_2 m\Omega}{4}\left(-2|w|^2t+\frac{\mathrm{i}(w^2-\bar{w}^2)}{2\Omega}\right)-\frac{\gamma_1}{4m\Omega}\left(2|w|^2t+\frac{\mathrm{i}(w^2-\bar{w}^2)}{2\Omega}\right)\right). \quad \text{(B.154)} \end{aligned}$$

Taking the inverse transform of $H(w,\bar{w},t)$ gives

$$\begin{aligned} Q(z,\bar{z},t) &= \frac{1}{\pi}\int\exp(-z\bar{w}+w\bar{z})\,H_0\big(w\exp(\mathrm{i}\Omega t),\bar{w}\exp(-\mathrm{i}\Omega t)\big) \\ &\quad\times\exp\left(\frac{\gamma_2 m\Omega}{4}\left(-2|w|^2t+\frac{\mathrm{i}(w^2-\bar{w}^2)}{2\Omega}\right)-\frac{\gamma_1}{4m\Omega}\left(2|w|^2t+\frac{\mathrm{i}(w^2-\bar{w}^2)}{2\Omega}\right)\right)\mathrm{d}^2w. \quad \text{(B.155)} \end{aligned}$$

Next, $H_0\big(w\exp(\mathrm{i}\Omega t),\bar{w}\exp(-\mathrm{i}\Omega t)\big)$ can be expressed as

$$H_0\big(w\exp(\mathrm{i}\Omega t),\bar{w}\exp(-\mathrm{i}\Omega t)\big)=\frac{1}{\pi}\int\exp\big(-w\exp(\mathrm{i}\Omega t)\bar{u}+\bar{w}\exp(-\mathrm{i}\Omega t)u\big)Q_0(u,\bar{u})\mathrm{d}^2u. \quad \text{(B.156)}$$

Putting these together we have

$$\begin{aligned} Q(z,\bar{z},t) &= \frac{1}{\pi^2}\iint\exp\big(-z\bar{w}+w\bar{z}-w\exp(\mathrm{i}\Omega t)\bar{u}+\bar{w}\exp(-\mathrm{i}\Omega t)u\big)Q_0(u,\bar{u}) \\ &\quad\times\exp\left(\frac{\gamma_2 m\Omega}{4}\left(-2|w|^2t+\frac{\mathrm{i}(w^2-\bar{w}^2)}{2\Omega}\right)-\frac{\gamma_1}{4m\Omega}\left(2|w|^2t+\frac{\mathrm{i}(w^2-\bar{w}^2)}{2\Omega}\right)\right) \\ &\quad\times\mathrm{d}^2w\,\mathrm{d}^2u. \quad \text{(B.157)} \end{aligned}$$

Defining $\alpha=z-\exp(-\mathrm{i}\Omega t)\,u$ and making the substitution $w=a+\mathrm{i}b$, we get

$$\begin{aligned} Q(z,\bar{z},t) &= \frac{1}{\pi^2}\iiint\exp\left(a\left(\bar{\alpha}-\alpha-\frac{\gamma_2 mb}{2}+\frac{\gamma_1 b}{2m\Omega^2}\right)-a^2\left(\frac{\gamma_2 m\Omega t}{2}+\frac{\gamma_1 t}{2m\Omega}\right)\right) \\ &\quad\times\exp\left(-b^2\left(\frac{\gamma_2 m^2\Omega^2t+\gamma_1 t}{2m\Omega}\right)+\mathrm{i}b(\bar{\alpha}+\alpha)\right)\mathrm{d}a\,\mathrm{d}b\,Q_0(u,\bar{u})\,\mathrm{d}^2u. \quad \text{(B.158)} \end{aligned}$$

Evaluating the integral for a we get

$$\begin{aligned} Q(z,\bar{z},t) &= \frac{1}{\pi^2}\sqrt{\frac{2m\Omega\pi}{\gamma_2 m^2\Omega^2t+\gamma_1 t}}\int\exp\left(\frac{m\Omega(\bar{\alpha}-\alpha)^2}{2(\gamma_2 m^2\Omega^2t+\gamma_1 t)}\right) \\ &\quad\times\int\exp\left(-b^2\left(\frac{4\Omega^2(\gamma_2 m^2\Omega^2t+\gamma_1 t)^2-(\gamma_2 m^2\Omega^2-\gamma_1)^2}{8m\Omega^3(\gamma_2 m^2\Omega^2t+\gamma_1 t)}\right)\right) \\ &\quad\times\exp\left(b\left(\frac{2\mathrm{i}m\Omega^3(\alpha+\bar{\alpha})(\gamma_2 m^2\Omega^2t+\gamma_1 t)-(\bar{\alpha}-\alpha)(\gamma_2 m^2\Omega^2-\gamma_1)}{2m\Omega^3(\gamma_2 m^2\Omega^2t+\gamma_1 t)}\right)\right)\mathrm{d}b \\ &\quad\times Q_0(u,\bar{u})\,\mathrm{d}^2u. \quad \text{(B.159)} \end{aligned}$$

Let us now evaluate the integral for b, we get

$$\begin{aligned} Q(z,\bar{z},t) &= \frac{1}{\pi^2}\sqrt{\frac{2m\Omega\pi}{\gamma_2 m^2\Omega^2 t+\gamma_1 t}}\sqrt{\frac{8\pi m\Omega^3(\gamma_2 m^2\Omega^2 t+\gamma_1 t)}{4\Omega^2(\gamma_2 m^2\Omega^2 t+\gamma_1 t)^2-(\gamma_2 m^2\Omega^2-\gamma_1)^2}} \\ &\quad\times\int\exp\left(\frac{m\Omega(\bar{\alpha}-\alpha)^2}{2(\gamma_2 m^2\Omega^2 t+\gamma_1 t)}\right) \\ &\quad\times\exp\left(\frac{\left(2\mathrm{i}m\Omega^3(\alpha+\bar{\alpha})(\gamma_2 m^2\Omega^2 t+\gamma_1 t)-(\bar{\alpha}-\alpha)(\gamma_2 m^2\Omega^2-\gamma_1)\right)^2}{2m\Omega^3(\gamma_2 m^2\Omega^2 t+\gamma_1 t)\left(4\Omega^2(\gamma_2 m^2\Omega^2 t+\gamma_1 t)^2-(\gamma_2 m^2\Omega^2-\gamma_1)^2\right)}\right) \\ &\quad\times Q_0(u,\bar{u})\,\mathrm{d}^2u. \end{aligned} \tag{B.160}$$

Rewriting neatly we get

$$\begin{aligned} Q(z,\bar{z},t) &= \frac{4m\Omega^2}{\pi}\sqrt{\frac{1}{4\Omega^2(\gamma_2 m^2\Omega^2 t+\gamma_1 t)^2-(\gamma_2 m^2\Omega^2-\gamma_1)^2}} \\ &\quad\times\int\exp\left(\frac{m\Omega(\bar{\alpha}-\alpha)^2}{2(\gamma_2 m^2\Omega^2 t+\gamma_1 t)}\right)\exp\left(\frac{-2(\alpha+\bar{\alpha})^2 m\Omega^3(\gamma_2 m^2\Omega^2 t+\gamma_1 t)}{4\Omega^2(\gamma_2 m^2\Omega^2 t+\gamma_1 t)^2-(\gamma_2 m^2\Omega^2-\gamma_1)^2}\right) \\ &\quad\times\exp\left(\frac{(\bar{\alpha}-\alpha)^2(\gamma_2 m^2\Omega^2-\gamma_1)^2}{2m\Omega^3(\gamma_2 m^2\Omega^2 t+\gamma_1 t)\left(4\Omega^2(\gamma_2 m^2\Omega^2 t+\gamma_1 t)^2-(\gamma_2 m^2\Omega^2-\gamma_1)^2\right)}\right) \\ &\quad\times\exp\left(\frac{-2\mathrm{i}(\bar{\alpha}^2-\alpha^2)(\gamma_2 m^2\Omega^2-\gamma_1)}{4\Omega^2(\gamma_2 m^2\Omega^2 t+\gamma_1 t)^2-(\gamma_2 m^2\Omega^2-\gamma_1)^2}\right)Q_0(u,\bar{u})\,\mathrm{d}^2u. \end{aligned} \tag{B.161}$$

As a simple case, when $\gamma_1=\gamma_2=\hbar=\Omega=k=m=1$, the solution reduces to

$$Q(z,\bar{z},t)=\frac{1}{\pi t}\int\exp\left(\frac{u\bar{z}\exp(-\mathrm{i}t)+z\bar{u}\exp(\mathrm{i}t)-|z|^2-|u|^2}{t}\right)Q_0(u,\bar{u})\,\mathrm{d}^2u, \tag{B.162}$$

where we substituted for α explicitly. □

Appendix C

Spherical harmonics, Husimi representation and other derivations

In this appendix we collect supporting material for the $\mathrm{SU}(2)$ analysis of Chapter 3. We review the properties of spherical harmonics and their role in harmonic analysis on the sphere, and provide detailed proofs of the propositions, lemmas, and theorems stated in the main text. Explicit derivations are given for the action of phase-space measurements and Lindblad dynamics on the density matrix in the $\{|s,m\rangle\}$ basis.

C.1 Harmonic analysis on S^2

We begin by considering the space of square-integrable functions on the sphere, $\mathcal{L}^2(S^2)$, which plays an important role in expressing quantum phase-space distributions for spin systems [102–104]. This Hilbert space is equipped with the inner product

$$\langle f, g\rangle_l = \int_{S^2} \overline{f(\theta,\phi)}\, g(\theta,\phi)\, \mathrm{d}\mu_\zeta^l \tag{C.1}$$

for each fixed l, where $\mathrm{d}\mu_\zeta^l$ is defined in (3.15) in terms of the spherical coordinates. A canonical orthonormal basis of functions on $\mathcal{L}^2(S^2)$ is provided by the spherical harmonics $Y_l^m(\theta,\phi)$ [73, 102, 103], defined by

$$Y_l^m(\theta,\phi) = (-1)^m \sqrt{\frac{(l-m)!}{(l+m)!}}\, P_l^m(\cos\theta)\, \mathrm{e}^{\mathrm{i}m\phi} \tag{C.2}$$

for $m \geq 0$, while for $m < 0$, Y_l^m is defined as the complex conjugate of Y_l^{-m}. Here P_l^m are the associated Legendre polynomials [35]. These functions satisfy the orthonormality condition

$$\int_{S^2} Y_l^m(\theta,\phi)\overline{Y_{l'}^{m'}(\theta,\phi)}\, \mathrm{d}\mu_\zeta^l = \delta_{ll'}\, \delta_{mm'}. \tag{C.3}$$

Any square-integrable function f with respect to the inner product (C.1) can be expanded in this

basis [35, 103] according to

$$f(\theta,\phi) = \sum_{m=-l}^{l} F_{l,m} Y_l^m(\theta,\phi), \tag{C.4}$$

with the expansion coefficients given by

$$F_{l,m} = \int f(\theta,\phi)\,\overline{Y_l^m(\theta,\phi)}\,\mathrm{d}\mu_\zeta^l\,. \tag{C.5}$$

The spherical harmonics satisfy the following form of the completeness condition [35, 103, 210]

$$\begin{aligned}\sum_{m=-l}^{l} Y_l^m(\theta,\phi)\overline{Y_l^m(\theta',\phi')} &= \sum_{m=-l}^{l} \frac{(l-m)!}{(l+m)!}\,P_l^m(\cos\theta)\,P_l^m(\cos\theta')\mathrm{e}^{\mathrm{i}m(\phi-\phi')}, \\ &= P_l\left(\cos\eta\right), \end{aligned} \tag{C.6}$$

where the final expression uses the spherical harmonics addition theorem [103], and $\cos\eta$ is given by

$$\cos\eta = \cos\theta\cos\theta' + \sin\theta\sin\theta'\cos(\phi-\phi')\,. \tag{C.7}$$

Lemma C.1. The function $P_l(\cos\eta)$, referred to as the l^{th} zonal harmonic, satisfies the following integral identity

$$\int P_l(\cos\eta)\,P_j(\cos\eta')\,\mathrm{d}\mu_{\zeta'}^l = \delta_{lj}\,P_j(\cos\eta''), \tag{C.8}$$

where $\cos\eta = \cos\theta\cos\theta' + \sin\theta\sin\theta'\cos(\phi-\phi')$, $\cos\eta' = \cos\theta\cos\theta'' + \sin\theta\sin\theta''\cos(\phi-\phi'')$, $\cos\eta'' = \cos\theta'\cos\theta'' + \sin\theta'\sin\theta''\cos(\phi'-\phi'')$.

Proof. Using the addition theorem and the orthonormality of spherical harmonics, we find

$$\begin{aligned}\int P_l(\cos\eta)\,P_j(\cos\eta')\,\mathrm{d}\mu_{\zeta'}^l &= \int \sum_{m=-l}^{l} Y_l^m(\theta,\phi)\overline{Y_l^m(\theta',\phi')} \sum_{k=-j}^{j} Y_j^k(\theta',\phi')\overline{Y_j^k(\theta'',\phi'')}\mathrm{d}\mu_{\zeta'}^l, \\ &= \sum_{m,k} Y_l^m(\theta,\phi)\overline{Y_j^k(\theta'',\phi'')}\int \overline{Y_l^m(\theta',\phi')}Y_j^k(\theta',\phi')\mathrm{d}\mu_{\zeta'}^l \\ &= \delta_{lj}\sum_m Y_l^m(\theta,\phi)\overline{Y_l^m(\theta'',\phi'')}, \\ &= \delta_{lj}\,P_j(\cos\eta''). \end{aligned} \tag{C.9}$$

□

The zonal harmonic $P_l(\cos\eta)$ serves as the reproducing kernel on $\mathcal{H}_l$, satisfying:

$$\int P_l(\cos\eta)\,P_l(\cos\eta')\,\mathrm{d}\mu_{\zeta'}^l = P_l(\cos\eta''). \tag{C.10}$$

More generally, we have:

Lemma C.2. For any square-integrable function f with respect to the inner product (C.1) we have

$$f(\theta,\phi) = \int P_l(\cos\eta)\, f(\theta',\phi')\, \mathrm{d}\mu^l_{\zeta'}\,. \tag{C.11}$$

Proof. Using the expansion (C.4) of f and definition (C.6) we find

$$\begin{aligned}
\int P_l(\cos\eta)\, f(\theta',\phi')\, \mathrm{d}\nu^l_{\zeta'} &= \int \sum_{k=-l}^{l} Y_l^k(\theta,\phi)\overline{Y_l^k(\theta',\phi')} \sum_{m=-l}^{l} C_{l,m} Y_l^m(\theta',\phi')\, \mathrm{d}\mu^l_{\zeta'},\\
&= \sum_{m,k=-l}^{l} C_{l,m} Y_l^k(\theta,\phi) \int \overline{Y_l^m(\theta',\phi')} Y_l^k(\theta',\phi')\, \mathrm{d}\mu^l_{\zeta'},\\
&= \sum_{m=-l}^{l} C_{l,m} Y_l^m(\theta,\phi),\\
&= f(\theta,\phi),
\end{aligned} \tag{C.12}$$

where we have made use of the orthogonality (C.3). □

Finally, any function $G(\cos\theta)$ that depends only on the polar angle can be expanded in terms of Legendre polynomials [35, 103]

$$G(\cos\theta) = \sum_{l=0}^{\infty} \lambda_l P_l(\cos\theta), \tag{C.13}$$

with the coefficients given by

$$\lambda_l = \frac{2l+1}{2} \int G(\cos\theta)\, P_l(\cos\theta)\, \sin\theta\, \mathrm{d}\theta. \tag{C.14}$$

C.2 Proofs of technical results

C.2.1 Proof of lemma 3.2

Proof. We verify the identity term by term. For the Hamiltonian contribution,

$$\begin{aligned}
\mathrm{Tr}\big(-\mathrm{i}[\hat{H},\hat{\rho}]\,\hat{A}\big) &= -\mathrm{i}\,\mathrm{Tr}(\hat{H}\hat{\rho}\hat{A} - \hat{\rho}\hat{H}\hat{A}),\\
&= -\mathrm{i}\,\mathrm{Tr}(\hat{\rho}\hat{A}\hat{H} - \hat{\rho}\hat{H}\hat{A}), \quad \text{(cyclicity of the trace)}\\
&= \mathrm{Tr}\big(\hat{\rho}\,\mathrm{i}[\hat{H},\hat{A}]\big).
\end{aligned} \tag{C.15}$$

For the jump term,

$$\mathrm{Tr}(\hat{L}_k\hat{\rho}\hat{L}_k^\dagger\hat{A}) = \mathrm{Tr}(\hat{\rho}\,\hat{L}_k^\dagger\hat{A}\hat{L}_k). \tag{C.16}$$

For the anticommutator term,

$$\begin{aligned}
\mathrm{Tr}\left(-\tfrac{1}{2}\{\hat{L}_k^\dagger\hat{L}_k,\hat{\rho}\}\,\hat{A}\right) &= -\tfrac{1}{2}\mathrm{Tr}\big((\hat{L}_k^\dagger\hat{L}_k)\hat{\rho}\hat{A} + \hat{\rho}(\hat{L}_k^\dagger\hat{L}_k)\hat{A}\big),\\
&= -\tfrac{1}{2}\mathrm{Tr}\big(\hat{\rho}\hat{A}(\hat{L}_k^\dagger\hat{L}_k) + \hat{\rho}(\hat{L}_k^\dagger\hat{L}_k)\hat{A}\big),\\
&= \mathrm{Tr}\left(\hat{\rho}\,\big(-\tfrac{1}{2}\{\hat{L}_k^\dagger\hat{L}_k,\hat{A}\}\big)\right).
\end{aligned} \tag{C.17}$$

Summing all contributions yields

$$\mathrm{Tr}\big(\mathcal{L}(\hat{\rho})\,\hat{A}\big) = \mathrm{Tr}\big(\hat{\rho}\,\mathcal{L}^{\dagger}(\hat{A})\big). \tag{C.18}$$

□

If the Lindblad operators are Hermitian, $\hat{L}_k^{\dagger} = \hat{L}_k$, then the superoperator is self-adjoint, $\mathcal{L}^{\dagger} = \mathcal{L}$, and the duality relation reduces to the symmetry

$$\mathrm{Tr}\big(\mathcal{L}(\hat{\rho})\,\hat{A}\big) = \mathrm{Tr}\big(\hat{\rho}\,\mathcal{L}(\hat{A})\big). \tag{C.19}$$

C.2.2 Proof of proposition 3.3

Proof. Taking the time derivative of (3.38) gives

$$\partial_t F^{(\sigma)}(\theta,\phi,t) = \mathrm{tr}\left(\dot{\hat{\rho}}\,\hat{w}^{(\sigma)}(\theta,\phi)\right) = \mathrm{tr}\left(\mathcal{L}(\hat{\rho})\,\hat{w}^{(\sigma)}(\theta,\phi)\right). \tag{C.20}$$

Using the result from Lemma we find that this is the same as writing

$$\partial_t F^{(\sigma)}(\theta,\phi,t) = \mathrm{tr}\left(\hat{\rho}\mathcal{L}(\hat{w}^{(\sigma)})(\theta,\phi)\right). \tag{C.21}$$

As the irreducible tensor operators are the eigenoperators of the Lindblad superoperator we find that from linearity

$$\mathcal{L}[\hat{w}^{(\sigma)}(\theta,\phi)] = \sum_{\ell,m}\sqrt{2\ell+1}\left(\frac{\binom{2s}{\ell}}{\binom{2s+\ell+1}{\ell}}\right)^{-\sigma/2}\overline{Y_\ell^m(\theta,\phi)}\Big(-\tfrac{\gamma}{2}\ell(\ell+1)\Big)\hat{T}^s_{\ell,m}. \tag{C.22}$$

Taking the trace of the above expression against $\hat{\rho}(t)$ we obtain

$$\partial_t F^{(\sigma)}(\theta,\phi,t) = \sum_{\ell,m}\sqrt{2\ell+1}\left(\frac{\binom{2s}{\ell}}{\binom{2s+\ell+1}{\ell}}\right)^{-\sigma/2}\Big(-\tfrac{\gamma}{2}\ell(\ell+1)\overline{\rho_{\ell,m}(t)}\Big)\overline{Y_\ell^m(\theta,\phi)}, \tag{C.23}$$

where $\rho_{\ell,m}(t) = \mathrm{Tr}(\hat{\rho}(\hat{T}^s_{\ell,m})^{\dagger})$.

Using the Hermiticity property of $\rho_{\ell,m}$ and the fact that $\overline{Y_l^m(\theta,\phi)} = (-1)^m Y_l^{-m}(\theta,\phi)$, the above expression can be expressed as

$$\partial_t F^{(\sigma)}(\theta,\phi,t) = \sum_{\ell,m}\sqrt{2\ell+1}\left(\frac{\binom{2s}{\ell}}{\binom{2s+\ell+1}{\ell}}\right)^{-\sigma/2}\Big(-\tfrac{\gamma}{2}\ell(\ell+1)\rho_{\ell,m}(t)\Big)Y_\ell^m(\theta,\phi), \tag{C.24}$$

Now observing that $\Delta_{\mathbb{S}^2}Y_\ell^m = -\ell(\ell+1)Y_\ell^m$ we obtain

$$\partial_t F^{(\sigma)}(\theta,\phi,t) = \tfrac{\gamma}{2}\,\Delta_{\mathbb{S}^2}\left(\sum_{\ell,m}\sqrt{2\ell+1}\left(\frac{\binom{2s}{\ell}}{\binom{2s+\ell+1}{\ell}}\right)^{-\sigma/2}\rho_{\ell,m}(t)\,Y_\ell^m(\theta,\phi)\right). \tag{C.25}$$

So the family of distributions $F^{(\sigma)}$ solve the heat equation on the phase-space. The solution to this

equation boils down to the evolution of the density matrix elements

$$\rho_{\ell,m}(t) = \mathrm{e}^{\left(-\frac{\gamma}{2}\ell(\ell+1)\right)}\rho_{\ell,m}(0), \tag{C.26}$$

and hence the solution to the heat equation is thus given by

$$F^{(\sigma)}(\theta,\phi,t) = \sum_{\ell,m} \mathrm{e}^{\left(-\frac{\gamma}{2}\ell(\ell+1)\right)} \sqrt{2\ell+1} \left(\frac{\binom{2s}{\ell}}{\binom{2s+\ell+1}{\ell}}\right)^{-\sigma/2} \rho_{\ell,m}(0)\, Y_\ell^m(\theta,\phi). \tag{C.27}$$

Now from the above expression it can be seen that

$$\sqrt{\frac{2\ell+1}{2s+1}} \left(\frac{\binom{2s}{\ell}}{\binom{2s+\ell+1}{\ell}}\right)^{-\sigma/2} \rho_{l,m}(0) = \int \overline{Y_l^m(\theta,\phi)}\, F^{(\sigma)}(\theta,\phi,0)\, \mathrm{d}\mu^l_{\theta,\phi}, \tag{C.28}$$

using the orthogonality of spherical harmonics. Substituting this in the solution we obtain

$$F^{(\sigma)}(\theta,\phi,t) = \sum_{\ell,m} \mathrm{e}^{\left(-\frac{\gamma}{2}\ell(\ell+1)\right)} \left[\int \overline{Y_l^m(\theta',\phi')}\, F^{(\sigma)}(\theta',\phi',0)\, \mathrm{d}\mu^l_{\theta',\phi'}\right] Y_l^m(\theta,\phi). \tag{C.29}$$

Summing over m using the addition theorem for spherical harmonics, gives the expression

$$F^{(\sigma)}(\theta,\phi,t) = \sum_{\ell=0}^{2s} \mathrm{e}^{\left(-\frac{\gamma}{2}\ell(\ell+1)\right)} \int P_\ell(\cos\eta)\, F^{(\sigma)}(\theta',\phi',0)\, \mathrm{d}\mu^\ell_{\theta',\phi'}, \tag{C.30}$$

where $\cos\eta = \cos\theta\cos\theta' + \sin\theta\sin\theta'\cos(\phi-\phi')$. □

C.2.3 Proof of proposition 3.4

Proof. The Lindbladian expression is rotationally invariant, since it sums over all m for fixed ℓ. By Schur's lemma, the action of any rotationally invariant superoperator on the irreducible subspace $\{\hat{T}^s_{\ell',m}\}_{m=-\ell'}^{\ell'}$ must be proportional to the identity. Therefore,

$$\mathcal{L}[\hat{T}^s_{\ell',m'}] = -\Gamma_{\ell'}\, \hat{T}^s_{\ell',m'}. \tag{C.31}$$

The scalar $\Gamma_{\ell'} \geq 0$ is obtained by computing, for example, the Hilbert–Schmidt inner product with $T^{(s)\dagger}_{\ell',m'}$:

$$\Gamma_{\ell'} = -\frac{\mathrm{tr}\left(T^{s\dagger}_{\ell',m'}\mathcal{L}[\hat{T}^s_{\ell',m'}]\right)}{\mathrm{tr}\left(T^{s\dagger}_{\ell',m'}\hat{T}^s_{\ell',m'}\right)}. \tag{C.32}$$

We first expand the state in the irreducible tensor operator basis:

$$\hat{\rho}(t) = \sum_{\ell=0}^{2s}\sum_{m=-\ell}^{\ell} \rho_{\ell,m}(t)\, \hat{T}^s_{\ell,m}. \tag{C.33}$$

We compute $\mathcal{L}[\hat{T}^s_{\ell',q}]$ term by term. By rotational invariance, the action of $\sum_m \hat{T}^s_{\ell,m}(\cdot)T^{s\,\dagger}_{\ell,m}$ on an oper-

ator must preserve the rank-ℓ subspace and be proportional to $\hat{T}^s_{\ell,q}$. Explicitly, the recoupling identity (see Varshalovich [105]) gives

$$\sum_{m=-\ell}^{\ell} \hat{T}^s_{\ell,m} \hat{T}^s_{\ell',q} \hat{T}^{s\,\dagger}_{\ell,m} = (2\ell+1)(-1)^{2s+\ell'} \begin{Bmatrix} s & s & \ell \\ s & s & \ell' \end{Bmatrix} \hat{T}^s_{\ell',q}. \tag{C.34}$$

Meanwhile, the anticommutator term yields

$$\frac{1}{2} \sum_m \{\hat{T}^{s\,\dagger}_{\ell,m} \hat{T}^s_{\ell,m}, \hat{T}^s_{\ell',q}\} = \frac{2\ell+1}{2s+1} \hat{T}^s_{\ell',q}, \tag{C.35}$$

since $\sum_m \hat{T}^{s\,\dagger}_{\ell,m} \hat{T}^s_{\ell,m} = \frac{2\ell+1}{2s+1} \mathbb{1}$. Combining these contributions, each ℓ sector contributes a coefficient

$$\Gamma_{\ell'} = \sum_{\ell=0}^{2s} -\gamma_\ell \left[\frac{2\ell+1}{2s+1} - (2\ell+1)(-1)^{2s+\ell'} \begin{Bmatrix} s & s & \ell \\ s & s & \ell' \end{Bmatrix} \right], \tag{C.36}$$

multiplying $\hat{T}^s_{\ell',q}$. Summing over ℓ yields the claimed formula for $\Gamma_{\ell'}$.

By construction, the $\hat{T}^s_{\ell,m}$ are eigenoperators of the superoperator defined by the Lindblad generator. That is,

$$\mathcal{L}[\hat{T}^s_{\ell,m}] = -\Gamma_\ell \, \hat{T}^s_{\ell,m}, \tag{C.37}$$

where the scalar eigenvalue Γ_ℓ depends only on the tensor rank ℓ, not on m. This follows from rotational invariance and the orthogonality of the $\hat{T}^s_{\ell,m}$ [105].

Substituting into the master equation, the coefficients obey

$$\frac{\mathrm{d}}{\mathrm{d}t} \rho_{\ell,m}(t) = -\Gamma_\ell \, \rho_{\ell,m}(t). \tag{C.38}$$

The solution is

$$\rho_{\ell,m}(t) = \mathrm{e}^{-\Gamma_\ell t} \, \rho_{\ell,m}(0). \tag{C.39}$$

Hence, the density operator evolves as

$$\hat{\rho}(t) = \sum_{\ell=0}^{2s} \sum_{m=-\ell}^{\ell} \mathrm{e}^{-\Gamma_\ell t} \, \rho_{\ell,m}(0) \, \hat{T}^s_{\ell,m}, \tag{C.40}$$

which proves the claim. □

C.3 Coherent state POVM in $|s, m\rangle$ basis

Proposition C.1. *The matrix elements $\rho^{(1)}_{m_1,m_2} = \langle s, m_1 | \hat{\rho}^{(1)} | s, m_2 \rangle$ of the state of the system after a single POVM measurement are given by*

$$\rho^{(1)}_{m_1,m_2} = \sum_{\lambda=\lambda_{\min}}^{\lambda_{\max}} \rho_{m_1+\lambda,m_2+\lambda} \, (-1)^\lambda \sum_{S=S_{\min}}^{S_{\max}} C^{S,m_2-m_1}_{s,-m_1-\lambda;s,m_2+\lambda} C^{S,m_2-m_1}_{s,-m_1;s,m_2} \left[\frac{\binom{2s}{S}}{\binom{2s+S+1}{S}} \right], \tag{C.41}$$

where $\lambda_{\min} = -s + \max(-m_1, -m_2)$, $\lambda_{\max} = s + \min(-m_1, -m_2)$, $S_{\min} = \max(0, |m_1 - m_2|)$, $S_{\max} = 2s$, *and*

$$C^{SM}_{s_1,m_1;s_2,m_2} = (\langle s_1, m_1| \otimes \langle s_2, m_2|)|S, M\rangle, \tag{C.42}$$

denotes the Clebsch-Gordan coefficients.

We remark that the state $|S, M\rangle$ appearing on the right side of (C.42) is defined as usual by the simultaneous eigenstates of Casimir operator $\hat{S}^2$ of the combined spin $\hat{S} = \hat{S}_1 \otimes \mathbb{1} + \mathbb{1} \otimes \hat{S}_2$ and $\hat{S}_z = \hat{S}_{1,z} \otimes \mathbb{1} + \mathbb{1} \otimes \hat{S}_{2,z}$, satisfying $\hat{S}^2 |S, M\rangle = S(S+1) |S, M\rangle$. By definition, therefore, we have

$$|S, M\rangle = \sum_{m_1,m_2} C^{SM}_{s_1,m_1;s_2,m_2} |s_1, m_1\rangle \otimes |s_2, m_2\rangle . \tag{C.43}$$

These coefficients satisfy orthogonality relations, ensuring different total spin states remain independent:

$$\sum_{m_1,m_2} C^{SM}_{s_1,m_1;s_2,m_2} C^{S'M}_{s_1,m_1;s_2,m_2} = \delta_{S,S'}, \tag{C.44}$$

where δ denotes the Kronecker delta. To establish the claim, we first express (3.16) in the $|s, m\rangle$ basis. Then performing the integration, we apply properties of the Clebsch-Gordan coefficients to derive the result in (C.41).

Proof. Let $\{\rho_{m_1,m_2}\}$ denote the elements of the initial density matrix in the $|s, m\rangle$ basis

$$\hat{\rho} = \sum_{m_1=-s}^{s} \sum_{m_2=-s}^{s} \rho_{m_1,m_2} |s, m_1\rangle \langle s, m_2| . \tag{C.45}$$

Using the completeness condition (3.6), the Husimi density function of the initial density matrix can be expanded in the form

$$Q(\theta, \phi) = \langle \zeta | \hat{\rho} | \zeta \rangle = \sum_{k=-s}^{s} \sum_{l=-s}^{s} \langle \zeta | s, k \rangle \langle s, k | \hat{\rho} | s, l \rangle \langle s, l | \zeta \rangle . \tag{C.46}$$

From (3.9) we have $\langle s, m|\zeta\rangle = D^s_{m,-s}(\phi, \theta, -\phi)$, so the expression reduces to

$$Q(\theta, \phi) = \sum_{k=-s}^{s} \sum_{l=-s}^{s} \rho_{k,l} \overline{(D^s_{k,-s}(\phi, \theta, -\phi))} (D^s_{l,-s}(\phi, \theta, -\phi)), \tag{C.47}$$

By substituting (C.47) in (3.16) and expressing $\hat{\rho}^{(1)}$ in the $|s, m\rangle$ basis, we obtain the matrix elements of $\hat{\rho}^{(1)}$ in terms of those of $\hat{\rho}$ as follows:

$$\begin{aligned} \rho^1_{m_1,m_2} \quad = \quad & \sum_{k=-s}^{s} \sum_{l=-s}^{s} \rho_{k,l} \\ & \times \int \overline{D^s_{k,-s}(\phi, \theta, -\phi)} (D^s_{l,-s}(\phi, \theta, -\phi)) (D^s_{m_1,-s}(\phi, \theta, -\phi)) \overline{D^s_{m_2,-s}(\phi, \theta, -\phi)} \, \mathrm{d}\mu^s_\zeta. \end{aligned} \tag{C.48}$$

We proceed to calculate the integral in the above equation, which we shall denote by I for convenience. By noting that the complex conjugate of the Wigner D-matrix is satisfies the relation [60,102,103,105]

$$D^s_{m_1,m_2}(\alpha,\beta,\gamma) = (-1)^{m_1-m_2}\overline{D^s_{-m_1,-m_2}(\alpha,\beta,\gamma)}\,, \tag{C.49}$$

we can express the integral I in the form

$$I = (-1)^{(2s+m_2+k)}\int D^s_{-k,s}(\phi,\theta,-\phi)D^s_{l,-s}(\phi,\theta,-\phi)D^s_{m_1,-s}(\phi,\theta,-\phi)D^s_{-m_2,s}(\phi,\theta,-\phi)\,\mathrm{d}\mu^s_\zeta\,. \tag{C.50}$$

The integrand is a product of four Wigner D-matrix elements. To simplify this, we shall reduce this to a product of two, which will allow us to apply the orthogonality relation of the Wigner D-matrices. Specifically, the product of two D-matrices can be expanded in terms of the Clebsch-Gordan coefficients [60,102,103,105]

$$D^{s_1}_{m_1k_1}(\alpha,\beta,\gamma)D^{s_2}_{m_2k_2}(\alpha,\beta,\gamma) = \sum_{S=|s_1-s_2|}^{s_1+s_2} C^{S,m_1+m_2}_{s_1,m_1;s_2,m_2}C^{S,k_1+k_2}_{s_1,k_1;s_2,k_2}D^S_{m_1+m_2,k_1+k_2}(\alpha,\beta,\gamma)\,. \tag{C.51}$$

Substituting (C.51) in the expression for I, we obtain

$$\begin{aligned} I &= (-1)^{(2s+m_2+k)}\sum_{S_1=0}^{2s}\sum_{S_2=0}^{2s} C^{S_1,l-k}_{s,-k;s,l}C^{S_2,m_1-m_2}_{s,m_1;s,-m_2}C^{S_1,0}_{s,s;s,-s}C^{S_2,0}_{s,-s;s,s} \\ &\quad\times(-1)^{(l-k)}\int \overline{D^{S_1}_{k-l,0}(\phi,\theta,-\phi)}\,D^{S_2}_{m_1-m_2,0}(\phi,\theta,-\phi)\,\mathrm{d}\mu^s_\zeta. \end{aligned} \tag{C.52}$$

To work out the integral I, we make use of the following orthogonality property of the Wigner D-matrices [60,102,103,105]

$$\int \overline{D^{s_1}_{m_1,k_1}(\phi,\theta,-\phi)}\,D^{s_2}_{m_2,k_2}(\phi,\theta,-\phi)\,\mathrm{d}\mu^s_\zeta = \frac{2s+1}{2s_1+1}\,\delta_{m_1,m_2}\delta_{k_1,k_2}\delta_{s_1,s_2} \tag{C.53}$$

to deduce that

$$I = (-1)^{(2s+m_2+l)}\sum_{S_1=0}^{2s}\sum_{S_2=0}^{2s} C^{S_1,l-k}_{s,-k;s,l}C^{S_2,m_1-m_2}_{s,m_1;s,-m_2}C^{S_1,0}_{s,s;s,-s}C^{S_2,0}_{s,-s;s,s}\delta_{S_1,S_2}\delta_{k-l,m_1-m_2}\,\frac{2s+1}{2S_1+1}. \tag{C.54}$$

Summing over S_2, and writing $S_1 = S$ for the remaining summation variable, we thus obtain

$$I = (-1)^{(2s+m_2+l)}\sum_{S=0}^{2s} C^{S,l-k}_{s,-k;s,l}C^{S,m_1-m_2}_{s,m_1;s,-m_2}C^{S,0}_{s,s;s,-s}C^{S,0}_{s,-s;s,s}\,\delta_{k-l,m_1-m_2}\,\frac{2s+1}{2S_1+1}. \tag{C.55}$$

Substituting (C.55) in (C.48) and replacing l with $k+m_2-m_1$, and noting that $(-1)^{2(s+m_2)}=1$, we find the following expression for the matrix elements of $\hat{\rho}^{(1)}$

$$\begin{aligned} \rho^{(1)}_{m_1,m_2} &= \sum_{k=k_{\min}}^{k_{\max}}\rho_{k,k+m_2-m_1} \\ &\quad\times\sum_{S=S_{\min}}^{S_{\max}}(-1)^{k-m_1}C^{S,m_2-m_1}_{s,-k;s,(k+m_2-m_1)}C^{S,m_1-m_2}_{s,m_1;s,-m_2}C^{S,0}_{s,-s;s,s}C^{S,0}_{s,s;s,-s}\,\frac{2s+1}{2S+1}\,, \end{aligned} \tag{C.56}$$

where $k_{\min} = -s + \max(0, m_1 - m_2)$, $k_{\max} = s + \min(0, m_1 - m_2)$, $S_{\min} = \max(0, |m_1 - m_2|)$, and $S_{\max} = 2s$. The above expression can be simplified further by utilising properties of the Clebsch-Gordan coefficients. Specifically, we make use of the following symmetry property

$$C^{S,M}_{s,m_1;s,m_2} = (-1)^{2s-S} C^{S,-M}_{s,-m_1;s,-m_2}. \tag{C.57}$$

Then we have $C^{S,0}_{s,-s;s,s} = (-1)^{2s-S} C^{S,0}_{s,s;s,-s}$ and $C^{S,m_1-m_2}_{s,m_1;s,-m_2} = (-1)^{2s-S} C^{S,m_2-m_1}_{s,-m_1;s,m_2}$. For the special case of $C^{S,0}_{s,-s;s,s}$ it can easily be shown that

$$C^{S,0}_{s,-s;s,s} = \langle s, -s; s, s | S, 0 \rangle = (-1)^{2s-S} \sqrt{2S+1} \sqrt{\frac{((2s)!)^2}{(2s-S)!(1+2s+S)!}}. \tag{C.58}$$

Substituting these in (C.56), we get

$$\rho^{(1)}_{m_1,m_2} = \sum_{k=k_{\min}}^{k_{\max}} \rho_{k,k+m_2-m_1} \sum_{S=S_{\min}}^{S_{\max}} (-1)^{k-m_1} C^{S,m_2-m_1}_{s,-k;s,(k+m_2-m_1)} C^{S,m_2-m_1}_{s,-m_1;s,m_2} \frac{\binom{2s}{S}}{\binom{2s+S+1}{S}}, \tag{C.59}$$

Making the substitution $k - m_1 = \lambda$, we finally arrive at the desired result

$$\rho^{(1)}_{m_1,m_2} = \sum_{\lambda=\lambda_{\min}}^{\lambda_{\max}} \rho_{m_1+\lambda,m_2+\lambda} (-1)^{\lambda} \sum_{S=S_{\min}}^{S_{\max}} C^{S,m_2-m_1}_{s,-m_1-\lambda;s,m_2+\lambda} C^{S,m_2-m_1}_{s,-m_1;s,m_2} \left[\frac{\binom{2s}{S}}{\binom{2s+S+1}{S}} \right], \tag{C.60}$$

where $\lambda_{\min} = -s + \max(-m_1, -m_2)$, $\lambda_{\max} = s + \min(-m_1, -m_2)$, $S_{\min} = \max(0, |m_1 - m_2|)$ and $S_{\max} = 2s$. This completes the proof. □

From (C.60) we observe that after a single iteration of the coherent state POVM measurement, the density matrix undergoes a significant transformation that involves a damping effect characterised by the presence of the Clebsch-Gordan coefficients, which impose a structured reduction of the off-diagonal elements of the matrix and a binomial factor that contributes to the overall suppression of coherences.

Proposition C.1 shows how the density matrix decoheres when the three spin components of the particle are monitored by the environment, when modelled through an SU(2) coherent state POVM. As indicated earlier, due to the lack of orthogonality of the coherent states, though, if the 'output' state $\hat{\rho}^{(1)}$ were monitored again through another POVM measurement, then we obtain a further-decohered state $\hat{\rho}^{(2)}$, and this process can carry on indefinitely. Hence to investigate the system's evolution through the process of decoherence, we iteratively apply the nonselective measurement process. Then the effect of decoherence after the k^{th} iteration of the coherent state POVM can be summarised as follows:

Proposition C.2. *After k iterations of the coherent state POVM measurement the matrix elements* $\langle s, m_1 | \hat{\rho}^{(k)} | s, m_2 \rangle$ *of the density matrix are given by*

$$\rho^{(k)}_{m_1,m_2} = \sum_{\lambda=\lambda_{\min}}^{\lambda_{\max}} \rho_{m_1+\lambda,m_2+\lambda} (-1)^{\lambda} \sum_{S=S_{\min}}^{S_{\max}} C^{S,m_2-m_1}_{s,-m_1-\lambda;s,m_2+\lambda} C^{S,m_2-m_1}_{s,-m_1;s,m_2} \left[\frac{\binom{2s}{S}}{\binom{2s+S+1}{S}} \right]^k, \tag{C.61}$$

where $\lambda_{\min} = -s + \max(-m_1, -m_2)$, $\lambda_{\max} = s + \min(-m_1, -m_2)$, $S_{\min} = \max(0, |m_1 - m_2|)$, *and* $S_{\max} = 2s$.

Proof. We prove this result by induction. For $k = 1$, (C.61) is evidently identical to (C.41), which has already been established. Now suppose that (C.61) is valid for k. Then from (C.41) we can write $\rho^{(k+1)}_{m_1,m_2}$ in terms of $\rho^{(k)}_{m_1,m_2}$ in the form

$$\rho^{(k+1)}_{m_1,m_2} = \sum_{\lambda=\lambda_{\min}}^{\lambda_{\max}} \rho^{(k)}_{m_1+\lambda,m_2+\lambda}(-1)^{\lambda} \sum_{S=S_{\min}}^{S_{\max}} C^{S,m_2-m_1}_{s,-m_1-\lambda;s,m_2+\lambda} C^{S,m_2-m_1}_{s,-m_1;s,m_2} \left[\frac{\binom{2s}{S}}{\binom{2s+S+1}{S}}\right], \tag{C.62}$$

where the summation ranges are the same as in (C.41). Next we substitute the expression (C.61) for $\rho^{(k)}$ in here to obtain

$$\begin{aligned}\rho^{k+1}_{\text{out},m_1,m_2} = & \sum_{\lambda=\lambda_{\min}}^{\lambda_{\max}} \sum_{\mu=\mu_{\min}}^{\mu_{\max}} \rho_{m_1+\mu+\lambda,m_2+\mu+\lambda}(-1)^{\mu} \sum_{S'=S'_{\min}}^{S'_{\max}} C^{S',m_2-m_1}_{s,-m_1-\lambda-\mu;s,m_2+\lambda+\mu} C^{S',m_2-m_1}_{s,-m_1-\lambda;s,m_2+\lambda} \\ & \times \left[\frac{\binom{2s}{S'}}{\binom{2s+S+1}{S'}}\right]^k (-1)^{\lambda} \sum_{S=S_{\min}}^{S_{\max}} C^{S,m_2-m_1}_{s,-m_1-\lambda;s,m_2+\lambda} C^{S,m_2-m_1}_{s,-m_1;s,m_2} \left[\frac{\binom{2s}{S}}{\binom{2s+S+1}{S}}\right], \end{aligned} \tag{C.63}$$

where $\mu_{\min} = -s+\max(-m_1-\lambda, -m_2-\lambda)$, $\mu_{\max} = s+\min(-m_1-\lambda, -m_2-\lambda)$, $S'_{\min} = \max(0, |m_1 - m_2|)$, and $S'_{\max} = 2s$. Making the substitution $\alpha = \lambda + \mu$, this becomes

$$\begin{aligned}\rho^{(k+1)}_{m_1,m_2} = & \sum_{\lambda=\lambda_{\min}}^{\lambda_{\max}} \sum_{\alpha=\alpha_{\min}}^{\alpha_{\max}} \rho_{m_1+\alpha,m_2+\alpha}(-1)^{\alpha} \sum_{S'=S'_{\min}}^{S'_{\max}} C^{S',m_2-m_1}_{s,-m_1-\alpha;s,m_2+\alpha} C^{S',m_2-m_1}_{s,-m_1-\lambda;s,m_2+\lambda} \left[\frac{\binom{2s}{S'}}{\binom{2s+S+1}{S'}}\right]^k \\ & \times \sum_{S=S_{\min}}^{S_{\max}} C^{S,m_2-m_1}_{s,-m_1-\lambda;s,m_2+\lambda} C^{S,m_2-m_1}_{s,-m_1;s,m_2} \left[\frac{\binom{2s}{S}}{\binom{2s+S+1}{S}}\right], \end{aligned} \tag{C.64}$$

where $\alpha_{\min} = -s + \max(-m_1, -m_2)$ and $\alpha_{\max} = s + \min(-m_1, -m_2)$. Rearranging the summations we have

$$\begin{aligned}\rho^{(k+1)}_{\text{out},m_1,m_2} = & \sum_{\alpha=\alpha_{\min}}^{\alpha_{\max}} \rho_{m_1+\alpha,m_2+\alpha}(-1)^{\alpha} \sum_{S'=S'_{\min}}^{S'_{\max}} \sum_{S=S_{\min}}^{S_{\max}} C^{S',m_2-m_1}_{s,-m_1-\alpha;s,m_2+\alpha} \left[\frac{\binom{2s}{S'}}{\binom{2s+S+1}{S'}}\right]^k \\ & \times C^{S,m_2-m_1}_{s,-m_1;s,m_2} \left[\frac{\binom{2s}{S}}{\binom{2s+S+1}{S}}\right] \sum_{\lambda=\lambda_{\min}}^{\lambda_{\max}} C^{S,m_2-m_1}_{s,-m_1-\lambda;s,m_2+\lambda} C^{S',m_2-m_1}_{s,-m_1-\lambda;s,m_2+\lambda}, \end{aligned} \tag{C.65}$$

but using the orthogonality (C.44) of Clebsch-Gordan coefficients we deduce that

$$\begin{aligned}\rho^{(k+1)}_{m_1,m_2} = & \sum_{\alpha=\alpha_{\min}}^{\alpha_{\max}} \rho_{m_1+\alpha,m_2+\alpha}(-1)^{\alpha} \sum_{S'=S'_{\min}}^{S'_{\max}} \sum_{S=S_{\min}}^{S_{\max}} C^{S',m_2-m_1}_{s,-m_1-\alpha;s,m_2+\alpha} \left[\frac{\binom{2s}{S'}}{\binom{2s+S+1}{S'}}\right]^k \\ & \times C^{S,m_2-m_1}_{s,-m_1;s,m_2} \left[\frac{\binom{2s}{S}}{\binom{2s+S+1}{S}}\right] \delta_{S,S'}. \end{aligned} \tag{C.66}$$

Summing over S' we thus obtain

$$\rho^{(k+1)}_{m_1,m_2} = \sum_{\alpha=\alpha_{\min}}^{\alpha_{\max}} \rho_{m_1+\alpha,m_2+\alpha}(-1)^{\alpha} \sum_{S=S_{\min}}^{S_{\max}} C^{S,m_2-m_1}_{s,-m_1-\alpha;s,m_2+\alpha} C^{S,m_2-m_1}_{s,-m_1;s,m_2} \left[\frac{\binom{2s}{S}}{\binom{2s+S+1}{S}}\right]^{k+1}, \tag{C.67}$$

where $\alpha_{\min} = -s + \max(-m_1, -m_2)$, $\alpha_{\max} = s + \min(-m_1, -m_2)$, $S_{\min} = \max(0, |m_1 - m_2|)$, and

$S_{\max} = 2s$. But this is just the claim (C.61) for the $k+1$ iteration, and hence completes the proof. □

In (C.61), we presented an explicit formula for the matrix elements of the density matrix $\hat{\rho}^{(k)}$ after k iterations of the coherent state POVM measurement, in the $\hat{S}_z$-basis. This expression highlights a key feature of the decoherence process which is the Clebsch-Gordan coefficients, which encode the angular momentum coupling structure of the system, remain unchanged, while the binomial damping factor $[\binom{2s}{S}/\binom{2s+S+1}{S}]^k$ is iteratively applied. Since this ratio lies strictly between zero and one for $S > 0$, we see that the iteration will exponentially suppress off-diagonal elements of the density matrix, thereby enhancing decoherence. The difference with the standard decoherence theory, when using an orthogonal POVM, is that the diagonal elements are also averaged in a certain manner.

This iterative structure reveals how decoherence induces decay in a structured way, with different entries decaying at different rates depending on their position and the Clebsch-Gordan decomposition, ultimately driving the matrix toward a diagonal, maximally mixed form.

The property that the density matrix $\hat{\rho}^{(k)}$ becomes proportional to the identity matrix in the limit $k \to \infty$ is a generic feature in all spin systems. Indeed, we have the following. In the limit $k \to \infty$, the density matrix $\hat{\rho}^{(k)}$ converges to the state of complete ignorance:

$$\lim_{k\to\infty} \rho^{(k)}_{m_1,m_2} = \frac{1}{2s+1}\,\delta_{m_1,m_2}\,. \tag{C.68}$$

C.4 Lindblad dynamics for the density matrix in $|s,m\rangle$ basis

The dynamical equation that we shall investigate is given by

$$\frac{\mathrm{d}\hat{\rho}}{\mathrm{d}t} = \gamma\left(\frac{1}{2}\hat{S}_+\hat{\rho}\hat{S}_- + \frac{1}{2}\hat{S}_-\hat{\rho}\hat{S}_+ + \hat{S}_z\hat{\rho}\hat{S}_z - s(s+1)\hat{\rho}\right), \tag{C.69}$$

where $\gamma > 0$ is a parameter that determines the decoherence rate and we used the identity $\hat{S}^2 = \hat{S}_x^2 + \hat{S}_y^2 + \hat{S}_z^2 = s(s+1)\mathbb{1}$.for the dynamical equation. The advantage of this formulation is that the matrix representation of the equation in the spin-z basis elements $|s,m\rangle$ can easily be obtained using (3.2) and (3.4). In particular, we find

$$\begin{aligned}\dot{\rho}_{m_1m_2} \;=\; & \gamma\Big[\frac{1}{2}\rho_{m_1-1,m_2-1}\sqrt{s(s+1)-m_1(m_1-1)}\sqrt{s(s+1)-m_2(m_2-1)}\\ & +\frac{1}{2}\rho_{m_1+1,m_2+1}\sqrt{s(s+1)-m_1(m_1+1)}\sqrt{s(s+1)-m_2(m_2+1)}\\ & +(m_1m_2-s(s+1))\rho_{m_1m_2}\Big].\end{aligned} \tag{C.70}$$

The general solution to this Lindblad equation can be expressed as follows:

Proposition C.3. *The solution to the Lindblad equation (C.70) is given, in the $|s,m\rangle$ basis, by*

$$\rho_{m_1m_2}(t) = \sum_{k=k_{\min}}^{k_{\max}} \rho_{k,\,k+m_2-m_1}(0)(-1)^{k-m_1} \sum_{S=S_{\min}}^{S_{\max}} C^{S,\,m_2-m_1}_{s,\,-k;\,s,\,k+m_2-m_1} C^{S,\,m_2-m_1}_{s,\,-m_1;\,s,\,m_2}\,\mathrm{e}^{-\frac{1}{2}S(S+1)\gamma t}, \tag{C.71}$$

where $\rho_{m_1 m_2}(t) = \langle s, m_1|\hat{\rho}(t)|s, m_2\rangle$*, and the summation limits are given by* $k_{\min} = -s + \max(0, m_1 - m_2)$, $k_{\max} = s + \min(0, m_1 - m_2)$, $S_{\min} = \max(0, |m_1 - m_2|)$, *and* $S_{\max} = 2s$.

We observe that the solution to the Lindblad equation (C.71) closely parallels the structure of the iterative POVM measurement (C.61): in both cases, all $S \neq 0$ terms are exponentially damped. The only distinction lies in the rates: POVM-induced damping depends on the total spin s, whereas the Lindblad solution features a universal, s-independent decay. Thus, the two mechanisms yield qualitatively identical decoherence, differing only by this quantitative factor.

Proof. Our strategy is to show that (C.71) satisfies the Lindblad equation (C.70), with a given initial condition. We begin by checking that the initial condition is satisfied by the postulated solution. Setting $t = 0$ in (C.71), we obtain

$$\rho_{m_1,m_2}(0) = \sum_{\lambda=\lambda_{\min}}^{\lambda_{\max}} \rho_{m_1+\lambda,m_2+\lambda}(0)(-1)^{\lambda} \sum_{S=S_{\min}}^{S_{\max}} C^{S,m_2-m_1}_{s,-m_1-\lambda;s,m_2+\lambda} C^{S,m_2-m_1}_{s,-m_1;s,m_2}. \tag{C.72}$$

Using the orthogonality relation (C.44) for the Clebsch-Gordan coefficients, we find

$$\rho_{m_1,m_2}(0) = \sum_{\lambda=\lambda_{\min}}^{\lambda_{\max}} \rho_{m_1+\lambda,m_2+\lambda}(0)\delta_{\lambda,0} = \rho_{m_1,m_2}(0), \tag{C.73}$$

and hence the initial condition is indeed satisfied. Next we work out the time derivative of the claimed solution (C.71):

$$\begin{aligned}\dot{\rho}_{m_1,m_2} &= -\frac{1}{2}\gamma \sum_{k=k_{\min}}^{k_{\max}} \rho_{k,k+m_2-m_1}(0)(-1)^{k-m_1} \sum_{S=S_{\min}}^{2s} C^{S,m_2-m_1}_{s,-k;s,k+m_2-m_1} C^{S,m_2-m_1}_{s,-m_1;s,m_2} \\ &\quad \times S(S+1)\, \mathrm{e}^{-\frac{1}{2}S(S+1)\gamma t}.\end{aligned} \tag{C.74}$$

This gives the left side of equation (C.70). On the other hand, substituting (C.71) on the right side of (C.70) gives

$$\begin{aligned}\dot{\rho}_{m_1,m_2} &= \gamma \sum_{k=k_{\min}}^{k_{\max}} \rho_{k,k+m_2-m_1}(0)(-1)^{k-m_1} \sum_{S=S_{\min}}^{2s} C^{S,m_2-m_1}_{s,-k;s,k+m_2-m_1} \\ &\quad \times \Bigg[C^{S,m_2-m_1}_{s,-m_1;s,m_2}(m_1 m_2 - s(s+1)) \\ &\quad -\frac{1}{2} C^{S,m_2-m_1}_{s,-m_1+1;s,m_2-1} \sqrt{s(s+1) - m_1(m_1-1)}\sqrt{s(s+1) - m_2(m_2-1)} \\ &\quad -\frac{1}{2} C^{S,m_2-m_1}_{s,-m_1-1;s,m_2+1} \sqrt{s(s+1) - m_1(m_1+1)}\sqrt{s(s+1) - m_2(m_2+1)} \Bigg] \\ &\quad \times \mathrm{e}^{-\frac{1}{2}S(S+1)\gamma t}.\end{aligned} \tag{C.75}$$

Since this substitution involves multiple terms, we will expand and simplify each term in detail to demonstrate that the resulting expression coincides with the time derivative worked out in (C.74). This will show that both sides of the differential equation agree, confirming that the proposed solution solves the Lindblad equation. To simplify the expression somewhat, let us define $A_{\pm}(s, m) =$

$\sqrt{s(s+1)-m(m\pm1)}$. Then the above equation reduces to

$$\begin{aligned}\dot{\rho}_{m_1,m_2} &= \gamma \sum_{k=k_{\min}}^{k_{\max}} \rho_{k,k+m_2-m_1}(0)(-1)^{k-m_1} \sum_{S=S_{\min}}^{2s} C^{S,m_2-m_1}_{s,-k;s,k+m_2-m_1} \\ &\times \left[C^{S,m_2-m_1}_{s,-m_1;s,m_2}(m_1m_2 - s(s+1)) - \frac{1}{2} C^{S,m_2-m_1}_{s,-m_1+1;s,m_2-1} A_-(s,m_1)A_-(s,m_2) \right. \\ &\left. -\frac{1}{2} C^{S,m_2-m_1}_{s,-m_1-1;s,m_2+1} A_+(s,m_1)A_+(s,m_2) \right] \mathrm{e}^{-\frac{1}{2}S(S+1)\gamma t}. \end{aligned} \tag{C.76}$$

To further simplify this expression, we employ the following form of the recursion relations for Clebsch-Gordan coefficients [102, 103]:

$$A_\pm(S,M)C^{S,M\pm1}_{s_1,m_1;s_2,m_2} = A_\pm(s_1,m_1\mp1)C^{S,M}_{s_1,m_1\mp1;s_2,m_2} + A_\pm(s_2,m_2\mp1)C^{S,M}_{s_1,m_1;s_2,m_2\mp1}. \tag{C.77}$$

Applying these relations with the relevant values of m_1 and m_2, we obtain the following four identities:

$$A_+(S,m_2-m_1)C^{S,m_2-m_1+1}_{s,-m_1+1;s,m_2} = A_-(s,m_1)C^{S,m_2-m_1}_{s,-m_1;s,m_2} + A_-(s,m_2)C^{S,m_2-m_1}_{s,-m_1+1;s,m_2-1}, \tag{C.78}$$

$$A_+(S,m_2-m_1)C^{S,m_2-m_1+1}_{s,-m_1;s,m_2+1} = A_+(s,m_1)C^{S,m_2-m_1}_{s,-m_1-1;s,m_2+1} + A_+(s,m_2)C^{S,m_2-m_1}_{s,-m_1;s,m_2}, \tag{C.79}$$

$$A_-(S,m_2-m_1)C^{S,m_2-m_1-1}_{s,-m_1;s,m_2-1} = A_-(s,m_1)C^{S,m_2-m_1}_{s,-m_1+1;s,m_2-1} + A_-(s,m_2)C^{S,m_2-m_1}_{s,-m_1;s,m_2}, \tag{C.80}$$

and

$$A_-(S,m_2-m_1)C^{S,m_2-m_1-1}_{s,-m_1-1;s,m_2} = A_+(s,m_1)C^{S,m_2-m_1}_{s,-m_1;s,m_2-1} + A_+(s,m_2)C^{S,m_2-m_1}_{s,-m_1-1;s,m_2+1}. \tag{C.81}$$

Multiplying (C.79) by $A_+(s,m_2)$ and (C.81) by $A_+(s,m_1)$, then adding the two expressions and rearranging terms, we obtain

$$\begin{aligned}A_+(s,m_1)A_+(s,m_2)C^{S,m_2-m_1}_{s,-m_1-1;s,m_2+1} &= \frac{1}{2}\Big(A_-(S,m_2-m_1)A_+(s,m_1)C^{S,m_2-m_1-1}_{s,-m_1-1;s,m_2} \\ &+A_+(s,m_2)A_+(S,m_2-m_1)C^{S,m_2-m_1+1}_{s,-m_1;s,m_2+1} - ((A_+(s,m_1))^2 + (A_+(s,m_2))^2)C^{S,m_2-m_1}_{s,-m_1;s,m_2}\Big). \end{aligned} \tag{C.82}$$

Similarly, multiplying (C.78) by $A_-(s,m_1)$ and (C.80) by $A_-(s,m_2)$, then adding the two expressions and rearranging terms, we obtain

$$\begin{aligned}A_-(s,m_1)A_-(s,m_2)C^{S,m_2-m_1}_{s,-m_1+1;s,m_2-1} &= \frac{1}{2}\Big(A_+(S,m_2-m_1)A_-(s,m_1)C^{S,m_2-m_1+1}_{s,-m_1+1;s,m_2} \\ &+A_-(s,m_2)A_-(S,m_2-m_1)C^{S,m_2-m_1-1}_{s,-m_1;s,m_2-1} - ((A_-(s,m_1))^2 + (A_-(s,m_2))^2)C^{S,m_2-m_1}_{s,-m_1;s,m_2}\Big). \end{aligned} \tag{C.83}$$

Next consider the sum of (C.82) and (C.83), which we denote by F:

$$\begin{aligned}
F &= A_-(s,m_1)A_-(s,m_2)C^{S,m_2-m_1}_{s,-m_1+1;s,m_2-1} + A_+(s,m_1)A_+(s,m_2)C^{S,m_2-m_1}_{s,-m_1-1;s,m_2+1} \\
&= \frac{1}{2}\Bigg[A_-(S,m_2-m_1)\Big(A_-(s,m_2)C^{S,m_2-m_1-1}_{s,-m_1;s,m_2-1} + A_+(s,m_1)C^{S,m_2-m_1-1}_{s,-m_1-1;s,m_2}\Big) \\
&\quad + A_+(S,m_2-m_1)\Big(A_+(s,m_2)C^{S,m_2-m_1+1}_{s,-m_1;s,m_2+1} + A_-(s,m_1)C^{S,m_2-m_1+1}_{s,-m_1+1;s,m_2}\Big) \\
&\quad - \big(A^2_-(s,m_1) + A^2_-(s,m_2) + A^2_+(s,m_1) + A^2_+(s,m_2)\big)C^{S,m_2-m_1}_{s,-m_1;s,m_2}\Bigg].
\end{aligned} \tag{C.84}$$

Applying the recursion identity (C.77) to each group of terms, this simplifies to

$$\begin{aligned}
F &= \frac{1}{2}\left[A^2_+(S,m_2-m_1) + A^2_-(S,m_2-m_1) - \sum_{\pm}\left(A^2_\pm(s,m_1) + A^2_\pm(s,m_2)\right)\right] C^{S,m_2-m_1}_{s,-m_1;s,m_2} \\
&= \left[S(S+1) + 2m_1m_2 - 2s(s+1)\right] C^{S,m_2-m_1}_{s,-m_1;s,m_2}.
\end{aligned} \tag{C.85}$$

Finally, substituting this in (C.76), we obtain

$$\begin{aligned}
\dot\rho_{m_1,m_2} &= \gamma \sum_{k=k_{\min}}^{k_{\max}} \rho_{k,k+m_2-m_1}(0)(-1)^{k-m_1} \sum_{S=S_{\min}}^{2s} C^{S,m_2-m_1}_{s,-k;s,k+m_2-m_1} \\
&\quad \times \left[C^{S,m_2-m_1}_{s,-m_1;s,m_2}\left(m_1m_2 - s(s+1) - \frac{S(S+1)}{2} - m_1m_2 + s(s+1)\right)\right] \mathrm{e}^{-\frac{1}{2}S(S+1)\gamma t}, \\
&= -\frac{1}{2}\gamma \sum_{k=k_{\min}}^{k_{\max}} \rho_{k,k+m_2-m_1}(0)(-1)^{k-m_1} \sum_{S=S_{\min}}^{2s} C^{S,m_2-m_1}_{s,-k;s,k+m_2-m_1} C^{S,m_2-m_1}_{s,-m_1;s,m_2} \\
&\quad \times S(S+1)\,\mathrm{e}^{-\frac{1}{2}S(S+1)\gamma t}.
\end{aligned} \tag{C.86}$$

This exactly matches the time derivative of (C.74), thus completing the proof. □

Appendix D

Hyperbolic harmonics, Husimi representation and other derivations

This appendix provides the supporting mathematical framework for the $\mathrm{SU}(1,1)$ analysis of Chapter 5. We review harmonic analysis on the hyperbolic plane and its connection to $\mathrm{SU}(1,1)$ representation theory, and give detailed proofs of the results stated in the main text. In particular, we discuss the role of $\mathrm{SU}(1,1)$ covariance in the construction of phase-space distributions and Lindblad-type dynamics, and derive the D-algebra relations for $\mathrm{SU}(1,1)$ coherent states. These results provide the technical foundation for understanding measurement-induced decoherence and covariant dynamics in the noncompact setting.

D.1 Harmonic analysis on the hyperbolic plane

In this section, we introduce the Hilbert space of square-integrable complex-valued functions defined over the hyperbolic plane $\mathbb{H}^2$ [35, 162, 166]. This space plays a central role in the harmonic analysis of $\mathrm{SU}(1,1)$ and underlies the phase-space formulation we adopt in this work. We denote this general space by $\mathcal{L}^2(\mathbb{H}^2)$, which is reducible under the group action.

The inner product $\langle\cdot,\cdot\rangle$ is defined for any pair of functions $F, G \in \mathcal{L}^2(\mathbb{H}^2)$

$$\langle F, G\rangle = \int_{\mathbb{H}^2} \overline{F(\tau,\phi)}\, G(\tau,\phi)\, \mathrm{d}\omega_{\tau,\phi}. \tag{D.1}$$

where, the integration is taken over the hyperbolic plane $\mathbb{H}^2$ using the invariant volume element [35, 162]

$$\mathrm{d}\omega_{\tau,\phi} = \frac{1}{2\pi}\sinh(\tau)\,\mathrm{d}\tau\,\mathrm{d}\phi, \tag{D.2}$$

where $\tau \in [0,\infty)$ is the radial (or hyperbolic distance) coordinate, and $\phi \in [0, 2\pi)$ is the angular coordinate in the upper sheet of the two-sheeted hyperboloid model of $\mathbb{H}^2$.

A complete orthogonal set of functions on the space $\mathcal{L}^2(\mathbb{H}^2)$, indexed by continuous and discrete

parameters $\lambda \in \mathbb{R}_{>0}$ and $\mu \in \mathbb{Z}$ respectively, is given by [35,162,174]

$$\psi_{\lambda,\mu}(\tau,\phi) = (-1)^{\mu} \frac{\Gamma\left(\frac{1}{2}+\mathrm{i}\lambda\right)}{\Gamma\left(\frac{1}{2}+\mathrm{i}\lambda+\mu\right)} P^{\mu}_{\mathrm{i}\lambda-\frac{1}{2}}(\cosh\tau)\, \mathrm{e}^{\mathrm{i}\mu\phi}, \tag{D.3}$$

where $P^{\mu}_{\mathrm{i}\lambda-\frac{1}{2}}(\cosh\tau)$ denotes the associated conical (or Mehler) functions [35,164,165,232–234], which arise as solutions to the associated Legendre differential equation with complex degree $\nu = \mathrm{i}\lambda - \frac{1}{2}$ and order μ, defined on the domain $\tau > 0$.

These functions form a complete orthogonal system on the hyperbolic plane

$$\lambda \tanh(\pi\lambda) \int \psi_{\lambda,\mu}(\tau,\phi)\, \overline{\psi_{\lambda',\mu'}(\tau,\phi)}\, \mathrm{d}\omega_{\tau,\phi} = \delta_{\mu\mu'}\, \delta(\lambda-\lambda'). \tag{D.4}$$

The conical functions $P^{\mu}_{\mathrm{i}\lambda-\frac{1}{2}}(\cosh\tau)$ admit an integral representation given by

$$P^{\mu}_{\mathrm{i}\lambda-\frac{1}{2}}(\cosh\tau) = \frac{1}{2\pi} \frac{\Gamma\left(\frac{1}{2}+\mathrm{i}\lambda+\mu\right)}{\Gamma\left(\frac{1}{2}+\mathrm{i}\lambda\right)} \int_0^{2\pi} (\cosh\tau + \sinh\tau\cos\theta)^{-\frac{1}{2}-\mathrm{i}\lambda}\, \mathrm{e}^{\mathrm{i}\mu\theta}\, \mathrm{d}\theta, \tag{D.5}$$

highlighting their role as eigenfunctions associated with the hyperbolic Laplacian.

An important property of the conical functions is that they are real-valued for real arguments and parameters

$$P^{\mu}_{\mathrm{i}\lambda-\frac{1}{2}}(x) = P^{\mu}_{-\mathrm{i}\lambda-\frac{1}{2}}(x), \tag{D.6}$$

which ensures that the radial part of the eigenfunction remains real when required.

The conical functions satisfy the following addition theorem [162,235,236]. For a fixed value of λ, the identity takes the form

$$\begin{aligned} P_{\mathrm{i}\lambda-\frac{1}{2}}(\cosh\eta) &= \sum_{\mu=-\infty}^{\infty} \psi_{\lambda,\mu}(\tau,\phi)\overline{\psi_{\lambda,\mu}(\tau',\phi')}, \\ &= \sum_{\mu=-\infty}^{\infty} \frac{|\Gamma\left(\frac{1}{2}+\mathrm{i}\lambda\right)|^2}{|\Gamma\left(\frac{1}{2}+\mathrm{i}\lambda+\mu\right)|^2} P^{\mu}_{\mathrm{i}\lambda-\frac{1}{2}}(\cosh(\tau)) P^{\mu}_{\mathrm{i}\lambda-\frac{1}{2}}(\cosh(\tau'))\mathrm{e}^{(\mathrm{i}\mu(\phi-\phi'))}, \end{aligned} \tag{D.7}$$

where $P_{\mathrm{i}\lambda-\frac{1}{2}}$ is referred to as the zonal hyperbolic harmonic [35,164,232–234] and $\cosh\eta = \cosh(\tau)\cosh(\tau') - \sinh(\tau)\sinh(\tau')\cos(\phi-\phi')$. These harmonics form a complete orthogonal basis for square-integrable, rotationally invariant functions on the hyperbolic space [164, 232–234, 237], satisfying the following orthogonality condition

$$\int P_{\mathrm{i}\lambda-\frac{1}{2}}(\cosh\eta) P_{\mathrm{i}\lambda'-\frac{1}{2}}(\cosh\eta)\, \sinh\rho\, \mathrm{d}\rho = \frac{\delta(\lambda-\lambda')}{\lambda\tanh\pi\lambda} \tag{D.8}$$

Any sufficiently well-behaved function $f(\cosh\tau)$ on the hyperbolic plane that depends only on the geodesic distance from a reference point (i.e., is zonal) can be expanded as a superposition of zonal

hyperbolic harmonics as

$$f(\cosh\tau) = \int_0^\infty a(\lambda) P_{\mathrm{i}\lambda-\frac{1}{2}}(\cosh\tau)\, \lambda \tanh(\pi\lambda)\, \mathrm{d}\lambda, \tag{D.9}$$

and the coefficient function $a(\lambda)$ is determined by the inverse transform

$$a(\lambda) = \int_0^\infty f(\cosh\tau) P_{\mathrm{i}\lambda-\frac{1}{2}}(\cosh\tau)\, \sinh\tau\, \mathrm{d}\tau. \tag{D.10}$$

This expansion is analogous to the Fourier-Bessel or spherical harmonic expansion for radial functions in Euclidean space and is referred to as the Mehler-Fock transform [232, 233, 237].

More generally, any square-integrable function $f(\tau,\phi) \in \mathcal{L}^2(\mathbb{H}^2)$ can be expanded in terms of the eigenfunctions of the hyperbolic Laplacian. As these eigenfunctions form a complete orthonormal basis on the hyperbolic plane, the expansion takes the form [162, 174, 232, 233, 237]

$$f(\tau,\phi) = \sum_{\mu=-\infty}^{\infty} \int_0^\infty \mathrm{d}\nu_\lambda\, \tilde{f}_{\lambda,\mu}\, \psi_{\lambda,\mu}(\tau,\phi), \tag{D.11}$$

where the Plancherel measure is given by $\mathrm{d}\nu_\lambda = \lambda \tanh(\pi\lambda)\, \mathrm{d}\lambda$, and the expansion coefficients $\tilde{f}_{\lambda,\mu}$ are obtained by projecting f onto the basis functions

$$\tilde{f}_{\lambda,\mu} = \int_{\mathbb{H}^2} f(\tau,\phi)\, \overline{\psi_{\lambda,\mu}(\tau,\phi)}\, \mathrm{d}\omega_{\tau,\phi}. \tag{D.12}$$

This expansion is known as the generalised Mehler-Fock transform [162, 174, 232, 233, 237].

Substituting (D.12) into (D.11) yields

$$f(\tau,\phi) = \sum_{\mu=-\infty}^{\infty} \int_0^\infty \mathrm{d}\nu_\lambda \left[\int_{\mathbb{H}^2} f(\tau',\phi')\, \overline{\psi_{\lambda,\mu}(\tau',\phi')}\, \mathrm{d}\omega_{\tau',\phi'} \right] \psi_{\lambda,\mu}(\tau,\phi). \tag{D.13}$$

Assuming convergence of the integrals and exchanging the order of integration and summation, we obtain

$$\begin{aligned} f(\tau,\phi) &= \int\int_{\mathbb{H}^2} \mathrm{d}\omega_{\tau',\phi'} \left[\int_0^\infty \mathrm{d}\nu_\lambda \sum_{\mu=-\infty}^{\infty} \psi_{\lambda,\mu}(\tau,\phi)\, \overline{\psi_{\lambda,\mu}(\tau',\phi')} \right] f(\tau',\phi'), \\ &= \int\int_{\mathbb{H}^2} \mathrm{d}\omega_{\tau',\phi'} \left[\int_0^\infty \mathrm{d}\nu_\lambda\, P_{\mathrm{i}\lambda-\frac{1}{2}}(\cosh\eta) \right] f(\tau',\phi'), \end{aligned} \tag{D.14}$$

where the quantity $\cosh\eta$ is the hyperbolic distance between the points (τ,ϕ) and (τ',ϕ') and is given by

$$\cosh\eta = \cosh\tau\cosh\tau' - \sinh\tau\sinh\tau'\cos(\phi-\phi'). \tag{D.15}$$

This expression demonstrates the reproducing kernel property of the Zonal hyperbolic functions, highlighting their role in reconstructing arbitrary functions via harmonic decomposition.

As a final mathematical ingredient, we now establish a key identity involving the product of two zonal spherical functions on the hyperbolic plane.

Lemma D.1. Let $P_{\mathrm{i}\lambda-\frac{1}{2}}(\cosh\eta)$ be the zonal spherical function on the hyperbolic plane. Then the following identity holds

$$\int P_{\mathrm{i}\lambda-\frac{1}{2}}(\cosh\eta')P_{\mathrm{i}\lambda'-\frac{1}{2}}(\cosh\eta'')\,\mathrm{d}\omega_{\tau'',\phi''} = \frac{\delta(\lambda-\lambda')}{\lambda\tanh(\pi\lambda)}\sum_{\mu=-\infty}^{\infty}\psi_{\lambda,\mu}(\tau,\phi)\,\overline{\psi_{\lambda',\mu}(\tau',\phi')}, \tag{D.16}$$

where

$$\begin{aligned}\cosh\eta' &= \cosh\tau''\cosh\tau' - \sinh\tau''\sinh\tau'\cos(\phi''-\phi'),\\ \cosh\eta'' &= \cosh\tau\cosh\tau'' - \sinh\tau\sinh\tau''\cos(\phi-\phi'').\end{aligned} \tag{D.17}$$

Proof. Using the addition theorem for eigenfunctions of the Laplace-Beltrami operator on the hyperbolic plane in (D.7), we expand the zonal functions as

$$P_{\mathrm{i}\lambda-\frac{1}{2}}(\cosh\eta') = \sum_{\mu=-\infty}^{\infty}\psi_{\lambda,\mu}(\tau'',\phi'')\,\overline{\psi_{\lambda,\mu}(\tau',\phi')}, \tag{D.18}$$

$$P_{\mathrm{i}\lambda'-\frac{1}{2}}(\cosh\eta'') = \sum_{\mu'=-\infty}^{\infty}\psi_{\lambda',\mu'}(\tau,\phi)\,\overline{\psi_{\lambda',\mu'}(\tau'',\phi'')}. \tag{D.19}$$

Substituting these expansions into the integral, we obtain

$$\begin{aligned}\int P_{\mathrm{i}\lambda-\frac{1}{2}}(\cosh\eta')P_{\mathrm{i}\lambda'-\frac{1}{2}}(\cosh\eta'')\,\mathrm{d}\omega_{\tau,\phi} &= \sum_{\mu,\mu'}\overline{\psi_{\lambda,\mu}(\tau',\phi')}\psi_{\lambda',\mu'}(\tau,\phi)\\ &\quad\times\int\psi_{\lambda,\mu}(\tau'',\phi'')\overline{\psi_{\lambda',\mu'}(\tau'',\phi'')}\,\mathrm{d}\omega_{\tau'',\phi''}.\end{aligned} \tag{D.20}$$

Rearranging the summation and using orthogonality of the eigenfunctions on the hyperbolic plane

$$\int\psi_{\lambda',\mu'}(\tau,\phi)\overline{\psi_{\lambda,\mu}(\tau,\phi)}\,\mathrm{d}\omega_{\tau,\phi} = \frac{\delta(\lambda-\lambda')\delta_{\mu\mu'}}{\lambda\tanh(\pi\lambda)}. \tag{D.21}$$

Substituting this back into the expression, we get the desired result and this completes the proof. □

D.2 Proofs of technical results

D.2.1 Proof of proposition 5.1

Proof. The density matrix of an $\mathrm{SU}(1,1)$ system with Bargmann index k can be expressed in the $|k,k+m\rangle$ basis as

$$\hat{\rho} = \sum_{m_1=0}^{\infty}\sum_{m_2=0}^{\infty}\rho_{m_1m_2}|k,k+m_1\rangle\langle k,k+m_2|. \tag{D.22}$$

A matrix element of the output density matrix $\hat{\rho}^{(1)}$ is then given by

$$\rho^{(1)}_{m_1,m_2} = \langle k,k+m_1|\hat{\rho}^{(1)}|k,k+m_2\rangle = \int Q(\tau,\phi)\,\langle k,k+m_1|\chi\rangle\langle\chi|k,k+m_2\rangle\,\mathrm{d}\mu^k_{\tau,\phi}, \tag{D.23}$$

where we have substituted (5.25). To evaluate this, we expand the Husimi function as

$$Q(\tau,\phi) = \langle\chi|\hat{\rho}|\chi\rangle = \sum_{p,q=0}^{\infty} \rho_{p,q}\, \langle\chi|k,k+p\rangle\langle k,k+q|\chi\rangle, \tag{D.24}$$

using the resolution of identity in (5.2). The overlaps are expressed in terms of Wigner D-matrices as

$$Q(\tau,\phi) = \sum_{p,q=0}^{\infty} \rho_{p,q}\, \overline{D^k_{k+p,k}(\phi,\tau,-\phi)}\, D^k_{k+q,k}(\phi,\tau,-\phi). \tag{D.25}$$

Substituting (D.25) into (D.23), we obtain

$$\begin{aligned}\rho^{(1)}_{m_1,m_2} \;=\; & \sum_{p,q=0}^{\infty} \rho_{p,q} \int \overline{D^k_{k+m_2,k}(\phi,\tau,-\phi)}\, D^k_{k+m_1,k}(\phi,\tau,-\phi) \\ & D^k_{k+q,k}(\phi,\tau,-\phi)\, \overline{D^k_{k+p,k}(\phi,\tau,-\phi)}\, \mathrm{d}\mu^k_{\tau,\phi}.\end{aligned} \tag{D.26}$$

Let us denote this integral by I, for brevity

$$I = \int \overline{D^k_{k+m_2,k}(\phi,\tau,-\phi)}\, D^k_{k+m_1,k}(\phi,\tau,-\phi) D^k_{k+q,k}(\phi,\tau,-\phi)\, \overline{D^k_{k+p,k}}(\phi,\tau,-\phi)\, \mathrm{d}\mu^k_{\tau,\phi}. \tag{D.27}$$

Using the complex conjugation identity [161]

$$\overline{D^k_{k+m,k}(\phi,\tau,-\phi)} = D^k_{k+m,k}(\phi,\tau,-\phi)\, \exp(2\mathrm{i}m\phi), \tag{D.28}$$

we simplify the integral as

$$I = \int \exp\left[2\mathrm{i}(m_2+p)\phi\right] \prod_{j=1}^{4} D^k_{a_j,k}(\phi,\tau,-\phi)\, \mathrm{d}\mu^k_{\tau,\phi}, \tag{D.29}$$

where $a_j \in \{k+m_1, k+m_2, k+q, k+p\}$.
We now employ the Clebsch-Gordan decomposition of Wigner D-matrices [169]

$$D^{k_1}_{k_1+p_1,k_1+m_1} D^{k_2}_{k_2+p_2,k_2+m_2} = \sum_{K=k_1+k_2}^{\infty} C^{K,k_1+k_2+m_1+m_2}_{k_1,k_1+m_1;k_2,k_2+m_2} C^{K,k_1+k_2+p_1+p_2}_{k_1,k_1+p_1;k_2,k_2+p_2} D^K_{K+m_1+m_2,K+p_1+p_2}, \tag{D.30}$$

and use the orthogonality of the D-matrix elements [161]

$$\int D^K_{K+a,K+b}(\phi,\tau,-\phi)\, \overline{D^{K'}_{K'+c,K'+d}(\phi,\tau,-\phi)}\, \mathrm{d}\mu^k_{\tau,\phi} = \frac{2k-1}{2K-1}\delta_{K,K'}\, \delta_{a,c}\, \delta_{b,d}. \tag{D.31}$$

Applying (D.30) to (D.29) gives

$$\begin{aligned} I = \sum_{K_1,K_2=2k}^{\infty} & C^{K_1,2k+m_1+q}_{k,k+m_1;\,k,k+q}\, C^{K_2,2k+m_2+p}_{k,k+m_2;\,k,k+p}\, C^{K_1,2k}_{k,k;\,k,k}\, C^{K_2,2k}_{k,k;\,k,k} \int \exp\left[2\mathrm{i}(m_2+p)\phi\right] \\ & \times D^{K_1}_{K_1+m_1+q,K_1}(\phi,\tau,-\phi)\, D^{K_2}_{K_2+m_2+p,K_2}(\phi,\tau,-\phi)\, \mathrm{d}\mu^k_{\tau,\phi}. \end{aligned} \tag{D.32}$$

Using (D.31) we find that I becomes

$$I = \sum_{K=2k}^{\infty} C^{K,2k+m_1+q}_{k,k+m_1;k,k+q} C^{K,2k+m_2+p}_{k,k+m_2;k,k+p} \left(C^{K,2k}_{k,k;k,k}\right)^2 \delta_{m_2+p,m_1+q} \frac{2k-1}{2K-1}. \tag{D.33}$$

Substituting this into (D.26) and changing summation variables via $p - m_1 = \lambda$, we obtain the final result

$$\rho^{(1)}_{m_1,m_2} = \sum_{\lambda=\lambda_{\min}}^{\lambda_{\max}} \rho_{m_1+\lambda,m_2+\lambda} \sum_{K=K_{\min}}^{\infty} C^{K,2k+m_1+m_2+\lambda}_{k,k+m_1;k,k+m_2+\lambda} C^{K,2k+m_1+m_2+\lambda}_{k,k+m_2;k,k+m_1+\lambda} \left(C^{K,2k}_{k,k;k,k}\right)^2 \frac{2k-1}{2K-1}, \tag{D.34}$$

where the summation limits are given by $\lambda_{\min} = \max(-m_1, -m_2)$, $\lambda_{\max} = \infty$, $K_{\min} = 2k + \min(0, m_1 - m_2)$, $K_{\max} = \infty$. This completes the proof. □

D.2.2 Proof of proposition 5.2

Proof. Using (5.40) and substituting for $\hat{\rho}^{(1)}$ from (5.25), we have for $F_1^{(\sigma)}(\chi)$,

$$F_1^{(\sigma)}(\chi) = \int \mathrm{d}\mu^k_{\chi'} \, \langle\chi'|\hat{\rho}|\chi'\rangle \, \langle\chi'| \, \hat{w}^{(\sigma)}(\chi)|\chi'\rangle. \tag{D.35}$$

Substituting for $\hat{w}^{(\sigma)}$ using (5.36) we get

$$F_1^{(\sigma)}(\chi) = \int \mathrm{d}\mu^k_{\chi'} \, \langle\chi'|\hat{\rho}|\chi'\rangle \, \frac{2}{2k-1} \int \mathrm{d}\mu^k_{\chi''} \int \mathrm{d}\nu_\lambda \, P_{\mathrm{i}\lambda-\frac{1}{2}}(\cosh\eta') \, \Phi_k(\lambda)^{-1/2-\sigma/2} \, |\langle\chi'|\chi''\rangle|^2. \tag{D.36}$$

where $\cosh\eta'$ is the angular distance between χ and χ''.

The overlap of coherent states (5.22) is a real-valued function that depends solely on $\cosh(\rho)$, it can be expanded in terms of conical (Mehler) functions using the Mehler-Fock transform (D.9,D.10)

$$|\langle\chi'|\chi''\rangle_k|^2 = \int \tilde{f}(\lambda) P_{\mathrm{i}\lambda-\frac{1}{2}}(\cosh\eta'') \, \mathrm{d}\nu_\lambda. \tag{D.37}$$

where $\cosh\eta''$ is the angular distance between χ' and χ''.

The spectral coefficient $\tilde{f}(\lambda)$ can be computed using known results from harmonic analysis on hyperbolic spaces [162, 232, 233]

$$\begin{aligned} \tilde{f}(\lambda) &= \int \cosh^{-4k}\left(\frac{\eta''}{2}\right) P_{\mathrm{i}\lambda-\frac{1}{2}}(\cosh\eta'') \sinh\eta'' \, \mathrm{d}\eta'' = 2\frac{|\Gamma(2k-\frac{1}{2}+\mathrm{i}\lambda)|^2}{\Gamma^2(2k)}, \\ &= \frac{2}{2k-1}\Phi_k(\lambda). \end{aligned} \tag{D.38}$$

Substituting for the overlap in (D.36) we get

$$\begin{aligned} F_1^{(\sigma)}(\chi) &= \int \mathrm{d}\mu^k_{\chi'} \, \langle\chi'|\hat{\rho}|\chi'\rangle \, \frac{2}{2k-1} \int \mathrm{d}\mu^k_{\chi''} \int \mathrm{d}\nu_\lambda \, P_{\mathrm{i}\lambda-\frac{1}{2}}(\cosh\eta') \, \Phi_k(\lambda)^{-1/2-\sigma/2} \\ &\quad \times \frac{2}{2k-1} \int \Phi_k(\lambda') P_{\mathrm{i}\lambda'-\frac{1}{2}}(\cosh\eta'') \, \mathrm{d}\nu_{\lambda'}. \end{aligned} \tag{D.39}$$

Here we use the orthogonality of the Mehler functions D.4

$$\int P_{\mathrm{i}\lambda-\frac{1}{2}}(\cosh(\eta'))P_{\mathrm{i}\lambda'-\frac{1}{2}}(\cosh(\eta''))\,\mathrm{d}\mu^k_{\chi''} = \frac{2k-1}{2}\frac{\delta(\lambda-\lambda')}{\lambda\tanh(\pi\lambda)}\sum_{\mu=-\infty}^{\infty}\psi_{\lambda,\mu}(\tau,\phi)\,\overline{\psi_{\lambda',\mu}(\tau',\phi')}, \quad \text{(D.40)}$$

where $\psi_{\lambda,\mu}$ are a complete set of orthogonal functions on the Hyperbolic plane.

Substituting this in the above expression and using the addition theorem (D.7) gives

$$F_1^{(\sigma)}(\chi) \;=\; \frac{2}{2k-1}\int \mathrm{d}\mu^k_{\chi'}\,\langle\chi'|\hat{\rho}|\chi'\rangle\int \mathrm{d}\nu_\lambda\, P_{\mathrm{i}\lambda-\frac{1}{2}}(\cosh\eta)\,\Phi_k(\lambda)^{1/2-\sigma/2}. \quad \text{(D.41)}$$

Identifying the integral for $F^{(\sigma)}$ we get

$$F_1^{(\sigma)}(\chi) \;=\; \frac{2}{2k-1}\int \mathrm{d}\mu^k_{\chi''}\int \mathrm{d}\nu_\lambda\, P_{\mathrm{i}\lambda-\frac{1}{2}}(\cosh\eta'')\,\Phi_k(\lambda)\,F^{(\sigma)}(\chi'). \quad \text{(D.42)}$$

□

D.2.3 Asymptotic limits of $\Phi_k(\lambda)$

Proposition D.1. *Let*

$$\Phi_k(\lambda) \;=\; \frac{(2k-1)\left|\Gamma\left(2k-\frac{1}{2}+\mathrm{i}\lambda\right)\right|^2}{\Gamma^2(2k)}, \quad \text{(D.43)}$$

with fixed $k>\frac{1}{2}$ and $\lambda\in\mathbb{R}$. Then we have

$$0<\Phi_k(\lambda)<1 \quad \textit{for all } \lambda\in\mathbb{R}. \quad \text{(D.44)}$$

Moreover, for $k=\frac{1}{2}$ one has $\Phi_{1/2}(\lambda)\equiv 0$. Finally, as $|\lambda|\to\infty$,

$$\Phi_k(\lambda) \;\sim\; \frac{(2k-1)\,2\pi}{\Gamma(2k)^2}\,|\lambda|^{4k-2}\,\mathrm{e}^{-\pi|\lambda|}. \quad \text{(D.45)}$$

Proof. Positivity is immediate since $|\Gamma(a+\mathrm{i}\lambda)|^2=\Gamma(a+\mathrm{i}\lambda)\Gamma(a-\mathrm{i}\lambda)>0$ for $a>0$ and real λ. Thus $\Phi_k(\lambda)>0$ for all λ; and if $k=\frac{1}{2}$ then the prefactor $(2k-1)$ vanishes, so $\Phi_{1/2}\equiv 0$.

For the upper bound, we evaluate at $\lambda=0$ to get

$$\Phi_k(0) \;=\; \frac{(2k-1)\,\Gamma^2\left(2k-\frac{1}{2}\right)}{\Gamma^2(2k)}. \quad \text{(D.46)}$$

By Gautschi's inequality [238] (for $x>0$), $\frac{\Gamma\left(x-\frac{1}{2}\right)}{\Gamma(x)} \;<\; x^{-1/2}$, and with $x=2k$ we obtain

$$\Phi_k(0) \;<\; (2k-1)\,\frac{1}{2k} \;=\; 1-\frac{1}{2k} \;<\; 1. \quad \text{(D.47)}$$

Moreover, for fixed $a>0$ the function $\lambda\mapsto|\Gamma(a+\mathrm{i}\lambda)|$ is strictly decreasing in $|\lambda|$ [239]; hence

$$\left|\Gamma\left(2k-\frac{1}{2}+\mathrm{i}\lambda\right)\right|^2 \;<\; \left|\Gamma\left(2k-\frac{1}{2}\right)\right|^2 \qquad (\lambda\neq 0), \quad \text{(D.48)}$$

which implies $\Phi_k(\lambda) < \Phi_k(0) < 1$ for all $\lambda \neq 0$.

Finally, the large-$|\lambda|$ behaviour follows from Stirling's formula for complex arguments [122, 123]

$$|\Gamma(a+\mathrm{i}\lambda)|^2 \;=\; \Gamma(a+\mathrm{i}\lambda)\Gamma(a-\mathrm{i}\lambda) \;\sim\; 2\pi\,|\lambda|^{2a-1}\,\mathrm{e}^{-\pi|\lambda|} \qquad (|\lambda|\to\infty)\,. \tag{D.49}$$

Setting $a = 2k - \frac{1}{2}$ (so $2a-1 = 4k-2$) yields

$$\left|\Gamma\left(2k-\frac{1}{2}+\mathrm{i}\lambda\right)\right|^2 \;\sim\; 2\pi\,|\lambda|^{4k-2}\,\mathrm{e}^{-\pi|\lambda|}\,, \tag{D.50}$$

and therefore

$$\Phi_k(\lambda) \;\sim\; \frac{(2k-1)\,2\pi}{\Gamma(2k)^2}\,|\lambda|^{4k-2}\,\mathrm{e}^{-\pi|\lambda|} \qquad (|\lambda|\to\infty)\,, \tag{D.51}$$

which establishes the claimed asymptotic decay. □

D.2.4 SU(1,1)-covariance of Lindblad generators

We consider Hermitian jump operators built from the $\mathrm{SU}(1,1)$ generators $\hat{K}_x, \hat{K}_y, \hat{K}_z$ and a time-homogeneous Lindblad generator

$$\mathcal{L}(\hat{\rho}) \;=\; \sum_{j=x,y,z} \gamma_j \left(\hat{K}_j\hat{\rho}\hat{K}_j - \frac{1}{2}\{\hat{K}_j^2,\hat{\rho}\}\right) \;\equiv\; \sum_{j=x,y,z}\gamma_j\,\mathcal{D}[\hat{K}_j]\hat{\rho}. \tag{D.52}$$

Let $\hat{U}_g$ be the unitary representation of $g \in \mathrm{SU}(1,1)$ on the system Hilbert space. We say that $\mathcal{L}$ is G-covariant iff

$$\mathcal{L}\big(\hat{U}_g\hat{\rho}\hat{U}_g^\dagger\big) \;=\; \hat{U}_g\,\mathcal{L}(\hat{\rho})\,\hat{U}_g^\dagger \qquad \forall g\in G,\ \forall\hat{\rho}. \tag{D.53}$$

Multiplying (D.53) on the left by $\hat{U}_g^\dagger$ and on the right by $\hat{U}_g$ gives the equivalent condition

$$\mathcal{L}(\hat{\rho}) \;=\; \hat{U}_g^\dagger\,\mathcal{L}\big(\hat{U}_g\hat{\rho}\hat{U}_g^\dagger\big)\,\hat{U}_g \qquad \forall g,\ \forall\hat{\rho}. \tag{D.54}$$

Using the identity

$$\hat{U}_g^\dagger\,\mathcal{D}[\hat{K}]\,\big(\hat{U}_g\hat{\rho}\hat{U}_g^\dagger\big)\,\hat{U}_g \;=\; \mathcal{D}[\hat{K}']\,\hat{\rho}, \qquad \hat{K}' = \hat{U}_g^\dagger\hat{K}\hat{U}_g, \tag{D.55}$$

we find that (D.54) is equivalent to

$$\sum_j \gamma_j\,\mathcal{D}[\hat{K}'_j]\,\hat{\rho} \;=\; \sum_j \gamma_j\,\mathcal{D}[\hat{K}_j]\,\hat{\rho} \qquad \forall g,\ \forall\hat{\rho}, \tag{D.56}$$

i.e. the set of dissipators must be invariant under conjugation of the jump operators, with the γ_j unchanged.

Rotation about $\hat{K}_z$. Let $\hat{U}_z(\alpha) = \mathrm{e}^{\mathrm{i}\alpha\hat{K}_z}$. Conjugating the generators with $\hat{U}_z$ gives [147]

$$\hat{K}'_x = \cos\alpha\,\hat{K}_x + \sin\alpha\,\hat{K}_y, \quad \hat{K}'_y = \cos\alpha\,\hat{K}_y - \sin\alpha\,\hat{K}_x, \quad \hat{K}'_z = \hat{K}_z. \tag{D.57}$$

For any linear combination $a\hat{A} + b\hat{B}$, we have the following result

$$\mathcal{D}[a\hat{A} + b\hat{B}]\hat{\rho} \;=\; a^2\mathcal{D}[\hat{A}]\hat{\rho} + b^2\mathcal{D}[\hat{B}]\hat{\rho} + ab\left(\hat{A}\hat{\rho}\hat{B} + \hat{B}\hat{\rho}\hat{A} - \frac{1}{2}\{\{\hat{A},\hat{B}\},\hat{\rho}\}\right). \tag{D.58}$$

Using the above result, the left-hand side of (D.56) becomes

$$\begin{aligned}\gamma_x\mathcal{D}[\hat{K}'_x] + \gamma_y\mathcal{D}[\hat{K}'_y] + \gamma_z\mathcal{D}[\hat{K}_z] \;=\; & (\gamma_x\cos^2\alpha + \gamma_y\sin^2\alpha)\,\mathcal{D}[\hat{K}_x] \\ & +(\gamma_x\sin^2\alpha + \gamma_y\cos^2\alpha)\,\mathcal{D}[\hat{K}_y] \\ & +(\gamma_x - \gamma_y)\sin\alpha\cos\alpha\;T_{xy} + \gamma_z\mathcal{D}[\hat{K}_z],\end{aligned} \tag{D.59}$$

where $T_{xy}(\hat{\rho}) = \hat{K}_x\hat{\rho}\hat{K}_y + \hat{K}_y\hat{\rho}\hat{K}_x - \frac{1}{2}\{\{\hat{K}_x,\hat{K}_y\},\hat{\rho}\}$. For equality with the right-hand side $\gamma_x\mathcal{D}[\hat{K}_x] + \gamma_y\mathcal{D}[\hat{K}_y] + \gamma_z\mathcal{D}[\hat{K}_z]$ for *all* α, the cross-term must vanish

$$(\gamma_x - \gamma_y)\sin\alpha\cos\alpha \equiv 0 \quad\Rightarrow\quad \gamma_x = \gamma_y = \gamma\,. \tag{D.60}$$

Boost along $\hat{K}_x$. Let $\hat{U}_x(\beta) = \mathrm{e}^{\mathrm{i}\beta\hat{K}_x}$. Conjugating the generators with $\hat{U}_x$ gives [147]

$$\hat{K}'_y = \cosh\beta\,\hat{K}_y - \sinh\beta\,\hat{K}_z, \qquad \hat{K}'_z = -\sinh\beta\,\hat{K}_y + \cosh\beta\,\hat{K}_z, \qquad \hat{K}'_x = \hat{K}_x. \tag{D.61}$$

We define $T_{yz}(\hat{\rho}) = \hat{K}_y\hat{\rho}\hat{K}_z + \hat{K}_z\hat{\rho}\hat{K}_y - \frac{1}{2}\{\{\hat{K}_y,\hat{K}_z\},\hat{\rho}\}$. Then we have

$$\begin{aligned}\gamma_y\mathcal{D}[\hat{K}'_y] + \gamma_z\mathcal{D}[\hat{K}'_z] \;=\; & (\gamma_y\cosh^2\beta + \gamma_z\sinh^2\beta)\,\mathcal{D}[\hat{K}_y] + (\gamma_y\sinh^2\beta + \gamma_z\cosh^2\beta)\,\mathcal{D}[\hat{K}_z] \\ & -(\gamma_y + \gamma_z)\sinh\beta\cosh\beta\;T_{yz}.\end{aligned} \tag{D.62}$$

Requiring equality with $\gamma_y\mathcal{D}[\hat{K}_y] + \gamma_z\mathcal{D}[\hat{K}_z]$ for *all* β, forces the cross-term to vanish:

$$(\gamma_y + \gamma_z)\sinh\beta\cosh\beta \equiv 0 \quad\Rightarrow\quad \gamma_z = -\gamma_y\,. \tag{D.63}$$

Combining (D.60) and (D.63) yields the *unique* coefficient pattern

$$\gamma_x = \gamma_y = \gamma, \qquad \gamma_z = -\gamma\,. \tag{D.64}$$

Therefore, the SU(1,1)-covariant second-order generator built from the triplet is

$$\mathcal{L}_{\mathrm{cov}}(\hat{\rho}) = \gamma\Big(\mathcal{D}[\hat{K}_x] + \mathcal{D}[\hat{K}_y] - \mathcal{D}[\hat{K}_z]\Big)\hat{\rho}. \tag{D.65}$$

This is the familiar "flipped" sign structure.
For completion, lets do the following

Boost along $\hat{K}_y$. Let $\hat{U}_y(\beta) = \mathrm{e}^{\mathrm{i}\beta\hat{K}_y}$. Conjugating the generators with $\hat{U}_y$ gives [147]

$$\hat{K}'_x = \cosh\beta\,\hat{K}_x - \sinh\beta\,\hat{K}_z, \quad \hat{K}'_z = -\sinh\beta\,\hat{K}_x + \cosh\beta\,\hat{K}_z, \quad \hat{K}'_y = \hat{K}_y. \tag{D.66}$$

By defining T_{xz} to be

$$T_{xz}(\hat{\rho}) = \hat{K}_x\hat{\rho}\hat{K}_z + \hat{K}_z\hat{\rho}\hat{K}_x - \frac{1}{2}\{\{\hat{K}_x,\hat{K}_z\},\hat{\rho}\}, \tag{D.67}$$

we find that

$$\begin{aligned}\gamma_x\mathcal{D}[\hat{K}'_x]+\gamma_z\mathcal{D}[\hat{K}'_z] &= (\gamma_x\cosh^2\beta+\gamma_z\sinh^2\beta)\,\mathcal{D}[\hat{K}_x]+(\gamma_x\sinh^2\beta+\gamma_z\cosh^2\beta)\,\mathcal{D}[\hat{K}_z]\\ &\quad -(\gamma_x+\gamma_z)\sinh\beta\cosh\beta\;T_{xz}.\end{aligned} \tag{D.68}$$

Requiring equality with $\gamma_x\mathcal{D}[\hat{K}_x]+\gamma_z\mathcal{D}[\hat{K}_z]$ for all β forces

$$(\gamma_x+\gamma_z)\sinh\beta\cosh\beta\equiv 0 \quad\Rightarrow\quad \gamma_z=-\gamma_x \tag{D.69}$$

For $\gamma>0$ the quadratic form above has signature $(+,+,-)$, so $\mathcal{L}_{\rm cov}$ is *not* of GKSL form (not completely positive) when viewed as an operator-level generator.

Casimir connection

If we introduce the adjoint action on operators (Heisenberg picture), the quadratic Casimir of $\mathfrak{su}(1,1)$ is $\hat{K}^2=\hat{K}_x^2+\hat{K}_y^2-\hat{K}_z^2$, and its image in the adjoint representation acts as

$$\rho_{\rm ad}(\hat{K}^2)\;:\;\hat{O}\mapsto[\hat{K}_x,[\hat{K}_x,\hat{O}]]+[\hat{K}_y,[\hat{K}_y,\hat{O}]]-[\hat{K}_z,[\hat{K}_z,\hat{O}]]. \tag{D.70}$$

The flipped generator in the Heisenberg picture is precisely

$$\mathcal{L}_{\rm cov}^{\dagger}\hat{O} \;=\; -\tfrac{\gamma}{2}\,\rho_{\rm ad}(\hat{K}^2)\,\hat{O}, \tag{D.71}$$

i.e. proportional to the adjoint action of the Casimir; since the Casimir is invariant, $\mathcal{L}_{\rm cov}$ is SU(1,1)-covariant.

Trace preservation and first moments

The Heisenberg adjoint of the Lindblad generator acts as

$$\mathcal{L}^{\dagger}\hat{O} \;=\; \sum_{j=x,y,z}\gamma_j\Big(\hat{K}_j\hat{O}\hat{K}_j-\frac{1}{2}\{\hat{K}_j^2,\hat{O}\}\Big)=-\frac{1}{2}\sum_{j=x,y,z}\gamma_j\,[\hat{K}_j,[\hat{K}_j,\hat{O}]], \tag{D.72}$$

where the last equality uses Hermiticity.

Trace preservation (TP). Using cyclicity of the trace and Hermiticity,

$$\begin{aligned}\operatorname{tr}\mathcal{L}(\hat{\rho}) &= \sum_j\gamma_j\Big(\operatorname{tr}[\hat{K}_j\hat{\rho}\hat{K}_j]-\frac{1}{2}\operatorname{tr}[\hat{K}_j^2\hat{\rho}]-\frac{1}{2}\operatorname{tr}[\hat{\rho}\hat{K}_j^2]\Big),\\ &= \sum_j\gamma_j\Big(\operatorname{tr}[\hat{\rho}\hat{K}_j^2]-\frac{1}{2}\operatorname{tr}[\hat{\rho}\hat{K}_j^2]-\frac{1}{2}\operatorname{tr}[\hat{\rho}\hat{K}_j^2]\Big)\;=\;0.\end{aligned} \tag{D.73}$$

Hence $\mathcal{L}$ is trace preserving, $\operatorname{tr}(\dot{\hat{\rho}})=0$.

First moments. For any observable $\hat{O}$,

$$\frac{\mathrm{d}}{\mathrm{d}t}\langle\hat{O}\rangle=\operatorname{tr}(\hat{O}\,\dot{\hat{\rho}})=\operatorname{tr}(\hat{O}\,\mathcal{L}(\hat{\rho}))=\operatorname{tr}(\hat{\rho}\,\mathcal{L}^{\dagger}\hat{O}). \tag{D.74}$$

Taking $\hat{O} = \hat{K}_a$ and using (D.72) together with the $\mathfrak{su}(1,1)$ commutators $[\hat{K}_x, \hat{K}_y] = -\mathrm{i}\hat{K}_z$, $[\hat{K}_y, \hat{K}_z] = \mathrm{i}\hat{K}_x$, $[\hat{K}_z, \hat{K}_x] = \mathrm{i}\hat{K}_y$, one finds the closed form

$$\mathcal{L}^\dagger \hat{K}_x = \frac{1}{2}(\gamma_y - \gamma_z)\,\hat{K}_x, \quad \mathcal{L}^\dagger \hat{K}_y = \frac{1}{2}(\gamma_x - \gamma_z)\,\hat{K}_y, \quad \mathcal{L}^\dagger \hat{K}_z = \frac{1}{2}(\gamma_x + \gamma_y)\,\hat{K}_z. \tag{D.75}$$

Therefore,

$$\frac{\mathrm{d}}{\mathrm{d}t}\langle \hat{K}_x\rangle = \frac{1}{2}(\gamma_y - \gamma_z)\,\langle \hat{K}_x\rangle, \quad \frac{\mathrm{d}}{\mathrm{d}t}\langle \hat{K}_y\rangle = \frac{1}{2}(\gamma_x - \gamma_z)\,\langle \hat{K}_y\rangle, \quad \frac{\mathrm{d}}{\mathrm{d}t}\langle \hat{K}_z\rangle = \frac{1}{2}(\gamma_x + \gamma_y)\,\langle \hat{K}_z\rangle. \tag{D.76}$$

Cases.

- **All-plus isotropic GKSL:** $\gamma_x = \gamma_y = \gamma_z = \gamma > 0$. Then we have $\mathcal{L}^\dagger \hat{K}_x = 0$, $\mathcal{L}^\dagger \hat{K}_y = 0$, $\mathcal{L}^\dagger \hat{K}_z = \gamma\,\hat{K}_z$. So the first moments are *not* all stationary, $\langle \hat{K}_x\rangle, \langle \hat{K}_y\rangle$ are constant, whereas $\langle \hat{K}_z\rangle$ grows/decays exponentially, $\frac{\mathrm{d}}{\mathrm{d}t}\langle \hat{K}_z\rangle = \gamma\langle \hat{K}_z\rangle$. (Trace is still preserved; TP does not imply stationarity of $\langle \hat{K}_a\rangle$.)

- **SU(1,1)-covariant ("flipped") pattern:** $\gamma_x = \gamma_y = \gamma$, $\gamma_z = -\gamma$. Then we have $\mathcal{L}^\dagger \hat{K}_x = \gamma\,\hat{K}_x$, $\mathcal{L}^\dagger \hat{K}_y = \gamma\,\hat{K}_y$, $\mathcal{L}^\dagger \hat{K}_z = \gamma\,\hat{K}_z$, i.e. all three first moments evolve with the same rate γ. This equality of eigenvalues on $\{\hat{K}_x, \hat{K}_y, \hat{K}_z\}$ is consistent with full SU(1,1) covariance.

D.2.5 Deriving the heat equation and its solution

Lemma D.2.

$$\langle\chi|f\hat{K}_+|\chi\rangle = \frac{\partial}{\partial\chi}\langle\chi|f|\chi\rangle + \frac{2k\bar{\chi}}{(1-|\chi|^2)}\langle\chi|f|\chi\rangle, \tag{D.77}$$

$$\langle\chi|f\hat{K}_z|\chi\rangle = \chi\frac{\partial}{\partial\chi}\langle\chi|f|\chi\rangle + \frac{2k|\chi|^2}{(1-|\chi|^2)}\langle\chi|f|\chi\rangle + k\langle\chi|f|\chi\rangle, \tag{D.78}$$

$$\langle\chi|f\hat{K}_-|\chi\rangle = \chi^2\frac{\partial}{\partial\chi}\langle\chi|f|\chi\rangle + \frac{2k|\chi|^2\chi}{(1-|\chi|^2)}\langle\chi|f|\chi\rangle + 2k\chi\langle\chi|f|\chi\rangle. \tag{D.79}$$

Proof. We begin by proving (D.77). Taking the derivative of the coherent state definition (5.13) with respect to χ, we find

$$\frac{\partial}{\partial\chi}|\chi\rangle = -\frac{k\bar{\chi}}{1-|\chi|^2}|\chi\rangle + \hat{K}_+|\chi\rangle. \tag{D.80}$$

Taking the adjoint of (5.13) gives

$$\langle\chi| = (1-|\chi|^2)^k\,\langle k,k|\exp(\bar{\chi}\hat{K}_-), \tag{D.81}$$

from which we compute

$$\frac{\partial}{\partial\chi}\langle\chi| = -\frac{k\bar{\chi}}{1-|\chi|^2}\langle\chi|. \tag{D.82}$$

Now consider

$$\begin{aligned}\frac{\partial}{\partial\chi}\langle\chi|f|\chi\rangle &= \frac{\partial}{\partial\chi}\left(\langle\chi|f|\chi\rangle\right) = \left(\frac{\partial}{\partial\chi}\langle\chi|\right)f|\chi\rangle + \langle\chi|f\left(\frac{\partial}{\partial\chi}|\chi\rangle\right), \\ &= -\frac{2k\bar{\chi}}{1-|\chi|^2}\langle\chi|f|\chi\rangle + \langle\chi|f\hat{K}_+|\chi\rangle. \end{aligned} \tag{D.83}$$

Rearranging the above expression gives

$$\langle\chi|f\hat{K}_+|\chi\rangle = \frac{\partial}{\partial\chi}\langle\chi|f|\chi\rangle + \frac{2k\bar{\chi}}{1-|\chi|^2}\langle\chi|f|\chi\rangle. \tag{D.84}$$

To evaluate $\langle\chi|f\hat{K}_z|\chi\rangle$, we use the Baker-Campbell-Hausdorff formula

$$\begin{aligned}\exp(\chi\hat{K}_+)\hat{K}_z\exp(-\chi\hat{K}_+) &= \hat{K}_z + [\chi\hat{K}_+,\hat{K}_z] + \frac{1}{2}[\chi\hat{K}_+,[\chi\hat{K}_+,\hat{K}_z]] + \cdots, \\ &= \hat{K}_z - \chi\hat{K}_+. \end{aligned} \tag{D.85}$$

We now rewrite the above expression as

$$\hat{K}_z = \chi\hat{K}_+ + \exp(\chi\hat{K}_+)\hat{K}_z\exp(-\chi\hat{K}_+). \tag{D.86}$$

Taking the expectation value with $\langle\chi|f$ and $|\chi\rangle$ and applying $\hat{K}_z|k,k\rangle = k|k,k\rangle$, we find

$$\langle\chi|f\hat{K}_z|\chi\rangle = \chi\langle\chi|f\hat{K}_+|\chi\rangle + k\langle\chi|f|\chi\rangle. \tag{D.87}$$

Substituting (D.77) yields (D.78).
To compute $\langle\chi|f\hat{K}_-|\chi\rangle$, we again use the BCH formula

$$\exp(\chi\hat{K}_+)\hat{K}_-\exp(-\chi\hat{K}_+) = \hat{K}_- - 2\chi\hat{K}_z + \chi^2\hat{K}_+. \tag{D.88}$$

Taking the expectation value and noting $\hat{K}_-|k,k\rangle = 0$, we get

$$0 = \langle\chi|f\hat{K}_-|\chi\rangle - 2\chi\langle\chi|f\hat{K}_z|\chi\rangle + \chi^2\langle\chi|f\hat{K}_+|\chi\rangle. \tag{D.89}$$

Solving for $\langle\chi|f\hat{K}_-|\chi\rangle$ and substituting the earlier results gives the expression in (D.79), completing the proof.
Taking Hermitian adjoints of the above results yields

$$\langle\chi|\hat{K}_-f|\chi\rangle = \frac{\partial}{\partial\bar{\chi}}\langle\chi|f|\chi\rangle + \frac{2k\chi}{1-|\chi|^2}\langle\chi|f|\chi\rangle, \tag{D.90}$$

$$\langle\chi|\hat{K}_zf|\chi\rangle = \langle\chi|\frac{\partial}{\partial\bar{\chi}}\langle\chi|f|\chi\rangle + \frac{2k|\chi|^2}{1-|\chi|^2}\langle\chi|f|\chi\rangle + k\langle\chi|f|\chi\rangle, \tag{D.91}$$

$$\langle\chi|\hat{K}_+f|\chi\rangle = \chi^2\frac{\partial}{\partial\bar{\chi}}\langle\chi|f|\chi\rangle + \frac{2k|\chi|^2\bar{\chi}}{1-|\chi|^2}\langle\chi|f|\chi\rangle + 2k\bar{\chi}\langle\chi|f|\chi\rangle. \tag{D.92}$$

□

We now demonstrate that the Husimi representation of (5.49) for the group $\mathrm{SU}(1,1)$ reduces to the heat equation on the Lobachevsky (hyperbolic) plane.

Proposition D.2. *The Husimi density function satisfies the following differential equation*

$$\frac{\mathrm{d}Q}{\mathrm{d}t} = \frac{\gamma}{2}(1-|\chi|^2)^2\frac{\partial^2 Q}{\partial\chi\partial\bar{\chi}}, \tag{D.93}$$

which is the diffusion equation in the Poincaré disk representation, $\gamma \in \mathbb{R}$ is the decoherence parameter.

Proof. We compute the Husimi symbols of the operators $\hat{K}_+$, $\hat{K}_-$, and $\hat{K}_z$, using the differential representations derived in Lemma D.2. In the Husimi picture, operator expectation values become differential operators acting on the Q-function.

$$\begin{aligned}
\frac{1}{2}(\langle\chi|\hat{K}_+\hat{\rho}\hat{K}_-|\chi\rangle) &= \frac{1}{2}\left(\bar{\chi}^2\frac{\partial}{\partial\bar{\chi}} + \frac{2k|\chi|^2\bar{\chi}}{(1-|\chi|^2)} + 2\bar{\chi}k\right)\left(\chi^2\frac{\partial}{\partial\chi} + \frac{2k|\chi|^2\chi}{(1-|\chi|^2)} + 2\chi k\right)Q(\chi), \\
&= \frac{1}{2}\left(|\chi|^4\frac{\partial^2 Q}{\partial\chi\partial\bar{\chi}} + \frac{2k|\chi|^2\bar{\chi}}{1-|\chi|^2}\frac{\partial Q}{\partial\bar{\chi}} + \frac{2k|\chi|^2\chi}{1-|\chi|^2}\frac{\partial Q}{\partial\chi} + \frac{2k|\chi|^4 Q}{(1-|\chi|^2)^2} + \frac{4k^2|\chi|^2 Q}{(1-|\chi|^2)^2}\right), \\
&= \frac{1}{2}\left(|\chi|^4\frac{\partial^2 Q}{\partial\chi\partial\bar{\chi}} + \frac{2k|\chi|^2\bar{\chi}}{1-|\chi|^2}\frac{\partial Q}{\partial\bar{\chi}} + \frac{2k|\chi|^2\chi}{1-|\chi|^2}\frac{\partial Q}{\partial\chi} + \frac{2k|\chi|^2(|\chi|^2+2k)Q}{(1-|\chi|^2)^2}\right).
\end{aligned} \tag{D.94}$$

Similarly, we can calculate $\langle\chi|\hat{K}_+\hat{\rho}\hat{K}_-|\chi\rangle$ to be

$$\begin{aligned}
\frac{1}{2}(\langle\chi|\hat{K}_+\hat{\rho}\hat{K}_-|\chi\rangle) &= \frac{1}{2}\left(\frac{\partial}{\partial\chi} + \frac{2k\bar{\chi}}{(1-|\chi|^2)}\right)\left(\frac{\partial}{\partial\bar{\chi}} + \frac{2k\chi}{1-|\chi|^2}\right)Q, \\
&= \frac{1}{2}\left(\frac{\partial^2 Q}{\partial\chi\partial\bar{\chi}} + \frac{2k}{(1-|\chi|^2)}\left(\bar{\chi}\frac{\partial Q}{\partial\chi} + \chi\frac{\partial Q}{\partial\chi}\right) + \frac{2kQ(1+2k|\chi|^2)}{(1-|\chi|^2)^2}\right).
\end{aligned} \tag{D.95}$$

And finally $\langle\chi|\hat{K}_z\hat{\rho}\hat{K}_z|\chi\rangle$ is calculated to be

$$\begin{aligned}
\langle\chi|\hat{K}_z\hat{\rho}\hat{K}_z|\chi\rangle &= \left(\bar{\chi}\frac{\partial}{\partial\bar{\chi}} + \frac{2k|\chi|^2}{1-|\chi|^2} + k\right)\left(\chi\frac{\partial}{\partial\chi} + \frac{2k|\chi|^2}{1-|\chi|^2} + k\right)Q, \\
&= |\chi|^2\frac{\partial^2 Q}{\partial\chi\partial\bar{\chi}} + k\frac{(1+|\chi|^2)}{(1-|\chi|^2)}\left(\chi\frac{\partial Q}{\partial\chi} + \bar{\chi}\frac{\partial Q}{\partial\bar{\chi}}\right) + \frac{2k(2k+1)|\chi|^2 Q}{(1-|\chi|^2)^2} + k^2 Q.
\end{aligned} \tag{D.96}$$

Combining the terms, gives the desired result and this completes the proof. □

We now transform this expression into hyperbolic polar coordinates on the Poincaré disk. Using the parametrisation $\chi = \tanh\left(\frac{\tau}{2}\right)\mathrm{e}^{-\mathrm{i}\phi}$ we compute the differential operators

$$\begin{aligned}
\frac{\partial}{\partial\chi} &= \cosh^2\left(\frac{\tau}{2}\right)\mathrm{e}^{\mathrm{i}\phi}\frac{\partial}{\partial\tau} + \frac{\mathrm{i}\mathrm{e}^{\mathrm{i}\phi}}{2\tanh\left(\frac{\tau}{2}\right)}\frac{\partial}{\partial\phi}, \\
\frac{\partial}{\partial\bar{\chi}} &= \cosh^2\left(\frac{\tau}{2}\right)\mathrm{e}^{-\mathrm{i}\phi}\frac{\partial}{\partial\tau} - \frac{\mathrm{i}\mathrm{e}^{-\mathrm{i}\phi}}{2\tanh\left(\frac{\tau}{2}\right)}\frac{\partial}{\partial\phi}.
\end{aligned} \tag{D.97}$$

Now using this we can calculate (D.93) in hyperbolic polar coordinates to be

$$\frac{\mathrm{d}Q(\tau,\phi)}{\mathrm{d}t} = \frac{\gamma}{2}\left(\frac{\partial^2}{\partial\tau^2} + \frac{1}{\sinh^2(\tau)}\frac{\partial^2}{\partial\phi^2} + \coth(\tau)\frac{\partial}{\partial\tau}\right)Q(\tau,\phi). \tag{D.98}$$

Appendix E

Stochastic processes, unravellings and other derivations

This appendix reviews the mathematical background on probability theory and stochastic processes needed for Chapter 6. We outline the key concepts of martingales, stochastic differential equations, and diffusion processes, and then provide detailed proofs of the propositions and technical results stated in the main text.

E.1 Mathematical background

Probability space and events

A probability space is a triple $(\Omega, \mathcal{F}, \mathbb{P})$, where Ω is the sample space of all possible outcomes, $\mathcal{F}$ is a σ-algebra of subsets of Ω called events, and $\mathbb{P}$ is a probability measure. The σ-algebra $\mathcal{F}$ satisfies closure under complementation and countable unions, ensuring that events can be consistently combined and measured. The measure $\mathbb{P} : \mathcal{F} \to [0, 1]$ assigns probabilities to events such that $\mathbb{P}(\Omega) = 1$ and is countably additive on disjoint collections. Each $\omega \in \Omega$ represents a realisation of the underlying random experiment, and an event $A \in \mathcal{F}$ is a well-defined question to which the model assigns a probability $\mathbb{P}(A)$. This structure provides the foundation for defining stochastic processes and the probabilistic evolution of quantum systems under continuous observation.

Random variables and distributions

Once a probability space $(\Omega, \mathcal{F}, \mathbb{P})$ is specified, observable quantities are represented by random variables, defined as measurable functions from Ω to a target measurable space $(\Gamma, \mathcal{G})$, where Γ is a set equipped with a σ-algebra $\mathcal{G}$. A function $X : \Omega \to \Gamma$ is measurable if the pre-image of every $G \in \mathcal{G}$ lies in $\mathcal{F}$, ensuring that the event "$X(\omega) \in G$" is a well-defined element of the probability space.

A particularly important case arises when $\Gamma = \mathbb{R}$ and $\mathcal{G}$ is the Borel σ-algebra, in which case X is called a real-valued random variable. Such variables are the probabilistic analogues of classical observables, assigning numerical values to outcomes $\omega \in \Omega$, and forming the foundation for defining stochastic processes.

Probability distribution and cumulative function

The probability distribution of a random variable X is given by its pushforward measure μ_X, defined on $(\mathbb{R}, \mathcal{B}(\mathbb{R}))$ via $\mu_X(B) = \mathbb{P}(X^{-1}(B))$ for all Borel sets $B \subseteq \mathbb{R}$. The associated cumulative distribution function (CDF) is $F_X(x) = \mathbb{P}(X \leq x)$, which gives the probability that the observable X takes a value less than or equal to x.

Expectation value

The expectation (or expected value) of a nonnegative random variable $X \geq 0$ is defined by the Lebesgue integral $\mathbb{E}[X] = \int_\Omega X(\omega)\,\mathrm{d}\mathbb{P}(\omega)$. For a general real-valued random variable X, the expectation is defined via its decomposition into positive and negative parts: $\mathbb{E}[X] = \mathbb{E}[X^+] - \mathbb{E}[X^-]$, where $X^+ = \max(X, 0)$ and $X^- = -\min(X, 0)$. The expectation exists whenever X is integrable, i.e., $\mathbb{E}[|X|] < \infty$.

Stochastic processes and filtrations

A stochastic process is a family of random variables $\{X_t\}_{t\geq 0}$ on a common probability space $(\Omega, \mathcal{F}, \mathbb{P})$, where each $X_t : \Omega \to \mathbb{R}$ is measurable and represents the state of the system at time t.

To formalise the temporal flow of information, we introduce a filtration $\{\mathcal{F}_t\}_{t\geq 0}$, an increasing family of sub-σ-algebras satisfying $\mathcal{F}_s \subseteq \mathcal{F}_t \subseteq \mathcal{F}$ for $0 \leq s \leq t$. The σ-algebra $\mathcal{F}_t$ encodes all events observable up to time t.

A process $\{X_t\}$ is adapted to the filtration if X_t is $\mathcal{F}_t$-measurable for each t, ensuring that its value depends only on information available up to that time.

Conditional expectation

Given a random variable X and a sub-σ-algebra $\mathcal{G} \subseteq \mathcal{F}$, the conditional expectation $\mathbb{E}[X|\mathcal{G}]$ is a $\mathcal{G}$-measurable random variable satisfying $\int_A \mathbb{E}[X|\mathcal{G}]\,\mathrm{d}\mathbb{P} = \int_A X\,\mathrm{d}\mathbb{P}, \quad \text{for all } A \in \mathcal{G}$. It represents the best estimate of X given the information contained in $\mathcal{G}$. When $\mathcal{G} = \mathcal{F}_t$, we write $\mathbb{E}_t[X] = \mathbb{E}[X|\mathcal{F}_t]$, denoting the expectation conditioned on information available up to time t.

Conditional expectation satisfies the tower property: $\mathbb{E}[\mathbb{E}[X|\mathcal{G}]] = \mathbb{E}[X]$, and more generally, $\mathbb{E}[\mathbb{E}[X|\mathcal{G}_2]|\mathcal{G}_1] = \mathbb{E}[X|\mathcal{G}_1]$ if $\mathcal{G}_1 \subseteq \mathcal{G}_2$. These identities are central to the analysis of multi-step stochastic processes and will be used extensively in the discussion of martingales and stochastic integrals.

Martingales and supermartingales

Let $\{X_t\}_{t\geq 0}$ be a stochastic process adapted to a filtration $\{\mathcal{F}_t\}$. It is called a *martingale* if $\mathbb{E}[|X_t|] < \infty$ for all t, and $\mathbb{E}[X_t|\mathcal{F}_s] = X_s$ for all $s < t$. Martingales represent "fair game" processes, with no systematic drift in the conditional mean. In physical contexts, they often correspond to conserved quantities under stochastic dynamics or unbiased measurement processes.

More generally, if $\mathbb{E}[X_t|\mathcal{F}_s] \leq X_s$, the process is a *supermartingale*; if $\mathbb{E}[X_t|\mathcal{F}_s] \geq X_s$, it is a *submartingale*. These describe processes with systematic drift, such as dissipative dynamics or measurement-induced information gain in quantum systems.

Brownian motion:

A real-valued process $\{W_t\}_{t\geq 0}$ is called a *standard Wiener process* (or Brownian motion) with respect to a filtration $\{\mathcal{F}_t\}$ if it satisfies $W_0 = 0$ almost surely; $t \mapsto W_t$ is almost surely continuous; the increment $W_t - W_s$ is independent of $\mathcal{F}_s$ and normally distributed with mean zero and variance $t - s$ for all $0 \leq s < t$; and $\{W_t\}$ is adapted to the filtration. Brownian motion models continuous, memoryless noise and serves as the fundamental source of randomness in the stochastic differential equations considered throughout this work.

Itô integral and Itô processes:

Let $\{a_t\}$ and $\{b_t\}$ be real-valued, progressively measurable processes satisfying

$$\mathbb{E}\left[\int_0^T |a_s|\,\mathrm{d}s + \int_0^T |b_s|^2\,\mathrm{d}s\right] < \infty \quad \text{for all } T > 0. \tag{E.1}$$

A process is progressively measurable with respect to $\{\mathcal{F}_t\}$ if, for each $t \geq 0$, its restriction to $[0, t]$ is measurable with respect to $\mathcal{B}([0, t]) \otimes \mathcal{F}_t$. This condition ensures that the process evolves causally and is compatible with the stochastic integral framework.

Given such processes, the evolution

$$X_t = X_0 + \int_0^t a_s\,\mathrm{d}s + \int_0^t b_s\,\mathrm{d}W_s \tag{E.2}$$

defines an *Itô process*. The first integral is interpreted in the standard Lebesgue sense, while the second is the *Itô integral*, defined as the limit in probability of stochastic Riemann sums of the form $\sum_k b_{t_k}(W_{t_{k+1}} - W_{t_k})$. The Itô integral is well-defined despite the nowhere-differentiable nature of Brownian paths and forms the foundation of stochastic calculus.

Itô's lemma (real version):

Let X_t be an Itô process as above, and let $f \in C^{2,1}(\mathbb{R} \times [0, \infty))$, meaning that $f(x, t)$ is twice continuously differentiable in x and once in t. Then the process $Y_t = f(X_t, t)$ satisfies the stochastic differential equation

$$\mathrm{d}f(X_t, t) = \left(\frac{\partial f}{\partial t} + a_t \frac{\partial f}{\partial x} + \frac{1}{2} b_t^2 \frac{\partial^2 f}{\partial x^2}\right)\mathrm{d}t + b_t \frac{\partial f}{\partial x}\,\mathrm{d}W_t. \tag{E.3}$$

This result is the stochastic analogue of the chain rule. The second-order term, absent in classical calculus, reflects the nonnegligible quadratic variation of Brownian paths and is central to the theory of stochastic evolution.

Stochastic differential equations (SDEs):

A *stochastic differential equation* is an equation of the form

$$\mathrm{d}X_t = a(X_t, t)\,\mathrm{d}t + b(X_t, t)\,\mathrm{d}W_t, \quad X_0 = x_0, \tag{E.4}$$

where a and b are prescribed functions. Under suitable Lipschitz and linear growth conditions, such equations admit a unique strong solution adapted to the filtration generated by the Brownian motion.

In quantum physics, SDEs are used to model the evolution of quantum states subject to continuous measurement, feedback, and interaction with an environment, culminating in the theory of stochastic Schrödinger equations.

Complex Itô calculus and Wirtinger derivatives

In many quantum applications, particularly those involving coherent states or wavefunctions, the natural variables of the system are complex-valued. To extend Itô calculus to this setting, we consider complex Itô processes and employ *Wirtinger calculus*, a convenient formalism for differentiating functions of complex variables.

Let $Z_t = X_t + \mathrm{i}Y_t$ be a complex-valued Itô process, where X_t and Y_t are real Itô processes. Then Z_t satisfies a stochastic differential equation of the form

$$\mathrm{d}Z_t = \mu(Z_t, t)\,\mathrm{d}t + \sigma(Z_t, t)\,\mathrm{d}W_t, \tag{E.5}$$

where μ and σ are complex-valued functions, and W_t is real Brownian motion.

Let $f(Z, \bar{Z}, t)$ be a complex-valued function of $Z \in \mathbb{C}$ and its complex conjugate $\bar{Z}$. The *Wirtinger derivatives* of f are defined as

$$\frac{\partial f}{\partial Z} = \frac{1}{2}\left(\frac{\partial f}{\partial X} - \mathrm{i}\frac{\partial f}{\partial Y}\right), \quad \frac{\partial f}{\partial \bar{Z}} = \frac{1}{2}\left(\frac{\partial f}{\partial X} + \mathrm{i}\frac{\partial f}{\partial Y}\right), \tag{E.6}$$

where $Z = X + \mathrm{i}Y$. A function $f(Z)$ is *holomorphic* if it is independent of $\bar{Z}$, i.e. $\partial f/\partial \bar{Z} = 0$.

For the case where $\mu, \sigma \in \mathbb{C}$ are constants (or adapted processes), and W_t is a standard real Wiener process, applying Itô's lemma in this complex setting gives

$$\begin{aligned} \mathrm{d}f(Z_t, \bar{Z}_t, t) \;=\; & \left(\frac{\partial f}{\partial t} + \mu\frac{\partial f}{\partial Z_t} + \bar{\mu}\frac{\partial f}{\partial \bar{Z}_t} + \frac{1}{2}\sigma^2\frac{\partial^2 f}{\partial Z_t^2} + \frac{1}{2}\bar{\sigma}^2\frac{\partial^2 f}{\partial \bar{Z}_t^2} + \frac{1}{2}|\sigma|^2\frac{\partial^2 f}{\partial Z_t \partial \bar{Z}_t}\right)\mathrm{d}t \\ & + \sigma\frac{\partial f}{\partial Z_t}\,\mathrm{d}W_t + \bar{\sigma}\frac{\partial f}{\partial \bar{Z}_t}\,\mathrm{d}W_t. \end{aligned} \tag{E.7}$$

When f is holomorphic, all terms involving $\bar{Z}_t$ vanish.

E.2 Proofs of technical results

E.2.1 Proof of lemma 6.1

Proof. We prove that the stochastic Schrödinger equation

$$\begin{aligned} \mathrm{d}|\psi_t\rangle \;=\; & -\frac{\mathrm{i}}{\hbar}\hat{H}|\psi_t\rangle\,\mathrm{d}t - \frac{\sigma^2}{8}\sum_k \left(\hat{L}^{k\dagger}\hat{L}^k - 2\overline{L_t^k}\hat{L}^k + |L_t^k|^2\right)|\psi_t\rangle\,\mathrm{d}t \\ & + \frac{\sigma}{2}\sum_k \left(\hat{L}^k - L_t^k\right)|\psi_t\rangle\,\mathrm{d}W_t^k, \end{aligned} \tag{E.8}$$

preserves the norm, where $L_t^k = \langle\psi_t|\hat{L}^k|\psi_t\rangle$. Define $N_t = \langle\psi_t|\psi_t\rangle$. By Itô's lemma,

$$\mathrm{d}N_t = \langle \mathrm{d}\psi_t|\psi_t\rangle + \langle\psi_t|\mathrm{d}\psi_t\rangle + \langle \mathrm{d}\psi_t|\mathrm{d}\psi_t\rangle. \tag{E.9}$$

We first calculate $\langle \mathrm{d}\psi_t|\psi_t\rangle$ to be

$$\begin{aligned}\langle \mathrm{d}\psi_t|\psi_t\rangle &= -\frac{\mathrm{i}}{\hbar}\langle\psi_t|\hat{H}|\psi_t\rangle\,\mathrm{d}t - \frac{\sigma^2}{8}\sum_k\left(\langle\psi_t|\hat{L}^{k\dagger}\hat{L}^k|\psi_t\rangle - 2|L_t^k|^2 + |L_t^k|^2\right)\mathrm{d}t \\ &\quad + \frac{\sigma}{2}\sum_k\left(\langle\psi_t|\hat{L}^{k\dagger}|\psi_t\rangle - \overline{L_t^k}\right)\mathrm{d}W_t^k.\end{aligned} \tag{E.10}$$

Taking the adjoint of the above equation gives

$$\begin{aligned}\langle\psi_t|\mathrm{d}\psi_t\rangle &= \frac{\mathrm{i}}{\hbar}\langle\psi_t|\hat{H}|\psi_t\rangle\,\mathrm{d}t - \frac{\sigma^2}{8}\sum_k\left(\langle\psi_t|\hat{L}^{k\dagger}\hat{L}^k|\psi_t\rangle - 2|L_t^k|^2 + |L_t^k|^2\right)\mathrm{d}t \\ &\quad + \frac{\sigma}{2}\sum_k\left(\langle\psi_t|\hat{L}^k|\psi_t\rangle - L_t^k\right)\mathrm{d}W_t^k.\end{aligned} \tag{E.11}$$

Finally the Itô correction term is calculated to be

$$\langle \mathrm{d}\psi_t|\mathrm{d}\psi_t\rangle = \left(\frac{\sigma}{2}\right)^2\sum_k\left\langle\left(\hat{L}^k - L_t^k\right)\psi_t\right|\left(\hat{L}^k - L_t^k\right)\psi_t\Big\rangle\,\mathrm{d}t = \frac{\sigma^2}{4}\sum_k\left(\langle\psi_t|\hat{L}^{k\dagger}\hat{L}^k|\psi_t\rangle - |L_t^k|^2\right)\mathrm{d}t. \tag{E.12}$$

Combining all three terms yields

$$\begin{aligned}\mathrm{d}N_t &= \left(-\frac{\sigma^2}{8}\sum_k(\langle\hat{L}^{k\dagger}\hat{L}^k\rangle - |L_t^k|^2)\right)\mathrm{d}t + \left(-\frac{\sigma^2}{8}\sum_k(\langle\hat{L}^{k\dagger}\hat{L}^k\rangle - |L_t^k|^2)\right)\mathrm{d}t \\ &\quad + \left(\frac{\sigma^2}{4}\sum_k(\langle\hat{L}^{k\dagger}\hat{L}^k\rangle - |L_t^k|^2)\right)\mathrm{d}t, \\ &= 0.\end{aligned} \tag{E.13}$$

Hence, the norm is preserved for all t, i.e.,

$$\langle\psi_t|\psi_t\rangle = \langle\psi_0|\psi_0\rangle = 1. \tag{E.14}$$

□

E.2.2 Proof of proposition 6.1

Proof. We want to compute the time evolution of the ensemble-averaged density matrix

$$\hat{\rho}_t = \mathbb{E}[\hat{R}_t] = \mathbb{E}\left[|\psi_t\rangle\langle\psi_t|\right]. \tag{E.15}$$

Applying Itô's product rule on $\hat{\rho}_t$ gives

$$\mathrm{d}(\hat{\rho}_t) = \mathrm{d}(|\psi_t\rangle\langle\psi_t|) = (\mathrm{d}|\psi_t\rangle)\langle\psi_t| + |\psi_t\rangle(\mathrm{d}\langle\psi_t|) + (\mathrm{d}|\psi_t\rangle)(\mathrm{d}\langle\psi_t|). \tag{E.16}$$

The first term is calculated to be

$$(\mathrm{d}|\psi_t\rangle)\langle\psi_t| = \left[-\frac{\mathrm{i}}{\hbar}\hat{H}|\psi_t\rangle\,\mathrm{d}t - \frac{\sigma^2}{8}\sum_k\left(\hat{L}^{k\dagger}\hat{L}^k - 2\overline{L_t^k}\hat{L}^k + |L_t^k|^2\right)|\psi_t\rangle\,\mathrm{d}t + \frac{\sigma}{2}\sum_k\left(\hat{L}^k - L_t^k\right)|\psi_t\rangle\,\mathrm{d}W_t^k\right]\langle\psi_t|. \tag{E.17}$$

Taking its adjoint gives the second term

$$|\psi_t\rangle(\mathrm{d}\langle\psi_t|) = |\psi_t\rangle\left[\frac{\mathrm{i}}{\hbar}\langle\psi_t|\hat{H}\,\mathrm{d}t - \frac{\sigma^2}{8}\sum_k\left(\langle\psi_t|\hat{L}^{k\dagger}\hat{L}^k - 2L_t^k\hat{L}^{k\dagger} + |L_t^k|^2\right)\mathrm{d}t + \frac{\sigma}{2}\sum_k\langle\psi_t|\left(\hat{L}^{k\dagger} - \overline{L_t^k}\right)\mathrm{d}W_t^k\right], \tag{E.18}$$

and finally the Itô correction term is calculated to be

$$(\mathrm{d}|\psi_t\rangle)(\mathrm{d}\langle\psi_t|) = \frac{\sigma^2}{4}\sum_k\left(\hat{L}^k - L_t^k\right)|\psi_t\rangle\langle\psi_t|\left(\hat{L}^{k\dagger} - \overline{L_t^k}\right)\mathrm{d}t. \tag{E.19}$$

Adding all three terms and taking the expectation value, all stochastic terms proportional to $\mathrm{d}W_t^k$ vanish. The remaining deterministic part yields

$$\frac{\mathrm{d}\hat{\rho}_t}{\mathrm{d}t} = -\frac{\mathrm{i}}{\hbar}\left[\hat{H},\hat{\rho}_t\right] + \sum_k\frac{\sigma^2}{8}\,\mathbb{E}\left[\hat{L}^k|\psi_t\rangle\langle\psi_t|\hat{L}^{k\dagger} - \frac{1}{2}\left\{\hat{L}^{k\dagger}\hat{L}^k, |\psi_t\rangle\langle\psi_t|\right\}\right]. \tag{E.20}$$

Taking expectation over the stochastic process and using linearity

$$\frac{\mathrm{d}\hat{\rho}_t}{\mathrm{d}t} = -\frac{\mathrm{i}}{\hbar}[\hat{H},\hat{\rho}_t] + \sum_k\frac{\sigma^2}{8}\left(\hat{L}^k\hat{\rho}_t\hat{L}^{k\dagger} - \frac{1}{2}\left\{\hat{L}^{k\dagger}\hat{L}^k,\hat{\rho}_t\right\}\right), \tag{E.21}$$

where $\hat{\rho}_t = \mathbb{E}[\hat{\rho}_t]$. This is the standard Lindblad master equation with decoherence rate $\gamma_k = \sigma^2/8$. □

E.2.3 Proof of proposition 6.2

Proof. We begin from the definition $|\alpha_t\rangle = \exp(\alpha_t\hat{a}^\dagger - \bar{\alpha}_t\hat{a})|0\rangle$. Using the Baker-Campbell-Hausdorff (BCH) formula [49], we may write the displacement operator in disentangled form

$$\begin{aligned}\exp(\alpha_t\hat{a}^\dagger - \bar{\alpha}_t\hat{a}) &= \exp(-|\alpha_t|^2/2)\exp(\alpha_t\hat{a}^\dagger)\exp(-\bar{\alpha}_t\hat{a}),\\ &= \exp(|\alpha_t|^2/2)\exp(-\bar{\alpha}_t\hat{a})\exp(\alpha_t\hat{a}^\dagger).\end{aligned} \tag{E.22}$$

We choose the first expression for convenience. Then by applying Itô's formula for vector-valued functions, we compute

$$\begin{aligned}\frac{\partial|\alpha_t\rangle}{\partial\alpha_t} &= \left(\hat{a}^\dagger - \frac{\bar{\alpha}_t}{2}\right)|\alpha_t\rangle,\\ \frac{\partial|\alpha_t\rangle}{\partial\bar{\alpha}_t} &= \left(\frac{\alpha_t}{2} - \hat{a}\right)|\alpha_t\rangle.\end{aligned} \tag{E.23}$$

Similarly, the second derivatives yield

$$\begin{aligned}\frac{\partial^2|\alpha_t\rangle}{\partial\alpha_t^2} &= \left(\hat{a}^{\dagger 2} - \hat{a}^\dagger\bar{\alpha}_t + \frac{(\bar{\alpha}_t)^2}{4}\right)|\alpha_t\rangle,\\ \frac{\partial^2|\alpha_t\rangle}{\partial(\bar{\alpha}_t)^2} &= \left(\hat{a}^2 - \hat{a}\alpha_t + \frac{\alpha_t^2}{4}\right)|\alpha_t\rangle.\end{aligned} \tag{E.24}$$

The mixed derivative is

$$\frac{\partial^2|\alpha_t\rangle}{\partial\alpha_t\partial\bar{\alpha}_t} = -\frac{1}{2}\left(\hat{a}\hat{a}^\dagger + \hat{a}^\dagger\hat{a} - \hat{a}\bar{\alpha}_t - \hat{a}^\dagger\alpha_t + \frac{|\alpha_t|^2}{2}\right)|\alpha_t\rangle, \tag{E.25}$$

which has been simplified (using $[\hat{a}, \hat{a}^\dagger] = 1$). Substituting for $\mathrm{d}\alpha_t$ from (6.7), the SDE simplifies to

$$\begin{aligned}\mathrm{d}|\alpha_t\rangle &= \frac{\sigma}{\sqrt{2}}\left(\hat{a}^\dagger - \frac{\bar{\alpha}_t}{2}\right)|\alpha_t\rangle\,\mathrm{d}W_t^x + \frac{\mathrm{i}\sigma}{\sqrt{2}}\left(\hat{a}^\dagger - \frac{\bar{\alpha}_t}{2}\right)|\alpha_t\rangle\,\mathrm{d}W_t^p\\ &\quad -\frac{\sigma}{\sqrt{2}}\left(\hat{a} - \frac{\alpha_t}{2}\right)|\alpha_t\rangle\,\mathrm{d}W_t^x + \frac{\mathrm{i}\sigma}{\sqrt{2}}\left(\hat{a} - \frac{\alpha_t}{2}\right)|\alpha_t\rangle\,\mathrm{d}W_t^p\\ &\quad -\frac{\sigma^2}{2}\left(\hat{a}\hat{a}^\dagger + \hat{a}^\dagger\hat{a} - \hat{a}\bar{\alpha}_t - \hat{a}^\dagger\alpha_t + \frac{|\alpha_t|^2}{2}\right)|\alpha_t\rangle\,\mathrm{d}t.\end{aligned} \tag{E.26}$$

□

E.2.4 Proof of proposition 6.6

Proof. Set $r_t = \beta - \alpha_t$, so that $P_t(\beta) = \exp(-|r_t|^2)$ with $|r_t|^2 = r_t\bar{r}_t$. First compute the differential of $|r_t|^2$ via Itô's lemma

$$\mathrm{d}|r_t|^2 = \mathrm{d}(r_t\bar{r}_t) = \bar{r}_t\,\mathrm{d}r_t + r_t\,\mathrm{d}\bar{r}_t + \mathrm{d}r_t\,\mathrm{d}\bar{r}_t. \tag{E.27}$$

Because $\mathrm{d}r_t = -\mathrm{d}\alpha_t$ and $\mathrm{d}\bar{r}_t = -\mathrm{d}\bar{\alpha}_t$, we have for $f_t = -|r_t|^2$,

$$\mathrm{d}f_t = -\,\mathrm{d}|r_t|^2 = \bar{r}_t\,\mathrm{d}\alpha_t + r_t\,\mathrm{d}\bar{\alpha}_t - \mathrm{d}\alpha_t\,\mathrm{d}\bar{\alpha}_t. \tag{E.28}$$

Insert the noise representation (6.7) to get the stochastic part of $\mathrm{d}f_t$

$$\begin{aligned}\bar{r}_t\,\mathrm{d}\alpha_t + r_t\,\mathrm{d}\bar{\alpha}_t &= \frac{\sigma}{\sqrt{2}}\Big[(\bar{r}_t + r_t)\,\mathrm{d}W_t^x + \mathrm{i}(\bar{r}_t - r_t)\,\mathrm{d}W_t^p\Big],\\ &= \sqrt{2}\sigma\Big(\mathrm{Re}[r_t]\,\mathrm{d}W_t^x + \mathrm{Im}[r_t]\,\mathrm{d}W_t^p\Big).\end{aligned} \tag{E.29}$$

The Itô correction in $\mathrm{d}f_t$ is $-\mathrm{d}\alpha_t\,\mathrm{d}\bar{\alpha}_t = -\sigma^2\,\mathrm{d}t$. Hence,

$$\mathrm{d}f_t = \sqrt{2}\sigma\Big(\mathrm{Re}[r_t]\,\mathrm{d}W_t^x + \mathrm{Im}[r_t]\,\mathrm{d}W_t^p\Big) - \sigma^2\,\mathrm{d}t. \tag{E.30}$$

Next, apply the Itô formula for the exponential $P_t = \exp(f_t)$

$$\mathrm{d}P_t = P_t\,\mathrm{d}f_t + \frac{1}{2}P_t\,(\mathrm{d}f_t)^2. \tag{E.31}$$

Since $(\mathrm{d}W_t^x)^2 = (\mathrm{d}W_t^p)^2 = \mathrm{d}t$ and $\mathrm{d}W_t^x\,\mathrm{d}W_t^p = 0$, the quadratic variation is

$$(\mathrm{d}f_t)^2 = 2\sigma^2\Big(\mathrm{Re}[r_t]^2 + \mathrm{Im}[r_t]^2\Big)\,\mathrm{d}t = 2\sigma^2\,|r_t|^2\,\mathrm{d}t. \tag{E.32}$$

Therefore,

$$\mathrm{d}P_t = \sqrt{2}\sigma\,\mathrm{Re}[r_t]\,P_t\,\mathrm{d}W_t^x \;+\; \sqrt{2}\sigma\,\mathrm{Im}[r_t]\,P_t\,\mathrm{d}W_t^p \;+\; \sigma^2\big(-1+|r_t|^2\big)\,P_t\,\mathrm{d}t. \tag{E.33}$$

Finally, expand $|r_t|^2 = |\beta-\alpha_t|^2 = |\beta|^2+|\alpha_t|^2-\beta\bar{\alpha}_t-\bar{\beta}\alpha_t$ to obtain

$$\sigma^2\big(-1+|r_t|^2\big) = \sigma^2\Big(-1+|\alpha_t|^2+|\beta|^2-\beta\bar{\alpha}_t-\bar{\beta}\alpha_t\Big), \tag{E.34}$$

which yields the stated SDE. □

E.2.5 Proof of proposition 6.7

Proof. We apply Itô's lemma to compute the differential of the rank-one projector $|\alpha_t\rangle\langle\alpha_t|$

$$\mathrm{d}(|\alpha_t\rangle\langle\alpha_t|) = \mathrm{d}|\alpha_t\rangle\langle\alpha_t| + |\alpha_t\rangle\mathrm{d}\langle\alpha_t| + \mathrm{d}|\alpha_t\rangle\mathrm{d}\langle\alpha_t|. \tag{E.35}$$

Substituting for $\mathrm{d}|\alpha_t\rangle$ from (6.9), we compute each term individually. First, the product $\mathrm{d}|\alpha_t\rangle\langle\alpha_t|$ gives:

$$\begin{aligned}\mathrm{d}|\alpha_t\rangle\langle\alpha_t| \;=\; & -\frac{\sigma^2}{2}\left(\hat{a}\hat{a}^\dagger+\hat{a}^\dagger\hat{a}-\hat{a}\bar{\alpha}_t-\hat{a}^\dagger\alpha_t+\frac{|\alpha_t|^2}{2}\right)|\alpha_t\rangle\langle\alpha_t|\,\mathrm{d}t+\frac{\sigma}{\sqrt{2}}\left(\hat{a}^\dagger-\hat{a}+\frac{\alpha_t-\bar{\alpha}_t}{2}\right)|\alpha_t\rangle\langle\alpha_t|\,\mathrm{d}W_t^x\\ & +\frac{\mathrm{i}\sigma}{\sqrt{2}}\left(\hat{a}^\dagger+\hat{a}-\frac{\alpha_t+\bar{\alpha}_t}{2}\right)|\alpha_t\rangle\langle\alpha_t|\,\mathrm{d}W_t^p.\end{aligned} \tag{E.36}$$

Similarly, the adjoint term $|\alpha_t\rangle\mathrm{d}\langle\alpha_t|$ yields

$$\begin{aligned}|\alpha_t\rangle\mathrm{d}\langle\alpha_t| \;=\; & -\frac{\sigma^2}{2}|\alpha_t\rangle\langle\alpha_t|\left(\hat{a}\hat{a}^\dagger+\hat{a}^\dagger\hat{a}-\hat{a}\bar{\alpha}_t-\hat{a}^\dagger\alpha_t+\frac{|\alpha_t|^2}{2}\right)\mathrm{d}t+\frac{\sigma}{\sqrt{2}}|\alpha_t\rangle\langle\alpha_t|\left(-\hat{a}^\dagger+\hat{a}-\frac{\alpha_t-\bar{\alpha}_t}{2}\right)\mathrm{d}W_t^x\\ & -\frac{\mathrm{i}\sigma}{\sqrt{2}}|\alpha_t\rangle\langle\alpha_t|\left(\hat{a}^\dagger+\hat{a}-\frac{\alpha_t+\bar{\alpha}_t}{2}\right)\mathrm{d}W_t^p.\end{aligned} \tag{E.37}$$

The second-order Itô correction is given by

$$\begin{aligned}\mathrm{d}|\alpha_t\rangle\mathrm{d}\langle\alpha_t| \;&=\; \frac{\sigma^2}{2}(\hat{a}^\dagger-\hat{a})|\alpha_t\rangle\langle\alpha_t|(\hat{a}-\hat{a}^\dagger)\mathrm{d}t+\frac{\sigma^2}{2}(\hat{a}^\dagger+\hat{a})|\alpha_t\rangle\langle\alpha_t|(\hat{a}+\hat{a}^\dagger)\mathrm{d}t\\ &=\; \sigma^2\hat{a}^\dagger|\alpha_t\rangle\langle\alpha_t|\hat{a}+\sigma^2\hat{a}|\alpha_t\rangle\langle\alpha_t|\hat{a}^\dagger\mathrm{d}t.\end{aligned} \tag{E.38}$$

Combining all three contributions, we obtain

$$\begin{aligned}\mathrm{d}(|\alpha_t\rangle\langle\alpha_t|) \;=\; & \sigma^2\hat{a}^\dagger|\alpha_t\rangle\langle\alpha_t|\hat{a}+\sigma^2\hat{a}|\alpha_t\rangle\langle\alpha_t|\hat{a}^\dagger-\sigma^2\left(\frac{1}{2}(\hat{a}^\dagger\hat{a}+\hat{a}\hat{a}^\dagger)|\alpha_t\rangle\langle\alpha_t|+\frac{1}{2}|\alpha_t\rangle\langle\alpha_t|(\hat{a}^\dagger\hat{a}+\hat{a}\hat{a}^\dagger)\right)\mathrm{d}t\\ & +\frac{\sigma}{\sqrt{2}}[(\hat{a}-\hat{a}^\dagger)\,|\alpha_t\rangle\langle\alpha_t|]\mathrm{d}W_t^x-\frac{\mathrm{i}\sigma}{\sqrt{2}}[(\hat{a}+\hat{a}^\dagger)\,|\alpha_t\rangle\langle\alpha_t|]\mathrm{d}W_t^p.\end{aligned} \tag{E.39}$$

Taking the expectation with respect to the noise (i.e., averaging over trajectories) yields the Lindblad-type evolution for the mixed state

$$\frac{\mathrm{d}\hat{\rho}_t}{\mathrm{d}t} = \sigma^2\left(\hat{a}^\dagger\hat{\rho}_t\hat{a}+\hat{a}\hat{\rho}_t\hat{a}^\dagger-\frac{1}{2}\{\hat{a}^\dagger\hat{a}+\hat{a}\hat{a}^\dagger,\hat{\rho}_t\}\right), \tag{E.40}$$

which is of Lindblad form. This confirms that the coherent-state SDE, when averaged, gives rise to a valid quantum dynamical semigroup. □

E.2.6 Proof of lemma 6.2

Proof. To prove the identity we compute the following using BCH formula [49]

$$\mathrm{e}^{-\zeta_t \hat{S}_+}\left(\hat{S}_- + 2\zeta_t \hat{S}_z - \zeta_t^2 \hat{S}_+\right)\mathrm{e}^{\zeta_t \hat{S}_+} = \hat{S}_- + 2\zeta_t \hat{S}_z - \zeta_t^2 \hat{S}_+ - \zeta_t[\hat{S}_+, \cdot\,] + \frac{\zeta_t^2}{2}[\hat{S}_+, [\hat{S}_+, \cdot\,]] + \cdots \tag{E.41}$$

Explicit evaluation using the commutation relations in (3.3) shows that all higher-order terms vanish, yielding

$$\mathrm{e}^{-\zeta_t \hat{S}_+}\left(\hat{S}_- + 2\zeta_t \hat{S}_z - \zeta_t^2 \hat{S}_+\right)\mathrm{e}^{\zeta_t \hat{S}_+} = \hat{S}_-. \tag{E.42}$$

Acting on the right side with $(1+|\zeta_t|^2)^{-s}|s,-s\rangle$ and $\mathrm{e}^{\zeta_t \hat{S}_+}$ on the left side of the above equation gives

$$\left(\hat{S}_- + 2\zeta_t \hat{S}_z - \zeta_t^2 \hat{S}_+\right)|\zeta_t\rangle \;=\; (1+|\zeta_t|^2)^{-s}\mathrm{e}^{\zeta_t \hat{S}_+}\hat{S}_-|s,-s\rangle. \tag{E.43}$$

But $\hat{S}_-|s,-s\rangle = 0$ by definition, so the identity holds. □

E.2.7 Proof of lemma 6.3

Proof. From Proposition 6.2, we have

$$\left(\hat{S}_- + 2\zeta_t \hat{S}_z - \zeta_t^2 \hat{S}_+\right)|\zeta_t\rangle = 0. \tag{E.44}$$

Multiplying both sides by $\bar{\zeta}_t$ and rearranging gives

$$\left(\hat{S}_-\bar{\zeta}_t + |\zeta_t|^2 \hat{S}_z\right)|\zeta_t\rangle = \left(\zeta_t^2\bar{\zeta}_t\hat{S}_+ - |\zeta_t|^2\hat{S}_z\right)|\zeta_t\rangle. \tag{E.45}$$

Adding $\hat{S}_+\zeta_t$ to both sides gives

$$\begin{aligned}\left(\hat{S}_+\zeta_t + \hat{S}_-\bar{\zeta}_t + |\zeta_t|^2\hat{S}_z\right)|\zeta_t\rangle &= \left(\hat{S}_+\zeta_t + \zeta_t^2\bar{\zeta}_t\hat{S}_+ - |\zeta_t|^2\hat{S}_z\right)|\zeta_t\rangle \\ &= (1+|\zeta_t|^2)\zeta_t\hat{S}_+|\zeta_t\rangle - |\zeta_t|^2\hat{S}_z|\zeta_t\rangle.\end{aligned} \tag{E.46}$$

We use the BCH identity as in Proposition 6.2 on the following expression to get

$$\begin{aligned}\mathrm{e}^{-\zeta_t\hat{S}_+}(\hat{S}_+\zeta_t - \hat{S}_z)\mathrm{e}^{\zeta_t\hat{S}_+} &= (\hat{S}_+\zeta_t - \hat{S}_z) - \zeta_t[\hat{S}_+, \hat{S}_+\zeta_t - \hat{S}_z] + \cdots, \\ &= \hat{S}_+\zeta_t - \hat{S}_z - \zeta_t\hat{S}_+ = -\hat{S}_z.\end{aligned} \tag{E.47}$$

Acting on $(1+|\zeta_t|^2)^{-s}|s,-s\rangle$ on both sides gives

$$(1+|\zeta_t|^2)^{-s}\mathrm{e}^{-\zeta_t\hat{S}_+}(\hat{S}_+\zeta_t - \hat{S}_z)\mathrm{e}^{\zeta_t\hat{S}_+}|s,-s\rangle = -(1+|\zeta_t|^2)^{-s}\hat{S}_z|s,-s\rangle. \tag{E.48}$$

Identifying the structure of (6.29) and using the fact that $\hat{S}_z|s,-s\rangle = -s|s,-s\rangle$ we find that

$$\mathrm{e}^{-\zeta_t\hat{S}_+}(\hat{S}_+\zeta_t - \hat{S}_z)|\zeta_t\rangle = (1+|\zeta_t|^2)^{-s}s\,|s,-s\rangle. \tag{E.49}$$

Multiplying on both sides by $e^{\zeta_t \hat{S}_+}$ we find that

$$(\hat{S}_+\zeta_t - \hat{S}_z)|\zeta_t\rangle = (\hat{S}_+\zeta_t - \hat{S}_z)|\zeta_t\rangle = s|\zeta_t\rangle. \tag{E.50}$$

and this implies that

$$\hat{S}_+\zeta_t|\zeta_t\rangle = (s + \hat{S}_z)|\zeta_t\rangle. \tag{E.51}$$

Substituting (E.51) in (E.46) we arrive at the desired result

$$(\hat{S}_+\zeta_t + \hat{S}_-\bar{\zeta}_t + |\zeta_t|^2\hat{S}_z)|\zeta_t\rangle = \left(\hat{S}_z + s(1 + |\zeta_t|^2)\right)|\zeta_t\rangle. \tag{E.52}$$

This concludes the proof. □

E.2.8 Proof of proposition 6.9

Proof. We apply the complex Itô formula for a vector-valued process $|\zeta_t\rangle$ defined by (6.29)

$$\mathrm{d}|\zeta_t\rangle = \partial_{\zeta_t}|\zeta_t\rangle\,\mathrm{d}\zeta_t + \partial_{\bar{\zeta}_t}|\zeta_t\rangle\,\mathrm{d}\bar{\zeta}_t + \frac{1}{2}\partial^2_{\zeta_t}|\zeta_t\rangle\,(\mathrm{d}\zeta_t)^2 + \frac{1}{2}\partial^2_{\bar{\zeta}_t}|\zeta_t\rangle\,(\mathrm{d}\bar{\zeta}_t)^2 + \partial_{\zeta_t}\partial_{\bar{\zeta}_t}|\zeta_t\rangle\,\mathrm{d}\zeta_t\mathrm{d}\bar{\zeta}_t. \tag{E.53}$$

We now compute each derivative term explicitly.

We start by taking the derivative of (6.29) with respect to ζ_t we get

$$\begin{aligned}\frac{\partial|\zeta_t\rangle}{\partial\zeta_t} &= -s(1 + |\zeta_t|^2)^{-s-1}\bar{\zeta}_t \exp(\hat{S}_+\zeta_t)|k,k\rangle + (1 + |\zeta_t|^2)^{-s}\hat{S}_+ \exp(\hat{S}_+\zeta_t)|s,-s\rangle,\\ &= -(1 + |\zeta_t|^2)^{-s-1}\bar{\zeta}_t \exp(\hat{S}_+\zeta_t)\hat{S}_z|s,-s\rangle + \hat{S}_+|\zeta_t\rangle,\end{aligned} \tag{E.54}$$

where we have used the fact that $\hat{S}_z|s,-s\rangle = -s|s,-s\rangle$. We now apply the BCH identity to get

$$\exp(\hat{S}_+\zeta_t)\hat{S}_z \exp(-\hat{S}_+\zeta_t) = \hat{S}_z + \zeta_t[\hat{S}_+, \hat{S}_z] = \hat{S}_z - \zeta_t\hat{S}_+. \tag{E.55}$$

Substituting this in the above equation we obtain

$$\begin{aligned}\frac{\partial|\zeta_t\rangle}{\partial\zeta_t} &= (1 + |\zeta_t|^2)^{-s-1}\bar{\zeta}_t(\hat{S}_z - \zeta_t\hat{S}_+) \exp(\hat{S}_+\zeta_t)|s,-s\rangle + \hat{S}_+|\zeta_t\rangle,\\ &= \frac{\bar{\zeta}_t\hat{S}_z - |\zeta_t^2|\hat{S}_+}{(1 + |\zeta_t^2|)}|\zeta_t\rangle + \hat{S}_+|\zeta_t\rangle = \frac{\hat{S}_+ + \hat{S}_z\bar{\zeta}_t}{(1 + |\zeta_t|^2)}|\zeta_t\rangle.\end{aligned} \tag{E.56}$$

Let us now calculate the derivative of $|\zeta_t\rangle$ with respect to $\bar{\zeta}$

$$\begin{aligned}\frac{\partial|\zeta_t\rangle}{\partial\bar{\zeta}} &= -s(1 + |\zeta_t|^2)^{-s-1}\zeta_t \exp(\zeta_t\hat{S}_+)|s,-s\rangle,\\ &= (1 + |\zeta_t|^2)^{-s-1}\zeta_t \exp(\zeta_t\hat{S}_+)\hat{S}_z|s,-s\rangle,\end{aligned} \tag{E.57}$$

and using the BCH formula as before we obtain

$$\frac{\partial|\zeta_t\rangle}{\partial\bar{\zeta}} = \zeta_t(1 + |\zeta_t|^2)^{-s-1}(\hat{S}_z - \zeta_t\hat{S}_+) \exp(\zeta_t\hat{S}_+)|s,-s\rangle = \frac{(-\zeta_t^2\hat{S}_+ + \zeta_t\hat{S}_z)}{1 + |\zeta_t|^2}|\zeta_t\rangle. \tag{E.58}$$

Applying the result from Proposition 6.2 in the above equation yields

$$\frac{\partial|\zeta_t\rangle}{\partial\bar{\zeta}_t} = -\frac{\zeta_t\hat{S}_z + \hat{S}_-}{(1+|\zeta_t|^2)}|\zeta_t\rangle. \tag{E.59}$$

We have now calculated the first derivatives of $|\zeta_t\rangle$, we will now use them to calculate the second derivatives. We start with

$$\frac{\partial^2|\zeta_t\rangle}{\partial\zeta_t^2} = \frac{\partial}{\partial\zeta_t}\left(\frac{\hat{S}_+ + \hat{S}_z\bar{\zeta}_t}{(1+|\zeta_t|^2)}|\zeta_t\rangle\right), \tag{E.60}$$

where we have substituted for $\frac{\partial|\zeta_t\rangle}{\partial\zeta_t}$ from (E.56). Using the product rule for differentiation the above equation becomes

$$\frac{\partial^2|\zeta_t\rangle}{\partial\zeta_t^2} = \frac{\partial}{\partial\zeta_t}\left(\frac{\hat{S}_+ + \hat{S}_z\bar{\zeta}_t}{(1+|\zeta_t|^2)}\right)|\zeta_t\rangle + \frac{\hat{S}_+ + \hat{S}_z\bar{\zeta}_t}{(1+|\zeta_t|^2)}\frac{\partial}{\partial\zeta_t}\Big(|\zeta_t\rangle\Big). \tag{E.61}$$

Applying the result from (E.56) again in the above expression and expanding yields

$$\frac{\partial^2|\zeta_t\rangle}{\partial\zeta_t^2} = \frac{-\hat{S}_+\bar{\zeta}_t - \hat{S}_z(\bar{\zeta}_t)^2}{(1+|\zeta_t|^2)^2}|\zeta_t\rangle + \frac{\hat{S}_+^2 + \hat{S}_+\hat{S}_z\bar{\zeta}_t + \hat{S}_z\hat{S}_+\bar{\zeta}_t + \hat{S}_z^2(\bar{\zeta}_t)^2}{(1+|\zeta_t|^2)^2}|\zeta_t\rangle. \tag{E.62}$$

Using the commutation relation $[\hat{S}_+, \hat{S}_z] = -\hat{S}_+$, we simplify the above equation to obtain

$$\frac{\partial^2|\zeta_t\rangle}{\partial\zeta_t^2} = \frac{\hat{S}_+^2 + 2\hat{S}_+\hat{S}_z\bar{\zeta}_t + \hat{S}_z^2(\bar{\zeta}_t)^2 - \hat{S}_z(\bar{\zeta}_t)^2}{(1+|\zeta_t|^2)^2}|\zeta_t\rangle. \tag{E.63}$$

Similarly, $\frac{\partial^2|\zeta_t\rangle}{\partial(\bar{\zeta}_t)^2}$ can be calculated to be

$$\frac{\partial^2|\zeta_t\rangle}{\partial(\bar{\zeta}_t)^2} = \frac{\hat{S}_-^2 + 2\hat{S}_-\hat{S}_z\zeta_t + \hat{S}_z^2(\zeta_t)^2 + \hat{S}_z(\zeta_t)^2}{(1+|\zeta_t|^2)^2}|\zeta_t\rangle. \tag{E.64}$$

Finally, we can calculate $\frac{\partial^2|\zeta_t\rangle}{\partial\zeta_t\partial\bar{\zeta}_t}$ as follows:

$$\frac{\partial^2|\zeta_t\rangle}{\partial\zeta_t\partial\bar{\zeta}_t} = \frac{\partial}{\partial\zeta_t}\frac{\partial}{\partial\bar{\zeta}_t}(|\zeta_t\rangle) = -\frac{\partial}{\partial\zeta_t}\left(\frac{\zeta_t\hat{S}_z + \hat{S}_-}{(1+|\zeta_t|^2)}|\zeta_t\rangle\right). \tag{E.65}$$

Using the product rule and expanding the expression we get

$$\frac{\partial^2|\zeta_t\rangle}{\partial\zeta_t\partial\bar{\zeta}_t} = \frac{-\zeta_t\hat{S}_z\hat{S}_+ - \bar{\zeta}_t\hat{S}_-\hat{S}_z - \hat{S}_-\hat{S}_+ - |\zeta_t|^2\hat{S}_z^2 + |\zeta_t|^2\hat{S}_z + \bar{\zeta}_t\hat{S}_- - \hat{S}_z(1+|\zeta_t|^2)}{(1+|\zeta_t|^2)^2}|\zeta_t\rangle, \tag{E.66}$$

and using the commutation relations in (3.3) we get

$$\frac{\partial^2|\zeta_t\rangle}{\partial\zeta_t\partial\bar{\zeta}_t} = \frac{-\hat{S}_-\hat{S}_+ - \hat{S}_+\hat{S}_- - 2\zeta_t\hat{S}_z\hat{S}_+ - 2\bar{\zeta}_t\hat{S}_z\hat{S}_- - 2|\zeta_t|^2\hat{S}_z^2}{2(1+|\zeta_t|^2)^2}|\zeta_t\rangle. \tag{E.67}$$

Applying the result from Lemma 6.3, (E.67) becomes

$$\frac{\partial^2|\zeta_t\rangle}{\partial\zeta_t\partial\bar{\zeta}_t} = \frac{-\hat{S}_-\hat{S}_+ - \hat{S}_+\hat{S}_- - 2\hat{S}_z^2 - 2s\hat{S}_z(1+|\zeta_t|^2)}{2(1+|\zeta_t|^2)^2}|\zeta_t\rangle. \tag{E.68}$$

Combining all derivative terms in the Itô expansion, we obtain the desired stochastic differential equation for $|\zeta_t\rangle$

$$\begin{aligned}
\mathrm{d}|\zeta_t\rangle &= \left(\frac{(\hat{S}_+ + \hat{S}_z\bar{\zeta}_t)|\zeta_t\rangle}{(1+|\zeta_t|^2)}\right)\mathrm{d}\zeta_\mathrm{t} - \left(\frac{(\hat{\mathrm{S}}_- + \hat{\mathrm{S}}_\mathrm{z}\zeta_\mathrm{t})|\zeta_\mathrm{t}\rangle}{(1+|\zeta_\mathrm{t}|^2)}\right)\mathrm{d}\bar{\zeta}_\mathrm{t} \\
&+\frac{1}{2}\left(\frac{\hat{S}_+^2 + 2\hat{S}_+\hat{S}_z\bar{\zeta}_t - \hat{S}_z(\bar{\zeta}_t)^2 + \hat{S}_z^2(\bar{\zeta}_t)^2}{(1+|\zeta_t|^2)^2}|\zeta_t\rangle\right)(\mathrm{d}\zeta_\mathrm{t})^2 \\
&+\frac{1}{2}\left(\frac{\hat{S}_-^2 + 2\hat{S}_-\hat{S}_z\zeta_t + \hat{S}_z(\zeta_t)^2 + \hat{S}_z^2(\zeta_t)^2}{(1+|\zeta_t|^2)^2}|\zeta_t\rangle\right)(\mathrm{d}\bar{\zeta}_\mathrm{t})^2 \\
&\frac{-1}{2}\left(\frac{\hat{S}_-\hat{S}_+ + \hat{S}_+\hat{S}_- + 2\hat{S}_z^2}{(1+|\zeta_t|^2)^2} + \frac{2s\hat{S}_z}{(1+|\zeta_t|^2)}\right)(\mathrm{d}\zeta_\mathrm{t})(\mathrm{d}\bar{\zeta}_\mathrm{t}).
\end{aligned} \tag{E.69}$$

Substituting (6.31) into (E.69), we obtain the SDE for the coherent state process $|\zeta_t\rangle$

$$\begin{aligned}
\mathrm{d}|\zeta_t\rangle &= -\frac{\sigma^2}{4}\left(\hat{S}_-\hat{S}_+ + \hat{S}_+\hat{S}_- + 2\hat{S}_z^2 + 2s\hat{S}_z(1+|\zeta_t|^2)\right)|\zeta_t\rangle\,\mathrm{d}t \\
&+\sigma\left(\frac{\hat{S}_+\zeta_t - \hat{S}_-\bar{\zeta}_t}{2|\zeta_t|}\right)\mathrm{d}W_t^\theta\,|\zeta_t\rangle - \sigma\left(\frac{\mathrm{i}(\hat{S}_+\zeta_t + \hat{S}_-\bar{\zeta}_t) + 2\mathrm{i}|\zeta_t|^2\hat{S}_z}{2|\zeta_t|}\right)\mathrm{d}W_t^\phi\,|\zeta_t\rangle.
\end{aligned} \tag{E.70}$$

and this concludes the proof of the Proposition. □

E.2.9 Proof of proposition 6.14

Proof. We compute the Itô differential of the rank-one projector $\hat{\rho}_t = |\zeta_t\rangle\langle\zeta_t|$ using Itô's product rule:

$$\mathrm{d}\hat{\rho}_t = \mathrm{d}|\zeta_t\rangle\langle\zeta_t| + |\zeta_t\rangle\mathrm{d}\langle\zeta_t| + \mathrm{d}|\zeta_t\rangle\mathrm{d}\langle\zeta_t|. \tag{E.71}$$

Using the relation from Lemma 6.3 and simplifying

$$\begin{aligned}
\mathrm{d}(\langle\zeta_t|)\mathrm{d}(|\zeta_t\rangle) &= \left(\frac{\sigma^2}{2}(\hat{S}_+|\zeta_t\rangle\langle\zeta_t|\hat{S}_- + \hat{S}_-|\zeta_t\rangle\langle\zeta_t|\hat{S}_+) + \frac{\sigma^2 s(1+|\zeta_t|^2)}{2}\hat{S}_z|\zeta_t\rangle\langle\zeta_t|\right. \\
&\left.+\frac{\sigma^2 s(1+|\zeta_t|^2)}{2}|\zeta_t\rangle\langle\zeta_t|\hat{S}_z + \sigma^2\hat{S}_z|\zeta_t\rangle\langle\zeta_t|\hat{S}_z\right)\mathrm{d}t.
\end{aligned} \tag{E.72}$$

Next, we compute the drift parts of $\mathrm{d}|\zeta_t\rangle\langle\zeta_t|$ and $|\zeta_t\rangle\mathrm{d}\langle\zeta_t|$, which are Hermitian conjugates. From (6.38), we extract the drift part of $\mathrm{d}|\zeta_t\rangle$ and simplify.

$\mathrm{d}(|\zeta_t\rangle)\langle\zeta_t|$ is calculated to be

$$\begin{aligned}
\mathrm{d}(|\zeta_t\rangle)\langle\zeta_t| &= \frac{-1}{2}\left(\frac{\hat{S}_-\hat{S}_+ + \hat{S}_+\hat{S}_- + 2\hat{S}_z^2}{(1+|\zeta_t|^2)^2} + \frac{2s\hat{S}_z}{(1+|\zeta_t|^2)}\right)\mathrm{d}t\frac{\sigma^2(1+|\zeta_t|^2)^2}{2}|\zeta_t\rangle\langle\zeta_t| \\
&+\sigma\left(\frac{\hat{S}_+\zeta_t - \hat{S}_-\bar{\zeta}_t}{2|\zeta_t|}\right)\mathrm{d}W_t^\theta|\zeta_t\rangle\langle\zeta_t| - \sigma\left(\frac{\mathrm{i}(\hat{S}_+\zeta_t + \hat{S}_-\bar{\zeta}_t)}{2|\zeta_t|} + \frac{2\mathrm{i}|\zeta_t|^2\hat{S}_z}{2|\zeta_t|}\right)\mathrm{d}W_t^\phi|\zeta_t\rangle\langle\zeta_t|.
\end{aligned} \tag{E.73}$$

and finally $|\zeta_t\rangle \mathrm{d}(\langle\zeta_t|)$ is calculated to be

$$\begin{aligned}|\zeta_t\rangle \mathrm{d}(\langle\zeta_t|) &= |\zeta_t\rangle\langle\zeta_t|\frac{-1}{2}\left(\frac{\hat{S}_-\hat{S}_+ + \hat{S}_+\hat{S}_- + 2\hat{S}_z^2}{(1+|\zeta_t|^2)^2} + \frac{2s\hat{S}_z}{(1+|\zeta_t|^2)}\right)\mathrm{d}t\frac{\sigma^2(1+|\zeta_t|^2)^2}{2} \\ &\quad -\sigma|\zeta_t\rangle\langle\zeta_t|\left(\frac{\hat{S}_+\zeta_t - \hat{S}_-\bar{\zeta}_t}{2|\zeta_t|}\right)\mathrm{d}W_t^\theta + \sigma|\zeta_t\rangle\langle\zeta_t|\left(\frac{\mathrm{i}(\hat{S}_+\zeta_t + \hat{S}_-\bar{\zeta}_t)}{2|\zeta_t|} + \frac{2\mathrm{i}|\zeta_t|^2\hat{S}_z}{2|\zeta_t|}\right)\mathrm{d}W_t^\phi. \quad \text{(E.74)}\end{aligned}$$

Adding all three contributions we obtain

$$\begin{aligned}\mathrm{d}(|\zeta_t\rangle\langle\zeta_t|) &= \frac{\sigma^2}{2}\Big[\hat{S}_+|\zeta_t\rangle\langle\zeta_t|\hat{S}_- + \hat{S}_-|\zeta_t\rangle\langle\zeta_t|\hat{S}_+ + 2\hat{S}_z|\zeta_t\rangle\langle\zeta_t|\hat{S}_z - \frac{1}{2}\Big(\hat{S}_-\hat{S}_+|\zeta_t\rangle\langle\zeta_t| + \hat{S}_+\hat{S}_-|\zeta_t\rangle\langle\zeta_t| + 2\hat{S}_z^2|\zeta_t\rangle\langle\zeta_t| \\ &\quad +|\zeta_t\rangle\langle\zeta_t|\hat{S}_-\hat{S}_+ + |\zeta_t\rangle\langle\zeta_t|\hat{S}_+\hat{S}_- + |\zeta_t\rangle\langle\zeta_t|2\hat{S}_z^2\Big)\Big]\mathrm{d}t - \sigma|\zeta_t\rangle\langle\zeta_t|\left(\frac{\hat{S}_+\zeta_t - \hat{S}_-\bar{\zeta}_t}{2|\zeta_t|}\right)\mathrm{d}W_t^\theta \\ &\quad +\sigma\left(\frac{\hat{S}_+\zeta_t - \hat{S}_-\bar{\zeta}_t}{2|\zeta_t|}\right)\mathrm{d}W_t^\theta|\zeta_t\rangle\langle\zeta_t| - \sigma\left(\frac{\mathrm{i}(\hat{S}_+\zeta_t + \hat{S}_-\bar{\zeta}_t)}{2|\zeta_t|} + \frac{2\mathrm{i}|\zeta_t|^2\hat{S}_z}{2|\zeta_t|}\right)\mathrm{d}W_t^\phi|\zeta_t\rangle\langle\zeta_t| \\ &\quad +\sigma|\zeta_t\rangle\langle\zeta_t|\left(\frac{\mathrm{i}(\hat{S}_+\zeta_t + \hat{S}_-\bar{\zeta}_t)}{2|\zeta_t|} + \frac{2\mathrm{i}|\zeta_t|^2\hat{S}_z}{2|\zeta_t|}\right)\mathrm{d}W_t^\phi. \quad \text{(E.75)}\end{aligned}$$

Taking the expectation, the terms linear in the Brownian motion $\mathrm{d}W_t$ vanish. The remaining drift terms yield

$$\begin{aligned}\frac{\mathrm{d}\hat{\rho}_t}{\mathrm{d}t} &= \sigma^2\left(\frac{\hat{S}_+}{\sqrt{2}}\hat{\rho}_t\frac{\hat{S}_-}{\sqrt{2}} + \frac{\hat{S}_-}{\sqrt{2}}\hat{\rho}_t\frac{\hat{S}_+}{\sqrt{2}} + \hat{S}_z\hat{\rho}_t\hat{S}_z\right) \\ &\quad -\frac{\sigma^2}{2}\left(\frac{\hat{S}_+\hat{S}_-}{2}\hat{\rho}_t + \frac{\hat{S}_-\hat{S}_+}{2}\hat{\rho}_t + \hat{S}_z^2\hat{\rho}_t + \hat{\rho}_t\hat{S}_z^2 + \hat{\rho}_t\frac{\hat{S}_+\hat{S}_-}{2} + \hat{\rho}_t\frac{\hat{S}_-\hat{S}_+}{2}\right). \quad \text{(E.76)}\end{aligned}$$

Rewriting in the standard Lindblad form, we recognize three effective jump operators $\hat{L}_1 = \frac{\hat{S}_+}{\sqrt{2}}$, $\hat{L}_2 = \frac{\hat{S}_-}{\sqrt{2}}$, $\hat{L}_3 = \hat{S}_z$. Alternatively in terms of $\hat{S}_x, \hat{S}_y, \hat{S}_z$, the equation can be written as

$$\begin{aligned}\frac{\mathrm{d}\hat{\rho}_t}{\mathrm{d}t} &= \sigma^2\left(\hat{S}_x\hat{\rho}_t\hat{S}_x + \hat{S}_y\hat{\rho}_t\hat{S}_y + \hat{S}_z\hat{\rho}_t\hat{S}_z\right) \\ &\quad -\frac{\sigma^2}{2}\left(\hat{S}_x^2\hat{\rho}_t + \hat{S}_y^2\hat{\rho}_t + \hat{S}_z^2\hat{\rho}_t + \hat{\rho}_t\hat{S}_z^2 + \hat{\rho}_t\hat{S}_y^2 + \hat{\rho}_t\hat{S}_x^2\right). \quad \text{(E.77)}\end{aligned}$$

□

E.2.10 Proof of lemma 6.4

Proof. To prove the identity we compute the following using BCH formula [49]

$$\mathrm{e}^{-\chi_t\hat{K}_+}\left(\hat{K}_- - 2\chi_t\hat{K}_z + \chi_t^2\hat{K}_+\right)\mathrm{e}^{\chi_t\hat{K}_+} = \hat{K}_- - 2\chi_t\hat{K}_z + \chi_t^2\hat{K}_+ - \chi_t[\hat{K}_+,\cdot] + \frac{\chi_t^2}{2}[\hat{K}_+,[\hat{K}_+,\cdot]] + \cdots \quad \text{(E.78)}$$

Explicit evaluation using the commutation relations in (5.7) shows that all higher-order terms vanish, yielding

$$\mathrm{e}^{-\chi_t\hat{K}_+}\left(\hat{K}_- - 2\chi_t\hat{K}_z + \chi_t^2\hat{K}_+\right)\mathrm{e}^{\chi_t\hat{K}_+} = \hat{K}_-. \quad \text{(E.79)}$$

Acting on the right side with $(1-|\chi_t|^2)^k|k,k\rangle$ and $e^{\chi_t \hat{K}_+}$ on the left side of the above equation gives

$$\left(\hat{K}_- - 2\chi_t \hat{K}_z + \chi_t^2 \hat{K}_+\right)|\chi_t\rangle \quad = \quad (1-|\chi_t|^2)^k e^{\chi_t \hat{K}_+}\hat{K}_-|k,k\rangle. \tag{E.80}$$

But $\hat{K}_-|k,k\rangle = 0$ by definition, so the identity holds. □

E.2.11 Proof of lemma 6.5

Proof. From Proposition 6.2, we have

$$\left(\hat{K}_- - 2\chi_t \hat{K}_z + \chi_t^2 \hat{K}_+\right)|\chi_t\rangle = 0. \tag{E.81}$$

Multiplying both sides by $\bar{\chi}_t$ and rearranging gives

$$\left(\hat{K}_-\bar{\chi}_t - |\chi_t|^2 \hat{K}_z\right)|\chi_t\rangle = \left(-\chi_t^2\bar{\chi}_t\hat{K}_+ + |\chi_t|^2\hat{K}_z\right)|\chi_t\rangle. \tag{E.82}$$

Adding $\hat{K}_+\chi_t$ to both sides gives

$$\begin{aligned}\left(\hat{K}_+\chi_t + \hat{K}_-\bar{\chi}_t + |\chi_t|^2\hat{K}_z\right)|\chi_t\rangle &= \left(\hat{K}_+\chi_t - \chi_t^2\bar{\chi}_t\hat{K}_+ + |\chi_t|^2\hat{K}_z\right)|\chi_t\rangle \\ &= (1-|\chi_t|^2)\chi_t\hat{K}_+|\chi_t\rangle + |\chi_t|^2\hat{K}_z|\chi_t\rangle.\end{aligned} \tag{E.83}$$

We use the BCH identity as in Proposition 6.4 on the following expression to get

$$\begin{aligned}e^{-\chi_t\hat{K}_+}(\hat{K}_+\chi_t - \hat{K}_z)e^{-\chi_t\hat{K}_+} &= (\hat{K}_+\chi_t - \hat{K}_z) - \chi_t[\hat{K}_+, \hat{K}_+\chi_t - \hat{K}_z] + \cdots, \\ &= \hat{K}_+\chi_t - \hat{K}_z - \chi_t\hat{K}_+ = -\hat{K}_z.\end{aligned} \tag{E.84}$$

Acting on $(1+|\chi_t|^2)^k|k,k\rangle$ on both sides gives

$$(1-|\chi_t|^2)^k e^{-\chi_t\hat{K}_+}(\hat{K}_+\chi_t - \hat{K}_z)e^{\chi_t\hat{K}_+}|k,k\rangle = -(1-|\chi_t|^2)^k\hat{K}_z|k,k\rangle. \tag{E.85}$$

Identifying the structure of (6.62) and using the fact that $\hat{K}_z|k,k\rangle = k|k,k\rangle$ we find that

$$e^{-\chi_t\hat{K}_+}(\hat{K}_+\chi_t - \hat{K}_z)|\chi_t\rangle = -(1-|\chi_t|^2)^k k\,|k,k\rangle. \tag{E.86}$$

Multiplying on both sides by $e^{\chi_t\hat{K}_+}$ we find that

$$(\hat{K}_+\chi_t - \hat{K}_z)|\chi_t\rangle = (\hat{K}_+\chi_t - \hat{K}_z)|\chi_t\rangle = -k|\chi_t\rangle. \tag{E.87}$$

and this implies that $\hat{K}_+\chi_t|\chi_t\rangle = (-k+\hat{K}_z)|\chi_t\rangle$. Substituting (E.2.11) in (E.83) we arrive at the desired result

$$(\hat{K}_+\chi_t + \hat{K}_-\bar{\chi}_t - |\chi_t|^2\hat{K}_z)|\chi_t\rangle = \left(\hat{K}_z - k(1-|\chi_t|^2)\right)|\chi_t\rangle. \tag{E.88}$$

This concludes the proof. □

E.2.12 Proof of proposition 6.15

.

Proof. This SDE captures the infinitesimal evolution of the quantum state along stochastic trajectories on the hyperbolic phase space. The derivation proceeds analogously to the $\mathrm{SU}(2)$ case and can be obtained by applying complex Itô calculus to the nonlinear map $\chi_t \mapsto |\chi_t\rangle$, using the same tools, the Baker-Campbell-Hausdorff (BCH) expansion, commutation relations from $\mathfrak{su}(1,1)$, and the identities satisfied by the coherent states, Lemmas 6.4,6.5.
Applying Itô's lemma for the coherent state process $|\chi_t\rangle$ we have

$$\mathrm{d}|\chi_t\rangle = \frac{\partial|\chi_t\rangle}{\partial\chi_t}\mathrm{d}\chi_t + \frac{\partial|\chi_t\rangle}{\partial\overline{\chi}_t}\mathrm{d}\overline{\chi}_t + \frac{1}{2}\frac{\partial^2|\chi_t\rangle}{\partial\chi_t^2}(\mathrm{d}\chi_t)^2 + \frac{1}{2}\frac{\partial^2|\chi_t\rangle}{\partial(\overline{\chi}_t)^2}(\mathrm{d}\overline{\chi}_t)^2 + \frac{\partial^2|\chi_t\rangle}{\partial\chi_t\partial\overline{\chi}_t}\mathrm{d}\chi_t\,\mathrm{d}\overline{\chi}_t. \tag{E.89}$$

Similar to the $\mathrm{SU}(2)$ case we calculate the derivatives of the coherent state $|\chi_t\rangle$ with respect to χ_t, $\overline{\chi}_t$ and subsequently higher order derivatives to complete the proof. We have the following results for the derivatives

$$\begin{aligned}
\frac{\partial|\chi_t\rangle}{\partial\chi_t} &= \frac{\hat{K}_+ - \hat{K}_z\bar{\chi}_t}{(1-|\chi_t|^2)}|\chi_t\rangle,\\
\frac{\partial|\chi_t\rangle}{\partial\bar{\chi}_t} &= \frac{(\chi_t^2\hat{K}_+ - \chi_t\hat{K}_z)}{1-|\chi_t|^2}|\chi_t\rangle,\\
\frac{\partial^2|\chi_t\rangle}{\partial\chi_t^2} &= \frac{\hat{K}_+^2 - 2\hat{K}_+\hat{K}_z\overline{\chi}_t + \hat{K}_z^2(\overline{\chi}_t)^2 - \hat{K}_z(\overline{\chi}_t)^2}{(1-|\chi_t|^2)^2}|\chi_t\rangle,\\
\frac{\partial^2|\chi_t\rangle}{\partial(\overline{\chi}_t)^2} &= \frac{\hat{K}_-^2 - 2\hat{K}_-\hat{K}_z\chi_t + \hat{K}_z^2(\chi_t)^2 + \hat{K}_z(\chi_t)^2}{(1-|\chi_t|^2)^2}|\chi_t\rangle,\\
\frac{\partial^2|\chi_t\rangle}{\partial\chi_t\partial\overline{\chi}_t} &= \frac{-\hat{K}_-\hat{K}_+ - \hat{K}_+\hat{K}_- + 2\chi_t\hat{K}_z\hat{K}_+ + 2\overline{\chi}_t\hat{K}_z\hat{K}_- - 2|\chi_t|^2\hat{K}_z^2}{2(1-|\chi_t|^2)^2}|\chi_t\rangle.
\end{aligned} \tag{E.90}$$

Substituting the derivatives in the expression for the Itô expansion of the coherent state we arrive at the result in the proposition

$$\begin{aligned}
\mathrm{d}|\chi_t\rangle &= \left(\frac{(\hat{K}_+ - \hat{K}_z\bar{\chi}_t)|\chi_t\rangle}{(1-|\chi_t|^2)}\right)\mathrm{d}\chi_t - \left(\frac{(\hat{K}_- - \hat{K}_z\chi_t)|\chi_t\rangle}{(1-|\chi_t|^2)}\right)\mathrm{d}\bar{\chi}_t\\
&+\frac{1}{2}\left(\frac{\hat{K}_+^2 - 2\hat{K}_+\hat{K}_z\bar{\chi}_t - \hat{K}_z(\bar{\chi}_t)^2 + \hat{K}_z^2(\bar{\chi}_t)^2}{(1-|\chi_t|^2)^2}|\chi_t\rangle\right)(\mathrm{d}\chi_t)^2\\
&+\frac{1}{2}\left(\frac{\hat{K}_-^2 - 2\hat{K}_-\hat{K}_z\chi_t + \hat{K}_z(\chi_t)^2 + \hat{K}_z^2(\chi_t)^2}{(1-|\chi_t|^2)^2}|\chi_t\rangle\right)(\mathrm{d}\bar{\chi}_t)^2\\
&\frac{-1}{2}\left(\frac{\hat{K}_-\hat{K}_+ + \hat{K}_+\hat{K}_- - 2\hat{K}_z^2}{(1-|\chi_t|^2)^2} + \frac{2k\hat{K}_z}{(1-|\chi_t|^2)}\right)(\mathrm{d}\chi_t)(\mathrm{d}\bar{\chi}_t),
\end{aligned} \tag{E.91}$$

and this concludes the proof. □

E.2.13 Proof of proposition 6.20

Proof. We apply Itô's lemma to $\mathrm{d}(|\chi_t\rangle\langle\chi_t|)$,

$$\mathrm{d}(|\chi_t\rangle\langle\chi_t|) = \mathrm{d}(|\chi_t\rangle)\langle\chi_t| + |\chi_t\rangle\mathrm{d}(\langle\chi_t|) + \mathrm{d}(\langle\chi_t|)\mathrm{d}(|\chi_t\rangle) \tag{E.92}$$

Similar to the SU(2) case we find the Itô correction term to be

$$\begin{aligned}\mathrm{d}(\langle\chi_t|)\mathrm{d}(|\chi_t\rangle) &= \frac{\sigma^2}{2}(\hat{K}_+|\chi_t\rangle\langle\chi_t|\hat{K}_- + \hat{K}_-|\chi_t\rangle\langle\chi_t|\hat{K}_+) + \frac{\sigma^2 k(1-|\chi_t|^2)}{2}\hat{K}_z|\chi_t\rangle\langle\chi_t| \\ &+\frac{\sigma^2 k(1-|\chi_t|^2)}{2}|\chi_t\rangle\langle\chi_t|\hat{K}_z - \sigma^2\hat{K}_z|\chi_t\rangle\langle\chi_t|\hat{K}_z. \end{aligned} \tag{E.93}$$

Similarly the drift terms, $\mathrm{d}(|\chi_t\rangle)\langle\chi_t|$, is calculated to be

$$\begin{aligned}\mathrm{d}(|\chi_t\rangle)\langle\chi_t| &= \frac{-1}{2}\left(\frac{\hat{K}_-\hat{K}_+ + \hat{K}_+\hat{K}_- - 2\hat{K}_z^2}{(1-|\chi_t|^2)^2} + \frac{2k\hat{K}_z}{(1-|\chi_t|^2)}\right)\mathrm{d}t\frac{\sigma^2(1-|\chi_t|^2)^2}{2}|\chi_t\rangle\langle\chi_t| \\ &+\sigma\left(\frac{\hat{K}_+\chi_t - \hat{K}_-\bar{\chi}_t}{2|\chi_t|}\right)\mathrm{d}W_t^\theta|\chi_t\rangle\langle\chi_t| \\ &-\sigma\left(\frac{\mathrm{i}(\hat{K}_+\chi_t + \hat{K}_-\bar{\chi}_t)}{2|\chi_t|} - \frac{2\mathrm{i}|\chi_t|^2\hat{K}_z}{2|\chi_t|}\right)\mathrm{d}W_t^\phi|\chi_t\rangle\langle\chi_t|. \end{aligned} \tag{E.94}$$

and finally $|\chi_t\rangle\mathrm{d}(\langle\chi_t|)$ is calculated to be

$$\begin{aligned}|\chi_t\rangle\mathrm{d}(\langle\chi_t|) &= |\chi_t\rangle\langle\chi_t|\frac{-1}{2}\left(\frac{\hat{K}_-\hat{K}_+ + \hat{K}_+\hat{K}_- - 2\hat{K}_z^2}{(1-|\chi_t|^2)^2} + \frac{2k\hat{K}_z}{(1-|\chi_t|^2)}\right)\mathrm{d}t\frac{\sigma^2(1-|\chi_t|^2)^2}{2} \\ &-\sigma|\chi_t\rangle\langle\chi_t|\left(\frac{\hat{K}_+\chi_t - \hat{K}_-\bar{\chi}_t}{2|\chi_t|}\right)\mathrm{d}W_t^\theta \\ &+\sigma|\chi_t\rangle\langle\chi_t|\left(\frac{\mathrm{i}(\hat{K}_+\chi_t + \hat{K}_-\bar{\chi}_t)}{2|\chi_t|} - \frac{2\mathrm{i}|\chi_t|^2\hat{K}_z}{2|\chi_t|}\right)\mathrm{d}W_t^\phi. \end{aligned} \tag{E.95}$$

Combining (E.93, E.94, E.95) we obtain

$$\begin{aligned}\mathrm{d}(|\chi_t\rangle\langle\chi_t|) &= \frac{\sigma^2}{2}\Bigg[\hat{K}_+|\chi_t\rangle\langle\chi_t|\hat{K}_- + \hat{K}_-|\chi_t\rangle\langle\chi_t|\hat{K}_+ - 2\hat{K}_z|\chi_t\rangle\langle\chi_t|\hat{K}_z \\ &-\frac{1}{2}\Big(\hat{K}_-\hat{K}_+|\chi_t\rangle\langle\chi_t| + \hat{K}_+\hat{K}_-|\chi_t\rangle\langle\chi_t| - 2\hat{K}_z^2|\chi_t\rangle\langle\chi_t| \\ &|\chi_t\rangle\langle\chi_t|\hat{K}_-\hat{K}_+ + |\chi_t\rangle\langle\chi_t|\hat{K}_+\hat{K}_- - |\chi_t\rangle\langle\chi_t|2\hat{K}_z^2\Big)\Bigg]\mathrm{d}t - \sigma|\chi_t\rangle\langle\chi_t|\left(\frac{\hat{K}_+\chi_t - \hat{K}_-\bar{\chi}_t}{2|\chi_t|}\right)\mathrm{d}W_t^\theta \\ &+\sigma\left(\frac{\hat{K}_+\chi_t - \hat{K}_-\bar{\chi}_t}{2|\chi_t|}\right)\mathrm{d}W_t^\theta|\chi_t\rangle\langle\chi_t| - \sigma\left(\frac{\mathrm{i}(\hat{K}_+\chi_t + \hat{K}_-\bar{\chi}_t)}{2|\chi_t|} - \frac{2\mathrm{i}|\chi_t|^2\hat{K}_z}{2|\chi_t|}\right)\mathrm{d}W_t^\phi|\chi_t\rangle\langle\chi_t| \\ &+\sigma|\chi_t\rangle\langle\chi_t|\left(\frac{\mathrm{i}(\hat{K}_+\chi_t + \hat{K}_-\bar{\chi}_t)}{2|\chi_t|} - \frac{2\mathrm{i}|\chi_t|^2\hat{K}_z}{2|\chi_t|}\right)\frac{(1-|\chi_t|^2)}{2|\chi_t|}\mathrm{d}W_t^\phi. \end{aligned} \tag{E.96}$$

Taking the expectation value of the above equation yields the desired result

$$\begin{aligned}\frac{\mathrm{d}\hat{\rho}_t}{\mathrm{d}t} &= \sigma^2\left(\frac{\hat{K}_+}{\sqrt{2}}\hat{\rho}_t\frac{\hat{K}_-}{\sqrt{2}} + \frac{\hat{K}_-}{\sqrt{2}}\hat{\rho}_t\frac{\hat{K}_+}{\sqrt{2}} - \hat{K}_z\hat{\rho}_t\hat{K}_z\right) - \frac{\sigma^2}{2}\left(\frac{\hat{K}_+\hat{K}_-}{2}\hat{\rho}_t + \frac{\hat{K}_-\hat{K}_+}{2}\hat{\rho}_t - \hat{K}_z^2\hat{\rho}_t\right) \\ &-\frac{\sigma^2}{2}\left(-\hat{\rho}_t\hat{K}_z^2 + \hat{\rho}_t\frac{\hat{K}_+\hat{K}_-}{2} + \hat{\rho}_t\frac{\hat{K}_-\hat{K}_+}{2}\right), \end{aligned} \tag{E.97}$$

□

Appendix F

Relativistic phase-space measurement and related derivations

This appendix contains detailed proofs of the propositions, lemmas, and technical results stated in Chapter 7. These proofs provide the rigorous foundation for the analysis of relativistic extensions of measurement-induced dynamics.

F.1 Proofs of technical results

F.1.1 Proof of proposition 7.2

Proof. Let $\Psi \in L^{2,h}(\Gamma^+)$. Then applying the forward and inverse transforms in succession yields:

$$\Psi(z) = (\mathcal{B}^{-1} \circ \mathcal{B})(\Psi)(z) = \int_{\mathcal{C}_+^\circ} \overline{A(q,\bar{z})}\, (\mathcal{B}\psi)(q)\, \mathrm{d}\nu_q. \tag{F.1}$$

Substituting the definition of $(\mathcal{B}\psi)(q)$, we get:

$$\begin{aligned} \Psi(z) &= \int_{\mathcal{C}_+^\circ} \overline{A(q,\bar{z})} \left[\int_\Gamma A(q,\bar{w})\, \Psi(w)\, \mathrm{d}\mu_w \right] \mathrm{d}\nu_q, \\ &= \int_\Gamma \Psi(w) \left[\int_{\mathcal{C}_+^\circ} \overline{A(q,\bar{z})}\, A(q,\bar{w})\, \mathrm{d}\nu_q \right] \mathrm{d}\mu_w. \end{aligned} \tag{F.2}$$

Let us now define $I(z^a)$ to be

$$I(z^a) = \frac{1}{8\pi^5} \int_{\mathcal{C}_+^\circ} \frac{1}{(-\mathrm{i}z^c z_c)^4} \exp\left(\frac{\mathrm{i}q_a z^a}{z^b z_b} \right) \psi(q) (q^d q_d)^2\, \mathrm{d}q^a. \tag{F.3}$$

Substituting for $\psi(q)$ in the above equation we have

$$\begin{aligned} I(z^a) &= \frac{1}{8\pi^5} \int_{\mathcal{C}_+^\circ} \frac{1}{(-\mathrm{i}z^c z_c)^4} \exp\left(\frac{\mathrm{i}q_a z^a}{z^b z_b} \right) \left[\int_{\Gamma^+} \frac{1}{(-\mathrm{i}\bar{w}^e \bar{w}_e)^4} \exp\left(-\frac{\mathrm{i}q_a \bar{w}^a}{\bar{w}^f \bar{w}_f} \right) \Psi(w)\, \mathrm{d}\mu_w \right] (q^d q_d)^2\, \mathrm{d}q^a, \\ &= \int_{\Gamma^+} \frac{1}{(-\mathrm{i}\bar{w}^e \bar{w}_e)^4} \frac{1}{(-\mathrm{i}z^c z_c)^4} \left[\int_{\mathcal{C}_+^\circ} \exp\left(-\frac{\mathrm{i}q_a \bar{w}^a}{\bar{w}^f \bar{w}_f} + \frac{\mathrm{i}q_a z^a}{z^b z_b} \right) (q^d q_d)^2\, \mathrm{d}q^a \right] \Psi(w)\, \mathrm{d}\mu_w. \end{aligned} \tag{F.4}$$

Let

$$m^a = \frac{\mathrm{i}z^a}{z^b z_b} - \frac{\mathrm{i}\bar{w}^a}{\bar{w}^c \bar{w}_c}, \tag{F.5}$$

then we have

$$I(z^a) = \frac{1}{8\pi^5} \int_{\Gamma^+} \frac{1}{(-\mathrm{i}\bar{w}^e \bar{w}_e)^4} \frac{1}{(-\mathrm{i}z^c z_c)^4} \left[\int_{\mathcal{C}_+^\circ} \exp\left(q_a m^a\right) (q^d q_d)^2 \, \mathrm{d}q^a \right] \Psi(w) \, \mathrm{d}\mu_w. \tag{F.6}$$

Let us now calculate the integral inside the square brackets. We define

$$Q(m) = \int_{\mathcal{C}_+^\circ} \exp\left(q_a m^a\right) (q^d q_d)^2 \, \mathrm{d}q^a. \tag{F.7}$$

We now switch to spherical polar coordinates for the spatial components, defining $R^2 = (q^1)^2 + (q^2)^2 + (q^3)^2$, and express the spatial part in terms of the radial coordinate R and angular variables such as θ, via $q^i = R\,\hat{n}^i(\theta, \varphi)$, where $i = 1, 2, 3$. The time component q^0 remains unchanged. The above integral now becomes

$$\begin{aligned} Q(m) &= \int_0^\infty \exp\left(q^0 m^0\right) \\ &\quad \times \int_{R<q^0} \int_{\theta=0}^{\pi} \int_{\phi=0}^{2\pi} \exp\left(-mR\cos(\theta)\right) ((q^0)^2 - R^2)^2 R^2 \sin(\theta) \, \mathrm{d}R \, \mathrm{d}\theta \, \mathrm{d}\phi \, \mathrm{d}q^0. \end{aligned} \tag{F.8}$$

Evaluating the integral for ϕ we obtain

$$\begin{aligned} Q(m) &= 2\pi \int_0^\infty \exp\left(q^0 m^0\right) \\ &\quad \times \int_{R<q^0} \int_{\theta=0}^{\pi} \exp\left(-mR\cos(\theta)\right) ((q^0)^2 - R^2)^2 R^2 \sin(\theta) \, \mathrm{d}R \, \mathrm{d}\theta \, \mathrm{d}\mathrm{q}^0. \end{aligned} \tag{F.9}$$

Using the fact

$$\frac{\mathrm{d}}{\mathrm{d}\theta} \left(\frac{R}{\xi} \exp\left(-R\xi\cos(\theta)\right) \right) = \exp\left(-R\xi\cos(\theta)\right) R^2 \sin(\theta). \tag{F.10}$$

we evaluate the integral for θ to obtain

$$\begin{aligned} Q(m) &= \frac{2\pi}{m} \int_0^\infty \exp\left(q^0 m^0\right) \\ &\quad \times \int_{R<q^0} \left[\left((q^0)^4 R + R^5 - 2(q^0)^2 R^3 \right) \exp\left(-mR\cos\theta\right) \right]_{\theta=0}^{\pi} \mathrm{d}R \, \mathrm{d}q^0. \end{aligned} \tag{F.11}$$

Substituting the limits we obtain

$$\begin{aligned} Q(m) &= \frac{2\pi}{m} \int_0^\infty \exp\left(q^0 m^0\right) \\ &\quad \times \int_{R=0}^{q^0} \left((q^0)^4 R + R^5 - 2(q^0)^2 R^3 \right) \left(\exp\left(mR\right) - \exp\left(-mR\right) \right) \, \mathrm{d}R \, \mathrm{d}q^0. \end{aligned} \tag{F.12}$$

We will now evaluate the integral for R to get

$$\begin{aligned} Q(m) &= 2\pi\int_0^\infty \exp(q^0m^0)\Bigg[\frac{(q^0)^5(\exp(mq^0)+\exp(-mq^0))}{m^2} - \frac{(q^0)^4(\exp(mq^0)-\exp(-mq^0))}{m^2\cdot m} \\ &+\frac{q^0(m^4(q^0)^4+20m^2(q^0)^2+120))(\exp(mq^0)+\exp(-mq^0))}{m^6} \\ &-\frac{(5(q^0)^2m^4+12m^2(q^0)^2+24)(\exp(mq^0)-\exp(-mq^0))}{m^6\cdot m} \\ &-\frac{2(q^0)^3(m^2(q^0)^2+6)(\exp(mq^0)+\exp(-mq^0))}{m^4} \\ &+\frac{6(q^0)^2(m^2(q^0)^2+2)(\exp(mq^0)-\exp(-mq^0))}{m^4\cdot m}\Bigg]\,\mathrm{d}q^0. \end{aligned} \tag{F.13}$$

and finally evaluating the integral for q^0 gives

$$\begin{aligned} Q(m) &= 2\pi\Bigg[\frac{96}{m^4.m}\left(\frac{1}{(m^0+m)^3}-\frac{1}{(m^0-m)^3}\right)+\frac{48}{m^4}\left(\frac{1}{(m^0+m)^4}+\frac{1}{(m^0-m)^4}\right) \\ &+\frac{120}{m^6}\left(\frac{1}{(m^0+m)^2}+\frac{1}{(m^0-m)^2}\right)+\frac{120}{m^6.m}\left(\frac{1}{(m^0+m)}-\frac{1}{(m^0-m)}\right)\Bigg], \\ &= \frac{1536\pi}{((m^0)^2-m^2)^4}=\frac{1536\pi}{(m^am_a)^4}, \end{aligned} \tag{F.14}$$

where we used the fact

$$\frac{\mathrm{d}}{\mathrm{d}\theta}\left(\left(\frac{(q^0)^4R}{m}+\frac{R^5}{m}-\frac{2q^0R^3}{m}\right)(\mathrm{e}^{mR\cos(\theta)})\right)=((q^0)^2-R^2)^2\mathrm{e}^{-mR\cos(\theta)}R^2\sin(\theta). \tag{F.15}$$

Substituting the result for $Q(m)$ into the integral for $I(z^a)$ we get

$$I(z^a) = \frac{192}{\pi^4}\int_{\Gamma^+}\frac{1}{(-\mathrm{i}\bar{w}^b\bar{w}_b)^4}\frac{1}{(-\mathrm{i}z^bz_b)^4}\frac{1}{(m^am_a)^4}\,\mathrm{d}\mu_w. \tag{F.16}$$

We will now expand m^am_a as follows:

$$\begin{aligned} m^am_a &= -\left(\frac{z^a}{z^bz_b}-\frac{\bar{w}^a}{\bar{w}^c\bar{w}_c}\right)\left(\frac{z_a}{z^bz_b}-\frac{\bar{w}_a}{\bar{w}^c\bar{w}_c}\right), \\ &= -\left(\frac{(z^a-\bar{w}^a)(z_a-\bar{w}_a)}{(\bar{w}^b\bar{w}_b)(z^cz_c)}\right). \end{aligned} \tag{F.17}$$

Substituting for m^am_a in the integral for $I(z^a)$ we obtain

$$\begin{aligned} I(z^a) &= \frac{192}{\pi^4}\int_{\Gamma^+}\frac{1}{(-\mathrm{i}z^bz_b)^4}\frac{1}{(-\mathrm{i}\bar{w}^b\bar{w}_b)^4}\left[\frac{1}{-\left(\frac{(z^a-\bar{w}^a)(z_a-\bar{w}_a)}{(\bar{w}^b\bar{w}_b)(z^cz_c)}\right)^4}\right]\Psi(w)\,\mathrm{d}\mu_w, \\ &= \int_{\Gamma^+}\frac{192}{\pi^4(g_{ab}(w^a-\bar{z}^a)(w^b-\bar{z}^b))^4}\,\Psi(w)\,\mathrm{d}\mu_w, \\ &= \Psi(z) \end{aligned} \tag{F.18}$$

□

F.1.2 Proof of proposition 7.3

Proof. Consider an arbitrary function $\phi \in L^2(\mathcal{C}^\circ_+)$. Then applying the inverse Bargmann transform followed by the forward transform yields:

$$\phi(q) = \left(\mathcal{B} \circ \mathcal{B}^{-1}\right) \phi(q) = \int_\Gamma A(q, \bar{z}) \left[\int_{\mathcal{C}^\circ_+} \overline{A(q', \bar{z})}\, \phi(q')\, \mathrm{d}\nu_{q'} \right] \mathrm{d}\mu_z. \tag{F.19}$$

Interchanging the order of integration gives:

$$\phi(q) = \int_{\mathcal{C}^\circ_+} \left[\int_{\Gamma^+} A(q, \bar{z})\, \overline{A(q', \bar{z})}\, \mathrm{d}\mu_z \right] \phi(q')\, \mathrm{d}\nu_{q'}. \tag{F.20}$$

Since this must hold for all ϕ, the integral kernel in brackets acts as the identity on $L^2(\mathcal{C}^\circ_+)$. Therefore, it must be the delta distribution

$$\int_{\Gamma^+} A(q, \bar{z})\, \overline{A(q', \bar{z})}\, \mathrm{d}\mu_z = \delta^{(4)}(q - q'). \tag{F.21}$$

Let us define $J(q)$ to be

$$J(q) = \int_{\Gamma^+} \frac{1}{(-\mathrm{i} \bar{z}^b \bar{z}_b)^4} \exp\left(-\frac{\mathrm{i} q_a \bar{z}^a}{\bar{z}^b \bar{z}_b} \right) \Psi(z^a)\, \mathrm{d}\mu_z. \tag{F.22}$$

Substituting for the Bargmann tranform we get

$$\begin{aligned} J(q) \;\; = \;\; & \frac{1}{8\pi^5} \int_{\Gamma^+} \frac{1}{(-\mathrm{i} \bar{z}^b \bar{z}_b)^4} \exp\left(-\frac{\mathrm{i} q_a \bar{z}^a}{\bar{z}^b \bar{z}_b} \right) \\ & \times \left[\int_{\mathcal{C}^\circ_+} \frac{1}{(i z^b z_b)^4} \exp\left(\frac{\mathrm{i} p_a z^a}{z^b z_b} \right) \psi(p) (p^a p_a)^2\, \mathrm{d}p^a \right], \end{aligned} \tag{F.23}$$

and rearranging the terms yields

$$J(q) \;\; = \;\; \frac{1}{8\pi^5} \int_{\mathcal{C}^\circ_+} \left[\int_{\Gamma^+} \frac{1}{(-\mathrm{i} z^c z_c)^4} \frac{1}{(-\mathrm{i} \bar{z}^b \bar{z}_b)^4} \exp\left(\frac{\mathrm{i} p_a z^a}{z^b z_b} - \frac{\mathrm{i} q_a \bar{z}^a}{\bar{z}^b \bar{z}_b} \right) \mathrm{d}\mu_z \right] \psi(p) (p^a p_a)^2\, \mathrm{d}p^a \tag{F.24}$$

Let us now examine the integral appearing inside the square brackets. To facilitate its evaluation, we perform a change of variables via the Kelvin transform, defined by

$$z^a = \frac{y^a}{y_b y^b}. \tag{F.25}$$

Under this transformation, the measure transforms as

$$\mathrm{d}\mu_z = \frac{1}{(y_b y^b)^8 (\bar{y}_c \bar{y}^c)^8}\, \mathrm{d}\mu_y = \left(\bar{z}_b \bar{z}^b\right)^4 \left(z_a z^a\right)^4 \mathrm{d}\mu_y. \tag{F.26}$$

The integral is now written as

$$J(q) = \frac{1}{8\pi^5} \int_{\mathcal{C}^\circ_+} \left[\int_{\Gamma^+} \exp\left(\mathrm{i} p_a y^a - \mathrm{i} q_a \bar{y}^a \right) \mathrm{d}\mu_y \right] \psi(p) (p^a p_a)^2\, \mathrm{d}p^a. \tag{F.27}$$

If $z^a = x^a - \mathrm{i}\, r^a$, with $r^0 > 0$ and $r^a r_a > 0$, then applying the Kelvin transform has the effect of

negating the time component r^0. More precisely, if

$$y^a = \frac{z^a}{z^b z_b}, \tag{F.28}$$

then one obtains $y^a = m^a - \mathrm{i}\, n^a$ with $n^0 < 0 \quad \text{and} \quad n^a n_a > 0$. Hence, the Kelvin transform maps the future tube to the past tube, inverting the sign of the imaginary time coordinate.

Substituting for y^a in terms of m^a, n^a, the inner integral can now be evaluated as follows:

$$\begin{aligned}\int_{\Gamma^+} \exp\left(\mathrm{i} q_a y^a - \mathrm{i} p_a \bar{y}^a\right) \mathrm{d}\mu_y &= \int_{\Gamma^+} \exp\left(\mathrm{i} q_a (m^a - \mathrm{i} n^a) - \mathrm{i} p_a (m^a + \mathrm{i} n^a)\right) \mathrm{d}^4 m\, \mathrm{d}^4 n, \\ &= (2\pi)^4 \delta^{(4)}(q^a - p^a) \int_{\mathcal{C}^\circ_-} \exp\left(n^a (q_a + p_a)\right) \mathrm{d}^4 n \end{aligned} \tag{F.29}$$

where we have used the fact that

$$\int_{\mathbb{R}^4} \mathrm{e}^{\mathrm{i}\,(q_a - p_a) m^a}\, \mathrm{d}m^a = (2\pi)^4 \delta^{(4)}(q^a - p^a), \tag{F.30}$$

where $\delta^{(4)}$ is a four dimensional delta function.

Let us introduce the vector $\xi^a = q^a + p^a$, with its spatial norm defined as $\xi^2 = (\xi^1)^2 + (\xi^2)^2 + (\xi^3)^2$, and similarly $R^2 = (n^1)^2 + (n^2)^2 + (n^3)^2$. We now consider the four-dimensional integral

$$\int_{\mathcal{C}^\circ_-} \exp\left(n^a \xi_a\right) \mathrm{d}^4 n = \int_{\mathcal{C}^\circ_-} \exp\left(n^0 \xi^0 - n^1 \xi^1 - n^2 \xi^2 - n^3 \xi^3\right) \mathrm{d}^4 n, \tag{F.31}$$

which in spherical coordinates can be written as

$$\begin{aligned}\int_{\mathcal{C}^\circ_-} \exp\left(n^a \xi_a\right) \mathrm{d}^4 n &= \int_{n^0=0}^{-\infty} \exp\left(n^0 \xi^0\right) \\ &\quad \times \int_{R<n^0} \int_{\theta=0}^{\pi} \int_{\phi=0}^{2\pi} \exp\left(-R\xi\cos(\theta)\right) R^2 \sin(\theta)\, \mathrm{d}R\, \mathrm{d}\theta\, \mathrm{d}\phi\, \mathrm{d}n^0. \end{aligned} \tag{F.32}$$

Evaluating the integral for ϕ gives

$$\begin{aligned}\int_{\mathcal{C}^\circ_-} \exp\left(n^a \xi_a\right) \mathrm{d}^4 n &= 2\pi \int_{n^0=0}^{-\infty} \exp\left(n^0 \xi^0\right) \\ &\quad \times \int_{n^1=0}^{n^0} \int_{\theta=0}^{2\pi} \exp\left(-R\xi\cos(\theta)\right) R^2 \sin(\theta)\, \mathrm{d}R\, \mathrm{d}\theta\, \mathrm{d}n^0. \end{aligned} \tag{F.33}$$

Using the fact

$$\frac{\mathrm{d}}{\mathrm{d}\theta}\left(\frac{R}{\xi}\exp\left(-R\xi\cos(\theta)\right)\right) = \exp\left(-R\xi\cos(\theta)\right) R^2 \sin(\theta). \tag{F.34}$$

we evaluate the integral for θ to obtain

$$\int_{\mathcal{C}^\circ_-} \exp\left(n^a \xi_a\right) \mathrm{d}^4 n = 2\pi \int_{n^0=0}^{-\infty} \exp\left(n^0 \xi^0\right) \int_{R<n^0} \left[\frac{R}{\xi}\exp\left(-R\xi\cos(\theta)\right)\right]_0^{\pi} \mathrm{d}R\, \mathrm{d}n^0, \tag{F.35}$$

and on substituting the limits we get

$$\int_{\mathcal{C}_-^\circ} \exp\left(n^a \xi_a\right) \mathrm{d}^4 n = 2\pi \int_{n^0=0}^{-\infty} \exp\left(n^0 \xi^0\right) \int_{R=0}^{n^0} \frac{R}{\xi} (\exp\left(R\xi\right) - \exp\left(-R\xi\right)) \, \mathrm{d}R \, \mathrm{d}n^0. \tag{F.36}$$

Now evaluating the integral for R yields

$$\begin{aligned} \int_{\mathcal{C}_-^\circ} \exp\left(n^a \xi_a\right) \mathrm{d}^4 n &= 2\pi \int_{n^0=0}^{-\infty} \exp\left(n^0 \xi^0\right) \Bigg(\frac{-1}{\xi^3} (\exp\left(\xi n^0\right) - \exp\left(-\xi n^0\right)) \\ &\quad + \frac{n^0}{\xi^2} (\exp\left(\xi n^0\right) + \exp\left(-\xi n^0\right)) \Bigg) \mathrm{d}n^0, \end{aligned} \tag{F.37}$$

and finally evaluating the integral for n^0 gives

$$\int_{\mathcal{C}_-^\circ} \exp\left(n^a \xi_a\right) \mathrm{d}^4 n = 2\pi \left(\frac{1}{\xi^3} \left[\frac{1}{\xi^0 + \xi} - \frac{1}{\xi^0 - \xi} \right] + \frac{1}{\xi^2} \left[\frac{1}{(\xi^0 + \xi)^2} + \frac{1}{(\xi^0 - \xi)^2} \right] \right). \tag{F.38}$$

Substituting the limits and simplifying yields

$$\begin{aligned} \int_{\mathcal{C}_-^\circ} \exp\left(n^a \xi_a\right) \mathrm{d}^4 n &= 2\pi \left(\frac{1}{\xi^3} \frac{-2\xi}{(\xi^0)^2 - (\xi^1)^2} + \frac{2}{\xi^2} \frac{(\xi^0)^2 + (\xi)^2}{((\xi^0)^2 - (\xi)^2)^2} \right), \\ &= \frac{8\pi}{(\xi^a \xi_a)^2}. \end{aligned} \tag{F.39}$$

From all the earlier calculations, we have derived the following result

$$\begin{aligned} \int_{\Gamma^+} \exp\left(\mathrm{i} q_a y^a - \mathrm{i} p_a \bar{y}^a\right) \mathrm{d}\mu_y &= (2\pi)^4 \delta^{(4)}(q^a - p^a) \frac{8\pi}{(q^c + p^c)^2 (q_c + p_c)^2}, \\ &= \frac{128\pi^5 \delta^{(4)}(q^a - p^a)}{((q^c + p^c)(q_c + p_c))^2}. \end{aligned} \tag{F.40}$$

So the Integral for $J(q)$ is evaluated to give

$$\begin{aligned} J(q) &= \frac{1}{8\pi^5} \int_{\mathcal{C}_+^\circ} \frac{128\pi^5 \delta^{(4)}(q^a - p^a)}{((q^c + p^c)(q_c + p_c))^2} \psi(p) (p^d p_d)^2 \, \mathrm{d}p^a, \\ &= \psi(q), \end{aligned} \tag{F.41}$$

and this completes the proof. □

F.1.3 Proof of proposition 7.5

Proof. On the future tube Γ^+, let the initial density kernel be denoted by $R(z, \bar{z})$. A nonselective phase-space measurement, performed by projecting onto coherent states but without recording the outcome, updates the density operator as

$$R^{(1)}(u, \bar{v}) = \int_{\Gamma^+} \frac{K(u, \bar{z}) \, K(z, \bar{v})}{K(z, \bar{z})} \, R(z, \bar{z}) \, \mathrm{d}\mu_z. \tag{F.42}$$

Now, express $R(z,\bar{z})$ using the inverse Bargmann transform

$$R(z,\bar{z}) = \iint_{\mathcal{C}_+^\circ \times \mathcal{C}_+^\circ} \overline{A(q,\bar{z})}\, \rho(q,q')\, A(q',\bar{z})\, \mathrm{d}\nu_q\, \mathrm{d}\nu_{q'}. \tag{F.43}$$

Substituting this into $R^{(1)}$, we obtain

$$R^{(1)}(u,\bar{v}) = \int_{\Gamma^+} \frac{K(u,\bar{z})\, K(z,\bar{v})}{K(z,\bar{z})} \left[\iint_{\mathcal{C}_+^\circ \times \mathcal{C}_+^\circ} \overline{A(q,\bar{z})}\, \rho(q,q')\, A(q',\bar{z})\, \mathrm{d}\nu_q\, \mathrm{d}\nu_{q'} \right] \mathrm{d}\mu_z. \tag{F.44}$$

Next, apply the forward Bargmann transform to map this back to the light-cone representation:

$$\rho^{(1)}(q,q') = \iint_{\Gamma^+ \times \Gamma^+} A(q,\bar{u})\, R^{(1)}(u,\bar{v})\, \overline{A(q',\bar{v})}\, \mathrm{d}\mu_u\, \mathrm{d}\mu_v. \tag{F.45}$$

Substituting the $R^{(1)}$ expression gives

$$\begin{aligned} \rho^{(1)}(q,q') \;=\; & \iint_{\Gamma^+ \times \Gamma^+} A(q,\bar{u}) \\ & \times \left[\int_{\Gamma^+} \frac{K(u,\bar{z})\, K(z,\bar{v})}{K(z,\bar{z})} \left(\iint_{\mathcal{C}_+^\circ \times \mathcal{C}_+^\circ} \overline{A(p,\bar{z})}\, \rho(p,p')\, A(p',\bar{z})\, \mathrm{d}\nu_p\, \mathrm{d}\nu_{p'} \right) \mathrm{d}\mu_z \right] \\ & \times \overline{A(q',\bar{v})}\, \mathrm{d}\mu_u\, \mathrm{d}\mu_v. \end{aligned} \tag{F.46}$$

Consider now the inner u and v integrals. Using the reproducing property of the Bergman kernel, we have

$$\int_{\Gamma^+} K(u,\bar{z})\, A(q,\bar{u})\, \mathrm{d}\mu_u = A(q,\bar{z}) \tag{F.47}$$

and

$$\int_{\Gamma^+} K(z,\bar{v})\, \overline{A(q',v)}\, \mathrm{d}\mu_v = \overline{A(q',\bar{z})}. \tag{F.48}$$

Hence, the bracket simplifies to

$$\rho^{(1)}(q,q') = \iint_{\mathcal{C}_+^\circ \times \mathcal{C}_+^\circ} \left[\int_{\Gamma^+} \frac{A(q,\bar{z})\, \overline{A(q',\bar{z})} A(p',\bar{z}) \overline{A(p,\bar{z})}}{K(z,\bar{z})}\, \mathrm{d}\mu_z \right] \rho(p,p')\, \mathrm{d}\nu_p\, \mathrm{d}\nu_{p'}. \tag{F.49}$$

Since $K(z,\bar{z})$ is strictly positive, one may absorb it into a redefinition of the measure if desired. This completes the transformation of the iterative phase-space measurement back to the light-cone density matrix picture.

We will now evaluate the inner integral

$$I = \int_{\Gamma^+} \frac{A(q,\bar{z})\, \overline{A(q',\bar{z})} A(p',\bar{z}) \overline{A(p,\bar{z})}}{K(z,\bar{z})}.\, \mathrm{d}\mu_z \tag{F.50}$$

Substituting for the explicit form of the Bargmann transform and the reproducing kernel on the future

tube Γ^+, the above equation becomes

$$I = \int_{\Gamma^+} \frac{1}{(z^c z_c)^8 (\bar{z}^d \bar{z}_d)^8} \frac{\exp\left(\frac{-\mathrm{i}q_a \bar{z}^a}{\bar{z}^b \bar{z}_b} - \frac{\mathrm{i}p'_a \bar{z}^a}{\bar{z}^b \bar{z}_b} + \frac{\mathrm{i}p_a z^a}{z^b z_b} + \frac{\mathrm{i}q'_a z^a}{z^b z_b}\right)}{\frac{192}{\pi^4 (g_{ef}(z^e - \bar{z}^e)(z^f - \bar{z}^f))^4}} \,\mathrm{d}\mu_z. \tag{F.51}$$

Now making the substituting $z^a = \frac{w^a}{w_c w^c}$, which corresponds to the Kelvin transform on the future tube, the measure transforms as $\mathrm{d}\mu_z = \frac{1}{w^8 \bar{w}^8} \mathrm{d}\mu_w$, where $w^2 = w^a w_a$. Hence, the integral above becomes

$$\begin{aligned} I &= \int_{\Gamma^-} \frac{w^{16} \bar{w}^{16} \exp\left(w^a(\mathrm{i}p_a + \mathrm{i}q'_a) - \bar{w}^a(\mathrm{i}q_a + \mathrm{i}p'_a)\right)}{\frac{192 w^8 \bar{w}^8}{\pi^4 (g_{cd}(w^c - \bar{w}^c)(w^d - \bar{w}^d))^4}} \frac{1}{w^8 \bar{w}^8} \,\mathrm{d}\mu_w, \\ &= \frac{\pi^4}{192} \int_{\Gamma^-} \exp\left(\mathrm{i}w^a(p_a + q'_a) - \mathrm{i}w^a(q_a + p'_a)\right) g_{cd}(w^c - \bar{w}^c)(w^d - \bar{w}^d)^4 \,\mathrm{d}\mu_w. \end{aligned} \tag{F.52}$$

Now let $w^a = m^a + \mathrm{i}n^a$, where $n^0 > 0$ and $n^a n_a > 0$. We have

$$\begin{aligned} I &= \frac{\pi^4}{192} \iint \exp\left(\mathrm{i}m^a(q'_a + p_a - q_a - p'_a)\right) \\ &\quad \times \exp\left(-n^a(p'_a + p_a + q'_a + q_a)\right)(-4n^c n_c)^4 \,\mathrm{d}m^a \mathrm{d}n^a. \end{aligned} \tag{F.53}$$

By letting

$$\xi_a = q_a + p_a + p'_a + q'_a, \tag{F.54}$$

and evaluating the integral for m^a we obtain

$$I = \frac{(2\pi)^4 (4\pi)^4}{192} \delta^{(4)}(q'_a + p_a - q_a - p'_a) \int \exp\left(-n^a \xi_a\right)(n^c n_c)^4 \,\mathrm{d}n^a. \tag{F.55}$$

The integral over the spatial components of n^a can be conveniently evaluated using spherical coordinates. Let

$$n^2 = (n^1)^2 + (n^2)^2 + (n^3)^2 = R^2, \tag{F.56}$$

where R denotes the spatial norm of the three-vector formed by the spatial parts of n^a. In spherical polar coordinates, the components are parametrised as

$$n^1 = R\sin\theta\cos\phi, \quad n^2 = R\sin\theta\sin\phi, \quad n^3 = R\cos\theta, \tag{F.57}$$

with $\theta \in [0, \pi]$ and $\phi \in [0, 2\pi)$. The measure in these coordinates becomes

$$d^3 n = R^2 \sin\theta \,\mathrm{d}R \,\mathrm{d}\theta \,\mathrm{d}\phi, \tag{F.58}$$

and the standard integration over the solid angle yields a factor of 4π. This representation simplifies the evaluation of integrals that depend only on n^2 by reducing them to a radial integral in R. From

the change of variables into spherical coordinates we get

$$J(\xi) = \int \exp\left(-n^a\xi_a\right)(n^a n_a)^4\,\mathrm{d}n^a \;=\; \int_{n^0=0}^{-\infty}\int_{R=0}^{n^0}\int_{\theta=0}^{\pi}\int_{\phi=0}^{2\pi}\exp\left(-n^0\xi^0 + R\xi\cos(\theta)\right) \times((n^0)^2 - R^2)^4\,R^2\,\sin(\theta)\,\mathrm{d}n^0\,\mathrm{d}R\,\mathrm{d}\theta\,\mathrm{d}\phi, \tag{F.59}$$

Evaluating the integral for ϕ gives

$$\begin{aligned} J(\xi) &= 2\pi\int_{n^0=0}^{\infty}\exp\left(-n^0\xi^0\right) \\ &\quad\times\int_{n=0}^{n^0}\int_{\theta=0}^{\pi}\exp\left(R\xi\cos(\theta)\right)((n^0)^2 - R^2)^4\,R^2\sin(\theta)\,\mathrm{d}\theta\,\mathrm{d}R\,\mathrm{d}n^0, \end{aligned} \tag{F.60}$$

Now evaluating the integral for θ gives

$$\begin{aligned} J(\xi) &= 2\pi\int_{n^0=0}^{\infty}\exp\left(-n^0\xi^0\right)\int_{R=0}^{n^0}((n^0)^2 - R^2)^4R^2\left[\frac{2\sinh(\xi R)}{\xi R}\right]\mathrm{d}R\,\mathrm{d}n^0, \\ &= \frac{4\pi}{\xi}\int_{n^0=0}^{\infty}\exp\left(-n^0\xi^0\right)\int_{R=0}^{n^0}((n^0)^2 - R^2)^4\,R\sinh(\xi R)\,\mathrm{d}R\,\mathrm{d}n^0, \end{aligned} \tag{F.61}$$

and evaluating the integral for R gives

$$\begin{aligned} J(\xi) &= \frac{4\pi}{\xi}\int_{n^0=0}^{\infty}\exp\left(-n^0\xi^0\right)\frac{384}{\xi^{10}} \\ &\times(\xi n^0(945 + 105(n^0\xi)^2 + (\xi n^0)^4)\cosh(\xi n^0) - 15(63 + 28((\xi n^0)^2 + (\xi n^0)^4))\sinh(\xi n^0))\,\mathrm{d}n^0, \end{aligned} \tag{F.62}$$

Finally evaluating the integral for n^0 gives

$$J(\xi) = \frac{384\times 4\times\pi}{\xi^{11}}\frac{15\times 256\xi^{11}}{(\xi^a\xi_a)^6} = \frac{384\times 4\times 15\times 256\times\pi}{(\xi^a\xi_a)^6}. \tag{F.63}$$

Substituting this result in the integral I, we get

$$I = \frac{2^{11}15\pi(2\pi)^4(4\pi)^4\,\delta^{(4)}(q'_a + p_a - q_a - p'_a)}{((q'^c + p^c + p'^c + q^c)(q_c + p_c + q'_c + p'_c))^6}. \tag{F.64}$$

Substituting the result for I in the integral for the coherent-state POVM measurement we get

$$\rho^{(1)}(q,q') = \int_{\mathcal{C}^\circ_+}\int_{\mathcal{C}^\circ_+}\frac{2^{11}15\pi(2\pi)^4(4\pi)^4\,\delta^{(4)}(q'_a + p_a - p'_a - q_a)}{((q^c + p^c + p'^c + q^c)(q_c + p_c + p'_c + q'_c))^6}\rho(p,p')\,\mathrm{d}\nu_{p'}\mathrm{d}\nu_p. \tag{F.65}$$

Evaluating the integral for p' yields

$$\rho^{(1)}(q,q') = \frac{(2^{11}\pi^9)15}{8\pi^5}\int_{\mathcal{C}^\circ_+}\frac{\rho(p,p+q'-q)}{((p^c + q'^c)(p_c + q'_c))^6}\,\mathrm{d}\nu_p. \tag{F.66}$$

By making the substitution $p - q = \lambda$, we get the desired result

$$\rho^{(1)}(q,q') = \frac{15\times 2^5}{\pi}\int_{\mathcal{C}^\circ_+}\frac{\rho(\lambda+q,\lambda+q')}{((q^c + \lambda^c + q'^c)(\lambda_c + q_c + q'_c))^6}((\lambda^d + q^d)(\lambda_d + q_d))^4\,\mathrm{d}\lambda^a. \tag{F.67}$$

□